

• REVIEW •

Multidisciplinary approach to understand the pathogenesis of gastric cancer

Juan Shang, AS Peña

Juan Shang, Hospital of Guangdong University of Technology, Guangzhou 510090, Guangdong Province, China
AS Peña, Laboratory of Immunogenetics and Department of Gastroenterology, VU University Medical Centre, PO Box 7057, 1007 MB Amsterdam, the Netherlands
Supported by the Foundation of Immunogenetics and Cluster I of VU University Medical Center, Amsterdam
Correspondence to: Juan Shang, Hospital of Guangdong University of Technology, Guangzhou 510090, Guangdong Province, China. juanshang@yahoo.com
Telephone: +86-20-38459380 Fax: +86-20-38458695
Received: 2004-10-01 Accepted: 2004-12-09

Abstract

Gastric carcinoma remains a common disease worldwide with a dismal prognosis. Therefore, it represents a very important health problem. It occurs with a high incidence in Asia and is one of the leading causes of cancer death in the world. Although the incidence and mortality of gastric carcinoma are decreasing in many countries, gastric cancer still represents the second most frequent malignancies in the world and the fourth in Europe. The 5-year survival rate of gastric carcinoma is low. The etiology and pathogenesis are not yet fully known. The study of gastric cancer is important in clinical medicine as well as in public health. Over the past 15 years, integrated research in molecular pathology has clarified the details of genetic and epigenetic abnormalities of cancer-related genes in the course of the development and progression of gastric cancer. Gastric cancer, as all cancers, is the end result of the interplay of many risk factors as well as protective factors. Although epidemiological evidence indicates that environmental factors play a major role in gastric carcinogenesis, the role of immunological, genetic, and immunogenetic factors are thought to contribute to the pathogenesis of gastric carcinoma. Among the environmental factors, diet and *Helicobacter pylori* are more amenable to intervention aimed at the prevention of gastric cancer. The aim of the present paper is to review and include the most recent published evidence to demonstrate that only a multidisciplinary approach will lead to the advancement of the pathogenesis and prevention of gastric cancer. On the immunogenetic research it is clear that evidence is accumulating to suggest that a genetic profile favoring the proinflammatory response increases the risk of gastric carcinoma.

Key words: Gastric cancer; *H pylori*; Immunogenetics; IL-1; Diet; Trefoil regulation; gp130

Shang J, Peña AS. Multidisciplinary approach to understand the pathogenesis of gastric cancer. *World J Gastroenterol* 2005; 11(27): 4131-4139
<http://www.wjgnet.com/1007-9327/11/4131.asp>

DISEASE DEFINITION AND CLASSIFICATION

The stomach wall is divided into three major areas: fundus, corpus, or body, and antrum and it has five layers: the inner lining (the mucosa) contains glands. Underneath is the submucosa; then is the layer of muscle; next is the subserosa. The outer layer is the serosa. Gastric cancers are malignancies arising in any part of stomach. Most gastric cancers arise in the antrum, the distal third of the stomach. The predominant site of gastric cancer occurrence has changed over the last 30 years^[1-6]. A large number of tumors involving the proximal stomach and gastro-esophageal junction have been found. The lesser curvature of the stomach is more frequently involved than the greater curvature.

Several different types of cancer can occur in the stomach. Adenocarcinoma, which starts in the glandular cells, is the most common cancer of the digestive tract and histology accounts for 90-95% of all gastric malignancies. It can spread to nearby lymph nodes (LN) and other areas of the body, such as the liver, pancreas, colon, lung, and ovaries. Other types of malignancy in the stomach are sarcoma arising from the cells of the muscle layer, and more common, lymphoma arising in the B and T cells of the lamina propria. The latter two types of malignancies have different prognosis and require different management than adenocarcinoma.

In this review we will concentrate in adenocarcinoma of the stomach mainly because other types have rarely been reported^[7,8].

Several classification systems are used for gastric cancer. Borrmann types, developed by Borrmann in 1923, identify five different types. This tissue classification of gastric cancer is characterized by the shape of the tumor on gastric mucosa and its pervading style in gastric wall.

Lauren developed the DIO system of the histomorphological classification, which assumes two main biological groups: diffuse gastric cancer (D) and intestinal gastric cancer (I), and other (O)^[9,10]. The former two groups account for 90% of all stomach cancers. The intestinal type is well differentiated and characterized by polypoid or fungating

lesions that may ulcerate centrally. Many evidences show that this type is strongly associated with *Helicobacter pylori* (*H. pylori*), and usually arises on a backdrop of chronic gastritis, gastric atrophy, and intestinal metaplasia^[11]. Clinically, the latter is present with diffuse thickening of the stomach wall, rather than a discernible mass. A genetic predisposition is presumed in young patients with a diffuse type of gastric cancer, in contrast to the intestinal type associated with older age^[12,13]. The intestinal type of adenocarcinoma has a better prognosis than the diffuse variant, most of which have spread beyond the confines of the stomach at the time of diagnosis. As with other cancers, stage is the most important determinant of outcome^[14].

According to the standard of WHO, the cellular classification in gastric carcinoma has these subtypes: papillary adenocarcinoma, tubular adenocarcinoma, mucinous adenocarcinoma, signet-ring cell carcinoma, squamous cell carcinoma, adenoacanthoma, undifferentiated carcinoma, unclassified carcinoma and carcinoid tumor.

The Fifth International Union Against Cancer tumor node metastasis (UICC TNM) classification, which was published in 1997, based on the number of metastatic LN, has proved to be a reliable and objective method as the principal assessing the extent and severity of disease and determining the prognosis of cancer patients^[15]. The new TNM classification not only is an objective, simple and reproducible system, but also a significant prognostic index for gastric cancer superior to the old classification. The new TNM classification represents a prognostic factor equally powerful to the old classification. Especially, the new N-classification is superior to the old N-classification in terms of the homogeneity of each N group^[16,17].

X-ray examination after taking barium meal may eventually contribute to detecting delayed gastric emptying quantitatively and indicates the degree of tumor infiltration. Similarly and more accurately, spiral CT is of help in the identification of the gross type, invasion to serous layer and adjacent organs of gastric cancer in its stage of progression. The CT scan is also valuable in detecting metastatic as hepatic, splenic, and abdominal apart from the involvement of LN near the lesion. Enhanced dynamic CT scan plays a significant role in the diagnosis of gastric carcinoma; early enhancing phase scanning is the technique of choice nowadays for demonstrating tumor lesions. Sophisticated scanning technique is mandatory in improving the diagnostic accuracy of gastric carcinoma^[18,19].

The ultrasound examination of stomach so far has been still a difficult technique that requires expertise. It can be used to observe the infiltration of the tumor into the lower layer of the mucous membrane. Endoscopic ultrasonography is very accurate in assessing the depth of tumor infiltration and the lymph node metastasis. It also can be used to determine the progress and prognosis of gastric carcinoma^[20].

DISEASE CHARACTERISTICS

Precancerous lesions of stomach

Six different pathological disorders have been described as increasing the risk for malignancy in the stomach. The following processes have been implicated as precancerous lesions.

Chronic atrophic gastritis There is evidence from animal model that nitrosamine plays a role in developing malignancy. Achlorhydria in atrophic gastritis allows bacterial colonization of the stomach, most extremely in places where overgrowth may cause nitrate reduction and transform the nitrate, which exist in many foods to potentially develop carcinogenic N-nitroso compounds^[21]. This occurs more often in antrum gastritis with intestinal metaplasia and non-typical proliferation. The course of gastritis is rather long and gastric cancer is believed to develop slowly over many years. Some patients present dyspepsia, vague abdominal fullness (after meal), irregular pain, belching, nausea, and vomiting, but not specific. Severe cardiac gastritis may produce glossitis and anemia.

Gastric polyps Familial adenomatous polyps are associated with upper gastrointestinal adenomas and adenocarcinoma. Based on Nakamura's classification^[22,23], hyperplastic polyps were further classified into the following subtypes: the foveolar epithelial type, fundic glandular hyperplastic type, and pyloric glandular hyperplastic type. It was found that atypical hyperplastic foci usually appear in the foveolar epithelial subtype, indicating a close relationship to cancer. This finding suggests that the subclassification of hyperplastic gastric polyp has a higher practical value in clinical application^[24].

Gastric ulcer Some gastric cancers are considered to transform from gastric ulcers, but with a low rate, 1-5% in China. Cancerous degeneration of ulcer was small and the epithelial regeneration at the ulcer's edge and benign fusion of the muscularis mucosa with the muscularis propria were very common. The cancerous tissue extending to node metastasis was rare. Therefore, the cancerous tissue down to the submucosa was found at the margin but not at the base of the ulcer. These patients should be thought seriously, specially if they are more than 45 years old, the symptoms of gastric ulcer are persistent 1 mo after treatment. These findings that conform well to Hauser's criteria blood test are positive. These results suggest that multiple biopsies should be taken from the edge of chronic ulcers. The most distinct feature of malignant ulcer was the lack of cancerous infiltration and muscular residue in the scar tissue of ulcer base. The existence of this type of ulcer clinically and pathomorphologically supports the viewpoint that gastric cancer ulcer can undergo malignant change^[25].

Cancer of gastric remnant Patients after gastrectomy have more opportunity to get vicious tumor than normal people, and the course from remnant stomach to gastric cancer is nearly 15-30 years. Refluxing of intragastric and bile after gastrectomy became the base of gastritis. Furthermore the pH is increased and is beneficial to the abnormal proliferation of cell, carcinogen such as nitrite transfer to nitrosamine. Bile salt, a carcinogen, sometimes can lead to cancer.

Cholecystitis It was found that both the content of various kinds of biliary acid salt and pH value of gastric juice were much higher in patients with gastric cancer, gastric ulcer, and chronic atrophic gastritis than in normal controls. Bile acid salt is known to be harmful to gastric mucosa and the damage becomes more severe with the increase of bile acid salt concentration and prolongation of exposure. Therefore,

our results suggest that the bile acid salt in the gastric juice is one of the carcinogenic factors^[26].

Pernicious anemia Pernicious anemia can lead to atrophic gastritis and is well known to be associated with gastric cancer. Pernicious anemia and autoimmune disease in general is rare in Chinese patients. There are few reports of pernicious anemia in Chinese patients and does not play a significant role as a predisposing cause of gastric cancer in China^[27,28].

Gastric schistosomiasis Gastric carcinoma has been found arising from schistosomiasis in the epidemic area of south China and this chronic inflammation has been linked to development of gastric cancer in this area of China^[29].

Early gastric cancer

The designation early gastric cancer (EGC) refers to a gastric carcinoma, which does not infiltrate beyond the submucosa. This definition is not influenced by absence or presence of metastases or by the diameter of the tumor. The 5-year survival of EGC is 90% or more. The diagnosis can regularly be made if, in the case of persistent vague upper abdominal complaints, an optimal radiological examination of the stomach is done. At even the slightest radiological suspicion, or if complaints persist in spite of negative radiological findings, gastroscopic examination and multiple-aimed biopsies should follow. Attention should be focused on the gastric angular incisure, antrum and lesser curvature to perform site-directed biopsy. Final diagnosis depended on the pathological diagnosis of the biopsy material. Pathologic diagnosis would be correct, provided the biopsy material was taken from the proper site^[30,31].

An investigation from Liaoning Province reported pathological characteristics of EGC in Chinese patients. The peak age of the patients was between 50 and 59 years. The incidence in female before 50 years was higher than that in male but reverse after this age. The most common site was in lower part of the stomach. Highly differentiated carcinomas were more frequently found in those cancer foci of no larger than 0.5 cm in diameter. More signet ring cell carcinomas were found. Lymphatic metastasis was more in type IIc+III and the least in type I. Comparing with the Japanese cases, it was found that the peak age of EGC patients in Japanese was 10 years older than that in Chinese patients and most of the tumor occurred in middle part of the stomach. Type III and mucinous adenocarcinoma was hardly found^[32].

The recurrence rate was higher in submucosal tumors than in mucosal tumors, in lymphatic and vascular vessel invasion-positive cases than in negative cases, in synchronous multiple gastric cancer than in solitary tumors, in tumors of 1.5 cm or more in diameter than in tumors of less than 1.5 cm. The rate of hematogenic metastasis to the liver or lung was 45.5%, and the recurrence in the residual stomach was 27.3% and in lymph node was 27.3%^[33].

Advanced gastric cancer

Because of the elusive nature of gastric disorders, gastric cancer usually is advanced when symptoms first appear. There are several characteristic routes by which gastric carcinoma will progress and metastasize: (1) by extension

and infiltration along the mucosal surface and stomach wall or lymphatic vessels, (2) via lymphatic or vascular embolism, probably to regional LN, (3) by direct extension into adjacent structures such as the pancreas, liver, or esophagus, and (4) by blood-borne spread. The pattern of metastatic spread of gastric cancer correlates with the size and the location of tumor. Lesions of the distal portion of the stomach usually metastasize to infra-pyloric, inferior gastric, and celiac LN. Tumors in the proximal portion often metastasize to pancreatic, pericardial, and gastric LN. With advanced gastric cancer, involvement of the left supraclavicular nodes may occur. Distant metastatic sites are the lung, adrenal glands, bone, liver, pancreas, and peritoneal cavity^[34].

Clinical syndromes

In the early stage, GC seldom showed significant symptoms, some of which are common to other, less serious gastrointestinal disorders (bloating, gas, and a sense of fullness). Some degrees of dysplasia occur, appetite loss, heartburn, vague abdominal fullness, flatus, excessive belching, and breath odor, mild or severe, were similar as in the presentation of chronic gastritis or gastric ulcer previously reported. Soon afterwards the difficulty in swallowing, particularly difficulty that increases over time, nausea and vomiting, abdominal pain and weight loss were on the rise. In the late stage some patients might vomit blood; have blood in the stools or black stools, tiredness due to anemia, abdominal pain and weight loss are aggravated, a decline in general health.

As other malignancies, early detection, early diagnosis, and early treatment remain the key to improve the survival of patients with resected cancer of the gastric cardia. Why residual tumor left at the resection edge and the presence of tumor thrombi do not influence survival needs to be further studied.

EPIDEMIOLOGY

The epidemiology of gastric cancer involves many features, since there are significant geographical, ethnical, and cultural factors influencing the prevalence of GC. It is more frequent in the developing world than in the developed world, more common in Asia than in Europe, and more in Latin America than in North America and Africa^[35]. Stomach cancer in China has distinct geographically different distribution. The morbidity in urban areas is higher than in rural areas, giving a difference of 1.9 times^[36]. According to an investigation between 1989 and 1999, in Linqu County of China, no reduction in GC mortality was observed in the highest risk population worldwide^[37].

The most recent estimates indicate that gastric cancer is the second most common cancer in the world after lung cancer. It represents 11% of all cancers in men and 7% of all cancers in women. In developing countries, lung cancer ranks first, representing 13% of all cancers and gastric cancer second (12%). In developed countries gastric cancer ranks fifth, representing 7% of all cancers, three-fourth of which occur in Asia. About 80% of the cases diagnosed in Asia occur in China and Japan. Steady decline in the rates of gastric cancer has been observed everywhere in the last few decades. However, the total number of new cases

diagnosed worldwide is increasing mainly because of increasing and aging of the population. It was estimated that there were 700 000 new cases in 1980, 755 000 in 1985, 900 000 in 1990, 1 013 000 in 1995, and 1 000 000 in 2000. This indicates that the impact of gastric cancer in public health is not decreasing^[4].

ETIOLOGY

Gastric cancer, of all cancers, is the end result of the interplay of many risk factors as well as protective factors. Genetic and environmental factors are likely to play a role in the etiology of the disease. Several factors are suspected to play a role in gastric carcinogenesis, including the effects of diet, exogenous chemicals, intragastric synthesis of carcinogens, genetic factors, infectious agents, and pathological conditions in the stomach (such as gastritis). According to Correa, there is evidence from pathology and epidemiology studies that gastric carcinogenesis develops with the following sequential stages: chronic gastritis; atrophy; intestinal metaplasia; and dysplasia. The initial stages of gastritis and atrophy have been linked to excessive salt intake and infection with *H pylori*^[38].

Environmental factors and gene polymorphisms involved in the susceptibility of gastric cancer

Several epidemiological evidences indicate that environmental factors play an important role in gastric carcinogenesis. The fact that immigrants exhibit incidence rates similar to those of their country of origin has led researchers to accept exogenous influences such as environment and diet. The investigation from China showed that the risk factors of gastric cancer were living in high incidence area for a long period, low economic income, low consumption of fresh vegetables and fruits and animal protein, high intake of sweet potato and ink fish and salted meat, eating and drinking too much at one meal and mental injury, and a family history of gastric cancer. High intake of grains and low intake of animal fat and proteins appear to be associated with a decreased risk. Diets rich in vitamins A and C are associated with low risk for gastric cancer. Controversy exists over the role of nitrates found in soil-grown foods, drinking water, and prepared foods. Because refrigeration and a high intake of ascorbic acid inhibit the formation of nitrates, it is postulated that the presence of these factors may account for decreasing gastric cancer. Neither smoking tobacco nor drinking alcohol has been demonstrated to increase the risk of gastric carcinoma^[32,39-44].

H pylori

Gastric carcinogenesis is a multistep and multifactorial process beginning with *H pylori*-associated gastritis in most cases. *H pylori* infection, together with other environmental factors and individual susceptibility, determine the final risk for the development of gastric cancer. The discovery of *H pylori* in the early 1980s has proved a turning point in understanding the pathogenicity of this malignancy. *H pylori* infection is common worldwide and about half of the human population believed to be infected. But only a small fraction of infected individuals develop gastric cancer.

Additional factors must be involved in the progression toward cancer^[45,46,50].

H pylori are highly host-adapted bacterial pathogens that establish a chronic infection in the human stomach and have no known animal or environmental reservoirs. It shows a high degree of genetic heterogeneity due to mutations and frequent recombination. In the past, specific genes have been identified which are associated with bacterial virulence. These genes (e.g., *vacA*, cytotoxin associated gene A (*cagA*), and *iceA*) have been studied individually, and distinct genotypes have been defined. There is accumulating evidence that the different genotypes of *H pylori* show a particular geographic distribution^[51]. *H pylori* strains containing the *cagA* protein are associated with more severe disease and harbor a 40-kb pathogenicity island (PAI) induce NF- κ B activation and interleukin (IL)-8 secretion in gastric epithelial cells. *H pylori* changes the expression of genes encoding growth factors and cytokine/chemokines and their receptors, apoptosis proteins, transcription factors, and metalloprotease-disintegrin proteins, and tissue inhibitors of metalloproteinases^[47].

H pylori stimulate endothelial cells to upregulate adhesion molecule expression and to increase the production of neutrophil-recruiting chemokines. The PAI encodes a bacterial type IV secretory system that secretes and translocates the *cagA* protein into host cells, where it is phosphorylated by a host-cell kinase and causes morphological changes. Innocenti *et al.*, found that several, but not all, *H pylori* strains are able to activate endothelial cells to express the adhesion molecules VCAM-1, ICAM-1, and E-selectin and to secrete neutrophil-recruiting chemokines, and therefore contribute to tissue damage and ulcer formation^[48,49]. Among people infected with *H pylori*, the virulence of the infecting strain is a major determinant which develops disease. Strains producing vacuolating cytotoxin activity are more commonly isolated from people with peptic ulcers than without. The gene encoding the toxin, *vacA*, varies between strains, especially in its signal sequence and mid regions. *vacA* genotype influence cytotoxin activity, and signal sequence type correlates closely with peptic ulceration. Infection with strains possessing *cagA* is more common among people with peptic ulceration or gastric adenocarcinoma than without. *CagA*+ *H pylori* infection is more closely associated with gastric cancers and peptic ulcers than *cagA*-infection. Because *cagA*+ infection may be associated with the development of atrophic gastritis, *cagA* infection is believed to be a risk factor for intestinal-type gastric cancer. But Deguchi *et al.*, reported that *cagA* infection is also associated with diffuse-type gastric cancer in Japan. They also found that all p53 alteration were in *H pylori*-positive gastric cancer and their mutations were more frequent in the *cagA* group, although the correlation between p53 mutation and *H pylori* infection did not reach statistical significance. p53 abnormality was clinically correlated with prognostic factors (e.g., tumor size, depth, lymph node metastasis) of gastric cancer. These findings indicated that *cagA*+ *H pylori* infection might have an important role in the development of gastric cancer with p53 mutation^[52].

The p53 tumor suppressor gene, located on chromosome

17p13, is one of the most commonly mutated genes in all types of human cancer. p53 codon 72, which produces variant proteins with an arginine (Arg) or proline (Pro), has been reported to be associated with cancers of the lung, esophagus, and cervix. Recently, studies in Japan suggested that the Pro/Pro genotype at p53 codon 72 contributes to susceptibility of diffuse-type gastric cancer patient with *H. pylori*-CG^[53]. The mutation of p53 and inactivation of p21WAF1 and p16 play an important role in carcinogenesis of stomach. However, *H. pylori* infection was not associated with the abnormal expression of these three genes in China^[54].

Human Chk1 and Chk2 are DNA damage-activated protein kinases that function as downstream mediators of ataxia-telangiectasia mutated, which are involved in G₂/M cell-cycle arrest. A study from Japan found a significant correlation between the levels of expression of Chk1 and p53 proteins in gastric carcinomas. Chk2 might be important in the checkpoint function in human gastric carcinomas with p53 mutation^[56]. Mutations of an oncogene, K-ras, may be involved in the early stage of carcinogenesis of the intestinal types. The incidence of K-ras mutations in gastric cancer is only 10%. However, by histological classifications, the incidence of K-ras mutation was more frequent in intestinal types than in diffuse types of gastric adenocarcinoma. In addition, K-ras mutations in *H. pylori*-associated chronic gastritis were significantly more frequent in gastric cancer patients than in cancer-free patients (50% *vs* 3.7%, $P = 0.037$)^[57].

No evidence for the involvement of antigastric antibodies in the stimulation of apoptosis was found. Therefore, host factors may be at least as important as bacterial factors in determining gastric mucosal responses to *H. pylori*^[55].

Interleukin gene polymorphisms and gastric cancer

The presence of *H. pylori* in gastric antrum is, in most cases, associated with mucosal inflammatory changes consisting of infiltration of a large number of polymorphonuclear and mononuclear phagocytes. *H. pylori* reside in the mucus layer overlying the epithelium and do not invade epithelial cells. However, accumulating evidence indicates that gastric infection with *H. pylori* induces the expression of several proinflammatory cytokines, including IL-1 β , IL-6, IL-8, IL-18 and TNF- α in gastric mucosa.

IL-1 β is a potent proinflammatory cytokine and powerful inhibitor of gastric acid secretion that is upregulated in the presence of *H. pylori* and is important in initiating and amplifying the inflammatory response to this infection. El-Omar *et al.*, reported that gene polymorphisms in the interleukin gene family of cytokines (IL-1 β -31C, IL-1 β -511T, and IL-1RN*2 alleles) are associated with an increased risk of both hypochlorhydria, in *H. pylori* negative infected first-degree relatives of gastric carcinoma^[58,59]. A study from Portugal supported the hypothesis that host genetic factors that affect IL-1 gene determine why some individuals infected with *H. pylori* develop gastric cancer while others do not^[60,61]. The polymorphism of promoter region -31C/T of IL-1 β gene and the polymorphism of IL-1RN genes 1/2 and 2/2 are associated with the susceptibility of gastric cancer in Chinese. Carrying -31T

allele increases the risk of gastric cancer. Polymorphism of IL-1RN and IL-1 β gene may be used as indicators of susceptibility of gastric carcinogenesis^[62]. A study from Japan investigated the polymorphism of -511 T-to-C located in the IL-1 β gene. According to these authors in view of the results for the IM or CAG without *H. pylori* group, the presence of the C allele may also indicate a risk of mucosal atrophy of the stomach in the Japanese population^[63].

Serum levels of IL-8 and nitrogen monoxide (NO) are correlated with CagA+*H. pylori* strain infection. Combined detection of serum level of IL-8, NO, and HP-CagA will contribute to the early diagnosis of precancerous lesion in the stomach^[64]. Secretion of IL-8 by gastric epithelial cell upon *H. pylori* infection is dependent on activation of NF- κ B^[65].

IL-18 is a recently identified cytokine (originally termed interferon γ -inducing factor) and is related to the IL-1 family both structurally and functionally. Recently research has showed that IL-18 was increased in a variety of human inflammatory conditions, including Crohn's disease, rheumatoid arthritis, and tuberculoid leprosy with pleiotropic immunomodulatory functions. It has been found that IL-18 mRNA expression was greater in *H. pylori*-positive than in *H. pylori*-negative patients with normal mucosa. But mature IL-18 protein and active caspase-1 p20 are present in mucosa of both *H. pylori*-infected and -uninfected subjects. The presence of the mature form of IL-18 in both normal and gastric mucosa suggests that gastric IL-18 has an important role in promoting local production of interferon-N and cell-mediated responses in the gastric mucosa^[47].

H. pylori induces the production of tumor necrosis factor- α (TNF- α), which is closely related to epithelial injury. TNF- α plays a crucial role in host defense against infection, but a high concentration of TNF- α may cause severe pathology. The gene for TNF- α is located within the class III region of the major histocompatibility complex, which is a highly polymorphic region. The most common exchanges are G to A transitions in the TNF- α promoter at positions -308 (-308A) and -238 (-238A), and these genetic changes have been reported to influence TNF- α concentrations. It is possible that increased TNF- α concentrations, as a result of -308A polymorphism, alter the immune response, which confers susceptibility to gastric disease with *H. pylori*-cagA subtype infection^[66]. In a study in Spain, these results suggest that TNF and LTA gene polymorphisms are related to the development of gastric and duodenal ulcer and may determine disease outcome in *H. pylori* infection^[67].

Wu *et al.*, have reported that no association was noted between gastric cancer and the distribution of IL-1 and TNF- α genotypes in Taiwanese Chinese. Logistic regression analysis revealed that *H. pylori* infection, cigarette smoking, and IL-10 genotype are independent risks for gastric cancer in the Taiwanese. Similar studies should be carried out in different populations and as Wu *et al.*, have correctly performed the risk of genotypes should be adjusted with confounding environmental risks^[68].

Genetic polymorphisms of some metabolizing enzymes

Environmental genotoxic chemical agents arising from the

diet, smoking, and air pollution are responsible for carcinogenesis in humans. It is generally accepted that the majority of carcinogenic chemical do not produce their biological effects *per se*, but require metabolic activation by host enzymes: phase I enzymes including cytochrome P450 enzyme and phase II enzymes including epoxide hydroxylase, *N*-acetyltransferase 2 (NAT2), and glutathione *S*-transferase (GSTs). Genetic polymorphisms have been recently shown in many of these enzymes, indicating that there are genetic differences among individuals in the ability to metabolize chemicals. Such genetic polymorphisms may affect the individual susceptibility to chemical carcinogenesis. From this point of view, the relationship between the genetic polymorphisms and carcinogenicity has been extensively examined to determine which polymorphic enzymes are highly associated with the susceptibility to cancers. Japanese researchers suggested that a combination of GSTM1 and NAT2 decreases the risk of gastric cancer in Japanese patients^[69]. A population-based case-control study in China suggested that the GSTP1 genotype seems not to be associated with the risk of gastric cancer and chronic gastritis in a high-risk Chinese population^[70]. The polymorphic genes of cytochrome P450, CYP2A6, and CYP2E1 have been implicated in increased susceptibility to certain malignancies. The CYP2A6 deletion was associated with gastric adenocarcinoma among Japanese population^[72].

KILLER/death receptor DR5

The KILLER/death receptor DR5 has been identified as a potent inducer of apoptosis, and mapped to chromosome 8p21-22, showing frequent allelic loss in gastric cancer. As stated before, the p53-induced apoptosis is an important biological process to prevent the development of cancer, and is mediated in part by expression of KILLER/DR5 only in cells with wild-type p53 protein, but not in those lacking p53 function. A report from Japan suspected that inactivation of KILLER/DR5 caused by mutations of KILLER/DR5 may be one of the possible escaping mechanisms against KILLER/DR5-mediated apoptosis and that inactivating mutation of KILLER/DR5 may contribute to the promotion or progression of a subset of gastric cancers^[71]. In Japan, another cancer registry-based study found that the incidence of gastric cancer was increased up to 5-fold in male relatives of early-onset prostate cancer patients. Currently unknown genes might contribute to the observed link between prostate and gastric cancer^[73].

E-cadherin

E-cadherin is a member of the cadherin family of calcium-dependent cell adhesion molecules. These molecules are localized in lateral cell-cell contacts of the epithelial cells and regulate the process of homophilic/homotypic adhesion between epithelial cells and play a role as a tumor suppressor gene. E-cadherin associates with α -catenin, β -catenin, and γ -catenin to form a complex that is essential for cell-cell communication and cell adhesion. Indeed, abnormal E-cadherin expression (characterized by loss, reduced, and/or cytoplasmic expression) has been observed in several types of carcinoma, and is frequently associated with poor differentiated/undifferentiated carcinomas and/or invasive

tumors. A co-operative study among Portugal, Germany, and Belgium reported that E-cadherin inactivation is significantly related with the diffuse histotype in gastric carcinoma, not only in "pure" diffuse carcinomas but also in the diffuse component of mixed tumors, β -catenin mRNA levels are increased in the vast majority of intestinal-type gastric cancers and this overexpression is independent of *H pylori* infection^[74,75].

Trefoil regulation, gp130, and gastric cancer

For a long time it was believed that the stomach and the intestine respond differently to inflammation. The immunological system of the stomach appears less fully developed than the intestine. This in part is due to the fact that nature has given the stomach a mechanism to protect itself with the production of hydrochloric acid and therefore an environment where only special bacteria, such as *H pylori* can survive. The intestine on the contrary is full of bacteria; however, seemingly ends in unrelated diseases. Inflammatory bowel disease and gastric cancer share in common an origin in chronic inflammation. An important and interesting finding that has arisen from research in mice with a "knock-in" mutation abrogating the Src-homology tyrosine phosphatase 2 (SHP2)-Ras-ERK signaling that developed gastric adenomas by 3 mo of age. Mice with a mutation eliminating the STAT1/3 signaling gp130 (Delta STAT)) showed impaired colonic mucosal wound healing^[76]. As stated in an editorial in Nature Medicine^[77], given the close interplay between the immune response and epithelial cells, it is not surprising that perturbations in signaling of immune system mediators play a key role in disease of the gut. It is the gp130 receptor, which binds the IL-6 family (IL-6 and IL-11) of cytokines that serve as an inflammation intersection between the stomach and the intestine. The homodimers of gp130, a transmembrane receptor β -chain, contain two discrete functional modules which signal through SHP-2/Erk and STAT1/3 that are responsible for the different behavior exhibited by the stomach and the intestine in response to inflammation. To understand the pathogenesis, it is necessary to understand the function of other family of genes called the trefoil factor (TFF) family that intimately appear to work with the gp130 molecule. Suemori *et al.*^[78], discovered in 1991 a group of small proteins designated intestinal trefoil factor. These authors demonstrated that it is primarily expressed and secreted onto the intestinal surface by goblet cells, suggesting that it may be an important component of intrinsic mechanisms for defending mucosal integrity. They are upregulated around areas of epithelial damage, ulceration, and neoplasia^[79].

IL-1 and IL-6 overexpression in chronic gastritis may lead to mucosal damage and gastric carcinogenesis through transcriptional repression of TFF1 and TFF2^[80]. TFF1 knockout mice developed multiple gastric adenomas and carcinomas, suggesting that TFF1 is a gastric-specific tumor-suppressor gene^[81]. The gp130 directly regulates the TFF genes. The trefoils are key downstream targets of the SHP2/Erk and STAT signaling pathways. The data also add to TFF1's credibility as a gastric-specific tumor-suppressor gene and TFF3's as a mediator of intestinal homeostasis. The hyperproliferative lesions was observed in the stomachs

of gp130 arise as a result of enhanced STAT3 activity in the absence of a counter-acting signal from the SHP2-Ras-Erk pathway rather than from the complete absence of (IL-6 and IL-11-mediated) gp130 signaling. IL-6 is likely to have an important role in the initial phase of intestinal wound healing. Furthermore, endogenous IL-11, unlike pharmacologically administered IL-11, seemed to have negligible effects on the intestinal epithelium.

In conclusion, although the incidence of gastric cancer is decreasing in some parts of the world, it still takes a significant toll among the inhabitants of Japan, China, Chile, Finland, Poland, Austria, Yugoslavia, and Costa Rica. The key to prevention of cancer of stomach lies in dietary intake. It is important to consume a balanced diet high in fresh fruits and vegetables and moderate amount of animal protein and fats. Salted, smoked, and pickled foods should be consumed in low quantities.

Screening and early detection programs are very useful. If detected at an early stage and treated aggressively, gastric cancer can be cured. As with all other forms of gastrointestinal cancers, gastric cancer is insidious in its onset and development. It usually infiltrates rapidly and can be disseminated throughout the body before overt signs of cancer are manifested. Overall 5-year survival rates are reported to range from about 8% to 16%. Gastric cancer mimics several other gastrointestinal maladies and diseases such as polyps, ulcers, dyspepsia, and gastritis. Some of the most difficult aspects of prevention and early detection are informing and motivating people at risk for the development of gastric cancer to seek medical attention for chronic "stomach problems". Inappropriate use of home remedies, self-medication, and misdiagnosis are major hurdles to overcome.

REFERENCES

- 1 **Gonzalez CA**, Sala N, Capella G. Genetic susceptibility and gastric cancer risk. *Int J Cancer* 2002; **100**: 249-260
- 2 **Ladero JM**, Agundez JA, Olivera M, Lozano L, Rodriguez-Lescure A, Diaz-Rubio M, Benitez J. N-acetyltransferase 2 single-nucleotide polymorphisms and risk of gastric carcinoma. *Eur J Clin Pharmacol* 2002; **58**: 115-118
- 3 **Yasui W**, Oue N, Kuniyasu H, Ito R, Tahara E, Yokozaki H. Molecular diagnosis of gastric cancer: present and future. *Gastric Cancer* 2001; **4**: 113-121
- 4 **Yamashita S**, Wakazono K, Sugimura T, Ushijima T. Profiling and selection of genes differentially expressed in the pylorus of rat strains with different proliferative responses and stomach cancer susceptibility. *Carcinogenesis* 2002; **23**: 923-928
- 5 **Alexander HR**, Grem JL, Pass HI, Hamilton M, McAtee N, Fraker DL, Allegra CJ. Neoadjuvant chemotherapy for locally advanced gastric adenocarcinoma. *Oncology* 1993; **7**: 37-42
- 6 **Powell J**, McConkey CC. Increasing incidence of adenocarcinoma of the gastric cardia and adjacent sites. *Br J Cancer* 1990; **62**: 440-443
- 7 **Xue ZQ**. Primary gastric malignant lymphoma-analysis of 32 cases. *Zhonghua Zhongliu Zazhi* 1989; **11**: 133-135
- 8 **Liu XF**, Huang YR. Primary gastric malignant lymphoma-analysis of 40 patients. *Zhonghua Zhongliu Zazhi* 1987; **9**: 298-301
- 9 **Lauren P**. Histogenesis of intestinal and diffuse types of gastric carcinoma. *Scand J Gastroenterol Suppl* 1991; **180**: 160-164
- 10 **Lauren PA**, Nevalainen TJ. Epidemiology of intestinal and diffuse types of gastric carcinoma. A time-trend study in Finland with comparison between studies from high- and low-risk areas. *Cancer* 1993; **71**: 2926-2933
- 11 **Lawrence W Jr**, Menck HR, Steele GD Jr, Winchester DP. The National Cancer Data Base report on gastric cancer. *Cancer* 1995; **75**: 1734-1744
- 12 **Taal BG**, van Loon HJ, Kahn N, de Jong D, Vasen HF, van 't Veer LJ. The role of genetic factors in the development of gastric cancer. *Ned Tijdschr Geneesk* 1999; **143**: 342-346
- 13 **Heiss MM**, Babic R, Allgayer H, Gruetzner KU, Jauch KW, Loehrs U, Schildberg FW. The prognostic impact of the urokinase-type plasminogen activator system is associated with tumour differentiation in gastric cancer. *Eur J Surg Oncol* 1996; **22**: 74-77
- 14 **Wang MX**. Pathological characteristics of early gastric cancer in 1477 Chinese patients. *Zhonghua Zhongliu Zazhi* 1993; **15**: 368-371
- 15 **Hyung WJ**, Noh SH, Yoo CH, Huh JH, Shin DW, Lah KH, Lee JH, Choi SH, Min JS. Prognostic significance of metastatic lymphnode ratio in T3 gastric cancer. *World J Surg* 2002; **26**: 323-329
- 16 **Wang Z**, Xu H, Wang S, Chen J. Relationship between new TNM classification and the prognosis and biological behavior of gastric cancer. *Zhonghua Waike Zazhi* 2000; **38**: 493-495
- 17 **Katai H**, Yoshimura K, Maruyama K, Sasako M, Sano T. Evaluation of the New International Union Against Cancer TNM staging for gastric carcinoma. *Cancer* 2000; **88**: 1796-1800
- 18 **Lu C**, Xu H, Zhang X. Judgement of gross type and local invasion of advanced gastric carcinoma by spiral computed tomography. *Zhonghua Zhongliu Zazhi* 2000; **22**: 235-237
- 19 **Jiang L**, Shi M, Hao Y. Two-phase dynamic CT findings of gastric carcinoma and its value for tumor detection and gross classification. *Zhonghua Zhongliu Zazhi* 1998; **20**: 374-376
- 20 **Yang A**, Lu X, Chen Y. The role of endoscopic ultrasonography and epidermal growth factor receptor assay in preoperative staging for gastric carcinoma. *Zhonghua Neike Zazhi* 1995; **34**: 743-746
- 21 **Stockbruegger RW**. Bacterial overgrowth as a consequence of reduced gastric acidity. *Scand J Gastroenterol Suppl* 1985; **111**: 7-16
- 22 **Nakamura T**, Nakano G. Histopathological classification and malignant change in gastric polyps. *J Clin Pathol* 1985; **38**: 754-764
- 23 **Muratani M**, Nakamura T, Nakano GI, Mukawa K. Ultrastructural study of two subtypes of gastric adenoma. *J Clin Pathol* 1989; **42**: 352-359
- 24 **Zhao GH**. Histopathological analysis of gastric polyps: classification and relationship to cancer. *Zhonghua Binglixue Zazhi* 1993; **22**: 279-281
- 25 **Zhao JS**. Comparative pathologic study on the peri-ulcer mucosal lesion around benign and malignant gastric ulcer. *Zhonghua Zhongliu Zazhi* 1992; **14**: 357-359
- 26 **Xu MR**. The relationship between bile acid and factors relative to gastric cancer. *Zhonghua Waike Zazhi* 1992; **30**: 719-721
- 27 **Au WY**, Hui CH, Chan LC, Liang RH, Kwong YL. Clinicopathological features of megaloblastic anaemia in Hong Kong: a study of 84 Chinese patients. *Clin Lab Haematol* 1998; **20**: 217-219
- 28 **Zuidema PJ**. A Chinese patient with pernicious anemia; a medical experience from the Indonesian period. *Ned Tijdschr Geneesk* 1996; **140**: 561-563
- 29 **Zhou XX**. Relationship between gastric schistosomiasis and gastric cancer, chronic gastric ulcer and chronic gastritis: pathological analysis of 79 cases. *Zhonghua Binglixue Zazhi* 1986; **15**: 62-64
- 30 **Dekker W**, Op Den Orth JO. Early gastric cancer. *Radiol Clin* 1977; **46**: 115-129
- 31 **Zhang B**, Cai J, Chen G. Diagnosis and treatment of early gastric cancer: an experience from 61 cases. *Zhonghua Zhongliu Zazhi* 1999; **21**: 383-385
- 32 **Wang R**. The epidemiological study of subtype risk factors of gastric cancer. *Zhonghua Liuxingbingxue Zazhi* 1993; **14**: 295-299

- 33 **Shan J**, Chen J, Wang S. Recurrence of early gastric cancer. *Zhonghua Yixue Zazhi* 1996; **76**: 750-752
- 34 **Macdonald JS**. Gastric cancer: chemotherapy of advanced Disease. *Hematol Oncol* 1992; **10**: 37-42
- 35 **Neugut AI**, Hayek M, Howe G. Epidemiology of gastric cancer. *Semin Oncol* 1996; **23**: 281-291
- 36 **Sun X**, Mu R, Zhou Y, Dai X, Qiao Y, Zhang S, Huangfu X, Sun J, Li L, Lu F. 1990-1992 mortality of stomach cancer in China. *Zhonghua Zhongliu Zazhi* 2002; **24**: 4-8
- 37 **Riecken B**, Pfeiffer R, Ma JL, Jin ML, Li JY, Liu WD, Zhang L, Chang YS, Gail MH, You WC. No impact of repeated endoscopic screens on gastric cancer mortality in a prospectively followed Chinese population at high risk. *Prev Med* 2002; **34**: 22-28
- 38 **Correa P**. Human gastric carcinogenesis: a multistep and multifactorial process-First American Cancer Society Award Lecture on Cancer Epidemiology and Prevention. *Cancer Res* 1992; **52**: 6735-6740
- 39 **Huang JQ**, Hunt RH. The evolving epidemiology of *Helicobacter pylori* infection and gastric cancer. *Can J Gastroenterol* 2003; **17** (Suppl): 18B-20
- 40 **Gill S**, Shah A, Le N, Cook EF, Yoshida EM. Asian ethnicity-related differences in gastric cancer presentation and outcome among patients treated at a canadian cancer center. *J Clin Oncol* 2003; **21**: 2070-2076
- 41 **Lee SA**, Kang D, Shim KN, Choe JW, Hong WS, Choi H. Effect of diet and *Helicobacter pylori* infection to the risk of early gastric cancer. *J Epidemiol* 2003; **13**: 162-168
- 42 **Kelley JR**, Duggan JM. Gastric cancer epidemiology and risk factors. *J Clin Epidemiol* 2003; **56**: 1-9
- 43 **La Vecchia C**, Franceschi S, Levi F. Epidemiological research on cancer with a focus on Europe. *Eur J Cancer Prev* 2003; **12**: 5-14
- 44 **El-Omar EM**, Chow WH, Rabkin CS. Gastric cancer and *H pylori*: Host genetics open the way. *Gastroenterology* 2001; **121**: 1002-1004
- 45 **Magnusson PKE**, Enroth H, Eriksson I, Held M, Nyren O, Engstrand L, Hansson LE, Gyllenstein UB. Gastric cancer and human leukocyte antigen: distinct DQ and DR alleles are associated with development of gastric cancer and infection by *Helicobacter pylori*. *Cancer Res* 2001; **61**: 2684-2689
- 46 **Cox JM**, Clayton CL, Tomita T, Wallace DM, Robinson PA, Crabtree JE. cDNA array analysis of cag pathogenicity island-associated *Helicobacter pylori* epithelial cell response genes. *Infect Immun* 2001; **69**: 6970-6980
- 47 **Salama N**, Guillemin K, McDaniel TK, Sherlock G, Tompkins L, Falkow S. A whole-genome microarray reveals genetic diversity among *Helicobacter pylori* strains. *Proc Natl Acad Sci USA* 2000; **97**: 14668-14673
- 48 **Innocenti M**, Thoreson AC, Ferrero RL, Stromberg E, Bolin I, Eriksson L, Svennerholm AM, Quiding-Jarbrink M. *Helicobacter pylori*-induced activation of human endothelial cells. *Infect Immun* 2002; **70**: 4581-4590
- 49 **Huang JQ**, Hunt RH. Review article: *Helicobacter pylori* and gastric cancer-the clinicians' point of view. *Aliment Pharmacol Ther* 2000; **14**(Suppl 3): 48-54
- 50 **Achtman M**, Azuma T, Berg DE, Ito Y, Morelli G, Pan ZJ, Suerbaum S, Thompson SA, van der Ende A, van Doorn LJ. Recombination and clonal groupings within *Helicobacter pylori* from different geographical regions. *Mol Microbiol* 1999; **32**: 459-470
- 51 **Van Doorn LJ**, Figueiredo C, Megraud F, Pena S, Midolo P, Queiroz DM, Carneiro F, Pegado MD, Sanna R, De Boer W, Schneeberger PM, Correa P, Ng EK, Atherton J, Blaser MJ, Quint WG. Geographic distribution of vacA allelic types of *Helicobacter pylori*. *Gastroenterology* 1999; **116**: 823-830
- 52 **Deguchi R**, Takagi A, Kawata H, Inoko H, Miwa T. Association between CagA+ *Helicobacter pylori* infection and p53, bax and transforming growth factor-beta-RII gene mutations in gastric cancer patients. *Int J Cancer* 2001; **91**: 481-485
- 53 **Hiyama T**, Tanaka S, Kitadai Y, Ito M, Sumii M, Yoshihara M, Shimamoto F, Haruma K, Chayama K. p53 Codon 72 polymorphism in gastric cancer susceptibility in patients with *Helicobacter pylori*-associated chronic gastritis. *Int J Cancer* 2002; **100**: 304-308
- 54 **Tian SF**, Xiong YY, Yu SP, Lan J. Relationship between *Helicobacter pylori* infection and expressions of tumor suppressor genes in gastric carcinoma and related lesions. *Aizheng* 2002; **21**: 970-973
- 55 **Moss SF**, Sordillo EM, Abdalla AM, Makarov V, Hanzely Z, Perez-Perez GI, Blaser MJ, Holt PR. Increased gastric epithelial cell apoptosis associated with colonization with cagA + *Helicobacter pylori* strains. *Cancer Res* 2001; **61**: 1406-1411
- 56 **Shigeishi H**, Yokozaki H, Oue N, Kuniyasu H, Kondo T, Ishikawa T, Yasui W. Increased expression of CHK2 in human gastric carcinomas harboring p53 mutations. *Int J Cancer* 2002; **99**: 58-62
- 57 **Hiyama T**, Haruma K, Kitadai Y, Masuda H, Miyamoto M, Tanaka S, Yoshihara M, Shimamoto F, Chayama K. K-ras mutation in *Helicobacter pylori*-associated chronic gastritis in patients with and without gastric cancer. *Int J Cancer* 2002; **97**: 562-566
- 58 **El-Omar EM**, Carrington M, Chow WH, McColl KE, Bream JH, Young HA, Herrera J, Lissowska J, Yuan CC, Rothman N, Lanyon G, Martin M, Fraumeni JF Jr, Rabkin CS. The role of interleukin-1 polymorphisms in the pathogenesis of gastric cancer. *Nature* 2001; **412**: 99
- 59 **El-Omar EM**, Carrington M, Chow WH, McColl KE, Bream JH, Young HA, Herrera J, Lissowska J, Yuan CC, Rothman N, Lanyon G, Martin M, Fraumeni JF Jr, Rabkin CS. Interleukin-1 polymorphisms associated with increased risk of gastric cancer. *Nature* 2000; **404**: 398-402
- 60 **Machado JC**, Pharoah P, Sousa S, Carvalho R, Oliveira C, Figueiredo C, Amorim A, Seruca R, Caldas C, Carneiro F, Sobrinho-Simoes M. Interleukin 1B and interleukin 1RN polymorphisms are associated with increased risk of gastric carcinoma. *Gastroenterology* 2001; **121**: 823-829
- 61 **Figueiredo C**, Machado JC, Pharoah P, Seruca R, Sousa S, Carvalho R, Capelinha AF, Quint W, Caldas C, van Doorn LJ, Carneiro F, Sobrinho-Simoes M. *Helicobacter pylori* and interleukin 1 genotyping: an opportunity to identify high-risk individuals for gastric carcinoma. *J Natl Cancer Inst* 2002; **94**: 1680-1687
- 62 **He X**, Jiang L, Fu B, Zhang X. Relationship between interleukin-1B and interleukin-1 receptor antagonist gene polymorphisms and susceptibility to gastric cancer. *Zhonghua Yixue Zazhi* 2002; **82**: 685-688
- 63 **Kato S**, Onda M, Yamada S, Matsuda N, Tokunaga A, Matsukura N. Association of the interleukin-1 beta genetic polymorphism and gastric cancer risk in Japanese. *J Gastroenterol* 2001; **36**: 696-699
- 64 **Song CF**, Sun LP, Dai WY, Yuan Y. Significance of serum level of NO and IL-8 in *Helicobacter pylori* associated gastric diseases. *Zhonghua Zhongliu Zazhi* 2003; **25**: 258-260
- 65 **Shi T**, Liu WZ, Gao F, Xiao SD. The role of nuclear factor kappa B in secretion of interleukin-8 by gastric cancer cell line SGC 7901 induced by *Helicobacter pylori*. *Zhonghua Yixue Zazhi* 2003; **83**: 133-136
- 66 **Yea SS**, Yang YI, Jang WH, Lee YJ, Bae HS, Paik KH. Association between TNF-alpha promoter polymorphism and *Helicobacter pylori* cagA subtype infection. *J Clin Pathol* 2001; **54**: 703-706
- 67 **Lanas A**, Garcia-Gonzalez MA, Santolaria S, Crusius JB, Serrano MT, Benito R, Pena AS. TNF and LTA gene polymorphisms reveal different risk in gastric and duodenal ulcer patients. *Genes Immun* 2001; **2**: 415-421
- 68 **Wu MS**, Wu CY, Chen CJ, Lin MT, Shun CT, Lin JT. Interleukin-10 genotypes associate with the risk of gastric carcinoma in Taiwanese Chinese. *Int J Cancer* 2003; **104**: 617-623
- 69 **Oda Y**, Kobayashi M, Ooi A, Muroishi Y, Nakanishi I. Genotypes of glutathione S-transferase M1 and N-acetyltransferase 2 in Japanese patients with gastric cancer. *Gastric Cancer* 1999; **2**: 158-164
- 70 **Setiawan VW**, Zhang ZF, Yu GP, Lu QY, Li YL, Lu ML, Wang MR, Guo CH, Yu SZ, Kurtz RC, Hsieh CC. GSTP1

- polymorphisms and gastric cancer in a high-risk Chinese population. *Cancer Causes Control* 2001; **12**: 673-681
- 71 **Park WS**, Lee JH, Shin MS, Park JY, Kim HS, Kim YS, Park CH, Lee SK, Lee SH, Lee SN, Kim H, Yoo NJ, Lee JY. Inactivating mutations of KILLER/DR5 gene in gastric cancers. *Gastroenterology* 2001; **121**: 1219-1225
 - 72 **Tsukino H**, Kuroda Y, Qiu D, Nakao H, Imai H, Katoh T. Effects of cytochrome P450 (CYP) 2A6 gene deletion and CYP2E1 genotypes on gastric adenocarcinoma. *Int J Cancer* 2002; **100**: 425-428
 - 73 **Ikonen T**, Matikainen M, Mononen N, Hyytinen ER, Helin HJ, Tammola S, Tammela TL, Pukkala E, Schleutker J, Kallionzemi OP, Koivisto PA. Association of E- polymorphism cadherin germ-line alterations with prostate cancer. *Clin Cancer Res* 2001; **7**: 3465-3471
 - 74 **Machado JC**, Soares P, Carneiro F, Rocha A, Beck S, Blin N, Berx G, Sobrinho-Simoes M. E-cadherin gene mutations provide a genetic basis for the phenotypic divergence of mixed gastric carcinomas. *Lab Invest* 1999; **79**: 459-465
 - 75 **Ebert MP**, Fei G, Kahmann S, Muller O, Yu J, Sung JJ, Malfertheiner P. Increased beta-catenin mRNA levels and mutational alterations of the APC and beta-catenin gene are present in intestinal-type gastric cancer. *Carcinogenesis* 2002; **23**: 87-91
 - 76 **Tebbutt NC**, Giraud AS, Inglese M, Jenkins B, Waring P, Clay FJ, Malki S, Alderman BM, Grail D, Hollande F, Heath JK, Ernst M. Reciprocal regulation of gastrointestinal homeostasis by SHP2 and STAT-mediated trefoil gene activation in gp130 mutant mice. *Nat Med* 2002; **8**: 1089-1097
 - 77 **Wang TC**, Goldenring JR. Inflammation intersection: gp130 balances gut irritation and stomach cancer. *Nat Med* 2002; **8**: 1080-1082
 - 78 **Suemori S**, Lynch-Devaney K, Podolsky DK. Identification and characterization of rat intestinal trefoil factor: tissue- and cell-specific member of the trefoil protein family. *Proc Natl Acad Sci USA* 1991; **88**: 11017-11021
 - 79 **Beck S**, Sommer P, Blin N, Gott P. 5'-flanking motifs control cell-specific expression of trefoil factor genes (TFF). *Int J Mol Med* 1998; **2**: 353-361
 - 80 **Dossinger V**, Kayademir T, Blin N, Gott P. Down-regulation of TFF expression in gastrointestinal cell lines by cytokines and nuclear factors. *Cell Physiol Biochem* 2002; **12**: 197-206
 - 81 **Park WS**, Oh RR, Park JY, Lee JH, Shin MS, Kim HS, Lee HK, Kim YS, Kim SY, Lee SH, Yoo NJ, Lee JY. Somatic mutations of the trefoil factor family 1 gene in gastric cancer. *Gastroenterology* 2000; **119**: 691-698

Science Editor Guo SY Language Editor Elsevier HK

• *Helicobacter pylori* •

Gastrin and antral G cells in course of *Helicobacter pylori* eradication: Six months follow up study

Aleksandra Sokic-Milutinovic, Vera Todorovic, Tomica Milosavljevic, Marjan Micev, Neda Drndarevic, Olivera Mitrovic

Aleksandra Sokic-Milutinovic, Tomica Milosavljevic, Clinic for Gastroenterology and Hepatology, Institute for Digestive Diseases, Clinical Center of Serbia, Serbia and Montenegro
Vera Todorovic, Neda Drndarevic, Olivera Mitrovic, Department of Immunohistochemistry and Electron Microscopy, Institute for Medical Research, Belgrade, Serbia and Montenegro
Marjan Micev, Pathology Department, Institute for Digestive Diseases, Clinical Center of Serbia, Serbia and Montenegro
Supported by a Grant From Serbian Ministry for Science, Technology and Development, No. 1752
Correspondence to: Aleksandra Sokic-Milutinovic, MD, MSc, Clinical Center of Serbia, Clinic for Gastroenterology and Hepatology, Koste Todorovica 6, Belgrade 11000, Serbia and Montenegro. asokic2002@yahoo.com
Telephone: +381-11-3617777-3734 Fax: +381-11-361-5432
Received: 2004-10-13 Accepted: 2004-11-23

Abstract

AIM: To assess long-term effects of *Helicobacter pylori* (*H. pylori*) eradication on antral G cell morphology and function in patients with and without duodenal ulcer (DU).

METHODS: Consecutive dyspeptic patients referred to the endoscopy entered the study. Out of 39 *H. pylori* positive patients, 8 had DU (*H. pylori* +DU) and 31 gastritis (*H. pylori* +G). Control groups consisted of 11 uninfected dyspeptic patients (CG1) and 7 healthy volunteers (CG2). Basal plasma gastrin (PGL), antral tissue gastrin concentrations (ATGC), immunohistochemical and electron microscopic characteristics of G cells were determined, prior to and 6 mo after therapy.

RESULTS: We demonstrated elevated PGL in infected patients compared to uninfected controls prior to therapy. Elevated PGL were registered in all *H. pylori*+patients (*H. pylori* +DU: 106.78 ± 22.72 pg/mL, *H. pylori* +G: 74.95 ± 15.63 , CG1: 68.59 ± 17.97 , CG2: 39.24 ± 5.59 pg/mL, $P < 0.01$). Successful eradication (e) therapy in *H. pylori*+patients lead to significant decrease in PGL (*H. pylori*+DU: 59.93 ± 9.40 and *H. pylori* +Ge: 42.36 ± 10.28 pg/mL, $P < 0.001$). ATGC at the beginning of the study were similar in infected and uninfected patients and eradication therapy lead to significant decrease in ATGC in *H. pylori* +gastritis, but not in DU patients. In the *H. pylori* +DU patients, the mean number of antral G cells was significantly lower in comparison with all other groups ($P < 0.01$), but after successful eradication was close to normal values found in controls. By contrast, G cell number and volume density were significantly decreased ($P < 0.01$) in *H. pylori* +Ge group after successful eradication therapy (294 ± 32 and 0.31 ± 0.02 , respectively), in comparison to values before eradication

(416 ± 40 and 0.48 ± 0.09). No significant change of the G cell/total endocrine cell ratio was observed during the 6 mo of follow up in any of the groups. A reversible increase in G cell secretory function was seen in all infected individuals, demonstrated by a more prominent secretory apparatus. However, differences between DU and gastritis group were identified.

CONCLUSION: *H. pylori* infection induces antral G cell hyperfunction resulting in increased gastrin synthesis and secretion. After eradication therapy complete morphological and functional recovery is observed in patients with gastritis. In the DU patients some other factors unrelated to the *H. pylori* infection influence antral G cell morphology and function.

© 2005 The WJG Press and Elsevier Inc. All rights reserved.

Key words: Gastrin; G cell; Duodenal ulcer; Gastritis; *Helicobacter pylori*

Sokic-Milutinovic A, Todorovic V, Milosavljevic T, Micev M, Drndarevic N, Mitrovic O. Gastrin and antral G cells in course of *Helicobacter pylori* eradication: Six months follow up study. *World J Gastroenterol* 2005; 11(27): 4140-4147
<http://www.wjgnet.com/1007-9327/11/4140.asp>

INTRODUCTION

Helicobacter pylori (*H. pylori*) causes chronic active type B gastritis and is involved in the pathogenesis of peptic ulcer disease (PUD) and gastric cancer^[1]. PUD symptoms were almost immediately attributed to the presence of *H. pylori* infection, however a positive correlation between the infection and non-ulcer dyspepsia (NUD) was acknowledged only after the results of meta-analysis^[2]. NUD should be considered in dyspeptic patients when symptoms persist for at least a month and endoscopy reveals neither peptic ulcer nor signs of gastric cancer^[3].

Gastrin is a secretory product of antral and duodenal G cells. Two main forms of gastrin (gastrin-17 and -34) are present in the circulation. About 95% of antral gastrin is gastrin-17^[3,4]. Stimuli for gastrin secretion are well identified and include food intake, presence of digested amino acids in the lumen, cholinergic stimuli, and antral alkalization^[3,4].

Although elevated serum gastrin levels are frequently observed in individuals with chronic *H. pylori* infection^[5-7], its pathophysiological significance in gastric mucosal inflammation remains unclear. Gastrin is capable of

up-regulating CXC chemokines in gastric epithelial cells and therefore may contribute to the progression of the inflammatory process in the stomach^[8]. Chronic hypergastrinemia is also associated with gastric argiophil cell hyperplasia in rats and humans and carcinoid tumor in Mongolian gerbils^[9]. In the antrum of *H pylori* infected gerbils and humans enhanced apoptosis is an early and transient cell cycle event whilst epithelial cell proliferation peaks later and is related to increased gastrin levels. Based on these findings it was suggested that gastrin-dependent mechanism might be responsible for epithelial cell growth in *H pylori* colonized gastric mucosa^[10,11]. It can be assumed that restored antral G cell function after *H pylori* eradication resulting in lower basal and meal-stimulated gastrin release would be a desirable event in both chronic gastritis and PUD. Most studies conducted so far focused on the effects of *H pylori* infection on gastric endocrine cells in patients with duodenal ulcer and came to different conclusions^[5,6]. There have been few reports concerning G cell morphology^[12-14] and/or gastrin secretion^[7] in patients with gastritis.

The aim of our study was to investigate changes in antral G cell morphology and function in dyspeptic patients with *H pylori* infection and its possible restoration in course of eradication therapy.

MATERIALS AND METHODS

Patients

We conducted an outpatient based prospective study in the Clinic for Gastroenterology and Hepatology, Clinical Center of Serbia, lasting for 6 mo after patients completed eradication therapy. Fifty consecutive dyspeptic patients referred to the endoscopy and seven healthy asymptomatic volunteers entered the study. Out of 39 *H pylori* positive patients had 31 histological signs of gastritis- *H pylori* +G and 8 DU- *H pylori* +DU. Control group 1 (CG1) consisted of 11 *H pylori* negative dyspeptic patients while 7 healthy asymptomatic volunteers were assigned to the control group 2 (CG2). All patients gave informed consent and the study protocol was approved by the local Ethics Committee. Mean age was 48 ± 15 years (28 males and 22 females), 21 were smokers and 21 had personal history of PUD. Exclusion criteria were in concordance with the recommendations from European *H pylori* Study Group^[15]. *H pylori* infection was diagnosed by rapid urease test (RUT), histology and serology. A patient was defined as *H pylori* positive if histology and at least one of the other applied diagnostic methods were positive.

Diagnostic methods

Routine endoscopy and biopsy samples Upper endoscopy was performed before therapy in all dyspeptic patients and repeated 6 mo after appropriate therapy. In healthy volunteers (CG2) endoscopy was performed only once. During endoscopy antral biopsy specimens, intended for routine histology, RUT test, determination of tissue gastrin levels, immunohistochemistry and electron microscopy were taken.

***H pylori* serology** Blood samples were taken from the patients after endoscopic examination and sera were

separated by centrifugation and stored at -20°C until analyzed. The concentration of anti- *H pylori* IgG antibodies was analyzed using the Pyloriset EIA-G IIITM (Orion Diagnostica, Finland), according to the manufacturers' instructions.

Therapy A triple eradication therapy consisting of omeprazole 20 mg twice a day (bid), amoxicillin 1 000 mg b.i.d. and metronidazole 500 mg b.i.d. was administered for 7 d in patients with *H pylori* infection. In uninfected patients, symptomatic therapy consisting of antacids, H_2 antagonists or proton pump inhibitors (PPIs) was prescribed for 2 wks. In the course of *H pylori* eradication, the disappearance of spiral bacteria from antral and corpus gastric mucosa, according to a negative RUT and histological examination, were observed.

Histological assessment Biopsies from antral and corpus mucosa were stained using hematoxylin- eosin and modified Giemsa staining procedure. Biopsy specimens were assessed according to the Sydney System^[16,17] by a single, experienced pathologist who was blinded to the clinical presentation, endoscopic data and RUT results of the patient.

Assessment of plasma and tissue gastrin levels

Plasma preparation Full blood samples for estimating fasting plasma gastrin levels were placed in ice/chilled tubes (5 mL) containing EDTA (2 mg) and proteinase inhibitor (Trasylol, 2 500 KIU). Plasma was extracted using standard procedure and stored below -70°C until further analysis.

Tissue extract preparation Each antral mucosa biopsy was washed with saline solution, measured and placed in to the tube together with 1 mL of distilled water. Gastrin extraction was performed in water bath on 95°C for 10 min, supernatant collected and after cooling stored below -70°C until further analysis.

Radioimmunoassay procedure (RIA) Plasma and tissue gastrin was determined under basal conditions using RIA protocol provided by Affiniti (UK) with rabbit antihuman gastrin-17 antiserum. Final dilutions were for plasma 1:100 000 and for the tissue 1:500 000. Intra-assay and inter-assay coefficients were 9.0 and 8.4 respectively. Sensitivity of the method was 1 pmol/L.

Evaluation of antral G cells

Immunohistochemistry Two antral biopsies from each patient were used for immunohistochemistry and light microscopic morphometry. These were fixed with 10% buffered formalin and embedded in paraffin in the usual manner. Only well-oriented antral mucosa biopsies that allowed assessment of the full mucosal thickness were studied. The sections were stained with different immunohistochemical methods in order to identify antral gastrin-producing cells and evaluate the ratio of antral G cells/all antral endocrine cells. Immunohistochemical staining for G cells was performed using rabbit anti human gastrin-17 (1:300 dilution, Code No A0568, DAKO A/S, Denmark) and peroxidase-labeled streptavidin biotin method (DAKO LSAB+/HRP, DAKO A/S, Denmark). In addition, sections were double immunostained with both polyclonal antibody to gastrin mentioned above and mAb to synaptophysin (1:50 dilution, Code No. A0010,

DAKO A/S, Denmark), using DAKO EnVision[®] double stain system (Code No. K1395). For double immunostaining, antisynaptophysin antibody was applied first with DAB as a chromogen, followed by antigastrin-17 antibody as the second antibody, with AEC as a chromogen. Negative controls were conjugated with normal horse serum^[18].

Routine electron microscopy The biopsy specimens of antral mucosa were immediately placed in a mixture of 2% glutaraldehyde in 0.2 mol/L sodium cacodylate buffer, pH 7.4, and fixed in the same fixative for 20 h at 4 °C. After postfixation for 1 h in 1% osmium tetroxide in cacodylate buffer, the specimens were dehydrated in graded ethanol and embedded in Epon 812[®], with mucosa surface perpendicular to the cutting surface. The blocks were sectioned with an LKB ultratome II. Ultra thin sections were double-stained with uranyl acetate and lead-citrate before examination in an Opton 109 electron microscope.

Morphometric analysis of G cells detected by immunohistochemistry Three 5-μm thick immunostained sections of antral mucosa at intervals of 50 μm were analyzed. Weibel multipurpose test system containing 42 points and 21 lines was used for evaluation of volume density and number of G cells^[19,20]. The total number of G cells per mm² of antral mucosa, as well as, ratio of antral G/total antral endocrine cells was calculated by examination of single or double immunostained sections. All sections were examined randomly by two histologists.

Morphometric analysis of G cells detected by electron microscopy G cells were identified as described previously^[21]. Morphometric analysis was performed using the methods described previously^[19,20]. Cell profile areas were estimated by drawings of G-cells using Camera Lucida attached to a Reichert microscope and analyzed with an image analyzing system (MOP 3 Video plan; Carl Zeiss)^[19,20].

Statistical analysis

Each time mean and SD was calculated for results presentation. A two sample paired or unpaired Student's *t*-test and Wilcoxon rank sum test and ANOVA were used. A *P* value less than 0.05 was considered significant.

RESULTS

Clinical data

Clinical and demographic characteristics of the patients are shown in Table 1. Out of 39 *H. pylori*-positive patients

eradication therapy was successful in 32 (82.1%). In all DU patients the infection was successfully treated, together with 24 patients with gastritis (*H. pylori* +Ge). In seven patients with gastritis eradication therapy failed (*H. pylori* +Gne). No significant difference in demographic and clinical data between *H. pylori*+Gne and *H. pylori*+Ge patients was observed.

Basal plasma gastrin levels (PGL)

Basal plasma gastrin-17 levels were compared between groups of patients at the beginning of the study. These findings are shown in Figure 1. PGL in *H. pylori*+DU patients were significantly higher at the beginning of the study than in any other group of patients irrespective of the presence of infection (*H. pylori* +DU: 106.78±22.72 pg/mL vs *H. pylori* +Ge: 74.95±15.63, *H. pylori*+Gne: 74.21±10.99, CG1: 68.59±17.97 and CG2: 39.24±5.59 pg/mL, *P*<0.001). Healthy asymptomatic controls (CG2) had significantly lower plasma gastrin levels than all other dyspeptic patients (*P*<0.01). After 6 mo, statistically significant decrease of PGL were observed in all successfully eradicated patients (*H. pylori*+DU: 59.93±9.40 and *H. pylori*+Ge: 42.36±10.28 pg/mL, *P*<0.001). However, no significant change was seen in other groups (*H. pylori*+Gne: 76.81±19.54 and CG1: 58.29±17.97 pg/mL, *P*>0.05).

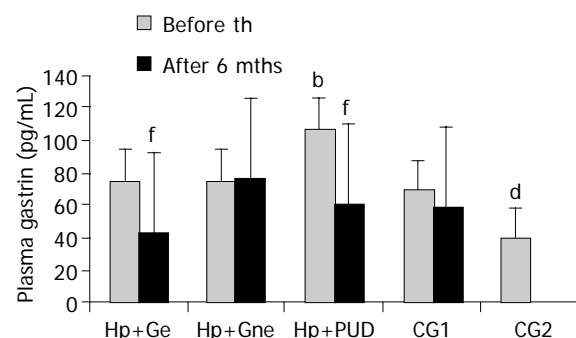


Figure 1 Basal plasma gastrin levels in patients with and without duodenal ulcer before and after eradication of *H. pylori* infection. *H. pylori*+Ge-*H. pylori*+eradicated patients with gastritis; *H. pylori*+Gne-*H. pylori*+non eradicated patients with gastritis; *H. pylori*+DU- patients with *H. pylori*+duodenal ulcer; CG1- *H. pylori* negative dyspeptic patients; CG2- asymptomatic volunteers; th-therapy; mths-months; ^a*P*<0.001 in *H. pylori*+DU vs all other groups, ^d*P*<0.01 in CG2 vs all other groups, ^f*P*<0.001 before vs after eradication therapy.

Table 1 Clinic and demographic data in *H. pylori* positive patients with DU and gastritis and in the control groups at the beginning of the study

	<i>H. pylori</i> +Ge (n = 24)	<i>H. pylori</i> + Gne (n = 7)	<i>H. pylori</i> +DU (n = 8)	CG1 (n = 11)	CG2 (n = 7)	<i>P</i>
Age (yr)	47±13	48±9	47±23	47±19	33±11	NS
Sex (males)	13	1	2	5	2	NS
Smokers	8	3	2	4	4	NS
Alcohol intake	12	3	1	1	1	NS
PH of PUD	8	0	6	7	0	NS
FH of PUD	11	3	5	6	3	NS

H. pylori +Ge-*H. pylori*+eradicated patients with gastritis; *H. pylori*+Gne-*H. pylori*+non eradicated patients with gastritis; *H. pylori* +DU- patients with *H. pylori*+duodenal ulcer; CG1-*H. pylori* negative dyspeptic patients; CG2- asymptomatic volunteers; PUD -peptic ulcer disease; PH-personal history; FH- family history; NS-not statistically significant.

Basal tissue gastrin concentrations

At the beginning of the study there was no significant difference ($P>0.05$) in antral tissue gastrin concentrations (ATGC) between groups of infected (*H pylori*+Ge: 0.23 ± 0.05 , *H pylori*+Gne: 0.23 ± 0.05 , *H pylori*+DU: 0.24 ± 0.03 pg/g wet weight) and uninfected patients (CG1: 0.22 ± 0.04 and CG2: 0.24 ± 0.03 pg/g wet weight). After successful eradication therapy significant decrease in ATGC was observed only in *H pylori*+Ge group (0.20 ± 0.05 pg/g wet weight, $P<0.05$), while in *H pylori*+DU group no significant change was observed (0.22 ± 0.04 pg/wet weight, $P>0.05$). ATGC in the *H pylori*+Gne and CG1 did not change significantly (0.26 ± 0.07 and 0.26 ± 0.06 pg/g wet weight, respectively, $P>0.05$). These findings are seen in Figure 2.

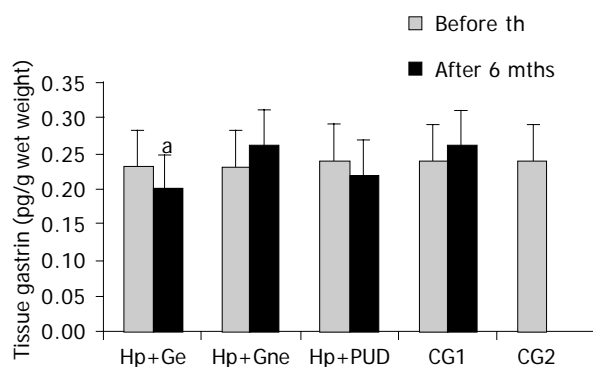


Figure 2 Antral tissue gastrin levels in patients with and without duodenal ulcer before and after eradication of *H pylori* infection. *H pylori* +Ge-*H pylori*+eradicated patients with gastritis; *H pylori*+Gne-*H pylori*+non eradicated patients with gastritis; *H pylori* +DU-patients with *H pylori*+duodenal ulcer; CG1- *H pylori* negative dyspeptic patients; CG2- asymptomatic volunteers; th-therapy; mths-months.

Antral G cell number

Antral G cell number was expressed as number of identified G cells per mm² of antral mucosa, G cell volume density (%) and a ratio of antral G/total antral endocrine cell count (Table 2). Antral G cell number remained unchanged after

6 mo of follow-up in *H pylori*+Gne (405 ± 32 vs 432 ± 18), CG1 (413 ± 61 vs 428 ± 80) and CG2 (426 ± 57) patients. In the *H pylori*+DU patients mean number of antral G cells per mm² of mucosa was lower at the beginning of the study (292 ± 20) than in any other group analyzed ($P<0.01$). At the end of the follow-up and after successful eradication of *H pylori* infection number of antral G cells identified in DU patients was increased (400 ± 32) and comparable to both control groups (CG1 and CG2). By contrast, in patients with gastritis successful treatment lead to a decrease in both antral G cell number (416 ± 40 vs 294 ± 32 , $P<0.01$) and volume density (0.48 ± 0.09 vs 0.31 ± 0.02 , $P<0.01$), as seen in Figure 3. However, no significant change of the G cell/ total endocrine cell ratio was observed during the 6 mo of follow up in any of the groups, including *H pylori* +Ge group (Figure 4).

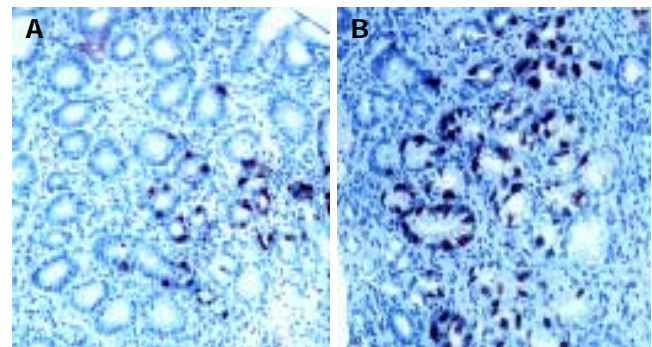


Figure 3 Pyloric gland area of *H pylori* associated gastritis before (A) and after eradication (B) therapy. DAKO LSAB+ immunohistochemical staining and diaminobezidine (DAB) as chromogen; x20 (A) and x10 (B). There is evident lower gastrin cell number after succesful eradication therapy.

Ultrastructural morphometric analysis of gastric antral G cell

Ultrastructural characteristics of antral G cells in healthy controls (Figure 5) and dyspeptic patients (Figure 6) before and after therapy were assessed using electron microscopy morphometric study (Table 3). Electron microscopy revealed

Table 2 Antral G cell in dyspeptic patients before and after eradication therapy-morphometric analysis on light microscopy

	<i>H pylori</i> +Ge (n = 24)	<i>H pylori</i> +Gne (n = 7)	<i>H pylori</i> +DU (n = 8)	CG1 (n = 11)	CG2 (n = 7)	P
G cell number (per mm ² of antral mucosa)						
Before therapy	416±40	405±32	292±20 ^a	413±61	426±57	0.05 ^a
After therapy	294±32 ^a	432±18	400±32 ^b	428±80	/	NS
P	0.05 ^a	NS	0.01 ^b	NS	/	
G cell volume density (%)						
Before therapy	0.48±0.09	0.43±0.11	0.42±0.02	0.48±0.03	0.44±0.02	NS
After therapy	0.31±0.02 ^a	0.40±0.04	0.43±0.01	0.50±0.03	/	NS
P	0.05	NS	NS	NS	/	
Antral G/ total antral endocrine cells ratio						
Before therapy	0.44±0.04	0.40±0.03	0.37±0.05	0.44±0.29	0.45±0.07	NS
After therapy	0.44±0.02	0.47±0.07	0.41±0.07	0.44±0.37	/	NS
P	NS	NS	NS	NS	/	

H pylori+Ge- *H pylori*+eradicated patients with gastritis; *H pylori*+Gne-*H pylori*+non eradicated patients with gastritis; *H pylori*+DU-patients with *H pylori*+duodenal ulcer; CG1-*H pylori* negative dyspeptic patients; CG2- asymptomatic volunteers; NS- $P>0.05$; ^a $P<0.05$; ^b $P<0.01$.

Table 3 Ultrastructural characteristics of antral G cell in dyspeptic patients before and after therapy assessed by electron microscopy morphometric study

Antral G cell	<i>H pylori</i> +Ge (n = 24)	<i>H pylori</i> +Gne (n = 7)	<i>H pylori</i> +DU (n = 8)	CG1 (n = 11)	CG2 (n = 7)	P
Number of cells analyzed						
Before therapy	93	30	33	55	37	
After therapy	113	31	30	47		
Cell profile surface (μm^2)						
Before therapy	142 \pm 14	138 \pm 20	188 \pm 14 ^a	130 \pm 10	136 \pm 10	0.05 ^a
After therapy	140 \pm 15	133 \pm 12	138 \pm 10 ^d	133 \pm 12	/	NS
P	NS	NS	0.001 ^d	NS	/	
Endoplasmatic reticulum (μm^2) (profile surface)						
Before therapy	6.9 \pm 2.3 ^a	6.2 \pm 2.3	17.9 \pm 2.3 ^b	5.3 \pm 0.9	5.5 \pm 0.9	^a 0.05; ^b 0.01
After therapy	5.0 \pm 2.3	6.0 \pm 1.0	5.7 \pm 1.3 ^d	5.5 \pm 0.7		NS
P	NS	NS	0.001 ^d	NS		
Volumen density of cytoplasmic granules						
Before therapy	17.3 \pm 1.9 ^a	13.1 \pm 3.2	47.0 \pm 4.9 ^b	14.6 \pm 2.7	13.6 \pm 2.7	^a 0.05; ^b 0.01
After therapy	9.7 \pm 1.1 ^b	14.2 \pm 3.1	17.3 \pm 1.9	13.2 \pm 2.0	/	NS
P	0.01 ^b	NS	NS	NS	/	
Number of cytoplasmic granules/cell profile						
Before therapy	232 \pm 18 ^a	199 \pm 34	330 \pm 13 ^b	190 \pm 37	196 \pm 21	^a 0.05; ^b 0.01
After therapy	180 \pm 13	202 \pm 45	220 \pm 31	196 \pm 20	/	NS
P	NS	NS	NS	NS	/	
Mean diameter of cytoplasmic granules (nm)						
Before therapy	220 \pm 23	245 \pm 11	327 \pm 23 ^a	237 \pm 4	227 \pm 7	0.01 ^a
After therapy	223 \pm 23	229 \pm 22	257 \pm 21 ^b	223 \pm 9	/	NS
P	NS	NS	0.01 ^b	NS	/	
Golgi apparatus (μm^2) (profile surface)						
Before therapy	2.9 \pm 0.10 ^b	2.10 \pm 0.3	3.33 \pm 0.10 ^a	2.11 \pm 0.33	2.05 \pm 0.23	0.01 ^a
After therapy	2.15 \pm 0.10	2.23 \pm 0.2	2.20 \pm 0.11 ^b	2.20 \pm 0.22	/	NS
P	0.01 ^b	NS	0.01 ^b	NS	/	

^aP<0.05, ^bP<0.01, ^dP<0.001 vs others.

changes in antral G cell morphology in all *H pylori*+patients. Namely, more prominent endoplasmatic reticulum (Figure 6B) and Golgi apparatus together with an increase in number and volume density of cytoplasmic granules (Figure 6A) were identified in all *H pylori* infected individuals. Antral G cells of *H pylori*+DU patients, however, exhibited some specific features, such as increased cell profile surface and increased mean diameter of cytoplasmic granules. It was

also found that G cells in DU patients, in comparison with healthy controls, have an increased proportion of dense core granules. In *H pylori*+Ge patients more granules per profile and higher volumen density, but similar diameter of secretory granules was identified when compared to the CG1 patients.

After successful eradication all those alterations were normalized and G cell ultrastructurally resembled to those found in CG2 group, with the exception of the diameter and volume density of cytoplasmic granules that remained higher in the *H pylori* +DU patients.

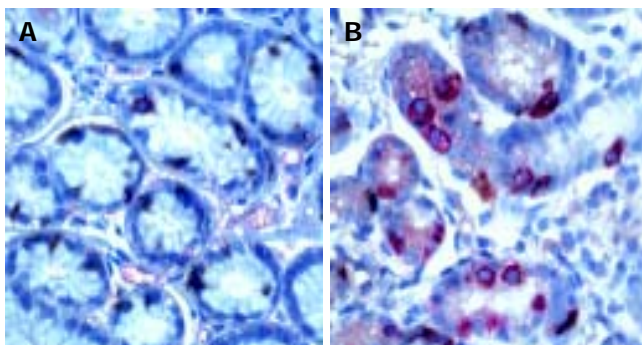


Figure 4 Synaptophysin and gastrin double immunostaining in pyloric gland of *H pylori*-associated gastritis before (A) and after (B) eradication therapy. DAKO EnVision double stain method; DAB is chromogen for G cells and aminoethylcarbazole (AEC) is chromogen for synaptophysin containing endocrine cells. x20 (A) and x10 (B). G cells (red)/ other endocrine cells (brown) ratio is equal before (A) and after (B) succesful eradication of *H pylori* infection.

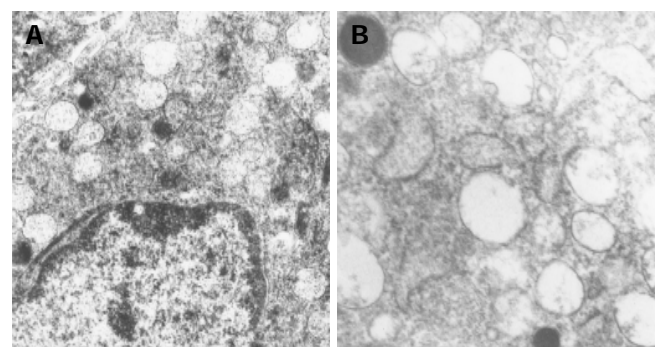


Figure 5 Electron micrographs of gastrin producing cells from healthy persons antral mucosa. Normal ultrastructure is characterized by the presence of numerous secretory granules of different electron density. Uranyl acetate, lead citrate; x8 400 (A) and x12 680 (B).

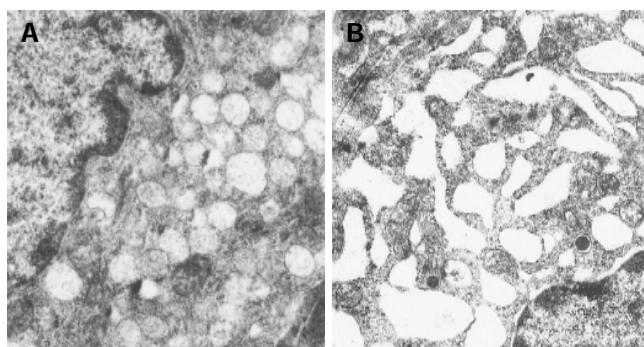


Figure 6 Electron micrographs of gastrin producing cells from *H pylori* infected individuals with gastritis (A) and duodenal ulcer (B) before eradication therapy. Uranyl acetate, lead citrate; x8 400 (both A and B). Note that total number of granules is higher than in controls and that dense core granules are more numerous in *H pylori*-patient with gastritis (A). Endoplasmic reticulum is very prominent in *H pylori*-patient with duodenal ulcer.

DISCUSSION

In our study, eradication therapy was successful in 82% (32/39) of all *H pylori* infected patients, all DU (100%, 8/8), and 77% of patients (24/31) with gastritis that accords with previously proposed acceptable eradication rate of approximately 80%^[2,22]. Eradication rate in our study is in line with results obtained with this eradication protocol that is, according to the literature, ranging from 53-81%^[23,24].

It is well known that *H pylori* leads to chronic gastritis and affects gastric acid secretion in virtually all infected individuals. The underlying mechanism responsible for changes in gastric acid secretion in *H pylori* infected individuals is not completely explained, however it is probably a result of impaired gastrin and somatostatin secretion and elevated proinflammatory cytokines in the infected gastric mucosa^[8,22,25]. Gastrin secretion and morphofunctional features of antral G cells in patients with *H pylori* infection and gastritis or DU was scarcely studied using a comparative study, before and after eradication of the infection.

In the present study, healthy asymptomatic individuals (CG2) had significantly lower plasma gastrin levels than all dyspeptic patients. Higher gastrin concentrations were registered in the plasma of *H pylori* infected individuals, both with gastritis and especially when duodenal ulcer was found on endoscopy. After 6 mo, significant decrease in plasma gastrin levels was registered in all successfully eradicated patients. However, no significant change was seen in other groups, including noneradicated patients with gastritis (*H pylori*+Gne) and dyspeptic patients without *H pylori* infection (CG1).

Higher basal plasma gastrin levels in *H pylori* infected patients and animals compared to the uninfected controls were previously reported by different authors^[3-6,10,25]. Our results showed that in infected patients with DU have significantly higher plasma levels of gastrin-17 when compared to *H pylori*-patients with gastritis, as was previously demonstrated both in adults by Kamada *et al.*^[26], and in children by Kato *et al.*^[27], but opposed to the results of other studies^[14]. After successful eradication of *H pylori* infection, plasma gastrin levels decreased markedly in both DU and gastritis patients, as demonstrated previously in adults^[1,26,28-30] and pediatric patients^[27,31] by other authors.

This change was not observed in non-eradicated patients and uninfected dyspeptic controls, implicating that decrease in plasma gastrin is directly related to the eradication of the bacterium from the stomach.

Antral tissue gastrin concentrations at the beginning of our study were similar in both infected (DU and gastritis group) and uninfected patients, as in other studies^[31,32]. Successful eradication therapy lead to a significant decrease in antral tissue gastrin concentrations in patients with gastritis, as seen in other studies^[33], but not in DU patients.

Immunohistochemical and ultrastructural examination of G cell morphology at the beginning of the study revealed significantly lower antral G cell number in *H pylori*+DU patients compared to all the other groups. However, after successful eradication antral G cell number was close to values observed in controls (both CG1 and CG2). By contrast, successful eradication therapy lead to a decrease in G cell number in the antrum of infected patients with gastritis. On the other hand no significant change in gastrin/total endocrine cell ratio was observed during the 6 mo of follow up, neither in infected nor uninfected patients.

Majority of authors agree that there is no significant difference in antral G cell number in infected and uninfected patients before therapy^[12,26,28,31,32]. Yacoub *et al.*, in a similar study, did not find differences in antral G, D, and EC cell densities and G/D, G/EC and D/EC cell ratios in DU patients^[13] compared to controls. On the other hand, a study by Chamouard *et al.*^[34], showed significantly lower number of antral G cells in DU patients, that is in agreement with the results of our study. The decrease in antral G cell number in subjects with DU (that can also correspond to the degranulation of very active gastrin-producing cells resulting in profound hypergastrinemia) could be related to the fact that the number of bacteria and/or severity of antral gastritis is greater in DU patients. Other possible explanation could be related to differences in *H pylori* strains that colonize the antrum of patients with DU. Namely, we previously reported that in Serbia and Montenegro there is high seroprevalence of *cagA*-positive *H pylori* strains in dyspeptic patients with and without peptic ulcer, while *VacA*-positive strains are more closely related to peptic ulcer disease^[35]. However, Gaider *et al.*, found *CagA*+ strains in 78% patients with *H pylori* infection and DU and described the absence of *CagA*+strains in individuals with antral G-cell hyperplasia^[36].

Based on the ultrastructural findings, we propose that in the *H pylori* +DU patients strongly stimulated remaining antral G cells, as a result of a compensatory mechanism, develop a strong synthetic and secretory phenotype before eradication therapy. In addition, after successful eradication all ultrastructural alterations registered in *H pylori*+DU patients were normalized to appearance expected in control group, excluding cytoplasmic granules volume density and their diameter which retained some higher values, but the observed difference was not statistically significant in comparison to values in healthy subjects. These findings suggest that remaining alterations in G cell morphology in DU should be attributed to an unknown host factor.

After successful *H pylori* eradication in dyspeptic patients with gastritis both unchanged^[35] and decreased^[31] antral G cell number was reported, that is consistent with

our results where eradication therapy lead to a decrease in antral G cell number.

Ultrastructural examinations in *H pylori*+ patients with gastritis at the beginning of the study revealed similar, but less prominent subcellular alterations of G cell morphology detected the DU patients. We confirmed in our study, previously reported, increased cytoplasmic cell granule index in patients with *H pylori*-related gastritis using electron microscopy and immunohistochemical examination of antral G cells^[12]. After successful eradication, all detected alterations were reversed and antral G cells had morphological features similar to those in healthy controls. This is consistent with the findings of Sugamata *et al.*^[14], demonstrating the reversibility of antral G cell morphology changes after elimination of the infection.

We identified total antral endocrine cell population and calculated number of G cells using double immunostaining for both synaptophysin and gastrin. Synaptophysin was considered an adequate pan-neuroendocrine marker based on the distribution background in the human antrum, while its importance in the other parts of gastrointestinal tract remains limited. The co-localization study revealed that synaptophysin immunoreactivity occurred in virtually all antral gastrin, somatostatin and serotonin-producing cells^[38]. In the antrum, proportion G cells accounts for 40% of all endocrine cells^[9], as described in all of our examined groups of patients and healthy controls. The fact that the antral G cells/total endocrine cell ratio remained unchanged after eradication of *H pylori* implicates that other gastric endocrine cell types disturbances are related with the presence of the infection. This finding is important for the understanding of the potential important role of other endocrine cell types and their interactive, functional relationship in gastric regulatory physiology in gastritis and peptic ulcer disease associated with *H pylori* infection. Namely, previous studies reported the increase in basal and gastrin-stimulated somatostatin-containing (D) cell activity in the early phase (4-8 wks) after *H pylori* eradication in gastric ulcers^[22] and gastritis^[39], suggesting that both antral G and D cell morphology and function should be considered in the gastric mucosal response to the presence of *H pylori* infection. Decreased antral D cell number in patients with *H pylori*-related chronic gastritis might be one of the reasons for the existing hypergastrinemia^[12].

Possible mechanisms responsible for hypergastrinemia in *H pylori* associated gastritis or duodenal ulcer could be different. Some recent studies indicated that ypergastrinemia related to *H pylori* infection is associated with enhanced activity of platelet activating factor (PAF) produced locally, in the affected gastric mucosa and higher expression of nuclear factor kappaB (NF-kappaB)^[40,41]. PAF may contribute to the hypergastrinemia of *H pylori* infection by stimulating gastrin release from G cells involving influx of extracellular calcium via L-type channels and activation of protein kinase C^[40]. NF-kappaB activation is considered crucial event in the production of proinflammatory molecules in *H pylori*-associated gastritis. In the uninflamed stomach, NF-kappaB was highly expressed and active in a subset of epithelial cells, which were identified as predominantly G cells. In accordance with this activity, antral

mucosa of infected individuals expressed high levels of the NF-kappaB target cytokine TNF-alpha, a well-documented stimulator of gastrin production. In patients with *H pylori*-associated gastritis, NF-kappaB activity was markedly enhanced and activation occurred preferentially in the epithelial cells^[41]. In addition, treatment of cultured canine antral G-cells with *H pylori* constituents enhances subsequent basal and bombesin-stimulated gastrin release suggesting that direct contact between *H pylori* and G-cells in the gastric antrum may be responsible for the hypergastrinemia seen in the infected individuals^[42].

In conclusion, it may be concluded that in *H pylori* infected patients with chronic gastritis, changes in morphology and function of antral G cell are completely reversible and attributable exclusively to the presence of the bacterium in the gastric mucosa. However, duodenal ulcer formation in infected individuals is partly attributable to the presence of the infection, but host factors are of importance as well, since more profound alterations are observed and a certain extent of antral G cell hyperfunction, resulting in prolonged hypergastrinemia, is detected. Further investigations are needed in order to identify relevant host characteristics leading to the ulcer formation including gene polymorphisms of proinflammatory cytokines involved in the control of gastric acid secretion.

REFERENCES

- 1 **Bobrzynski A.** Hormonal, secretory and morphological alterations in gastric mucosa in the course of *Helicobacter pylori* eradication in patients with duodenal ulcer and non-ulcer dyspepsia. *J Physiol Pharmacol* 1997; **48**: S4-S16
- 2 **Hunt RH, Huang JQ.** The case for treatment of dyspeptic patient infected with *H pylori*. *Eur J Surg Suppl* 1998; **582**: 6-10
- 3 **Dockray GJ.** Gastrin and gastric epithelial physiology. *J Physiol* 1999; **518**: 315-324
- 4 **Kaneko H, Konagaya T, Kusugami K.** *Helicobacter pylori* and gut hormones. *J Gastroenterol* 2002; **37**: 77-86
- 5 **Gisbert JP, Boixeda D, Vila T, De Rafael L, Redondo C, De Argila CM.** Basal and stimulated gastrin levels and gastric acid output five months after therapy for *Helicobacter pylori* eradication in duodenal ulcer patients. *J Clin Gastroenterol* 1996; **22**: 90-95
- 6 **Haruma K, Sumii K, Okamoto S, Yoshihara M, Kajiyama G, Wagner S.** *Helicobacter pylori* infection associated with low antral somatostatin content in young adults: implications for the pathogenesis of hypergastrinemia. *Scand J Gastroenterol* 1995; **30**(6 Pt 1): 550-553
- 7 **Feldman M, Cryer B, Lee E.** Effects of *Helicobacter pylori* gastritis on gastric secretion in healthy human beings. *Am J Physiol Gastrointest Liver Physiol* 1998; **274**(6 Pt 1): G1011-G1017
- 8 **Hiraoka S, Miyayaki Y, Kitamura S, Toyota M, Kiyohara T, Shinomura Y, Mukaida N, Matsuzawa Y.** Gastrin induces CXC chemokine expression in gastric epithelial cells through activation of NF-kB. *Am J Physiol Gastrointest Liver Physiol* 2001; **281**: G735-742
- 9 **Sugiyama A, Ikeno T, Maruta F, Kawasaki S, Hayama M, Ota H, Yoshiyawa A, Nakajuma K, Fukushima M, Honda T.** Long-term *Helicobacter* colonization produces G cell hyperplasia and carcinoid tumor in Mongolian gerbils. *J Cell Mol Med* 2000; **4**: 308-309
- 10 **Peek RM Jr, Wirth HP, Moss SF, Yang M, Abdalla AM, Tham KT, Zhang T, Tang LH, Modlin IM, Blaser MJ.** *Helicobacter pylori* alters gastric epithelial cell cycle events and gastric acid secretion in Mongolian gerbils. *Gastroenterology* 2000; **118**: 48-59
- 11 **Drndarevic N, Todorovic V, Micev M, Sokic-Milutinovic A,**

- Milosavljevic T, Spuran M. Assessment of epithelial cell proliferation in gastric mucosal biopsies of patients with *Helicobacter pylori* infection. *Gut* 2003; **52**: A151
- 12 **Tzaneva M.** Light and microscopic immunohistochemical investigation on G and D cells in antral mucosa in *Helicobacter pylori* related gastritis. *Exp Toxicol Pathol* 2001; **52**: 523-528
 - 13 **Yacoub WR,** Thomson ABR, Hooper P, Jewell LD. Immunocytochemical and morphometric studies of gastrin-, somatostatin- and serotonin-producing cells in the stomach and duodenum of patients with acid peptic disorders. *Can J Gastroenterol* 1996; **10**: 395-400
 - 14 **Sugamata M,** Ihara T, Todate A, Sugamata M, Hirakawa R, Yoshida Y, Yamanaka T, Miyata M, Miura M. Ultrastructural study of antral G cells in patients with duodenal ulcer: effect of *Helicobacter pylori* eradication. *Helicobacter* 1997; **2**: 118-122
 - 15 **Malfertheiner P,** Megraud F, O' Morain CO, Bell D, Bianchi Porro G, Deltenre M, Forman D, Gasbarrini G, Jaup B, Misiewicz JJ, Pajares J, Quina M, Rauws E. Current European concepts in the management of *Helicobacter pylori* infection – the Maastricht consensus report. *Eur J Gastroenterol Hepatol* 1997; **9**: 91-92
 - 16 **Goodwin CS.** The Sydney system – microbial gastritis. *J Gastroenterol Hepatol* 1991; **6**: 223-235
 - 17 **Dixon MF,** Genta RM, Yardley JH, Correa P. Classification and grading of gastritis. The updated Sydney System. *Am J Surg Pathol* 1996; **20**: 1161-1181
 - 18 **Sternberg LA.** Immunohistochemistry. New York: Z Wiley and Sons 1986
 - 19 **Koko V,** Todorovic V, Varagic J, Micev M, Korac A, Bajcetic M, Cakic-Milosevic M, Nedeljkovic M, Drndarevic N. Gastrin producing G-cells after chronic ethanol and low protein nutrition. *Ind J Exp Biol* 1998; **36**: 1093-1101
 - 20 **Todorovic V,** Koko V, Varagic J, Lackovic V, Vuzevski V, Milin J. Effects of chronic ethanol administration on the serotonin-producing cells in rat antral and duodenal mucosa. *Histol Histopathol* 1993; **8**: 285-296
 - 21 **Bordi C,** D' Adda T, Azzoni C, Ferraro G. Classification of gastric endocrine cells at light and electron microscopical levels. *Microsc Res Techn* 2000; **48**: 258-271
 - 22 **Hayakawa T,** Kaneko H, Konagaya T, Shinoyaki K, Kasahara A, Funaki Y, Mori S, Yokoi T, Hirooka Y, Kusugami K, Kakunu S. Enhanced somatostatin secretion into the gastric juice with recovery of basal acid output after *Helicobacter pylori* eradication in gastric ulcers. *Gastroenterol Hepatol* 2003; **18**: 505-511
 - 23 **Lind T,** Van Zanten SV, Unge P, Spiller R, Bayerdorffer E, O'Morain C, Bardhan K, Bradette M, Chiba N, Wrangstadh M. Eradication of Hp using one week triple therapies combining omeprazole with two antimicrobials: the MACH I study. *Helicobacter* 1996; **1**: 138-144
 - 24 **Bayerdorffer E,** Lind T, Dite P, Dev Bardhan K, O'Morain C, Delchier JC, Spiller R, Van Zanten SV, Sipponen P, Megraud F, Zeijlon L. Omeprazole, amoxycillin and metronidazole for the cure of Hp infection. *Eur J Gastroenterol Hepatol* 1999; **11**: S19-S22
 - 25 **Zhao CM,** Wang X, Friis-Hansen L, Waldum HL, Halgunset J, Waldstrom T, Chen D. Chronic *Helicobacter pylori* infection results in gastric hypoacidity and hypergastrinemia in wild-type mice but vagally induced hypersecretion in gastrindeficient mice. *Regul Pept* 2003; **15**: 161-170
 - 26 **Kamada T,** Haruma K, Kawaguchi H, Yoshihara M, Sumii K, Kajiyama G. The association between antral G and D cells and mucosal inflammation, atrophy, and *Helicobacter pylori* infection in subjects with normal mucosa, chronic gastritis and duodenal ulcer. *Am J Gastroenterol* 1998; **93**: 748-752
 - 27 **Kato S,** Oyawa K, Koike T, Sekine H, Ohara S, Minoura T, Iinuma K. Effect of *Helicobacter pylori* infection on gastric acid secretion and meal-stimulated serum gastrin in children. *Helicobacter* 2004; **9**: 100-105
 - 28 **Park SM,** Lee HR, Kim JG, Park JW, Jung G, Han SH, Cho JH, Kim MK. Effect of *Helicobacter pylori* infection on antral gastrin and somatostatin cells and on serum gastrin concentrations. *Korean J Int Med* 1999; **14**: 15-20
 - 29 **Kim JH,** Park HJ, Cho JS, Lee KS, Lee SI, Park IS, Kim CK. Relationship of cagA to serum gastrin concentrations and antral G, D cell densities in *Helicobacter pylori* infection. *Yonsei Med J* 1999; **40**: 301-306
 - 30 **Williams MP,** Usselman B, Chilton A, Sercombe J, Nwokolo CU, Pounder RE. Eradication of *Helicobacter pylori* increases nocturnal intragastric acidity during dosing with rabeprazole, omeprazole, lansoprazole and placebo. *Aliment Pharmacol Ther* 2003; **17**: 775-783
 - 31 **Queiroz DM,** Mendes EN, Rocha GA, Moura SB, Resende LM, Barbosa AJ, Coehlo LG, Passos MC, Castro LP, Oliveira CA. Effect of *Helicobacter pylori* eradication on antral gastrin- and somatostatin-immunoreactive cell density and gastrin and somatostatin concentrations. *Scand J Gastroenterol* 1993; **28**: 858-864
 - 32 **Odum L,** Petersen HD, Andersen IB, Hansen BF, Rehfeld JF. Gastrin and somatostatin in *Helicobacter pylori* infected antral mucosa. *Gut* 1994; **35**: 615-618
 - 33 **Kwan CP,** Tytgat GN. Antral G cell hyperplasia: a vanishing disease? *Eur J Gastroenterol Hepatol* 1995; **7**: 1099-1103
 - 34 **Chamouard P,** Walter P, Wittersheim C, Demuynck P, Meunier O, Baumann R. Antral and fundic D-cell numbers in *Helicobacter pylori* infection. *Eur J Gastroenterol Hepatol* 1997; **9**: 361-365
 - 35 **Sokic Milutinovic A,** Wex T, Todorovic V, Milosavljevic T, Malfertheiner P. Anti- CagA and anti-VacA antibodies in *Helicobacter pylori* infected patients with and without peptic ulcer disease in Serbia and Montenegro. *Scand J Gastroenterol* 2004; **30**: 222-226
 - 36 **Gaidar IuA,** Stepanova EV, Mosiichuk LN, Demeshkina LV, Shekhetova GA, Beshpalova EV, Kudriavtseva VE, Vcherashiaia NN. Particular features of the relationship of *Helicobacter pylori* and G cells in patients with duodenal ulcer, with special reference to the *Helicobacter pylori* strain. *Lik Sprava* 2001; **4**: 176-177
 - 37 **Graham DY,** Lew GM, Lechago J. Antral G-cell and D-cell numbers in *Helicobacter pylori* infection: effect of *H. pylori* eradication. *Gastroenterology* 1993; **104**: 1655-1660
 - 38 **Portela-Gomes GM,** Stridsberg M, Johansson H, Grimelius L. Co-localization of synaptophysin with different neuroendocrine hormones in the human gastrointestinal tract. *Histochem Cell Biol* 1999; **111**: 49-54
 - 39 **Milutinovic AS,** Todorovic V, Milosavljevic T, Micev M, Spuran M, Drndarevic N. Somatostatin and D cells in patients with gastritis in the course of *Helicobacter pylori* eradication: a six-month, follow-up study. *Eur J Gastroenterol Hepatol* 2003; **15**: 755-766
 - 40 **Beales IL.** Effect of platelet-activating factor on gastrin-release from cultured rabbit G-cells. *Dig Dis Sci* 2001; **46**: 301-306
 - 41 **Van Den Brink GR,** Ten Kate EJ, Ponsioen CY, Rive MM, Tytgat GN, van Deventer SJ, Peppelenbosch MP. Expression and activation of NF/kappa B in the antrum of the human stomach. *J Immunol* 2000; **164**: 3353-3359
 - 42 **Beales IL,** Calam J. *Helicobacter pylori* increases gastrin release from cultured canine antral- G-cells. *Eur J Gastroenterol Hepatol* 2000; **12**: 641-644

• *Helicobacter pylori* •

Enhanced plasma ghrelin levels in *Helicobacter pylori*-colonized, interleukin-1-receptor type 1-homozygous knockout (IL-1R1^{-/-}) mice

Yuka Abiko, Hidekazu Suzuki, Tatsuhiro Masaoka, Sachiko Nomura, Kumiko Kurabayashi, Hiroshi Hosoda, Kenji Kangawa, Toshifumi Hibi

Yuka Abiko, Hidekazu Suzuki, Tatsuhiro Masaoka, Sachiko Nomura, Kumiko Kurabayashi, Toshifumi Hibi, Department of Internal Medicine and Center for Integrated Medical Research, Keio University School of Medicine, Shinjuku-ku, Tokyo 160-8582, Japan
Hiroshi Hosoda, Kenji Kangawa, Department of Biochemistry, National Cardiovascular Center Research Institute, Suita, Osaka 565-8565, Japan

Supported by a Grant-in-Aid for Scientific Research C (2) from the Japan Society for the Promotion of Science (JSPS) (15590686, to H.S.), and a grant from the Keio University School of Medicine
Correspondence to: Hidekazu Suzuki, MD, PhD, Assistant Professor, Department of Internal Medicine, School of Medicine, Keio University, 35 Shinanomachi, Shinjuku-ku, Tokyo 160-8582, Japan. hsuzuki@sc.itc.keio.ac.jp

Telephone: +81-3-5363-3914 Fax: +81-3-5363-3967

Received: 2004-10-14 Accepted: 2004-11-29

which is also induced by the infection, resulting in the body weight loss of mice with *H. pylori* infection.

© 2005 The WJG Press and Elsevier Inc. All rights reserved.

Key words: Ghrelin; *H. pylori*; IL-1; Body weight; Myeloperoxidase

Abiko Y, Suzuki H, Masaoka T, Nomura S, Kurabayashi K, Hosoda H, Kangawa K, Hibi T. Enhanced plasma ghrelin levels in *Helicobacter pylori*-colonized, interleukin-1-receptor type 1-homozygous knockout (IL-1R1^{-/-}) mice. *World J Gastroenterol* 2005; 11(27): 4148-4153

<http://www.wjgnet.com/1007-9327/11/4148.asp>

Abstract

AIM: Ghrelin is an endogenous ligand for the growth hormone secretagogue receptor, and it plays a role in stimulating the growth hormone secretion, food intake, body weight gain and gastric motility. Eradication of *Helicobacter pylori* (*H. pylori*) was shown to be associated with increase of the body weight. On the other hand, *H. pylori* infection evokes the release of gastric IL-1 β . The present study was designed to investigate the involvement of the gastric IL-1 signal in the ghrelin dynamics in *H. pylori*-colonized mice.

METHODS: Twelve-week-old female IL-1-receptor type 1-homozygous-knockout mice (IL-1R1^{-/-}) and their wild-type littermates (WT) were orally inoculated with *H. pylori* (Hp group), while other cohorts received oral inoculation of culture medium (Cont group). Thirteen weeks after the inoculation, the mice were examined. The plasma and stomach ghrelin levels and the gastric preproghrelin mRNA were measured.

RESULTS: Although the WT mice with *H. pylori* infection showed a significantly decreased body weight as compared with that of the animals without *H. pylori* infection, *H. pylori* infection did not influence the body weight of the IL-1R1-knockout (IL-1R1^{-/-}) mice. In the *H. pylori*-infected IL-1R1^{-/-} mice, the total and active ghrelin levels in the plasma were significantly increased, and the gastric ghrelin level was decreased. No significant differences were noted in the gastric preproghrelin mRNA expression.

CONCLUSION: Ghrelin secretion triggered by *H. pylori* infection might be suppressed by IL-1 β , the release of

INTRODUCTION

Ghrelin, an endogenous ligand for the growth hormone secretagogue receptor (GHS-R), stimulates growth hormone (GH) release from cultured pituitary cells in a dose-dependent manner^[1], and is produced and secreted from the A-like cells found mainly in the oxyntic glands of the gastric fundus^[2]. Ghrelin is now known to play a role in not only GH release, but also in controlling the appetite and body weight. Since both parenterally and intracerebro-ventricularly administered ghrelin have been shown to stimulate food intake and increase the body weight of mice and rats with free access to food, even those animals with GH deficiency^[3,4], the control of appetite and body weight may be independent of GH release. Ghrelin, a 28-amino-acid peptide, is activated when its third serine residue is acylated by n-octanoic acid, and GHS-R is responsive to the first four or five residues including the octanoylated serine residue of the whole ghrelin peptide^[5]. GHS-R has been shown to be present in the pituitary, hypothalamus, adrenal glands, thyroid, pancreas, myocardium, spleen and testes^[1,6-8]. Ghrelin stimulates the expression of both NPY and AGRP mRNA in the hypothalamus. The central orexigenic effect of ghrelin is mediated by the NPY/AGRP-expressing neurons in the hypothalamus^[3,9-11]. On the other hand, ghrelin has also been reported to suppress vagal afferent activity^[2]. The peripheral orexigenic effect of ghrelin may be mediated, at least in part, by its suppressive effect on the vagal afferent activity.

IL-1 β is a pro-inflammatory cytokine that mediates the cachectic process by stimulating the expression and release of leptin^[12] and/or by mimicking the effect on the hypothalamus of excessive negative-feedback signaling from

leptin^[13]. Cachexia is a condition characterized by wasting, emaciation, feebleness and inanition. It was recently reported that the levels of both ghrelin peptide and ghrelin mRNA in the stomach were up-regulated in a mouse model of cancer cachexia^[14]. In cachectic mice with increased plasma levels of IL-1 β , the plasma concentrations of ghrelin also increased with the progression of cachexia^[15]. This result suggests that a close relationship might exist between the ghrelin dynamics and the cachectic process mediated by IL-1. IL-1 β is an anorexigenic substance, just like CCK, leptin, gastrin-related protein and bombesin, and antagonizes the actions of ghrelin. Asakawa *et al.*, reported that parenterally administered IL-1 β decreased NPY mRNA expression in the hypothalamus and preproghrelin mRNA expression in the stomach, and that intraperitoneally administered ghrelin inhibited the severity of IL-1 β -induced anorexia.

Helicobacter pylori (*H pylori*) infection is known to be a major pathogenetic factor in the development of gastritis, peptic ulcer disease and gastric malignancy^[16,17]. Attachment of *H pylori* to the gastric mucosa induces inflammation, which is associated with the release of various cytokines, including IL-1 β ^[18]. Although the importance of the anorexigenic effect of IL-1 β in cases with *H pylori* infection has not yet been clarified, it has been observed clinically that *H pylori* eradication is often followed by improvement of some nutritional parameters, such as the body weight and the serum levels of total cholesterol, total protein and albumin^[19]. We recently reported that *H pylori* infection could modify the plasma and gastric ghrelin dynamics in Mongolian gerbils^[20]. In humans, however, *H pylori* infection has been reported not to be associated with any changes of the plasma ghrelin levels^[21,22], although eradication of *H pylori* has been shown by some to be associated with increases of the plasma ghrelin levels^[23]. Therefore, regulation of the ghrelin dynamics and its influence on the body weight control in cases with *H pylori* infection still remains to be clarified.

We designed the present study to investigate the role of the gastric IL-1 signal in the regulation of the ghrelin dynamics and its influence on the body weight control under in cases with *H pylori* infection.

MATERIALS AND METHODS

Animal procedures

All experiments and procedures carried out on the animals were approved by the Keio University Animal Research Committee (No. 023009). Twelve-week-old, specific-pathogen-free female interleukin-1 (IL-1)-receptor type 1-homozygous-knockout mice (IL-1R1^{-/-}) on a C57BL/6 background (The Jackson Lab., Bar Harbor, ME, USA) and their wild-type cohorts as controls (WT) were used for the study. The Sydney Strain of *H pylori* (SS1) was grown from frozen stocks at 37 °C under microaerobic conditions for 24–36 h in lysed horse-blood agar supplemented with antibiotics, harvested in Brucella broth, and administered to the mice immediately after being harvested. Six IL-1R1^{-/-} mice and five WT mice were orally inoculated with *H pylori* (1.5 \times 10⁸ CFU/mL, 0.5 mL), while another six IL-1R1^{-/-} mice and five WT mice were orally inoculated with the culture medium alone as control. A week later, each animal

was inoculated again with the aforementioned bacterial strain. Thirteen weeks after the first inoculation, all the mice were examined under ether anesthesia. The mice were then deprived of food for 17 h before being killed. The body weight of each mouse was measured just before the examination.

Confirmation of Infection

H pylori infection was diagnosed by determining the number of CFUs in a microaerobic bacterial culture. Briefly, the diluted homogenates of the stomachs were plated on to Brucella agar plates containing 10% horse blood, 2.5 μ g/mL amphotericin B, 9 μ g/mL vancomycin, 0.32 μ g/mL polymyxin B, 5 μ g/mL trimethoprim, and 50 μ g/mL 2, 3, 5-triphenyl-tetrazolium chloride. The plates were then incubated at 37 °C in a microaerobic atmosphere for 7 d^[24]. All of the *H pylori* inoculated animals were confirmed as *H pylori* positive by this procedure in the present study.

Measurement of plasma ghrelin levels

Whole-blood samples were obtained from the right ventricle in tubes containing EDTA-2Na (1 mg/mL blood) and aprotinin (500 kIU/mL blood). The tubes were centrifuged and the plasma samples were stored at -80 °C.

Plasma total ghrelin was measured using the Desacyl-Ghrelin ELISA Kit (Mitsubishi Kagaku Medical, Inc., Ibaraki, Japan), and plasma active ghrelin was measured using the Active Ghrelin ELISA Kit (Mitsubishi Kagaku Medical, Inc., Ibaraki, Japan). Total ghrelin, i.e., active plus inactive ghrelin, was measured using an antibody directed against the C-terminal end (residues 1 to 11) of ghrelin, while an antibody directed against the N-terminal end of ghrelin (residues 13 to 28) was used for the measurement of active ghrelin. The plasma samples were placed in testing wells coated with the ghrelin antibodies. Then, the plate with the wells was incubated for 2 h at room temperature. After incubation, the samples were washed and diluted HRP was added to the wells. The plate was then incubated again for 1 h at room temperature. The samples were washed and substrate solution was added to the wells. The plate was incubated for a further 30 min at room temperature under shade conditions. After the reaction, a reagent was added to stop the reaction, and the absorbance of each well was measured at 450 nm.

Measurement of myeloperoxidase activity

Immediately after the mice were sacrificed, the stomachs of the animals were removed and opened along the greater curvature. Tissue samples of the gastric mucosa were collected in tubes containing PBS and protease inhibitors (100 μ mol/L phenylmethylsulfonyl fluoride, 10 μ g/mL aprotinin) and sonicated over ice in 30 consecutive 0.5 s bursts at 0.5 s intervals, at a power setting of 150 W (VCX 50; Sonics and Materials, Inc., Newton, CT, USA). The total protein content in the homogenates was measured by modified Lowry's method^[25], as described by Smith *et al.*^[26].

Myeloperoxidase (MPO) activity, as an index of tissue-associated neutrophil accumulation, was determined by a modification of Grisham *et al.*'s method^[27]. Aliquots containing 100 μ L of the mucosal homogenates were

centrifuged at 8 000 r/min for 15 min at 4 °C to separate the pellets of insoluble cellular debris. The pellets were rehomogenized in an equal volume of 0.05 mol/L potassium phosphate buffer (pH 5.4) containing 0.5%-hexadecyltrimethylammonium bromide. The samples were then centrifuged at 8 000 r/min for 15 min at 4 °C and the supernatants were reserved. The MPO activity in the supernatants was assessed by measuring the H₂O₂-dependent oxidation of 3, 3', 5, 5'-tetramethylbenzidine. One unit of enzyme activity was defined as the amount of MPO that caused a change in the absorbance of 1.0/min at 655 nm, at 25 °C.

Measurement of the gastric ghrelin levels

Fresh whole-anterior-wall specimens of the glandular stomach were frozen immediately after collection in liquid nitrogen and stored at -80 °C. Each sample was boiled for five min in a 10-fold volume of water to inactivate the intrinsic proteases. The solution was adjusted to 1N acetic acid by addition of 180 microliter acetic acid after cooling, and the tissue was homogenized. The supernatant was lyophilized and subjected to RIA to measure the ghrelin level. The extraction efficiency of tissue ghrelin was more than 95%.

Two RIA techniques were used for measuring ghrelin, as described previously^[28]. Briefly, ghrelin levels were measured using two polyclonal rabbit antibodies raised against an N terminal (1-11) (Gly1-Lys11) or C terminal (13-28) (Gln13-Arg28) fragment of rat ghrelin. Two tracer ligands were synthesized: [Tyr29]-rat ghrelin for antirat ghrelin (1-11) antiserum and [Tyr12]-rat ghrelin [13-28] for antirat ghrelin [13-28] antiserum. The RIA incubation mixtures containing 100 µL of either standard ghrelin or unknown samples containing 200 µL of antiserum diluted in RIA buffer containing 0.5% normal rabbit serum, were initially incubated for 12 h. Then, the mixture was incubated for 36 h after the addition of 100 µL of ¹²⁵I labeled tracer (15 000 cpm). Antirabbit IgG goat serum (100 µL) was added followed by incubation for an additional 24 h. Free and bound tracers were then separated by centrifugation at 3 000 r/min for 30 min. Following aspiration of the supernatant, the radioactivity in the pellet was quantified using a gamma counter (ARC-600; Aloka, Tokyo, Japan). All assays were performed at 4 °C. The antirat ghrelin (1-11) antiserum specifically recognized the n-octanoylated form of rat ghrelin, but not the des-acyl form. The antirat ghrelin (13-28) antiserum recognized both the acylated and des-acyl forms of rat ghrelin equally efficiently. Both antisera were equally cross-reactive with human and gerbil ghrelin, and did not recognize the other enteric peptides. The respective intra- and interassay coefficients of variation for the N terminal RIA were 3% and 6%, and for the C terminal RIA were 6% and 9%.

Measurement of the preproghrelin mRNA expression level in the stomach

Total RNA was extracted from the stomach of the mice using the RNeasy Mini Kit (Qiagen). A TaqMan quantitative real-time RT-PCR was performed to detect preproghrelin mRNA and GAPDH mRNA using the ABI PRISM 7700 sequence detection system (PE Applied Biosystems)^[29].

The following primers were used to amplify preproghrelin mRNA: forward-ghrelin (5'-GGA ATC CAA GAA GCC ACC AGC-3'), reverse-ghrelin (5'-GCT CCT GAC AGC TTG ATG CCA-3'), and Taqman-ghrelin (5'-FAM-AAC TGC AGC CAC GAG CTC TGG AAG GC-TAMRA-3'). The following primers were used to amplify GAPDH mRNA as the internal control: forward primer (5'-TTC AAC GGC ACA GTC AAG GC-3'), reverse primer (5'-GCC TTC TCC ATG GTG GTG AAG-3'), and Taqman probe (5'-FAM-CCC ATC ACC ATC TTC CAG GAG CGA GA-TAMRA-3').

The preproghrelin mRNA expression levels were normalized using the GAPDH mRNA expression levels.

Statistical analysis

All the data were expressed as the mean±SE. The data were analyzed using one-way analysis of variance, followed by Scheffe's multiple comparison tests. A value of *P*<0.05 was considered to denote statistical significance.

RESULTS

Among the WT mice, the *H. pylori*-infected mice showed a significantly reduced body weight as compared to the uninfected and control mice (*P*<0.001). Although the basic body weight of the IL-1R1^{-/-} mice was lower than that of the WT mice, no further reduction of the body weight of these mice was observed after *H. pylori* infection (Table 1).

H. pylori infection increased the MPO activity in the gastric mucosa in both the WT (*P*<0.01) and IL-1R1^{-/-} (*P*<0.01) mice, although in the IL-1R1^{-/-} mice, the increase was significantly less marked (*P*<0.05) (Figure 1).

Table 1 Body weight of the mice at the time of the examination

Wild type mice (g)		IL-1R1 ^{-/-} mice (g)	
Not-infected	Infected	Not-infected	Infected
26.0±0.71	22.1±0.54 ^b	23.4±0.51	23.1±0.34

Among the wild-type mice, the body weight of *H. pylori*-infected mice (*n* = 4) was lower than that of the uninfected mice (*n* = 5); on the other hand, among the IL-1R1^{-/-} mice, no significant difference in the body weight was noted between the infected (*n* = 6) and uninfected (*n* = 6) mice. ^b*P*<0.001 vs the uninfected mice.

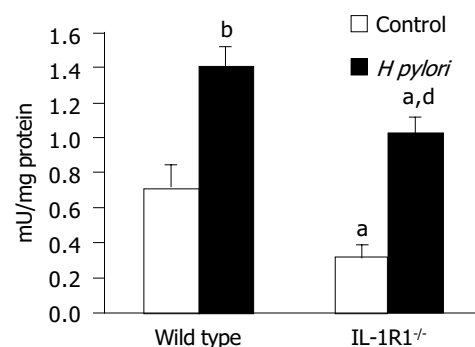


Figure 1 Myeloperoxidase (MPO) activity in the stomach. Both wild-type (filled column: *n* = 4) and IL-1R1^{-/-} (spotted filled column: *n* = 6) mice with *H. pylori* infection showed increased MPO activity as compared with the uninfected wild-type (clear column: *n* = 5) and IL-1R1^{-/-} (spotted clear column: *n* = 5). ^a*P*<0.05 vs the wild-type mice, ^b*P*<0.001, ^d*P*<0.01 vs the uninfected mice.

Among the WT mice, the *H pylori*-infected animals showed no significant increase of the plasma total ghrelin levels as compared to the uninfected and control mice. In the case of the IL-1R1^{-/-} mice, although simple lack of the IL-1 signal did not affect the plasma total ghrelin dynamics, *H pylori* infection of these mice was associated with a marked increase of the plasma total ghrelin levels ($P < 0.05$; compared with the uninfected mice, $P < 0.001$; compared with the wild-type mice) (Figure 2).

The same tendency was shown for the plasma active ghrelin dynamics. Among the WT mice, the *H pylori*-infected mice showed a tendency towards increase in the plasma active ghrelin levels as compared to the uninfected and control mice, but the increase was not statistically significant. On the other hand, in the IL-1R1^{-/-} mice, while a simple lack of the IL-1 signal did not affect the plasma active ghrelin dynamics, *H pylori* infection of these animals was associated with a marked increase of the plasma active ghrelin levels ($P < 0.01$; compared with the uninfected mice, $P < 0.05$; compared with the wild-type mice) (Figure 3).

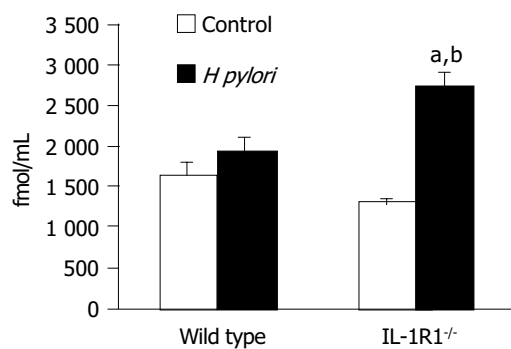


Figure 2 The total ghrelin levels in the plasma. Although neither simple lack of the IL-1 signal (spotted clear column: $n = 4$) nor *H pylori* infection alone (filled column: $n = 4$) was associated with any changes in the total plasma ghrelin levels as compared with the levels in the uninfected wild-type mice (clear column: $n = 5$), *H pylori* infection induced a marked increase of the total plasma ghrelin levels in the IL-1R1^{-/-} mice (spotted filled column: $n = 6$). ^a $P < 0.05$ vs the uninfected mice. ^b $P < 0.001$ vs the wild-type mice.

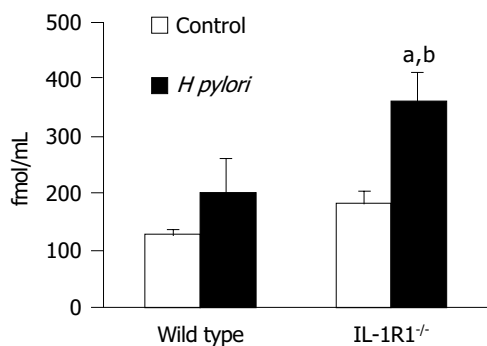


Figure 3 The active ghrelin levels in the plasma. Neither simple lack of the IL-1 signal (spotted clear column: $n = 6$) nor *H pylori* infection alone (filled column: $n = 3$) was associated with any changes in the total plasma ghrelin levels as compared with the levels in the uninfected wild-type mice (clear column: $n = 5$). *H pylori* infection induced a marked increase of the plasma active ghrelin levels in the IL-1R1^{-/-} mice (spotted filled column: $n = 6$). ^a $P < 0.05$ vs the wild-type mice; ^b $P < 0.01$ vs the uninfected mice.

In contrast to the effects of *H pylori* on the plasma ghrelin dynamics, the ghrelin levels in the stomach, both total and active, were significantly decreased in the *H pylori*-infected IL-1R1^{-/-} mice ($P < 0.05$) (Figure 4A and B), indicating that ghrelin is secreted into the blood from its stores in the stomach.

Preproghrelin mRNA expression, evaluated in comparison with the expression of GAPDH mRNA, was not modified by either *H pylori* infection or lack of the IL-1 signal, or both (Figure 5). These results suggest that the stomach ghrelin stores were not replenished after ghrelin secretion into the blood.

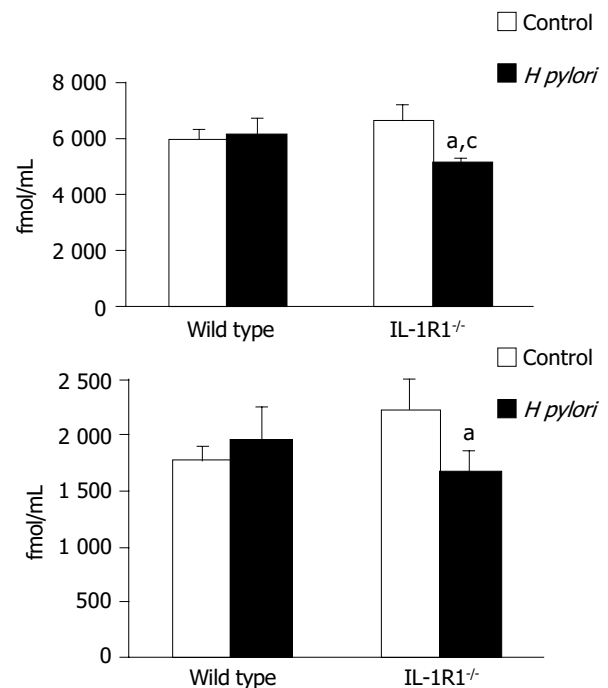


Figure 4 The gastric (A: total, B: active) ghrelin levels. Although neither a simple lack of the IL-1 signal (spotted clear column: (A) $n = 5$, (B) $n = 5$) nor *H pylori* infection alone (filled column: (A) $n = 5$, (B) $n = 5$) was associated with any changes in the gastric ghrelin levels as compared with the levels in the uninfected wild-type mice (clear column: (A) $n = 5$, (B) $n = 5$), *H pylori* infection induced a marked decrease of the a) total and b) active gastric ghrelin levels in the IL-1R1^{-/-} mice (spotted filled column: (A) $n = 6$, (B) $n = 5$). ^a $P < 0.05$ vs the uninfected mice; ^c $P < 0.05$ vs the wild-type mice.

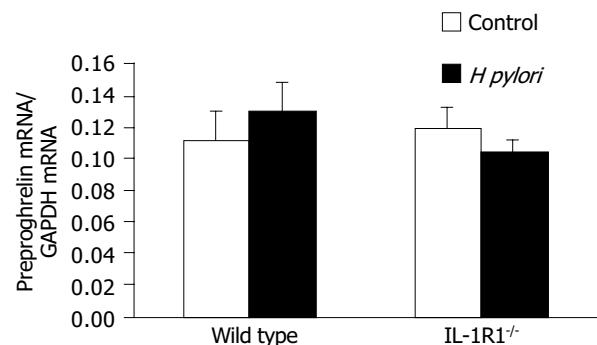


Figure 5 Preproghrelin mRNA levels in the gastric mucosa. No significant differences were observed among the uninfected wild-type mice (clear column: $n = 5$), uninfected IL-1R1^{-/-} mice (spotted clear column: $n = 6$), *H pylori*-infected wild-type mice (filled column: $n = 5$) and *H pylori*-infected IL-1R1^{-/-} mice (spotted filled column: $n = 6$).

DISCUSSION

It is widely known that *H. pylori* infection is associated with loss of body weight. In the present study, although *H. pylori*-infected wild-type (WT) mice showed body weight loss, no such weight loss was observed in IL-1R1^{-/-} mice with *H. pylori* infection (Table 1). On the other hand, although an increase in the level of gastric mucosal neutrophil accumulation was noted in both WT and IL-1R1^{-/-} mice with *H. pylori* infection, the neutrophil accumulation was significantly less marked in *H. pylori*-infected IL-1R1^{-/-} mice than in *H. pylori*-infected WT mice (Figure 1), indicating that the lack of the IL-1 signal could affect the regulatory mechanisms of both body weight and gastric mucosal inflammation.

It has previously been reported that the administration of lipopolysaccharide (LPS) is associated with a reduction in the plasma levels of ghrelin^[30, 31] and increase in the plasma levels of IL-1 β ^[31]. According to the study by Burgess *et al.*^[32], while intracerebroventricular administration of LPS greatly reduced the food intake in WT mice, no such effect was observed in mice deficient in the IL-1 β -converting enzyme. In addition, as mentioned above, it has been reported that injection of IL-1 β was followed by a decrease in the gastric preproghrelin mRNA expression^[9]. These results suggest that the anorexigenic effect of LPS may be mediated by IL-1 β and ghrelin, a downstream molecule in the cascade. The production of IL-1 β might be enhanced by LPS and the release of ghrelin might be suppressed by IL-1 β .

We recently reported from a study in Mongolian gerbils, that the plasma levels of ghrelin are enhanced for a restricted period after *H. pylori* inoculation^[20]. In the present study, while the plasma levels of ghrelin showed no significant increase in the WT mice with *H. pylori* infection, the levels were significantly elevated in IL-1R1^{-/-} mice with *H. pylori* infection (Figure 2, 3), indicating that IL-1 may suppress ghrelin secretion, as mentioned above. As in Mongolian gerbils, *H. pylori* infection also stimulates ghrelin secretion in mice, but the secretion is suppressed by IL-1 β , a mediator whose production is also enhanced by *H. pylori* infection. Therefore, in IL-1-signal-deficient mice with *H. pylori* infection, ghrelin production and release into the blood occurs unopposed by the inhibitory action of IL-1 on these processes.

Contrary to the observations on the ghrelin dynamics, the gastric expression of leptin mRNA, one of the important anorexigenic peptides produced by adipocytes, is significantly increased by *H. pylori* infection^[33]; expression of this mRNA is also significantly enhanced by IL-1 administration^[12]. The central pathway of appetite control by ghrelin is reported to be mediated by neuropeptide Y (NPY)-expressing neurons in the hypothalamus. Ghrelin increases the activity of NPY-expressing neurons, and hence food intake^[9, 10]. The same NPY-expressing neurons in the hypothalamus have also been reported to be involved in the suppression of appetite by leptin. Leptin decreases the mRNA expression of NPY in the neurons of the hypothalamus^[11], thereby suppressing food intake and causing loss of body weight^[3, 11]. The effects of ghrelin and leptin are considered to be competitively regulated by the hypothalamic NPY-expressing neurons.

Thus, in the WT mice, *H. pylori* infection stimulates both

ghrelin secretion and IL-1 β release, but excessive ghrelin secretion is suppressed by IL-1 β , whereas leptin secretion, also stimulated by *H. pylori*, is promoted by IL-1 β . The competitive actions of ghrelin and leptin in the hypothalamic NPY-expressing neurons result in a decrease of the appetite and body weight of WT mice with *H. pylori* infection. On the other hand, in the *H. pylori*-infected IL-1R1^{-/-} mice, the inhibitory effect of the IL-1 signal on ghrelin secretion is absent, and the enhanced ghrelin secretion combined with the enhanced leptin secretion might result in a dominant effect of ghrelin on the appetite control, and body weight loss does not become manifest in these animals.

While the secretion of stored gastric ghrelin is affected by *H. pylori*, the gastric preproghrelin mRNA expression was not significantly enhanced by *H. pylori* infection in the present study (Figure 5). While in Mongolian gerbils, *H. pylori* infection was associated with increased plasma ghrelin levels and decreased gastric ghrelin and preproghrelin mRNA expression^[20], the infection in mice had no significant effect on any of the above three parameters. According to Asakawa *et al.*^[9], IL-1 administration reduced gastric preproghrelin mRNA expression; this may be the reason why the IL-1-receptor-knockout mice in the present study did not show any changes of the gastric preproghrelin mRNA expression. Thus, there may be species differences in the hormone dynamics and their reactivity to stimulation, such as in the event of *H. pylori* infection.

In conclusion, ghrelin secretion triggered by *H. pylori* infection might be suppressed by IL-1 β , resulting in body weight loss of the infected mice.

ACKNOWLEDGMENTS

A part of the present data was presented in the Topic Forum of Digestive Disease Week on May, 17th, 2004, in New Orleans, USA.

REFERENCES

- 1 Kojima M, Hosoda H, Date Y, Nakazato M, Matsuo H, Kangawa K. Ghrelin is a growth-hormone-releasing acylated peptide from stomach. *Nature* 1999; **402**: 656-660
- 2 Date Y, Murakami N, Toshinai K, Matsukura S, Nijima A, Matsuo H, Kangawa K, Nakazato M. The role of the gastric afferent vagal nerve in ghrelin-induced feeding and growth hormone secretion in rats. *Gastroenterology* 2002; **123**: 1120-1128
- 3 Nakazato M, Murakami N, Date Y, Kojima M, Matsuo H, Kangawa K, Matsukura S. A role for ghrelin in the central regulation of feeding. *Nature* 2001; **409**: 194-198
- 4 Wren AM, Small CJ, Ward HL, Murphy KG, Dakin CL, Taheri S, Kennedy AR, Roberts GH, Morgan DG, Ghatei MA, Bloom SR. The novel hypothalamic peptide ghrelin stimulates food intake and growth hormone secretion. *Endocrinology* 2000; **141**: 4325-4328
- 5 Bednarek MA, Feighner SD, Pong SS, McKee KK, Hreniuk DL, Silva MV, Warren VA, Howard AD, Van Der Ploeg LH, Heck JV. Structure-function studies on the new growth hormone-releasing peptide, ghrelin: minimal sequence of ghrelin necessary for activation of growth hormone secretagogue receptor 1a. *J Med Chem* 2000; **43**: 4370-4376
- 6 Gaytan F, Barreiro ML, Caminos JE, Chopin LK, Herington AC, Morales C, Pinilla L, Paniagua R, Nistal M, Casanueva FF, Aguilar E, Dieguez C, Tena-Sempere M. Expression of ghrelin and its functional receptor, the type 1a growth hor-

- mone secretagogue receptor, in normal human testis and testicular tumors. *J Clin Endocrinol Metab* 2004; **89**: 400-409
- 7 **Guan XM**, Yu H, Palyha OC, McKee KK, Feighner SD, Sirinathsinghi DJ, Smith RG, Van der Ploeg LH, Howard AD. Distribution of mRNA encoding the growth hormone secretagogue receptor in brain and peripheral tissues. *Brain Res Mol Brain Res* 1997; **48**: 23-29
 - 8 **Gnanapavan S**, Kola B, Bustin SA, Morris DG, McGee P, Fairclough P, Bhattacharya S, Carpenter R, Grossman AB, Korbonits M. The tissue distribution of the mRNA of ghrelin and subtypes of its receptor, GHS-R, in humans. *J Clin Endocrinol Metab* 2002; **87**: 2988
 - 9 **Asakawa A**, Inui A, Kaga T, Yuzuriha H, Nagata T, Ueno N, Makino S, Fujimiya M, Niiijima A, Fujino MA, Kasuga M. Ghrelin is an appetite-stimulatory signal from stomach with structural resemblance to motilin. *Gastroenterology* 2001; **120**: 337-345
 - 10 **Kamegai J**, Tamura H, Shimizu T, Ishii S, Sugihara H, Wakabayashi I. Central effect of ghrelin, an endogenous growth hormone secretagogue, on hypothalamic peptide gene expression. *Endocrinology* 2000; **141**: 4797-4800
 - 11 **Shintani M**, Ogawa Y, Ebihara K, Aizawa-Abe M, Miyanaga F, Takaya K, Hayashi T, Inoue G, Hosoda K, Kojima M, Kangawa K, Nakao K. Ghrelin, an endogenous growth hormone secretagogue, is a novel orexigenic peptide that antagonizes leptin action through the activation of hypothalamic neuropeptide Y/Y1 receptor pathway. *Diabetes* 2001; **50**: 227-232
 - 12 **Sarraf P**, Frederich RC, Turner EM, Ma G, Jaskowiak NT, Rivet DJ 3rd, Flier JS, Lowell BB, Fraker DL, Alexander HR. Multiple cytokines and acute inflammation raise mouse leptin levels: potential role in inflammatory anorexia. *J Exp Med* 1997; **185**: 171-175
 - 13 **Inui A**. Cancer anorexia-cachexia syndrome: are neuropeptides the key? *Cancer Res* 1999; **59**: 4493-4501
 - 14 **Hanada T**, Toshinai K, Kajimura N, Nara-Ashizawa N, Tsukada T, Hayashi Y, Osuye K, Kangawa K, Matsukura S, Nakazato M. Anti-cachectic effect of ghrelin in nude mice bearing human melanoma cells. *Biochem Biophys Res Commun* 2003; **301**: 275-279
 - 15 **Hanada T**, Toshinai K, Date Y, Kajimura N, Tsukada T, Hayashi Y, Kangawa K, Nakazato M. Upregulation of ghrelin expression in cachectic nude mice bearing human melanoma cells. *Metabolism* 2004; **53**: 84-88
 - 16 **Marshall BJ**, Warren JR. Unidentified curved bacilli in the stomach of patients with gastritis and peptic ulceration. *Lancet* 1984; **1**: 1311-1315
 - 17 **Uemura N**, Okamoto S, Yamamoto S, Matsumura N, Yamaguchi S, Yamakido M, Taniyama K, Sasaki N, Schlemper RJ. *Helicobacter pylori* infection and the development of gastric cancer. *N Engl J Med* 2001; **345**: 784-789
 - 18 **Yamaoka Y**, Kita M, Kodama T, Sawai N, Kashima K, Imanishi J. Induction of various cytokines and development of severe mucosal inflammation by cagA gene positive *Helicobacter pylori* strains. *Gut* 1997; **41**: 442-451
 - 19 **Furuta T**, Shirai N, Xiao F, Takashima M, Hanai H. Effect of *Helicobacter pylori* infection and its eradication on nutrition. *Aliment Pharmacol Ther* 2002; **16**: 799-806
 - 20 **Suzuki H**, Masaoka T, Hosoda H, Ota T, Minegishi Y, Nomura S, Kangawa K, Ishii H. *Helicobacter pylori* infection modifies gastric and plasma ghrelin dynamics in Mongolian gerbils. *Gut* 2004; **53**: 187-194
 - 21 **Gokcel A**, Gumurdulu Y, Kayaselcuk F, Serin E, Ozer B, Ozsahin AK, Guvener N. *Helicobacter pylori* has no effect on plasma ghrelin levels. *Eur J Endocrinol* 2003; **148**: 423-426
 - 22 **Suzuki H**, Masaoka T, Hosoda H, Nomura S, Ohara T, Kangawa K, Ishii H, Hibi T. Plasma ghrelin concentration correlates with the levels of serum pepsinogen I and pepsinogen I/II ratio-a possible novel and non-invasive marker for gastric atrophy. *Hepatogastroenterology* 2004; **51**: 1249-1254
 - 23 **Nwokolo CU**, Freshwater DA, O'Hare P, Randeva HS. Plasma ghrelin following cure of *Helicobacter pylori*. *Gut* 2003; **52**: 637-640
 - 24 **Takahashi S**, Keto Y, Fujita H, Muramatsu H, Nishino T, Okabe S. Pathological changes in the formation of *Helicobacter pylori*-induced gastric lesions in Mongolian gerbils. *Dig Dis Sci* 1998; **43**: 754-765
 - 25 **Lowry OH**, Rosebrough NJ, Farr AL, Randall RJ. Protein measurement with the Folin phenol reagent. *J Biol Chem* 1951; **193**: 265-275
 - 26 **Smith PK**, Krohn RI, Hermanson GT, Mallia AK, Gartner FH, Provenzano MD, Fujimoto EK, Goeke NM, Olson BJ, Klenk DC. Measurement of protein using bicinchoninic acid. *Anal Biochem* 1985; **150**: 76-85
 - 27 **Grisham MB**, Hernandez LA, Granger DN. Xanthine oxidase and neutrophil infiltration in intestinal ischemia. *Am J Physiol* 1986; **251**: G567-574
 - 28 **Hosoda H**, Kojima M, Matsuo H, Kangawa K. Ghrelin and des-acyl ghrelin: two major forms of rat ghrelin peptide in gastrointestinal tissue. *Biochem Biophys Res Commun* 2000; **279**: 909-913
 - 29 **Masaoka T**, Suzuki H, Hosoda H, Ota T, Minegishi Y, Nagata H, Kangawa K, Ishii H. Enhanced plasma ghrelin levels in rats with streptozotocin-induced diabetes. *FEBS Lett* 2003; **541**: 64-68
 - 30 **Basa NR**, Wang L, Arteaga JR, Heber D, Livingston EH, Tache Y. Bacterial lipopolysaccharide shifts fasted plasma ghrelin to postprandial levels in rats. *Neurosci Lett* 2003; **343**: 25-28
 - 31 **Zuckerman SH**, Shellhaas J, Butler LD. Differential regulation of lipopolysaccharide-induced interleukin 1 and tumor necrosis factor synthesis: effects of endogenous and exogenous glucocorticoids and the role of the pituitary-adrenal axis. *Eur J Immunol* 1989; **19**: 301-305
 - 32 **Burgess W**, Gheusi G, Yao J, Johnson RW, Dantzer R, Kelley KW. Interleukin-1 β -converting enzyme-deficient mice resist central but not systemic endotoxin-induced anorexia. *Am J Physiol* 1998; **274**: R1829-1833
 - 33 **Azuma T**, Suto H, Ito Y, Ohtani M, Dojo M, Kuriyama M, Kato T. Gastric leptin and *Helicobacter pylori* infection. *Gut* 2001; **49**: 324-329

• BASIC RESEARCH •

Mechanisms of action of leptin in preventing gastric ulcer

Edward O. Adeyemi, Salim A. Bastaki, Irwin S. Chandranath, Mohammed Y. Hasan, Mohammed Fahim, Abdu Adem

Edward O. Adeyemi, Department of Internal Medicine, Faculty of Medicine and Health Sciences, UAE University, Al Ain, United Arab Emirates

Salim A. Bastaki, Irwin S. Chandranath, Mohammed Y. Hasan, Abdu Adem, Department of Pharmacology, Faculty of Medicine and Health Sciences, UAE University, Al Ain, United Arab Emirates
Mohammed Fahim, Department of Physiology, Faculty of Medicine and Health Sciences, UAE University, Al Ain, United Arab Emirates
Supported by the Faculty of Medicine and Health Sciences Research Grant, UAE University, United Arab Emirates

Correspondence to: Professor Abdu Adem, Department of Pharmacology, FMHS, UAE University, PO Box 17666, Al Ain, United Arab Emirates. abdu.adem@uaeu.ac.ae

Telephone: +971-3-7137522 Fax: +971-3-7672033

Received: 2004-10-23 Accepted: 2005-01-13

also suggest that leptin prevents ulcer formation by increasing the activities of the cyclo-oxygenase and/or nitric oxide pathways and by increasing mucus secretion.

© 2005 The WJG Press and Elsevier Inc. All rights reserved.

Key words: Indomethacin; Acidified ethanol; Gastric ulcer; Prostaglandin; Ranitidine; Omeprazole; Lansoprazole; *N*⁶-nitro L-arginine methyl ester; Wistar rats

Adeyemi EO, Bastaki SA, Chandranath IS, Hasan MY, Fahim M, Adem A. Mechanisms of action of leptin in preventing gastric ulcer. *World J Gastroenterol* 2005; 11(27): 4154-4160

<http://www.wjgnet.com/1007-9327/11/4154.asp>

Abstract

AIM: To investigate the effects of leptin (1-20 µg/kg) on acidified ethanol (AE)- and indomethacin (Indo)-induced gastric lesions in rats and compare it with ranitidine, lansoprazole, and omeprazole and to determine its mechanisms of actions.

METHODS: Gastric ulcers, which were approximately 1 mm in width, formed in the glandular portion of the gastric mucosa produced by oral administration of either AE or Indo were taken as ulcer index. The inhibitory effect of subcutaneous administration of leptin, two proton pump inhibitors (PPIs) lansoprazole and omeprazole, or H₂-receptor antagonist ranitidine 30 min before AE or Indo was evaluated. A radioimmunoassay was used to determine the PGE₂ concentration in the homogenate of the glandular portion of the stomach. We performed histological study of the glandular stomach for the evaluation of total, acidic, and sulfated mucus content.

RESULTS: Subcutaneous administration of leptin, two PPIs lansoprazole and omeprazole or H₂-receptor antagonist ranitidine 30 min before AE or Indo produced a dose-dependent and reproducible inhibition of gastric ulcers (GUs). This inhibition was found to be more potent than other antagonists used. In *N*⁶-nitro L-arginine methyl ester (L-NAME)-pretreated animals, the ulcer prevention ability of leptin in AE-induced ulcer was significantly reduced, compared to rats without L-NAME pretreatment. However, the ulcer prevention ability of leptin was not altered by L-NAME treatment in Indo-induced ulcers. Leptin produced a dose-dependent increase in PGE₂ level in the gastric glandular tissues. Leptin also increased mucus secretion.

CONCLUSION: The results of the present study show that leptin inhibits GU formation by AE or Indo in a dose-dependent and reproducible manner in rats. The results

INTRODUCTION

Peptic ulcer is caused by a break in the mucosal integrity, close to the acid-secreting areas of the gastrointestinal tract. It is a disease that was characterized by remissions and exacerbations before the era of gastric acid secretion modifying drugs or *Helicobacter pylori* (*H. pylori*). It is often located in the stomach (gastric ulcer, GU), in the proximal duodenum (duodenal ulcer), rarely in the esophagus, jejunum (distal to a gastrojejunal anastomosis) or the Meckel's diverticulum, containing ectopic gastric mucosa. Development of a peptic ulcer depends on the balance between the known aggressive factors and mucosal defense mechanisms. Some of the aggressive factors are gastric acid^[1,2], bile salts, abnormal motility^[3], pepsin, use of nonsteroidal anti-inflammatory drugs (NSAID)^[4], infection with micro-organisms (*H. pylori*, herpes simplex and others). Mucus secretion, gastroduodenal bicarbonate production^[5], prostaglandin synthesis^[6], cholecystokinin and somatostatin^[7], cellular regeneration, and normal tissue microcirculation protect against ulcer formation.

Leptin, a 167-amino acid peptide hormone, is secreted by the adipocytes into the circulation, lowers the body weight by decreasing appetite and increasing energy expenditure^[8-10]. It has also been found to be present in the gastric mucosa^[11], and this has been thought to control food intake in man. Another way of interpreting the presence of leptin in the gastric mucosa is to invoke its ability to function as a mucosal defense factor in the stomach. Indeed, a Polish group of workers showed recently that leptin has a gastro-protective effect in rats^[12]. Much more recently, a Turkish group of workers showed that leptin has a gastro-protective effect on mucosal injury induced by ischemia reperfusion^[13]. To date, there is a dearth of information in the literature about the mechanism by which leptin prevents ulcer formation in the stomach. Thus, the primary aim of this project was to investigate the effect of leptin on PGE₂ synthesis on ulcer formation by

indomethacin (Indo), a NSAID, or acidified ethanol (AE) in rats. The second aim was to study the role of leptin in relation to other established anti-ulcer agents, such as ranitidine^[14] and PPIs^[15] on peptic ulcer prevention in rats.

MATERIALS AND METHODS

The following drugs and chemicals were used for the experiments: absolute alcohol (BDH, Poole, UK), hydrochloric acid (BDH), lansoprazole (Sigma, St. Louis, MO, USA), omeprazole (Astra, Uppsala, Sweden), Indo (Sigma, UK), L-NAME (Sigma, UK) and high sensitivity prostaglandin E₂ Chemiluminescence Enzyme Immunoassay Kit (Assay Designs Inc., MI, USA). Leptin was a generous gift from Amgen Inc., USA. All solutions were freshly prepared and diluted in normal saline.

Experimental protocols

Wistar rats weighing 200–250 g were fasted for 18 h in wire mesh cages to avoid coprophagy. The animals were deprived of food but had free access to water *ad libitum*. The temperature of the animal room was maintained at 22±2 °C and a 12–12 h dark-light cycle was maintained. All animals used for the study had an ethical clearance from the Animal Users' Committee of the Faculty of Medicine, United Arab Emirates University.

Indomethacin-induced ulceration and effect of leptin treatment

Indo (30 mg/kg) was administered orally to induce GUs in 18-h fasted Wistar rats. Gastric lesions were formed 6 h after Indo administration. The rats were divided into different groups of six animals each and Indo was given to each animal 30 min after administering leptin (1–50 µg/kg, subcutaneously) or normal saline (1 mL/kg, subcutaneously), and the animals were killed 6 h later by cervical dislocation and exsanguinations. The abdomen was incised, the stomach removed and cut open along the greater curvature and rinsed with water to remove any adherent food particles and mucus. The opened stomach was spread on a sheet of cork so as to have a clear macroscopic view of the gastric mucosa. The total lengths of the hemorrhagic lesions, which were approximately 1 mm in width formed in the glandular portion of the gastric mucosa, were taken as ulcer index. An observer unaware of the drug treatments confirmed the ulcer index. The percentage reduction of the ulcer index in the drug-treated groups was calculated from the saline-treated groups.

Indomethacin-induced ulceration: comparison of leptin with ranitidine

The ability of different doses of leptin (1–50 µg/kg) and a fixed dose of ranitidine (50 mg/kg), all administered subcutaneously, to prevent the formation of Indo-induced GU was studied. The rats were killed 6 h after administering Indo by cervical dislocation and exsanguinations. The abdomen was incised and the stomach removed and the ulcer index was determined as described above. The reduction of the ulcer in the drug-treated groups was calculated as a percentage of the ulcer index in the saline-treated group.

Indomethacin-induced ulceration: comparison of leptin with two proton pump inhibitors

In another experiment, 10 µg/kg each of lansoprazole and

omeprazole, or 10 µg/kg of leptin was administered 30 min before the animals received Indo orally. The rest of the experiment and determination of the ulcer index were performed as described earlier.

Acidified ethanol-induced ulceration and effect of leptin treatment

AE was administered orally to induce GUs in rats. We used 60% ethanol in 150 mmol/L HCl as an ulcerogenic agent, based on earlier observation that ethanol 50% and above caused a reproducible model of gastric damage^[16,17]. Gastric lesions were formed 1 h after administering AE. The rats were divided into different groups of six animals each and each group received either saline (1 mL/kg) or leptin (1–20 µg/kg), subcutaneously. Thirty minutes later, AE was given orally to each animal at a dose of 1 mL per rat and the animals were killed 1 h later by cervical dislocation and exsanguinations. The ulcer index was determined as described above.

Leptin ulcer prevention ability in indomethacin pre-treated rats

In order to study the influence of prostaglandin on the cytoprotective activity of leptin, Indo was administered at a dose of 10 mg/kg subcutaneously (a dose, which inhibits prostaglandin synthesis, but does not induce gastric ulceration) to one group of animals followed by subcutaneous administration of leptin (10 µg/kg), 30 min later. AE was given to each animal 30 min after drug administration and the animals were killed 1 h later. The stomachs were subsequently removed to measure the ulcer index as described earlier.

Leptin ulcer prevention ability in L-NAME pre-treated rats

In another group of animals, N^G-nitro L-arginine methyl ester (L-NAME, 25 mg/kg), an inhibitor of nitric oxide synthase activity, was administered subcutaneously 15 min before giving leptin (10 µg/kg, subcutaneously). AE was given orally 30 min later and the animals were killed 1 h after ethanol administration to determine the ulcer index. In another group of L-NAME-pretreated animals, Indo was given orally instead of AE to induce ulcers, and the animals were killed 6 h later to determine the ulcer index.

Effect of leptin on prostaglandin E₂ (PGE₂) levels in the gastric mucosa

The glandular portion of the control and leptin-treated rat stomachs were homogenized in 1.5 mL of Tris buffer (50 mmol/L; pH 7.5) containing 10 µg/mL Indo to prevent further cyclo-oxygenase activity at 0 °C. The tissue homogenate was acidified by addition of 2 mmol/L HCl to a pH of 3.5, and allowed to settle at 4 °C for 15 min before centrifuging the samples in a microcentrifuge at 1 000 r/min for 5 min to remove the tissue debris. The supernatant was harvested and stored at -20 °C until assayed, usually within 24 h. A radioimmunoassay was used to determine the PGE₂ concentration in the supernatant according to the instructions of the manufacturer (Assay Designs Inc., MI, USA). The assay is based on the competitive binding technique by which PGE₂ present in a sample competes with a fixed amount of alkaline phosphatase-labeled PGE₂ for sites on a mouse mAb. During incubation, the mouse mAb is bound to the

goat anti-mouse antibody coated onto the microtiter well plate. Following a wash to remove excess conjugate and unbound sample, a substrate solution is added to the wells to determine the bound enzyme activity. Immediately following the color development, the luminescence is read in a luminometer. The intensity of the color is inversely proportional to the concentration of PGE_2 in the sample. A standard curve was constructed from a series of known concentrations of PGE_2 solution provided by the kit manufacturer, and the PGE_2 concentrations of the unknown samples were determined by interpolation.

Determination of mucus in glandular mucosa

We performed histological study of the glandular stomach for the evaluation of total, acidic, and sulfated mucus content. Cross-sectional areas of the portion of the gland stained red by periodic acid Schiff (PAS) were measured to give the total glycoprotein present in the gastric pits. The Alcian Blue (AB) method at pH 1 was used to measure the sulfated macromolecular content in the gastric pits, whereas at pH 2.5 were used to measure the total acidic mucus content.

The glandular portion of the stomach was fixed in Zamboni fixative overnight. Smaller pieces cut from the glandular portion was dehydrated with ethanol and embedded in paraffin. Two series of sections (6 $\mu\text{mol/L}$ thick) were made by cutting the block in a plane perpendicular to the mucosal surface. Sections, after being deparaffinized

and hydrated to distilled water and placed in acetic acid solution, were stained with PAS and/or AB (pH 2.5 and 1). They were serially dehydrated in 95% ethyl alcohol, absolute alcohol, and xylene and mounted in resinous medium. The sections were evaluated in a randomized blinded fashion by a histologist who was unaware of the experimental protocol.

Statistical analysis

All results were expressed as mean \pm SE. Ulcer index obtained for test drugs and saline controls were compared using one-way ANOVA. A two-tailed P value <0.05 was considered significant.

RESULTS

Indo caused a marked ulceration of the stomach in those rats given normal saline (Figures 1A-D). Figure shows hemorrhagic lesions on the glandular area of the rat stomach caused by AE (A) and Indo (C) in the absence (A and C) and presence (B and D) of 10 $\mu\text{g/kg}$ leptin. A significant inhibition of the hemorrhagic lesions due to the leptin treatment was evident. When the animals were treated with leptin (1-50 $\mu\text{g/kg}$), there was a dose-dependent increase of the ulcer prevention ability of leptin, against Indo and formed a plateau at a dose of 20 $\mu\text{g/kg}$ leptin. The ulcer index at each of the leptin concentrations from 5-50 $\mu\text{g/kg}$ was significantly less ($P<0.05$) than the ulcer index in normal saline-treated rats (Figure 2A).

Figure 2B reveals the degree of preventing Indo-induced

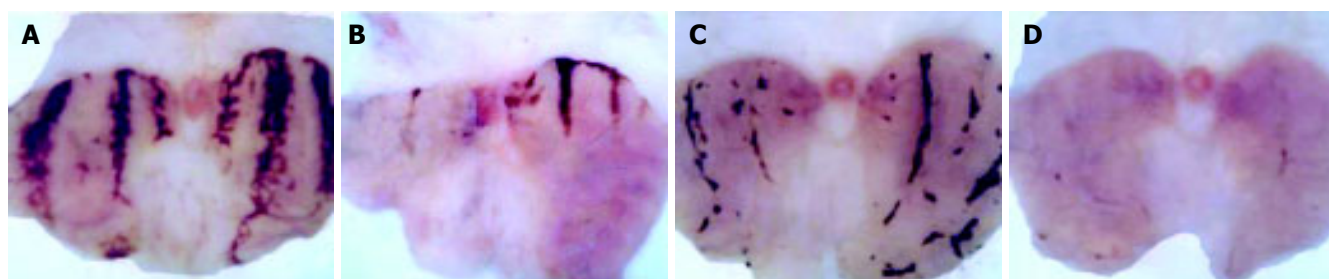


Figure 1 Photomicrograph of macroscopic appearance of the glandular mucosa, showing the effect of AE (A) and Indo (C) in the absence (A and C) and presence

of 10 $\mu\text{g/kg}$ dose of leptin (B and D). These photographs are typical of six such tissues.

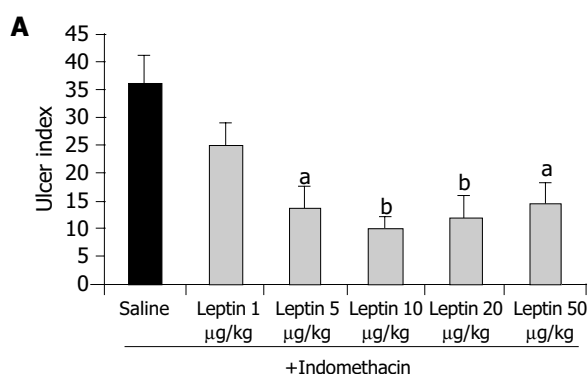
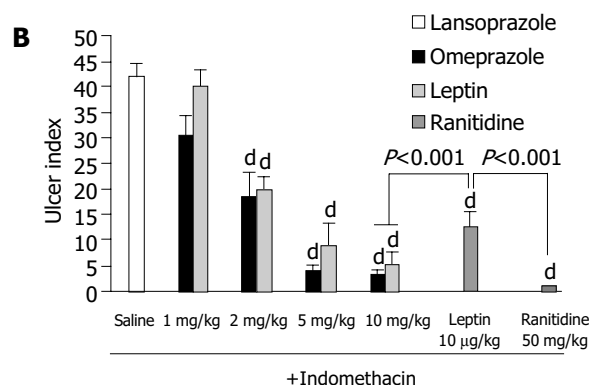


Figure 2 A: The ulcer indices of saline and different concentrations of leptin (1-50 $\mu\text{g/kg}$) against Indo. Each value is a mean \pm SE. Asterisks indicate significant difference when compared to saline control ($^aP<0.05$, $^bP<0.01$); **B:** The degree of prevention of Indo-induced ulcerations after treatment with different doses of



lansoprazole and omeprazole (each used at 1-10 mg/kg), leptin (10 $\mu\text{g/kg}$) and ranitidine (50 mg/kg). Each value is a mean \pm SE. Asterisks indicate significant difference ($^dP<0.001$) when compared to saline control.

ulcerations when the animals were treated with lansoprazole and omeprazole, each used at a dose of 1, 2, 5, and 10 mg/kg. There was a profound inhibition of ulcer formation at 10 mg/kg of both lansoprazole and omeprazole. The difference between the drug-treated group (lansoprazole or omeprazole at 2-10 mg/kg) and the saline-treated group was significant ($P<0.001$); with lansoprazole showing a slightly more powerful inhibition than omeprazole but the difference between them was not statistically significant. The leptin ulcer inhibition at 10 μ g/kg dosage was significantly less ($P<0.001$) than that achieved with lansoprazole or omeprazole, each administered at 10 mg/kg (1 000 times the dose of leptin used; Figure 2B). When the rats were treated with 50 mg/kg of ranitidine (5 000 times the dose of leptin), the ulcer prevention activity was significantly higher ($P<0.001$) than that achieved with 10 μ g/kg leptin (Figure 2B).

When the animals were treated with increasing doses of leptin (1-10 μ g/kg), lansoprazole (1-20 mg/kg) and omeprazole (0.5-10 mg/kg) 30 min before they received AE, there was a dose-dependent inhibition of ulcer formation by leptin and each of the PPIs (Figure 3).

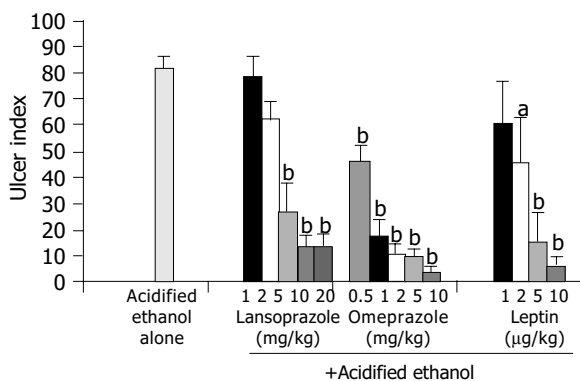


Figure 3 The effect of increasing doses of leptin (1-10 μ g/kg), lansoprazole (1-10 mg/kg), and omeprazole (0.5-10 mg/kg) on AE-induced ulceration in rats. Each value is a mean \pm SE. Asterisks indicate significant difference, $^aP<0.05$, $^bP<0.001$ vs controls.

Leptin (10 μ g/kg) produced a significant ($P<0.001$) inhibition of Indo-induced ulcers in L-NAME-pretreated animals, which was not statistically significantly different from the ulcer index for leptin in animals without L-NAME pretreatment (Figure 4).

Leptin caused a profound ulcer inhibition, which was significantly greater ($P<0.001$) for 10 μ g/kg of leptin than saline-treated controls when AE was used to induce gastric ulceration in Indo-pretreated animals (Figure 5). When ulcer induction was performed with AE in L-NAME-pretreated rats, there was a significantly greater degree ($P<0.001$) of GU inhibition by leptin than saline-treated controls (Figure 5). However, the inhibition by leptin of AE-induced ulcer formation was significantly less ($P<0.001$) in the presence of L-NAME than in its absence (Figure 5). Injection of increasing doses of leptin to the animals before AE led to increasing degrees of peptic ulcer prevention and higher tissue concentrations of PGE₂ (Figure 6). Leptin increased

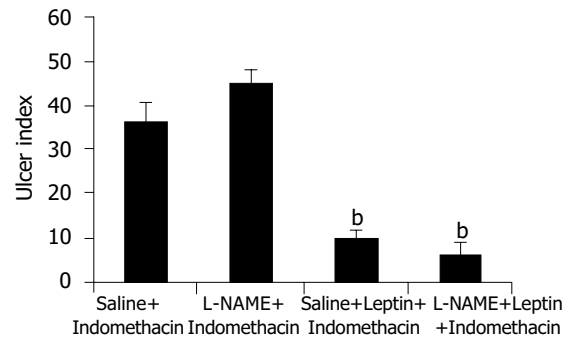


Figure 4 The ulcer prevention ability of leptin (10 μ g/kg), when Indo was used to induce ulcer in L-NAME-pretreated animals. Each value is a mean \pm SE. Asterisks indicate significant difference, $^bP<0.001$ vs controls.

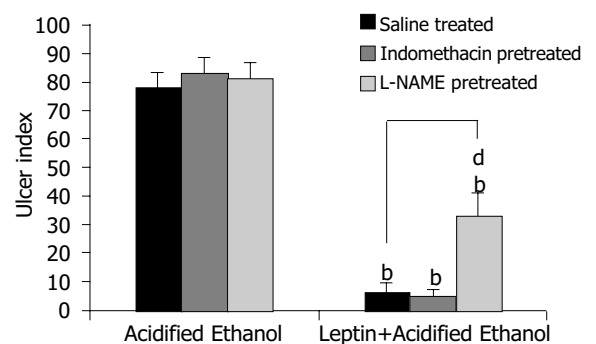


Figure 5 The ulcer prevention ability of leptin (10 μ g/kg), in AE-induced ulcer after Indo or L-NAME pretreatment. Each value is a mean \pm SE. Asterisks indicate significant difference, $^bP<0.001$ vs controls. $^dP<0.001$ shows the significant difference in the effect of leptin on saline-treated and L-NAME-pretreated rats.

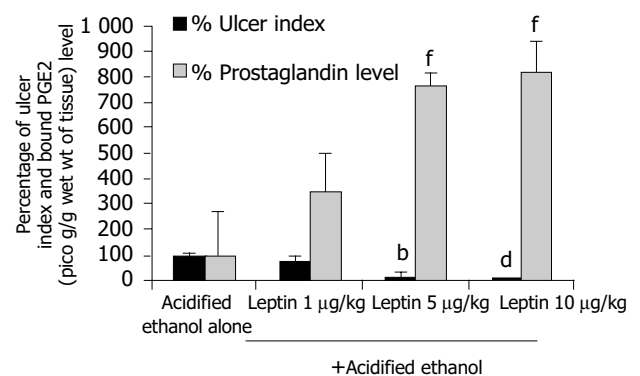


Figure 6 The effect of increasing doses of leptin (1-10 μ g/kg) on AE-induced ulcer and prostaglandin E₂ levels in the gastric glandular mucosa in rats. Each value is a mean \pm SE. $^bP<0.01$, $^dP<0.001$ indicate significant difference in percentage ulcer index compared to AE-treated rats taken as 100%. $^fP<0.01$ shows the significant difference in the level of prostaglandin E₂ compared to AE-treated rats taken as 100%.

mucus secretion (Figures 7D, F) and prevented injury to the epithelial layer (Figures 7A-C) thus showing the involvement of mucus as the mechanism of gastroprotection.

DISCUSSION

Leptin is a peptide that is produced by the adipocytes and it

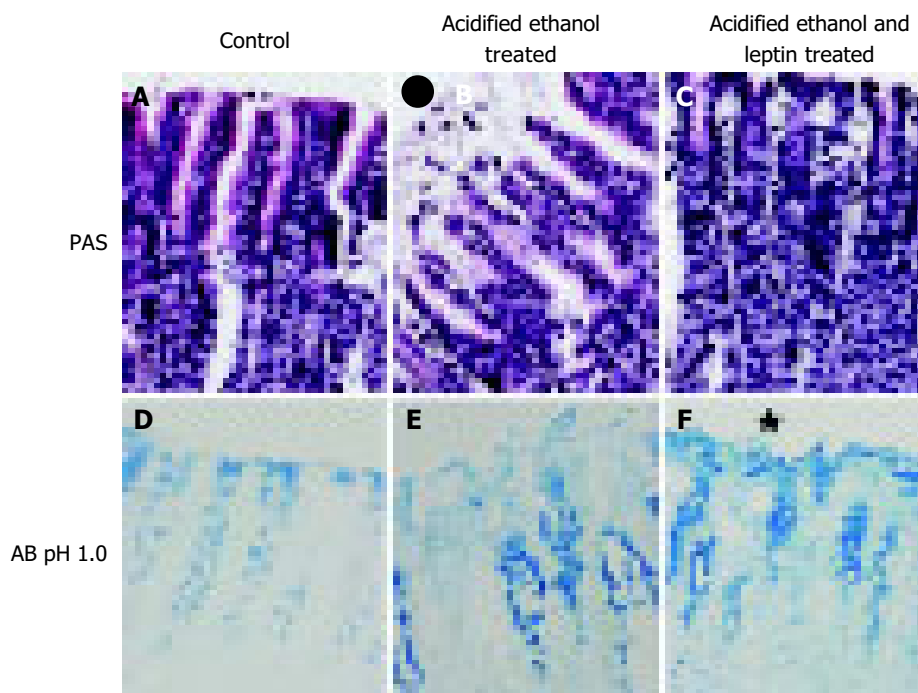


Figure 7 Gastric mucosal layer of rats stained with PAS showing (A) normal epithelium from control rats; (B) damaged epithelium (●) and (C) repaired epithelium after leptin treatment. Lower panel shows the AB (pH 1.0) staining

showing mucus in (D) normal epithelium; (E) loss of epithelial mucus due to AE (★) and (F) presence of epithelial mucus after leptin treatment (bar = 6 μ m; magnification 40 \times).

regulates the function of the satiety center in the hypothalamus^[8]. Although it has also been found in the stomach^[11] its function in the stomach is not clear. In this study, we investigated the property of leptin as an ulcer-preventing agent in an experimental animal model. Our results showed that exogenous leptin demonstrated profound ulcer prevention ability in rats when their gastric mucosa was exposed to ulcer-inducing agents, such as Indo and AE. Exogenous administration of leptin increased the leptin levels in the blood plasma, fundus, and antrum of the stomach^[18,19]. The basal leptin concentration did not prevent by itself the ulcerogenic effect of Indo or AE. However, exogenously administered leptin prevented this effect indicating a pharmacological action of leptin.

Indo is a well-known ulcerogenic agent. In this study, Indo produced hemorrhagic lesions in the gastric mucosa 6 h after its ingestion, which is in accord with previous reports^[20-23]. In Indo-induced ulceration, the ulcer prevention ability of leptin was dose-dependent, reaching a maximum at 10 μ g/kg. No further increase was observed when the leptin dose was doubled. Indeed, its ulcer prevention ability was reduced at a higher leptin dose of 50 μ g/kg. This phenomenon may be explained by an increase in gastric acid secretion that was observed in this study (unpublished data). At this dosage, the leptin ulcer prevention ability was significantly less ($P < 0.05$) than that achieved with ranitidine, which was used at 50 mg/kg, 5 000 times the dose of leptin. However, the ulcer prevention ability of leptin at 10 μ g/kg compares well with that of omeprazole or lansoprazole, each used at 10 mg/kg, 1 000 times the dose at which leptin was employed.

AE, a well-known ulcerogenic agent, was used in the study to produce gastric mucosal damage by causing areas

of focal hyperemia and hemorrhage^[22,24,25]. Moreover, intragastric ethanol increases vascular permeability and vascular damage in capillaries near the luminal surface and not in the deeper muscularis mucosa that might indicate a role for impaired blood flow in the production of AE-induced gastric lesions. Leptin demonstrated a profound ulcer prevention ability, which compared well with that of each of the PPIs, lansoprazole and omeprazole, when AE was employed as an ulcerogenic agent. This is in line with previous reports^[12] that leptin has gastro-protective effect on the gastric mucosal injury induced by topical application of 75% ethanol.

It was interesting to note that the leptin ulcer prevention ability was slightly greater in AE- than in Indo-induced ulceration, although it did not reach statistical level of significance. This may be due to the fact that the AE-induced ulcers are formed superficially at the epithelial layer unlike that induced by Indo, which affects the deeper layer, the submucosa. This profound effect of inhibiting AE-induced ulcer formation by leptin was maintained, even when the animals were pretreated with low dose of Indo. However, a competition in the production of gastric mucosal PGE₂ between Indo (inhibition) and leptin (stimulation) cannot be ruled out. In AE-induced ulceration, evaluation of the effect of leptin on gastric tissue prostaglandin synthesis revealed a dose-dependent increase of gastric mucosal PGE₂ concentration^[26]. This finding suggests that leptin might act in part via the cyclo-oxygenase pathway in preventing ulcer formation. Furthermore our findings that leptin stimulated mucus secretion support the notion that this peptide acted by stimulating PGE₂ production. It has been reported previously that PGE₂ stimulates mucus secretion^[26-28]. In contrast to our results Brzozowski *et al.*^[12], reported that

prostaglandins are not involved in the gastro-protective effect of leptin. The contradictory finding observed in our present results could be due to methodological differences in inducing ulcer.

The influence of leptin-induced histamine release, which has a protective effect on the gastric mucosa, was reported by several workers^[13,29]. Morimoto *et al.*^[29], have reported that histamine release in the hypothalamus was significantly increased by leptin administration. Erkasap *et al.*^[13], have reported that leptin exerts a cytoprotective effect by increasing gastric tissue histamine content which in turn maintain the gastric mucosal blood flow, thereby suggesting that histamine is involved in the prevention of ischemia reperfusion-induced gastric mucosal injury. Goiot *et al.*^[30], reported that the co-existence of leptin and STAT-3 proteins in antral cells provide evidence for the involvement of leptin in the control of gastric secretions. Konturek *et al.*^[31], have investigated the effect of leptin on gastric acid secretion using *H. pylori*-positive and -negative patients and reported that gastric meal- and CCK-induced leptin is capable of inhibiting basal and meal stimulated gastric H⁺ secretion in *H. pylori*-positive patients. But in *H. pylori*-negative patients the release of leptin was reduced in response to CCK and meal. We have shown that subcutaneous administration of low doses of leptin (1-50 µg/kg) potentiates the gastric acid stimulating effect of dimaprit, an H₂ receptor agonist, and pentagastrin, a gastrin receptor agonist, in anaesthetized rats (results not shown). The variation in our results and those of others may be due to the methodological approach towards the evaluation of leptin effect. Taken together our data and those of Azuma *et al.*^[32], Morimoto *et al.*^[29], Erkasap *et al.*^[13], and Konturek *et al.*^[19], suggested that, in addition to the local effect of leptin, a generalized effect of leptin could not be ruled out.

Pretreatment of the animals with L-NAME (25 mg/kg, subcutaneously), an inhibitor of the nitric oxide synthase, before AE-induced gastric ulcerations, reduced the peptic ulcer prevention ability of leptin (10 µg/kg) significantly. However, it did not blot it out completely. This finding suggests that the peptic ulcer prevention ability of leptin does not depend solely on the nitric oxide pathway. This again is in line with the observation of Brzozowski *et al.*^[12], that L-NAME reduced the ulcer-preventing ability of leptin against AE. Brzozowski *et al.*^[33], have also investigated the effect of centrally and intraperitoneally administered leptin and reported that its gastro-protective action, accompanied by increased gastric blood flow and increased plasma gastrin levels, depends on vagal activity and involves hyperemia mediated by NO.

Our results may have consequences for the clinical practice. Based on our data, one would want to recommend the use of leptin subcutaneously in a pilot study in humans, in order to assess its efficacy as an ulcer prevention drug in patients in the intensive care unit, who are prone to develop stress ulcers^[34] during the course of their treatment. Another potential area for its use is among patients with active rheumatoid arthritis^[35] who need to use NSAID for their inflammatory joint disease. This is mainly because the existing epidemiological data support a causal relationship between NSAID use and the development of clinically

important ulcer disease or its complications, including upper GI bleeding.

In conclusion, we have shown that leptin, at low doses (1-10 µg/kg), has ulcer prevention ability, which is comparable to that of ranitidine, an H₂-receptor antagonist or omeprazole and lansoprazole. The ulcer prevention ability of leptin varies according to the ulcerogenic agent used. It is more effective in inhibiting AE-induced than Indo-induced ulcers. The ulcer prevention ability of leptin in AE-induced ulcer involves the cyclooxygenase and the nitric oxide pathways, whereas it acts only via the cyclooxygenase pathway in preventing Indo-induced ulcers.

ACKNOWLEDGMENTS

We would like to thank Amgen Inc., USA, for kindly donating the leptin, which was used in this study. We would also like to thank Dr. Eric Mensah-Brown for his help in studying the photomicrographs and Mr. Naseer Omar for assisting in animal experiments and Dr. Edward Adeyemi who passed away at the end of the year 2004.

REFERENCES

- 1 Magalhaes AF, Macedo C, Hauck JR, Carvalhaes A, De Nucci G, Magna LA, Pedrazzoli J Jr. Acid suppression with ranitidine plus oral triple therapy improves ulcer healing but not *Helicobacter pylori* eradication. *Hepatogastroenterology* 1998; **45**: 2161-2164
- 2 Brown LF, Wilson DE. Gastroduodenal ulcers: causes, diagnosis, prevention and treatment. *Compr Ther* 1999; **25**: 30-38
- 3 Azuma T, Dodge M, Ito S, Yamazaki Y, Miyaji H, Ito Y, Suttie H, Kuriyama M, Kato T, Kohli Y. Bile reflux due to disturbed gastric movement is a cause of spontaneous gastric ulcer in W/W^v mice. *Dig Dis Sci* 1999; **44**: 1177-1183
- 4 Gaw AJ, Williams LV, Spraggs CF, Jordan CC. Role of pepsin in the development of indomethacin-induced antral ulceration in the rat. *Aliment Pharmacol Ther* 1995; **9**: 167-172
- 5 Hogan DL, Ainsworth NA, Isenberg J. Review article: Gastroduodenal bicarbonate secretion. *Aliment Pharmacol Ther* 1994; **8**: 475-478
- 6 Peskar BM, Maricic N. Role of prostaglandins in gastro protection. *Dig Dis Sci* 1998; **43**(Suppl 9): 23S-29
- 7 Brzozowski T, Konturek PC, Konturek SJ, Kwiecien S, Pajdo R, Brzozowska I, Hahn EG. Involvement of endogenous cholecystokinin and somatostatin in gastroprotection induced by intraduodenal fat. *J Clin Gastroenterol* 1998; **27**(Suppl 1): S125-137
- 8 Zhang Y, Proenca R, Maffei M, Barone M, Leopold L, Friedman JM. Positional cloning of the mouse obese gene and its human homologue. *Nature* 1994; **372**: 425-432
- 9 Halaas JL, Gajiwala KS, Maffei M. Weight reducing effects of the plasma protein encoded by the obese gene. *Science* 1995; **269**: 543-546
- 10 Pellemounter MA, Cullen MJ, Baker MB, Hecht R, Winters D, Boone T. Effects of the obese gene product on body weight regulation in ob/ob mice. *Science* 1995; **269**: 540-543
- 11 Bado A, Lévassieur S, Attoub S, Kermorgant S, Laigneau JP, Bortoluzzi MN, Moizo L, Lehy T, Guerre-Millo M, Le Marchand-Brustel Y, Lewin MJ. The stomach is a source of leptin. *Nature* 1998; **394**: 790-793
- 12 Brzozowski T, Konturek PC, Konturek SJ, Pajdo R, Duda A, Pierzchalski P, Bielanski W, Hahn EG. Leptin in gastro protection induced by cholecystokinin or by a meal. Role of vagal and sensory nerves and nitric oxide. *Eur J Pharmacol* 1999; **374**: 263-266
- 13 Erkasap N, Uzuner K, Serteser M. Gastroprotective effect of

- leptin on gastric mucosal injury induced by ischaemia-reperfusion is related to gastric histamine content in rats. *Peptides* 2003; **24**: 1181-1187
- 14 **Lazzaroni M**, Bianchi Porro G. Prophylaxis and treatment of non-steroidal anti-inflammatory drug-induced upper gastrointestinal side effects. *Dig Liver Dis* 2001; **33**(Suppl 2): S44-48
- 15 **Warzecha Z**, Dembinski A, Brzozowski T. Histamine in stress ulcer prophylaxis in rats. *J Physiol Pharmacol* 2001; **52**: 407-421
- 16 **Nishida A**, Takinami Y, Yuki H. YM022{®}-1-[2,3-dihydro-1-(2'-methylphenacyl)-2-oxo-5-phenyl-1H-1,4benzodiazepin-3-yl]-3 (methylphenyl)urea, a potent and selective gastrin/cholecystokinin-B receptor antagonist, prevents gastric and duodenal lesions in rats. *J Pharmacol Exp Ther* 1994; **270**: 1256-1261
- 17 **Mercer DW**, Cross JM, Barreto JC. Cholecystokinin is a potent protective agent against alcohol-induced gastric injury in the rat. *Dig Dis Sci* 1995; **40**: 651-660
- 18 **Sobhani I**, Bado A, Vissuzaine C, Buyse M, Kermogrant S, Laigneau JP, Attoub S, Lehy T, Henin D, Mignon M, Lewin MJ. Leptin secretion and leptin receptor in the human stomach. *Gut* 2000; **47**: 178-183
- 19 **Konturek PC**, Brzozowski T, Sulekova Z, Meixner H, Hahn EG, Konturek SJ. Enhanced expression of leptin following acute gastric injury in rat. *J Physiol Pharmacol* 1999; **50**: 587-595
- 20 **Kasuya Y**, Urushidani T, Okabe S. Effects of various drugs and vagotomy on indomethacin-induced gastric ulcers in the rat. *Jap J Pharmacol* 1979; **29**: 670-673
- 21 **Ueki S**, Takeuchi K, Okabe S. Gastric motility is an important factor in the pathogenesis of indomethacin-induced gastric mucosal lesions in rats. *Dig Dis Sci* 1988; **33**: 209-216
- 22 **Bastaki SMA**, Chandranath SI, Singh J. Comparison of the antisecretory and antiulcer activity of epidermal growth factor, urogastrone and transforming growth factor alpha and its derivative in rodents *in vivo*. *Mol Cell Biochem* 2002; **236**: 83-94
- 23 **Chandranath SI**, Bastaki SMA, Singh J. Comparative study on the activity of lansoprazole, omeprazole and PD-136450 on acidified ethanol- and indomethacin-induced gastric lesions in the rat. *Clin Exp Pharmacol Physiol* 2002; **29**: 173-180
- 24 **Lacy ER**, Ito S. Microscopic analysis of ethanol damage to rat gastric mucosa after treatment with a prostaglandin. *Gastroenterology* 1982; **83**: 619-625
- 25 **Szabo S**, Trier J, Brown A. Early vascular injury and increased vascular permeability in gastric mucosal injury caused by ethanol in the rat. *Gastroenterology* 1985; **88**: 228-236
- 26 **Bastaki SMA**, Chandranath SI, Adem A. The role of prostaglandin E₂ in the prevention of ability of leptin. *Gut* 2004; **53** (Suppl 3): A77
- 27 **Wallace JL**, Tigley AW. New insights into prostaglandins and mucosal defense. *Aliment Pharmacol Ther* 1995; **9**: 227-235
- 28 **Bastaki SMA**, Wallace JL. Pathogenesis of nonsteroidal anti-inflammatory drug gastropathy: clues to preventive therapy. *Can J Gastroenterol* 1999; **13**: 123-127
- 29 **Morimoto T**, Yamamoto Y, Yamatodani A. Leptin facilitates histamine release from the hypothalamus in rats. *Brain Res* 2000; **868**: 367-369
- 30 **Goiot H**, Attoub S, Kermogrant S, Laigneau JP, Lardeux B, Lehy T, Lewin MJ, Bado A. Antral mucosa expresses functional leptin receptors coupled to STAT-3 signaling, which is involved in the control of gastric secretions in the rat. *Gastroenterology* 2001; **121**: 1417-1427
- 31 **Konturek JW**, Konturek SJ, Kwiecien N, Bielanski W, Pawlik T, Rembiasz K, Domschke W. Leptin in the control of gastric secretion and gut hormones in humans infected with *Helicobacter pylori*. *Scand J Gastroenterol* 2001; **36**: 1148-1154
- 32 **Azuma T**, Suto H, Ito Y, Ohtani M, Dojo M, Kuriyama M, Kato T. Gastric leptin and *Helicobacter pylori* infection. *Gut* 2001; **49**: 324-329
- 33 **Brzozowski T**, Konturek PC, Pajdo R, Kwiecien S, Ptak A, Sliwowski Z, Drozdowicz D, Pawlik M, Konturek SJ, Hahn EG. Brain-gut axis in gastroprotection by leptin and cholecystokinin against ischemia-reperfusion induced gastric lesions. *J Physiol Pharmacol* 2001; **52**: 583-602
- 34 **Overmier JB**, Murison R. Anxiety and helplessness in the face of stress predisposes, precipitates and sustains gastric ulceration. *Behav Brain Res* 2000; **110**: 161-164
- 35 **Hochberg MC**. Association of nonsteroidal anti-inflammatory drugs with upper gastrointestinal disease: epidemiological and economic considerations. *J Rheumatol* 1992; **19** (Suppl 36): 63-67

• BASIC RESEARCH •

Differentiation of embryonic stem cells into insulin-producing cells promoted by Nkx2.2 gene transfer

Akira Shiroy, Shigehiko Ueda, Yukiteru Oujy, Ko Saito, Kei Moriya, Yuko Sugie, Hiroshi Fukui, Shigeaki Ishizaka, Masahide Yoshikawa

Akira Shiroy, Yukiteru Oujy, Kei Moriya, Yuko Sugie, Shigeaki Ishizaka, Masahide Yoshikawa, Division of Developmental Biology, Department of Parasitology, Nara Medical University, Kashihara, Nara 634-8521, Japan

Shigehiko Ueda, Ko Saito, Hiroshi Fukui, Department of Gastroenterology and Hepatology, Nara Medical University, Kashihara, Nara 634-8521, Japan

Correspondence to: Masahide Yoshikawa, Division of Developmental Biology, Department of Parasitology, Nara Medical University, 840 Shijo-cho, Kashihara, Nara 634-8521,

Japan. myoshika@naramed-u.ac.jp

Telephone: +81-744-29-8857 Fax: +81-744-24-7122

Received: 2004-11-29 Accepted: 2005-01-05

ability to differentiate into insulin-producing cells.

© 2005 The WJG Press and Elsevier Inc. All rights reserved.

Key words: Embryonic stem cells; Insulin; Nkx2.2; Dithizone

Shiroy A, Ueda S, Oujy Y, Saito K, Moriya K, Sugie Y, Fukui H, Ishizaka S, Yoshikawa M. Differentiation of embryonic stem cells into insulin-producing cells promoted by Nkx2.2 gene transfer. *World J Gastroenterol* 2005; 11(27): 4161-4166
<http://www.wjgnet.com/1007-9327/11/4161.asp>

Abstract

AIM: To investigate the ability of a genetically altered embryonic stem (ES) cell line to generate insulin-producing cells *in vitro* following transfer of the Nkx2.2 gene.

METHODS: Hamster Nkx2.2 genes were transferred into mouse ES cells. Parental and Nkx2.2-transfected ES cells were initiated toward differentiation in embryoid body (EB) culture for 5 d and the resulting EBs were transferred to an attached culture system. Dithizone (DTZ), a zinc-chelating agent known to selectively stain pancreatic beta cells, was used to detect insulin-producing cells. The outgrowths were incubated in DTZ solution (final concentration, 100 µg/mL) for 15 min before being examined microscopically. Gene expression of the endocrine pancreatic markers was also analyzed by RT-PCR. In addition, insulin production was determined immunohistochemically and its secretion was examined using an ELISA.

RESULTS: DTZ-stained cellular clusters appeared after approximately 14 d in the culture of Nkx2.2-transfected ES cells (Nkx-ES cells), which was as much as 2 wk earlier, than those in the culture of parental ES cells (wt-ES). The frequency of DTZ-positive cells among total cultured cells on day 28 accounted for approximately 1.0% and 0.1% of the Nkx-ES- and wt-ES-derived EB outgrowths, respectively. The DTZ-positive cellular clusters were found to be immunoreactive to insulin, while the gene expressions of pancreatic-duodenal homeobox 1 (PDX1), proinsulin 1 and proinsulin 2 were observed in the cultures that contained DTZ-positive cellular clusters. Insulin secretion was also confirmed by ELISA, whereas glucose-dependent secretion was not demonstrated.

CONCLUSION: Nkx2.2-transfected ES cells showed an

INTRODUCTION

It has been proposed that approximately 150 million people worldwide have diabetes mellitus, which may double by 2025, and 5-10% of those suffer from type 1 diabetes, for which injections of insulin are unavoidable. Transplantation of pancreatic islets for type 1 diabetes is a promising therapeutic strategy^[1], however, an inadequate supply of donor islets is a major obstacle. Thus, embryonic stem (ES) cells are being considered as a potential source for generating insulin-producing cells. ES cells come from clonal cell lines derived from the inner cell mass of developing blastocysts^[2,3], and are able to proliferate *in vitro* and have shown a capacity to differentiate into a broad spectrum of derivatives of all three embryonic germ layers including hematopoietic cells, cardiomyocytes, smooth muscle cells, neurons, hepatocytes, and insulin-producing cells^[4-10]. We recently reported the appearance of the islet-like cellular clusters containing insulin-producing cells in embryoid body (EB) outgrowth cultures with the use of a zinc-chelating substance, dithizone (DTZ)^[11]. However, the development of islet-like cellular clusters was found in only a small portion of the EB outgrowths and required long-term cultures of more than 3 wk.

Nkx2.2 and Nkx6.1 are NK-homeodomain genes expressed in early pancreatic progenitor cells as well as neurogenin-3 (Ngn3)-expressing islet precursor cells, and are considered to be β -cell competence factors^[12-14]. Nkx2.2 mutants completely lack insulin expression^[14], while Nkx6.1 mutants show a less dramatic impaired differentiation of β -cells^[15]. Further, Nkx2.2 expression lasts for a longer period of time in differentiated islet cells. These findings suggest that Nkx2.2 is a critical transcription factor in early pancreatic endocrine development and the following differentiation into pancreatic β -cells.

In the present study, we generated Nkx2.2-expressing

cell lines by transfection of the Nkx2.2 gene into undifferentiated ES cells, and investigated their ability to differentiate into insulin-producing cells in EB outgrowth cultures. We found that insulin-producing cells appeared as much as 2 wk earlier in the EB outgrowths derived from Nkx2.2-transfected ES (Nkx-ES) cells than in those from parental ES (wt-ES) cells. Further, the frequency of insulin-producing cells on culture d 28 was approximately 1% in the Nkx-ES-derived EB outgrowths, a 10-fold greater efficiency as compared to that on the wt-ES-derived EB outgrowths. These results suggest that Nkx2.2 acts to promote the differentiation of ES cells into insulin-producing cells.

MATERIALS AND METHODS

Murine ES cell lines

We utilized a mouse ES cell line, EB3 (129/SvJ mouse ES cells, a kind gift from Dr. Hitoshi Niwa, RIKEN Center for Developmental Biology, Kobe, Japan)^[15], which was a subline derived from E14tg2a ES cells^[16] and carried the blasticidin S-resistant selection marker gene driven by the Oct-3/4 promoter (active under undifferentiated status)^[17]. Undifferentiated EB3 cells were maintained on gelatin-coated dishes without feeder cells in the maintenance medium, which was knockout-DMEM medium (Gibco-BRL) supplemented with 10% fetal bovine serum (FBS; GIBCO/BRL), 0.1 mmol/L of 2-mercaptoethanol (Sigma), 10 mmol/L of non-essential amino acids (GIBCO/BRL), L-glutamine, and 1 000 U/mL of leukemia inhibitory factor (LIF; GIBCO/BRL).

Generation of Nkx2.2-expressing ES (Nkx-ES) cells

The hamster Nkx2.2 gene was obtained from the plasmid pBAT12.shNkx2.2 (kindly provided by Dr. M. German, University of California, San Francisco). The cDNA was inserted into the BstXI-stuffer site of the expression vector pPyCAGIRESzeocinpA^[18]. The constructed plasmid pPyCAGIRESzeocinpA-Nkx2.2 contained the zeocin resistance gene driven by the chicken β -actin promoter. The Nkx2.2 vector (20 μ g) was transfected using a lipofection method with lipofectAmine (GIBCO/BRL). Transfected ES cells were selected by growth in the presence of 20 μ g/mL of zeocin, and three clones expressing Nkx2.2 (Nkx-ES) were established. Undifferentiated Nkx-ES cells were maintained in the same manner as undifferentiated wt-ES cells.

EB outgrowths with non-selective differentiation

The method used for the EB outgrowths has been previously described^[11]. Briefly, undifferentiated ES cells were dissociated into single-cell suspensions and then cultured in hanging drops to induce embryoid body (EB) formation at an initial cell density of 500 cells per drop (20 μ L) of ES cell-medium in the absence of LIF. After 5 d in a hanging drop culture, the resulting EBs were plated in plastic 30-mm gelatin-coated dishes (five EBs per dish), and then allowed to attach and form outgrowth cultures. A half amount of culture medium was replenished with new medium every 2 d. The culture medium used was the maintenance medium lacking LIF and known differentiation-inducing factors.

Throughout the whole culture, no growth factors or cytokines including insulin were added to the culture medium.

Dithizone (DTZ)-staining

A DTZ (Merck, Whitehouse Station, NJ, USA) stock solution was prepared with 50 mg of DTZ in 5 mL of dimethylsulfoxide (DMSO) and stored briefly at -15 °C. The staining solution was filtered through a 0.2 μ m nylon filter and then used as a DTZ working solution. *In vitro* DTZ staining was performed by adding 10 μ L of the stock solution to 1 mL of culture medium, then the culture dishes were incubated at 37 °C for 15 min in the DTZ solution. After the dishes were rinsed thrice with HBSS, clusters stained crimson red were examined using a stereomicroscope. After examination, the dishes were refilled with DMEM containing 10% FBS. Although the stain completely disappeared from the cells after 5 h, the cultures that had not been treated with DTZ were used for RT-PCR and insulin secretion studies to avoid the influence of the treatment. In some experiments, the number of DTZ-stained cells in the cultures was determined by counting crimson red cells after trypsinization following DTZ stain.

RT-PCR

Total RNA was extracted from the cells using TRIzol (GIBCO/BRL). DNase-treated total RNA was used for the first-strand cDNA. This reaction was performed using M-MLV Reverse Transcriptase (Promega) and Random Primer (Takara Bio Inc.), following the protocols of the manufacturers. cDNA samples were subjected to PCR amplification with specific primers under linear conditions in order to reflect the original amount of the specific transcript. The cycling parameters were as follows: denaturation at 94 °C for 1 min, annealing at 52-60 °C for 1 min (depending on the primer), elongation at 72 °C for 1 min (35 cycles), and a final extension for 20 min at 72 °C. The PCR primers and the lengths of the amplified products were as follows: β -actin (TGAAGTGGCTGACTGCTGTG and CATCCTTGGCCTCAGCATAG, 174 bp); pro-insulin 1 (GTTGGTGCACCTTCCTACCCCTG and GTAGAGGGAGCAGATGCTGGTG, 300 bp); pro-insulin 2 (GTGGATGCGCTTCCTGCCCCTG and GTAGAGGGAGCAGATGCTGGTG, 300 bp); PDX1 (GGCCACACAGCTCTACAAGG and TTCCACTTCATGCGACGGTT, 582 bp); and mouse-nkx2.2 (TGACCAACACAAAGACGGGGT and GCACGTTTCATCTTGTCGTA, 650 bp). A set of mouse-nkx2.2 primers was used for the detection of hamster Nkx2.2.

Immunocytochemistry

Cells in culture dishes were fixed with 4% paraformaldehyde in phosphate-buffered solution and immunocytochemistry was carried out using a standard protocol. As the primary antibody for Nkx2.2, mouse anti-chick Nkx2.2 mAb (Hybridoma Bank, University of Iowa) was used at a dilution of 1:40. For detection of the primary antibody, a biotinylated anti-mouse antibody, ABC kit (VECTASTAIN Elite ABC KIT), and DAB (Dojindo; Kumamoto, Japan) were utilized according to the manufacturers' instructions.

For detection of the primary antibody, a fluorescent labeled secondary antibody, goat anti-guinea pig IgG conjugated with fluorescein-5-isothiocyanate (Cappel 57000, ICN Pharmaceuticals, Inc., OH, USA), was utilized according to the manufacturer's instructions. All nuclei were stained with DAPI (Dojindo; Kumamoto, Japan).

Insulin detection assay

Cells in the culture dishes were washed thrice with PBS and pre-incubated in Krebs Ringer bicarbonate buffer (KRBB) containing 2.8 mmol/L of glucose for 1 h, then placed in 1 000 μ L of KRBB with 2.8 mmol/L of glucose for 2 h. Next, the supernatant was collected and the dishes were rinsed thrice with PBS, after which the cells were re-incubated with KRBB containing 25.5 mmol/L of glucose for 2 h. Subsequently, conditioned medium samples were collected, and insulin levels were measured using an enzyme immunoassay (Mouse Insulin ELISA TMB Kit AKRIN-011T, Shibayagi Co., Ltd. Gunma, Japan) that detects mouse insulin in a range between 156 and 10 000 pg/mL with no cross-reactivity to C-peptide.

RESULTS

Establishment of Nkx2.2-expressing ES cell lines

ES cells were transfected with the Nkx2.2 expression vector and selected with zeocin. Three stable clones at a time were obtained and screened for Nkx2.2 expression by RT-PCR and three clones with a high expression of Nkx2.2 were finally selected (Figure 1A). Subsequently, immunocytochemistry showed that all three clones expressed Nkx2.2 protein (Figure 1B). Each Nkx-ES clone demonstrated similar results in the following experiments, thus representative results from only clone 3 are shown.

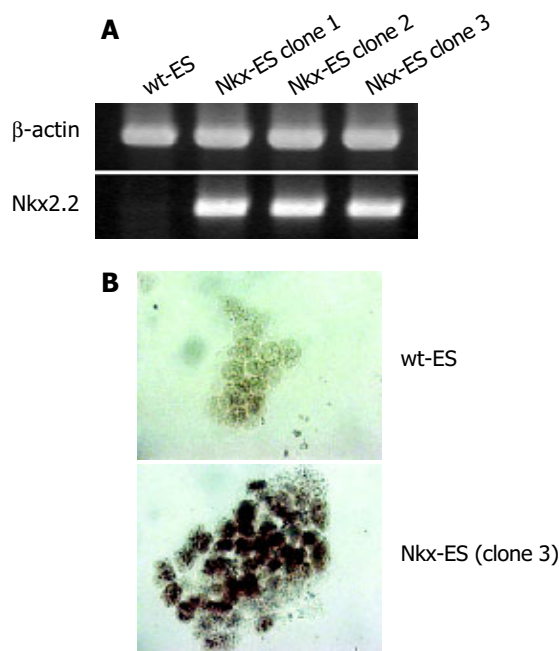


Figure 1 Expression of Nkx2.2 in parental (wt-ES cells) and Nkx2.2-transfected ES cells (Nkx-ES cells). **A:** Nkx-ES cells, but not wt-ES cells, expressed Nkx2.2 mRNA; **B:** Nkx2.2 protein was mainly observed in the nuclei of Nkx-ES cells. Original magnification, $\times 200$.

Early appearance of DTZ-stained cells in EB outgrowths

DTZ, a zinc-chelating agent, is known to selectively stain pancreatic β -cells crimson red^[19-21] and we previously demonstrated that DTZ stain could also be applied for the detection of ES-derived insulin-producing cells. Figure 2 shows the outline of the EB outgrowth culture and results of DTZ-staining. DTZ-positive cellular clusters appeared as much as 2 wk earlier in the EB outgrowths derived from Nkx-ES cells. On d 14, DTZ-positive cells were already present in the EB outgrowths derived from Nkx-ES cells (Figure 2D), whereas they were absent in those from wt-ES cells (Figure 2A). On d 21, distinct DTZ-positive cellular clusters were observed in the Nkx-ES-derived EB outgrowths (Figure 2E), while they were obscure in the differentiating wt-ES cultures (Figure 2B). In the wt-ES-derived EB outgrowths, DTZ-positive cellular clusters became distinct on d 28 (Figure 2C). The appearance of DTZ-positive clusters on d 28 in Nkx-ES-derived EB outgrowths was quite similar to that seen on d 21 (Figures 2E and F).

DTZ-stained clusters that appeared in Nkx-ES-derived EB outgrowths were frequently larger than those in wt-ES-derived EB outgrowths. To estimate the frequency of the emerged DTZ-stained cells in the cultures, the number of DTZ-stained red cells was directly counted under a microscope after trypsinization following the treatment with DTZ. The percentages of DTZ-stained cells among total cells on day 28 were $1.0 \pm 0.2\%$ of the Nkx-ES-derivatives and less than 0.1% of the wt-ES-derivatives.

Gene expression and immunohistochemistry of differentiating EB outgrowths

Pdx 1, a key transcriptional factor of pancreatic differentiation, was faintly detected in Nkx-ES cells and completely absent in wt-ES cells on d 0. Thereafter, Pdx 1 was expressed in all EB outgrowths on d 14, 21, and 28 as well as in isolated mouse islets. In contrast, Nkx2.2 was not detected on d 14, faintly detected on d 21, and clearly detected on d 28 in the differentiating wt-ES cells. In addition, pro-insulin 1 and 2 were detected on d 14 in the Nkx-ES-derived EB outgrowths, though not until d 28 in the wt-ES-derived EB outgrowths. To confirm the expression of insulin protein, we performed an immunohistochemistry examination in parallel with the DTZ-stain examination (Figure 3B). Immunoreactivity against insulin was found to coincide with the DTZ-stained culture areas within the EB outgrowths. In Nkx-ES-derived EB outgrowths, insulin-immunoreactivity was detected as early as on d 14, whereas it did not become positive until d 28 in the wt-ES-derived EB outgrowths. No immunoreactivity was found on d 14 or 21 in the wt-ES-derived EB outgrowths.

Insulin secretion

EB outgrowths on d 28 were used for the detection of released insulin. Insulin concentrations in culture media of wt-ES-derived EB outgrowths incubated with 2.8 and 25 mmol/L of glucose were 163 ± 38 and 191 ± 31 pg/mL, respectively, while those in media of Nkx-ES-derived EB outgrowths were 525 ± 132 and 660 ± 171 pg/mL with 25.5 mmol/L of glucose, respectively. Glucose-dependent insulin secretion was not observed in wt-ES- or Nkx-ES-

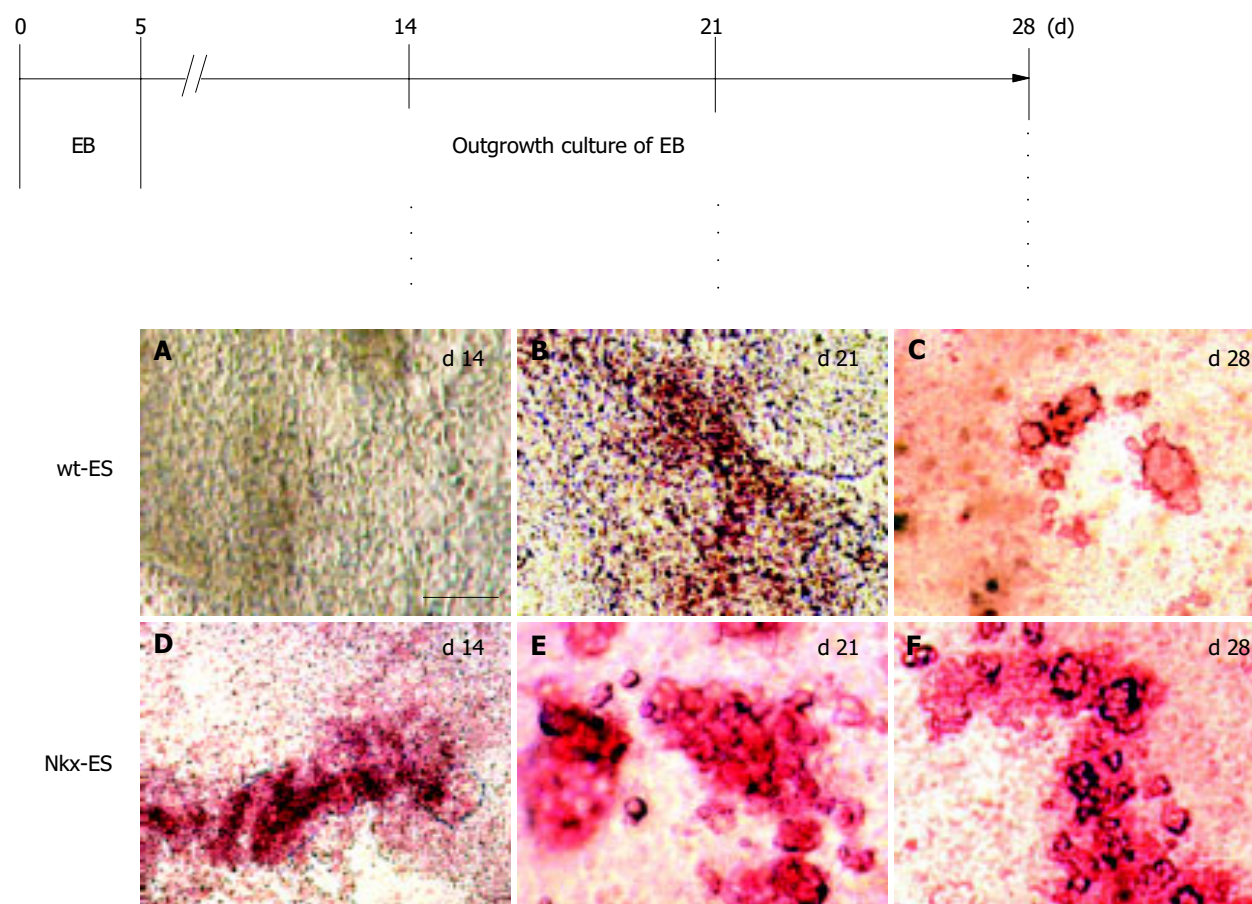


Figure 2 A-F: Early appearance of insulin-producing cells in EB outgrowths. An outline of the culture processes and results of DTZ-staining are shown. Scale

bar represents 100 μm in length.

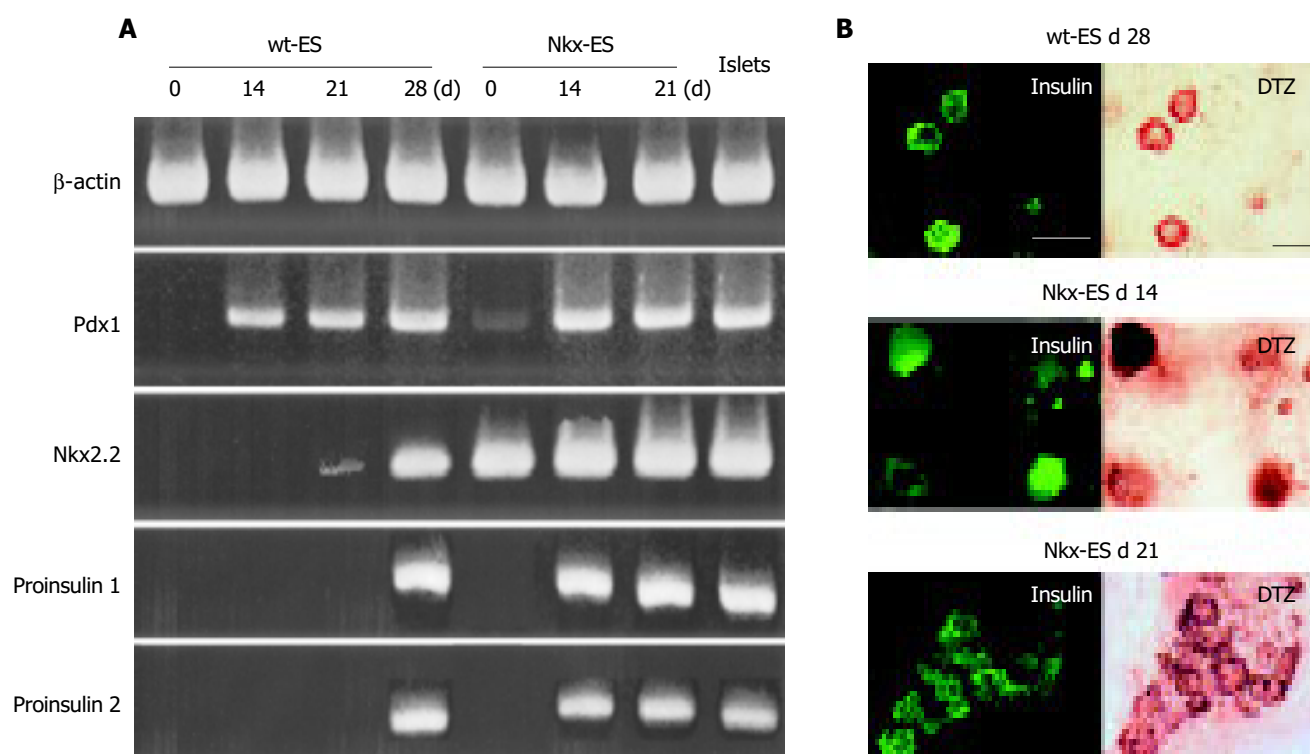


Figure 3 Gene expression and immunohistochemistry findings for differentiating EB outgrowths. **A:** The expression of Pdx 1, Nkx2.2, pro-insulin 1 and pro-insulin 2 was examined in differentiating wt-ES cells and Nkx-ES cells; **B:**

Insulin-immunoreactivity was examined in the EB outgrowths with DTZ-staining. Scale bars represent 100 μm in length.

derived EB outgrowth cultures, whereas secreted insulin was detected in the Nkx-ES-derived EB outgrowth cultures, in amounts several times greater than in the wt-ES-derived EB outgrowth cultures.

DISCUSSION

The homeodomain transcription factor Nkx2.2 is one of the key transcription factors in pancreatic β -cell differentiation and expressed throughout all development periods, as well as broadly in the initial pancreatic precursor population, and in Ngn3-expressing islet progenitor cells and differentiated islet cells^[12,13,22]. Mice homozygous for a null mutation of Nkx2.2 develop severe hyperglycemia leading to death shortly after birth, because of the lack of insulin-producing β -cells^[14], and show a variety of functional defects in the islet cells that produce endocrine hormones other than insulin. In the present study, we examined genetically altered ES cells after transfection of the Nkx2.2 gene to determine their ability to differentiate into insulin-producing cells *in vitro*.

To assess the effect of the exogenous Nkx2.2 transgene on generation of insulin-producing ES-derived cells, we considered that an EB-based 1-step culture protocol^[11,15,23] that supported natural differentiation of ES cells would be better than an EB-based multi-step protocol^[24] that directed an oriented differentiation of ES cells toward pancreatic cell lineages using serum-free culture followed by a combination of growth factors. Since a promoted induction of insulin-producing cells was expected, a less efficient differentiation protocol was better suited to demonstrate the promoted action than a more sophisticated and efficient protocol. In addition, some investigators have speculated that the insulin-immuno-positive nature of cultured cells derived in an EB-based multi-step method is due to the incorporation of insulin from the culture medium^[25,26], while it is also suspected that such insulin-incorporated cells are apoptotic. Therefore, in the present study, EBs are simply allowed to attach and grow in gelatin-coated dishes in media containing FCS without growth factors, including insulin.

Since the emergence of insulin-producing cells among the simple EB outgrowths was expected to be rare, we used DTZ to locate those that produced insulin. DTZ is a zinc-binding substance, and known to stain crimson red the pancreatic islets from such animals, as mice, dogs and pigs, as well as those from human beings^[19-21]. We previously reported that DTZ-stained cellular clusters appeared in EB outgrowths and that the clusters demonstrated characteristics similar to pancreatic islets^[11]. In the present study, DTZ-stained cellular clusters appeared 2 wk earlier in the Nkx-ES-derived EB outgrowths, as compared to the wt-ES-derived EB outgrowths. Those cellular clusters were immunopositive for insulin and the presence of secreted insulin was confirmed by ELISA. Further, in addition to an early emergence, an increased frequency of DTZ-stained cells was also observed in the Nkx-ES-derived EB outgrowths. These results suggest that the fate of differentiating cells was favorably affected toward the generation of insulin-producing cells.

In spite of our success, the DTZ-positive cellular fraction still accounted for only 1% of the differentiated Nkx-ES cells. To achieve a more efficient generation of insulin-

producing cells from ES cells *in vitro*, controlled regulation of other transcriptional factors that are involved in pancreatic β -cell differentiation might be necessary. Indeed, a highly efficient production of insulin-producing cells from ES cells has been reported by the expression of exogenously transfected pdx-1, pax 4, or Nkx6.1^[27-29].

The precise mechanisms by which Nkx-ES cells promote the induction of insulin-producing cells is unknown, thus sequential analyses of a number of transcription factors that are involved in pancreatic β -cell differentiation must be examined in differentiating Nkx-ES cells. Although we have not performed such an analysis, an important finding to investigate is the early expression of insulin seen in the present differentiating Nkx-ES cells. Nkx2.2 expression preceded insulin expression in differentiating wt-ES cells (Figure 3A), which has also been seen in the pancreatic β -cell development^[30]. Therefore, Nkx-ES cells may directly skip to that process following Nkx2.2 expression. Glucose-dependent insulin secretion was not observed in the cultures of ES-derived insulin-secreting cells, which we considered may have been due to the high concentration of glucose present in the culture media, in which the ES cells were allowed to differentiate until the insulin detection assay.

In summary, we generated gene-engineered Nkx2.2-expressing ES cells and demonstrated their ability to induce insulin-producing cells *in vitro*. Our results show that gene-engineered ES may be a useful source of insulin-producing cells.

REFERENCES

- 1 **Shapiro AM**, Lakey JR, Ryan EA, Korbitt GS, Toth E, Warnock GL, Kneteman NM, Rajotte RV. Islet transplantation in seven patients with type 1 diabetes mellitus using a glucocorticoid-free immunosuppressive regimen. *N Engl J Med* 2000; **343**: 230-238
- 2 **Evans MJ**, Kaufman MH. Establishment in culture of pluripotent cells from mouse embryos. *Nature* 1981; **292**: 154-156
- 3 **Martin GR**. Isolation of a pluripotent cell line from early mouse embryos cultured in medium conditioned by teratocarcinoma stem cells. *Proc Natl Acad Sci USA* 1981; **78**: 7634-7638
- 4 **Assady S**, Maor G, Amit M, Itskovitz-Eldor J, Skorecki KL, Tzukerman M. Insulin production by human embryonic stem cells. *Diabetes* 2001; **50**: 1691-1697
- 5 **Hori Y**, Rulifson IC, Tsai BC, Heit JJ, Cahoy JD, Kim SK. Growth inhibitors promote differentiation of insulin-producing tissue from embryonic stem cells. *Proc Natl Acad Sci USA* 2002; **99**: 16105-16110
- 6 **Kahan BW**, Jacobson LM, Hullett DA, Ochoada JM, Oberley TD, Lang KM, Odorico JS. Pancreatic precursors and differentiated islet cell types from murine embryonic stem cells: an *in vitro* model to study islet differentiation. *Diabetes* 2003; **52**: 2016-2024
- 7 **Moritoh Y**, Yamato E, Yasui Y, Miyazaki S, Miyazaki J. Analysis of insulin-producing cells during *in vitro* differentiation from feeder-free embryonic stem cells. *Diabetes* 2003; **52**: 1163-1168
- 8 **Segev H**, Fishman B, Ziskind A, Shulman M, Itskovitz-Eldor J. Differentiation of human embryonic stem cells into insulin-producing clusters. *Stem Cells* 2004; **22**: 265-274
- 9 **Blyszczuk P**, Wobus AM. Stem cells and pancreatic differentiation *in vitro*. *J Biotechnol* 2004; **113**: 3-13
- 10 **Lester LB**, Kuo HC, Andrews L, Nauert B, Wolf DP. Directed differentiation of rhesus monkey ES cells into pancreatic cell phenotypes. *Reprod Biol Endocrinol* 2004; **2**: 42
- 11 **Shiroy A**, Yoshikawa M, Yokota H, Fukui H, Ishizaka S,

- Tatsumi K, Takahashi Y. Identification of insulin-producing cells derived from embryonic stem cells by zinc-chelating dithizone. *Stem Cells* 2002; **20**: 284-292
- 12 **Schwitzgebel VM**, Scheel DW, Conners JR, Kalamaras J, Lee JE, Anderson DJ, Sussel L, Johnson JD, German MS. Expression of neurogenin 3 reveals an islet cell precursor population in the pancreas. *Development* 2000; **127**: 3533-3542
- 13 **Sander M**, Sussel L, Conners J, Scheel D, Kalamaras J, Dela Cruz F, Schwitzgebel V, Hayes-Jordan A, German M. Homeobox gene Nkx6.1 lies downstream of Nkx2.2 in the major pathway of beta-cell formation in the pancreas. *Development* 2000; **127**: 5533-5540
- 14 **Sussel L**, Kalamaras J, Hartigan-O'Connor DJ, Meneses JJ, Pedersen RA, Rubenstein JL, German MS. Mice lacking the homeodomain transcription factor Nkx2.2 have diabetes due to arrested differentiation of pancreatic beta cells. *Development* 1998; **125**: 2213-2221
- 15 **Yamada T**, Yoshikawa M, Takaki M, Torihashi S, Kato Y, Nakajima Y, Ishizaka S, Tsunoda Y. *In vitro* functional gut-like organ formation from mouse embryonic stem cells. *Stem Cells* 2002; **20**: 41-49
- 16 **Hooper M**, Hardy K, Handyside A, Hunter S, Monk M. HPRT-deficient (Lesch-Nyhan) mouse embryos derived from germline colonization by cultured cells. *Nature* 1987; **326**: 292-295
- 17 **Niwa H**, Miyazaki J, Smith AG. Quantitative expression of Oct-3/4 defines differentiation, dedifferentiation or self-renewal of ES cells. *Nat Genet* 2000; **24**: 372-376
- 18 **Niwa H**, Burdon T, Chambers I, Smith A. Self-renewal of pluripotent embryonic stem cells is mediated via activation of STAT3. *Genes Dev* 1998; **12**: 2048-2060
- 19 **Latif ZA**, Noel J, Alejandro R. A simple method of staining fresh and cultured islets. *Transplantation* 1988; **45**: 827-830
- 20 **Clark SA**, Borland KM, Sherman SD, Rusack TC, Chick WL. Staining and *in vitro* toxicity of dithizone with canine, porcine, and bovine islets. *Cell Transplant* 1994; **3**: 299-306
- 21 **Shewade YM**, Umrani M, Bhonde RR. Large-scale isolation of islets by tissue culture of adult mouse pancreas. *Transplant Proc* 1999; **31**: 1721-1723
- 22 **Watada H**, Scheel DW, Leung J, German MS. Distinct gene expression programs function in progenitor and mature islet cells. *J Biol Chem* 2003; **278**: 17130-17140
- 23 **Yamada T**, Yoshikawa M, Kanda S, Kato Y, Nakajima Y, Ishizaka S, Tsunoda Y. *In vitro* differentiation of embryonic stem cells into hepatocyte-like cells identified by cellular uptake of indocyanine green. *Stem Cells* 2002; **20**: 146-154
- 24 **Lumelsky N**, Blondel O, Laeng P, Velasco I, Ravin R, McKay R. Differentiation of embryonic stem cells to insulin-secreting structures similar to pancreatic islets. *Science* 2001; **292**: 1389-1394
- 25 **Rajagopal J**, Anderson WJ, Kume S, Martinez OI, Melton DA. Insulin staining of ES cell progeny from insulin uptake. *Science* 2003; **299**: 363
- 26 **Sipione S**, Eshpeter A, Lyon JG, Korbitt GS, Bleackley RC. Insulin expressing cells from differentiated embryonic stem cells are not beta cells. *Diabetologia* 2004; **47**: 499-508
- 27 **Miyazaki S**, Yamato E, Miyazaki J. Regulated expression of pdx-1 promotes *in vitro* differentiation of insulin-producing cells from embryonic stem cells. *Diabetes* 2004; **53**: 1030-1037
- 28 **Blyszczuk P**, Czyz J, Kania G, Wagner M, Roll U, St-Onge L, Wobus AM. Expression of Pax4 in embryonic stem cells promotes differentiation of nestin-positive progenitor and insulin-producing cells. *Proc Natl Acad Sci USA* 2003; **100**: 998-1003
- 29 **Leon-Quinto T**, Jones J, Skoudy A, Burcin M, Soria B. *In vitro* directed differentiation of mouse embryonic stem cells into insulin-producing cells. *Diabetologia* 2004; **47**: 1442-1451
- 30 **Soria B**. *In-vitro* differentiation of pancreatic beta-cells. *Differentiation* 2001; **68**: 205-219

Science Editor Guo SY Language Editor Elsevier HK

• BASIC RESEARCH •

Comparison of murine cirrhosis models induced by hepatotoxin administration and common bile duct ligation

Ming-Ling Chang, Chau-Ting Yeh, Pei-Yeh Chang, Jeng-Chang Chen

Ming-Ling Chang, Chau-Ting Yeh, Liver Research Unit, Department of Hepatogastroenterology, Chang Gung Memorial Hospital, Taoyuan, Taiwan, China

Pei-Yeh Chang, Jeng-Chang Chen, Department of Surgery, Chang Gung Children's Hospital, Taoyuan, Taiwan, China

Supported by the Chang Gung Memorial Hospital, Taoyuan, Taiwan, China, CMRPG 33014, CMRPG 33063 and CMRP 800

Correspondence to: Jeng-Chang Chen, Department of Surgery, Chang Gung Children's Hospital, 5 Fu-Shin Street, Kweishan, 333, Taoyuan, Taiwan, China. jengchang@so-net.net.tw

Telephone: +886-3-3281200-8227 Fax: +886-3-3287261

Received: 2004-10-20 Accepted: 2004-12-23

Key words: Common bile duct ligation; Fibrosis; Hepatotoxin; Liver; Mice

Chang ML, Yeh CT, Chang PY, Chen JC. Comparison of murine cirrhosis models induced by hepatotoxin administration and common bile duct ligation. *World J Gastroenterol* 2005; 11(27): 4167-4172

<http://www.wjgnet.com/1007-9327/11/4167.asp>

Abstract

AIM: To build up the research models of hepatic fibrosis in mice.

METHODS: Inbred wild-type FVB/N mice were either treated with alpha-naphthyl-isothiocyanate (ANIT), allyl alcohol (AA), carbon tetrachloride (CCl₄), 3,5-diethoxycarbonyl-1,4-dihydrocollidine (DDC), and silica, or subjected to common bile duct ligation (CBDL) to induce hepatic injury. Liver biopsies were performed every 4 wk to evaluate hepatic fibrosis over a period of 6 mo. Cumulative cirrhosis and survival curves were constructed by life table method and compared with Wilcoxon test.

RESULTS: Under the dosages used, there was neither mortality nor cirrhosis in AA and silica-treated groups. DDC and ANIT caused cirrhosis within 4-12 and 12-24 wk, respectively. Both showed significantly faster cirrhosis induction at high dosages without significant alteration of survival. The duration for cirrhosis induction by CCl₄ ranged from 4 to 20 wk, mainly dependent upon the dosage. However, the increase in CCl₄ dosage significantly worsened survival. Intraperitoneal CCl₄ administration resulted in better survival in comparison with gavage administration at high dosage, but not at medium and low dosages. After CBDL, all the mice developed liver cirrhosis within 4-8 wk and then died by the end of 16 wk.

CONCLUSION: CBDL and administrations of ANIT, CCl₄, and DDC ensured liver cirrhosis. CBDL required the least amount of time in cirrhosis induction, but caused shortened lives of mice. It was followed by DDC and ANIT administration with favorable survival. As for CCl₄, the speed of cirrhosis induction and the mouse survival depended upon the dosages and the administration route.

INTRODUCTION

Being the final outcome of chronic liver damage regardless of the underlying etiologies, hepatic fibrosis demands thorough study. The studies of hepatic fibrosis rely upon the availability of animal models. Although no experimental model exactly reproduces human liver fibrosis by etiologies, animal models serve to improve our understanding of pathogenetic mechanisms of liver fibrosis. In view of the cost-effectiveness in inducing hepatic injuries, hepatotoxin administration and common bile duct ligation (CBDL) were considered as useful methods^[1].

In recent years, advances in molecular biology have helped to generate a transgenic mouse model of liver fibrosis^[2]. This represents a new form of perturbation analysis whereby selective expression of novel or altered genes are used to perturb a complex system so that the information about the changes during development, functioning and malfunctioning can be deduced^[3]. This approach potentially allows development of animal models with liver fibrosis that are inducible and genetically similar to that of man. A reliable and reproducible model of hepatic fibrosis in wild-type control mice will aid to unveil the pathologic mechanisms deduced from genetic and molecular approaches. However, informative data of mouse hepatic fibrosis generated in the laboratory remained lacking in the literature because rats had long been the most common animal model for studying hepatic fibrosis induced by various chemical or surgical hepatic injuries^[1]. Since different animal models display distinct characteristics in the nature of pathogenesis of fibrosis or cirrhosis, the data acquired from rats could not apply to mice without bias^[4-8]. This urged us to set up a mouse model of hepatic fibrosis using CBDL or the administration of various hepatotoxins including alpha-naphthyl-isothiocyanate (ANIT)^[9,10], silica^[11], carbon tetrachloride (CCl₄)^[12-14], 3,5-diethoxycarbonyl-1,4-dihydrocollidine (DDC)^[15,16], and allyl alcohol (AA)^[17-19]. This study mainly focused on the strain of FVB/N inbred mice, which have been widely used to generate a variety of transgenic lines owing to their high reproduction rate and easy access in microinjection^[20,21].

MATERIALS AND METHODS

Mice

Inbred FVB/N mice (8-10 wk old) were obtained from the National Laboratory Animal Center (Taipei, Taiwan). All animals received care as outlined in the "Guides for the Care and Use of Laboratory Animals" prepared by the Committee of Animal Research, Chang Gung Memorial Hospital. Mice were supplied with food and water and exposed to a 12-h light-dark cycle. Ten mice (five males and five females) composed a group to which surgical CBDL or a hepatotoxin via intraperitoneal (IP) or oral gavage (OG) administration at the same dosage was given during a period of 6 mo.

Methods to induce hepatic injuries

ANIT (Sigma Chemical Co., St. Louis, MO, USA) ANIT was dissolved in corn oil and administered via IP or OG route, respectively. For each route of administration, there were three subgroups according to the maintenance dose as follows: 25 mg/kg (low dosage), 50 mg/kg (medium dosage) and 125 mg/kg (high dosage). After a single loading dose of 100 mg/kg, the maintenance doses were given twice a week. Additionally, there was a modified method of OG administration with a single loading dose of 100 mg/kg and subsequent maintenance doses of 50 mg/kg for the 1st and 2nd mo, 75 mg/kg for the 3rd and 4th mo, and 100 mg/kg for the 5th and 6th mo.

AA (Sigma Chemical Co.) AA was prepared in double distilled water and administered via OG route for five subgroups according to the dosages as follows: 0.2, 0.4, 0.6, 0.8, and 1.0 mmol/kg twice a week.

CCl₄ (Sigma Chemical Co.) The mice were fed via OG or IP route with CCl₄ (density = 1.594 kg/L) diluted in double distilled water. As for each route of administration, they were further subgrouped into three according to the maintenance doses as follows: 0.8 g/kg (low dosage), 1.6 g/kg (medium dosage) and 2.0 g/kg (high dosage). After a single loading dose of 2.4 g/kg, the maintenance doses were then administered twice a week.

DDC (Sigma Chemical Co.) The mice were fed via OG with DDC in corn oil twice a week. They were subgrouped by four different dosages as follows: 0.25, 0.5, 2.5, and 5 mg. In addition, 0.1% DDC contained diet (Purina Mills TestDiet, St. Louis, MO, USA) was used as the 5th subgroup.

Silica (US Silica Company, Berkeley Springs, WV, USA) Silica was dissolved in Dulbecco's modified eagle media and given subcutaneously at the dose of 3.5 g/kg, or intraperitoneally at the dose of 1.6 g/kg twice a week.

CBDL The surgical procedure was performed under sterile conditions. The mice were anesthetized with isoflurane. Midline laparotomy was performed for exploring the hepatic hilum and identifying CBD. Under the dissecting microscope, CBD was then isolated, doubly ligated and transected between two ligatures.

Liver biopsy

Liver biopsy demanded survival procedures and sterile techniques. After anesthesia with isoflurane, midline laparotomy was performed to expose the mouse liver. A liver block sized 0.5 cm in diameter was taken and then the cut surface was sutured for hemostasis. Serial biopsy was

performed monthly (per 4 wk) for each mouse till cirrhosis was well documented by histopathology. At the first liver biopsy, ascites, and intra-abdominal adhesion were examined and recorded.

Histopathology

Mouse livers from biopsies were fixed in 10% neutral buffered formaldehyde solution and embedded in paraffin. Sections, 4 μ m in thickness, were stained with hematoxylin and eosin. Fatty change of hepatocytes was recorded when hepatocytes showed fat accumulation, balloon-like swelling or formation of fat cysts. For liver necrosis, there were the disorganization of liver cell cords, homogeneous cytoplasm, pyknotic nuclei and periportal infiltration of inflammatory cells. Fibrosis was defined as the presence of fibrous scarring band in the liver parenchyma by Mason's trichrome collagen stain. Once the irregular zones of fibrosis developed and surrounded the remaining parenchymal tissues to display a pattern of nodularity under microscope, cirrhosis was diagnosed.

Statistical analysis

For survival and cirrhosis rate analyses, life table method was used. The length of time intervals used in this study was 4 wk. Any mouse which died, or whose liver was pathologically documented to be cirrhotic was considered to have experienced an event. When a mouse died before cirrhosis was confirmed at cirrhosis rate analysis, it was counted as a withdrawal and treated the same way as cases lost to follow-up. Plots were constructed with weeks after inducing liver injury vs survival or cirrhosis rate. The Wilcoxon test was employed to compare the curves. Differences were regarded as significant if a *P* value was less than 0.05.

RESULTS

Mouse survival

During the period of 6 mo, none of the 260 mice enrolled in this study died of the procedures for CBDL, liver biopsy or administration of hepatotoxins. There was no mortality case in the AA and silica groups. As for the other groups, 71 mice died in the course of this study. Among the 71 deaths, 20 occurred before cirrhosis could be histopathologically confirmed (pre-cirrhotic) and the remaining 51 after cirrhosis was found (post-cirrhotic). Nineteen of the 20 pre-cirrhotic deaths occurred in the CCl₄ group. As for the post-cirrhotic deaths, there were 4 in the ANIT group, 26 in the CCl₄ group, 11 in the DDC group and 10 in the CBDL group. The case numbers of mortality in each subgroup were listed in Table 1. Mortality had been found in all the CCl₄ subgroups, ranging from 40% to 100%. In the DDC group, mortality was mainly post-cirrhotic, and seen in 2.5 and 5 mg and 0.1% diet subgroup. All the mice in CBDL group had post-cirrhotic death by the end of 16 wk. The overall comparison for the survival curves in the ANIT and DDC groups could not reach any statistical significance (*P* = 0.0823 and 0.1227, respectively), whereas there was a significant difference in the CCl₄ subgroup (*P* < 0.0001). Pairwise comparisons for survival curves of the six CCl₄ subgroups showed that the

low dosage (IP0.8 and OG0.8) was significantly better than the medium dosage (IP1.6 and OG1.6, Figure 1, $P = 0.0010$ – 0.0317), and the medium dosage was also superior to the high dosage (IP2.0 and OG2.0, Figure 1, $P = 0.0002$ – 0.0044). Considering the administration routes, IP route compared favorably in survival with OG route at the high dosage ($P = 0.0221$), but not at the medium and low dosages ($P = 0.7899$ and 0.5902 , respectively).

Table 1 Case number of pre-cirrhotic and post-cirrhotic deaths

	Pre-cirrhotic death	Post-cirrhotic death
ANIT OG 25 mg/kg	0	0
ANIT OG 50 mg/kg	0	0
ANIT OG 125 mg/kg	0	3
ANIT IP 25 mg/kg	0	0
ANIT IP 50 mg/kg	0	0
ANIT IP 125 mg/kg	1	0
ANIT modified	0	1
AA OG from 0.2 to 1.0 mmol/kg	0	0
CCl ₄ OG 0.8 g/kg	0	5
CCl ₄ OG 1.6 g/kg	2	7
CCl ₄ OG 2.0 g/kg	5	5
CCl ₄ IP 0.8 g/kg	4	0
CCl ₄ IP 1.6 g/kg	6	1
CCl ₄ IP 2.0 g/kg	2	8
DDC OG 0.25 mg	0	0
DDC OG 0.5 mg	0	1
DDC OG 2.5 mg	0	3
DDC OG 5 mg	0	4
DDC 0.1% diet	0	3
Silica (SC 3.5 g/kg or IP 1.6 g/kg)	0/0	0/0
CBDL	0	10

OG: Oral gavage; IP: intraperitoneal; SC: subcutaneous.

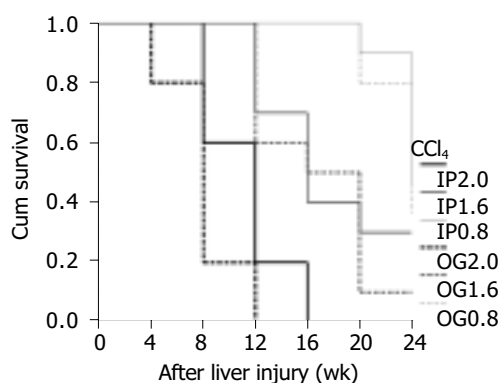


Figure 1 Survival curves of six CCl₄ subgroups are shown. The number immediately behind the IP or OG indicates the dosage of CCl₄ used in g/kg.

Ascites and intraabdominal adhesion

Ascites was universally found at laparotomy when the hepatotoxins were administered via IP route. In the CBDL group, there were only three mice presenting with ascites at the subsequent laparotomy. Intraabdominal adhesion existed in over 50 % of cases (ranging from 50% to 100%) when IP route or CBDL was used. Additionally, granuloma-like masses were intraperitoneally identified in all the cases of silica IP subgroup and in nine cases of ANIT IP subgroups

(two for 25 mg/kg, one for 50 mg/kg and six for 125 mg/kg).

Histopathology

The case numbers of histopathological findings in each subgroup were listed in Table 2. Fatty change was seen mainly in the ANIT and CCl₄ groups, and sporadically in the AA group (1 for 0.8 mmol/kg and 2 for 1.0 mmol/kg). Bile lakes were the common findings in the DDC and CBDL groups. Liver necrosis and fibrosis were demonstrated almost in all the cases of the ANIT, CCl₄, DDC, and CBDL groups, two cases of the AA group (one for 0.8 mmol/kg and the other for 1.0 mmol/kg), but none of the silica group. The necrosis and fibrosis were detected at the first or second liver biopsy (4–8 wk after liver injury). Liver fibrosis in the two mice from the AA group did not progress to cirrhosis by the end of this study. Cirrhotic nodules could be identified in 30 mice (42.9%) of ANIT group ($n = 70$), 32 mice (53.3%) of CCl₄ group ($n = 60$), 39 mice (78.0%) of DDC group ($n = 50$) and all the mice (100%) of CBDL group ($n = 10$). DDC subgroup with higher dosages (2.5 and 5 mg) and 0.1% diet could substantially reach 100% successful rate of cirrhosis induction as seen in the CBDL group.

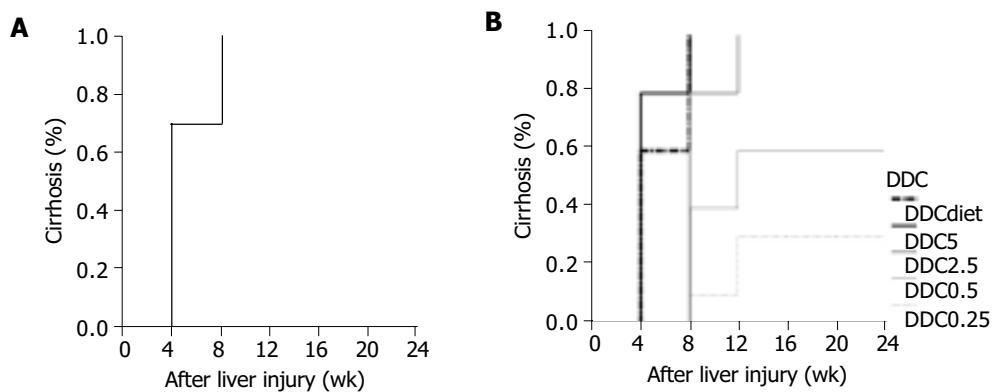
Durations required for cirrhosis induction

Results from life table analysis for the durations were presented in the curves with weeks after inducing liver injury *vs* cirrhosis rate. CBDL represented a rapid method to induce liver cirrhosis with 70–100% of successful rate within 4–8 wk (Figure 2A). DDC caused liver cirrhosis within 4–12 wk (Figure 2B). Statistical analysis revealed that the lower the DDC dosage, the longer the time spent by DDC in inducing cirrhosis among 0.5, 2.5 and 5 mg subgroups (DDC0.5 *vs* DDC2.5, $P = 0.0387$ and DDC2.5 *vs* DDC5, $P = 0.0004$). There was no significant difference between 0.25 and 0.5 mg DDC subgroups ($P = 0.1311$). DDC 0.1% diet required significantly less time to induce cirrhosis than DDC 0.25 mg ($P = 0.0001$), 0.5 mg ($P = 0.0008$) and 2.5 mg ($P = 0.0032$), but was not significantly different from 5 mg subgroups ($P = 0.3415$). As for CCl₄, the duration for inducing cirrhosis was quite variable, ranging from 4 to 20 wk (Figure 3A). The IP and OG high dosages (2.0 g/kg) of CCl₄ spent significantly less time in cirrhosis induction than IP and OG low dosages (0.8 g/kg) of CCl₄ ($P = 0.0005$ – 0.0209). There was no difference of the cirrhosis curves between IP and OG administrations at the high ($P = 0.1760$) and low ($P = 0.1661$) dosages, whereas OG administration compared favorably in cirrhosis induction than IP administration at the medium dosage (1.6 g/kg) of CCl₄ ($P = 0.0060$). The OG medium dosage (OG1.6) had no significant difference from the high dosage ($P = 0.1852$ for OG2.0 and $P = 0.7241$ for IP2.0), and the IP medium dosage (IP1.6) had no significant difference from the low dosage ($P = 0.8822$ for OG0.8 and $P = 0.1514$ for IP0.8). Cirrhosis caused by ANIT did not show up until 12–24 wk (Figure 3B). The high dosage of ANIT significantly spent less time in cirrhosis induction than the medium ($P = 0.0002$ – 0.0263) and low dosages ($P = 0.0002$ – 0.0027), whereas the medium dosage could not be significantly superior to the low dosage ($P = 0.0904$ – 1.0000). At the same ANIT dosage used, there was no significant difference of cirrhosis curves between OG and

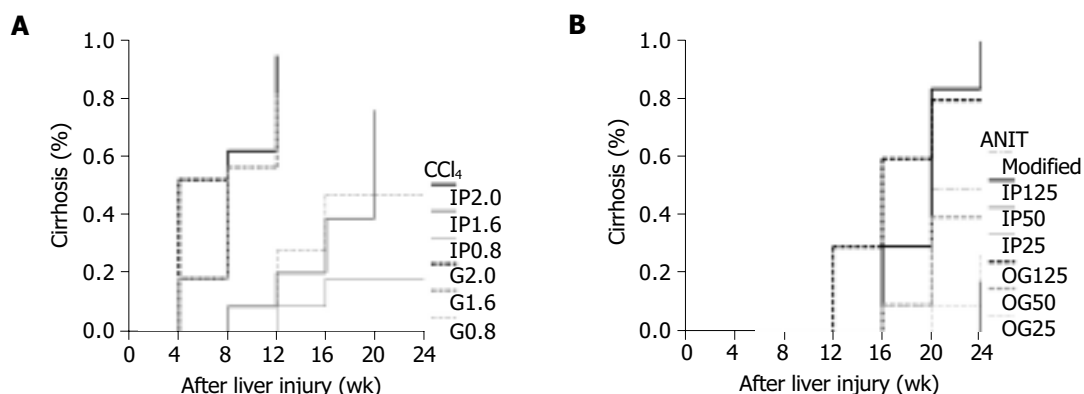
Table 2 Histopathological changes after inducing liver injuries

	Fatty change	Necrosis/fibrosis	Cirrhosis	Bile lake
ANIT OG 25 mg/kg	0	10	2	0
ANIT OG 50 mg/kg	4	10	4	0
ANIT OG 125 mg/kg	5	10	8	0
ANIT IP 25 mg/kg	0	9	1	0
ANIT IP 50 mg/kg	1	10	1	0
ANIT IP 125 mg/kg	4	10	9	0
ANIT modified	4	10	5	0
AA OG from 0.2 to 1.0 mmol/kg	3 ¹	2 ²	0	0
CCl ₄ OG 0.8 g/kg	4	10	5	0
CCl ₄ OG 1.6 g/kg	5	10	8	0
CCl ₄ OG 2.0 g/kg	8	10	5	0
CCl ₄ IP 0.8 g/kg	3	10	2	0
CCl ₄ IP 1.6 g/kg	5	10	4	0
CCl ₄ IP 2.0 g/kg	6	10	8	0
DDC OG 0.25 mg	0	10	3	6
DDC OG 0.5 mg	0	10	6	9
DDC OG 2.5 mg	0	10	10	10
DDC OG 5 mg	0	10	10	10
DDC 0.1% diet	0	10	10	9
Silica (SC 3.5 g/kg or IP 1.6 g/kg)	0/0	0/0	0/0	0/0
CBDL	0	10	10	10

OG: oral gavage; IP: intraperitoneal; SC: subcutaneous. ¹1 for 0.8 mmol/kg and 2 for 1.0 mmol/kg; ²1 for 0.8 mmol/kg and 1 for 1.0 mmol/kg.

**Figure 2** Cirrhosis rates of CBDL and DDC groups. **A:** The cirrhosis curve for CBDL group is shown; **B:** The cirrhosis curves for 5 DDC subgroups are

shown. The number immediately behind DDC indicates its dosage used in mg per mouse. DDC diet represents 0.1% DDC contained diet.

**Figure 3** Cirrhosis rates of CCl₄ and ANIT groups. **A:** The cirrhosis curves for six CCl₄ subgroups are shown. The number immediately behind the IP or OG indicates the dosage of CCl₄ used in g/kg; **B:** The cirrhosis curves for seven

ANIT subgroups are shown. The number immediately behind the IP or OG indicates the dosage of ANIT used in mg/kg.

IP administrations ($P = 0.2444$ for high dosage, $P = 0.0904$ for medium dosage, and $P = 0.5032$ for low dosage). The modified method for ANIT administration compared

favorably in cirrhosis induction only with IP low dosage and IP medium dosage ($P = 0.0349$, for both), but poorly with OG high dosage ($P = 0.0303$).

DISCUSSION

In this 6-mo study of experimental cirrhosis induction, AA and silica were ineffective in inducing liver fibrosis let alone cirrhosis. AA administration in the drinking water (50 ppm equivalent to 0.08–0.11 mmol/kg per d) for 15 wk has no effect on the histopathological examination of rat livers^[19]. Moreover, IP injection of AA in rats only produced variable periportal liver necrosis predominantly at 6–12 h, followed by restitutive proliferation of periportal necrosis to repopulate the necrotic zone. Eventually, the liver architecture was essentially restored by 1 wk^[18]. It indicated that AA merely induced short-term toxicity in rats. Although we had observed liver necrosis and fibrosis in two mice with OG administration of 0.8 and 1.0 mmol/kg AA, this liver damage was transient and insufficient to result in cirrhosis. It suggested that rats and FVB/N mice had similar hepatotoxic resistance to AA. As for silica, subcutaneous or IP administration was reported to cause liver fibrosis and cirrhosis in nude mice at 12 mo and in (C57BL/6×BALB/c) F₁ mice at 18 mo^[22]. Thus, a 6-mo duration might not be long enough for silica to cause hepatic injury with subsequent fibrosis and cirrhosis in FVB/N mice. As a result, a longer-term administration of silica might be required for inducing liver cirrhosis in FVB/N mice. A major drawback with silica administration was the granuloma formation at the injection site. This might be of concern to subsequent laparotomy for liver biopsy when the IP route is used.

The IP or OG administration of ANIT, CCl₄ or DDC could effectively lead to liver fibrosis within 4–8 wk. All the liver fibrosis in mice did not always progress to microscopic cirrhotic nodules by the end of 24 wk. It suggested that restitutive response of mice to the injuries by those hepatotoxins sometimes restore liver architecture. ANIT has been used for years to study cholangiolitic hepatotoxicity in laboratory animals^[9,10]. This study showed that ANIT usually led to mouse cirrhosis within 12–24 wk after administration. Mortality was only seen in the subgroups with high dosage and modified administration. However, there was no significant difference among the survival curves of all the ANIT subgroups. The high dosage of ANIT could more rapidly induce liver cirrhosis than the medium or low dosage. At the same dosage of ANIT, it made no significant difference between IP and OG administrations in cirrhosis induction. The modified method by gradual increase of ANIT dosage could not substantially provide any benefit in cirrhosis induction in this study. Overall, ANIT model required a longer period for the formation of cirrhosis. This might provide more time for researchers to investigate the progression of liver fibrosis.

CCl₄ has been used extensively for decades to induce liver injury in various experimental models to elucidate the mechanisms behind hepatotoxicity^[23]. Also, it was commonly used as a hepatotoxic agent in transgenic mice to evaluate liver fibrosis and cirrhosis on the basis of the selective expression of some novel or altered genes^[13,14,24]. We experienced that the major problem in association with the use of CCl₄ to induce liver fibrosis or cirrhosis had been the high mortality rates of mice, accounting for 40–100 % in those subgroups. Animals might die before or after cirrhosis was found. The higher CCl₄ dosage was associated with the worse survival

curve. The duration required for cirrhosis induction by CCl₄ was quite variable, ranging from 4 to 20 wk, mainly depending upon the dosage. The high dosage (2.0 g/kg) of CCl₄ could rapidly cause liver cirrhosis within 4–12 wk, but led to poor survival. Under the circumstances, IP administration will be suggested since IP route posed better survival than OG route only at the high dosage of CCl₄. The low dosage (0.8 g/kg) of CCl₄ required 12–24 wk to successfully induce cirrhosis. At the low dosage, it was shown that the administration routes had no influence on the survival and the cirrhosis induction. At the medium dosage (1.6 g/kg) of CCl₄, OG administration was more rapid to induce cirrhosis than IP administration, but did not significantly differ in survival curves from IP administration. Nevertheless, the high mortality rate along with the use of CCl₄ must be taken into consideration since it will prematurely terminate the sequential studies or observations of liver fibrosis or cirrhosis. Furthermore, CCl₄ might not be an ideal solvent for investigating hepatocarcinoma since liver carcinogenesis might be due to the genotoxic chemical carcinogen effect of CCl₄ itself as well as CCl₄-induced liver cirrhosis^[25,26].

DDC did not result in pre-cirrhotic death, but tended to lead to post-cirrhotic death at higher dosage (2.5 and 5 mg) and 0.1% DDC diet. The overall comparison for all survival curves of those DDC subgroups led to the insignificant difference. It took about 4–12 wk for DDC to successfully induce cirrhosis. Except 0.25 mg DDC subgroup, the successful rate of cirrhosis induction was quite satisfactory. The higher the dosage of DDC we used, the lesser the time we needed to induce cirrhosis. DDC 0.1% diet could not be superior to 5 mg DDC subgroup in cirrhosis induction. A major concern of DDC use was the high proportion of bile lake formation. This might cause some biases in observing the relationship between cirrhosis and its sequelae.

CBDL represented a rapid and consistent method to induce liver fibrosis and cirrhosis. Hepatocellular injuries were caused by cholestasis, leading to liver dysfunction, promoting fibrogenesis and ultimately resulting in liver failure and death. All the mice with CBDL rapidly progressed to cirrhosis within 4–8 wk after operation, and died by the end of 16 wk. The rapid progression to cirrhosis and death by CBDL might limit its application in chronic fibrosis studies and make it difficult to carry out a long-term investigation of liver cirrhosis. A major technical problem was the reversibility of histological changes due to recanalization of bile ducts^[1]. In our tested animals, the bile ducts remained totally obstructed till their death in view of bile lakes at final pathology and the coloration of peritoneum and auricle. The successful obstruction by CBDL might be due to the fact that CBD was doubly ligated and transected between two ligatures^[27]. Besides, intraabdominal adhesion could be an obstacle for subsequent survival laparotomy to study CBDL livers.

In summary, CBDL and hepatotoxins of ANIT, CCl₄ and DDC could be effective in causing liver fibrosis of mice. CBDL rapidly and irreversibly led to liver fibrosis and subsequently to cirrhosis within 4–8 wk, but inevitably caused mortality by the end of 16 wk. As a result, CBDL was suitable for creating a mouse model for the short-term study of liver fibrogenesis. Although CCl₄ had been commonly used for inducing liver fibrosis and cirrhosis, the duration

required for cirrhosis induction varied (4-20 wk) and mainly depended upon the dosage. It could be used in mice for studying both acute and chronic liver fibrogenesis. A major drawback in association with CCL₄ use was a relatively high mortality. DDC could effectively induce cirrhosis within 4-12 wk. The time required for cirrhosis induction by DDC was quite similar to that of CBDL, but the survival experience was better in the DDC group. ANIT slowly induced liver cirrhosis in mice. The duration from initial liver inflammatory damage to cirrhosis formation by ANIT was more than 12 wk after administration. Thus, ANIT was quite a good toxin for a long-term study of fibrosis progression into cirrhosis.

ACKNOWLEDGMENTS

We thank Dr. Yun-Fan Liaw for his suggestions, helpful discussions and support.

REFERENCES

- 1 Wu J, Norton PA. Animal models of liver fibrosis. *Scand J Gastroenterol* 1996; **31**: 1137-1143
- 2 Sanderson N, Factor V, Nagy P, Kopp J, Kondaiah P, Wakefield L, Roberts AB, Sporn MB, Thorgeirsson SS. Hepatic expression of mature transforming growth factor beta 1 in transgenic mice results in multiple tissue lesions. *Proc Natl Acad Sci USA* 1995; **92**: 2572-2576
- 3 Hanahan D. Transgenic mice as probes into complex systems. *Science* 1989; **246**: 1265-1275
- 4 Quick DJ, Shuler ML. Use of in vitro data for construction of a physiologically based pharmacokinetic model for naphthalene in rats and mice to probe species differences. *Biotechnol Prog* 1999; **15**: 540-555
- 5 Lindstrom AB, Yeowell-O'Connell K, Waidyanatha S, McDonald TA, Golding BT, Rappaport SM. Formation of hemoglobin and albumin adducts of benzene oxide in mouse, rat, and human blood. *Chem Res Toxicol* 1998; **11**: 302-310
- 6 Cunningham ML, Bucher JR. Pharmacodynamic responses of F344 rats to the mouse hepatocarcinogen oxazepam in a 90-d feed study. *Toxicol Appl Pharmacol* 1998; **149**: 41-48
- 7 Watt KC, Buckpitt AR. Species differences in the regio- and stereoselectivity of 1-nitronaphthalene metabolism. *Drug Metab Dispos* 2000; **28**: 376-378
- 8 Dill JA, Lee KM, Bates DJ, Anderson DJ, Johnson RE, Chou BJ, Burka LT, Roycroft JH. Toxicokinetics of inhaled 2-butoxyethanol and its major metabolite, 2-butoxyacetic acid, in F344 rats and B6C3F1 mice. *Toxicol Appl Pharmacol* 1998; **153**: 227-242
- 9 Palmeira CM, Ferreira FM, Rolo AP, Oliveira PJ, Santos MS, Moreno AJ, Cipriano MA, Martins MI, Seica R. Histological changes and impairment of liver mitochondrial bioenergetics after long-term treatment with alpha-naphthyl-isothiocyanate (ANIT). *Toxicology* 2003; **190**: 185-196
- 10 Ohta Y, Kongo M, Sasaki E, Harada N. Change in hepatic antioxidant defense system with liver injury development in rats with a single alpha-naphthylisothiocyanate intoxication. *Toxicology* 1999; **139**: 265-275
- 11 Williams AO, Knapton AD. Hepatic silicosis, cirrhosis, and liver tumors in mice and hamsters: studies of transforming growth factor beta expression. *Hepatology* 1996; **23**: 1268-1275
- 12 Natsume M, Tsuji H, Harada A, Akiyama M, Yano T, Ishikura H, Nakanishi I, Matsushima K, Kaneko S, Mukaida N. Attenuated liver fibrosis and depressed serum albumin levels in carbon tetrachloride-treated IL-6-deficient mice. *J Leukoc Biol* 1999; **66**: 601-608
- 13 Brenner DA, Veloz L, Jaenisch R, Alcorn JM. Stimulation of the collagen alpha 1 (I) endogenous gene and transgene in carbon tetrachloride-induced hepatic fibrosis. *Hepatology* 1993; **17**: 287-292
- 14 Inagaki Y, Truter S, Bou-Gharios G, Garrett LA, de Crombrughe B, Nemoto T, Greenwel P. Activation of Proalpha2(I) collagen promoter during hepatic fibrogenesis in transgenic mice. *Biochem Biophys Res Commun* 1998; **250**: 606-611
- 15 Preisegger KH, Factor VM, Fuchsbichler A, Stumptner C, Denk H, Thorgeirsson SS. Atypical ductular proliferation and its inhibition by transforming growth factor beta1 in the 3,5-diethoxycarbonyl-1,4-dihydrocollidine mouse model for chronic alcoholic liver disease. *Lab Invest* 1999; **79**: 103-109
- 16 Fickert P, Trauner M, Fuchsbichler A, Stumptner C, Zatloukal K, Denk H. Bile acid-induced Mallory body formation in drug-primed mouse liver. *Am J Pathol* 2002; **161**: 2019-2026
- 17 Alam K, Nagi MN, Al-Shabanah OA, Al-Bekairi AM. Beneficial effect of nitric oxide synthase inhibitor on hepatotoxicity induced by allyl alcohol. *J Biochem Mol Toxicol* 2001; **15**: 317-321
- 18 Yavorkovsky L, Lai E, Ilic Z, Sell S. Participation of small intraportal stem cells in the restitutive response of the liver to periportal necrosis induced by allyl alcohol. *Hepatology* 1995; **21**: 1702-1712
- 19 Carpanini FM, Gaunt IF, Hardy J, Gangolli SD, Butterworth KR, Lloyd AG. Short-term toxicity of allyl alcohol in rats. *Toxicology* 1978; **9**: 29-45
- 20 Taketo M, Schroeder AC, Mobraaten LE, Gunning KB, Hanten G, Fox RR, Roderick TH, Stewart CL, Lilly F, Hansen CT. FVB/N: an inbred mouse strain preferable for transgenic analyses. *Proc Natl Acad Sci USA* 1991; **88**: 2065-2069
- 21 Perret-Gentil MI, Murray L, Bird DJ, Ladiges WC. Evaluation of FVB/N mice as recipients for transgenic embryos. *Lab Anim Sci* 1999; **49**: 427-428
- 22 Ebbesen P. Chirality of quartz. Fibrosis and tumour development in dust inoculated mice. *Eur J Cancer Prev* 1991; **1**: 39-41
- 23 Plaa GL. Chlorinated methanes and liver injury: highlights of the past 50 years. *Annu Rev Pharmacol Toxicol* 2000; **40**: 42-65
- 24 Schnur J, Olah J, Szepesi A, Nagy P, Thorgeirsson SS. Thioacetamide-induced hepatic fibrosis in transforming growth factor beta-1 transgenic mice. *Eur J Gastroenterol Hepatol* 2004; **16**: 127-133
- 25 Zalatinai A, Lapis K. Simultaneous induction of liver cirrhosis and hepatocellular carcinomas in F-344 rats: establishment of a short hepatocarcinogenesis model. *Exp Toxicol Pathol* 1994; **46**: 215-222
- 26 Beddowes EJ, Faux SP, Chipman JK. Chloroform, carbon tetrachloride and glutathione depletion induce secondary genotoxicity in liver cells via oxidative stress. *Toxicology* 2003; **187**: 101-115
- 27 Prado IB, dos Santos MH, Lopasso FP, Iriya K, Laudanna AA. Cholestasis in a murine experimental model: lesions include hepatocyte ischemic necrosis. *Rev Hosp Clin Fac Med Sao Paulo* 2003; **58**: 27-32

• BASIC RESEARCH •

Tetramethylpyrazine stimulates cystic fibrosis transmembrane conductance regulator-mediated anion secretion in distal colon of rodents

Qiong He, Jin-Xia Zhu, Ying Xing, Lai-Ling Tsang, Ning Yang, Dewi Kenneth Rowlands, Yiu-Wa Chung, Hsiao-Chang Chan

Qiong He, Jin-Xia Zhu, Ying Xing, Ning Yang, Department of Physiology, Medical School, Zhengzhou University, Zhengzhou 450052, Henan Province, China

Qiong He, Jin-Xia Zhu, Lai-Ling Tsang, Ning Yang, Dewi Kenneth Rowlands, Yiu-Wa Chung, Hsiao-Chang Chan, Epithelial Cell Biology Research Center, Department of Physiology, Faculty of Medicine, The Chinese University of Hong Kong, Shatin, Hong Kong, China

Supported by the Innovation and Technology Fund of Hong Kong, China

Correspondence to: Dr. Hsiao-Chang Chan, Epithelial Cell Biology Research Center, Department of Physiology, Faculty of Medicine, The Chinese University of Hong Kong, Shatin, NT, Hong Kong, China. hsiaoChan@cuhk.edu.hk

Telephone: +852-2609-6839 Fax: +852-2603-5022

Received: 2004-08-19 Accepted: 2004-10-05

Abstract

AIM: To investigate the effect of tetramethylpyrazine (TMP), an active compound from *Ligustium Wollichii Franchet*, on electrolyte transport across the distal colon of rodents and the mechanism involved.

METHODS: The short-circuit current (I_{sc}) technique in conjunction with pharmacological agents and specific inhibitors were used in analyzing the electrolyte transport across the distal colon of rodents. The underlying cellular signaling mechanism was investigated by radioimmunoassay analysis (RIA) and a special mouse model of cystic fibrosis.

RESULTS: TMP stimulated a concentration-dependent rise in I_{sc} , which was dependent on both Cl^- and HCO_3^- , and inhibited by apical application of diphenylamine-2,2'-dicarboxylic acid (DPC) and glibenclamide, but resistant to 4,4'-diisothiocyanatostilbene-2,2'-disulfonic acid disodium salt hydrate (DIDS). Removal of Na^+ from basolateral solution almost completely abolished the I_{sc} response to TMP, but it was insensitive to apical Na^+ replacement or apical Na^+ channel blocker, amiloride. Pretreatment of colonic mucosa with BAPTA-AM, a membrane-permeable selective Ca^{2+} chelator, did not significantly alter the TMP-induced I_{sc} . No additive effect of forskolin and 3-isobutyl-1-methylxanthine (IBMX) was observed on the TMP-induced I_{sc} , but it was significantly reduced by a protein kinase A inhibitor, H_{89} . RIA results showed that TMP (1 mmol/L) elicited a significant increase in cellular cAMP production, which was similar to that elicited by the adenylate cyclase activator, forskolin (10 μ mol/L). The TMP-elicited I_{sc} as well as forskolin- or IBMX-induced I_{sc} were abolished in

mice with homozygous mutation of the cystic fibrosis transmembrane conductance regulator (CFTR) presenting defective CFTR functions and secretions.

CONCLUSION: TMP may stimulate cAMP-dependent and CFTR-mediated Cl^- and HCO_3^- secretion. This may have implications in the future development of alternative treatment for constipation.

© 2005 The WJG Press and Elsevier Inc. All rights reserved.

Key words: Tetramethylpyrazine; Ligustrazine; Colonic mucosa; Cl^- ; HCO_3^- ; cAMP; CF mice

He Q, Zhu JX, Xing Y, Tsang LL, Yang N, Rowlands DK, Chung YW, Chan HC. Tetramethylpyrazine stimulates cystic fibrosis transmembrane conductance regulator-mediated anion secretion in distal colon of rodents. *World J Gastroenterol* 2005; 11(27): 4173-4179

<http://www.wjgnet.com/1007-9327/11/4173.asp>

INTRODUCTION

Constipation presents a massive impact on health services, and the epidemiology investigation has demonstrated that the prevalence of constipation in many areas around the world is significantly high^[1,2]. Studies have shown that constipation results primarily from changes in gastrointestinal motility^[3]. In addition, alterations in regulating fluid and electrolyte transport across gut epithelia may represent another contributing factor in the pathophysiology of constipation^[4].

The mammalian colon is the final station of the gastrointestinal tract, where the organism has the last opportunity to modify the electrolyte contents in the feces with balanced absorptive and secretory activities. The epithelial layer covering the inner surface of colon is a typical electrolyte-transporting epithelium, which under physiological conditions absorbs water, sodium and chloride while secreting NaCl as well as potassium and bicarbonate through a number of ion channels, carriers, and pumps, located either on the luminal or on the basolateral membrane. Epithelial Na^+ channels populated in the apical membranes of the absorptive cells in the colon, which are amiloride-sensitive and well-known targets for mineralocorticoids, are responsible for Na^+ absorption^[5]. Cystic fibrosis transmembrane conductance regulator (CFTR), a cAMP-dependent Cl^- channel, is predominantly expressed in colonic

crypts^[6,7] and known to mediate both Cl^- ^[8,9] and HCO_3^- secretion^[10,11]. Disturbance of ion transport, like cholera toxin and cystic fibrosis (CF) may result in diarrhea^[12] or constipation^[13] with severe pathological consequences^[9].

The traditional therapeutic proposals, such as the employment of cathartic medications, stool softeners, lubricant grease, and enemas have some effects on constipation, but their side effects have restricted their use^[14].

In our previous study, we have observed that Bak Foong Pill, consisting of more than 20 herbal ingredients, a well known Chinese remedy widely used for treating gynecological disorders, exerts a stimulatory effect on anion secretion by the human colonic epithelia cell line T₈₄ primarily via the cAMP pathway with minor contribution from the Ca^{2+} pathway^[15]. This result highlights the potential for exploring an active component of Bak Foong Pills for treatment of constipation or other obstructive bowel syndromes in patients.

Tetramethylpyrazine (TMP, $\text{C}_8\text{H}_{12}\text{N}_2$, molecular weight 136.20), also known as ligustrazine, is the active compound extracted from one of the component herbs of Bak Foong Pill, *Ligustium Wollichii*. TMP is used in clinic to treat cardiovascular disorders because of its multitude of biological effects such as improving blood circulation and metabolism of cardiac muscle, increasing coronary flow, decreasing oxygen consumption, lowering blood pressure and inhibiting thrombosis^[16-18]. TMP may act as an inhibitor of phosphodiesterase (PDE) to increase intracellular cAMP thereby exerting its antiplatelet and vasodilatation effects^[19]. On the other hand, the effect of TMP on the release of calcium from internal stores has also been reported^[17]. Therefore, it is possible that TMP may be the active compound responsible for mediating the effect of Bak Foong Pills. The focus of this study was to investigate the effect of TMP on water and electrolyte transport properties of native mammalian colon with the hope of exploring new alternative treatment for constipation or obstructive bowel syndromes.

MATERIALS AND METHODS

Materials

TMP was purchased from the Fourth Pharmaceutical Factory of Beijing (Beijing, China). 3-Isobutyl-1-methylxanthine (IBMX), amiloride, DIDS, BAPTA-AM, POP and POPOP were obtained from Sigma Chemical Company (St. Louis, MO, USA). Calbiochem (San Diego, CA, USA) was the source for bumetanide, forskolin, TTX, H₈₉, and glibenclamide. Diphenylamine-2,2'-dicarboxylic acid (DPC) was purchased from Riedel de Haen Chemicals (Hannover, Germany). cAMP measurement kit was purchased from the Institute of Atomic Energy Science (Beijing, China). Stock solutions of all the chemicals were dissolved in DMSO. Final DMSO concentrations never exceeded 1 mL/L. Preliminary experiments indicated that the vehicle did not alter any baseline electrophysiological parameters.

Krebs-Henseleit (KH) solution contained (in mmol/L): 117, NaCl; 4.7, KCl; 1.2, MgCl_2 ; 1.2, KH_2PO_4 ; 24.8, NaHCO_3 ; 2.5, CaCl_2 ; 11.1, glucose. The solution was continuously bubbled with 95% O_2 and 50 mL/L CO_2 to

maintain the pH at 7.4. In Cl^- free solution, NaCl, KCl, and CaCl_2 were replaced by sodium gluconate, potassium gluconate, and calcium gluconate, respectively^[20]. When HCO_3^- free solution was used, NaHCO_3 was replaced by NaCl, and the solution was buffered with 10 mmol/L Hepes with a pH of 7.4 when gassed with 100% O_2 . In the Cl^- and HCO_3^- free solutions, NaCl and NaHCO_3 were replaced by sodium gluconate, KCl by potassium gluconate, and CaCl_2 by calcium gluconate. The solution was buffered with 10 mmol/L Hepes with a pH of 7.4 when gassed with 100% O_2 . In all solutions, the osmolarity was adjusted to 290 mOsm/L with D-mannitol if necessary.

Methods

Tissue preparation Adult male Sprague-Dawley rats (Laboratory Animal Services Center at The Chinese University of Hong Kong) ranging in age from 8 to 12 wk had free access to standard rodent laboratory food and water until the day of the experiments. The animals were killed by CO_2 asphyxiation in accordance with a protocol approved by Animal Research Ethics Committee of the Chinese University of Hong Kong. Segments of distal colon about 5 cm proximal to the anus were quickly removed, cut along the mesenteric border into a flat sheet and flushed with ice-cold KH solution. The tissues were pinned flat with the mucosal side down in a Sylgard-lined petri dish containing ice-cold oxygenated solution. The serosa, submucosa, and muscular layer were stripped away with fine forceps to obtain a mucosa preparation. Two to three of these stripped mucosal preparations were obtained from one animal. TTX was used to exclude possible involvement of neuronal circuitry.

CFTR mice CFTR mice, B6.129P2-*Cftr*^{*tm1Unc1*}, were purchased from Jackson's Laboratory (Bar Harbor, ME 04609, USA) and then bred in Laboratory Animal Services Center at The Chinese University of Hong Kong by mating heterozygous pairs genotyped by PCR amplification of genomic DNA isolated from the animals' tails, as described previously^[21]. Homozygous CFTR mutation (-/-) mice and their littermate wild-type CFTR (+/+) controls were utilized in the study. Preparation of mouse colonic mucosa was similar to that described for the rat. Mice were cared for in accordance with the Laboratory Animal Services Center of the Chinese University of Hong Kong guidelines.

Short circuit current measurement The short-circuit current (I_{sc}) was measured *in vitro* in Ussing chambers^[22]. Flat sheets of distal colon with intact mucosa were mounted between two halves of modified Ussing chambers, in which the total cross-sectional area was 0.45 cm². The mucosal and serosal surfaces of tissues were bathed with 10 mL of KH solution by recirculation from a reservoir maintained at 37 °C during the experiment. The solution was gassed with 95% O_2 and 50 mL/L CO_2 to maintain the pH at 7.4. An equilibration period of 30 min was given before the experiments. The tissues were continuously short-circuited, and the transepithelial potential difference (PD) was measured through Ag/AgCl reference electrodes (World Precision Instruments, Sarasota, Boca Raton, FL, USA) connected to a preamplifier that was connected in turn to a voltage clamp amplifier (DVC 1000; World Precision

Instruments). Voltage offset of two voltage electrodes and fluid resistance were adjusted and compensated prior to the onset of each measurement. At 0.5 intervals, a transepithelial PD of 0.1 mV (U) was applied to the tissue and the change in current (I) was measured. The tissue conductance (G_t) and the open-circuit PD could be calculated from these values according to Ohm's law ($G_t = I/U$ and $\text{PD} = I/G_t$). Drugs could be added directly to the apical or basolateral side of epithelium. Responses were continuously recorded on a chart recorder. The change in I_{SC} was calculated on the basis of the value before and after stimulation and normalized as current per unit area of epithelium ($\mu\text{A}/\text{cm}^2$), according to which, the total transmembrane charges ($\mu\text{C}/\text{cm}^2$) for 30 min could be calculated. The methodology for tissue preparation and measurement of electrical parameters across the mucosal sheets was described earlier^[23,24].

Measurement of cAMP Cytosolic cAMP concentrations were measured by radioimmunoassay analysis (RIA). After a 20-min period of equilibration in normal KH solution at 37 °C, the isolated mucosal sheet was treated with TMP, forskolin, TMP with IBMX, TMP with IBMX and forskolin. The mucosal sheet without treatment could act as control. The mucosal sheets were further incubated for 2 min and then rapidly frozen in liquid nitrogen and weighed 50.0 mg frozen tissue precisely. The tissues were homogenized in 2 mL of 1 N perchloric acid using a glass homogenizer. The homogenate was centrifuged at 1 000 r/min, 600 μL of the supernatant was extracted and neutralized with 300 μL of 20% KOH. The sediment was discarded after centrifugation. Six hundred microliters of the supernatant was extracted and evaporated in an electrothermal blast drier at 80 °C and the residue was dissolved in 200 μL TE buffer for further measurement. The amount of cAMP was determined by RIA with a ^3H -labeled cAMP kit (Institute of Atomic Energy Science). Procedures were performed according to the manufacturer's instructions.

Statistical analysis

Results were expressed as mean \pm SE. The number of experiments represented independent measurements on separate stripped mucosal preparation (two to three of these tissue preparations were obtained from one animal).

Comparisons between groups of data were made by either the Student's *t*-test (two-group comparison) or one-way ANOVA with Newman-Keuls post hoc test (three or more-group comparison). $P < 0.05$ was considered statistically significant. EC_{50} values were determined by nonlinear regression using GraphPad Prism software.

RESULTS

TMP-induced I_{SC} response in rat distal colon

Addition of TMP to either the apical or basolateral membrane could elicit I_{SC} responses with a greater response obtained with basolateral challenge. The present study only focused on the responses elicited by basolateral addition of TMP. As shown in Figure 1, the TMP response was concentration-dependent with an apparent EC_{50} of 0.994 mmol/L. At a concentration greater than 3 mmol/L, TMP induced a biphasic response with a fast transient peak followed by a sustained plateau.

To exclude possible involvement of enteric nervous system, 1 $\mu\text{mol/L}$ TTX was added to the basolateral side before the administration of TMP and no significant change in the TMP-evoked increase in I_{SC} was observed.

Ion basis of TMP-evoked I_{SC}

The increase in I_{SC} could be attributed to either enhanced movement of positive charges from the luminal to the serosal side (i.e., Na^+) or movement of negative charges into the lumen (i.e., Cl^- and/or HCO_3^-). Ion substitution experiments were conducted to determine the ionic basis for the increases in I_{SC} induced by TMP (Figure 2). When extracellular Cl^- or HCO_3^- was removed, the TMP-induced response measured by total charge transfer per unit area over a 30-min period was reduced by 58.4% ($n = 5$, $P < 0.01$) and 70.8% ($n = 4$, $P < 0.01$), respectively. When both Cl^- and HCO_3^- were replaced, 98.1% ($n = 6$, $P < 0.001$) of the response was abolished, indicating substantial contribution of Cl^- and HCO_3^- to the TMP-induced response (Figure 2A).

To test whether the TMP-induced I_{SC} responses were due to electrogenic Na^+ absorption, apical Na^+ was replaced but it did not reduce the TMP response ($n = 6$), excluding electrogenic Na^+ absorption across the colonic mucosa.

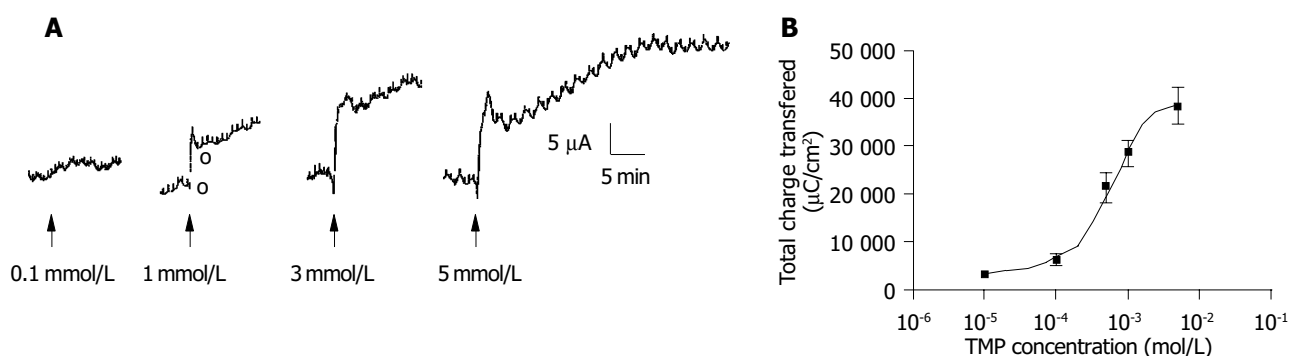


Figure 1 Effect of TMP on ion transport across rat colonic mucosa. **A:** Representative recordings of I_{SC} response to TMP (0.1, 1.0, 3.0, and 5.0 mmol/L) added to basolateral side. Arrowheads indicate the time of addition of TMP; **B:** Concentration-response curve of TMP with response indicated by the total

charge transfer per unit area over a 30-min period. Each data point was obtained from at least four individual experiments. Values are mean \pm SE of maximal increase in I_{SC} .

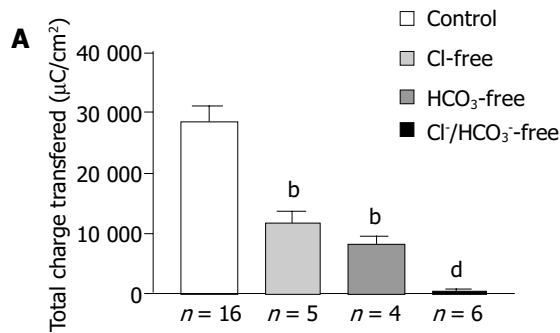
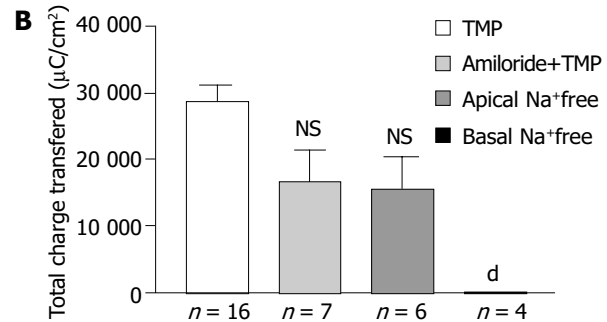


Figure 2 Ionic basis of TMP-induced I_{SC} . **A:** One millimole per liter of TMP-induced I_{SC} response (total charge transfer per unit area over 30-min period) obtained in various solutions was plotted with normal KH solution as the control; **B:** Summarized data showing the effect of 1 mmol/L of TMP-evoked



I_{SC} response in the apical presence of amiloride (0.1 mmol/L), apical Na⁺ removal, and basolateral Na⁺ removal from the bath solution. Values are mean±SE; ^b $P<0.001$, ^d $P<0.01$ vs control. NS, not significant.

However, removing Na⁺ from basolateral or bilateral bathing solution abolished TMP-induced I_{SC} response by 99.5% ($n = 4$, $P<0.001$, Figure 2B), suggesting that both Cl⁻ and HCO₃⁻ secretion might involve transport mechanisms that depend on basolateral Na⁺.

Effect of ion channel blockers

To investigate whether the TMP-induced I_{SC} response was mediated by activation of the apical anion channel, different anion channel blockers were used. As shown in Figure 3, the TMP-induced I_{SC} was completely inhibited by apical application of glibenclamide (1 mmol/L, $n = 9$), which has previously been shown to block CFTR^[25] or DPC (2 mmol/L, $n = 10$, data not shown). However, the TMP-induced I_{SC} response was not sensitive to apical addition of DIDS (100, 500 μmol/L, and 1 mmol/L, $n = 5$), known to block the Ca²⁺-activated Cl⁻ channel.

Amiloride, an inhibitor of the epithelial Na⁺ channel, was also used to assess the involvement of Na⁺ absorption. In our preparation of rat colonic mucosa, a small amount of amiloride-sensitive current was observed under basal conditions. However, we did not detect any decrement of TMP-induced I_{SC} response following apical amiloride (0.1 mmol/L) pretreatment ($n = 7$, Figure 2B).

Involvement of the second messengers

To address whether [Ca²⁺]_i was involved in mediating TMP-evoked anion secretion, BAPTA-AM (100 μmol/L), a membrane-permeable selective Ca²⁺ chelator, was

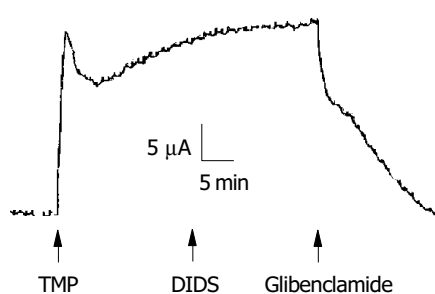


Figure 3 Effect of Cl⁻ channel blockers. Representative I_{SC} recording with arrows indicating the response to TMP (5 mmol/L, basolateral) and apical addition of channel blockers DIDS (100 mmol/L) and glibenclamide (1 mmol/L).

added bilaterally to the colonic mucosa for 45 min prior to the addition of TMP. The subsequent TMP-evoked I_{SC} was slightly reduced but not significant ($n = 6$, $P>0.05$, Figure 4).

To test whether TMP exploited the cAMP pathway, the additive effect of forskolin (10 μmol/L, $n = 7$) or IBMX (100 μmol/L, $n = 6$) was examined. As shown in Figure 5A, no further increase in I_{SC} by TMP was observed when the I_{SC} was first elicited by the adenylate cyclase (AC) activator, forskolin, or PDE inhibitor, IBMX. Similarly, little or reduced forskolin or IBMX-induced I_{SC} response was observed if the I_{SC} was first activated by TMP (data not shown), indicating significant overlapping of the TMP signaling pathway with the cAMP-dependent one. This possibility was further tested by examining the effect of the protein kinase A (PKA) inhibitor, H₈₉. The I_{SC} response to TMP could be blocked by 91.7% upon bilateral pretreatment with 5 μmol/L H₈₉ ($n = 7$, Figure 5B).

It is also possible that TMP may alter arachidonic acid metabolism affecting production of prostaglandins (PG), which are also known to be a mediator of other secretagogues of intestinal secretion^[26]. Therefore, the effect of PG synthesis inhibitor, indomethacin, on TMP-induced I_{SC} increase was also determined. In the presence of basolateral indomethacin (10 μmol/L), the TMP-induced I_{SC} response reduced but substantial response remained with concentration-dependent characteristics (Figure 6). The indomethacin-insensitive TMP response could be inhibited by H₈₉ (data not shown), consistent with the involvement of the cAMP pathway.

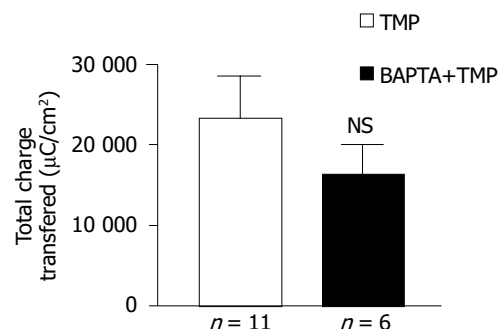


Figure 4 Effect of BAPTA-AM on TMP-evoked I_{SC} . Values are mean±SE; NS, not significant.

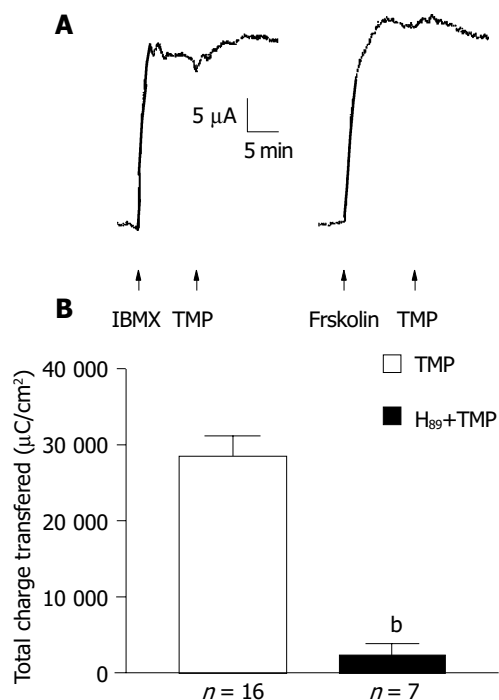


Figure 5 Involvement of cAMP in TMP-induced I_{sc} response. **A**: Representative recordings of I_{sc} response to IBMX (100 $\mu\text{mol/L}$), forskolin (10 $\mu\text{mol/L}$) without and subsequent challenge of TMP (1 mmol/L); **B**: Effect of H₈₉ (5 $\mu\text{mol/L}$) on TMP (1 mmol/L)-induced I_{sc} response. Values are mean \pm SE; ^b $P < 0.001$ vs control.

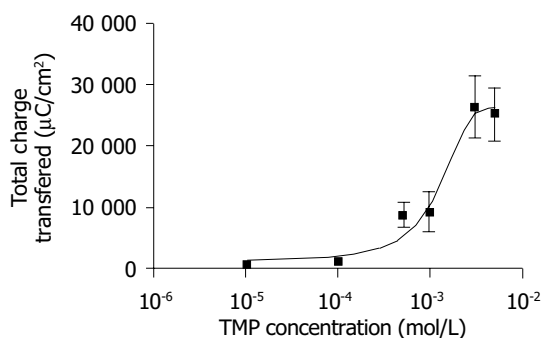


Figure 6 Concentration-response curve for TMP-induced transmembrane charges (30 min) in the presence of indomethacin (10 $\mu\text{mol/L}$). Each data point was obtained from at least four individual experiments. Values are mean \pm SE of maximal increase in charge.

Intracellular cAMP measurement

RIA was performed to study the effect of TMP on colonic epithelial intracellular cAMP levels and the results are shown in Figure 7. The intracellular cAMP content could be stimulated from a basal level of 20.0 ± 5.8 nmol/L ($n = 9$) to 45.8 ± 5.0 nmol/L ($n = 6$, $P < 0.005$) in response to AC activator forskolin (10 $\mu\text{mol/L}$), or to 48.8 ± 9.9 nmol/L ($n = 10$, $P < 0.05$) in response to TMP (1 mmol/L).

Effect of TMP on CF mouse colonic mucosa

Since CFTR is a cAMP-dependent Cl^- channel, the involvement of the cAMP-dependent pathway as shown above suggests that the secretory response elicited by TMP may be mediated by CFTR. To test this hypothesis, mutant CF mice with homozygous mutation of CFTR (-/-) were

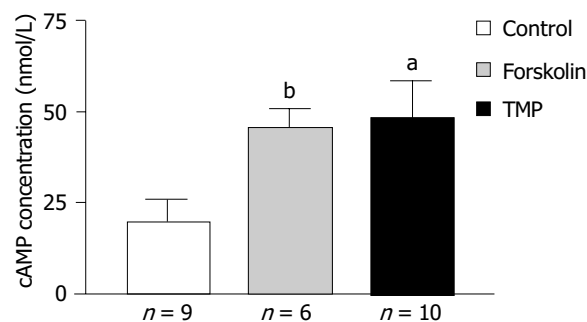


Figure 7 Effect of TMP on intracellular cAMP level. Each column represents mean \pm SE; ^a $P < 0.05$, ^b $P < 0.01$ vs control (KHS).

used and the effect of TMP on colonic mucosa was compared to that obtained from the wild type, CFTR (+/+). TMP (5 mmol/L) added to the basolateral side of the wild type colonic mucosa produced a sustained increase in I_{sc} response ($n = 3$, Figure 8A), which mimicked the forskolin-induced I_{sc} response ($n = 3$, Figure 8B). The same concentration of TMP was used to challenge colonic mucosa from CF mice and no TMP response was observed ($n = 5$, Figure 8C), neither with addition of forskolin (10 $\mu\text{mol/L}$, $n = 3$) or IBMX (100 $\mu\text{mol/L}$, $n = 3$), indicating that both TMP-induced Cl^- and HCO_3^- secretion was mediated by CFTR.

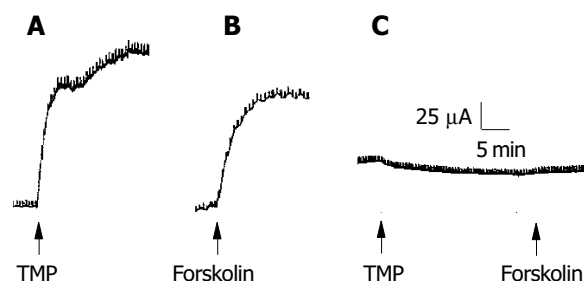


Figure 8 A-C: TMP-induced I_{sc} response in colonic mucosa of mice with CFTR wild-type and homozygous mutation.

DISCUSSION

The present study has demonstrated a stimulatory effect of TMP on colonic anion secretion but not Na^+ absorption. The TMP-induced increase in I_{sc} is not considered to be mediated by electrogenic Na^+ absorption because it was not inhibited by apical addition of amiloride, the epithelial sodium channel blocker, or by Na^+ removal from apical side. Previous studies have also shown that isolated rat distal colon is largely devoid of electrogenic Na^+ transport^[27]. However, replacement of extracellular Cl^- and HCO_3^- ions, or addition of Cl^- channel blockers, greatly attenuated the TMP-induced I_{sc} , suggesting that TMP has a primary effect on the anion secretion by the colon of rodents. It is interesting to note that both Cl^- and HCO_3^- secretions seem to be Na^+ -dependent since Na^+ removal from basolateral solution almost completely abolished the TMP-induced I_{sc} , suggesting involvement of basolateral

Na^+ -dependent transporting mechanisms, i.e., both Na^+ - HCO_3^- cotransporter^[28] and Na^+ - K^+ - 2Cl^- cotransporter^[29] are implicated in secondary active Cl^- and HCO_3^- secretion in many epithelia including the intestine.

The results of the present study suggest that CFTR is the likely candidate pathway for apical Cl^- and HCO_3^- exit since the TMP-evoked anion secretion was completely inhibited by glibenclamide and DPC, which are known to block CFTR^[25,30], but not by DIDS which has no effect on the activity and conductance of CFTR^[31]. The strong evidence indicating the involvement of CFTR came from the studies on CF mice with CFTR homozygous mutation. The complete abolition of the TMP-induced response in CFTR mutated colonic mucosa suggests that both TMP-stimulated Cl^- and HCO_3^- secretions are mediated by CFTR, which is consistent with an important role of CFTR in HCO_3^- as well as Cl^- secretion in many epithelial tissues^[32]. It is interesting to note that removing Cl^- or HCO_3^- alone from the bathing solution resulted in 58.4% and 70.8% attenuation in TMP-induced I_{SC} , respectively. The summated inhibition is more than 100%, suggesting interaction between the two ions, possibly during their transport by CFTR. The phenomena that the presence of one ion interferes with the transport of another ion have been previously reported to be associated with CFTR^[33]. In native guinea pig pancreatic duct cells, CFTR is between 3-5 times more selective for Cl^- over HCO_3^- ; however, extracellular HCO_3^- significantly inhibits CFTR current carried by Cl^- . The interaction between Cl^- and HCO_3^- secretion may also have physiological bearing in the colon, the details of which, especially the role of CFTR, remain to be elucidated.

The involvement of CFTR also suggests that the effect of TMP is mediated primarily by the cAMP-dependent pathway since CFTR is a cAMP-activated Cl^- channel^[34] and mainly responsible for cAMP-dependent anion secretion^[35]. The amount of cAMP available to activate PKA to phosphorylate CFTR is determined by the balance between cAMP production by AC and cAMP hydrolysis by PDE^[36]. cAMP can be stimulated either by activation of AC or inhibition of PDE. The observation that TMP failed to further increase the I_{SC} , or lack of additive effect after a maximal stimulation with forskolin (AC activator) or IBMX (PDE inhibitor) suggests that the signaling pathway mediating the effect of TMP may overlap with the cAMP pathway. These indicate that TMP, forskolin and IBMX share a common intracellular pathway (i.e., a rise in $[\text{cAMP}]_i$). This notion is further supported by the inhibition of the TMP responses by H_{89} , an inhibitor of PKA, which is the primary target for intracellular cAMP. The present results obtained from RIA studies demonstrate an enhancement of intracellular cAMP by TMP in the rat colon.

While there is no question about the involvement of cAMP in mediating the TMP effect, how TMP activates intracellular cAMP remains to be elucidated. Previous studies reported that the antiplatelet activity of TMP is due to the enhancement of intracellular cAMP by acting as a PDE inhibitor^[19]. Although we do not have any substantial evidence to support this, the asymmetrical I_{SC} response to apical and basolateral challenge of TMP suggests differential distribution of the component(s) of the signaling pathway

involved. In this regard, it is interesting to note that PDE subtypes are differently localized in the apical and basolateral membrane domains of T_{84} colonic epithelial cells^[8]. Therefore, the more potent effect of TMP observed when applied to the basolateral membrane can be explained by the presence of greater amount of a certain PDE subtype in the basolateral domain of the colonic mucosa, if TMP is indeed acting as a PDE inhibitor. Further studies along this line are necessary in order to understand the detail mechanism of cAMP activation by TMP.

It should be mentioned that while the TMP effect does not appear to involve the enteric nervous system, portion of the TMP effect could be blocked by indomethacin, an inhibitor of PG synthesis, indicating the involvement of PG which is well known for its function as the mediator of other secretagogues and acts by stimulating AC in the intestinal epithelium^[37]. The present studies also demonstrate that both the indomethacin-sensitive and indomethacin-insensitive TMP response could be blocked by H_{89} indicating the involvement of cAMP in both cases. Therefore, TMP may indirectly activate cAMP via PG, apart from its possible direct action as a PDE inhibitor.

Although previous studies demonstrating effects of TMP on cardiac vascular function^[17] have suggested its action on the Ca^{2+} pathway, the present results suggest that TMP acts primarily on the cAMP but not on the Ca^{2+} pathway, at least for the concentration range used in the present study. However, it should be noted that the treatment with BAPTA-AM in the present study did appear to reduce the TMP response although the effect was not significant. Therefore, TMP might have a minor action on the Ca^{2+} -dependent pathway, which may also be TMP concentration dependent. We have preliminary data indicating increased Ca^{2+} involvement with increased TMP concentrations. Further studies using direct Ca^{2+} measurement may be required to clarify this.

The effect of TMP on colonic anion secretion by a primary action on the cAMP pathway is consistent with our previous studies with Bak Foong Pills, indicating that TMP may be an active compound responsible for mediating the stimulatory effect of Bak Foong Pills on colonic anion secretion previously observed^[15]. Since Cl^- secretion is the main driving force for fluid secretion across the colon^[9], and HCO_3^- secretion at the luminal surface is considered to have a decisive influence on a constant pH microclimate sustenance^[38], the ability of TMP to enhance the secretion of these anions secretion may have implications in future development of alternative treatment for constipation. Most importantly, as an active compound of many popular traditional Chinese medicines, TMP has been in clinical use with trivial side effects and few clinically relevant drug interactions reported. Taken together, TMP may have therapeutic potential for treatment of constipation caused by disturbance of electrolyte and fluid transport in the GI tract.

REFERENCES

- 1 Pan G, Lu S, Ke M, Han S, Guo H, Fang X. Epidemiologic study of the irritable bowel syndrome in Beijing: stratified randomized study by cluster sampling. *Chin Med J* 2000; **113**: 35-39

- 2 **Bommelaer G**, Dorval E, Denis P, Czernichow P, Frexinos J, Pelc A, Slama A, El Hasnaoui A. Prevalence of irritable bowel syndrome in the French population according to the Rome I criteria. *Gastroenterol Clin Biol* 2002; **26**: 1118-1123
- 3 **Belai A**, Wheeler H, Burnstock G. Innervation of the rat gastrointestinal sphincters: Changes during development and aging. *Int J Dev Neurosci* 1995; **13**: 81-95
- 4 **Burleigh DE**. Evidence for a functional cholinergic deficit in human colonic tissue resected for constipation. *J Pharm Pharmacol* 1988; **40**: 55-57
- 5 **Dawson DC**. Ion channels and colonic salt transport. *Annu Rev Physiol* 1991; **53**: 321-339
- 6 **Sood R**, Bear C, Auerbach W, Reyes E, Jensen T, Kartner N, Riordan JR, Buchwald M. Regulation of CFTR expression and function during differentiation of intestinal epithelial cells. *EMBO J* 1992; **11**: 2487-2494
- 7 **Strong TV**, Boehm K, Collins FS. Localization of cystic fibrosis transmembrane conductance regulator mRNA in the human gastrointestinal tract by *in situ* hybridization. *J Clin Invest* 1994; **93**: 347-354
- 8 **O'Grady SM**, Jiang X, Maniak PJ, Birmachew W, Scribner LR, Bulbulian B, Gullikson GW. Cyclic AMP-dependent Cl secretion is regulated by multiple phosphodiesterase subtypes in human colonic epithelial cells. *J Membr Biol* 2002; **185**: 137-144
- 9 **Kunzelmann K**, Mall M. Electrolyte transport in the mammalian colon: mechanisms and implications for disease. *Physiol Rev* 2002; **82**: 245-289
- 10 **Clarke LL**, Harline MC. Dual role of CFTR in cAMP-stimulated HCO₃⁻ secretion across murine duodenum. *Am J Physiol* 1998; **274**(4 Pt 1): G718-726
- 11 **Seidler U**, Blumenstein I, Kretz A, Viellard-Baron D, Rossmann H, Colledge WH, Evans M, Ratcliff R, Gregor M. A functional CFTR protein is required for mouse intestinal cAMP-, cGMP- and Ca²⁺-dependent HCO₃⁻ secretion. *J Physiol* 1997; **505**: 411-423
- 12 **Lencer WI**, Delp C, Neutra MR, Madara JL. Mechanism of cholera toxin action on a polarized human intestinal epithelial cell line: role of vesicular traffic. *J Cell Biol* 1992; **117**: 1197-1209
- 13 **Ewe K**. Intestinal transport in constipation and diarrhoea. *Pharmacology* 1988; **36**: 73-84
- 14 **Campillos Paez MT**, Valles Ugarte ML, San Laureano Palomero T, Perez Hernansaiz M. Constipation and laxative consumption in the elderly. *Aten Primaria* 2000; **26**: 430-432
- 15 **Zhu JX**, Chan YM, Tsang LL, Chan LN, Zhou Q, Zhou CX, Chan HC. Cellular signaling mechanisms underlying pharmacological action of Bak Foong Pills on gastrointestinal secretion. *Jpn J Physiol* 2002; **52**: 129-134
- 16 **Xu J**, Li YK, Liang ZJ. Effects of tetramethylpyrazine and ferulic acid alone or combined on vascular smooth muscle, blood viscosity and toxicity. *Zhongguo Zhongyao Zazhi* 1992; **17**: 680-682
- 17 **Liu SY**, Sylvester DM. Antiplatelet activity of tetramethylpyrazine. *Thromb Res* 1994; **75**: 51-62
- 18 **Lin LN**, Wang WT, Xu ZJ. Clinical study on ligustrazine in treating myocardial ischemia and reperfusion injury. *Zhongguo Zhongxiyijiehe Zazhi* 1997; **17**: 261-263
- 19 **Lin CI**, Wu SL, Tao PL, Chen HM, Wei J. The role of cyclic AMP and phosphodiesterase activity in the mechanism of action of tetramethylpyrazine on human and dog cardiac and dog coronary arterial tissues. *J Pharm Pharmacol* 1993; **45**: 963-966
- 20 **Kenyon JL**, Gibbons WR. Effects of low-chloride solutions on action potentials of sheep cardiac Purkinje fibers. *J Gen Physiol* 1977; **70**: 635-660
- 21 **Snouwaert JN**, Brigman KK, Latour AM, Malouf NN, Boucher RC, Smithies O, Koller BH. An animal model for cystic fibrosis made by gene targeting. *Science* 1992; **257**: 1083-1088
- 22 **Ussing HH**, Zerahn K. Active transport of sodium as the source of electric current in the short-circuited isolated frog skin. *Acta Physiol Scand* 1951; **23**: 110-127
- 23 **Strabel D**, Diener M. Evidence against direct activation of chloride secretion by carbachol in the rat distal colon. *Eur J Pharmacol* 1995; **274**: 181-191
- 24 **Andres H**, Rock R, Bridges RJ, Rummel W, Schreiner J. Submucosal plexus and electrolyte transport across rat colonic mucosa. *J Physiol* 1985; **364**: 301-312
- 25 **Schultz BD**, DeRoos AD, Venglarik CJ, Singh AK, Frizzell RA, Frizzell RA, Bridges RJ. Glibenclamide blockade of CFTR chloride channels. *Am J Physiol* 1996; **271**(2 Pt 1): L192-200
- 26 **Mall M**, Bleich M, Schürlein M, Kuhr J, Seydewitz HH, Brandis M, Greger R, Kunzelmann K. Cholinergic ion secretion in human colon requires coactivation by cAMP. *Am J Physiol Gastrointest Liver Physiol* 1998; **275**(6 Pt 1): G1274-1281
- 27 **Foster ES**, Zimmerman TW, Hayslett JP, Binder HJ. Corticosteroid alteration of active electrolyte transport in rat distal colon. *Am J Physiol* 1983; **245**(5 Pt 1): G668-675
- 28 **Bachmann O**, Rossmann H, Berger UV, Colledge WH, Ratcliff R, Evans MJ, Gregor M, Seidler U. cAMP-mediated regulation of murine intestinal/pancreatic Na⁺/HCO₃⁻ cotransporter subtype pNBC1. *Am J Physiol Gastrointest Liver Physiol* 2003; **284**: 37-45
- 29 **Haas M**, Forbush B. The Na⁺-K⁺-Cl⁻ cotransporter of secretory epithelia. *Annu Rev Physiol* 2000; **62**: 515-534
- 30 **Ito Y**, Mizuno Y, Aoyama M, Kume H, Yamaki K. CFTR-Mediated anion conductance regulates Na⁺-K⁺-pump activity in Calu-3 human airway cells. *Biochem Biophys Res Commun* 2000; **274**: 230-235
- 31 **Greger R**. Role of CFTR in the colon. *Annu Rev Physiol* 2000; **62**: 467-491
- 32 **Geibel JP**, Singh S, Rajendran VM, Binder HJ. HCO₃⁻ secretion in the rat colonic crypt is closely linked to Cl⁻ secretion. *Gastroenterology* 2000; **118**: 101-107
- 33 **Gray MA**, O'Reilly C, Winpenny J, Argent B. Functional interactions of HCO₃⁻ with cystic fibrosis transmembrane conductance regulator. *JOP* 2001; **2**: 207-211
- 34 **Dalemans W**, Barbry P, Champigny G, Jallat S, Dott K, Dreyer D, Crystal RG, Pavirani A, Lecocq JP, Lazdunski M. Altered chloride ion channel kinetics associated with the F508 cystic fibrosis mutation. *Nature* 1991; **354**: 526-528
- 35 **Barrett KE**, Keely SJ. Chloride secretion by the intestinal epithelium: molecular basis and regulatory aspects. *Annu Rev Physiol* 2000; **62**: 535-572
- 36 **Kopito RR**. Biosynthesis and degradation of CFTR. *Physiol Rev* 1999; **79**(1 Suppl): S167-173
- 37 **Craven PA**, DeRubertis FR. Stimulation of rat colonic mucosal prostaglandin synthesis by calcium and carbamylcholine: relationship to alterations in cyclic nucleotide metabolism. *Prostaglandins* 1981; **21**: 65-81
- 38 **Genz AK**, v Engelhardt W, Busche R. Maintenance and regulation of the pH microclimate at the luminal surface of the distal colon of guinea-pig. *J Physiol* 1999; **517**: 507-519

• BASIC RESEARCH •

Procedure for preparing peptide-major histocompatibility complex tetramers for direct quantification of antigen-specific cytotoxic T lymphocytes

Xian-Hui He, Li-Hui Xu, Yi Liu

Xian-Hui He, Key Laboratory of Ministry of Education of China for Tissue Transplantation and Immunology, Jinan University, Guangzhou 510632, Guangdong Province, China
Li-Hui Xu, Institute of Bioengineering, Jinan University, Guangzhou 510632, Guangdong Province, China

Yi Liu, Department of Dermatology, First Affiliated Hospital, Zhengzhou University, Zhengzhou 450052, Henan Province, China
Supported by the National Natural Science Foundation of China, No. 30230350 and No. 30371651, and Major State Basic Research Development Program of China, 973 Program, No. G2000057006
Correspondence to: Dr. Xian-Hui He, Key Laboratory of Ministry of Education of China for Tissue Transplantation and Immunology, Jinan University, 601 Huangpu Road West, Guangzhou 510632, Guangdong Province, China. thehx@jnu.edu.cn
Telephone: +86-20-85220679 Fax: +86-20-85221337
Received: 2004-08-18 Accepted: 2004-11-19

Abstract

AIM: To establish a simplified method for generating peptide-major histocompatibility complex (MHC) class I tetramers.

METHODS: cDNAs encoding the extracellular domain of human lymphocyte antigen (HLA)-A*0201 heavy chain (A2) and β_2 -microglobulin (β_2m) from total RNA extracted from leukocytes of HLA-A2⁺ donors were cloned into separate expression vectors by reverse transcription-polymerase chain reaction. The recombinant A2 and β_2m proteins were expressed in *Escherichia coli* strain BL21(DE3) and recovered from the inclusion body fraction. Soluble A2 proteins loaded with specific antigen peptides were refolded by dilution from the heavy chain in the presence of light chain β_2m and HLA-A2-restricted peptide antigens. The refolded A2 monomers were biotinylated with a commercial biotinylation enzyme (BirA) and purified by low pressure anion exchange chromatography on a Q-Sepharose (fast flow) column. The tetramers were then formed by mixing A2 monomers with streptavidin-PE in a molar ratio of 4:1. Flow cytometry was used to confirm the expected tetramer staining of CD8⁺ T cells.

RESULTS: Recombinant genes for HLA-A*0201 heavy chain (A2) fused to a BirA substrate peptide (A2-BSP) and mature β_2m from HLA-A2⁺ donor leukocytes were successfully cloned and highly expressed in *E. coli*. Two soluble monomeric A2-peptide complexes were reconstituted from A2-BSP in the presence of β_2m and peptides loaded with either human cytomegalovirus pp65₄₉₅₋₅₀₃ peptide (NLVPMVATV, NLV; designated as A2-NLV) or influenza virus matrix

protein Mp58-66 peptide (GILGFVFTL, GIL; designated as A2-GIL). Refolded A2-NLV or A2-GIL monomers were biotinylated and highly purified by single step anion exchange column chromatography. The tetramers were then formed by mixing the biotinylated A2-NLV or A2-GIL monomers with streptavidin-PE, leading to more than 80% multiplication as revealed by SDS-PAGE under non-reducing, unboiled conditions. Flow cytometry revealed that these tetramers could specifically bind to CD8⁺ T cells from a HLA-A2⁺ donor, but failed to bind to those from a HLA-A2⁻ donor.

CONCLUSION: The procedure is simple and efficient for generating peptide-MHC tetramers.

© 2005 The WJG Press and Elsevier Inc. All rights reserved.

Key words: Major histocompatibility complex; HLA-A2; Tetramers; Cytomegalovirus; Immune responses; Cytotoxic T lymphocytes

He XH, Xu LH, Liu Y. Procedure for preparing peptide-major histocompatibility complex tetramers for direct quantification of antigen-specific cytotoxic T lymphocytes. *World J Gastroenterol* 2005; 11(27): 4180-4187

<http://www.wjgnet.com/1007-9327/11/4180.asp>

INTRODUCTION

Cytotoxic T lymphocytes (CTLs), or CD8⁺ T cells, play a critical role in the clearance of viral infections and the eradication of tumors^[1]. A better understanding of cellular immunity against viruses and/or tumor cells requires careful analysis of the responding CD8⁺ T cells, particularly in terms of their numbers and effector functions^[2]. Because specific CD8⁺ T cells are often vastly outnumbered by irrelevant T cells, quantification of antigen-specific T cells often requires *in vitro* culture and re-stimulation, which may introduce bias in the results^[2]. The standard method for deriving specific CTL frequency information is limiting dilution analysis (LDA)^[2]. However, accumulating evidence indicates that this technique may significantly underestimate the number of specific CTLs, because it does not detect cells that lack proliferative potential^[2,3]. This limitation has been overcome by the introduction of peptide-major histocompatibility complex (MHC) class I tetrameric complex technology^[3-6], which initiates a profound revolution in the field of cellular immunology^[7-10]. Peptide-MHC tetramer-based assays have enabled direct flow cytometric quantification^[3-6], phenoty-

ping^[3,8-11] and even functional analysis^[8,11] of antigen-specific CD8⁺ T cells. Thus, peptide-MHC tetramer technology is a powerful tool for evaluating the fundamental aspects of T-cell immunity.

Though tetramer technology for direct quantification of the frequency and/or function of antigen-specific CTLs has been generally accepted, wide application of tetramer strategies is limited by the complex procedures necessary for tetramer production^[3]. Moreover, the expression level of recombinant human MHC class I heavy chain in *Escherichia coli* is usually minimal due to the low translation frequency of human proteins in *E. coli*^[12]. To address these problems, we sought to develop a simplified and efficient method for production of peptide-MHC class I tetramers. We constructed prokaryotic expression vectors for recombinant human lymphocyte antigen (HLA)-A2 heavy chain and β_2m -microglobulin (β_2m) proteins, in which nucleotide residues in the translation initiation region (TIR) were substituted to the preferred codons for *E. coli*^[13] and decreased the G/C content in this region^[14]. The recombinant A2 and β_2m proteins were overexpressed in *E. coli* in the form of inclusion bodies, thus facilitating their high purity isolation by simple washing and centrifugation. Further simple procedures allowed us to establish an efficient, streamlined procedure for the preparation of HLA-A2 tetramers. This improved procedure should facilitate the general application of tetramer technology in both basic research and clinical applications.

MATERIALS AND METHODS

Materials

E. coli strain DH5 α was stored in our laboratory. *E. coli* strain BL21(DE3) and plasmid pET-3c were purchased from Novagen (Madison, WI, USA). *Nde*I, *Bam*HI, T4 DNA ligase and high fidelity DeepVent Taq polymerase were purchased from New England Biolabs (Beverly, MA, USA). The TRIzol reagent and ThermoScript reverse transcription-polymerase chain reaction (RT-PCR) system were obtained from Invitrogen (Carlsbad, CA, USA). Q-Sepharose (fast flow) was obtained from Amersham (Uppsala, Sweden). Mouse anti-human monoclonal antibodies CD3-FITC, CD8-CyChrome and HLA-A2-FITC were purchased from PharMingen (San Diego, CA, USA). Streptavidin R-phycoerythrin (PE) conjugate (streptavidin-PE) was purchased from Molecular Probes (Eugene, OR, USA). Protein molecular mass markers were obtained from Sigma (St. Louis, MO, USA). The biotinylation enzyme, BirA, was purchased from Avidity (www.avidity.com). The NLVPMVATV (NLV) peptide derived from pp65 (pp65₄₉₅₋₅₀₃) of HCMV^[11], and the GILGFVFTL (GIL) peptide derived from the matrix protein (Mp₅₈₋₆₆) of the influenza A virus^[15], were synthesized by BioAsia (Shanghai, China) and purified to >98%. All other chemicals were from Sigma and were analytically pure.

Cloning of HLA-A*0201 heavy chain and β_2m cDNAs

Heparinized human peripheral blood was collected from three HLA-A2 positive (identified by anti-human HLA-A2-FITC staining and flow cytometric analysis) donors by venipuncture. Total RNA was extracted from freshly isolated

PBMCs using the TRIzol reagent. cDNAs were synthesized from the isolated RNA using the ThermoScript RT-PCR system according to the recommended procedure. PCR amplification of the resultant cDNA was performed in a total volume of 50 μ L containing high fidelity DeepVent Taq polymerase. For amplification of β_2m , PCR was performed with an initial denaturation for 2 min at 94 °C, followed by 35 cycles of 94 °C for 30 s, 55 °C for 30 s and 72 °C for 1 min, and a final extension for 10 min at 72 °C. The primers (5'-ATA TCC ATA TGT CTC GCT CCG TGG CCT TAG-3' and 5'-AAC TAG GGA TCC TTA CAT GTC TCG ATC CCA C-3') were designed to amplify the entire coding sequence of human β_2m cDNA. For amplification of the mature HLA-A*0201 heavy chain, PCR was performed as above except that the extension time at 72 °C was 1.5 min and the primers (5'-TAT ACA TAT GGG CTC TCA CTC CAT GAG GTA TTT C-3' and 5'-AAC CAG GGA TCC TAC ACT TTA CAA GCT GTG AGA G-3') were designed to amplify the entire coding sequence of mature A2. The resultant PCR products were cloned into the *Nde*I-*Bam*HI sites of the pET-3c vector. Randomly selected clones were *Nde*I/*Bam*HI digested and screened for the presence of a correctly sized insert. Several independent clones were submitted for DNA sequencing of the HLA-A*0201 heavy chain cDNA using the dye-labeled deoxy-terminator protocol on a 377 automated DNA sequencer (Applied Biosystems). The cloned β_2m cDNA was also confirmed by DNA sequencing analysis.

Construction of expression vector for mature β_2m

To create a β_2m expression construction with optimized codon usage and G/C content, the DNA fragment for mature β_2m was PCR amplified from the cloned β_2m cDNA using specific primers (5'-AT ATC CAT ATG ATT CAA CGT ACT CCA AAA ATT CAA GTT TAC TCA CGT CAT CC-3' and 5'-CGA CTG GAT CCT TAC ATG TCT CGA TCC CAC TTA AC-3'). The underlined codons were optimized for expression in *E. coli*^[13] by synonymous substitutions from ATC, CAG, AAG, CAG to ATT, CAA, AAA and CAA, respectively. These alterations also reduced the G/C content in the TIR. The resulting PCR product was inserted into the *Nde*I-*Bam*HI sites of the pET-3c vector, and a positive clone with a correct sized insert was confirmed by DNA sequencing. This recombinant plasmid was designated as pET- β_2m .

Construction of expression vector for extracellular domain of HLA-A2 heavy chain fused with BirA substrate peptide (BSP)

To construct an expression vector in which the HLA-A2 heavy chain was fused with BSP, the DNA fragment encoding a Gly-Ser linker and a BSP (LHHILDAQKMWVWVNR) was fused to the 3' end of the cDNA encoding the extracellular domain of the HLA-A2 heavy chain (1-275) by PCR amplification from cloned HLA-A2 heavy chain cDNA with specific primers (5'-ATA CAT ATG GGT TCT CAT TCT ATG CGT TAT TTT TTT ACA TCT GTT TCC CGG CCC GGC CGC-3' and the 3' primer 5'-GCG CGG ATC CTT AAC GAT GAT TCC ACA CCA TTT TCT GTG CAT CCA GAA TAT GAT GCA GAG AGC CCG GCT CCC ATC TCA GGG T-3'). The underlined codons were

optimized for expression in *E. coli*^[13], and reduced the G/C content without any changes in amino acid sequence. These codons were changed from GGC, CAC, TCC, AGG, TTC, TTC, TCC and GTG, respectively. The resultant PCR product was *NdeI/BamHI* digested and subcloned into plasmid pET-3c. Clones with correct sized inserts were verified by direct sequencing, and the recombinant plasmid was designated as pET-A2-BSP.

Expression and isolation of recombinant A2-BSP and β_2m proteins

BL21(DE3) competent cells were transformed with either pET- β_2m or pET-A2-BSP, single colonies were used to inoculate 100 mL of LB medium, and cultures were incubated at 37 °C overnight until cells reached the stationary phase. Each stationary culture was diluted 10-fold with fresh LB medium (to 1 L) and incubated at 37 °C for a further 2 h, 0.4 mmol/L isopropyl β -D-thiogalactopyranoside (IPTG) was added, and cells were incubated for an additional 4 h. Cells were collected by centrifugation, and insoluble protein aggregates (inclusion bodies) were purified essentially as described^[16]. In brief, each cell pellet was re-suspended in 50 mmol/L Tris-HCl buffer (pH 8.0) containing 1 mmol/L EDTA, 0.1 mmol/L phenylmethylsulfonyl fluoride (PMSF) and 10 mmol/L dithiothreitol (DTT), and then sonicated on ice. The insoluble pellet was collected by centrifugation and washed with washing buffer (50 mmol/L Tris-HCl pH 8.0, 100 mmol/L NaCl, 1 mmol/L EDTA, 1 mmol/L DTT and 5 g/L Triton X-100), followed by three more rounds of sonication, centrifugation and collection. The pellet was washed three more times with washing buffer without Triton X-100 and the isolated inclusion body pellet was dissolved in 20 mmol/L 2-(N-morpholino)ethanesulfonic acid (pH 6.0, containing 8 mol/L urea, 10 mmol/L EDTA, and 0.1 mmol/L DTT). The insoluble material was pelleted by centrifugation and removed. The protein concentration of the remaining solution was determined by measuring $A_{280\text{ nm}}$ and $A_{260\text{ nm}}$, and calculated according to the empirical formula ($1.45 \times A_{280\text{ nm}} - 0.74 \times A_{260\text{ nm}} = \text{protein concentration in mg/mL}$). The protein solution was immediately frozen at -70 °C.

Refolding of monomeric HLA-A2

The HLA-A2 monomers were refolded essentially as described by Garboczi and Wiley^[17], with slight modifications. Briefly, 2 mg of peptide (NLV or GIL peptide) dissolved in DMSO was added in drops to 200 mL of pre-chilled refolding buffer (100 mmol/L Tris-HCl pH 8.0, containing 400 mmol/L L-arginine, 2 mmol/L EDTA, 5 mmol/L reduced glutathione, 0.5 mmol/L oxidized glutathione and 0.2 mmol/L PMSF). Then, 6 mg A2-BSP in 1 mL injection buffer containing 3 mol/L guanidine-HCl pH 4.2, 10 mmol/L sodium acetate and 10 mmol/L EDTA was forcefully injected to the stirring reaction through a 26-gauge needle as close to the stir bar as possible. Five micrograms of β_2m was injected similarly, and the refolding mixture was incubated at 10 °C for 3 d. At the end of the incubation, 200 mL of the refolding mixture was concentrated to 5 mL with an ultrafiltration apparatus (Amicon, Millipore, Bedford, MA, USA) containing a 10 ku molecular mass cut-off membrane,

and dialyzed against 10 mmol/L Tris-HCl buffer (pH 8.0, containing 0.2 mmol/L PMSF). The refolded monomeric HLA-A2 was centrifuged to eliminate precipitates, and then biotinylated.

Biotinylation and purification of monomeric HLA-A2

The refolded HLA-A2 was enzymatically biotinylated by incubation with BirA according to the procedure provided by the supplier (Avidity Co.). The biotinylated HLA-A2 was dialyzed against 10 mmol/L Tris-HCl buffer (pH 8.0, containing 0.2 mmol/L PMSF) and loaded onto an anion-exchanger Q-Sepharose column (2 cm×8 cm) equilibrated with the same buffer. The column was eluted with a 0-300 mmol/L NaCl linear gradient, and 1.5 mL fraction was collected. Fractions exhibiting both HLA-A2 heavy chain and β_2m bands upon SDS-PAGE analysis were pooled and concentrated to 300 μ L. The buffer of the biotinylated HLA-A2 was changed to 0.01 mol/L phosphate-buffered saline (PBS, pH 7.4) containing 0.2 mmol/L PMSF and 2 mmol/L EDTA through ultrafiltration.

Tetramerization of soluble HLA-A2 monomers

HLA-A2 tetramers were formed by mixing the biotinylated proteins with streptavidin-PE at a molar ratio of 4:1. Tetramers were analyzed by SDS-PAGE of samples prepared without boiling, in a loading buffer that contained no reducing reagent^[10].

Tetramer staining and flow cytometry

Peripheral blood mononuclear cells (PBMCs) were separated from 3 mL whole blood of two volunteers (over 40 years) by centrifugation over a Ficoll-Hypaque density gradient (Lymphoprep; NYCOMED, Norway). For staining, 1×10^6 cells suspended in 50 μ L PBS containing 20 mL/L fetal calf serum and 1 g/L sodium azide were incubated on ice for 1 h with 10 μ L of CD3-FITC, 10 μ L of CD8-CyChrome and 1 μ g of HLA-A2 tetramer. After being washed, the cells were fixed in 300 μ L of 10 g/L paraformaldehyde and detected on a FACSCalibur flow cytometer (Becton Dickinson, San Jose, CA, USA). For each sample, 50 000 events were collected and analyzed with the CELLQuest software (Becton Dickinson). The results were expressed as the percentages of tetramer-binding cells in the total T cell population.

RESULTS

Cloning of cDNA for HLA-A*0201 heavy chain and β_2m

The cDNA encoding the mature HLA-A2 heavy chain was RT-PCR amplified from total RNA of three HLA-A2 positive donors (identified as such by flow cytometry after anti-HLA-A2-FITC staining). The DNA fragments with the expected length (1 100 bp) were inserted into pET-3c, and eight independently transformed DH5a clones were identified to have the correct insert (Figure 1). DNA sequencing of these clones showed that six clones from donors 1 and 2 contained the cDNA for HLA-A*0201 heavy chain (designated pET-A2), while those from donor 3 contained the cDNA for HLA-A*0207 heavy chain. The cDNA sequence for HLA-A*0201 was submitted to GenBank (accession number AY191309).

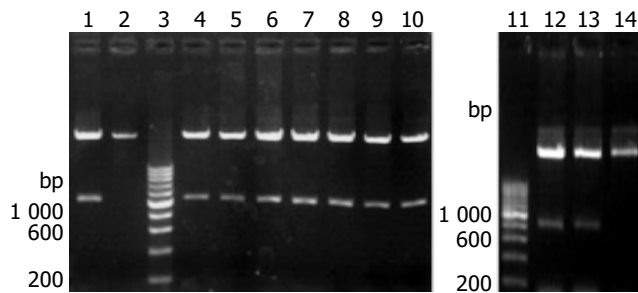


Figure 1 Identification of clones with correct sized inserts, using *NdeI/BamHI* double digestion. Lanes 1 and 4-8: pET-A2 clones from donors 1 and 2; lanes 2 and 14: pET-3c; lanes 3 and 11: 200-bp DNA ladder; lanes 9 and 10: pET-A2 clones from donor 3; lanes 12 and 13: pET-A2-BSP.

Similarly, the cDNA encoding β_2m was cloned from the total RNA of one donor and inserted into pET-3c (data not shown). The sequence was verified by DNA sequencing and found to be identical to the published one (submitted to GenBank, accession number AY187687).

Construction of expression vectors for recombinant A2-BSP and β_2m proteins

According to Altman's strategy^[3], the DNA fragment encoding a Gly-Ser linker and a BSP (LHHILDAQKMVWNHR) was fused to the 3' end of the DNA fragment encoding the extracellular domain of HLA-A*0201 heavy chain (residues from 1 to 275) by PCR amplification of plasmid pET-A2. In order to increase the expression level in *E. coli*, our primers introduced synonymous substitutions at the 5' region, intended to reduce the G/C content of the TIR and to optimize codons for the bias usage of *E. coli*^[13,14]. The amplified DNA fragment (900 bp) was inserted into pET-3c. Two clones with the correct insert were confirmed by DNA sequencing, and the generated expression vector was designated as pET-A2-BSP (Figure 1).

The expression vector for mature β_2m was similarly constructed by PCR amplification using cloned β_2m cDNA as template. The codons at the 5' region were optimized for better expression of β_2m in *E. coli*. The sequence of the insert was verified by DNA sequencing, and the vector was designated as pET- β_2m .

Refolding and biotinylation of monomeric HLA-A2

The expression vectors pET-A2-BSP and pET- β_2m were transformed into *E. coli* BL21(DE3). The cells showed leaky expression of the two proteins, and the expression levels increased dramatically after induction with IPTG (Figure 2). The molecular mass of the recombinant β_2m was approximately 12 ku, which was consistent with that of native human β_2m , while the engineered A2 heavy chain-BSP fusion protein (A2-BSP) had the expected molecular mass of 33 ku. The expression levels of these two recombinant proteins accounted for more than 20% of the total cellular proteins (Figure 2). The yields were approximately 32 and 50 mg/L for A2-BSP and β_2m , respectively. Western blotting showed that the recombinant β_2m could react with antibodies against human native β_2m (data not shown). HLA-A2 heavy chain expression was not analyzed by Western blotting, because

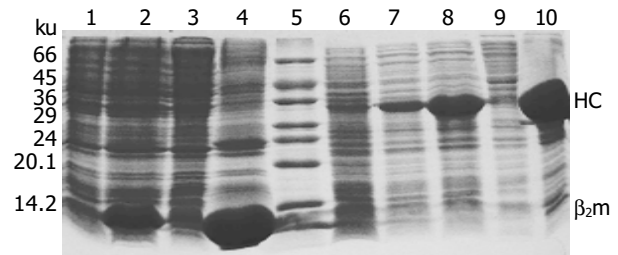


Figure 2 SDS-PAGE (150 g/L) analyses of recombinant A2-BSP and β_2m proteins expressed in *E. coli* strain BL21(DE3). Lane 1: BL21 (pET- β_2m) before IPTG induction; lane 2: BL21 (pET- β_2m)+IPTG; lane 3: supernatant of BL21 (pET- β_2m) lysate; lane 4: washed inclusion body of β_2m ; lane 5: MW marker; lane 6: BL21 (pET-3c)+IPTG; lane 7: BL21 (pET-A2-BSP) before IPTG induction; lane 8: BL21 (pET-A2-BSP)+IPTG; lane 9: supernatant of BL21 (pET-A2-BSP) lysate; lane 10: washed inclusion body of A2-BSP. HC: heavy chain.

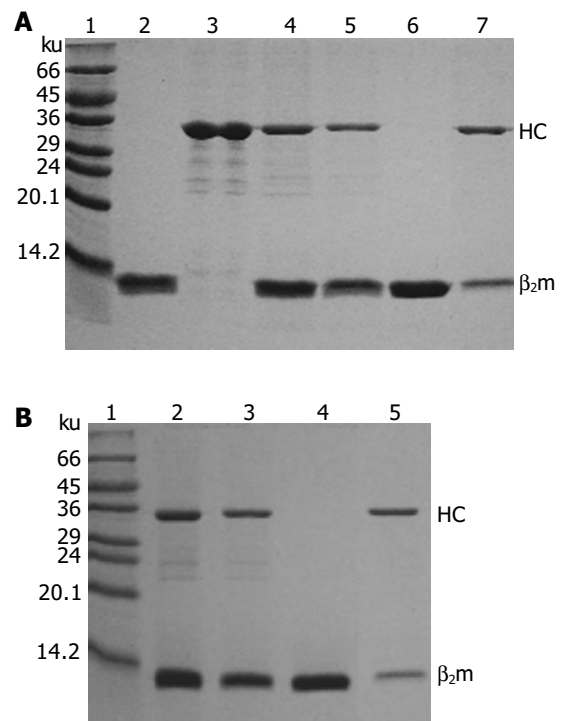


Figure 3 Analyses of refolded A2-GIL (A) and A2-NLV (B) monomers after purification and biotinylation with SDS-PAGE (150 g/L). In (A) lane 1: protein MW marker; lane 2: solubilized β_2m ; lane 3: solubilized A2-BSP; lane 4: refolded A2-GIL monomer; lane 5: biotinylated A2-GIL monomer; lane 6: peak I (β_2m) (Figure 4); lane 7: peak II (purified A2-GIL). In (B) lane 1: protein MW marker; lane 2: refolded A2-NLV monomer; lane 3: biotinylated A2-NLV monomer; lane 4: peak I (β_2m); lane 5: peak II (purified A2-NLV). HC: heavy chain.

no suitable antibody was available. Both A2-BSP and β_2m were largely expressed in the insoluble fraction (inclusion bodies), which facilitated purification through simple washing and centrifugation (Figure 3, lanes 2 and 3).

Monomeric HLA-A2 was refolded by dilution of A2-BSP and β_2m with refolding buffer in the presence of HLA-A*0201-restricted antigenic peptides. Two peptides were used to reconstitute the HLA-A2 complex. One was the immunodominant NLVPMVATV (NLV) peptide, which was derived from pp65 (pp65₄₉₅₋₅₀₃) of HCMV^[11] and used to

reconstitute the HLA-A2-NLV (hereafter referred to as A2-NLV) complex. The other was the predominant CTL epitope GILGFVFTL (GIL) peptide derived from the matrix protein (Mp₅₈₋₆₆) of influenza A virus^[15], which was used to reconstitute the HLA-A2-GIL (referred to as A2-GIL) complex. The yield of refolding was about 10-15%. The refolded A2-NLV and A2-GIL complexes appeared as two bands (A2-BSP and β_2m) on SDS-PAGE (Figure 3). After biotinylation, each complex was purified by single Q-Sepharose column chromatography. Typically, three peaks eluted from the column, as shown by monitoring of absorbance at 280 nm (Figure 4). Soluble β_2m eluted as the first peak. The second peak comprised the desired soluble HLA-A2 complex (A2-NLV or A2-GIL) consisting of a heavy chain and β_2m (Figure 3), which was of 95% purity as analyzed with the PhotoCapt Ver11.01 software (Vilber Lourmat, France). The fractions in this peak were pooled and concentrated by ultrafiltration. The third peak contained non-protein materials with a much higher absorbance at 260 nm than at 280 nm. Refolding without peptide (negative control) yielded no stable HLA-A2 complex.

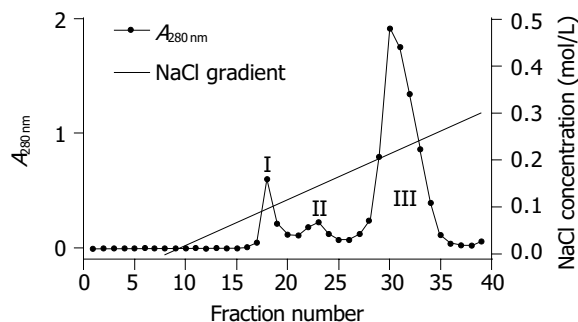


Figure 4 A typical elution profile of biotinylated HLA-A2 monomer from Q-Sepharose (fast flow) column (2 cm x 8 cm).

Formation of HLA-A2 tetramers

HLA-A2 tetramers were formed by mixing the biotinylated A2-NLV or A2-GIL monomers with streptavidin-PE at a 4:1 molar ratio. SDS-PAGE analysis of the HLA-A2 tetramers could be used to estimate the extent of tetramer formation, because the complex formed between streptavidin and biotin was stable in the absence of boiling treatment and DTT^[10]. As shown in Figure 5, the single main band observed in the lanes of monomeric A2-NLV or A2-GIL corresponded to the 33 ku heavy chain, as β_2m quickly migrated to the bottom of the gel. Software analysis (PhotoCapt Ver11.01) showed that the amount of heavy chain in the A2-NLV tetramer lane was about 10-20% of that in the lane containing monomeric HLA-A2, indicating that about 80% of the A2-NLV monomer formed multimers with streptavidin-PE. The A2-GIL tetramer showed a similar extent of multimer formation.

Staining of CTLs with HLA-A2 tetramers

Finally, the A2-NLV and A2-GIL tetramers were tested by flow cytometry for their abilities to identify HCMV- or influenza-specific CD8⁺ T cells in freshly isolated PBMCs

from HLA-A2 positive and negative donors. PBMCs were analyzed by three-color flow cytometry after A2-NLV and A2-GIL tetramer staining. Background staining was performed with streptavidin-PE instead of the tetramers.

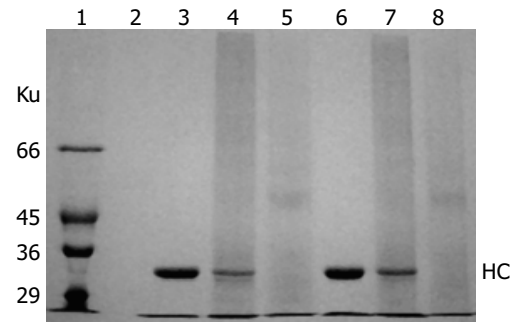


Figure 5 SDS-PAGE (75 g/L) analyses of A2-NLV and A2-GIL tetramers under non-reducing conditions without boiling. Lane 1: protein MW marker; lane 2: empty; lane 3: A2-NLV monomer (5 µg); lane 4: A2-NLV tetramer (5 µg A2-NLV monomer + 8 µg streptavidin-PE); lanes 5 and 8: streptavidin-PE (8 µg); lane 6: A2-GIL monomer (5 µg); lane 7: A2-GIL tetramer (5 µg A2-GIL monomer + 8 µg streptavidin-PE). HC: heavy chain.

Subpopulations of CD8⁺ T cells specific for either pp65₄₉₅₋₅₀₃ or Mp₅₈₋₆₆ epitopes were found in HLA-A2 positive donors by A2-NLV or A2-GIL tetramer staining. Of the total T cells, 0.19% were stained by the A2-NLV tetramer, while 0.17% bound to the A2-GIL tetramer (Figure 6). However, only 0.07% and 0.12% of T cells from the HLA-A2 negative donor were nonspecifically stained by the A2-NLV or A2-GIL tetramers, respectively, which was comparable to the control staining with streptavidin-PE (0.06%). This result suggests that these tetramers are quite specific for MHC-restricted T cells.

DISCUSSION

As the current method of limiting dilution assay (LDA) tends to underestimate CTL frequency^[2,3], other methods have been sought for the quantification of antigen-specific CD8⁺ T cells in immune responses. T cell antigen receptors (TCR) expressed on CD8⁺ T cells can recognize peptide-MHC complexes, the specific ligands on the antigen-presenting cells (APCs). Therefore, direct staining of CD8⁺ T cells with their soluble cognate ligands should be an ideal approach. However, the strategy initially failed because soluble monomeric peptide-MHC complexes have low affinities for the T-cell receptor (TCR)^[1-3]. This obstacle has been overcome by Altman *et al.*^[3]. Tetramer reagents have been shown to bind specifically to cognate T cells in numerous systems, allowing fast and direct quantification of antigen-specific T cells by flow cytometry^[3,4,8,9,18-20]. Thus, tetramer-based assays have become a powerful new technology for detecting antigen-specific T cells^[4,8,21]. However, the general application of this strategy is limited by the complex, labor intensive protocols required for preparing specific peptide-MHC tetramers.

It is difficult to prepare a large amount of MHC class I heavy chain, because the translation efficiency in *E. coli* is very

low. However, optimization of codons in the TIR has been shown to increase translation efficiency^[14]. Sato *et al.*^[12], found that the expression of wild type HLA-A*2402 heavy chain in *E. coli* is undetectable, whereas a synonymous mutant in which the TIR mammalian usage codons are replaced by those of *E. coli*, can be expressed at high levels. Lakey *et al.*^[22], showed that the production of recombinant mycobacterial proteins increases 54-fold following selective replacement of low-usage *E. coli* codons in mycobacterial proteins with high-usage *E. coli* codons. In addition, the high G/C content in the TIR can block the expression of human proteins in *E. coli*^[14]. The previous paper did not include a detailed description of the expression vector or *E. coli* system, instead of referring readers to the system used by Garboczi^[17], in which no codon or G/C content changes were described. In the present study, recombinant proteins were expressed largely in the form of inclusion bodies, which greatly facilitated isolation and purification of the refolded peptide-MHC complexes, thus simplifying the tetramer preparation procedure. In addition to the difficulty in obtaining a large amount of MHC heavy chain, the practical application of tetramers is also limited by the complexity of the necessary

preparation procedures. In this study, we reconstituted the monomeric HLA-A2 complexes based on the dilution strategy described by Garboczi^[17]. After biotinylation, the HLA-A2 monomer could be highly purified by single step ion-exchange chromatography. It should be noted that the purification in the present study was carried out in a low pressure chromatography system requiring no HPLC facilities, whereas the previous protocol included three purification steps with high performance column chromatography^[3].

The results of this study indicate that the generated reagents can be used for the detection of antigen-specific T cells. Our novel procedure for generating tetramers should be applicable for preparing other HLA-A2 tetramers or for generating tetramers of other human MHC class I alleles.

Tetramer technology is primarily used to determine the frequency of antigen-specific T cells^[3-5], and has been extensively used in evaluating the dynamics of cytomegalovirus (CMV)-specific CTL responses in humans^[5-7,9,11]. It is generally believed that adults over 40 years in developing countries are almost 100% CMV positive^[9], and that the pp65₄₉₅₋₅₀₃ NLV peptide (NLVPMVATV) is the predominant CMV epitope presented by HLA-A2 molecules^[11,23]. Quantification

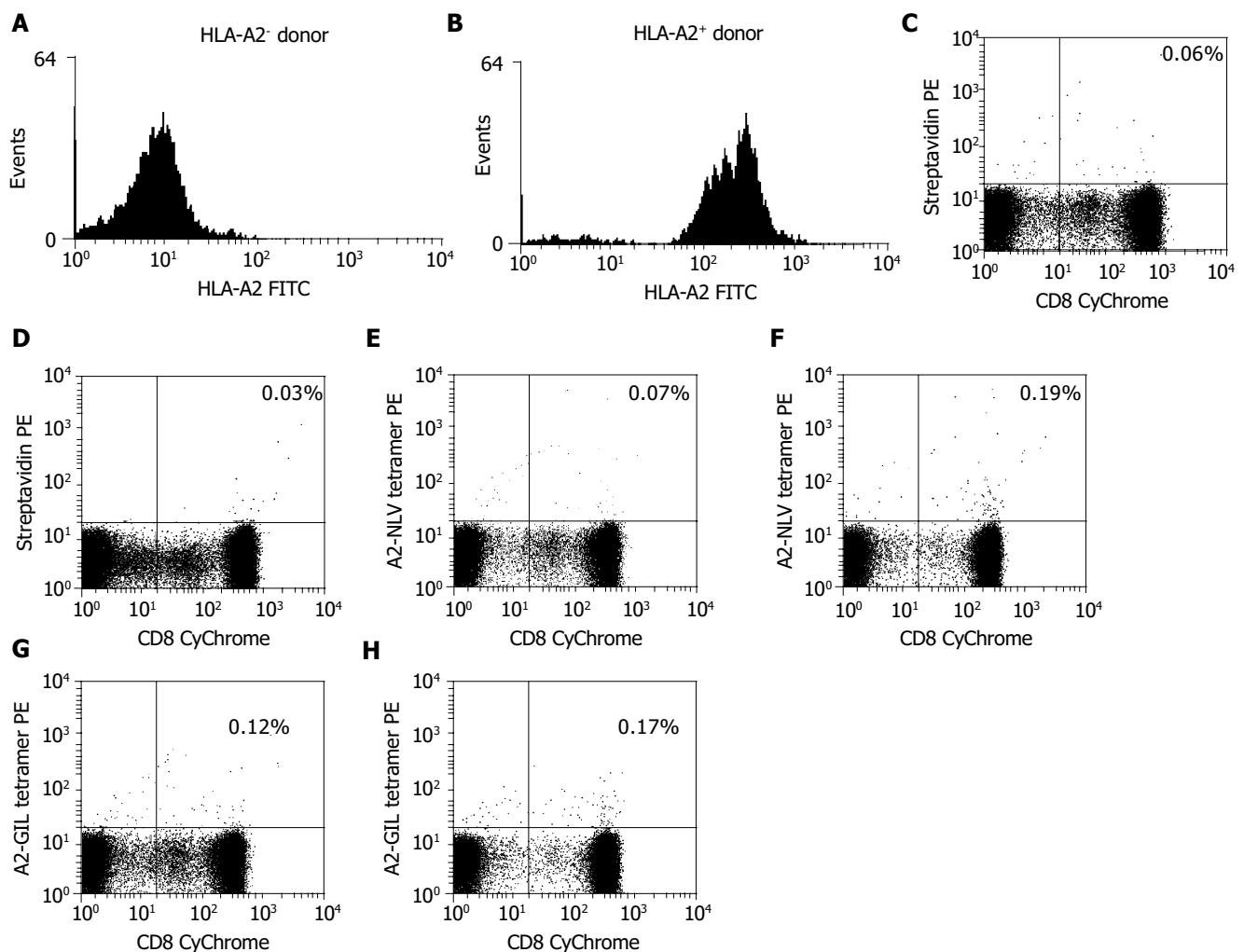


Figure 6 Flow cytometry of antigen-specific CD8⁺ T cells stained with A2-NLV tetramer (panels E and F) and A2-GIL tetramer (panels G and H) from both HLA-

A2 positive (B) and negative (A) donors. Background staining was performed with streptavidin-PE instead of the tetramers (C and D).

of specific T cells in the peripheral blood of healthy CMV carriers using an A2-NLV tetramer demonstrated that the percentage of NLV-specific CTLs in CMV carriers is about 0.02-6.19% within the CD8⁺ T cell population^[24]. In our study, tetramer staining showed that there were 0.19% NLV-specific CTLs among total T cells from the peripheral blood of a randomly selected HLA-A2-positive volunteer over 40 years, confirming again that NLV dominates the HLA-A2-restricted cellular immune response against CMV^[23]. There is substantial evidence that quantification of NLV-specific CTLs by tetramers is of clinical significance^[5-7,9,11,24,25]. Despite antiviral therapy, CMV remains an important cause of morbidity and mortality after allogeneic stem cell transplantation (SCT)^[26]. Through direct quantification of CMV-specific CD8⁺ T cells using A2-NLV tetramers, several studies demonstrated that recovery of CMV-specific CD8⁺ T cells after SCT is critical for protection against CMV disease^[6,7,25]. Accordingly, enumeration of HLA-restricted, CMV-specific CD8⁺ T cells by tetramer technology in grafts, and monitoring of these cells after SCT may constitute a rapid and sensitive tool for identifying SCT recipients at risk for developing CMV disease. Hence, tetramer technology is of value both in the development of novel transplant protocols and in clinical management of individual cases^[5-7,9,25].

It is also possible to combine tetramer staining with other flow cytometry-based assays to gain more phenotypic or even functional information on antigen-specific CTLs^[3,8,10,12]. For example, tetramer staining can be combined with intracellular detection of cytokines (e.g. interferon- γ), chemokines (e.g. macrophage inflammatory protein 1 α), and cytotoxins (e.g. perforin/granzymes) following *in vitro* antigen/mitogen stimulation to assess the functional status of tetramer-positive T cells^[27,28]. Moreover, tetramers can be used in the isolation of antigen-specific cells for characterization and even expansion of immunotherapeutic use^[11,25,29]. Conjugation of a specific tetramer with antibodies against a tumor-associated antigen has been used to redirect CMV-specific CTLs to kill tumor cells by binding to the surface of tumor cells and sensitizing them to lysis by tetramer-specific CTLs, suggesting the potential therapeutic application of tetramers^[30]. Thus, tetramer technology has opened new routes for further study of T-cell responses and tumor immunotherapy.

In summary, we have established a simplified and efficient procedure for generating peptide-MHC tetramers, a highly specific and very useful reagent with a number of important applications in cellular immune response studies. The present method may provide an alternative method for the preparation of MHC class I tetramers, and promote the use of this exciting technology.

REFERENCES

- Harty JT, Tvinneim AR, White DW. CD8⁺ T cell effector mechanisms in resistance to infection. *Annu Rev Immunol* 2000; **18**: 275-308
- Doherty PC, Christensen JP. Accessing complexity: the dynamics of virus-specific T cell responses. *Annu Rev Immunol* 2000; **18**: 561-592
- Altman JD, Moss PA, Goulder PJ, Barouch DH, McHeyzer-Williams MG, Bell JI, McMichael AJ, Davis MM. Phenotypic analysis of antigen-specific T lymphocytes. *Science* 1996; **274**: 94-96
- Meidenbauer N, Hoffmann TK, Donnenberg AD. Direct visualization of antigen-specific T cells using peptide-MHC class I tetrameric complexes. *Methods* 2003; **31**: 160-171
- Gratama JW, Cornelissen JJ. Diagnostic potential of tetramer-based monitoring of cytomegalovirus-specific CD8⁺ T lymphocytes in allogeneic stem cell transplantation. *Clin Immunol* 2003; **106**: 29-35
- Gratama JW, van Esser JW, Lamers CH, Tournay C, Lowenberg B, Bolhuis RL, Cornelissen JJ. Tetramer-based quantification of cytomegalovirus (CMV)-specific CD8⁺ T lymphocytes in T-cell-depleted stem cell grafts and after transplantation may identify patients at risk for progressive CMV infection. *Blood* 2001; **98**: 1358-1364
- Cwynarski K, Ainsworth J, Cobbold M, Wagner S, Mahendra P, Apperley J, Goldman J, Craddock C, Moss PA. Direct visualization of cytomegalovirus-specific T-cell reconstitution after allogeneic stem cell transplantation. *Blood* 2001; **97**: 1232-1240
- Xu XN, Screaton GR. MHC/peptide tetramer-based studies of T cell function. *J Immunol Methods* 2002; **268**: 21-28
- Lacey SF, Diamond DJ, Zaia JA. Assessment of cellular immunity to human cytomegalovirus in recipients of allogeneic stem cell transplants. *Biol Blood Marrow Transplant* 2004; **10**: 433-447
- Bousso P. Generation of MHC-peptide tetramers: a new opportunity for dissecting T-cell immune responses. *Microbes Infect* 2000; **2**: 425-429
- Bodinier M, Peyrat MA, Tournay C, Davodeau F, Romagne F, Bonneville M, Lang F. Efficient detection and immunomagnetic sorting of specific T cells using multimers of MHC class I and peptide with reduced CD8 binding. *Nat Med* 2000; **6**: 707-710
- Sato Y, Sahara H, Tsukahara T, Kondo M, Hirohashi Y, Nabeta Y, Kawaguchi S, Ikeda H, Torigoe T, Ichimiya S, Tamura Y, Wada T, Yamashita T, Goto M, Takasu H, Sato N. Improved generation of HLA class I/peptide tetramers. *J Immunol Methods* 2002; **271**: 177-184
- Andersson SG, Kurland CG. Codon preferences in free-living microorganisms. *Microbiol Rev* 1990; **54**: 198-210
- Song ZL, Pan QH, Wang J, Yang Y, Zhu DM, Chen XJ, Liu CL, Hong A. Cloning and high expression of hbFGF with a new strategy. *Yichuan Xuebao* 2002; **29**: 84-89
- Brosterhus H, Brings S, Leyendeckers H, Manz RA, Miltenyi S, Radbruch A, Assenmacher M, Schmitz J. Enrichment and detection of live antigen-specific CD4⁺ and CD8⁺ T cells based on cytokine secretion. *Eur J Immunol* 1999; **29**: 4053-4059
- He XH, Xu LH, Liu Y, Zeng YY. Cloning of human β_2 -microglobulin gene and its high expression in *Escherichia coli*. *Shengwu Gongcheng Xuebao* 2004; **20**: 99-103
- Garboczi DN, Hung DT, Wiley DC. HLA-A2-peptide complexes: refolding and crystallization of molecules expressed in *Escherichia coli* and complexed with single antigenic peptides. *Proc Natl Acad Sci USA* 1992; **89**: 3429-3433
- Trudeau JD, Kelly-Smith C, Verchere CB, Elliott JF, Dutz JP, Finegood DT, Santamaria P, Tan R. Prediction of spontaneous autoimmune diabetes in NOD mice by quantification of autoreactive T cells in peripheral blood. *J Clin Invest* 2003; **111**: 217-223
- Skinner PJ, Haase AT. In situ tetramer staining. *J Immunol Methods* 2002; **268**: 29-34
- Ferrari G, Neal W, Ottinger J, Jones AM, Edwards BH, Goepfert P, Betts MR, Koup RA, Buchbinder S, McElrath MJ, Tartaglia J, Weinhold KJ. Absence of immunodominant anti-Gag p17 (SL9) responses among Gag CTL-positive, HIV-uninfected vaccine recipients expressing the HLA-A*0201 allele. *J Immunol* 2004; **173**: 2126-2133
- Gratama JW, Kern F. Flow cytometric enumeration of antigen-specific T lymphocytes. *Cytometry* 2004; **58**: 79-86
- Lahey DL, Voladri RK, Edwards KM, Hager C, Samten B, Wallis RS, Barnes PF, Kernodle DS. Enhanced production of recombinant *Mycobacterium tuberculosis* antigens in *Escherichia coli* by replacement of low-usage codons. *Infect Immun* 2000; **68**: 233-238
- Wills MR, Carmichael AJ, Mynard K, Jin X, Weekes MP,

- Plachter B, Sissons JG. The human cytotoxic T-lymphocyte (CTL) response to cytomegalovirus is dominated by structural protein pp65: frequency, specificity, and T-cell receptor usage of pp65-specific CTL. *J Virol* 1996; **70**: 7569-7579
- 24 **Hassan-Walker AF**, Vargas Cuero AL, Mattes FM, Klenerman P, Lechner F, Burroughs AK, Griffiths PD, Phillips RE, Emery VC. CD8⁺ cytotoxic lymphocyte responses against cytomegalovirus after liver transplantation: correlation with time from transplant to receipt of tacrolimus. *J Infect Dis* 2001; **183**: 835-843
- 25 **Einsele H**, Roosnek E, Rufer N, Sinzger C, Riegler S, Loffler J, Grigoleit U, Moris A, Rammensee HG, Kanz L, Kleihauer A, Frank F, Jahn G, Hebart H. Infusion of cytomegalovirus (CMV)-specific T cells for the treatment of CMV infection not responding to antiviral chemotherapy. *Blood* 2002; **99**: 3916-3922
- 26 **Broers AE**, van Der Holt R, van Esser JW, Gratama JW, Henzen-Logmans S, Kuenen-Boumeester V, Lowenberg B, Cornelissen JJ. Increased transplant-related morbidity and mortality in CMV-seropositive patients despite highly effective prevention of CMV disease after allogeneic T-cell-depleted stem cell transplantation. *Blood* 2000; **95**: 2240-2245
- 27 **Appay V**, Nixon DF, Donahoe SM, Gillespie GM, Dong T, King A, Ogg GS, Spiegel HM, Conlon C, Spina CA, Havlir DV, Richman DD, Waters A, Easterbrook P, McMichael AJ, Rowland-Jones SL. HIV-specific CD8⁺ T cells produce antiviral cytokines but are impaired in cytolytic function. *J Exp Med* 2000; **192**: 63-75
- 28 **Lichterfeld M**, Yu XG, Waring MT, Mui SK, Johnston MN, Cohen D, Addo MM, Zaunders J, Alter G, Pae E, Strick D, Allen TM, Rosenberg ES, Walker BD, Altfeld M. HIV-1-specific cytotoxicity is preferentially mediated by a subset of CD8⁺ T cells producing both interferon-gamma and tumor necrosis factor-alpha. *Blood* 2004; **104**: 487-494
- 29 **Keenan RD**, Ainsworth J, Khan N, Bruton R, Cobbold M, Assenmacher M, Milligan DW, Moss PA. Purification of cytomegalovirus-specific CD8 T cells from peripheral blood using HLA-peptide tetramers. *Br J Haematol* 2001; **115**: 428-434
- 30 **Robert B**, Guillaume P, Luescher I, Romero P, Mach JP. Antibody-conjugated MHC class I tetramers can target tumor cells for specific lysis by T lymphocytes. *Eur J Immunol* 2000; **30**: 3165-3170

Science Editor Wang XL and Guo SY Language Editor Elsevier HK

• CLINICAL RESEARCH •

Association of polymorphic alleles of *CTLA4* with inflammatory bowel disease in the Japanese

Haruhisa Machida, Kazuhiro Tsukamoto, Chun-Yang Wen, Yukiko Narumi, Saburo Shikuwa, Hajime Isomoto, Fuminao Takeshima, Yohei Mizuta, Norio Niikawa, Ikuo Murata, Shigeru Kohno

Haruhisa Machida, Hajime Isomoto, Yohei Mizuta, Fuminao Takeshima, Shigeru Kohno, Second Department of Internal Medicine, Nagasaki University School of Medicine, 1-7-1 Sakamoto, Nagasaki 852-8501, Japan

Kazuhiro Tsukamoto, Yukiko Narumi, Ikuo Murata, Department of Pharmacotherapeutics, Nagasaki University Graduate School of Biomedical Sciences, 1-14 Bunkyo-machi, Nagasaki 852-8521, Japan

Chun-Yang Wen, Department of Molecular Pathology, Atomic Bomb Disease Institute, Nagasaki University Graduate School of Biomedical Sciences, 1-12-4 Sakamoto, Nagasaki 852-8523, Japan

Saburo Shikuwa, Department of Gastroenterology, National Hospital Organization Nagasaki Medical Center, 2-1001-1 Kubara, Omura 856-8562, Japan

Norio Niikawa, Department of Human Genetics, Nagasaki University Graduate School of Biomedical Sciences, 1-12-4 Sakamoto, Nagasaki 852-8523, Japan

Correspondence to: Kazuhiro Tsukamoto, MD, PhD, Department of Pharmacotherapeutics, Nagasaki University Graduate School of Biomedical Sciences, 1-14 Bunkyo-machi, Nagasaki 852-8521, Japan. ktsuka@net.nagasaki-u.ac.jp

Telephone: +81-95-819-2448 Fax: +81-95-819-2895

Received: 2004-11-04 Accepted: 2004-11-23

Abstract

AIM: To examine an association between the cytotoxic T-lymphocyte antigen 4 (*CTLA4*) gene that plays a role in downregulation of T-cell activation and inflammatory bowel disease consisting of ulcerative colitis (UC) and Crohn's disease (CD) in the Japanese.

METHODS: We studied 108 patients with UC, 79 patients with CD, and 200 sex-matched healthy controls, with respect to three single nucleotide polymorphisms (SNPs) in *CTLA4*, such as C-318T in the promoter region, A+49G in exon 1 and G+6230A in the 3' untranslated region (3'-UTR) by a PCR-restriction fragment length polymorphism method, and to an (AT)_n repeat polymorphism in 3'-UTR by fragment analysis with fluorescence-labeling on denaturing sequence gels. Frequency of alleles and genotypes and their distribution were compared statistically between patients and controls and among subgroups of patients, using χ^2 and Fisher exact tests.

RESULTS: The frequency of "A/A" genotype at the G+6230A SNP site was statistically lower in UC patients than in controls (3.7% vs 11.0%, $P = 0.047$, odds ratio (OR) = 0.311). Moreover, the frequency of "G/G" genotype at the A+49G SNP site was significantly higher in CD

patients with fistula (48.6%) than those without it (26.2%) ($P = 0.0388$, OR=2.67).

CONCLUSION: The results suggest that *CTLA4* located at 2q33 is a determinant of UC and responsible for fistula formation in CD in the Japanese.

© 2005 The WJG Press and Elsevier Inc. All rights reserved.

Key words: Ulcerative colitis; *CTLA4* gene; Disease-susceptible gene; Crohn's disease; Fistula formation

Machida H, Tsukamoto K, Wen CY, Narumi Y, Shikuwa S, Isomoto H, Takeshima F, Mizuta Y, Niikawa N, Murata I, Kohno S. Association of polymorphic alleles of *CTLA4* with inflammatory bowel disease in the Japanese. *World J Gastroenterol* 2005; 11(27): 4188-4193

<http://www.wjgnet.com/1007-9327/11/4188.asp>

INTRODUCTION

Chronic inflammatory bowel disease (IBD) is a multifactorial disorder characterized by non-specific inflammation of the gastrointestinal tract, resulting in intestinal malabsorption and immune defense abnormalities, especially an exaggerated T-cell response^[1,2]. Ulcerative colitis (UC) and Crohn's disease (CD) are common major forms of IBD. Although the etiology of IBD remains unknown, both environmental and genetic factors may contribute to the occurrence of this disorder^[3,4]. Genome-wide linkage analyses and candidate gene-based association studies have shown possible IBD-susceptibility loci at 16q12 (IBD1), 12p13 (IBD2), 6p21 (IBD3), 14q11 (IBD4), 5q31-q33 (IBD5), 19p13 (IBD6), 1p36 (IBD7), and 16p (IBD8)^[5-7]. The caspase activating recruitment domain 15/nucleotide oligomerization domain 2 gene (*CARD15/NOD2*) located at 16q12 is one of them, and its mutations were associated with CD in the Caucasians, but not in the Japanese^[8-11]. This may be due to different genetic background between the races.

As a candidate gene susceptible to IBD, we focused on the cytotoxic T-lymphocyte antigen 4 (*CTLA4*) gene located at 2q33, because CTLA4 is a T-cell receptor that binds to B7-1 (CD80) and B7-2 (CD86) during antigenic stimulation of T cells, and plays a role in downregulation of T-cell activation against another competitive receptor, CD28, which operates on upregulation of T-cell activation^[12-14]. Since *CTLA4*-deficient mice developed a lethal lymphoproliferative

disease characterized by massive T-lymphocytic infiltration in all tissues^[15,16], diminution of downregulation of T-cell activation through CTLA4 may result in an exaggerated T-cell response and subsequent continuous inflammation in the gastrointestinal mucosae, probably leading to the development of IBD. Three single nucleotide polymorphisms (SNPs) in the human *CTLA4*, i.e., a C-318T SNP in the promoter region^[17], an A+49G SNP in exon 1^[12], and a G+6230A SNP in the 3' untranslated region (3'-UTR)^[18], and an (AT)_n repeat polymorphism in 3'-UTR^[19] have been reported. Current studies showed an association of *CTLA4* polymorphic alleles with inhibitory function of CTLA4 at the mRNA and protein levels in peripheral blood mononuclear cells^[20,21], and also with various autoimmune diseases, such as Graves' disease^[18,22], rheumatoid arthritis^[23], multiple sclerosis^[24], type I diabetes mellitus^[18,25], Hashimoto's disease^[18,26], and others^[27-29], of which pathoetiology is probably similar to IBD. However, there was no association of two *CTLA4* SNPs, C-318T and A+49G, with IBD in both the Dutch and Chinese populations^[30].

In this study, we examined on whether three *CTLA4* SNPs, C-318T, A+49G, and G+6230A, and an (AT)_n repeat polymorphism in 3'-UTR are associated with IBD in the Japanese.

MATERIALS AND METHODS

Subjects

The subjects studied comprised 108 patients with UC, 79 patients with CD, and 200 gender-matched unrelated healthy volunteers as controls (Table 1). All participants were Japanese who were randomly recruited from eight general health clinics in the Nagasaki district, Japan. The study protocol was approved by the Committee for the Ethical Issue on Human Genome and Gene Analysis in Nagasaki University, and written informed consent was obtained from each participant. Diagnosis of IBD was made according to endoscopic, radiological, histological, and clinical criteria provided by both the Council for International Organizations of Medical Sciences in WHO and the International Organization for the Study of Inflammatory Bowel Disease^[31-33]. Patients with indeterminate colitis, multiple sclerosis, systemic lupus erythematosus, or other recognized autoimmune diseases were excluded from the subjects studied.

Table 1 Clinical characteristics of study subjects

Characteristics	Patients with		Controls
	UC	CD	
Number of subjects	108	79	200
Age range (yr)	14-83	17-75	20-60
Age (mean±SD)	44.0±16.9 ^b	34.5±12.7	32.5±11.1
Male/female (%)	57 (52.8)/51 (47.2)	47 (59.5)/32 (40.5)	125 (62.5)/75 (37.5)

^bP<0.01 vs controls.

Patients with UC were classified into three subgroups according to age at onset (<40 or ≥40 years), localization and extension of disease (pancolitis, left-sided colitis, or proctitis), and presence or absence of colectomy as an

indicator of severity. Likewise, patients with CD were divided into subgroups according to age at onset (<40 or ≥40 years), localization and extension of lesions (ileum, ileocolon, or colon), presence or absence of fistula, and performance of operation such as partial resection of intestine, and stricture plasty.

Determination of three SNPs and (AT)_n repeat polymorphism

Genomic DNA was extracted from whole blood of each subject using the DNA Extractor WB-rapid Kit (Wako, Osaka, Japan) according to the manufacturer's protocol. Presence or absence of polymorphic alleles at three SNP sites in the human *CTLA4*, a C/T SNP at nt -318 (C-318T) in the promoter region^[17], an A/G SNP at nt +49 in exon 1 (A-49G)^[12], and a G/A SNP at nt +6 230 (G+6230A) in 3'-UTR^[18], were determined with the PCR-restriction fragment length polymorphism methods. Polymorphic region was amplified by PCR with a GeneAmp PCR System 9700 thermal cycler (Applied Biosystems, Foster City, CA, USA) using 150 µg of genomic DNA in a 25-µL reaction solution containing 10 mmol/L Tris-HCl (pH 8.3), 50 mmol/L KCl, 1.5 mmol/L MgCl₂, 0.2 mmol/L each dNTPs, 15 pmol of forward primer: 5'-AATGAATTGGACTGGATGG-3' and reverse primer: 5'-TTACGAGAAAGGAAGCCGTG-3' for C-318T SNP^[17]; forward primer: 5'-CTGAACACCGCTC-CCATAAA-3' and reverse primer: 5'-CCTCCTCCATCTT-CATGCTC-3' for A+49G SNP; or forward primer: 5'-TGATTCATTCAGTATCTGGTGGAG-3' and reverse primer: 5'-AGGGGAGGTGAAGAACCCTGT-3' for G+6230A SNP, and 1 U Taq DNA polymerase. The amplification protocol comprised initial denaturation at 94 °C for 5 min, 35 cycles of denaturation at 94 °C for 30 s, annealing at 60 °C (C-318T), at 65 °C (A+49G), and at 62 °C (G+6230A) for 30 s, and extension at 72 °C for 30 s, and final extension at 72 °C for 5 min. The PCR products were digested with *Mse*I (New England BioLabs Inc., Beverly, MA, USA), *Bln*I (New England BioLabs Inc.), and *Tai*I (MBI Fermentas Inc., Hanover, MD, USA), to detect C-318T, A+49G, and G+6230A, respectively. All these products were subjected to electrophoresis on a 6% polyacrylamide gels and visualized with UV transilluminator (Alpha Innotech Co., San Leandro, CA, USA).

A (AT)_n repeat polymorphism in 3'-UTR of *CTLA4*^[19] was investigated by fragment analysis with fluorescence-labeling on denaturing sequence gels. Polymorphic region was amplified by PCR using 150 µg of genomic DNA in a 25-µL reaction solution containing 10 mmol/L Tris-HCl (pH 8.3), 50 mmol/L KCl, 1.5 mmol/L MgCl₂, 0.2 mmol/L each dNTPs, 15 pmol of forward primer labeled with 6-carboxyfluorescein dye (Applied Biosystems): 5'-GCCAG-TGATGCTAAAGGTTG-3' and reverse primer: 5'-AACATACGTGGCTCTATGCA-3', and 1 U Taq DNA polymerase. The amplification protocol comprised initial denaturation at 94 °C for 5 min, 35 cycles of denaturation at 94 °C for 30 s, annealing at 64 °C for 30 s, and extension at 72 °C for 30 s, and final extension at 72 °C for 5 min. The PCR products were analyzed on a 6% denaturing sequence gel with an internal size marker, GeneScan 500XL ROX (Applied Biosystems), by ABI Prism 377 genetic analyzer and ABI Prism 3100 genetic analyzer (Applied Biosystems).

Statistical analysis

Gender and age values between UC or CD patients and controls were evaluated by χ^2 -test and unpaired Student's *t*-test, respectively. Allele frequencies were estimated by the gene-counting method, and χ^2 -test was used to identify significant departures from the Hardy–Weinberg equilibrium. SNP and genotype frequencies and their distributions were compared between UC or CD patients and controls, between individuals with and without a genotype, and among subgroups of UC or CD patients, using χ^2 and Fisher exact tests. Odds ratio (OR) with 95% confidence interval was calculated by multiple logistic regression analysis using the JMP program package (version 5, SAS Institute Inc., Cary, NC, USA) and the StatView program package (version 5, SAS Institute Inc.). A *P* value of 0.05 or less was considered statistically significant.

RESULTS

Frequencies and distributions of CTLA4 polymorphic alleles

We identified frequencies and distributions of alleles at the

three SNP sites and seven alleles of the (AT)_{*n*} repeat polymorphism of *CTLA4* among the subjects examined (Table 2). Distributions of *CTLA4* polymorphic alleles in our study population well corresponded to the Hardy–Weinberg equilibrium (Table 2). The results imply that the population we studied has a homogeneous genetic background. The alleles, “C” at nt -384, “A” at nt +49, “G” at nt +6 230, and “(AT)₇” in 3'-UTR, are wild types, while other alleles are variants. Since the frequencies of two alleles, (AT)₂₀ and (AT)₂₂, were very low (<2%), they were not considered for subsequent multiple logistic regression analysis. There were no significant differences in frequency of any alleles between IBD and controls.

Frequencies and distributions of CTLA4 genotypes

Of a total of 108 UC patients, 4 (3.7%) had “A/A” genotype at the G+6230A SNP site, the incidence being significantly lower than that (22/200, 11.0%) in the controls (*P* = 0.047, OR = 0.311) (Tables 3 and 4). There were no significant

Table 2 Distribution of *CTLA4* polymorphic alleles among study subjects

Polymorphic site	Allele	Number (%) of alleles in		Controls
		UC	CD	
nt -318	C	192 (88.9)	140 (88.6)	362 (90.5)
	T	24 (11.1)	18 (11.4)	38 (9.5)
nt +49	A	84 (38.9)	59 (37.3)	159 (39.8)
	G	132 (61.1)	99 (62.7)	241 (60.2)
nt +6 230	G	158 (73.1)	115 (72.8)	278 (69.5)
	A	58 (26.9)	43 (27.2)	122 (30.5)
(AT) _{<i>n</i>} in 3'-UTR	(AT) ₇	107 (49.5)	83 (52.5)	205 (51.3)
	(AT) ₁₅	45 (20.8)	22 (13.9)	82 (20.5)
	(AT) ₁₆	50 (23.1)	35 (22.2)	87 (21.8)
	(AT) ₁₇	3 (1.4)	15 (9.5)	16 (4.0)
	(AT) ₁₈	11 (5.1)	1 (0.6)	8 (2.0)
	(AT) ₂₀	0	2 (1.3)	0
	(AT) ₂₂	0	0	2 (0.5)
Total number of alleles		216	158	400

Table 3 Distribution of *CTLA4* genotypes among study subjects

Polymorphic site	Genotype	Number (%) of subjects with genotype		Controls (<i>n</i> = 200)
		UC (<i>n</i> = 108)	CD (<i>n</i> = 79)	
nt -318	C/C	84 (77.8)	63 (79.8)	163 (81.5)
	C/T	24 (22.2)	14 (17.7)	36 (18.0)
	T/T	0	2 (2.5)	1 (0.5)
nt +49	A/A	14 (13.0)	9 (11.4)	33 (16.5)
	A/G	56 (51.8)	41 (51.9)	93 (46.5)
	G/G	38 (35.2)	29 (36.7)	74 (37.0)
nt +6 230	G/G	54 (50.0)	39 (49.4)	100 (50.0)
	G/A	50 (46.3)	37 (46.8)	78 (39.0)
	A/A	4 (3.7)	3 (3.8)	22 (11.0)
(AT) _{<i>n</i>} in 3'-UTR	(AT) ₇ /(AT) ₇	52 (48.1)	41 (51.9)	101 (50.5)
	(AT) ₇ /(AT) ₁₅	2 (1.9)	1 (1.3)	1 (0.5)
	(AT) ₇ /(AT) ₁₆	1 (0.9)	0	2 (1.0)
	(AT) ₁₅ /(AT) ₁₅	16 (14.8)	5 (6.3)	31 (15.5)
	(AT) ₁₅ /(AT) ₁₆	11 (10.2)	9 (11.4)	18 (9.0)
	(AT) ₁₅ /(AT) ₁₇	0	2 (2.5)	1 (0.5)
	(AT) ₁₆ /(AT) ₁₆	18 (16.7)	13 (16.4)	30 (15.0)
	(AT) ₁₆ /(AT) ₁₇	2 (1.9)	0	6 (3.0)
	(AT) ₁₆ /(AT) ₁₈	0	0	1 (0.5)
	(AT) ₁₇ /(AT) ₁₇	0	6 (7.6)	3 (1.5)
	(AT) ₁₇ /(AT) ₁₈	1 (0.9)	1 (1.3)	3 (1.5)
	(AT) ₁₈ /(AT) ₁₈	5 (4.6)	0	2 (1.0)
	(AT) ₂₀ /(AT) ₂₀	0	1 (1.3)	0
	(AT) ₂₂ /(AT) ₂₂	0	0	1 (0.5)

Table 4 Number of subjects with or without “G” allele at the G+6230A SNP site of *CTLA4*

Genotype	Number (%) of subjects with genotype		
	UC (n = 108)	CD (n = 79)	Control (n = 200)
G/G+G/A	104 (96.3)	76 (96.2)	178 (89.0)
A/A	4 (3.7) ^a	3 (3.8)	22 (11.0)

^aP<0.05 vs controls (P = 0.047, OR = 0.311).

differences in frequency of genotypes at three other polymorphic sites between patients with IBD and the controls.

Frequencies and distributions of genotypes among UC and CD subgroups classified according to clinical features were shown in Tables 5 and 6, respectively. With respect to A+49G SNP, the frequency of “G/G” genotype was significantly higher in CD patients with fistula (48.6%) than

Table 5 Number of UC patients classified by clinical features

Polymorphic site	Genotype	Number of patients (n = 108, %)	Age at onset (yr)	
			<40	≥40
C-318T	C/C	84 (77.8)	55	29
	C/T	24 (22.2)	18	6
	T/T	0	0	0
A+49G	A/A	14 (13.0)	8	6
	A/G	56 (51.8)	40	16
	G/G	38 (35.2)	25	13
G+6230A	G/G	54 (50.0)	39	15
	G/A	50 (46.3)	31	19
	A/A	4 (3.7)	3	1
(AT) _n in 3'-UTR	(AT) ₇ /(AT) ₇	52 (48.1)	33	19
	(AT) ₇ /(AT) _x or others	56 (51.9)	40	16
(Continued)				
Location			Colectomy	
Pancolitis	Left-sided colitis	Proctitis	Yes	No
42	29	13	7	77
10	13	1	1	23
0	0	0	0	0
9	4	1	0	14
28	20	8	3	53
15	18	5	5	33
20	27	7	6	48
28	15	7	2	48
4	0	0	0	4
31	14	7	1	51
23	26	7	7	49

Table 6 Number of CD patients classified by clinical features

Polymorphic site	Genotype	Number of patients (n = 79, %)	Age at onset (yr)			
			<40	≥40		
C-318T	C/C	63 (79.8)	54	9		
	C/T	14 (17.7)	12	2		
	T/T	2 (2.5)	2	0		
A+49G	A/A	9 (11.4)	8	1		
	A/G	41 (51.9)	35	6		
	G/G	29 (36.7)	25	4		
G+6230A	G/G	39 (49.4)	35	4		
	G/A	37 (46.8)	30	7		
	A/A	3 (3.8)	3	0		
(AT) _n in 3'-UTR	(AT) ₇ /(AT) ₇	41 (51.9)	34	7		
	(AT) ₇ /(AT) _x or others	38 (48.1)	34	4		
(Continued)						
Location of lesion			Operation		Fistula	
Ileocolon	Ileum	Colon	Yes	No	Presence	Absence
40	14	9	33	30	27	36
11	1	2	9	5	8	6
2	0	0	2	0	2	0
7	2	0	5	4	5	4
25	11	5	20	21	14	27
21	2	6	19	10	18	11
25	5	7	21	18	19	20
25	8	4	22	15	18	19
1	2	0	1	2	0	3
27	10	4	24	17	19	22
26	9	3	20	18	17	21

those without it (26.2%) ($P = 0.0388$, $OR = 2.67$; Table 7). There were no significant differences in frequency of other genotypes among any other subgroups of IBD patients.

Table 7 Relationship between genotype at the A+49G SNP site and presence/absence of fistula in CD patients

Genotype	No. (%) of patients	
	With fistula ($n = 37$)	Without fistula ($n = 42$)
A/A+A/G	19 (51.4)	31 (73.8)
G/G	18 (48.6) ^a	11 (26.2)

^a $P < 0.05$ vs without fistula ($P = 0.0388$, $OR = 2.67$).

DISCUSSION

We have shown that “A/A” genotype at the G+6230A SNP site of *CTLA4* is associated with insusceptibility to UC. This suggests that individuals with “A/A” genotype at nt +6 230 may have some resistance to UC, or reversely, those with “G/G” or “G/A” genotypes are susceptible to UC. Moreover, “G/G” genotype at the A+49G SNP site was more frequently observed in CD patients with fistula than those without it. These findings suggest that *CTLA4* is one of genetic factors for the predisposition to the onset and/or development of UC and CD. However, since the number of UC patients with “A/A” genotype at the G+6230A SNP site in our study population is small (Table 5), it remains to be confirmed whether the association is reproducible in larger Japanese samples as well as in other populations. Although a previous study in the Dutch and Chinese populations did not find an association between *CTLA4* and IBD, it never dealt with the G+6230A SNP site^[30]. Therefore, the present study is the first report on an association of *CTLA4* polymorphisms with IBD.

CTLA4 consists of four exons that encode leader peptide, ligand-binding domain, transmembrane domain, and cytoplasmic tail, respectively. In humans, there are two isoforms of *CTLA4*, which are a full-length isoform (*f*/*CTLA4* transcript) and a soluble isoform (*s*/*CTLA4* transcript) which lacks exon 3 by alternative splicing. Especially, *s*/*CTLA4* is secreted and circulating in human sera^[34,35]. It binds CD80/86 molecules and subsequently inhibits T-cell proliferation *in vitro*^[35]. Expression of the human *CTLA4* mRNA isoforms by alternative splicing correlates genotype, G+6230A SNP^[18]. The ratio of *s*/*CTLA4* to *f*/*CTLA4* at mRNA level in unstimulated T cells was 50% lower in individuals with “G/G” genotype at nt +6 230 than in those with “A/A” genotype^[18]. Although expression of *CTLA4* isoforms at protein level and activities of T-cell signal pathway were not examined, individuals with “G/G” genotype at nt +6 230 may reduce the production of *s*/*CTLA4* transcript, and subsequently diminish the inhibition of T-cell activation, probably leading to an increase in T-cell proliferation and chronic inflammation in epithelial cells of the colon. Moreover, the A+6230G SNP was associated with the susceptibility to autoimmune diseases, i.e., Grave’s disease, autoimmune hypothyroidism, and type 1 diabetes mellitus^[18]. As well as these autoimmune diseases, autoantibodies against

colonic epithelial cells, such as anticolon antibodies, antitropomyosin antibodies, and antineutrophil cytoplasmic antibodies, are frequently found in sera of patients with UC^[36-38]. Thus, it is plausible that UC is also an autoimmune disease and some genetic factors are common between UC and autoimmune diseases.

Fistula formation in CD patients is one of the indicators of severity. Our results indicated that CD patients with “G/G” genotype at nt +49 more frequently had fistula. Since intracellular distribution of CTLA4 in individuals with “G/G” genotype at nt +49 was qualitatively different from that with “A/A”, and downregulation of T-cell activation in individuals with “G/G” genotype was reduced^[39], CD patients with “G/G” genotype may show progressive and severe clinical course. It remains to be investigated why the A+49G SNP is associated with fistula formation in Japanese CD patients.

In conclusion, our study showed that *CTLA4* is one of the determinants of UC and responsible for fistula formation in CD in the Japanese.

ACKNOWLEDGMENTS

We are grateful to physicians, patients, and volunteers for participating in this study. We thank Miss Naoko Sakemi and Dr. Hiroshi Soda for their support.

REFERENCES

- 1 **Fiocchi C.** Inflammatory bowel disease: etiology and pathogenesis. *Gastroenterology* 1998; **115**: 182-205
- 2 **Farrell RJ, Peppercorn MA.** Ulcerative colitis. *Lancet* 2002; **359**: 331-340
- 3 **Yang H, Taylor KD, Rotter JJ.** Inflammatory bowel disease. I. Genetic epidemiology. *Mol Genet Metab* 2001; **74**: 1-21
- 4 **Watts DA, Satsangi J.** The genetic jigsaw of inflammatory bowel disease. *Gut* 2002; **50** (Suppl 3): 31-36
- 5 **Taylor KD, Yang H, Rotter JJ.** Inflammatory bowel disease. II. Gene mapping. *Mol Genet Metab* 2001; **74**: 22-44
- 6 **Cho JH, Nicolae DL, Ramos R, Fields CT, Rabenau K, Corradino S, Brant SR, Espinosa R, LeBeau M, Hanauer SB, Bodzin J, Bonen DK.** Linkage and linkage disequilibrium in chromosome band 1p36 in American Chaldeans with inflammatory bowel disease. *Hum Mol Genet* 2000; **9**: 1425-1432
- 7 **Hampe J, Frenzel H, Mirza MM, Croucher PJ, Cuthbert A, Mascheretti S, Huse K, Platzer M, Bridger S, Meyer B, Nurnberg P, Stokkers P, Krawczak M, Mathew CG, Curran M, Schreiber S.** Evidence for a NOD2-independent susceptibility locus for inflammatory bowel disease on chromosome 16p. *Proc Natl Acad Sci USA* 2002; **99**: 321-326
- 8 **Hugot JP, Chamaillard M, Zouali H, Lesage S, Cezard JP, Belaiche J, Almer S, Tysk C, O’Morain CA, Gassull M, Binder V, Finkel Y, Cortot A, Modigliani R, Laurent-Puig P, Gower-Rousseau C, Macry J, Colombel JF, Sahbatou M, Thomas G.** Association of NOD2 leucine-rich repeat variants with susceptibility to Crohn’s disease. *Nature* 2001; **411**: 599-603
- 9 **Ogura Y, Bonen DK, Inohara M, Nicolae DL, Chen FF, Ramos R, Britton H, Moran T, Karaliuskas R, Duerr RH, Achkar JP, Brant SR, Bayless TM, Kirschner BS, Hanauer SB, Nunez G, Cho JH.** A frameshift mutation in NOD2 associated with susceptibility to Crohn’s disease. *Nature* 2001; **411**: 603-606
- 10 **Inoue N, Tamura K, Kinouchi Y, Fukuda Y, Takahashi S, Ogura Y, Inohara N, Nunez G, Kishi Y, Koike Y, Shimosegawa T, Shimoyama T, Hibi T.** Lack of common NOD2 variants in Japanese patients with Crohn’s disease. *Gastroenterology* 2002; **123**: 86-91
- 11 **Yamazaki K, Takazoe M, Tanaka T, Kazumori T, Nakamura**

- U. Absence of mutation in the NOD2/CARD15 gene among 483 Japanese patients with Crohn's disease. *J Hum Genet* 2002; **47**: 469-472
- 12 **Harper K**, Balzano C, Rouvier E, Mattei MG, Luciani MF, Golstein P. CTLA-4 and CD28 activated lymphocyte molecules are closely related in both mouse and human as to sequence, message expression, gene structure, and chromosomal location. *J Immunol* 1991; **147**: 1037-1044
 - 13 **Karandikar NJ**, Vanderlugt CL, Walunas TL, Miller SD, Bluestone JA. CTLA-4: a negative regulator of autoimmune disease. *J Exp Med* 1996; **184**: 783-788
 - 14 **Salomon B**, Bluestone JA. Complexities of CD28/B7: CTLA-4 costimulatory pathways in autoimmunity and transplantation. *Annu Rev Immunol* 2001; **19**: 225-252
 - 15 **Waterhouse P**, Penninger JM, Timms E, Wakeham A, Shahinian A, Lee KP, Thompson CB, Griesser H, Mak TW. Lymphoproliferative disorders with early lethality in mice deficient in CTLA-4. *Science* 1995; **270**: 985-988
 - 16 **Liu Z**, Geboes K, Hellings P, Maerten P, Heremans H, Vandenbergh P, Boon L, van Kooten P, Rutgeerts P, Ceuppens JL. B7 interactions with CD28 and in chronic experimental colitis. *J Immunol* 2001; **167**: 1830-1838
 - 17 **Deichmann K**, Heinzmann A, Brüggelno E, Forster J, Kuehr J. An Mse I RFLP in the human CTLA4 promoter. *Biochem Biophys Res Commun* 1996; **225**: 817-818
 - 18 **Ueda H**, Howson JM, Esposito L, Heward J, Snook H, Chamberlain G, Rainbow DB, Hunter KM, Smith AN, Di Genova G, Herr MH, Dahlman I, Payne F, Smyth D, Lowe C, Twells RC, Howlett S, Healy B, Nutland S, Rance HE, Everett V, Smink LJ, Lam AC, Cordell HJ, Walker NM, Bordin C, Hulme J, Motzo C, Cucca F, Hess JF, Metzker ML, Rogers J, Gregory S, Allahabadia A, Nithiyananthan R, Tuomilehto-Wolf E, Tuomilehto J, Bingley P, Gillespie KM, Undlien DE, Ronningen KS, Guja C, Ionescu-Tirgoviste C, Savage DA, Maxwell AP, Carson DJ, Patterson CC, Franklyn JA, Clayton DG, Peterson LB, Wicker LS, Todd JA, Gough SC. Association of the T-cell regulatory gene CTLA4 with susceptibility to autoimmune disease. *Nature* 2003; **423**: 506-511
 - 19 **Polymeropoulos MH**, Rath DS, Xiao H, Merrill CR. Dinucleotide repeat polymorphisms at the human CTLA4 gene. *Nucleic Acids Res* 1991; **19**: 4018
 - 20 **Kouki T**, Sawai Y, Gardine CA, Fisfalen ME, Alegre ML, DeGroot LJ. CTLA-4 gene polymorphism at position 49 in exon 1 reduces the inhibitory function of CTLA-4 and contributes to the pathogenesis of Grave's disease. *J Immunol* 2000; **165**: 6606-6611
 - 21 **Ligers A**, Teleshova N, Masterman T, Huang WX, Hillert J. CTLA-4 gene expression is influenced by promoter and exon 1 polymorphisms. *Genes Immunol* 2001; **2**: 145-152
 - 22 **Kosta K**, Watson PF, Weetman AP. A CTLA-4 gene polymorphism is associated with both Grave's disease and autoimmune hypothyroidism. *Clin Endocrinol* 1997; **46**: 551-554
 - 23 **Rodríguez MR**, Núñez-Roldán A, Aguilar F, Valenzuela A, García A, Gonzalez-Escribano MF. Association of the CTLA4 3' untranslated region polymorphism with the susceptibility to rheumatoid arthritis. *Hum Immunol* 2002; **63**: 76-81
 - 24 **Harbo HF**, Celius EG, Vardal F, Spurkland A. CTLA4 promoter and exon 1 dimorphisms in multiple sclerosis. *Tissue Antigens* 1999; **53**: 106-110
 - 25 **Marrohn MP**, Raffel LJ, Garchon HJ, Jacob CO, Serrano-Rios M, Martinez Larrad MT, Teng WP, Park Y, Zhang ZX, Goldstein DR, Tao YW, Beaurain G, Bach JF, Huang HS, Luo DF, Zeidler A, Rotter JJ, Yang MC, Modilevsky T, Maclaren NK, She JX. Insulin-dependent diabetes mellitus (IDDM) is associated with CTLA4 polymorphisms in multiple ethnic groups. *Hum Mol Genet* 1997; **6**: 1275-1282
 - 26 **Donner H**, Braun J, Seidl C, Rau H, Finke R, Ventz M, Walfish PG, Usadel KH, Badenhoop K. Codon 17 polymorphism of the cytotoxic T lymphocyte antigen 4 gene in Hashimoto's thyroiditis and Addison's disease. *J Clin Endocrinol Metab* 1997; **82**: 4130-4132
 - 27 **Ahmed S**, Ihara K, Kanemitsu S, Nakashima H, Otsuka T, Tsuzaka K, Takeuchi T, Hara T. Association of CTLA-4 but not CD28 gene polymorphisms with systemic lupus erythematosus in the Japanese population. *Rheumatology* 2001; **40**: 662-667
 - 28 **Ligers A**, Xu C, Saarinen S, Hillert J, Olerup O. The CTLA-4 gene is associated with multiple sclerosis. *J Neuroimmunol* 1999; **97**: 182-190
 - 29 **Agarwal K**, Jones DEJ, Daly AK, James OFW, Vaidya B, Pearce S, Bassemidine MF. CTLA-4 gene polymorphism confers susceptibility to primary biliary cirrhosis. *J Hepatol* 2000; **32**: 538-541
 - 30 **Xia B**, Crusius JBA, Wu J, Zwiers A, Zwiers A, van Bodegraven AA, Peña AS. CTLA4 gene polymorphisms in Dutch and Chinese patients with inflammatory bowel disease. *Scand J Gastroenterol* 2002; **37**: 1296-1300
 - 31 **Podolsky DK**. Inflammatory bowel disease (1). *N Eng J Med* 1991; **325**: 928-937
 - 32 **Podolsky DK**. Inflammatory bowel disease (2). *N Eng J Med* 1991; **325**: 1008-1016
 - 33 **Lennard-Jones JE**. Classification of inflammatory bowel disease. *Scand J Gastroenterol Suppl* 1989; **170**: 2-6
 - 34 **Magistrelli G**, Jeannin P, Herbault N, Benoit De Coignac A, Gauchat JF, Bonnefoy JY, Delneste Y. A soluble form of CTLA-4 generated by alternative splicing is expressed by nonstimulated human T cells. *Eur J Immunol* 1999; **29**: 3596-3602
 - 35 **Oaks MK**, Hallett KM, Penwell RT, Stauber EC, Warren SJ, Tector AJ. A native soluble form of CTLA-4. *Cell Immunol* 2000; **201**: 144-153
 - 36 **Fiocchi C**, Roche JK, Michener WM. High prevalence of antibodies to intestinal epithelial antigens in patients with inflammatory bowel disease and their relatives. *Ann Intern Med* 1989; **110**: 786-794
 - 37 **Geng X**, Biancone L, Dai HH, Lin JJ, Yoshizaki N, Dasgupta A, Pallone F, Das KM. Tropomyosin isoforms in intestinal mucosa: production of autoantibodies to tropomyosin isoforms in ulcerative colitis. *Gastroenterology* 1998; **114**: 912-922
 - 38 **Duerr RH**, Targan SR, Landers CJ, Sutherland LR, Shanahan F. Antineutrophil cytoplasmic antibodies in ulcerative colitis: comparison with other colitis/diarrheal illness. *Gastroenterology* 1991; **100**: 1590-1596
 - 39 **Maurer M**, Loserth S, Kolb-Maurer A, Ponath A, Wiese S, Kruse N, Rieckmann P. A polymorphism in the human cytotoxic T-lymphocyte antigen 4 (CTLA4) gene (exon 1 +49) alters T-cell activation. *Immunogenetics* 2002; **54**: 1-8

• CLINICAL RESEARCH •

Patients with primary biliary cirrhosis have increased serum total antioxidant capacity measured with the crocin bleaching assay

George Notas, Niki Miliaraki, Marilena Kampa, Fillipos Dimoulis, Erminia Matrella, Adam Hatzidakis, Elias Castanas, Elias Kouroumalis

George Notas, Fillipos Dimoulis, Erminia Matrella, Elias Kouroumalis, Laboratory of Gastroenterology and Hepatology, University of Crete, Faculty of Medicine, Heraklion 71003, Greece
Niki Miliaraki, Laboratory of Clinical Chemistry, University of Crete, Faculty of Medicine, Heraklion 71003, Greece

Marilena Kampa, Elias Castanas, Laboratory of Experimental Endocrinology, University of Crete, Faculty of Medicine, Heraklion 71003, Greece

Adam Hatzidakis, Department of Radiology, University of Crete, Faculty of Medicine, Heraklion 71003, Greece

Co-first-author: Niki Miliaraki

Correspondence to: Dr. George Notas, Laboratory of Gastroenterology and Hepatology, University of Crete, School of Medicine, PO Box 2208, Heraklion 71003, Greece. gnotas@med.uoc.gr

Telephone: +30-810-394634 Fax: +30-810-394634

Received: 2004-09-11 Accepted: 2004-10-18

and this maybe related to the pathophysiology of the disease. UDCA treatment restores the levels of CTAC to control levels.

© 2005 The WJG Press and Elsevier Inc. All rights reserved.

Key words: Antioxidants; Serum total antioxidant capacity; Primary biliary cirrhosis; Chronic hepatitis C; Viral HCV cirrhosis; Ursodeoxycholic acid

Notas G, Miliaraki N, Kampa M, Dimoulis F, Matrella E, Hatzidakis A, Castanas E, Kouroumalis E. Patients with primary biliary cirrhosis have increased serum total antioxidant capacity measured with the crocin bleaching assay. *World J Gastroenterol* 2005; 11(27): 4194-4198

<http://www.wjgnet.com/1007-9327/11/4194.asp>

Abstract

AIM: The balance between oxidants and antioxidants can play an important role in the initiation and development of liver diseases. Recently, we have described a new automated method for the determination of total antioxidant capacity (TAC) in human serum and plasma.

METHODS: We measured TAC and corrected TAC (CTAC -abstraction of interactions due to endogenous uric acid, bilirubin and albumin) in 52 patients with chronic liver diseases (41 patients with primary biliary cirrhosis (PBC), 10 patients with chronic hepatitis C and 13 patients with viral HCV cirrhosis) as well as in 10 healthy controls. In 23 PBC patients measurement were also done 6 mo after treatment with ursodeoxycholic acid (UDCA). The TAC assay was based on a modification of the crocin bleaching assay. The results were correlated with routine laboratory measurements and the histological stage of PBC.

RESULTS: There were no significant differences in TAC between the various groups. However, CTAC was considerably increased in the PBC group compared to controls and cirrhotics. Analysis of these patients according to disease stages showed that this increase was an early phenomenon observed only in stages I and II compared to controls, cirrhotics and patients with chronic hepatitis C). After 6 mo of treatment with UDCA, levels of CTAC decreased to those similar to that of controls.

CONCLUSION: Patients in the early stages of PBC present with high levels of corrected total antioxidant capacity

INTRODUCTION

Evidence of enhanced production of free radicals or significant decrease of antioxidant defense have been reported in all types of liver damage. A large number of studies have focused on the pathogenetic significance of oxidative stress in liver injury as well as on therapeutic interventions with antioxidant and metabolic scavengers^[1-4]. Primary biliary cirrhosis (PBC) is a chronic granulomatous cholestatic disorder characterized by a possible immunological attack on bile ducts leading to fibrosis, cirrhosis, liver failure, and death. Several studies suggest that oxidant stress plays a key role in the progression of this disease^[5-7].

Circulation of oxidative molecules has been incriminated in lipoprotein oxidation and the generation of increased arterial deposits, ultimately leading to atherosclerosis^[8-11]. However marked hypercholesterolemia, typical of severe longstanding cholestasis in PBC patients, is not associated with an excess risk of cardiovascular disease^[12]. Since the antioxidant status in PBC has been reported to be compromised, with several important components of the antioxidant defense mechanism being significantly decreased^[5] there is a disagreement between these data.

Recently, we have introduced a new automated method for the estimation of the plasma total antioxidant capacity^[13]. In the present study we assayed and evaluated the levels of antioxidant capacity in patients with chronic liver diseases, by this method. In addition, we have also corrected these results per a number of analytes, directly affecting redox potential, thus introducing the concept of "corrected antioxidant capacity". Our results indicate that, although the total

antioxidant capacity of patients with chronic liver diseases do not differ significantly from normal subjects, the corrected antioxidant capacity is increased in PBC patients, indicating that a counterbalancing mechanism might be present.

MATERIALS AND METHODS

Patient population

The study included 41 Greek patients with PBC (35 women and 6 men, median age 62 years, range 31-85 years) followed up at the Department of Gastroenterology of the University Hospital of Heraklion, Crete. Thirty-seven of them were positive for antimitochondrial antibody (AMA)-M2 testing by immunofluorescence and by ELISA. All patients had typical biochemical pattern. Liver histology consistent with PBC was available in 38 patients. Three patients with clinical evidence of portal hypertension (esophageal varices) and positive AMA-M2 were not submitted to liver biopsy. At the time of diagnosis 25 patients (median age 58 years, range 31-71) were in histological stage I or II and 16 patients (median age 67 years, range 54-85) were in histological stage III or IV, according to Ludwig *et al.*, criteria^[14]. Laboratory data and clinical details at the time of diagnosis and prior to initiation of UDCA therapy are shown in Table 1. All patients were negative for markers of hepatitis B and C.

UDCA at a dose of 15 mg/(kg • d) was administered to all patients. Serum levels of TAC were measured in all patients prior to initiation of UDCA therapy. In 23 patients (14 in stages I-II and 9 in stages III-IV) TAC was also measured after 6 mo of UDCA therapy. No patients were withdrawn from treatment during this 6-mo period.

A group of 13 patients (8 men and 5 women, median age 53 years, range 41-64 years) with biopsy-proven postviral HCV liver cirrhosis was also enrolled. Another group of 10 patients (5 men and 5 women, median age 36 years, range 22-49 years), with biopsy-proven chronic hepatitis C was also included in the study as disease controls. No patient used alcohol. Finally, 10 healthy volunteers, matched to the PBC population for age and sex, served as a reference group.

In another group of 10 cirrhotic PBC patients and in all 13 control cirrhotics TAC levels estimations were also made in blood taken from the hepatic vein during catheterization for the measurement of wedged hepatic pressure done for assessment of portal hypertension. The group of PBC patients catheterized had been receiving UDCA treatment for at least 1 year.

Blood was collected from all patients and controls and was immediately centrifuged at 4 °C. All serum samples were stored at -70 °C until assayed. The study was approved by the local hospital Ethics committee, and written informed consent was obtained from all patients.

Determination of TAC

Plasma total antioxidant capacity (TAC) was measured on an Olympus AU-600 analyzer using the TAC kit (Medikon SA, Gerakas, Greece) as described previously^[13]. Briefly, antioxidants in the sample inhibit the bleaching of crocin from ABAP [2,2-azobis-(2-amidinopropane) dihydrochloride] to a degree that is proportional to their concentration. The assay was performed at 37 °C in the following steps: 2 µL

of sample, calibrator or control were mixed with 250 µL of crocin reagent (R1) and incubated for 160 s. Subsequently, 250 µL of ABAP (R2) were added and the decrease in absorbance at 450 nm was measured 26 s later. Values of TAC were expressed as mmol/L.

Routine clinical chemistry

Plasma uric acid, albumin, total bilirubin, alkaline phosphatase, aminotransferases, and γ-glutamyl transpeptidase were determined on an Olympus AU-600 analyzer using Olympus reagents provided by Medicon Hellas (Gerakas, Greece).

Statistical analysis

Statistical analysis of data was performed by the use of the SyStat v 10.0 program (SPSS Inc, Chicago, IL, USA), and the Origin v 5.0 program (MicroCal, Northampton, MA, USA). Paired and unpaired *t*-test were used where applicable. A *P* value less than 0.05 was considered statistically significant.

RESULTS

Total and corrected plasma antioxidant capacity in chronic liver diseases (Table 1)

Figure 1 presents levels of TAC in the several groups tested. It appears that TAC values are slightly elevated in PBC patients, but this was not of statistical significance. No statistically significant differences between any of the groups could be identified. Since all patients did not have decompensated disease, our results show that the total antioxidant capacity is unaltered in non-hospitalized patients.

Table 1 TAC and CTAC in patients and controls

Group	TAC (mmol/L)	CTAC (mmol/L)
Control	1.493±0.059	0.797±0.057
Cirrhotics	1.532±0.095	0.723±0.069
PBC	1.664±0.062	1.012±0.068
PBC I-II	1.691±0.080	1.096±0.077
PBC III-IV	1.593±0.086	0.789±0.117
CAH	1.477±0.080	0.875±0.072

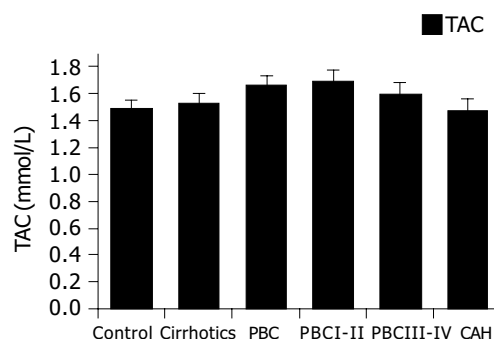


Figure 1 Total plasma antioxidant capacity in chronic liver diseases. Slightly elevated TAC levels were found in PBC patients.

As TAC is a complex measurement, that is affected by a number of serum constituents, including bilirubin, we also calculated the corrected TAC. Corrected TAC (CTAC) is depicted in Figure 2. As stated in our previous work¹³, this

calculated parameter represents the fraction of circulating antioxidants, after elimination of interference by endogenous metabolites. Our previous work has shown that uric acid and bilirubin, and in a lesser degree albumin, are the major endogenous substances linearly interfering with coefficients of 0.11, 0.11, and 0.01 mmol/L of TAC per mg/dL respectively. We have therefore assayed these analytes and subtracted their interferences from the obtained values of TAC to estimate possible modifications of the antioxidant activity, without those interferences. Increased levels of CTAC in patients with PBC compared to controls ($P<0.05$) and cirrhotics ($P<0.01$) were found (Figure 2). Further analysis shows that this increase is mainly attributed to early PBC patients (stages I and II $P<0.01$, compared to controls, cirrhotics and patients with chronic hepatitis C), while late PBC patients (stages III and IV) had CTAC levels similar to controls.

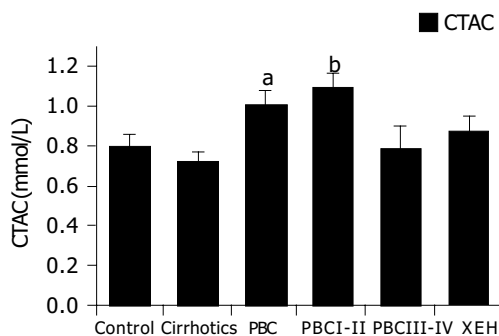


Figure 2 Corrected plasma antioxidant capacity in chronic liver diseases. Increased levels of CTAC were found in PBC patients. Only early PBC patients (stages I and II) had high CTAC levels. ^a $P<0.05$, ^b $P<0.01$ vs controls.

UDCA treatment reduces TAC and CTAC values to control levels (Table 2)

In 23 patients that received 6 mo of UDCA therapy a reduction of both TAC and CTAC was noticed as shown in Figure 3. Reduction was significant in the early stages of PBC. In late stages, a reduction of CTAC was also noted but this was at the limit of statistical significance.

Table 2 TAC and CTAC in PBC patients before and after UDCA treatment

Group		Before UDCA	After UDCA	Significance
PBC Total	TAC	1.697±0.077	1.289±0.093	<0.001
	CTAC	1.068±0.071	0.601±0.093	<0.001
PBC I-II	TAC	1.762±0.082	1.243±0.124	<0.001
	CTAC	1.169±0.076	0.660±0.115	<0.001
PBC III-IV	TAC	1.527±0.184	1.410±0.049	NS
	CTAC	0.789±0.153	0.448±0.091	NS

CTAC values are higher in peripheral blood samples compared to hepatic vein samples (Table 3)

Hepatic vein samples, taken during catheterization for estimation of portal hypertension had lower values of both TAC and CTAC as shown in Figure 4 compared to peripheral

vein samples. This was significant only for the cirrhotic patients. In the treated PBC patients a similar trend was observed but it did not reach statistical significance.

Table 3 TAC and CTAC in serum samples collected from hepatic and peripheral vein in cirrhotic and PBC patients

Group		Hepatic	Peripheral	Significance
Cirrhotics	TAC	1.357±0.052	1.532±0.095	<0.05
	CTAC	0.563±0.031	0.757±0.073	<0.05
PBC	TAC	1.494±0.074	1.587±0.071	NS
	CTAC	0.821±0.032	0.913±0.042	NS

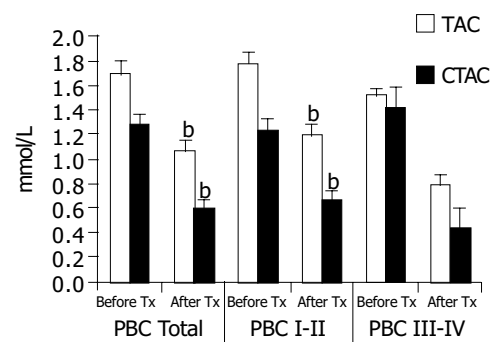


Figure 3 UDCA treatment reduces TAC and CTAC values. A significant reduction of CTAC was observed in the early stages of PBC. In late stages, a reduction of CTAC was also noted but this was at the limit of statistical significance. ^b $P<0.001$ vs TAC.

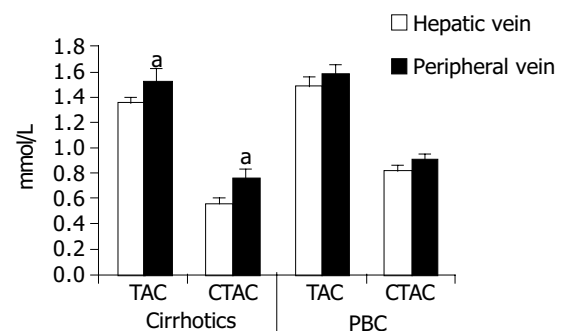


Figure 4 CTAC values are higher in peripheral blood samples compared to hepatic vein samples. Hepatic vein samples had lower values of both TAC and CTAC compared to peripheral vein samples. This was significant only for the cirrhotic patients. In the treated PBC patients a similar trend was observed but it did not reach statistical significance. ^a $P<0.05$ vs others.

DISCUSSION

Production of reactive species, including free radicals, is an integral part of human metabolism. Because of the high potential to damage vital biological systems, reactive species have now been incriminated in aging and in more than 100 disease states^[15,16]. A complex system of neutralizing antioxidants exists in plasma and intra- and extracellular fluids, but an imbalance (oxidant stress) between free radical production and use can cause damage to DNA, lipids, proteins, and other biomolecules^[5]. Nevertheless, most markers of oxidative

damage have not been fully validated^[17]. Endogenous antioxidant defenses (superoxide dismutases, H₂O₂-removing enzymes, metal binding proteins) are inadequate to prevent damage completely, so diet-derived antioxidants are important in maintaining health^[16,18,19]. The sum of endogenous plus food-derived antioxidants represents the total antioxidant capacity of extracellular fluid. The overall antioxidant capacity may give more relevant biological information compared to that obtained by the measurement of individual parameters, as it considers the cumulative effect of all antioxidants present in plasma and body fluids^[20].

A great variety of methods have been proposed for the assay of total antioxidant activity or capacity of serum or plasma^[20,21]. Many researchers have stressed the distinction between antioxidant *activity* and antioxidant *capacity*: *Antioxidant activity* corresponds to the rate constant of a single antioxidant against a given free radical; *antioxidant capacity*, on the other hand, is the number of moles of a given free radical scavenged by a test solution, independently of the capacity of any one antioxidant present in the mixture. In the case of plasma being a heterogeneous solution of diverse antioxidants the antioxidant status is better reflected by antioxidant capacity rather than activity. This capacity is a combination of all redox chain antioxidants, including several analytes such as thiol bearing proteins, and uric acid. An increase of antioxidant capacity of plasma indicates absorption of antioxidants and improved *in vivo* antioxidant status^[22], or the result of the activation of an adaptation mechanism to oxidative stress. It should be noted that, due to the participation of diverse metabolites to the antioxidant capacity of human plasma, its increase may not be necessarily a desirable condition. Indeed, in some cases, such as renal failure (uric acid), icteric status (bilirubin), hepatic damage (hypoalbuminemia) the variation of several metabolites modify plasma antioxidant capacity in a deleterious direction, a situation returning to normal values after correction of the underlying disease^[23]. Recently, we have introduced a new automated method for the assay of the plasma antioxidant activity, based on crocin bleaching. This method (the TAC assay) gives an estimation of the integrated plasma antioxidant capacity. Furthermore, we also determine the interference of a number of endogenous analytes, such as uric acid, and bilirubin, which have been found to produce a major interference of TAC, while albumin results in a smaller interference^[13].

In the present work, we have simultaneously assayed TAC and the concentrations of these analytes in patients with chronic liver diseases. As reported in the results no differences between TAC levels of the study groups were noted but patients in early stages of PBC had higher levels of CTAC. Other researchers have reported low total antioxidant capacity in PBC patients. Aboutwerat *et al.*, reported that oxidant stress, as reflected in a spectrum of lipid peroxidation and antioxidant markers, is a significant feature of early-stage PBC. They also reported that the total antioxidant capacity in whole serum (measured with an enhanced chemiluminescent technique) was significantly reduced in PBC patients but was normal in protein-free serum, suggesting that protein-bound components make an important contribution^[5]. Floreani *et al.*, measured a number

of antioxidant substances in both primary biliary cirrhosis and primary sclerosing cholangitis patients and reported significantly lower levels of retinol, alpha-tocopherol, total carotenoids, lutein, zeaxanthin, lycopene, alpha- and beta-carotene in these patients compared to healthy controls^[24]. Discrepancies among these studies and our results could be attributed to different factors:

1. The different methods of assay of TAC, measuring a number of discrete molecules. The TAC assay, used in the present study is an integrator of the totality of antioxidants circulating at a given time point in the blood.

2. The distinction of activity and capacity discussed previously. Indeed, through chain oxidative-reduction reactions, a number of antioxidants measured at a given time point may not act as antioxidants *per se*^[25].

Calculation of the corrected TAC (in which the interference of a number of endogenous metabolites has been subtracted) appears to provide a better estimate of the real antioxidant activity of the organism. However, the interpretation of the changes in plasma or serum antioxidant capacity depends upon not only the method used in detecting these changes, but also the conditions under which the plasma or serum antioxidant capacity is determined, because the determined antioxidant capacity reflects changes in a dynamic system. Furthermore an increased antioxidant capacity in plasma or serum is not necessarily a desirable condition if it is due to an adaptive response to increased oxidative stress at an early stage^[21]. Our finding of increased CTAC in the early stages of PBC may reflect such an early response.

Ursodeoxycholic acid has been reported of having a marginal therapeutic effect for primary biliary cirrhosis^[26]. Ursodeoxycholic acid treatment reduces intracellular hydrophobic bile acid levels and thereby may have a cytoprotective effect on cell membranes^[27]. It has also been reported that UDCA reduced the deoxycholic acid-associated loss of the mitochondrial membrane potential and decreased the production of reactive oxygen species^[28-30]. Our finding of TAC and CTAC reduction after UDCA treatment especially in the early stages of PBC maybe an indication that UDCA contributes to the normalization of the oxidative status in PBC patients.

Finally this is the first report that presents evidence of increased total antioxidant capacity originating from the periphery compared to the hepatic veins in patients with viral cirrhosis. Although the group of PBC patients used in this study had received UDCA treatment a similar trend can be noticed. Whether this is a feature of cirrhosis or a universal phenomenon cannot be concluded from our data. Although similar measurements cannot be performed in normal subjects, it would be interesting to further validate this result with studies on a bigger PBC population.

In conclusion, CTAC is considerably increased in the serum of PBC patients of stages I and II, but not in patients with viral cirrhosis or chronic hepatitis C. This increased antioxidant capacity in serum maybe due to an adaptive response to increased oxidative stress. Treatment with UDCA decreased the levels of CTAC to values similar to those of controls indicating a possible normalizing effect of UDCA on the oxidative status in PBC patients. Further study is needed for the finding of higher levels of CTAC in blood

samples drawn from peripheral veins compared to samples from hepatic veins in cirrhotic patients.

ACKNOWLEDGMENTS

G. Notas is a recipient of the Manasaki scholarship (University of Crete).

REFERENCES

- 1 Jones BE, Czaja MJ. III. Intracellular signaling in response to toxic liver injury. *Am J Physiol* 1998; **275**(5 Pt 1): G874-G878
- 2 Kaplowitz N. Mechanisms of liver cell injury. *J Hepatol* 2000; **32**: 39-47
- 3 Loguercio C, Federico A. Oxidative stress in viral and alcoholic hepatitis. *Free Radic Biol Med* 2003; **34**: 1-10
- 4 Mori N, Hirayama K. Long-term consumption of a methionine-supplemented diet increases iron and lipid peroxide levels in rat liver. *J Nutr* 2000; **130**: 2349-2355
- 5 Aboutwerat A, Pemberton PW, Smith A, Burrows PC, McMahon RF, Jain SK, Warnes TW. Oxidant stress is a significant feature of primary biliary cirrhosis. *Biochim Biophys Acta* 2003; **1637**: 142-150
- 6 Paradis V, Kollinger M, Fabre M, Holstege A, Poynard T, Bedossa P. *In situ* detection of lipid peroxidation by-products in chronic liver diseases. *Hepatology* 1997; **26**: 135-142
- 7 Ono M, Sekiya C, Ohhira M, Ohhira M, Namiki M, Endo Y, Suzuki K, Matsuda Y, Taniguchi N. Elevated level of serum Mn-superoxide dismutase in patients with primary biliary cirrhosis: possible involvement of free radicals in the pathogenesis in primary biliary cirrhosis. *J Lab Clin Med* 1991; **118**: 476-483
- 8 Sigal E, Laughton CW, Mulkins MA. Oxidation, lipoxygenase, and atherogenesis. *Ann NY Acad Sci* 1994; **714**: 211-224
- 9 Stam H, Hulsmann WC, Jongkind JF, van der Kraaij AM, Koster JF. Endothelial lesions, dietary composition and lipid peroxidation. *Eicosanoids* 1989; **2**: 1-14
- 10 Lyons TJ. Glycation and oxidation: a role in the pathogenesis of atherosclerosis. *Am J Cardiol* 1993; **71**: 26B-31B
- 11 Offermann MK, Medford RM. Antioxidants and atherosclerosis: a molecular perspective. *Heart Dis Stroke* 1994; **3**: 52-57
- 12 Longo M, Crosignani A, Battezzati PM, Squarcia GC, Invernizzi P, Zuin M, Podda M. Hyperlipidaemic state and cardiovascular risk in primary biliary cirrhosis. *Gut* 2002; **51**: 265-269
- 13 Kampa M, Nistikaki A, Tsaousis V, Maliaraki N, Notas G, Castanas E. A new automated method for the determination of the Total Antioxidant Capacity (TAC) of human plasma, based on the crocin bleaching assay. *BMC Clin Pathol* 2002; **2**: 3
- 14 Ludwig J, Dickson ER, McDonald GS. Staging of chronic nonsuppurative destructive cholangitis (syndrome of primary biliary cirrhosis). *Virchows Arch A Pathol Anat Histol* 1978; **379**: 103-112
- 15 Ames BN, Shigenaga MK, Hagen TM. Oxidants, antioxidants, and the degenerative diseases of aging. *Proc Natl Acad Sci USA* 1993; **90**: 7915-7922
- 16 Halliwell B, Gutteridge JM, Cross CE. Free radicals, antioxidants, and human disease: where are we now? *J Lab Clin Med* 1992; **119**: 598-620
- 17 McCall MR, Frei B. Can antioxidant vitamins materially reduce oxidative damage in humans? *Free Radic Biol Med* 1999; **26**: 1034-1053
- 18 Halliwell B. Free radicals, antioxidants, and human disease: curiosity, cause, or consequence? *Lancet* 1994; **344**: 721-724
- 19 Halliwell B. Antioxidants in human health and disease. *Annu Rev Nutr* 1996; **16**: 33-50
- 20 Ghiselli A, Serafini M, Natella F, Scaccini C. Total antioxidant capacity as a tool to assess redox status: critical view and experimental data. *Free Radic Biol Med* 2000; **29**: 1106-1114
- 21 Prior RL, Cao G. *In vivo* total antioxidant capacity: comparison of different analytical methods. *Free Radic Biol Med* 1999; **27**: 1173-1181
- 22 Cao G, Booth SL, Sadowski JA, Prior RL. Increases in human plasma antioxidant capacity after consumption of controlled diets high in fruit and vegetables. *Am J Clin Nutr* 1998; **68**: 1081-1087
- 23 Jackson P, Loughrey CM, Lightbody JH, McNamee PT, Young IS. Effect of hemodialysis on total antioxidant capacity and serum antioxidants in patients with chronic renal failure. *Clin Chem* 1995; **41**: 1135-1138
- 24 Floreani A, Baragiotta A, Martines D, Naccarato R, D'odorico A. Plasma antioxidant levels in chronic cholestatic liver diseases. *Aliment Pharmacol Ther* 2000; **14**: 353-358
- 25 Barbaste M, Berke B, Dumas M, Soulet S, Delaunay JC, Castagnino C, Arnaudinaud V, Cheze C, Vercauteren J. Dietary antioxidants, peroxidation and cardiovascular risks. *J Nutr Health Aging* 2002; **6**: 209-223
- 26 Glud C, Christensen E. Ursodeoxycholic acid for primary biliary cirrhosis. *Cochrane Database Syst Rev* 2002; **1**: CD000551
- 27 Szalay F. Treatment of primary biliary cirrhosis. *J Physiol Paris* 2001; **95**: 407-412
- 28 Rodrigues CM, Fan G, Wong PY, Kren BT, Steer CJ. Ursodeoxycholic acid may inhibit deoxycholic acid-induced apoptosis by modulating mitochondrial transmembrane potential and reactive oxygen species production. *Mol Med* 1998; **4**: 165-178
- 29 Rodrigues CM, Fan G, Ma X, Kren BT, Steer CJ. A novel role for ursodeoxycholic acid in inhibiting apoptosis by modulating mitochondrial membrane perturbation. *J Clin Invest* 1998; **101**: 2790-2799
- 30 Rodrigues CM, Ma X, Linehan-Stieers C, Fan G, Kren BT, Steer CJ. Ursodeoxycholic acid prevents cytochrome c release in apoptosis by inhibiting mitochondrial membrane depolarization and channel formation. *Cell Death Differ* 1999; **6**: 842-854

Science Editor Guo SY Language Editor Elsevier HK

• CLINICAL RESEARCH •

Sclerosing cholangitis following severe trauma: Description of a remarkable disease entity with emphasis on possible pathophysiologic mechanisms

Johannes Benninger, Rainer Grobholz, Yurdaquel Oeztuerk, Christoph H. Antoni, Eckhart G. Hahn, Manfred V. Singer, Richard Strauss

Johannes Benninger, Yurdaquel Oeztuerk, Eckhart G. Hahn, Richard Strauss, Department of Medicine I, Friedrich-Alexander-University Erlangen-Nuremberg, Ulmenweg 18, Erlangen D-91054, Germany

Christoph H. Antoni, Manfred V. Singer, Department of Medicine II, Ruprecht-Karls-University Heidelberg, University Hospital Mannheim, Theodor-Kutzer-Ufer 1-3, Mannheim D-68135, Germany

Rainer Grobholz, Department of Pathology, Ruprecht-Karls-University Heidelberg, University Hospital Mannheim, Theodor-Kutzer-Ufer 1-3, Mannheim D-68135, Germany

Correspondence to: Johannes Benninger, Department of Medicine I, Friedrich-Alexander-University Erlangen-Nuremberg, Ulmenweg 18, Erlangen D-91054,

Germany. johannes.benninger@med1.imed.uni-erlangen.de

Telephone: +49-9131-85-35204 Fax: +49-9131-85-209

Received: 2004-08-26 Accepted: 2004-09-06

cholestasis after severe trauma.

© 2005 The WJG Press and Elsevier Inc. All rights reserved.

Key words: Life-threatening trauma; Arterial hypotension; Cholestasis; Ischemia of intrahepatic bile ducts; Secondary sclerosing cholangitis; Posttraumatic sclerosing cholangitis

Benninger J, Grobholz R, Oeztuerk Y, Antoni CH, Hahn EG, Singer MV, Strauss R. Sclerosing cholangitis following severe trauma: Description of a remarkable disease entity with emphasis on possible pathophysiologic mechanisms. *World J Gastroenterol* 2005; 11(27): 4199-4205

<http://www.wjgnet.com/1007-9327/11/4199.asp>

Abstract

AIM: Persistent cholestasis is a rare complication of severe trauma or infections. Little is known about the possible pathomechanisms and the clinical course.

METHODS: Secondary sclerosing cholangitis was diagnosed in five patients with persistent jaundice after severe trauma (one burn injury, three accidents, one power current injury). Medical charts were retrospectively reviewed with regard to possible trigger mechanisms for cholestasis, and the clinical course was recorded.

RESULTS: Diagnosis of secondary sclerosing cholangitis was based in all patients on the primary sclerosing cholangitis (PSC)-like destruction of the intrahepatic bile ducts at cholangiography after exclusion of PSC. In four patients, arterial hypotension with subsequent ischemia may have caused the bile duct damage, whereas in the case of power current injury direct thermal damage was assumed to be the trigger mechanism. The course of secondary liver fibrosis was rapidly progressive and proceeded to liver cirrhosis in all four patients with a follow-up >2 years. Therapeutic possibilities were limited.

CONCLUSION: Posttraumatic sclerosing cholangitis is a rare but rapidly progressive disease, probably caused by ischemia of the intrahepatic bile ducts via the peribiliary capillary plexus due to arterial hypotension. Gastroenterologists should be aware of this disease in patients with persistent

INTRODUCTION

For a long time it is known that after severe trauma marked cholestasis can occur^[1-3]. Different reasons were held responsible for this including hepatic hypoxia, inflammation, and mass transfusions^[1,4]. Unfortunately, cholangiographic studies to detect changes of the bile ducts to exclude obstructive jaundice were not done, primarily as most of these studies were performed in the pre-ERCP era.

On the other side, gastroenterologists are occasionally confronted with patients with a history of persistent cholestasis who have survived life-threatening events with long-term stays in intensive care units. In the diagnostic work-up ERC in some of these patients shows a PSC-like picture with strictures and dilatations of the intrahepatic bile ducts.

Except one recent report by Engler *et al.*^[5], these patients are characterized badly in the literature. Therefore, we report on five patients with secondary sclerosing cholangitis after life-threatening injuries in order to demonstrate the clinical course, evaluate measures for diagnosis, and discuss possible trigger mechanisms for posttraumatic sclerosing cholangitis.

MATERIALS AND METHODS

All five patients (one woman and four men; age 18-71 years) presented with acute or persistent cholestasis. Three of them were seen as outpatients between January 2001 and June 2003, 4 to 22 mo after occurrence of cholestasis (Table 1). Patient 5 was seen as consultant during the initial stay of the patient on the intensive care unit of a burn clinic after

occurrence of jaundice, patient 1 is a former case of one of the hospitals that has already been published and who was re-evaluated^[6].

Time between the occurrence of cholestasis and definitive diagnosis ranged between 2 and 27 mo.

All patients experienced life-threatening injuries and needed long-term treatment on intensive care units (ICU) (from 23 to 88 d, Table 1). Mechanical ventilation was necessary in all patients (from 13 to 62 d). Temporary acute renal failure occurred in patients 3 and 4 (maximum creatinine 3.6 mg/dL [-1.0] on d 5 and 1.6 mg/dL on d 4, respectively). In all patients several surgeries had to be performed (without abdominal surgery), in three of them pleural drainages were necessary.

The charts of these patients at their initial hospital stay were intensely reviewed, especially concerning periods of hypotension, therapy with vasopressors and RBC units, septic fever, antibiotics, mechanical ventilation, and liver function tests to find triggers for subsequent bile duct damage. Pre-injury liver function tests were documented if available. Diagnostic work-up included ERC, liver biopsy, imaging studies of the liver and vessels of the liver hilus (ultrasound, doppler ultrasound, CT, and/or MRI), and the exclusion of other liver diseases (e.g. viral hepatitis, hereditary, and autoimmune liver diseases). Liver biopsies (also from hospitals outside) were re-evaluated by one pathologist. The further course was observed and recorded.

For the purpose of the study an increase in liver function tests more than twice above the upper limit of normal was defined abnormal.

RESULTS

Before the trauma no patient had known liver disease. No comorbidities were present with the exception of patient 3 (arterial hypertension, cardiac arrhythmias). No patient reported about alcohol abuse. On hospital admission patient 5 (power current injury) had increased values of ALT (alanine aminotransferase) and AST (aspartate aminotransferase) due to direct thermal cell damage. In all other patients liver function tests were normal on admission. No other liver diseases or thrombosis of hepatic artery and veins were found.

Early course

In all patients as the first sign of bile duct damage a permanent increase of GGT (gamma glutamyl transferase) twice above the upper limit of normal was first documented between d 4 and 11 (Table 2). Alkaline phosphatase (AP) and bilirubin rose during the next 2 weeks in all but patient 1 in whom bilirubin increased after four weeks and patient 2 whose bilirubin levels according to a milder course of cholestasis reached twice the upper limit of normal only once. Aminotransferases always increased secondary to signs of cholestasis (Table 2). As an example the early course (first month) of AST, ALT, GGT, AP, and bilirubin in patient 3 is shown in Figure 1A.

Possible reasons for bile duct damage

Details of different parameters during intensive care of the patients are shown in Table 2.

Table 1 Summary of patients' characteristics

	Patient 1	Patient 2	Patient 3	Patient 4	Patient 5
Sex	Female	Male	Male	Male	Male
Age (yr)	56	41	56	71	18
Initial event	Room fire	Motorbike accident	Tractor accident	Fall from a raised hide	Power current accident and fall
Injuries	Burn injury: 34 % of body surface (hands, head, neck, back)	Polytrauma with avulsions (left subclavian artery, forearm, anterior tibial artery) and fractures (left humeral shaft, pelvis, both lower legs)	Polytrauma with serial rib fracture, hemothorax, pleural effusion, fracture of right joint ankle	Polytrauma with burst fractures of lumbar spine, paraplegia, rib fractures, pneumothorax	Burn injury (36 % of body surface), multiple rib fractures, hemothorax, fractures of the thoracic vertebrae 5 to 9
Intensive care (d)	58	23	34	26	88
Time from occurrence of cholestasis until diagnosis (mo)	4	27	4	13	2
Treatment start with UDCA	mo 4	mo 22	mo 4	mo 13	mo 1
Follow-up(mo)	55 (death)	48	41	33	12
Complications	Liver cirrhosis (Child-Pugh C), variceal bleeding, death due to liver insufficiency	Small intrahepatic gallstones after 6 mo (endoscopically extracted), liver cirrhosis (Child-Pugh A)	unbearable pruritus during first year, liver cirrhosis (Child-Pugh A)	liver cirrhosis (Child-Pugh B), recurrent stomal bleeding	-

UDCA: urso deoxycholic acid.

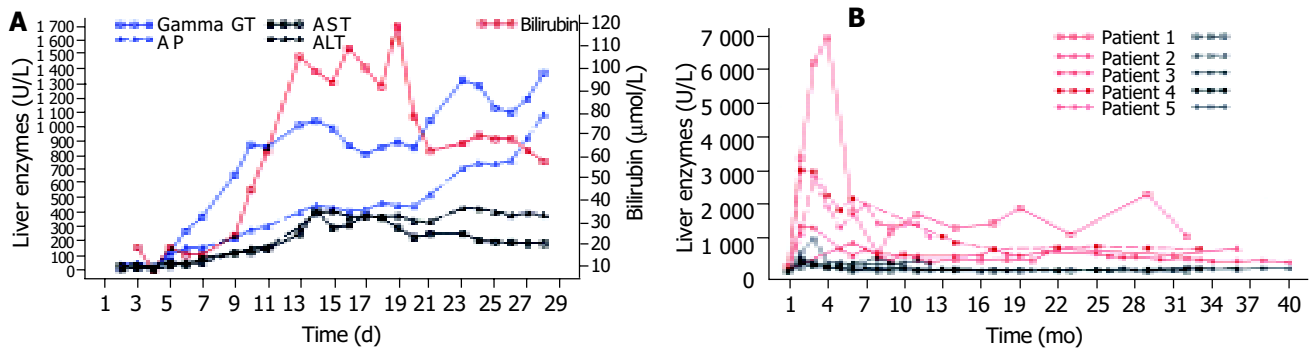


Figure 1 A: Liver function tests of patient 3 in the first month showing the strong increase of cholestasis followed by a milder rise of aminotransferases; **B:** Long-time course of AP (red) and ALT (black) of all patients showing the initial strong

increase of AP with a subsequent slow decrease and only a mild initial rise of ALT with nearly normal values in the long term.

Severe arterial hypotension with a systolic blood pressure of ≤ 70 mmHg as a possible cause of bile duct ischemia occurred in four patients. Only patient 5 experienced no hemodynamic instability throughout the whole course. In contrast to all other patients aminotransferases were already increased at clinic admission and nearly normalized during the following days. According to the pattern of his burns current flow through the body was diagnosed. Therefore, a direct thermal damage of the intrahepatic bile ducts can be suspected.

Two patients (patients 2 and 3) suffered of sudden strong blood loss requiring mass transfusions in patient 2 (30 RBC units, 11 fresh frozen plasma units, and four platelet concentrates during the first four hours after hospital admission), whereas a moderate decrease of the hemoglobin occurred in the other patients. After ICU admission all patients received parenteral nutrition via central venous lines, and additional enteral feeding via a nasogastric tube was

started in all cases between d 2 and 5.

Imaging findings

Imaging findings are shown in Table 3.

Ultrasound Ultrasound was repeatedly performed in all patients. Depending on the time since occurrence of cholestasis different findings were recorded (Table 3).

In the early phase (first 2 mo) the liver was described as normal or enlarged with homogeneous or hyperechoic parenchyma, bile ducts were normal in all patients, gallbladder sludge was seen in four patients. Later on liver parenchyma got more and more inhomogeneous and signs of liver cirrhosis (nodularity/irregularity of liver surface, inhomogeneous parenchyma, splenomegaly) occurred. Intrahepatic bile ducts showed segmental dilatation in two patients after 12 to 24 mo, whereas the common bile duct remained normal in all patients.

Table 2 Patients' data and important findings during the early course at the intensive care unit

	Patient 1	Patient 2	Patient 3	Patient 4	Patient 5
Time of increase of liver function tests $> 2 \times$ ULN (d)					
GGT ¹	10 ¹	6	5	4	11
AP	18	18	9	12	15
Bilirubin	36	6 ²	10	8	13
AST	18	52	9	12	16
ALT	18	23	9	7	19
Mechanical ventilation (d)	36;	13;	25;	16;	62;
	PEEPmax. 6 mmHg; FiO ₂ not documented	PEEPmax. 10 mmHg; FiO ₂ max. 0.6	PEEPmax. 8 mmHg; FiO ₂ max. 0.6	PEEPmax. 15 mmHg; FiO ₂ max. 0.7	PEEPmax. 20 mmHg; FiO ₂ max. 0.6
Severe hypotension (systolic blood pressure < 70 mm Hg) ³	d 1 (2 h)	d 1 (45 min)	d 2 (30 min) and d 3 (60 min)	d 1 (30 min)	None
Vasopressor therapy	Dobutamine d 1-8 dopamine d 1-18 norepinephrine d 1-7	None	Norepinephrine d 3-5 and d 9-17	Norepinephrine d 2-4	None
Minimum hemoglobin ³	7.3 g/dL (d 3)	2.4 g/dL (d 1)	7.2 g/dL (d 3)	8.6 g/dL (d 1)	7.9 g/dL (d 4)
Transfusions (RBC units) ³	30	34	10	10	24
Fever (> 38.0 °C)	d 7-16	d 6-13	d 2-25	d 5-17	d 2-20
Antibiotics ³	Cefotaxim, imipenem, sulbactam, mezlocillin	None	Piperacillin/sulbactam	None	Piperacillin/tazobactam, ciprofloxacin, meropenem, levofloxacin, fluconazol

ALT: alanine aminotransferase; AP: alkaline phosphatase; AST: aspartate aminotransferase; FiO₂max.: maximum fraction of inspired oxygen; GGT: gamma glutamyl transferase; PEEPmax.: maximum positive end-expiratory pressure; ULN: upper limit of normal ¹No control of liver function tests between d 4 and 10; ²A bilirubin value $2 \times$ ULN was noted only once at d 6; ³Until increase of GGT $\geq 2 \times$ ULN.

Table 3 Diagnostic findings in posttraumatic sclerosing cholangitis during the course of the disease (ultrasound, MRT/MRCP, ERCP, and liver histology)

	Patient 1	Patient 2	Patient 3	Patient 4	Patient 5
1 - 2 mo					
Ultrasound	L normal, BD normal, GB sludge	L normal, BD normal, GB sludge	L normal, BD normal, GB sludge	L normal, BD normal, GB sludge	L enlarged, hyperechoic, BD normal, GB contracted, splenomegaly
ERC	Stenoses and loss of IHBD, CBD normal, GB normal	-	IHBD irregular, CBD normal, GB normal	-	-
MRT/MRCP	-	-	-	L normal, BD normal, GB normal	-
4 - 6 mo					
Ultrasound	L cirrhosis, BD normal, GB stones	L inhomogeneous, BD normal	L inhomogeneous with hyperechoic areas alongside the IHBD, BD normal, GB normal,	-	L enlarged, BD normal, BD normal, splenomegaly
ERC	-	-	IHBD: multifocal short strictures and dilatations, CBD normal, GB normal (Figure 2)	-	IHBD irregular, beaded appearance, CBD normal, GB normal
Liver histology	Substantial cholestasis; inflammation of the portal tracts, liver lobules, and sporadically the bile ducts; feathery degeneration of hepatocytes; fibrosis around bile ducts; regenerative bile duct proliferations	Portal tract inflammation, occasionally lymphocytes in bile duct epithelium; several necrotic foci with foamy macrophages in the liver acini; bridging fibrosis; regenerative bile duct proliferations	Canalicular bile thrombi; edematously swollen portal tracts; inflammatory infiltrates, esp. around bile ducts; occasionally feathery degeneration of hepatocytes; minimal fibrosis	-	-
12 - 24 mo					
Ultrasound	L inhomogeneous cirrhosis BD normal, GB stones and sludge, splenomegaly, distinct ascites	L enlarged, inhomogeneous, hyperechoic areas segment 7/8, IHBD slightly dilated, CBD normal, GB stones, splenomegaly	L cirrhosis, BD normal, GB normal, splenomegaly	L cirrhosis, IHBD slightly dilated, CBD normal, GB normal, splenomegaly	-
ERC	stenoses and loss of IHBD, CBD normal, GB normal	IHBD: loss and stenoses of right-sided bile ducts, a long, stretched running left bile duct (suitable to liver hypertrophy), CBD normal, GB stones	-	IHBD: multifocal high-grade strictures and dilatations on the left side, bile ducts on the right side not presentable, CBD normal	-
MRT/MRCP	-	L atrophy of right liver, hypertrophy of left liver; reduced signal intensity of segments 2 and 3 and partly 7 and 8; IHBD segmentally dilated, CBD pseudoobstruction, GB stones, splenomegaly	L macronodular cirrhosis, CBD pseudoobstruction, splenomegaly	-	-
Liver histology	No cholestasis; complete liver cirrhosis	-	Occasionally canalicular cholestasis; mild portal inflammation (predominantly lymphocytes); some regenerative bile duct proliferations; mild fibrosis; (sampling error ?)	Substantial cholestasis (bile thrombi in dilated canaliculi); occasionally lymphocytes in the epithelium of bile ducts; numerous regenerative bile duct proliferations in the periphery of portal tracts; cirrhosis (Figure 4)	

BD: bile ducts; CBD: common bile duct; GB: gallbladder; IHBD: intrahepatic bile ducts; L: liver.

Computed tomography CT scans performed in patient 1 18 mo and in patient 3 10 d and 4 mo after the onset of cholestasis confirmed sonographic findings.

MRT/MRCP MRT/MRCP in patient 3 in the early phase showed normal abdominal findings. In two patients MRT/MRCP was performed after 2 years. In patient 2 MRT/MRCP disclosed atrophy of the right liver, hypertrophy of the left liver, a reduced signal intensity in segments 2 and 3 and partly 7 and 8, and peripheral segmental dilatation of intrahepatic bile ducts rather unusual findings (Figure 2). In patient 3 signs of liver cirrhosis with large nodules and inhomogeneous liver parenchyma were present.

ERC Diagnostic ERC was performed in all patients. Together with the history it led to diagnosis in all patients. Already three weeks after first signs of cholestasis slight changes of the intrahepatic bile ducts were noticed (patient 3). After four to six months multifocal strictures and dilatations of the intrahepatic bile ducts (comparable to lesions in primary sclerosing cholangitis) occurred (Figure 3), that were also present after 12-24 mo. The common bile duct and the cystic duct were normal in all patients at all times.

Liver histology

Liver biopsy was performed in four patients (in no one in the acute phase), at least once in three patients and three times in one patient (patient 3) (Table 3). After 4-6 mo

portal inflammation (predominantly lymphocytes) with involvement of the bile ducts, necrosis of periportal hepatocytes, fibrosis of different degree, and depending on the biochemical extent of cholestasis bile thrombi were present. After 12-24 mo complete liver cirrhosis was diagnosed in patients 1 and 4, whereas in patient 3 only mild fibrosis was diagnosed, possibly due to a sampling error (clinically cirrhosis). Inflammation of the portal tracts with involvement of bile ducts was still present. Regenerative bile duct proliferations were a prominent feature. As an example liver histology of patient 4 is shown in Figure 4.

Follow-up, treatment, and complications

The patients were followed between 12 and 55 mo after trauma (Table 1).

The long-time courses of AP and ALT of all patients are shown in Figure 1B.

All patients were treated with ursodeoxycholic acid after different periods of time (Table 1).

Liver cirrhosis was diagnosed clinically and/or histologically in all four patients with a follow-up of >2 years. It occurred already at mo 5 in patient 4. In this case it was diagnosed macroscopically during colostomy which was performed due to fecal incontinence following paraplegia. Decompensation of liver cirrhosis with large amounts of ascites occurred in patient 1 already after 18 mo. This patient died after 55 mo due to hepatic insufficiency.

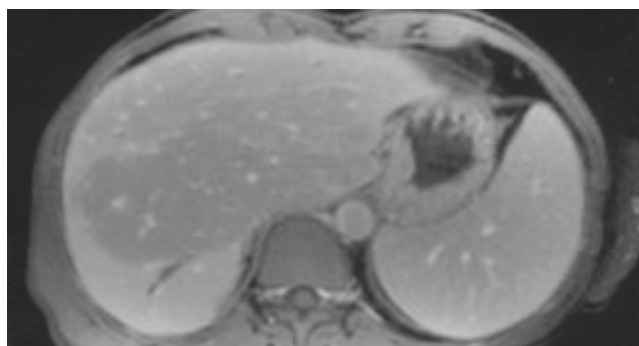


Figure 2 MRT of patient 2 (T1-weighted after contrast medium) showing an area centrally in the liver with reduced signal intensity, a dilatation of the bile duct in segment 6, and splenomegaly.



Figure 3 ERCP of patient 3 showing a normal cystic and common bile duct, but multifocal short strictures and dilatations of the intrahepatic bile ducts (4 mo after occurrence of cholestasis).

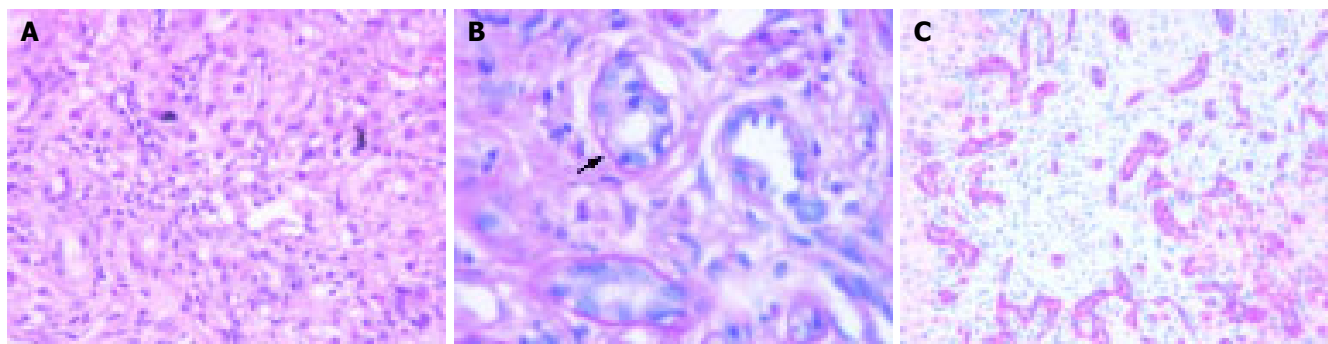


Figure 4 Liver histology of patient 4 (13 mo after occurrence of cholestasis). **A:** Portal inflammation, severe cholestasis with bile thrombi, HE (20x); **B:** Lymphocytic infiltration of a small bile duct (arrow). Periodic acid Schiff's reaction

after treatment with diastase (100x); **C:** Immunostaining for cytokeratin 7. Regenerative bile duct proliferations show a strong expression of cytokeratin 7 (25x).

Liver transplantation was planned for patient 3 after 4 mo, but due to improvement of liver function tests and clinical symptoms transplantation was cancelled. Patient 5 is designated for liver transplantation.

DISCUSSION

Cholestasis is common in long-term ICU patients. However, in most cases it is mild and resolves within weeks after clinical improvement of the patient.

Secondary sclerosing cholangitis after trauma ("posttraumatic SC") is a rare and probably underdiagnosed complication of severe trauma with to our knowledge only two publications in the literature^[5,6]. Our patients shared the following findings, thus leading to the diagnosis: (1) a severe, life-threatening trauma; (2) slowly increasing signs of cholestasis with a secondary moderate rise of aminotransferases; (3) the typical PSC-like appearance of the intrahepatic bile ducts with multifocal strictures and dilatations; and (4) the exclusion of other liver diseases. All patients except patient 5 had normal liver function tests at hospital admission. After a few days a slow, but constant increase of signs of cholestasis was noted with a subsequent rise of aminotransferases that never exceeded 15 times of ULN. This differs from "shock liver" where an acute elevation of the aminotransferases to at least 20 times ULN is required for diagnosis^[7]. According to our results ERC is of essential importance for the diagnosis. Probably earlier than MRC, ERC best shows the PSC-like bile duct changes (multifocal strictures and dilatations, beaded appearance) that occur only intrahepatically in posttraumatic SC. The possibility to aspirate bile for microbiological examination is another advantage of ERC compared to all non-invasive imaging procedures as to our experience and some case reports in the literature in some intensive care patients with severe, long-lasting infections requiring mechanical ventilation jaundice may be caused by secondary bacterial or fungal cholangitis without preexisting biliary obstruction^[8,9]. The value of ultrasound, CT, and MRT in the early course is to exclude obvious biliary obstruction, later they may help to diagnose secondary development of liver cirrhosis.

Posttraumatic SC seems to be rapidly progressive. Liver cirrhosis was diagnosed clinically or by liver biopsy in all patients with a follow-up of more than 2 years, in one patient already after 5 mo, in the others after 18-24 mo. After decompensation of liver cirrhosis at mo 18 and esophageal variceal bleeding at mo 22, one patient died after 55 mo due to hepatic insufficiency. This rapidly progressive course compares well with the experience of Engler *et al.*^[5]. In their series all four patients with a follow-up of more than 2 years developed liver cirrhosis, three of them during the second year.

All patients were treated with UDCA after 1-22 mo. As this was an uncontrolled retrospective study clear conclusions concerning the therapeutic value of UDCA are not possible, but the efficacy seems to be rather limited. In patients with posttraumatic SC and end-stage liver disease liver transplantation may be the only therapeutic option. In contrast to Engler *et al.* we are not convinced that endoscopic interventions for treatment of strictures (dilatation or

stenting) are beneficial as bile duct strictures were multifocal and localized intrahepatically in all of our patients. This is comparable to PSC where only patients with a dominant extrahepatic stricture appear to have some potential benefit from endoscopic treatment^[10]. Even in the patients of Engler *et al.*^[5], endoscopic therapy (with the additional risk of secondary bacterial cholangitis) did not stop disease progression. However, for diagnostic reasons early ERC appears necessary.

Interestingly, bilirubin levels of all patients decreased without intervention after 2-6 mo. Proliferation of bile ducts in the portal tracts with metaplasia of hepatocytes may have improved bile flow. This phenomenon was also described in drug-induced prolonged cholestasis with ductopenia^[11]. However, posttraumatic SC progresses in spite of decreasing bilirubin levels.

What are the possible mechanisms for posttraumatic sclerosing cholangitis? As shown in Table 2 we examined several factors that are discussed in the literature, which could have contributed to bile duct damage^[5,6,12]. In our opinion the dominant cause is arterial hypotension with subsequent ischemia of the intrahepatic bile ducts which occurred in four of the five patients in the early course after the accident (in patient 5 according to the pattern of burns current flow through the body was diagnosed suggesting a direct thermal damage of the intrahepatic bile ducts). It can be assumed that through temporary hypoperfusion, possibly aggravated by vasopressor therapy, an ischemic damage of the intrahepatic bile duct epithelium occurred which led to secondary scarring of the bile ducts and subsequent cholestasis. In contrast to shock liver the initial damage is not characterized by rapidly increasing aminotransferases as the liver via the portal vein - seems to be perfused sufficiently. After the acute ischemic phase, parallel to bile duct changes, increasing signs of cholestasis occur. Later, aminotransferases raise secondary to bile duct obstruction as in other obstructive bile duct diseases. Possibly due to the non-reversible scarring of the bile ducts with persistence of cholestasis and comparable to experimental bile duct ligation liver fibrosis and cirrhosis develop rather quickly^[13].

In all of our patients only the intrahepatic bile ducts were affected. The reason may be the blood supply of the bile ducts^[14-16]. Whereas the extrahepatic biliary system seems to be well supplied, mainly by two parallel to the common bile duct running arteries which are fed by branches of eight arteries on the average (retroduodenal artery, gastroduodenal artery, left and right hepatic artery, *etc.*), the intrahepatic ducts are supplied by a nonaxial network of small arteries deriving only from the right and left hepatic artery. They form a plexus of arterioles, venules, and capillaries within the peribiliary adventitia with a second plexus within the biliary wall primarily composed of capillaries ("peribiliary capillary plexus"). This structure, possibly especially the blood supply via the left and right hepatic artery as functional end arteries, may cause the vulnerability of the intrahepatic bile ducts to ischemic events. Except in the periphery of the liver portal-venous blood plays no role in the supply of the bile ducts.

Other factors like systemic inflammation or transfusions

may contribute to progressing cholestasis in some patients, but may be of minor importance.

In conclusion, after severe, life-threatening injuries a small number of patients develop jaundice that is caused by multiple intrahepatic bile duct strictures. The main trigger may be ischemia and subsequent damage of the bile ducts due to transient arterial hypotension. Slowly progressive cholestasis after severe injury in patients without prior liver disease is the hallmark of posttraumatic sclerosing cholangitis. The diagnosis is confirmed by ERC. The major characteristics of posttraumatic SC are summarized in Table 4. The course of this form of secondary sclerosing cholangitis appears to be rather progressive without promising therapeutic options (except probably liver transplantation). Gastroenterologists should be aware of this disease in patients with cholestasis after severe trauma.

Table 4 Characteristics of posttraumatic sclerosing cholangitis

1	No former liver disease
2	Severe life-threatening injury with temporary severe arterial hypotension
3	Slowly increasing signs of cholestasis
4	Secondary moderate rise of aminotransferases
5	PSC-like appearance of intrahepatic bile ducts (multifocal strictures and dilatations)
6	Exclusion of other liver diseases (esp. hepatic artery thrombosis)

ACKNOWLEDGMENTS

The authors thank the surgical hospitals, the Berufsgenossenschaftliche Unfallklinik Ludwigshafen and the Clinic Nuremberg, both Germany, for the permission to analyze the medical files and therefore enabling this paper.

REFERENCES

- Nunes G, Blaisdell FW, Margaretten W. Mechanism of hepatic dysfunction following shock and trauma. *Arch Surg* 1970; **100**: 546-556
- Champion HR, Jones RT, Trump BF, Decker R, Wilson S, Stega M, Nolan J, Crowley RA, Gill W. Post-traumatic hepatic dysfunction as a major etiology in post-traumatic jaundice. *J Trauma* 1976; **16**: 650-657
- Hartley S, Scott AJ, Spence M. Benign postoperative jaundice complicating severe trauma. *N Z Med J* 1977; **86**: 174-178
- Te Boekhorst T, Urlus M, Doesburg W, Yap SH, Goris RJA. Etiologic factors of jaundice in severely ill patients. *J Hepatol* 1988; **7**: 111-117
- Engler S, Elsing C, Flechtenmacher C, Theilmann L, Stremmel W, Stiehl A. Progressive sclerosing cholangitis after septic shock: a new variant of vanishing bile duct disorders. *Gut* 2003; **52**: 688-693
- Schmitt M, Koelbl CB, Mueller MK, Verbeke CS, Singer MV. Sclerosing cholangitis after burn injury. *Z Gastroenterol* 1997; **35**: 929-934
- Seeto RK, Fenn B, Rockey DC. Ischemic hepatitis: Clinical presentation and pathogenesis. *Am J Med* 2000; **109**: 109-113
- Scheppach W, Druge G, Wittenberg G, Mueller JG, Gassel AM, Gassel HJ, Richter F. Sclerosing cholangitis and liver cirrhosis after extrabiliary infections: Report on three cases. *Crit Care Med* 2001; **29**: 438-441
- Domagk D, Bisping G, Poremba C, Fegeler W, Domschke W, Menzel J. Common bile duct obstruction due to candidiasis. *Scand J Gastroenterol* 2001; **36**: 444-446
- Lee YM, Kaplan MM. Practice guideline committee of the ACG. American college of gastroenterology. Management of primary sclerosing cholangitis. *Am J Gastroenterol* 2002; **97**: 528-534
- Degott C, Feldmann G, Larrey D, Durand-Schneider AM, Grange D, Machayekhi JP, Moreau A, Potet F, Benhamou JP. Drug-induced prolonged cholestasis in adults: a histological semiquantitative study demonstrating progressive ductopenia. *Hepatology* 1992; **15**: 244-251
- Labori KJ, Bjornbeth BA, Raeder MG. Aetology and prognostic implication of severe jaundice in surgical trauma patients. *Scand J Gastroenterol* 2003; **38**: 102-108
- Johnstone JM, Lee EG. A quantitative assessment of the structural changes the rat's liver following obstruction of the common bile duct. *Br J Exp Pathol* 1976; **57**: 85-94
- Batts KP. Ischemic cholangitis. *Mayo Clin Proc* 1998; **73**: 380-385
- Northover JM, Terblanche J. A new look at the arterial supply of the bile duct in man and its surgical implications. *Br J Surg* 1979; **66**: 379-384
- Cho KJ, Lunderquist A. The peribiliary vascular plexus: The microvascular architecture of the bile duct in the rabbit and in clinical cases. *Radiology* 1983; **147**: 357-364

Science Editor Li WZ Language Editor Elsevier HK

• CLINICAL RESEARCH •

Thermo-chemo-radiotherapy for advanced bile duct carcinoma

Terumi Kamisawa, Yuyang Tu, Naoto Egawa, Katsuyuki Karasawa, Tadayoshi Matsuda, Kouji Tsuruta, Atsutake Okamoto

Terumi Kamisawa, Yuyang Tu, Naoto Egawa, Department of Internal Medicine, Tokyo Metropolitan Komagome Hospital, 3-18-22 Honkomagome, Bunkyo-ku, Tokyo, Japan

Katsuyuki Karasawa, Tadayoshi Matsuda, Department of Radiology, Tokyo Metropolitan Komagome Hospital, 3-18-22 Honkomagome, Bunkyo-ku, Tokyo, Japan

Kouji Tsuruta, Atsutake Okamoto, Department of Surgery, Tokyo Metropolitan Komagome Hospital, 3-18-22 Honkomagome, Bunkyo-ku, Tokyo, Japan

Correspondence to: Dr. Terumi Kamisawa, Department of Internal Medicine, Tokyo Metropolitan Komagome Hospital, 3-18-22 Honkomagome, Bunkyo-ku, Tokyo, Japan. kamisawa@cick.jp

Telephone: +81-3-3823-2101 Fax: +81-3-3824-1552

Received: 2004-12-28 Accepted: 2005-01-13

Abstract

AIM: Complete resection of the bile duct carcinoma is sometimes difficult by subepithelial spread in the duct wall or direct invasion of adjacent blood vessels. Nonresected extrahepatic bile duct carcinoma has a dismal prognosis, with a life expectancy of about 6 mo to 1 year. To improve the treatment results of locally advanced bile duct carcinoma, we have been conducting a clinical trial using regional hyperthermia in combination with chemoradiation therapy.

METHODS: Eight patients complaining of obstructive jaundice with advanced extrahepatic bile duct underwent thermo-chemo-radiotherapy (TCRT). All tumors were located in the upper bile duct and involved hepatic bifurcation, and obstructed the bile duct completely. Radiofrequency capacitive hyperthermia was administered simultaneously with chemotherapeutic agents once weekly immediately following radiotherapy at 2 Gy. We administered heat to the patient for 40 min after the tumor temperature had risen to 42 °C. The chemotherapeutic agents employed were cis-platinum (CDDP, 50 mg/m²) in combination with 5-fluorouracil (5-FU, 800 mg/m²) or methotrexate (MTX, 30 mg/m²) in combination with 5-FU (800 mg/m²). Number of heat treatments ranged from 2 to 8 sessions. The bile duct at autopsy was histologically examined in three patients treated with TCRT.

RESULTS: In respect to resolution of the bile duct, there were three complete regression (CR), two partial regression (PR), and three no change (NC). Mean survival was 13.2±10.8 mo (mean±SD). Four patients survived for more than 20 mo. Percutaneous transhepatic biliary drainage (PTBD) tube could be removed in placement of self-expandable metallic stent into the patency-restored bile duct after TCRT. No major side effects occurred. At

autopsy, marked hyalinization or fibrosis with necrosis replaced extensively bile duct tumor and wall, in which suppressed cohesiveness of carcinoma cells and degenerative cells were sparsely observed.

CONCLUSION: Although the number of cases is rather small, TCRT in the treatment of locally advanced bile duct carcinoma is promising in raising local control and thus, long-term survival.

© 2005 The WJG Press and Elsevier Inc. All rights reserved.

Key words: Hyperthermia; Chemotherapy; Radiotherapy; Bile duct carcinoma

Kamisawa T, Tu Y, Egawa N, Karasawa K, Matsuda T, Tsuruta K, Okamoto A. Thermo-chemo-radiotherapy for advanced bile duct carcinoma. *World J Gastroenterol* 2005; 11(27): 4206-4209

<http://www.wjgnet.com/1007-9327/11/4206.asp>

INTRODUCTION

Extrahepatic bile duct carcinomas are typically slow-growing and locally invasive tumors, which spread along nerves and invade adjacent vascular structures^[1]. Optimal treatment of these tumors includes complete surgical resection with negative histologic margins^[2]. However, complete resection is sometimes difficult by local extension, which occurs perineurally, via lymphatic channels, by subepithelial spread in the duct wall, and by direct invasion of adjacent blood vessels^[3]. Nonresected extrahepatic bile duct carcinoma has a dismal prognosis, with a life expectancy of about 6 mo to 1 year^[4].

Hyperthermia has been used in combination with radiation therapy and chemotherapy, and is considered to be effective for certain type of tumors^[5]. We have been conducting a clinical trial of regional hyperthermia in combination with chemoradiotherapy for advanced extrahepatic bile duct carcinoma. In this study, clinical effectiveness of thermo-chemo-radiotherapy (TCRT) for locally advanced extrahepatic bile duct carcinoma was evaluated.

MATERIALS AND METHODS

Study patients

Eight patients complaining of obstructive jaundice with advanced extrahepatic bile duct underwent TCRT. All tumors were located in the upper bile duct and involved hepatic bifurcation. Bile duct was completely obstructed on

percutaneous transhepatic or endoscopic retrograde cholangiography. Six patients underwent percutaneous transhepatic biliary drainage (PTBD). Unresectable reasons were involvement of the portal vein ($n = 5$) and extensive involvement of hepatic hilus ($n = 3$, Table 1). None of them showed distant metastasis.

Table 1 Cases with bile duct carcinoma treated with thermo-chemo-radiotherapy

Case	Age (yr)	Sex	Unresectable reasons
1	70	m	Extensive involvement of hepatic hilus
2	57	m	Involvement of the portal vein
3	73	m	Extensive involvement of hepatic hilus
4	70	m	Involvement of the portal vein
5	70	f	Involvement of the portal vein
6	78	m	Involvement of the portal vein
7	65	m	Involvement of the portal vein
8	71	m	Extensive involvement of hepatic hilus

Thermo-chemo-radiotherapy (TCRT) techniques

The heating equipment was radiofrequency (RF) capacitive heating device, Thermotron RF-8 (Yamamoto Vinita Company, Osaka, Japan)^[6]. The patient lay in the prone position. The target was sandwiched with upper and lower electrodes, and 8 MHz RF wave was applied. We administered heat to the patient for 40 min after the tumor temperature had risen to 42 °C. Tumor temperature was measured continuously using a needle thermosensor on each heating. The thermosensor was inserted beside the tumor from the skin surface through 18-G angiocatheter under the aid of ultrasonography. The chemotherapeutic agents employed were cis-platinum (CDDP, 50 mg/m²) in combination with 5-fluorouracil (5-FU, 800 mg/m²) or methotrexate (MTX, 30 mg/m²) in combination with 5-FU (800 mg/m²). The hyperthermia and chemotherapeutic agents were administered simultaneously once weekly immediately following radiotherapy at 2 Gy. Usually it started within 15 min after the irradiation (Figure 1). Number of heat treatments ranged from 2 to 8 sessions (mean±SD, 4.5±2.5). Two cases were retreated (Table 2).

Table 2 Thermo-chemo-radiotherapy in each case

Case	Heat session	Chemotherapy	Dose of radiation (Gy)
1	×4, ×4	MTX + 5Fu	50+40
2	×2, ×6	CDDP + 5Fu	46
3	×6	MTX + 5Fu	56
4	×4	MTX + 5Fu	56
5	×4	CDDP + 5Fu	50
6	×2	CDDP + 5Fu	46
7	×2	MTX + 5Fu	50
8	×2	MTX + 5Fu	16

MTX: Methotrexate, 5Fu: 5-fluorouracil, CDDP: cis-platinum.

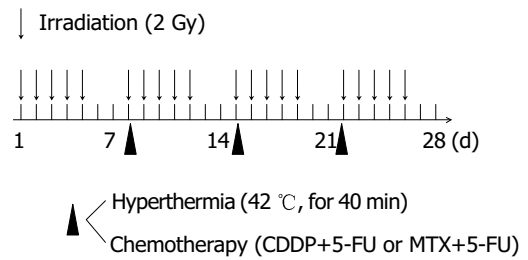


Figure 1 Schedule of TCRT.

Response and toxicity criteria

The effectiveness of TCRT on the advanced bile duct carcinoma was evaluated about resolution of biliary obstruction by cholangiography. Response of obstructed bile duct was graded as complete regression (CR: more than 80% resolution), partial regression (PR: more than 50% and less than 80% resolution), and no change (NC).

We examined histologically the state of the bile duct at autopsy in three patients with advanced bile duct carcinoma treated with TCRT.

Side effects were evaluated and graded according to the National Cancer Institute Common Toxicity Criteria^[7].

RESULTS

Effectiveness of TCRT

In respect to resolution of the bile duct, there were 3 CR, 2 PR, and 3 NC. CR rate and CR+PR rate was 38% and 63%. Mean survival was 13.2±10.8 mo. Four patients survived for more than 20 mo (Table 3). We placed self-expandable metallic stent into the patency-restored bile duct for prevention of restenosis ($n = 1$) and partially resolved bile duct ($n = 2$) after TCRT for improvement of patients' quality of life (Figures 2A and B). In these three patients, PTBD tube could be withdrawn.

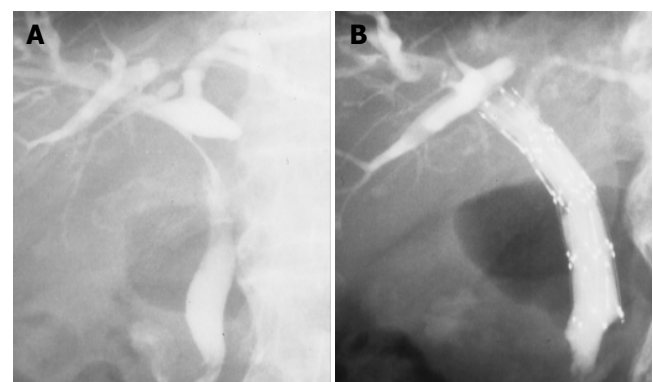


Figure 2 A: Completely obstructed upper bile duct was partially resolved after TCRT; B: self-expandable metallic stent was placed into the patency-restored bile duct, and PTBD tube could be removed.

Histological findings at autopsy in patients treated with TCRT

Marked hyalinization or fibrosis with necrosis replaced extensively bile duct tumor and wall, in which suppressed

Table 3 Effectiveness of thermo-chemo-radiotherapy and survival months

Case	Resolution of the bile duct	Survival months
1	Complete response	33
2	Complete response	22
3	Complete response	22
4	Partial response	21.5
5	Partial response	6
6	No change	13.5
7	No change	4
8	No change	2.5

cohesiveness of carcinoma cells and degenerative cells were sparsely observed. Carcinoma cells were also detected peripherally. Common bile duct of two cases was not completely obstructed, though it was partly obstructed with debris or necrotic mass.

Complication of TCRT

Treatment complications by TCRT were nausea and vomiting (grades 1 and 2, five cases), gastritis (grade 2, three cases), leukocytopenia (grade 2, three cases), and thrombocytopenia (grade 1, one case). These complications were successfully treated conservatively.

DISCUSSION

Optimal treatment of bile duct carcinoma is complete surgical resection with negative histologic margins^[2]. However, complete resection is sometimes difficult by local extension, especially when the tumor located near the hepatic bifurcation. Deeply invaded tumors are apt to spread to the intrahepatic bile duct or the connective tissues in the hepatoduodenal ligament, with encasement of major vessels. Moreover, tumor cells that spread to the ligament often cannot be cleared away completely, even when dissection of the tissue is performed. In nonresected cases, tumor involving the hepatic hilus frequently induces the development of obstructive jaundice which cannot be under control, resulting in early death from cholangitis. One of the desirable strategies for advanced bile duct carcinoma appears to control over involvement of the hepatic hilar bile duct and the hepatoduodenal ligament.

We have treated advanced gallbladder carcinoma with TCRT and reported the effectiveness^[8]. Then, we undertook a preliminary study involving TCRT for unresectable bile duct carcinomas. In respect to resolution of the bile duct, there were three CR and two PR of eight treated cases. Four patients survived for more than 20 mo. PTBD tube could be removed in three patients, in whom self-expandable metallic stent was placed into the patency-restored bile duct after TCRT.

Hyperthermia involves two biological interactions with radiation, a radiosensitizing effect^[9,10] and a direct cytotoxic effect on tumor cells^[11]. When the target lesion is heated up to around 42 °C, the cancer-killing effect of radiation or anticancer drug is enhanced^[12]. Experimental studies strongly

suggest that the extracellular pH of the tumor and a hypoxic environment sensitize tumor cells to direct heat killing^[13]. Hyperthermia in combination with radiotherapy for superficial malignancies has contributed to a better rate of complete response and reduction in the rate of recurrence compared with radiotherapy alone^[14]. Data on hyperthermia for deep-seated tumors were still preliminary, because the heating and thermal measurement techniques were not yet established. However, the effectiveness of TCRT for deep-seated tumors has been recently revealed by prospective randomized studies^[15,16]. The treatment protocol of TCRT was established and its effectiveness was evidenced by Sugimachi and his colleagues^[17]. They treated esophageal carcinoma with TCRT and demonstrated significant improvement in the clinical effectiveness and 5-year survival ratio. Anatomically, the bile duct is located near the abdominal wall, which is advantageous to heating and thermal measurement. Thus, it seems that TCRT may be a favorable treatment strategy for advanced bile duct carcinoma.

In conclusion, although our clinical trial was preliminary and the number of patients was small, the results were better than we expected. We prefer HCRT in place of aggressive surgical approach for patients with locally advanced bile duct carcinoma.

REFERENCES

- 1 Suzuki M, Takashima T, Ouchi K, Matsuno S. The development and extension of hepatohilar bile duct carcinoma. A three-dimensional tumor mapping in the intrahepatic biliary tree visualized with the aid of a graphics computer system. *Cancer* 1989; **64**: 658-666
- 2 Klempnauer J, Ridder GJ, Werner M, Weimann A, Picklmayr R. What constitutes long-term survival after surgery for hilar cholangiocarcinoma? *Cancer* 1997; **79**: 26-34
- 3 Sakamoto E, Nimura Y, Hayakawa N, Kamiya J, Kondo S, Nagino M, Kanai M, Miyachi M, Uesaka K. The pattern of infiltration at the proximal border of hilar bile duct carcinoma: a histologic analysis of 62 resected cases. *Ann Surg* 1998; **227**: 405-411
- 4 D'Angelica MI, Jarnagin WR, Blumgart LH. Resectable hilar cholangiocarcinoma: surgical treatment and long-term outcome. *Surg Today* 2004; **34**: 885-890
- 5 Arcangeli G, Cividalli A, Nervi C, Creton G, Lovisolo G, Mauro F. Tumor control and therapeutic gain with different schedules of combined radiotherapy and local external hyperthermia in human cancer. *Int J Radiat Oncol Biol Phys* 1983; **9**: 1125-1134
- 6 Hiraoka M, Jo S, Akuta K, Nishimura Y, Takahashi M, Abe M. Radiofrequency capacitive hyperthermia for deep-seated tumors. II. Effects of thermoradiotherapy. *Cancer* 1987; **60**: 128-135
- 7 Appendix A Grading of toxicity. Manual of oncologic therapeutics. Philadelphia: J.B. Lippincott 1989
- 8 Okamoto A, Tsuruta K, Ishiwata J, Isawa T, Kamisawa T, Tanaka Y. Treatment of T3 and T4 carcinomas of the gallbladder. *Int Surg* 1996; **81**: 130-135
- 9 Arcangeli G, Casale C, Colistro F, Benassi M, Lovisolo G, Begnozzi L. One versus four heat treatments in combination with radiotherapy in metastatic mammary carcinoma. *Int J Radiat Oncol Biol Phys* 1991; **21**: 1569-1574
- 10 Kim JH, Hahn EW, Ahmed SA. Combination hyperthermia and radiation therapy for malignant melanoma. *Cancer* 1982; **50**: 478-482
- 11 Overgaard J. Effect of hyperthermia on malignant cells *in vivo*. A review and hypothesis. *Cancer* 1977; **37**: 2637-2648

- 12 **Song CW.** Effect of local hyperthermia and blood flow and microenvironment: a review. *Cancer Res* 1984; **44**(10 Suppl): 4721S-4730
- 13 **Lin JC, Levitt SH, Song CW.** Relationship between vascular thermotolerance and intratumor pH. *Int J Radiat Oncol Biol Phys* 1992; **22**: 123-129
- 14 **Perez CA, Gillespie B, Pajak T, Hornback NB, Emani B, Rubin P.** Quality assurance problems in clinical hyperthermia and their impact on therapeutic outcome: a report by the radiation therapy oncology group. *Int J Radiat Oncol Biol Phys* 1989; **16**: 551-558
- 15 **Harima Y, Nagata K, Harima K, Oka A, Ostapenko VV, Shikata N, Ohnishi T, Tanaka Y.** Bax and Bcl-2 protein expression following radiationtherapy versus radiation plus thermoradiotherapy in stage IIIB cervical carcinoma. *Cancer* 2000; **88**: 132-138
- 16 **Van der Zee J, Gonzalez Gonzalez D, van Rhoon GC, van Dijk JD, van Putten WL, Hart AA.** Comparison of radiotherapy plus hyperthermia in locally advanced pelvic tumors: a prospective randomized multicenter trial. Dutch Deep Hyperthermia Group. *Lancet* 2000; **335**: 1119-1125
- 17 **Sugimachi K, Matsuda H, Ohno S, Fukuda A, Matsuoka H, Mori M, Kuwano H.** Long term effects of hyperthermia combined with chemotherapy and irradiation of the treatment of patients with carcinoma of the esophagus. *Surg Gynecol Obstet* 1988; **167**: 319-323

Science Editor Guo SY Language Editor Elsevier HK

• CLINICAL RESEARCH •

Effect of itopride, a new prokinetic, in patients with mild GERD: A pilot study

Yong Sung Kim, Tae Hyeon Kim, Chang Soo Choi, Young Woo Shon, Sang Wook Kim, Geom Seog Seo, Yong Ho Nah, Myung Gyu Choi, Suck Chei Choi

Yong Sung Kim, Tae Hyeon Kim, Chang Soo Choi, Young Woo Shon, Geom Seog Seo, Yong Ho Nah, Suck Chei Choi, Department of Internal Medicine, School of Medicine, Wonkwang University and Digestive Disease Research Institute, Iksan, South Korea

Sang Wook Kim, Department of Internal Medicine, School of Medicine, Chonbuk National University, Jeonju, South Korea

Myung Gyu Choi, Department of Internal Medicine, School of Medicine, Catholic University, Seoul, South Korea

Supported by the 2004 Research Fund of Wonkwang University
Correspondence to: Dr. Suck Chei Choi, Department of Internal Medicine, School of Medicine, Wonkwang University, Iksan, South Korea. medcsc@wmc.wonkwang.ac.kr

Telephone: +82-63-850-1075 Fax: +82-63-854-7675

Received: 2004-09-29 Accepted: 2004-10-18

Abstract

AIM: Itopride is a newly developed prokinetic agent, which enhances gastric motility through both antidopaminergic and anti-acetylcholinesterasic actions. The importance of esophageal motor dysfunction in the pathogenesis of gastro-esophageal reflux disease (GERD) makes it interesting to examine the effect of itopride on esophageal acid exposure.

METHODS: The effect of itopride on esophageal acid reflux variables for 24 h was studied in 26 patients with GERD symptoms, pre-entry total acid exposure time (pH<4) of more than 5% and mild esophagitis (Savary-Miller grades I, II) proven by endoscopy. Ambulatory 24-h pH-metry and symptom assessment were performed after treatments with 150 or 300 mg itopride thrice a day (t.i.d.) for 30 d in random order, using an open label method. For evaluating the safety of itopride, blood biochemical laboratory test was performed and the serum prolactin level was also examined before and after treatment.

RESULTS: Total symptom score was significantly decreased after treatment in 150- or 300-mg group. Itopride 300 mg was significantly effective than 150 mg on decreasing the total per cent time with pH<4, total time with pH<4 and DeMeester score. No serious adverse effects were observed with administration of itopride in both groups.

CONCLUSION: Itopride 100 mg t.i.d. is effective on decreasing pathologic reflux in patient with GERD and therefore it has the potential to be effective in the treatment of this disease.

Key words: Gastro-esophageal reflux disease; Itopride

Kim YS, Kim TH, Choi CS, Shon YW, Kim SW, Seo GS, Nah YH, Choi MG, Choi SC. Effect of itopride, a new prokinetic, in patients with mild GERD: A pilot study. *World J Gastroenterol* 2005; 11(27): 4210-4214

<http://www.wjgnet.com/1007-9327/11/4210.asp>

INTRODUCTION

Gastro-esophageal reflux disease (GERD) is characterized by the reflux of gastric content into esophagus with or without histological changes. However, the excessive reflux of gastric acid induces some complications such as esophagitis, esophageal stenosis, cancer, or Barrett's esophagus. Pathogenesis of GERD are lower esophageal sphincter (LES) dysfunction, abnormal clearing capacity of refluxed materials, delayed gastric emptying and abnormal resistance of esophageal mucosa to gastric acid, but the primary motor dysfunction is regarded as the most important factor in general^[1,2]. Therefore, prokinetic agent that restores gastric motility with increasing of LES and esophageal motility has been developed and used frequently in the treatment of GERD^[3]. There are several prokinetic agents such as bethanechol, metoclopramide, domperidone, and cisapride that potentiate acetylcholine effects on smooth muscle of gastrointestinal tract or antagonize the activity of dopamine.

However, these prokinetic agents have some limitations for prescribing to GERD patients, because they show uncertain efficacies on GERD except for cisapride and have some problems in safety^[4,5]. Especially, cisapride accelerates the esophageal acid clearance by an enhancement of esophageal propulsive motility, which strengthens LES and stimulates the gastric emptying. So it is regarded that cisapride has the same efficacy as an inhibitor of gastric acid secretion for GERD. In spite of these predominant effects, cisapride is restricted to use because of a safety problem that it provokes arrhythmia.

Itopride, a new type of the prokinetic agent, acts both as a dopamine D₂ receptor antagonist and as an acetylcholine esterase inhibitor. It accelerates gastric emptying, improves gastric tension and sensitivity, and has an anti-emetic action. And also, itopride was identified to have equivalent efficacy with cisapride in functional dyspepsia. These mechanisms of itopride may be useful to GERD patients, but no clinical data are available from them as yet.

The aim of this pilot study is to evaluate the efficacy of

itopride for the treatment of GERD by evaluating the improvement of the clinical symptom and esophageal pH change.

MATERIALS AND METHODS

Study design

This study was performed prospectively to evaluate the efficacy and dose-response of itopride for the treatment of GERD by estimating ambulatory 24-h pH-metry and clinical symptoms before and after treatment. Patients satisfying the entry criteria were assigned to two groups by the randomization allocation schedule and received either 150 or 300 mg of itopride per day.

Inclusion/exclusion criteria

Twenty-six patients (range 18-65 years) who visited the Department of Internal Medicine in Wonkwang University and agreed to participate in this study were recruited based on the following entry criteria:

Inclusion criteria were (1) more than moderate heartburn symptom; (2) more than one upper dyspeptic symptoms such as regurgitation, epigastric pain, nausea, vomiting, dysphagia, chest pain lasting for more than 4 wk; (3) less than grade II esophagitis by Savary-Miller classification by endoscopic examination; (4) abnormal acid exposure on 24-h pH-metry (fraction of time of >5% with pH below 4).

For each symptom, the severity scores are as follows: 0 (none) = absent; 1 (mild) = symptom was not spontaneously reported but elicited upon specific questions; 2 (moderate) = symptom needs to be treated but not interfered with normal activities; 3 (severe) = symptom interfered with normal activities; 4 (very severe) = impossible to do normal activities due to symptom.

Exclusion criteria were the following: (1) acute esophagitis related to strong stimuli; (2) corrosive esophagitis by a toxicant; (3) esophagitis or some symptoms by inflammatory infection or radiotherapy; (4) regular use of H₂ blockers, prokinetic or anticholinergic agents for previous 4 wk; (5) previous gastrointestinal surgery; (6) inflammatory bowel disease; (7) cardiological, respiratory, gastrointestinal disease, endocrine metabolic disease and neuro-psychological disease; (8) clinically significant hepatic or renal dysfunction; (9) pregnancy or lack of adequate contraception in the case of women at child-bearing age; (10) patients who are inappropriate to this study by investigator's opinion.

Study procedures

This study was approved by the institutional review board of Wonkwang University Hospital and informed consent was obtained from patients for inclusion in this study. The patients were asked about basic information and previous treatment history. And they were screened as physical examination, vital sign and lab examination. Any drugs that could influence the study were postponed for at least 1 wk before that examination.

The baseline symptom of GERD was evaluated by questionnaire. Endoscopic examination was performed to check the organic lesion like cancer or ulcer, and to evaluate the severity of esophagitis. After examination, ambulatory

24-h pH-metry was carried out.

Patients who met the entry criteria were allocated randomly to 150- or 300-mg group of itopride. Fifty or 100 mg of itopride was administered thrice per day for 4 wk. After treatment of itopride for 4 wk, physical examination, vital sign, laboratory test, and symptoms of GERD were evaluated and ambulatory 24-h pH-metry was performed.

Efficacy parameters were (1) changes in acid reflux episodes measured by ambulatory pH-metry such as number of reflux episodes, number of reflux episodes lasting for more than 5 min, duration of longest episodes, % time with pH <4, and DeMeester score; (2) changes in subjective symptom of patient with GERD.

Safety parameters were (1) results of laboratory test (biochemistry, complete blood count, urinalysis and prolactin level); (2) occurrences of adverse events after the treatment. If adverse events occurred, the time of onset, duration, severity, relationship to itopride and the requirement of treatment were evaluated.

Statistical analysis

Two sample *t*-test and paired *t*-test were used for continuous variables presented as a normal distribution; Wilcoxon signed rank test and Wilcoxon rank sum test were used for those not presented as a normal distribution. And χ^2 test or Fisher's exact test was used for categorical variables. All data were statistically analyzed with SAS package (version 8.0) and differences with a value of *P*<0.05 were considered significant.

RESULTS

Patients' characteristics

The mean age and body weight of patients in 150-mg group were 44±9 years and 64±11 kg, those of patients in 300-mg group were 45±12 years and 61±12 kg. Seven were men, six were women in 150-mg group and five were men, eight were women in 300-mg group.

Baseline characteristics of patients in two groups are detailed in Table 1 and no statistical differences were noted

Table 1 Clinical characteristics of patients

		150 mg	300 mg	<i>P</i>
Age (yr)		44±9	45±12	0.814 ¹
Sex	Male	7	5	0.734
	Female	6	8	
Weight		64±11	61±12	0.428 ¹
Duration of reflux disease	<6 mo	5	2	0.412
	6 mo–2 yr	6	8	
	>2 yr	2	3	
Pre-medication	Yes	2	1	0.828
	No	11	12	
Endoscopy (Savary-Miller grade)	0	5	7	0.717
	I	7	5	
	II	1	1	
Drinking	Yes	2	3	0.884
	No	11	10	
Smoking	Yes	3	3	1
	No	10	10	

P value by χ^2 test except for ¹two sample *t*-test.

in the past history, smoking and drinking history and endoscopic results.

Efficacy of itopride on GERD symptoms

A significant improvement of all symptoms including heartburn, a main symptom of GERD, was identified after the 150 and 300 mg of itopride treatment compared with the pre-treatment (Figure 1A). No statistically significant differences were found between two groups in the symptom improvement (Figure 2B).

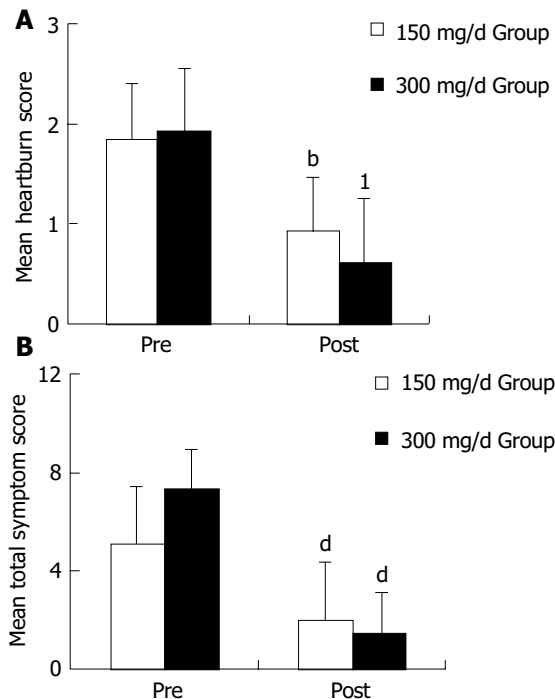


Figure 1 A: Change in mean heartburn score after treatment of itopride. The heartburn score of patients with GERD was improved in both groups of itopride significantly. ^b $P < 0.0001$, ¹ $P = 0.0006$ vs pretreatment by paired *t*-test; B: Change in mean total symptom score after treatment of itopride. The mean total symptom score of patients with GERD was improved in both groups of itopride significantly. ^d $P < 0.0001$ vs pretreatment by paired *t*-test.

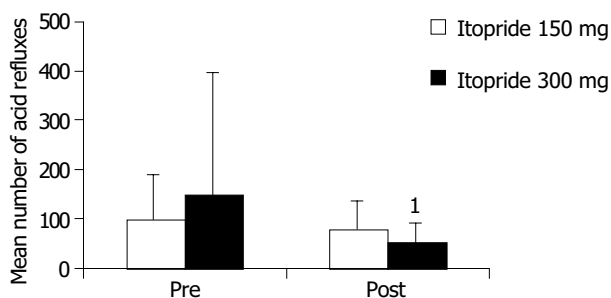


Figure 2 Change in mean number of acid refluxes after itopride treatment. Mean number of acid refluxes was significantly improved in 300-mg group. ¹ $P = 0.057$ vs pretreatment by Wilcoxon's signed rank test.

Efficacy of itopride on esophageal acid reflux variables

Among the acid reflux variables recorded, total time of

pH<4, per cent time with pH<4 and DeMeester score were significantly improved in 300-mg group compared with the pre-treatment (Figure 2). In 150-mg group, itopride significantly reduced the duration of longest episode compared with the pre-treatment. The individual values of acid reflux variable before and after treatment with 150 or 300 mg of itopride are given in Table 2.

Safety of itopride

Itopride was well tolerated and only minor adverse events were reported. There were no significant changes in the mean level of prolactin with the 4-wk treatment of 150- or 300-mg itopride (Figure 3). In two patients of the 300-mg group, prolactin level was increased over 15 ng/mL, but there were no adverse events like lacteal secretion.

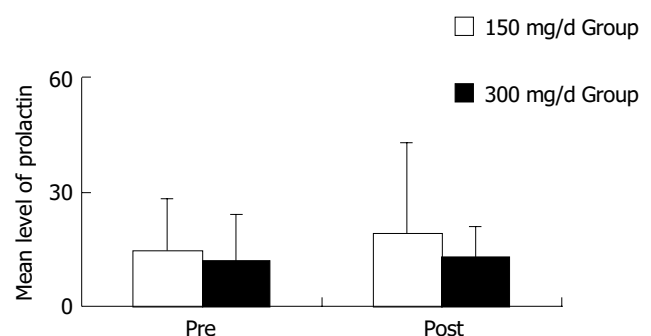


Figure 3 Change in mean level of prolactin after itopride treatment. The level of prolactin was not changed after treatment of itopride in GERD.

DISCUSSION

The result of this pilot study demonstrates that itopride decreases esophageal acid reflux and relieved symptoms without any significant adverse event in patients with GERD. These results show that itopride can improve the pathologic conditions of GERD.

The aims of treatment for GERD are relief of symptoms and healing of damaged lesion if endoscopic or pathologic examinations revealed mucosal damage of esophagus. Currently, it is being considered that long-term treatment is required because GERD has been regarded as chronic-relapsing disease like hypertension and diabetes mellitus^[12,13].

Among several therapeutic drugs, a prokinetic agent has been used for the treatment and improvement of pathogenic mechanism of GERD such as gastrointestinal motility disorder, incompetent LES relaxation, impaired esophageal acid clearance, and prolonged gastric emptying. Among the kinds of prokinetic drugs, many studies have focused on the effect of cisapride on GERD. In one of them, cisapride increased tones of esophageal peristalsis and LES dose-dependency in healthy subjects^[14,15]. On the contrary, in the other study, cisapride did not have any influence on the postprandial esophageal peristalsis, gastric acid^[16] and LES pressure^[17] in healthy subjects.

Even though this study does not confirm the efficacy of itopride on the esophageal peristalsis and LES, considering that itopride improves symptoms of the patients with GERD and decreases acid reflux effectively, we can speculate that

Table 2 Changes of acid reflux variables and DeMeester score in 26 patients with GERD after treatment with 150 or 300 mg of itopride

Variable	Group (mg/d)	Itopride Tx.	n	Mean	SD	P
Number of acid refluxes	150	Pre	12	99.25	88.57	0.97
		Post	12	76.92	60.53	
	300	Pre	13	150.77	246.15	0.057
		Post	13	52.23	39.79	
Number of acid refluxes longer than 5 min	150	Pre	12	6.08	5.32	0.287
		Post	12	3.83	5.32	
	300	Pre	13	6.23	5.12	0.054
		Post	13	2.69	2.5	
Longest time acid refluxes (min)	150	Pre	12	30.55	33.37	0.018
		Post	12	14.09	11.03	
	300	Pre	13	30.25	56.4	0.289
		Post	13	20.78	33.64	
Total time below pH 4 (min)	150	Pre	12	138.42	98.56	0.16
		Post	12	92.09	78.07	
	300	Pre	13	145.08	86.1	0.011
		Post	13	71.77	51.43	
Fraction time below pH 4 (%)	150	Pre	12	11.13	9.26	0.211
		Post	12	10.12	12.69	
	300	Pre	13	11.2	6.69	0.005
		Post	13	5.27	3.57	
DeMeester score	150	Pre	12	32.5	16.96	0.16
		Post	12	22.89	18.75	
	300	Pre	13	44.48	37.5	0.007
		Post	13	19.56	14.72	

itopride exerts some effects on improving esophageal motor dysfunction. Further studies will be required for making out the effect of itopride on the esophageal motor dysfunction of GERD.

From the viewpoint of improving symptom and healing mucosa, it was observed that administration of cisapride 10 mg four times a day (q.i.d.) and 20 mg twice a day (b.i.d.) improved the esophageal reflux compared with placebo, and cisapride had the same effect as H₂ blocker on treatment of patients with mild esophagitis^[6,7]. Additionally, it was reported that a combination therapy with cisapride and H₂ blocker was more effective than monotherapy in patients with severe reflux esophagitis^[18].

Although a few studies on functional dyspepsia show that the efficacy of itopride was equivalent to that of cisapride^[11], this is the first study reporting that administration of itopride for 4 wk improves symptoms of GERD including heartburn (the main symptom of GERD) in both 150- and 300-mg group. So hereafter, additional studies will be required for evaluating the effect of itopride monotherapy or combination therapy with H₂ receptor inhibitors on the esophagitis with mucosal damage as the initial and maintenance treatment.

The most standard method to measure the variation of esophageal acid is ambulatory 24-h pH-metry. In other studies using a similar method, cisapride 10 mg q.i.d. for 8 wk was more effective than placebo in terms of decreasing the number of reflux episodes, duration of longest episode, and percent time with pH<4. These results suggest that cisapride is useful for acid reflux in patients with GERD^[19].

In the study of mosapride 40 mg every day (q.d.) for 2 d, it reduced the number of reflux episodes, the number of reflux episodes >5 min, and percent time with pH<4 and improved acid clearance time^[20]. In this study, itopride

100 mg t.i.d. for 4 wk was effective in decreasing percent time with pH<4 and DeMeester score. In this regard, it can be considered that itopride has a similar effect on decreasing acid reflux as cisapride or mosapride, although it is different in the action mechanism or duration of treatment from cisapride or mosapride^[9,10].

The action mechanism of itopride on the reflux variables is unclear so far. But, dual mechanism of itopride, acetylcholine esterase inhibitory action and antagonistic activity on dopamine D₂ receptor, which is known to inhibit activities of acetylcholine^[21], seems to make this drug effective on promoting the esophageal and gastrointestinal movement and on improving acid clearance. It has been known that the threshold of itopride to promote gastrointestinal motility is higher than that of cisapride, metoclopramide and domperidone^[8].

Prokinetic drugs that inhibit dopamine D₂ receptor may elicit some adverse events such as fatigue, confusion, extrapyramidal symptom, and hyperprolactinemia that cause lacteal secretion or breast enlargement. Although there was no extensive study concerned about safety of itopride, the development of extrapyramidal symptom or hyperprolactinemia was uncommon with the administration of usual dosage of itopride (150 mg/d). In this study, there was no hyperprolactinemia and extrapyramidal symptoms in 150-mg group of itopride and there were two cases showing over 15 ng/mL of prolactin level in 300-mg group of itopride without adverse events like lacteal secretion^[22].

Taken together, these results demonstrate that the administration of 150 or 300 mg of itopride for 4 wk improves symptoms of GERD and that the administration of 300 mg of itopride for 4 wk improves mild esophagitis and pathologic acid reflux. Therefore, itopride can be useful for treatment of the patients with GERD.

REFERENCES

- 1 **Lundell L**, Myers JC, Jamieson GG. Is motility impaired in the entire upper gastrointestinal tract in patients with gastro-oesophageal reflux disease? *Scand J Gastroenterol* 1996; **31**: 131-135
- 2 **Rydberg L**, Ruth M, Lundell L. Does oesophageal motor function improve with time after successful antireflux surgery? Results of a prospective, randomized clinical study. *Gut* 1997; **41**: 82-86
- 3 **Achem SR**, Robinson M. A prokinetic approach to treatment of gastroesophageal reflux disease. *Dig Dis* 1998; **16**: 38-46
- 4 **Ramirez B**, Richter JE. Review article: promotility drugs in the treatment of gastro-oesophageal reflux disease. *Aliment Pharmacol Ther* 1993; **7**: 5-20
- 5 **Kim YB**, Song CW, Kim HR, Lee SW, Bak YT, Hyun JH, Moon JS, Park HC. The incidence of gastroesophageal reflux disease and the effect of cisapride in patients with epigastric soreness. *Korean J Gastrointestinal Motility* 2000; **6**: 168-195
- 6 **Richter JE**, Long JF. Cisapride for gastroesophageal reflux disease: a placebo-controlled, double-blind study. *Am J Gastroenterol* 1995; **90**: 423-430
- 7 **Castell DO**, Sigmund C Jr, Patterson D, Lambert R, Hasner D, Clyde C, Zeldis JB. Cisapride 20 mg b.i.d. provides symptomatic relief of heartburn and related symptoms of chronic mild to moderate gastroesophageal reflux disease. CIS-USA-52 Investigator Group. *Am J Gastroenterol* 1998; **93**: 547-552
- 8 **Iwanaga Y**, Miyashita N, Morikawa K, Mizumoto A, Kondo Y, Itoh Z. A novel water-soluble dopamine-2 antagonist with anticholinesterase activity in gastrointestinal motor activity. Comparison with domperidone and neostigmine. *Gastroenterology* 1990; **99**: 401-408
- 9 **Iwanaga Y**, Miyashita N, Mizutani F, Morikawa K, Kato H, Ito Y, Itoh Z. Stimulatory effect of N-[4-[2-(dimethylamino)ethoxy] benzyl]-3,4-dimethoxybenzamide hydrochloride (HSR-803) on normal and delayed gastrointestinal propulsion. *Jpn J Pharmacol* 1991; **56**: 261-269
- 10 **Choi MG**, Choo KY, Kim BW, Choi H, Park SH, Oh JH, Han SW, Kim JK, Chung IS, Chung KW, Sun HS. The effect of itopride on proximal gastric tone and visceral perception in healthy human. *Kor J Gastroenterol* 2000; **36**: 293-301
- 11 **Kim JK**, Moon SB, Choi H, Kim SW, Chung KW, Sun HS, Lee HY, Hong SS. An effectiveness and safety of Itopride versus Cisapride in functional dyspepsia. *Kor J Gastroenterol* 1999; **33**: 749-756
- 12 **DeVault KR**. Overview of medical therapy for gastroesophageal reflux disease. *Gastroenterol Clin North Am* 1999; **28**: 831-845
- 13 **DeVault KR**, Castell DO. Updated guidelines for the diagnosis and treatment of gastroesophageal reflux disease. The Practice Parameters Committee of the American College of Gastroenterology. *Am J Gastroenterol* 1999; **94**: 1434-1442
- 14 **Gilbert RJ**, Dodds WJ, Kahrilas PJ, Hogan WJ, Lipman S. Effect of cisapride, a new prokinetic agent, on esophageal motor function. *Dig Dis Sci* 1987; **32**: 1331-1336
- 15 **Ceccatelli P**, Janssens J, Vantrappen G, Cucchiara S. Cisapride restores the decreased lower oesophageal sphincter pressure in reflux patients. *Gut* 1988; **29**: 631-635
- 16 **Wallin L**, Kruse-Andersen S, Madsen T, Boesby S. Effect of cisapride on the gastro-oesophageal function in normal human subjects. *Digestion* 1987; **37**: 160-165
- 17 **Holloway RH**, Downton J, Mitchell B, Dent J. Effect of cisapride on postprandial gastro-oesophageal reflux. *Gut* 1989; **30**: 1187-1193
- 18 **Galmiche JP**, Brandstatter G, Evreux M, Hentschel E, Kerstan E, Kratochvil P, Reichel W, Schutze K, Soule JC, Vitaux J. Combined therapy with cisapride and cimetidine in severe reflux oesophagitis: a double blind controlled trial. *Gut* 1988; **29**: 675-681
- 19 **Nah YH**, Song JH. Effect of Cisapride on ambulatory 24 - hour esophageal pH profile in gastroesophageal reflux disease. *Kor J Gastroenterol* 1990; **22**: 515-521
- 20 **Ruth M**, Hamelin B, Rohss K, Lundell L. The effect of mosapride, a novel prokinetic, on acid reflux variables in patients with gastro-oesophageal reflux disease. *Aliment Pharmacol Ther* 1998; **12**: 35-40
- 21 **Glavin GB**, Szabo S. Dopamine in gastrointestinal disease. *Dig Dis Sci* 1990; **35**: 1153-1161
- 22 **Perkel MS**, Hersh T, Moore C, Davidson ED. Metoclopramide therapy in fifty-five patients with delayed gastric emptying. *Am J Gastroenterol* 1980; **74**: 231-236

Science Editor Guo SY Language Editor Elsevier HK

• CLINICAL RESEARCH •

Clinical analysis of multiple primary malignancies in the digestive system: A hospital-based study

Hui-Yun Cheng, Cheng-Hsin Chu, Wen-Hsiung Chang, Tzu-Chi Hsu, Shee-Chan Lin, Chuan-Chuan Liu, An-Ming Yang, Shou-Chuan Shih

Hui-Yun Cheng, Chuan-Chuan Liu, An-Ming Yang, Shou-Chuan Shih, Health Evaluation Center, Mackay Memorial Hospital, Taipei, Taiwan, China

Hui-Yun Cheng, Cheng-Hsin Chu, Wen-Hsiung Chang, Shee-Chan Lin, An-Ming Yang, Shou-Chuan Shih, Department of Internal Medicine, Mackay Memorial Hospital, Taipei, Taiwan, China
Tzu-Chi Hsu, Department of Surgery, Mackay Memorial Hospital, Taipei, Taiwan, China

Cheng-Hsin Chu, Shou-Chuan Shih, Mackay Medicine, Nursing and Management College, Taipei, Taiwan, China

Correspondence to: Dr. Shou-Chuan Shih, Department of Internal Medicine, Mackay Memorial Hospital, No. 92, Section 2, Chung Shan North Road, Taipei, Taiwan, China. hychey@msl.mmh.org.tw
Telephone: +886-2-25433535-2860

Received: 2004-11-05 Accepted: 2004-12-08

lesions, based on an awareness of the possibility of second and third cancers, and multidisciplinary treatment strategies will substantially increase the survival of these patients.

© 2005 The WJG Press and Elsevier Inc. All rights reserved.

Key words: Multiple primary malignancies; Digestive system

Cheng HY, Chu CH, Chang WH, Hsu TC, Lin SC, Liu CC, Yang AM, Shih SC. Clinical analysis of multiple primary malignancies in the digestive system: A hospital-based study. *World J Gastroenterol* 2005; 11(27): 4215-4219
<http://www.wjgnet.com/1007-9327/11/4215.asp>

Abstract

AIM: To analyze the characteristics of multiple primary malignancies (MPMs) of digestive system; including incidence, types of tumor combinations, time intervals between development of multiple tumors, clinical course, and prognostic factors affecting survival and mortality.

METHODS: Data from a total of 129 patients treated from January 1991 to December 2000 for pathologically proved MPMs, including at least one originating from the digestive system, were reviewed retrospectively.

RESULTS: Among 129 patients, 120 (93.02%) had two primary cancers and 9 (6.98%) had three primary cancers. The major sites of MPMs of the digestive system were large intestine, stomach, and liver. Associated non-digestive cancers included 40 cases of gynecological cancers, of which 31 were carcinoma of cervix and 10 cases of genitourinary cancers, of which 5 were bladder cancers. Other cancers originated from the lung, breast, nasopharynx, larynx, thyroid, brain, muscle, and skin. Reproductive tract cancers, especially cervical, ovarian, bladder, and prostate cancers were the most commonly associated non-GI cancers, followed by cancer of the lung and breasts. Forty-three cases were synchronous, while the rest (86 cases) were metachronous cancers. Staging of MPMs and treatment regimes correlated with the prognosis between survival and non-survival groups.

CONCLUSION: As advances in cancer therapy bring about a progressively larger percentage of long-term survivors, the proportion of patients with subsequent primary lesions will increase. Early diagnosis of these

INTRODUCTION

Many types of cancer, when treated early and aggressively, can be cured. The potential, however, for cancer to occur independently a second time, or more often, in the same patients remains an ever present risk. Interest in multiple primary malignancies (MPMs) is long-standing since Warren and Gates in 1932. He proposed that each suspected primary tumor (1) must be clearly malignant as determined by histological evaluation; (2) must be geographically separate and distinct. The lesion should be separated by normal appearing mucosa. If a secondary neoplasm is contiguous to the initial primary tumor or is separated by mucosa with intraepithelial neoplastic changes, the two should be considered as confluent growth rather than multi-centric carcinomas; and (3) the possibility that the second neoplasm represents a metastasis should be excluded. The observation that the invasive carcinoma arises from an overlying epithelium, which demonstrates a transition from carcinoma *in situ* to invasive carcinoma, is helpful, and when the separate foci have significant differences in histology, the diagnosis of separate primary cancers is appropriate^[1,2].

Multiple primary cancers may be synchronous or metachronous depending on the interval between their diagnosis. Synchronous cancers are diagnosed simultaneously or within an interval of about 6 mo, and metachronous cancers are secondary cancers that developed more than 6 mo after the diagnosis of primary cancers usually after treatment of primary lesions^[2].

MPMs were classified into four types: (1) multicentric, if the two distinct carcinomata arise in the same organ or tissue; (2) systemic, if they arise on anatomically or

functionally allied organs of the same system (colon and rectum cancers), (3) paired organs, as in the breasts, and (4) random, if they occur as a co-incidental or accidental association in unrelated sites^[3].

The development of more sophisticated invasive and non-invasive diagnostic tools has made it possible to detect cancer at an early stage. Furthermore, it has contributed to the detection of synchronous occult tumors, which were formerly overlooked.

An individual developing more than one primary tumor in anatomically and functionally unrelated organs may be considered as cancer-prone. People with a family history of cancer will inherit genetic cancer susceptibility as a risk factor for cancer. Gene mutations influence cancer susceptibility through changes of metabolism and catabolism of carcinogens. Tumor suppressor genes, such as *p53* and *FHIT*, may be candidates for target genes of these risk factors^[4]. Genetic instability is also considered as a driving force behind carcinogenesis and the alterations of the length of single repetitive genomic sequences or microsatellite instability, implicating impaired DNA repair mechanism^[5]. People with newly diagnosed cancers and survivors of earlier cancers who have genetic cancer susceptibility, therefore, have an increased risk of MPMs.

This study has analyzed the incidence of MPMs in digestive system, as well as the different tumor combinations, time interval between occurrence of tumors, staging, clinical course, and prognostic features of survival and non-survival groups.

The purpose of this study is to determine whether certain organs or systems are particularly susceptible to second or third primary cancers and, by clarifying this tendency, to aid in the early diagnosis of these lesions.

MATERIALS AND METHODS

Retrospective data from a total of 9 807 patients treated at the Mackay Memorial Hospital from January 1991 to December 2000 for pathologically proven cancer were reviewed from the Cancer Registry. Of these, 246 patients had multiple primary cancers, among which 129 (58 males and 71 females) had MPMs in the digestive system and were included in this study.

The histological criteria described by Warren and Gates^[1] and Moertel *et al.*^[3], were used for diagnosing multiple separate primary malignancies.

Clinical histories, diagnostic methods, histology, staging, and clinical course of each tumor were reviewed in all patients. The age at the onset of the primary cancer and the time intervals between two or more cancers were recorded. The distribution of the digestive and associated non-digestive cancers in these 129 patients was also investigated. Fifty-two patients had received previous radiotherapy or chemotherapy for their first cancers, and interval between the first and second cancers were recorded. All tumors had been staged according to the American Joint Committee on Cancer TNM staging system^[6]. The prognostic factors between survival and non-survival groups were analyzed for double primary cancers.

The differences between groups were analyzed by Student's *t*-test for continuous variables and the χ^2 test for

categorical data. A *P* value of <0.05 was considered as statistical significance.

RESULTS

Among the 9 807 pathologically proven cancer patients, 246 had MPMs, with an incidence of 2.5%. Among these, 129 (52.43%), including 58 males (44.96%) and 71 females (55.04%), had MPMs of the digestive system. One hundred and twenty patients (93.02%) had two primary malignancies, and nine (6.98%) had three primary malignancies. The age at onset of the primary cancers ranged from 29 to 89 years (mean 60.3 ± 13.05 years) in double cancers, and 43 to 68 years (mean 50.22 ± 7.9 years) in triple cancers. Forty-three patients (35.8%) were over 65 years of age. Fifty-two patients (40.3%) had received previous radiotherapy or chemotherapy for their first cancer. The interval between the first and second cancers was 0.5-28 years (mean 8.1 ± 2.5 years) and 0.5-5 years (mean 3.2 ± 3.7 years) in the 32 patients receiving radiotherapy and the 17 patients receiving chemotherapy respectively.

The distribution and incidence of MPMs of the digestive system are shown in Table 1. The major site for MPMs of the digestive system was the large intestine (colon, 23.17%; rectum, 25.82%), followed by the stomach (23.17%) and liver (15.23%).

Distributions of associated non-digestive cancers in patients with MPMs are shown in Table 2. There were

Table 1 Distribution of MPMs in digestive tract

Site	Number of MPMs	Total number	Incidence (%)	% in GI MPMs
Esophagus	8	374	2.14	5.29
Stomach	35	1 770	1.98	23.17
Small bowel	3	76	3.95	1.98
Ampulla Vater	3	76	3.95	1.98
Liver	23	2 081	1.11	15.23
Gall bladder	2	58	3.45	1.32
Pancreas	3	303	0.99	1.98
Colon	35	1 010	3.47	23.17
Rectum	39	1 059	3.68	25.82

From January 1991 to December 2000.

Table 2 Distribution of associated non-GI cancers in patients with MPMs in digestive system

Site	n (%)	%
Gynecological cancers	40	45.97
Cervix	31/40 (77.50)	
Endometrium	2/40 (5)	
Ovary	7/40 (17.50)	
Genitourinary cancers	10	11.49
Bladder	5/10 (50)	
Kidney	2/10 (20)	
Prostate	3/10 (30)	
Lung	10	11.49
NPC	5	5.74
Breast	10	11.49
Skin	4	4.59
Thyroid gland	2	2.29
Neuromuscular tumor	2	2.29
Tongue	2	2.29
Gum	1	1.14
Brain	1	1.14

40 cases (45.97%) with gynecological cancers, of which 31 cases (77.5%) were carcinoma of uterine cervix; 10 cases (11.49%) with genitourinary cancer, among which 5 (50%) had bladder cancers and 3 (30%) had prostate cancers.

The most common tumor combination in double primary malignancies (both cancers originating from the digestive tract) was colon and rectum (10 cases), as shown in Tables 5-8.

The most common tumor combination in double primary malignancies (at least one originating from the digestive system) was rectum and cervical cancer (14 cases) and shown in Table 4.

Nine patients had triple cancers (Table 9). Mean time interval between diagnosis of the first and second primary cancer was 7.2 ± 3.86 years and for the second and third cancer was 5.24 ± 3.85 years. Two out of these nine patients had initial squamous cell cancers of cervix and nasopharynx

Table 3 Distribution of synchronous and metachronous MPMS in digestive system

Site	Synchronous (n)	Metachronous (n)	
		(1)	(2)
Colon ¹	13	10	19
Stomach ¹	8	3	11
Liver ¹	6	1	7
Esophagus ¹	0	1	1
Others ¹	0	2	1
Double GI	16	30	0
Total	43	47	39

¹Exclude double GI cases. (1): Primary GI tract cancer, secondary cancers of other sites. (2): Primary cancers of other sites, secondary GI tract cancers.

Table 4 Distribution of MPMS in large intestine: 42 cases¹

Subgroup	Large intestine	n	Non-GI cancers	n
(1)	Colon	5	Cervix	1
			Larynx	1
			Lung	1
			Uterus	1
			Left breast	1
	Rectum	5	Ovary	1
			Cervix	2
			Right breast	1
			Bladder	1
			Bladder	1
(2)	Colon	7	Cervix	2
			Ovary	1
			Thyroid	1
			Right thigh	1
			Bladder	1
	Rectum	12	Nose	1
			Cervix	9
			Right breast	1
			Thyroid	1
			Brain	1
(3)	Colon	7	Cervix	3
			Ovary	4
	Rectum	6	Cervix	3
			Left breast	1
			Lung	2

¹Excluding double primary GI tract cancers (22 cases). (1): Primary GI tract cancer, secondary cancers of other sites. (2): Primary cancers of other sites, secondary GI tract cancers. (3): Synchronous.

and developed synchronous adenocarcinoma of rectum and colon, with disease intervals of 9.4 and 5.9 years respectively.

Most of the tumors in double or triple primary malignancies were diagnosed at stages 3 or 4. Synchronous cancers were found in 43 cases, while 86 cases had metachronous cancers, among which 13 cases developed secondary cancers more than 10 years after diagnosis of primary malignancies (Tables 3 and 10).

There were no significant differences between the survival and non-survival groups in terms of age, gender, and time interval between first and second primary cancers. However, stage of tumor, especially stages 1-3 and radical treatment regimes correlated with prognosis in these two groups.

Table 5 Distribution of MPMS in stomach: 22 cases¹

Subgroup	Stomach	n	Non-GI cancers	n
(1)	Adenocarcinoma	3	Right breast	2
			NPC	1
(2)	Adenocarcinoma	11	Cervix	4
			Prostate	2
			Bladder	1
			Left kidney	1
			Tongue	1
			Larynx	1
			NPC	1
			NPC	2
(3)	Adenocarcinoma	8	Lung	3
			Prostate	1
			Bladder	1
			Skull	1
			Skull	1

¹Exclude double GI cases (12 cases). (1): Primary GI tract cancer, secondary cancers of other sites. (2): Primary cancers of other sites, secondary GI tract cancers. (3): Synchronous.

Table 6 Distribution of MPMS in liver: 14 cases¹

Subgroup	Liver	n	Non-GI cancers	n
(1)	Hepatoma	1	Bladder	1
(2)	Hepatoma	7	Cervix	4
			Right breast	2
			Right leg	1
(3)	Hepatoma	6	Gum	1
			Skull	1
			Right kidney	1
			Lung	3

¹Exclude double GI cases (10 cases). (1): Primary GI cancer, secondary cancers of other sites. (2): Primary cancers of other sites, secondary GI cancers. (3): Synchronous.

Table 7 Distribution of synchronous double GI MPMS: 16 cases

Site	n	Site	n
Esophagus	2	Stomach	1
		Gall bladder	1
Stomach	3	Rectum	1
		Gall bladder	1
		Sigmoid colon	1
Duodenum	1	Sigmoid colon	1
Sigmoid colon	3	Appendix	1
		Rectum	2
Rectum	3	Ascending colon	3
Liver	4	Hepatic flexure	1
		Stomach	3

Table 8 Distribution of metachronous double GI MPMs: 30 cases

1 st cancer	n	2 nd cancer	n
Esophagus	3	Stomach	1
		Liver	2
Stomach	4	Rectum	1
		Esophagus	1
		Liver	1
		Pancreatic head	1
GIST of ileum	1	Liver	1
Ampulla Vater	2	Liver	2
Appendix	2	Rectum	2
Cecum	2	Stomach	2
Colon	6	Liver	2
		Stomach	1
		Pancreatic head	3
Rectum	10	Stomach	1
		Liver	1
		Transverse colon	5
		Esophagus	3

Table 9 Sites and dates of diagnosis of triple primary cancers (nine cases)

Age (yr)/sex	First primary	Second primary	Third primary
68/Female	3/84 Cervix	6/93 Rectum	6/93 Sigmoid colon
46/Female	9/85 Cervix	8/88 Rectum	8/95 Ascending colon
49/Female	8/84 Ovary	10/86 Cervix	3/90 Rectum
47/Female	8/79 Breast	9/89 Cervix	10/97 Liver
50/Male	6/82 Stomach	5/85 Skin	4/91 Ascending colon
45/Male	8/84 Stomach	3/86 Prostate	1/92 Ascending colon
43/Male	3/89 Nasopharynx	2/95 Sigmoid colon	2/95 Rectum
46/Female	1/84 Larynx	4/88 Sigmoid colon	3/91 Esophagus
58/Female	3/71 Right breast	6/82 Sigmoid colon	6/92 Ascending colon

The age listed is that at the time of diagnosis of the first primary.

Table 10 Demographic and clinical data in survival and non-survival groups¹

	Survival n = 40	Non-survival n = 80	P
Median age (yr)	61.50±13.60 (29–84)	60.00±14.78 (30–89)	0.46
Gender			
Male	16	39	0.18
Female	24	41	0.18
Time interval (mo)	32.78±27.07	32.98±18.58	0.49
Staging			
Stage 1	14	2	<0.01 ^b
Stage 2	19	2	<0.01 ^b
Stage 3	6	41	0.04 ^a
Stage 4	1	35	0.16
Treatment regimes ²			
Radical	36	16	<0.01 ^b
Palliative	2	36	0.08
Supportive	2	28	0.08

¹Excluding triple primary cancers nine cases. ²Radical treatment includes radical surgery±radiotherapy±chemotherapy. Palliative treatment includes palliative surgery±radiotherapy±chemotherapy. ^aP<0.05, ^bP<0.01 vs others.

DISCUSSION

The presence of a single tumor does not offer immunity against the development of second, third, or additional

primary malignant lesions in the same patient. Multiple primary malignant tumors in the same individual are experienced more frequently as advances in cancer treatment prolong life. Improved survival rates for patients with neoplastic disease, largely due to early diagnosis, allow more patients to survive long enough to develop subsequent primary tumors.

The incidence of MPMs has been carried out by the review of cancer registries in several countries, and ranged from 0.7 to 11%^[7-10]. In our study, the incidence of MPMs was 2.21%, which was similar to the 2.6% as reported by Okamoto *et al.*^[11].

In our study, the major site of MPMs in the digestive system was the large intestine, followed by stomach and liver. Cancers of the large intestine, particularly hereditary nonpolyposis colorectal cancers, were associated with increased frequencies of endometrial and ovarian cancers^[12]. However, MPMs of large intestine in our study were most commonly associated with carcinoma of cervix (17 cases) and stomach (8 cases), while only two were associated with carcinoma of endometrium and six were with ovarian cancers. The significance of these differences may be due to the fact that carcinoma of cervix is much more common than endometrial cancer in our country. Unfortunately, no genetic evaluation was performed in our patients.

The predilection of MPMs for the large intestine is noted in numerous reports in the literatures^[13-15]. In our series, 49 of 129 patients (37.98%) had colorectal malignancy as the first primary lesion. Of these, seven (14.28%) had a second primary cancer in the colon or rectum and four (8.16%) had a second primary cancer in the stomach. The interval between the diagnosis of the first primary colorectal cancer and the development of the second colorectal carcinoma averaged 7 years, and ranged from 1½ to 14 years. This suggests that patients without evidence of disease for 5 years after operation of colorectal cancers still require careful follow-up studies of gastrointestinal tract.

Genitourinary cancers, especially cervical and ovarian cancers, bladder and prostate cancers were the common associated non-GI cancers, followed by cancers of lung and breast. Thus, attention should be paid to these sites during the period of post-operative follow-up of the first primary cancer.

The majority of MPMs may occur as a result of random chance^[16]. Nonetheless, different mechanisms have been considered to be involved in MPMs, such as intense exposure to carcinogens, the effects of chemo- and/or radiotherapy and the influence of genetic predisposition.

Both the chemo- and radiotherapy have been shown to be carcinogenic in several reports^[17,18]. In our study, 52 patients (40.3%) had received previous radiotherapy or chemotherapy for their first cancer, and the interval between the first and second cancers was 0.5–28 years (mean 8.1 years) and 0.5–5 years (mean 3.2 years) in the 32 patients receiving radiotherapy and the 20 patients receiving chemotherapy respectively. This suggests that radiotherapy and/or chemotherapy may play an important role in the development of MPMs.

The main problem in proving a correlation between antineoplastic therapies and secondary cancer may be

attributable to detection bias rather than to carcinogenic therapy^[19]. Beyond an increased zeal in searching, diagnostic agents and methods have improved such that the detection of cancer today is enhanced by improvements in technology, cytogenetics, and surveillance.

Based on a pooled analysis involving 316 relatives of 12 families, Lynch *et al.*^[20], have demonstrated a 21.5% incidence of MPMs, a consistent 3% risk for a second primary cancer in each year of survival following the first onset, and a significantly higher 6.9% risk per year for the development of a third primary cancer following the second neoplasm.

In our study, there were no significant differences between the survival and non-survival groups in terms of age, gender, and time intervals between first and second primary cancers. Only stage of tumors, especially stages 1-3, and radical treatment regimes correlated with prognosis in these two groups.

Two important inferences can be obtained from our analysis: (1) the early diagnosis of a second primary lesion may alter survival rate. Hence more intensive surveillance and appropriate cytogenetic and molecular studies should be developed in order to improve strategies to detect MPMs, and (2) multidisciplinary treatment strategies are important to ameliorate quality of life and survival rates in patients with MPMs.

It is fundamental that patients who have been treated for cancers require careful follow-up studies. When symptoms and signs of tumor develop in a patient who has been treated for an initial cancer, they should not be assumed to represent metastases. The possibility of a localized and curable second primary cancer should be considered and evaluated. As advances in cancer therapy bring about a progressively large percentage of long-term survivors, the proportion of patients with subsequent primary lesions will increase. Early diagnosis of these lesions, based on an awareness of the possibility of second and third cancers, and multidisciplinary treatment will substantially increase the survival of these patients.

REFERENCES

- 1 Warren S, Gates O. Multiple primary malignant tumors: A survey of the literature and statistical study. *Am J Cancer* 1932; **16**: 1358-1414
- 2 Kapsinow R. Multiple primary cancer. A classification with report of cases. *J La State Med Soc* 1962; **114**: 194-200
- 3 Moertel CG, Dockerty MB, Baggenstoss AH. Multiple primary malignant neoplasms. II. Tumors of different tissues or organs. *Cancer* 1961; **14**: 231-237
- 4 Morita M, Saeki H, Mori M, Kuwano H, Sugimachi K. Risk factors for esophageal cancer and the multiple occurrence of carcinoma in the upper aerodigestive tract. *Surgery* 2002; **131** (1 Suppl): S1-6
- 5 Sardi I, Franchi A, Bocciolini C, Mechi C, Frittelli A, Bruschini L, Gallo O. Microsatellite instability as biomarker for risk of multiple primary malignancies of the upper aerodigestive tract. *Oncol Rep* 2001; **8**: 393-399
- 6 American Joint Committee on Cancer. Manual for staging cancer. 4th ed. Philadelphia: JB Lippincott 1992: 75-82
- 7 Coleman MP. Multiple primary malignant neoplasms in England and Wales, 1971-1981. *Yale J Biol Med* 1986; **59**: 517-531
- 8 Levi F, Randimbson L, Te VC, Rolland-Portal I, Franceschi S, La Vecchia C. Multiple primary cancers in the Vaud Cancer Registry, Switzerland, 1974-89. *Br J Cancer* 1993; **67**: 391-395
- 9 Tsukuma H, Fujimoto I, Hanai A, Hiyama T, Kitagawa T, Kinoshita N. Incidence of second primary cancers in Osaka residents, Japan, with special reference to cumulative and relative risks. *Jpn J Cancer Res* 1994; **85**: 339-345
- 10 Frodin JE, Ericsson J, Barlow L. Multiple primary malignant tumors in a national cancer registry-reliability of reporting. *Acta Oncol* 1997; **36**: 465-469
- 11 Okamoto N, Morio S, Inoue R, Akiyama K. The risk of a second primary cancer occurring in five-year-survivors of an initial cancer. *Jpn J Clin Oncol* 1987; **17**: 205-213
- 12 Watson P, Lynch HT. Extracolonic cancer in hereditary nonpolyposis colorectal cancer. *Cancer* 1993; **71**: 677-685
- 13 Rosenthal I, Baronofsky ID. Prognostic and therapeutic implications of polyps in metachronous colic carcinoma. *JAMA* 1960; **172**: 37-41
- 14 Polk HC Jr, Spratt JS Jr, Butcher HR Jr. Frequency of multiple primary malignant neoplasms associated with colorectal carcinoma. *Am J Surg* 1965; **109**: 71-75
- 15 Bachulis BL, Williams RD. Multiple primary malignancies. *Arch Surg* 1966; **92**: 537-540
- 16 Robinson E, Neugut AI. Clinical aspects of multiple primary neoplasms. *Cancer Detect Prev* 1989; **13**: 287-292
- 17 Brumback RA, Gerber JE, Hicks DG, Strauchen JA. Adenocarcinoma of stomach following irradiation and chemotherapy for lymphoma in young patients. *Cancer* 1984; **54**: 994-998
- 18 Sandler RS, Sandler DP. Radiation-induced cancers of the colon and rectum: assessing the risk. *Gastroenterology* 1983; **84**: 51-57
- 19 Craig SL, Feinstein AR. Antecedent therapy versus detection bias as causes of neoplastic multimorbidity. *Am J Clin Oncol* 1999; **22**: 51-56
- 20 Lynch HT, Harris RE, Lynch PM, Guirgis HA, Lynch JF, Bardawil WA. Role of heredity in multiple primary cancer. *Cancer* 1977; **40**(4 Suppl): 1849-1854

• CLINICAL RESEARCH •

Surgical experience in splitting donor liver into left lateral and right extended lobes

Ji-Qi Yan, Thomas Becker, Michael Neipp, Cheng-Hong Peng, Rainer Lueck, Frank Lehner, Hong-Wei Li, Juergen Klempnauer

Ji-Qi Yan, Cheng-Hong Peng, Hong-Wei Li, Department of Surgery, Ruijin Hospital Affiliated to Shanghai Second Medical University, Shanghai 200025, China

Ji-Qi Yan, Thomas Becker, Michael Neipp, Rainer Lueck, Frank Lehner, Juergen Klempnauer, Department of Abdominal and Transplant Surgery, Medical School of Hannover, Carl-Neuberg-Str. 1, Hannover 30625, Germany

Supported by the DAAD Foundation

Correspondence to: Ji-Qi Yan, MD, Department of Surgery, Ruijin Hospital Affiliated to Shanghai Second Medical University, Shanghai 200025, China. jiqiyan@yahoo.com

Telephone: +86-21-64370045 Fax: +86-21-64333548

Received: 2004-10-09 Accepted: 2004-11-19

Yan JQ, Becker T, Neipp M, Peng CH, Lueck R, Lehner F, Li HW, Klempnauer J. Surgical experience in splitting donor liver into left lateral and right extended lobes. *World J Gastroenterol* 2005; 11(27): 4220-4224

<http://www.wjgnet.com/1007-9327/11/4220.asp>

Abstract

AIM: To outline the surgical experience with donor liver splitting in split liver transplantation.

METHODS: From March 1 to September 1 in 2004, 10 donor livers were split *ex situ* into a left lateral lobe (segments II and III) and a right extended lobe (segments I, IV-VIII) in Medical School of Hannover, and thereafter split liver transplantation was performed successfully in 19 cases. The average age, weight and ICU staying period of the donors were 32.7 years (15-51 years), 64.5 kg (45-75 kg) and 2.4 d (1-8 d) respectively.

RESULTS: The average weight of the whole graft and the left lateral lobe was 1 322.6 g (956-1 665 g) and 281.8 g (198-373 g) respectively, and the average ratio of left lateral lobe to the whole graft was 0.215 (0.178-0.274). The average graft to recipient weight ratio (GRWR) of the left lateral lobe and the right extended lobe reached 2.44% (1.22-5.41%) and 1.73% (1.31-2.30%) respectively. On average it took approximately 105 min (85-135 min) to split the donor liver. Five donor organs showed anatomic variation including the left hepatic vein variation in two cases, the left hepatic artery variation in two cases and the bile duct variation in one case.

CONCLUSION: Split liver transplantation has become a mature surgical technique to expand the donor pool with promising results. In the process of graft splitting, close attention needs to be paid to potential anatomic variations, especially to variations of the left hepatic vein, the left hepatic artery, and the bile duct.

© 2005 The WJG Press and Elsevier Inc. All rights reserved.

Key words: Split; Donor liver; Anatomic variation

INTRODUCTION

Orthotopic liver transplantation (OLT) has been widely accepted as an effective treatment for end-stage liver diseases. The advent of new immunosuppressive agents and refinement of the surgical techniques have accounted for remarkable progress in the years since the first OLT was performed in 1963. Thousands of patients who would have died otherwise have been saved by the improved results of organ transplantation. However, the past two decades have also witnessed an exceptional increase in the number of patients awaiting liver transplantation, and the ever-growing great disparity between demand and supply of donor organs has become the major limiting factor for further expansion of liver transplantation. Hence, a death rate on the waiting of 10-15% would even be underestimated^[1]. Historically, the situation has been worse for children because of the difficulty of finding size-matched donor organs^[2]. However, the development of a reduced-size liver transplant technique has provided a first step to alleviate this problem^[3-5]. Although such technique does not increase the number of grafts available, it shifts available organs from adult to pediatric recipient. Obviously, split liver transplantation, first successfully performed in the Medical School of Hannover^[6], is becoming an efficient approach to expand the donor pool for both adults and children.

MATERIALS AND METHODS

From March 1 to September 1 in 2004, a total of 10 donor livers were split *ex situ* in Medical School of Hannover. All these donor livers were divided into a left lateral lobe (segments II and III) and a right extended lobe (segments I, IV-VIII), and thus making available split liver transplantation to 19 patients (in 6 cases the right extended lobe was sent to another transplantation center). The average age and weight of those 10 brain death donors were 32.7 years (15-51 years) and 64.5 kg (45-75 kg) respectively. Before the organ procurement, the average ICU stay of the donors was 2.4 d (1-8 d), and the average serum level of AST, creatinine, sodium and total bilirubin was 53.0 IU/L (14-122 IU/L), 0.91 mg/dL (0.40-1.25 mg/dL), 148.5 mmol/L (137-158 mmol/L), and 0.70 mg/dL (0.09-1.60 mg/dL) respectively.

Ten pediatric patients, three boys and seven girls, received left lateral lobe liver transplantation. The average age and weight of the pediatric recipients were 48.1 mo (5-82 mo) and 14.3 kg (6.9-23.8 kg) respectively. Indications included seven cases of congenital biliary atresia (one child receiving liver re-transplantation due to chronic rejection after the first transplant), two cases of progressive familial intrahepatic cholestasis and one case of acute liver failure. Nine adult or adolescent patients, five males and four females, received right extended lobe liver transplantation. The average age and weight of the adult recipients were 30.7 years (10-49 years) and 64.1 kg (39.9-88.5 kg) respectively. Indications included four cases of postnecrotic cirrhosis, two cases of primary sclerosing cholangitis, one case of Wilson's disease, one case of autosomal recessive polycystic kidney deficiency combined with liver fibrosis, and one case of acute liver necrosis caused by ligation of the hepatic artery due to rupture of the hepatic arterial aneurysm. Two patients were emergency cases, one due to postnecrotic cirrhosis and the other due to acute liver necrosis (Tables 1 and 2).

The key to successful liver division is to share vascular and biliary structures between the two sides but without handicapping either, and preferably to provide either graft with single first order arterial and biliary elements. Normally, the inferior vena cava, the common bile duct, and the main trunk of the portal vein as well as the hepatic artery are preserved for the right extended graft. We emphasize on performing dissection of the hepatic hilum only from the left side and always keeping the right side untouched, the steps of *ex situ* splitting the donor liver into a left lateral lobe and a right extended lobe were described briefly as

follows: (1) completing the conventional bench hepatic graft preparation and resecting the gallbladder, briefly checking the portal vein, the hepatic artery, the bile duct, and the hepatic vein; (2) exposing the left hepatic artery and identifying the segment IV artery, and then transecting the left hepatic artery distally to the origin of segment IV artery; (3) isolating and transecting the left portal vein, and ligating the branches supplying segment IV originating from left portal vein; (4) splitting the liver parenchyma step by step along with umbilical scissure from downward to upward, and the various tiny vessels and bile ducts handled with ligation or metal clips; (5) exposing the left hepatic vein when dividing close to suprahepatic inferior vena cava, and then transecting the left hepatic vein leaving a suitable stump; (6) finally transecting the bile duct connecting the two parts of donor liver; and (7) injecting cold preservation solution via portal vein, hepatic artery as well as bile duct to check for leaks. None of these 10 cases of donor livers was applied cholangiography or angiography in the process of splitting.

RESULTS

All the 10 donor livers were split successfully into a left lateral lobe (segments II and III) and a right extended lobe (segments I, IV-VIII), and subsequently split liver transplantation was performed in 19 cases. The average weight of the whole graft before splitting was 1 322.6 g (956-1 665 g), and the average weight of the left lateral lobe and the right extended lobe after splitting was 281.8 g (198-373 g) and 1 075.8 g (726-1 299 g) respectively. The average ratio of left lateral lobe to total graft was 0.215

Table 1 Basic data of donors

	Age/Sex	Height (cm)/weight (kg)	ICU (d)	AST (IU/L)	Crea (mg/dL)	Na (mmol/L)	BIL (mg/dL)	Whole graft weight (g)
1	15/M	168/70	1	22	1.20	152	1.60	1 290
2	35/M	185/50	3	14	1.10	152	0.63	1 580
3	46/F	176/70	2	16	0.80	153	0.09	1 296
4	43/F	175/70	2	122	1.25	158	0.48	1 435
5	37/F	170/75	8	77	1.22	137	0.28	1 665
6	51/F	160/45	2	28	0.40	146	0.70	1 000
7	40/F	170/65	2	23	0.59	138	0.10	1 209
8	15/F	175/65	1	94	1.01	153	1.56	1 225
9	27/F	175/75	2	30	0.70	155	0.88	956
10	18/F	165/60	1	105	0.80	144	0.71	1 570

Table 2 Basic data of recipients receiving left lateral lobe and right extended lobe liver transplantation

	Patients receiving left lateral lobe				Patients receiving right extended lobe			
	Age (m) /sex	Weight (kg)	Graft weight (g)	GRWR (%)	Age (yr) /sex	Weight (kg)	Graft weight (g)	GRWR (%)
1	74/F	18.6	242	1.30	46/M	80.0	1 048	1.31
2	50/F	15.0	281	1.87	42/F	88.5	1 299	1.47
3	72/F	15.7	318	2.03	49/M	70.5	978	1.39
4	78/F	21.9	275	1.26	17/M	60.5	1 160	1.92
5	5/M	6.9	373	5.41	49/F	63.0	1 292	2.05
6	20/F	10.0	274	2.74	-	-	-	-
7	11/F	7.1	268	3.72	14/F	64.6	941	1.46
8	8/M	7.8	270	3.46	26/M	55.0	955	1.73
9	82/M	16.2	198	1.22	10/M	39.9	758	1.90
10	81/F	23.8	319	1.34	23/F	54.5	1 251	2.30

The right extended lobe from case 6 was sent to the other center.

(0.178-0.274). The average GRWR of the left lateral lobe and the right extended lobe reached 2.44% (1.22-5.41%) and 1.73% (1.31-2.30%) respectively. The average weight ratio of donor to pediatric recipient was 5.47 (2.52-10.87). The average time required to split the donor liver was 105 min (85-135 min).

A total number of five anatomic variations occurred in the process of graft splitting. The left hepatic vein variation occurred in two cases, where the segment II hepatic vein, the segment III hepatic vein and the middle hepatic vein draining separately into inferior vena cava appeared to be a trifurcation at the junction. In order to obtain a sufficiently long left hepatic vein, some part of the lateral wall of the middle hepatic vein and suprahepatic inferior vena cava was sacrificed, the defect was repaired with part of donor common iliac vein (Figures 1 and 2). Two donor organs had anatomical variations of the left hepatic artery. In one case with the segment IV artery arising very distal from the left hepatic artery, only 3 mm of the common trunk of segments II and III arteries could be obtained after painstakingly dissecting the liver parenchyma of the left lateral lobe. There was one case where the replaced left hepatic artery originated from the left gastric artery (Figure 3). Although partial blood supply of the segment II liver from the segment IV artery could be identified, the diameter of this branch was less than 2 mm with quite good backflow under perfusion, consequently no reconstruction was required. Finally there was the anatomical bile duct variation. In this case the union of segments II and III bile ducts was right to the umbilical fissure resulting in two separate

openings of bile duct on the cutting surface of left lateral lobe. Fortunately in this case the distance between the two bile duct openings was quite close and in the shape of a figure '8'; therefore, one opening could be achieved by plastic reconstruction (Figure 4).

DISCUSSION

Pichlmayr *et al.*^[6], reported the first clinical attempt of split liver transplantation in 1988, and 1 year later Bismuth *et al.*^[7], described two patients with fulminant hepatic failure, each receiving a split graft. In 1990, Broelsch *et al.*^[8], presented the first series of 30 split liver transplantations in 21 children and 5 adults. In this early experience, patient survival was inferior to that reported in series of cadaveric whole-size orthotopic liver transplants. Despite skepticism as to the lasting role of split liver transplantation, several European centers, faced with an increasing waiting list of death rate due to the scarcity of donor organs, pursued the split liver options. In 1995, the results of a collective experience of 50 donor livers, providing 100 grafts during a 5-year period from the European Split Liver Registry^[9] demonstrated no significant difference when compared to conventional whole-sized OLT during the same period.

With the present improved surgical techniques, it is commonly acceptable to split the donor liver into two transplantable grafts, one for a pediatric and the other for an adult recipient. A series comprising 110 consecutive split liver transplantations in 55 adults and 55 pediatric recipients showed that patient survival of split liver transplantation

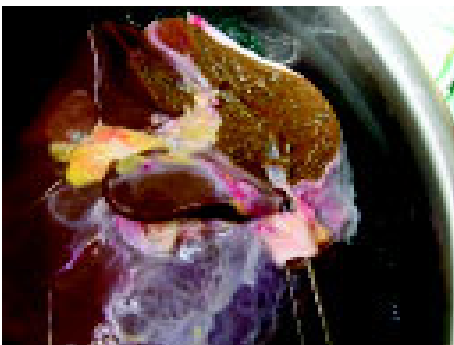


Figure 1 Partial defect of MHV and IVC after splitting.

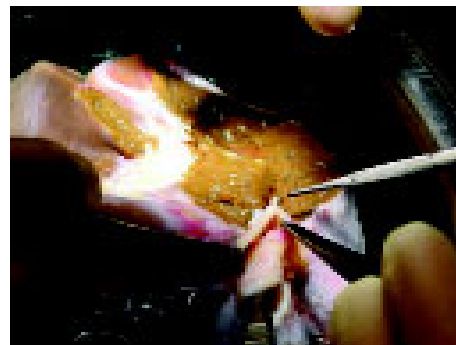


Figure 2 Repair of defect of MHV and IVC by part of common iliac vein.

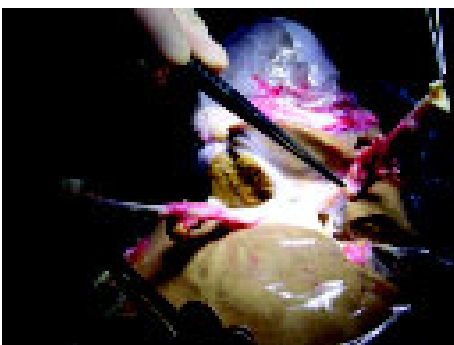


Figure 3 Left replaced hepatic artery originating from the left gastric artery, with segment II blood supply partially from a small branch of segment IV artery.

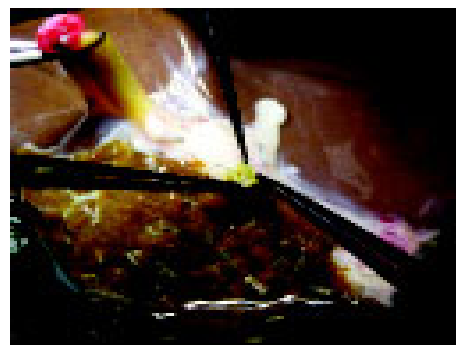


Figure 4 Appearance after plastic reconstruction of separate openings of segments II and III bile ducts nearby.

was not significantly different from whole-organ OLT^[10]. Similar results are also reported by Broering *et al.*^[11]. Such view is strongly evidenced by more and more current clinical data^[12-15]. Our experience with more than 150 cases of split liver transplantation since 1988 has confirmed these results. Between 1993 and 1999, split liver transplantation activities increased in central Europe from 1.2% to 10.4%^[16]. Currently split liver transplantations make up more than 20% of all liver transplantations performed at the Medical School of Hannover. With the refinement of surgical skill, split liver transplantation could even be applied in the cases of retransplantation and emergency.

What kind of donor liver is suitable for splitting calls for thorough consideration and evaluation whenever an organ donor is available. Besides meeting the basic prerequisites regarding the donor livers, the following factors are worth to be considered based on our experience and opinions from other authors^[10,11,17]: (1) a donor age below 50 years and above 10 years; (2) hemodynamic stability, if in use of vasopressor, maintaining good blood pressure at least; (3) the preferable donor ICU stay less than 5 d; and (4) no status of hypernatremia, a serum sodium concentration of <170 mmol/L or even better <150 mmol/L. Although donor parameters are critical when selecting livers for a splitting procedure, the experience accumulated over the years clearly indicates that the most reliable basis for the decision on splitting is the judgment of an experienced transplant surgeon. Microscopic examination should become a kind of supplement to macroscopic observation. It is pivotal to scrutinize whether the donor liver has a soft consistency, a sharp edge and is well perfused. One has to appreciate the frank remark of Busuttill on criteria for splittable donor livers^[10]: "I think that the ultimate exclusion criterion is when you go and look at the liver, if the liver does not look good, you do not split it."

With the current technique, it is quite reliable to split a donor liver into a left lateral lobe (segments II and III) and a right extended lobe (segments I, IV-VIII) for one child recipient and one adult recipient. Our results confirmed that the right extended liver lobe would account for about 80% of the standard volume in humans, and can be allocated like a full-size liver if careful consideration is given to recipient selection^[18]. Actually in our group the maximum weight of recipients was up to 88.5 kg with satisfactory outcome of transplantation. In this study, the average GRWR of the right extended lobe was 1.73%. For the right extended lobe graft 1% GRWR is sufficient for the low risk recipient in stable condition and good nutritional status. However, GRWR should be not less than 1.5% for the high risk recipient with decompensatory liver function and severe portal hypertension^[19,20]. For the left lateral lobe graft the ideal weight ratio of donor to child should be 3-10 times.

Compared to splitting liver into a full left lobe and a full right lobe^[21,22], fewer anatomical variations might occur when splitting liver into a left lateral lobe and a right extended lobe. Nevertheless, it is crucial for the success of the subsequent liver transplantation how the various potential variations are handled in the process of splitting. Considering that the left liver lobe is more constant regarding anatomical variations,

it can be said that the more one stays on the left, the fewer anatomical variants one is confronted with.

In most of cases, the left hepatic vein joins the middle hepatic vein, thus forming the common trunk entering the antero-left surface of the inferior vena cava^[23]. Instead of joining the segment II hepatic vein to form the left hepatic vein, the segment III hepatic vein seldom joins the middle hepatic vein individually with the probability for about 5-10%. The diameter of the extrahepatic portion of the left hepatic vein is around 10 mm, and the smaller diameter less than 7 mm is sufficient to suspect such circumstance. In the present study, left hepatic vein variation occurred in two cases, the segments II and III draining of hepatic veins appeared with the middle hepatic vein as a trifurcation. Under certain circumstances, the dividing line needs to be moved slightly to the right slightly in order to guarantee one venous drainage from the graft of left lateral lobe. The defect of middle hepatic vein and inferior vena cava could be repaired by the common iliac vein from the donor.

Intrahepatic portal venous variations can be seen in approximately 20% of the population^[24]. However, unless the rare absence of a portal vein bifurcation with only 0.9% possibility, will it become the contradiction of graft splitting. In the majority of cases the portal vein inflow to segment IV is accomplished by the left umbilical section of the left portal vein. However, those branches originating from umbilical section will inevitably be transected. Fortunately, in most cases the additional portal vein branches to segment IV arising from the portal vein bifurcation and the right portal vein could be expected. By preserving these veins and moving the transection line to the left, partial portal vein supply to segment IV can be achieved.

Variations of the hepatic artery are comparatively frequent^[25]. Only 50-70% of livers present with "normal" anatomy^[26,27]. If the left main hepatic artery originates from the left gastric artery (10-15%) both the length and the diameter of this artery would be adequate for the anastomosis in the recipient. Such a situation occurred in one case. Although one branch from the segment IV artery supplying segment II could be identified, no reconstruction was required with small diameter and good backflow under perfusion. Since in most cases the portal vein supply to segment IV has to be sacrificed in the process of splitting, arterial supply will largely determine survival of this segment, and therefore, every effort should be made to preserve the segment IV artery. In most cases the segment IV artery originates from the left hepatic artery, and its origin should have some distance to the union of segments II and III arteries. The segment IV artery rarely arises far distal from the left hepatic artery, and the three arteries of segments II, III, and IV might form a trifurcation at their origins. A similar situation occurred in one of our cases when with painstaking efforts only a length of 3 mm of the common trunk of segments II and III arteries could be obtained at last. In case the segment IV artery has to be cut down, it is suggested to anastomose it with the stump of the left hepatic artery on the backtable.

Close attention should also be paid to variations of bile ducts. During the initial period of left lateral split liver transplantation, many groups isolated the main left hepatic

duct next to the main bile duct bifurcation when harvesting the left lateral lobe, in order to create a nice bile duct stump for anastomosis. However, this technique seems to be associated with a high rate of biliary complications on both grafts for the following reasons. First, leaving the long stump of bile duct with the left lateral graft might result in ischemic necrosis due to damaging the parabiliary vascular plexus in the isolation of the left hepatic duct^[8]. Second, a high incidence of damage to the segments I and IV bile duct of the right extended graft might occur with such a method^[28]. Therefore, we kept the connective tissue surrounding bile ducts untouched, and only used a metal probe or Arrow[®] catheter to identify the trend of bile duct, and transected bile duct as the last step of the whole splitting procedure. Although in 15% of donor livers the union of segments II and III bile ducts is located right to the umbilical fissure, which means two separate openings of bile duct appear on the cutting surface of the left lateral graft, we would still rather keep the transecting line curving a little to the left in order to retain an undamaged segment IV bile duct. If the distance between two separate bile duct openings is quite close, they might be merged into one through plastic reconstruction.

Undoubtedly, split liver transplantation has become a well-established approach to extend the donor pool for both pediatric and adult patients. Careful donor and recipient selection, good knowledge of the liver anatomy, excellent surgical skills and meticulous postoperative management all contribute to the success of each case of split liver transplantation.

REFERENCES

- 1 **Abouljoud M**, Yoshida A, Dagher F, Moonka D, Brown K. Living donor and split-liver transplantation: an overview. *Transplant Proc* 2003; **35**: 2772-2774
- 2 **Emond JC**, Whittington PF, Thistlethwaite JR, Alonso EM, Broelsch CE. Reduced-size orthotopic liver transplantation: use in the management of children with chronic liver disease. *Hepatology* 1989; **10**: 867-872
- 3 **Bismuth H**, Houssin D. Reduced-sized orthotopic liver graft in hepatic transplantation in children. *Surgery* 1984; **95**: 367-372
- 4 **Broelsch CE**, Emond JC, Thistlethwaite JR, Whittington PF, Zucker AR, Baker AL, Aran PF, Rouch DA, Lichtor JL. Liver transplantation including the concept of reduced-size liver transplants in children. *Ann Surg* 1988; **208**: 410-420
- 5 **Otte JB**, de Ville de Goyet J, Solak E, Alberti D, Moulin D, de Hemptinne B, Veyckemans F, van Obbergh L, Carlier M, Clapuyt P. Size reduction of the donor liver is a safe way to alleviate the shortage of size-matched organs in pediatric liver transplantation. *Ann Surg* 1990; **211**: 146-157
- 6 **Pichlmayr R**, Ringe B, Gubernatis G, Hauss J, Bunzendahl H. Transplantation of a donor liver to 2 recipients (splitting transplantation)-a new method in the further development of segmental liver transplantation. *Langenbecks Arch Chir* 1988; **373**: 127-130
- 7 **Bismuth H**, Morino M, Castaing D, Gillon MC, Descorps Declere A, Saliba F, Samuel D. Emergency orthotopic liver transplantation in two patients using one donor. *Br J Surg* 1989; **76**: 722-724
- 8 **Broelsch CE**, Emond JC, Whittington PF, Thistlethwaite JR, Baker AL, Lichtor JL. Application of reduced size liver transplants as split grafts, auxiliary orthotopic grafts and living related segmental transplants. *Ann Surg* 1990; **212**: 368-377
- 9 **de Ville de Goyet J**. Split liver transplantation in Europe-1988 to 1993. *Transplantation* 1995; **59**: 1371-1376
- 10 **Ghobrial RM**, Yersiz H, Farmer D, Amersi F, Goss J, Chen P, Dawson S, Lerner S, Nissen N, Imagawa D, Colquhoun S, Arnout W, McDiarmid SV, Busuttil RW. Predictors of survival after *in vivo* split liver transplantation: analysis of 110 consecutive patients. *Ann Surg* 2000; **232**: 312-323
- 11 **Broering DC**, Topp S, Schaefer U, Fisher L, Gundlach M, Sterneck M, Schoder V, Pothmann W, Rogiers X. Split liver transplantation and risk to the adult recipient: analysis using matched pairs. *J Am Coll Surg* 2002; **195**: 648-657
- 12 **Renz JF**, Yersiz H, Reichert PR, Hisatake GM, Farmer DG, Emond JC, Busuttil RW. Split-liver transplantation: a review. *Am J Transplant* 2003; **3**: 1323-1335
- 13 **Moreno A**, Meneu JC, Moreno E, Garcia I, Loinaz C, Jimenez C, Gomez R, Abradelo M, Calvo J, Fundora Y, Ortiz C. Results in split liver transplantation. *Transplant Proc* 2003; **35**: 1810-1811
- 14 **Gridelli B**, Spada M, Petz W, Bertani A, Lucianetti A, Colledan M, Altobelli M, Alberti D, Guizzetti M, Riva S, Melzi ML, Stroppa P, Torre G. Split-liver transplantation eliminates the need for living-donor liver transplantation in children with end-stage cholestatic liver disease. *Transplantation* 2003; **75**: 1197-1203
- 15 **Deshpande RR**, Bowles MJ, Vilca-Melendez H, Srinivasan P, Girlanda R, Dhawan A, Mieli-Vergani G, Muiesan P, Heaton ND, Rela M. Results of split liver transplantation in children. *Ann Surg* 2002; **236**: 248-253
- 16 **Klempnauer J**, Schrem H, Becker T, Nashan B, Luck R. Liver transplantation today. *Transplant Proc* 2002; **33**: 3433-3435
- 17 **Emond JC**, Freeman RB Jr, Renz JF, Yersiz H, Rogiers X, Busuttil RW. Optimizing the use of donated cadaver livers: analysis and policy development increase the application of split-liver transplantation. *Liver Transpl* 2002; **8**: 863-872
- 18 **Renz JF**, Emond JC, Yersiz H, Ascher NL, Busuttil RW. Split-liver transplantation in the United States: outcomes of a national survey. *Ann Surg* 2004; **239**: 172-181
- 19 **Heaton N**. Small-for-size liver syndrome after auxiliary and split liver transplantation: donor selection. *Liver Transpl* 2003; **9**: S26-S28
- 20 **Macros A**. Split-liver transplantation for adult recipients. *Liver Transpl* 2000; **6**: 707-709
- 21 **Yersiz H**, Renz JF, Hisatake G, Reicher PR, Feduska NJ, Lerner S, Farmer DG, Ghobrial RM, Geevarghese S, Baquerizo A, Chen P, Busuttil RW. Technical and logistical consideration of *in situ* split liver transplantation for two adults: Part I. Creation of left segment II, III, IV and right segment I, V-VIII grafts. *Liver Transpl* 2001; **7**: 1077-1080
- 22 **Yersiz H**, Renz JF, Hisatake G, Reicher PR, Feduska NJ, Lerner S, Farmer DG, Ghobrial RM, Geevarghese S, Baquerizo A, Chen P, Busuttil RW. Technical and logistical consideration of *in situ* split liver transplantation for two adults: Part II. Creation of left segment I-IV and right segment V-VIII grafts. *Liver Transpl* 2002; **8**: 78-81
- 23 **Noujaim HM**, Mirza DF, Mayer DA, De Ville De Goyet J. Hepatic vein reconstruction in *ex situ* split-liver transplantation. *Transplantation* 2002; **74**: 1018-1021
- 24 **Atri M**, Bret PM, Fraser-Hill MA. Intrahepatic portal venous variations: prevalence with US. *Radiology* 1992; **184**: 157-158
- 25 **Hiatt JR**, Gabbay J, Busuttil RW. Surgical anatomy of the hepatic arteries in 1000 cases. *Ann Surg* 1994; **220**: 50-52
- 26 **Kawarada Y**, Das BC, Taoka H. Anatomy of the hepatic hilar area: the plate system. *J Hepatobiliary Pancreat Surg* 2000; **7**: 580-586
- 27 **Hardy KJ**, Jones RM. Hepatic artery anatomy in relation to reconstruction in liver transplantation: some unusual variations. *Aust N Z J Surg* 1994; **64**: 437-440
- 28 **Stapleton GN**, Hickman R, Terblanche J. Blood supply of the right and left hepatic ducts. *Br J Surg* 1998; **85**: 202-207

• BRIEF REPORTS •

Evaluation of serum cathepsin B and D in relation to clinicopathological staging of colorectal cancer

Elzbieta Skrzydlewska, Mariola Sulkowska, Andrzej Wincewicz, Mariusz Koda, Stanislaw Sulkowski

Elzbieta Skrzydlewska, Department of Analytical Chemistry, Medical University of Bialystok, Poland

Mariola Sulkowska, Andrzej Wincewicz, Mariusz Koda, Stanislaw Sulkowski, Department of Pathology, Medical University of Bialystok, Poland

Supported by the Polish State Committee for Scientific Research, No. 3 PO5B 07922

Correspondence to: Professor Elzbieta Skrzydlewska MD, PhD, Department of Analytical Chemistry, Medical University of Bialystok, Mickiewicza 2, 15-230 Bialystok, Poland. skrzydle@amb.edu.pl

Telephone: +48-85-7485707 Fax: +48-85-7485707

Received: 2004-10-19 Accepted: 2005-01-05

© 2005 The WJG Press and Elsevier Inc. All rights reserved.

Key words: Proteases; Cathepsin D; Cathepsin B; Colorectal cancer

Skrzydlewska E, Sulkowska M, Wincewicz A, Koda M, Sulkowski S. Evaluation of serum cathepsin B and D in relation to clinicopathological staging of colorectal cancer. *World J Gastroenterol* 2005; 11(27): 4225-4229

<http://www.wjgnet.com/1007-9327/11/4225.asp>

Abstract

AIM: Proteolytic degradation of the extracellular matrix facilitates cancer invasion and promotes metastasis. The study aims at evaluation of preoperative and postoperative serum cathepsins B and D levels in correlation with selected anatomoclinical features of colorectal cancer.

METHODS: Blood samples were collected from 63 colorectal cancer patients before curative operation of the tumor 10 d later. Blood that was obtained from 20 healthy volunteers, served as a control. The activity of cathepsin B was measured with Bz-DL-arginine-pNA as a substrate at pH 6.0, while cathepsin D activity was determined with urea-denatured hemoglobin (pH 4.0).

RESULTS: The preoperative and postoperative activities of cathepsin B were significantly ($P < 0.00001$) lower in serum of colorectal cancer patients than in control group. However, postoperative values of this protease were significantly increased in comparison with preoperative ones ($P = 0.031$). Activity of cathepsin D appeared to be significantly higher in colorectal cancer sera ($P < 0.00001$) compared with controls. No statistically significant differences between preoperative and postoperative activity of cathepsin D were noted ($P = 0.09$). We revealed a strong linkage of cathepsins' levels with lymph node status and pT stage of colorectal cancer.

CONCLUSION: Blood serum activities of cathepsin B and D depend on the time of sampling, tumor size and lymph node involvement. Significantly, increased activity of cathepsin D could indicate a malignant condition of the large intestine. In our work, the serum postoperative decrease of cathepsin B activity appears as an obvious concomitant of local lymph node metastasis-the well-known clinicopathological feature of poor prognosis.

INTRODUCTION

Normal cells undergo several changes to converse into invasive malignant clones with metastatic capability. Progress of these alternations is manifested in distinguishable histological and temporal stages-for instance: normal tissue, hyperplasia with a high incidence of proliferating cells, dysplasia with the induction of angiogenesis that precedes following metamorphosis of observed cell clusters into tumors with metastasis. Analysis of the subsequent stages of tumor progression has provided a multistage theory of carcinogenesis on the basis of genetic changes that include activation of oncogenes, inactivation of tumor suppressor genes, and altered expression of tumor-associated molecules.

Cellular transformation provokes tissue remodeling inside neoplastic lesions and in the periphery of the tumor. Disorders in stroma or extracellular matrix (ECM) play an essential role in cancer progression. It is suggested that perturbation of the tissue microenvironment may be sufficient to induce tumor formation. Moreover, local carcinomatous invasion and metastasis also require the destruction of the EMC during local dissemination of malignant cells, angiogenesis, intravasation and extravasation. These processes are enabled by multiple degradation of stromal structure which is achieved due to cooperation of various specific intra- and extracellular proteases. Lysosomal aspartyl and cysteine enzymes-cathepsin D and B are the most important of intracellular proteases that participate in stromal destruction, which facilitates tumor invasion of deeper tissue layers^[1]. These enzymes can act directly by proteolysis of EMC components or indirectly by costimulation of a cascade of other proteases such as metalloproteases or elastase, which then decompose protein elements of the EMC and basal membranes. This stromal disarrangement allows migration of malignant cells to different regions and compartments of the human body, what accelerates tumor growth and favors metastasis. Not only does overexpression of cathepsin B and D in cancer cells reflect intensity of

neoplasm development, but also increased serum activity of mentioned proteases does the same as well. Apart from mentioned functions, independently of its catalytic activity human cathepsin D stimulates tumor growth as a direct or indirect mitogenic factor for cancer cells^[1]. Cathepsin D affects tumor angiogenesis in a mysterious way. It was suggested that cathepsin D might favor angiogenesis by releasing ECM-bound bFGF^[2]. Suggestions of its proangiogenic function contrast with the fact that pro-cathepsin D is responsible for the generation of specific inhibitor of angiogenesis-angiostatin^[3]. Now it is presumed that cathepsin D may stimulate endothelial cell growth via a paracrine loop, acting as a protein ligand, by directly or indirectly triggering a yet unidentified cell surface receptor^[4].

Increased expression, enhanced secretion and cell surface association of cathepsin B were found in different types of tumor cells especially in their more malignant variants^[5]. Last studies have revealed that augmented production and release of cathepsin B in tumor cells lead to tumor cell growth, invasion and metastasis^[6]. This cathepsin may act at the contact regions of tumor cells and basement membrane or interstitial stroma. Low pH is necessary for activation of secreted precursors to active forms, which degrade the protein components of basement membranes and interstitial connective matrix including laminin, fibronectin, elastin, and various types of collagen^[7]. Cathepsin B split fibronectin into smaller parts and change conformation of this protein components. In such a way the CS-1 sequence and alternatively spliced type III connecting segment (IIICS) are uncovered, exposed and recognized by the integrin $\alpha_4\beta_1$ -receptor^[8]. Thereby, cathepsin B may be involved in cellular signal transduction beside extracellular protein degradation.

Therefore, the aim of this work was to investigate the activity of lysosomal proteases-cathepsin B and D in blood serum and their potential impact on cancer progression and metastasis in cases of colorectal cancer.

MATERIALS AND METHODS

The study included 63 patients (42 men and 21 women) with a mean age of 64 years that were required to undergo a colorectal cancer operation. Thirty tumors were located in the rectum and 33 were found in the colon. The patients had no preoperative chemo- or radiotherapy. All the patients were monitored after the operation. Two independent pathologists assessed conventional histopathological parameters (including AJCC/UICC TNM stage, tumor type and grade of differentiation). Differentiation and histological type of the tumors was determined following the World Health Organization guidelines. Fifty-eight colorectal cancers were classified histopathologically as adenocarcinoma and 5 as mucinous adenocarcinoma: 43 cases with G2 grade and 15 cases with G3 grade. Because of too small a number of tumors that were classified as pT1, pT2 and pT4 patients were divided into two groups: five tumors comprised pT1+pT2 group and 53 cancer cases belonged to pT3+pT4 group. Forty-six percent patients had involved lymph nodes at the time of diagnosis.

Biochemical analysis

The blood samples were collected from colorectal cancer

patients twice: before and 10 d after the curative operation. The blood was centrifuged at 4 °C and the serum samples were stored at -80 °C until examination. The control group included of 20 healthy volunteers (12 men and 8 women) with a mean age of 59 years. The control blood samples were collected only once. Serum was gained from collected blood and the activity of cathepsin B was determined with Bz-DL-arginine-pNA as a substrate at pH 6.0^[9], while the cathepsin D activity was measured with urea-denatured hemoglobin (pH 4.0)^[10].

RESULTS

The preoperative and postoperative activities of cathepsin B were significantly ($P < 0.00001$) smaller than in control group. However, postoperative values of this protease were significantly increased in comparison with preoperative ones ($P = 0.031$). On the other hand the activity of aspartyl protease-cathepsin D appeared to be significantly higher ($P < 0.00001$) in comparison with the control group data. In addition, no statistically significant differences between preoperative and postoperative activity were noted ($P = 0.09$, Table 1).

Table 1 Activity of cathepsin B and D in serum of patients with colorectal carcinoma

	Healthy people (n = 20)	Control serum	66.9±2.8
	Colorectal patients (n = 63)	Before operation1 (serum sample a) After operation (serum sample b)	7.9±8.5 ^{1b} 21.0±8.7 ^f
Cathepsin B nmolPNA/mL			
	Healthy people (n = 20)	Control serum	30.2±2.2
	Colorectal patients (n = 63)	Before operation (serum sample a) After operation (serum sample b)	58.7±24.2 ^{2d} 49.9±16.9 ^b
Cathepsin D nmol Tyr/mL			

Statistical differences: ¹ $P = 0.031$ -comparison between cathepsin B serum samples a and b. ² $P = 0.09$ -comparison between cathepsin D serum samples a and b. ^b $P < 0.00001$, ^d $P < 0.00001$, ^b $P < 0.00001$, ^f $P < 0.00001$ vs control serum.

We revealed a strong linkage of cathepsins' levels with lymph node status and pT stage of colorectal cancer. As referred to TNM classification, patient group of pT1 and pT2 tumors showed significantly higher preoperative serum activity of cathepsin B than it was detected in preoperative serum of patients with tumors classified to pT3 and pT4 group ($P = 0.0057$). This trend of differences was not apparent enough to reach a level of statistical significance in case of postoperative serum values of cathepsin B. We assume that statistical significance could not be achieved in analysis of homologous postoperative data because of wide variation of postoperative cathepsin B values in set of patients with pT1 and pT2. Similarly values of cathepsin D before operations (serum sample A) were more increased with nearly statistical significance in pT1 and pT2 vs pT3 and pT4 groups respectively ($P = 0.053$).

As shown in Table 2, node-negative (N-) colorectal cancer patients displayed significantly higher postoperative

serum levels of cathepsin B in opposition to patients with lymph node involvement (N+) ($P = 0.0054$). These groups of patients did not significantly differ in cathepsin B levels before operation. We drew out a similar comparison between activities of cathepsin D in node negative and node positive sets of colorectal cancer-but inversely to cathepsin B-remarkable distinction of cathepsin D serum levels appeared before surgery. Namely, the preoperative serum activity of cathepsin D was increased in node negative (N-) *vs* node positive (N+) colorectal cancer patients with statistical significance ($P = 0.019$).

DISCUSSION

Cancer development is characterized by severe disarrangement of the intra- and extracellular metabolism and structural alterations. Cancer cells overexpress and secrete a large proportion of lysosomal proteases-cathepsins. The activity increase of cathepsin B and D was discovered to be statistically significant in both the neoplastic tissue cytosol and homogenate, compared to the cytosol and homogenate of adjacent healthy tissue^[11]. Marked tissue immunoreactivity of cathepsin B and D takes place in carcinoma of uterus, ovary, lung, intestines and many other organs^[12-15]. Moreover, it was reported that tumor cell lines secrete cathepsin B and D^[16]. On the other hand it was reported that serum cathepsin B level did not differ significantly both in benign and malignant neoplasms of ovaries^[17]. In cancers there was elevated serum value of cystatin C in comparison with benign ovarian tumors and controls, which negatively affected the amount of cathepsin B. However, ovarian cancer cells are strongly positive for cathepsin B in immunohistochemical analysis, while benign ovarian tumors lacked any positive reaction of this kind^[17].

It is suggested that colorectal cancer development is enhanced by oxidative stress. Oxidative stress is maintained as the effect of excessive concentration of lipid hydroperoxides in the vascular net and their participation in the oxidant generation. The other possible explanation might be overproduction of oxidants by inflammatory and/or cancer cells and suppression of antioxidant system in cancer cells. In these conditions free radicals may enhance lipid peroxidation.

Products of this process are responsible for membrane alteration. Reactive oxygen species cause protein damage and as a result changes in biological function of active proteins and membrane permeability for intracellular compounds may appear due to increased susceptibility for drugs that induce apoptosis of neoplastic cells^[1,18]. It may explain translocation of cathepsins from lysosomes via cytosol and cellular membrane into body fluids.

As we have demonstrated in our previous works, generation of free radicals accompanies the development of cancer^[18]. Reactive oxygen species cause an oxidative damage of cell membranes which results in an increase of membrane permeability. That implies influx of cathepsin D to extracellular fluid. Therefore, elevated activity of cathepsin D is observed in the serum as an evidence for impairment of general cellular functions like maintenance of the barrier between intracellular and extracellular environment. Advancement of tumor growth and neoplastic spreading across the whole organism seem to reflect the severity of cellular damage. Cathepsin B -cysteine protease is so sensitive to free radicals, that the latter probably inactivate cathepsin B. Thereby it would explain why serum activity of cathepsin B is lower in serum of patients with colorectal cancer in comparison to serum values of this protease in healthy volunteers. Production of free radicals is upregulated and activity of cathepsin B falls down along with the enlargement of tumors and neoplastic extent into lymph nodes. This statement is supported by our present study in which we detected lower levels of cathepsin B in group pT3 and pT4 *vs* pT1 and pT2 as well as in node positive (N+) *vs* node negative (N-) patients after surgery. Total resection of cancer could contribute to limit ROS generation and by means of the inactivation of cathepsin B, ROS generation was reduced enough which is shown in the results obtained.

The concentrations of cathepsin B and D were increased also in the blood serum of patients with other carcinomas^[19-21]. Additionally, the increase of cathepsin B correlated with the advancement of cancer assessed with Duke's scale. Moreover patients with both elevated levels of cathepsin B and CEA were classified as the group of poor prognosis^[20]. Nevertheless, in our present investigations, we discovered

Table 2 Correlation of serum cathepsin B and D activity and clinicopathological findings

Variable		n = 63	Cathepsin B (nmol/L pNA/mL)				Cathepsin D (nmol Tyr/mL)			
			Before operation	P	After operation	P	Before operation	P	After operation	P
Sex	M	42	19.1±8.9	NS	21.7±9.1	NS	59.4±26.3	NS	49.5±16.3	NS
	F	21	15.3±6.6		19.6±7.9		57.0±19.2		50.9±18.4	
Age (yr)	≤60	16	20.4±12.3	NS	17.4±8.0	P = 0.064	54.2±17.0	NS	51.7±22.0	NS
	>60	47	17.02±6.6		22.4±8.7		60.2±26.1		49.3±14.7	
Tumor site	Rectum	30	16.5±7.4	NS	18.4±7.6	NS	59.8±21.6	NS	51.2±19.9	NS
	Colon	33	19.1±9.2		23.5±9.1		57.7±26.3		48.8±13.6	
HPtype	Adc.	58	18.1±8.4	NS	21.02±8.9	NS	58.7±24.4	NS	50.7±17.0	NS
	Adc. m.	5	10.1±9.3		20.9±7.0		56.0±21.2		43.2±14.2	
pT	pT 1+2	5	25.3±0.7	P = 0.0057	30.3±18.7	NS	76.8±23.0	P = 0.053	48.8± 16.5	NS
	pT 3+4	53	17.1±8.5		20.3±7.3		56.7±23.6		50.1± 17.0	
G	2	43	18.8±8.8	NS	21.5±9.2	NS	62.5±25.5	NS	50.4±17.3	NS
	3	15	15.8±7.3		19.9±7.7		50.3±18.8		49.2±16.2	
N	(-)	34	18.5±8.5	NS	23.9±8.9	P = 0.0054	65.9±26.5	P = 0.019	49.7±17.2	NS
	(+)	29	17.03±8.4		17.3±7.1		49.1±16.7		50.3±16.6	

Statistical differences: see Table 1.

only the increase of cathepsin D while levels of cathepsin B were decreased in sera of colorectal cancer patients.

Overexpression of cathepsins may prelude the loss of integrity of ECM protein components. It is known that cathepsin D as endopeptidase degrades ECM proteins and proteins of the basal epithelium as well as many intracellular and endocytosed proteins. It occurs mainly in phagosome-like acid vesicles with acidic pH where EMC components are trapped^[22]. Cathepsin D may cooperate with cathepsin B in the process of proteolysis and cancer progression. Cathepsin D probably activates cysteine procathepsins B and L^[23]. Cathepsin B activates the urokinase-type plasminogen which can subsequently activate the plasmin-metalloproteinases proteolytic pathway^[24,25]. Moreover, cathepsin B may change the balance of metalloproteinases and their inhibitors and directly cleave and inactivate some of MMPs inhibitors -TIMP-1 and TIMP-2^[26]. In such a way cathepsin B assists tumor cells in their detachment from ECMs and metastasis. Furthermore during proteolysis of interstitial extracellular structure some ECMs-bound growth factors, e.g. bFGF, EGF, TGF- β , IGF-I and VEGF, may get free from their chains of connections to the matrix and thanks to the fact that they can escape to join suitable receptors of stromal and tumor cells which indicates their bioavailability for growth modulation^[27].

Cathepsin B can multiply the effect of protein digestion and disarrangement by triggering trypsinogen activation^[28]. Lysosomal cathepsin B activates trypsinogen *in vitro* and the intensity of trypsinogen activation improves with acidic pH^[15,29]. Human trypsinogen is produced on a wide scale by human colorectal cells^[30]. Anyway further findings in colon cancer cell lines suggest that this production is limited only to such trypsin levels that are enough to activate PAR-2 receptor on the same cancer cells in possible autocrine/paracrine manner^[31]. It is worth mentioning that trypsin triggers matrilysin (matrix metalloproteinase-7) activity. So it is an important factor of colorectal cancer progression as immunohistochemical labeling of trypsin correlated with the depth of carcinomatous infiltration, lymphatic and venous involvement, metastasis, recurrence and shorter overall survival of patients^[32]. In our study the activity of cathepsin B could be insufficient to recruit trypsinogen activation in volume that would significantly affect tumor invasion as we detected lower cathepsin B activities in colorectal cancer compared with healthy volunteers.

The role of cathepsin B is supposed to be diverse. Namely, it can promote neoplastic invasion by lysis of EMC protein nets. Furthermore, by paracrine loop, it could cause death of neighboring cancer cells directly by proteolytic damage of cell membranes and changes in structure superficial cell receptors. Indirectly cathepsin B might act as TNF- α -induced apoptotic second messenger that mediates damage of mitochondria and release cytochrome c from these organelles^[33]. Thus, the components of cellular producer cathepsin B can be responsible for harmful suicidal injury. It can explain why higher serum levels of cathepsin B were associated with smaller size of tumor.

Cathepsin comes from two kinds of cells: carcinomatous ones and inflammatory cells that constitute immunologic response to neoplasm. According to our present results, we

suspect that along with progression of colorectal cancer, inflammatory cells might become significant producers of cathepsins. We observed lower activity of cathepsins in cases of larger tumors (pT3 and pT4 group) in comparison with smaller ones (pT1 and pT2 group) in measurements before surgery. The cause of it, can be a more escalated immunologic reaction in the onset and early stages of cancer than in advanced and late phases of neoplastic disease. Simultaneously, the outflow of cathepsins into extracellular environment destroys stromal protein structure, which is suspected to facilitate neoplastic spreading, but on the other hand, it can influence the vitality of cancer cells. So cathepsins particularly cathepsin B (probably in lower concentrations that do not induce trypsinogen activity) may disable neoplastic cells in such a way that they cannot forcibly invade surroundings despite promoting invasion by proteolysis of the interstitium. This action of cathepsin B is presumably responsible for relatively higher postoperative levels of serum cathepsin B in case of node negative patients *vs* node positive ones.

Blood serum activity of cathepsin B and D depends on the time of sampling, tumor size and lymph node involvement. Significantly increased activity of cathepsin D could indicate malignant colorectal condition. However, decreased activity of cathepsin B indicates that also different mechanisms besides proteolytic ones, participate in cancer invasion and metastasis. In comparison with analogous higher activity in node negative colorectal cancers, the significant downfall of postoperative cathepsin B activity coexisted with cancerous node involvement. Therefore, in our work, the decrease of this serum protease levels appears as an obvious concomitant of local lymph node metastasis the well-known clinicopathological feature of poor prognosis.

REFERENCES

- 1 Berchem G, Glondou M, Gleizes M, Brouillet JP, Vignon F, Garcia M, Liaudet-Coopman E. Cathepsin-D affects multiple tumor progression steps *in vivo*: proliferation, angiogenesis and apoptosis. *Oncogene* 2002; **21**: 5951-5955
- 2 Briozzo P, Badet J, Capony F, Pieri I, Montcourrier P, Barritault D, Rochefort H. MCF7 mammary cancer cells respond to bFGF and internalize it following its release from extracellular matrix: a permissive role of cathepsin D. *Exp Cell Res* 1991; **194**: 252-259
- 3 Morikawa W, Yamamoto K, Ishikawa S, Takemoto S, Ono M, Fukushima J, Naito S, Nozaki C, Iwanaga S, Kuwano M. Angiostatin generation by cathepsin D secreted by human prostate carcinoma cells. *J Biol Chem* 2000; **275**: 8912-8920
- 4 Glondou M, Coopman P, Laurent-Matha V, Garcia M, Rochefort H, Liaudet-Coopman E. A mutated cathepsin-D devoid of its catalytic activity stimulates the growth of cancer cells. *Oncogene* 2001; **20**: 6920-6929
- 5 Campo E, Munoz J, Miquel R, Palacin A, Cardesa A, Sloane BF, Emmert-Buck MR. Cathepsin B expression in colorectal carcinomas correlates with tumor progression and shortened patient survival. *Am J Pathol* 1994; **145**: 301-309
- 6 Talieri M, Papadopoulou S, Scorilas A, Xynopoulos D, Arnogiannis N, Plataniotis G, Yotis J, Agnanti N. Cathepsin B and cathepsin D expression in the progression of colorectal adenoma to carcinoma. *Cancer Lett* 2004; **205**: 97-106
- 7 Buck MR, Karustis DG, Day NA, Honn KV, Solane BF. Degradation of extracellular-matrix proteins by human cathepsins B from normal and tumor tissues. *Biochem J* 1992; **282**: 273-277
- 8 Ugarova TP, Ljubimov AV, Deng L, Plow EF. Proteolysis regulates exposure of the IIICS-1 adhesive sequence in plasma

- fibronectin. *Biochemistry* 1996; **35**: 10913-10921
- 9 **Tawatari T**, Kawabata Y, Katunuma M. Crystallization and properties of cathepsin B from rat liver. *Eur J Biochem* 1979; **102**: 279-289
 - 10 **Barrett AJ**. Cathepsin D and other carboxyl proteinases In: Proteinases in mammalian cells and tissues. *North Holland Publishing Company* 1977: 240-243
 - 11 **Lah TT**, Kalman E, Najjar D, Gorodetsky E, Brennan P, Somers R, Daskal I. Cells producing cathepsins D, B, and L in human breast carcinoma and their association with prognosis. *Hum Pathol* 2000; **31**: 149-160
 - 12 **Ioachim EE**, Goussia AC, Machera M, Tsianos EV, Kappas AM, Agnantis NJ. Immunohistochemical evaluation of cathepsin D expression in colorectal tumors: a correlation with extracellular matrix components, p53, pRb, bcl-2, c-erbB-2, EGFR and proliferation indices. *Anticancer Res* 1999; **19**: 2147-2155
 - 13 **Matsuo K**, Kobayashi I, Tsukuba T, Kiyoshima T, Ishibashi Y, Miyoshi A, Yamamoto K, Sakai H. Immunohistochemical localization of cathepsins D and E in human gastric cancer: a possible correlation with local invasive and metastatic activities of carcinoma cells. *Hum Pathol* 1996; **27**: 184-190
 - 14 **Chabowski A**, Sulkowska M, Sulkowski S, Famulski W, Skrzydłewska E, Kisielewski W. Immunohistochemical evaluation of cathepsin D expression in colorectal cancer. *Folia Histochem Cytobiol* 2001; **39**: 153-154
 - 15 **Brouillet JP**, Dufour F, Lemamy G, Garcia M, Schlup N, Grenier J, Mani JC, Rochefort H. Increased cathepsin D level in the serum of patients with metastatic breast carcinoma detected with a specific pro-cathepsin D immunoassay. *Cancer* 1997; **79**: 2132-2136
 - 16 **van der Stappen JW**, Williams AC, Maciewicz RA, Paraskeva C. Activation of cathepsin B, secreted by a colorectal cancer cell line requires low pH and is mediated by cathepsin D. *Int J Cancer* 1996; **67**: 547-554
 - 17 **Nishikawa H**, Ozaki Y, Nakanishi T, Blomgren K, Tada T, Arakawa A, Suzumori K. The role of cathepsin B and cystatin C in the mechanisms of invasion by ovarian cancer. *Gynecol Oncol* 2004; **92**: 881-886
 - 18 **Skrzydłewska E**, Kozusko B, Sulkowska M, Bogdan Z, Kozłowski M, Snarska J, Puchalski Z, Sulkowski S, Skrzydłowski Z. Antioxidant potential in esophageal, stomach and colorectal cancers. *Hepatogastroenterology* 2003; **50**: 126-131
 - 19 **Amiguet JA**, Jimenez J, Monreal JJ, Hernandez MJ, Lopez-Vivanco G, Vidan JR, Conchillo F, Liso P. Serum proteolytic activities and antiproteases in human colorectal carcinoma. *J Physiol Biochem* 1998; **54**: 9-13
 - 20 **Kos J**, Nielsen HJ, Krasovec M, Christensen IJ, Cimerman N, Stephens RW, Brunner N. Prognostic values of cathepsin B and carcinoembryonic antigen in sera of patients with colorectal cancer. *Clin Cancer Res* 1998; **4**: 1511-1516
 - 21 **Strojan P**, Budihna M, Smid L, Vrhovec I, Skrk J. Cathepsin D in tissue and serum of patients with squamous cell carcinoma of the head and neck. *Cancer Lett* 1998; **130**: 49-56
 - 22 **Sis B**, Sagol O, Kupelioglu A, Sokmen S, Terzi C, Fuzun M, Ozer E, Bishop P. Prognostic significance of matrix metalloproteinase-2, cathepsin D, and tenascin-C expression in colorectal carcinoma. *Pathol Res Pract* 2004; **200**: 379-387
 - 23 **Nishimura Y**, Kawabata T, Kato K. Identification of latent procathepsins B and L in microsomal lumen: characterization of enzymatic activation and proteolytic processing *in vitro*. *Arch Biochem Biophys* 1988; **261**: 64-71
 - 24 **Ikeda Y**, Ikata T, Mishiro T, Nakano S, Ikebe M, Yasuoka S. Cathepsins B and L in synovial fluids from patients with rheumatoid arthritis and the effect of cathepsin B on the activation of pro-urokinase. *J Med Invest* 2000; **47**: 61-75
 - 25 **Levicar N**, Kos J, Blejec A, Golouh R, Vrhovec I, Frkovic-Grazio S, Lah TT. Comparison of potential biological markers cathepsin B, cathepsin L, stefin A and stefin B with urokinase and plasminogen activator inhibitor-1 and clinicopathological data of breast carcinoma patients. *Cancer Detect Prev* 2002; **26**: 42-49
 - 26 **Kostoulas G**, Lang A, Nagase H, Baici A. Stimulation of angiogenesis through cathepsin B inactivation of the tissue inhibitors of matrix metalloproteinases. *FEBS Lett* 1999; **455**: 286-290
 - 27 **Hirtenlehner K**, Pec M, Kubista E, Singer CF. Influences of stroma-derived growth factors on the cytokine expression pattern of human breast cancer cell lines. *Arch Gynecol Obstet* 2002; **266**: 108-113
 - 28 **Halangk W**, Lerch MM, Brandt-Nedelev B, Roth W, Ruthenburger M, Reinheckel T, Domschke W, Lippert H, Peters C, Deussing J. Role of cathepsin B in intracellular trypsinogen activation and the onset of acute pancreatitis. *J Clin Invest* 2000; **106**: 773-781
 - 29 **Teich N**, Bodeker H, Keim V. Cathepsin B cleavage of the trypsinogen activation peptide. *BMC Gastroenterol* 2002; **2**: 16
 - 30 **Williams SJ**, Gotley DC, Antalis TM. Human trypsinogen in colorectal cancer. *Int J Cancer* 2001; **93**: 67-73
 - 31 **Ducroc R**, Bontemps C, Marazova K, Devaud H, Darmoul D, Laburthe M. Trypsin is produced by and activates protease-activated receptor-2 in human cancer colon cells: evidence for new autocrine loop. *Life Sci* 2002; **70**: 1359-1367
 - 32 **Yamamoto H**, Iku S, Adachi Y, Imsumran A, Taniguchi H, Nosho K, Min Y, Horiuchi S, Yoshida M, Itoh F, Imai K. Association of trypsin expression with tumor progression and matrilysin expression in human colorectal cancer. *J Pathol* 2003; **199**: 176-184
 - 33 **Foghsgaard L**, Wissing D, Mauch D, Lademann U, Bastholm L, Boes M, Elling F, Leist M, Jaattela M. Cathepsin B acts as a dominant execution protease in tumor cell apoptosis induced by tumor necrosis factor. *J Cell Biol* 2001; **153**: 999-1010

• BRIEF REPORTS •

Fecal loading in the cecum as a new radiological sign of acute appendicitis

Andy Petroianu, Luiz Ronaldo Alberti, Renata Indelicato Zac

Andy Petroianu, Luiz Ronaldo Alberti, Renata Indelicato Zac,
Alfa Institute of Gastroenterology of the Hospital of Clinics of the
Federal University of Minas Gerais, Avenida Alfredo, Balena, 110-
2 andar, Belo Horizonte, MG, Brazil
Correspondence to: Professor Andy Petroianu, Avenida Afonso
Pena, 1626 apto. 1901, Belo Horizonte, MG 30130-005,
Brazil. petroianu@medicina.ufmg.br
Telephone: +55-31-3274-7744 Fax: +55-31-3274-7744
Received: 2004-10-13 Accepted: 2004-12-08

Abstract

AIM: Although the radiological features of acute appendicitis have been well documented, the value of plain radiography has not been fully appreciated. The aim of this study was to determine the frequency of the association of acute appendicitis with images of fecal loading in the cecum.

METHODS: Plain abdominal radiographs of 400 patients operated upon for acute appendicitis ($n = 100$), acute cholecystitis ($n = 100$), right acute pelvic inflammatory disease ($n = 100$) and right nephrolithiasis ($n = 100$) were assessed. The presence of fecal loading was recorded and the sensitivity and specificity of this sign for acute appendicitis were calculated.

RESULTS: The presence of fecal loading in the cecum occurred in 97 patients with acute appendicitis, 13 patients with acute cholecystitis, 12 patients with acute inflammatory pelvic disease and 19 patients with nephrolithiasis. The sensitivity of this sign for appendicitis was 97% and its specificity to this disease was 85.3%. Its positive predictive value for appendicitis was 68.7%; however, its negative predictive value for appendicitis was 98.8%.

CONCLUSION: The present study suggests that the presence of radiological images of fecal loading in the cecum may be a useful sign of acute appendicitis, and the absence of this sign probably excludes this disease. This is the first description of fecal loading as a radiological sign for acute appendicitis.

© 2005 The WJG Press and Elsevier Inc. All rights reserved.

Key words: Appendicitis; Radiography; Cecum; Fecal loading; Diagnosis

Petroianu A, Alberti LR, Zac RI. Fecal loading in the cecum as a new radiological sign of acute appendicitis. *World J Gastroenterol* 2005; 11(27): 4230-4232
<http://www.wjgnet.com/1007-9327/11/4230.asp>

INTRODUCTION

Abdominal pain in the right lower quadrant is probably one of the most challenging problems in Medicine^[1-4]. In most patients, acute appendicitis is diagnosed on the basis of clinical examination, white blood cell count, abdominal radiographic studies, and abdominal ultrasound^[1-5]. However, the less than perfect accuracy of these exams leads to a high rate of misdiagnosis leading to a rate of negative appendicectomies of about 15%^[1,2,6,7]. In order to avoid the unnecessary removal of the appendix, other investigation methods, such as computed tomography and abdominal scintigraphy have been proposed, without real advantages^[2-5].

In the presence of acute abdominal pain, abdominal radiographs are relevant and helpful, but little significance is attached to this exam in appendicitis although associated radiological features have been documented, such as localized adynamic ileum (51-81% of cases), increase in soft-tissue density in the right lower quadrant (12-33%), appendicoliths (7-14%) and deformity of cecum (4-5%)^[1,5,8-10]. The aim of this prospective study was to evaluate an apparently new sign present in the plain abdominal radiography of patients with acute appendicitis, i.e., images of fecal loading in the cecum. This sign was studied comparatively with other patients presenting acute right abdominal pain due to other diseases. This is the first description of fecal loading as a radiological sign for acute appendicitis.

MATERIALS AND METHODS

Four hundred consecutive patients with acute right abdominal pain were prospectively studied at the Alfa Institute of Gastroenterology of the Hospital of Clinics and Hospital Julia Kubitshek between 2002 and 2004. No patient was discarded from this investigation.

Plain abdominal radiographies were obtained for all patients before treatment in order to verify the presence of fecal images in the cecum. These patients were divided into the following four groups, with 100 patients each, according to their disease.

Acute appendicitis

Patients of both sexes (62 men and 38 women) ranging in age from 10 to 73 (28.3 ± 12.2) years. All patients were operated for acute appendicitis and the diagnosis was confirmed in all cases by histologic examination of the removed appendix. Fifty of the patients with positive fecal loading in the cecum during the appendicitis period were submitted to a new plain abdominal radiography on the

second postoperative day, to verify the presence of this sign after the appendicectomy.

Acute cholecystitis

Patients of both sexes (30 men and 70 women) ranging in age from 17 to 75 (mean 49.4 ± 16.3 years). All patients were operated for acute cholecystitis and the diagnosis was confirmed in all cases by histologic examination of the removed gallbladder. Eight of these cases presented acute cholangitis as well.

Right pelvic inflammatory disease

Women of the age from 20 to 45 (mean 32.3 ± 8.1 years). The complaint of these cases was due to right hydrosalpingitis (69 cases), right Fallopian pregnancy (14 cases), rupture of a right ovarian cyst (12 cases) and torsion of the right ovary (5 cases). The diagnoses were confirmed in all cases by clinical follow-up, pelvic ultrasound, laparoscopy, and surgical procedures.

Right nephrolithiasis

Patients of both sexes (42 men and 58 women) ranging in age from 10 to 73 (43.5 ± 14.3) years. The diagnosis was confirmed in all these cases by plain abdominal radiography, urography, ultrasound and CT scan.

The radiological image studied was cecal intraluminal mass consisting of a mixture of soft tissue and internal gas bubble like feces, suggesting fecal impaction, or residual feces. The amount of fecal material and consequent cecal dilatation were considered.

The sensitivity and specificity of this radiological sign, as well as its positive and negative predictive values for acute appendicitis were calculated.

The present study followed the Ethics Principles of Research in Humans, according to World Medical Association Helsinki Declaration, adopted in 1964 and amended in 1996, and was approved by the Ethical Committee of the Department of Surgery of the Medical School of the Federal University of Minas Gerais, Belo Horizonte, Brazil. All exams performed on these patients are routinely employed in the presence of acute abdominal pain in the hospitals where this investigation was carried out.

RESULTS

Table 1 describes the presence of fecal loading in the cecum of the patients of the four groups (Figure 1A). Some of these radiographs showed cecal dilatation by the large amount of fecal mass (Figure 1B).

The sensitivity of this sign was 97% for acute appendicitis, 13% for acute cholecystitis, 12% for right acute pelvic inflammatory disease and 19% for right nephrolithiasis. The specificity of fecal loading in the cecum for acute appendicitis was 85.3%. The positive predictive value of this sign for acute appendicitis was 68.7%; however, its negative predictive value for appendicitis was 98.8%.

On the second postoperative day, only two of the 50 patients with previous positive radiological sign preserved the fecal loading in the cecum. In the other 48 patients, this sign disappeared from the cecum.

Table 1 Presence of fecal loading in plain abdominal radiographs of 400 patients with right acute abdominal pain divided into four groups ($n = 100$ each)

Disease	Fecal loading			
	Present		Absent	
	<i>n</i>	(%)	<i>n</i>	(%)
Acute appendicitis	97	97	3	3
Acute cholecystitis	13	13	87	87
Right pelvic inflammatory disease	12	12	88	88
Right nephrolithiasis	19	19	81	81

DISCUSSION

Although a few studies have suggested that plain abdominal radiography is not helpful anymore in patients with acute abdominal pain, its indiscriminate use remains the rule in most emergency units^[6,8,9-11]. However, the radiological signs described in the literature are not constant or characteristic of appendicitis. Recent investigations have called into question the value of routine use of plain abdominal radiography in patients with suspected appendicitis^[1,3,4,9]. Many physicians consider ultrasound studies as standard in acute abdominal pain, believing the impact of radiograph is not of value.

In this prospective study, the association of acute

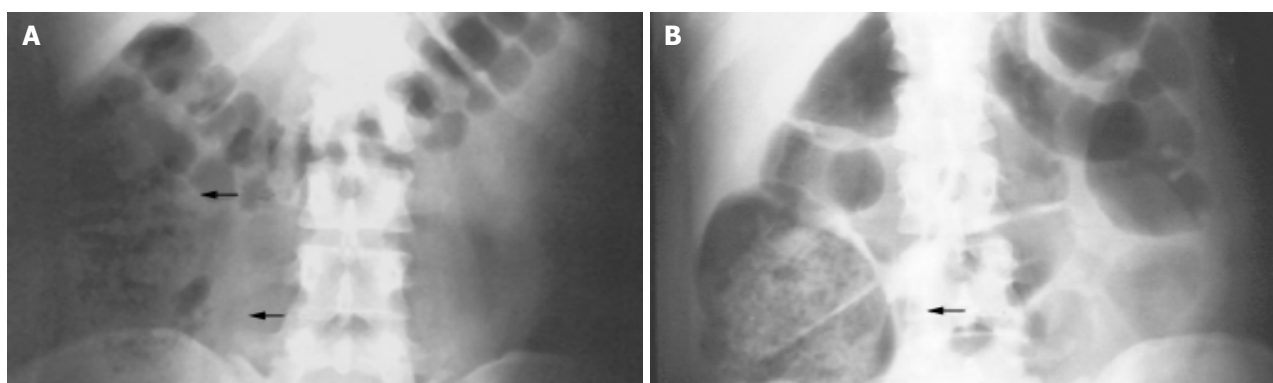


Figure 1 Plain radiographs of the abdomen in the presence of acute appendicitis, showing the fecal loading (cecal intraluminal mass consisting of a mixture of soft tissue and internal gas bubble like feces). **A:** The image of fecal loading in the

cecum (arrow) and right colon (arrow); **B:** The film of another patient with acute appendicitis. Observe residual gross fecal loading with consequent dilatation of the cecum (arrow).

appendicitis with images of fecal loading in the cecum had a sensitivity of 97% and a specificity of 85.3% when compared with other common causes of acute right abdominal pain. This rate is higher than the frequency of other clinical, laboratory, or radiological signs associated with acute appendicitis.

Another important result of the present study is based on the predictive value. According to these data, the possibility of appendicitis in the presence of fecal loading in the cecum is 68.7%. However, the absence of this sign practically excludes the diagnosis of appendicitis, which may occur in only 1.2% of cases.

We could not understand the pathophysiology to answer why appendicitis could lead to fecal loading in the cecum. However, we believe it is worth supposing that this sign may be related to a local ileum of the cecum with stool, which occurred in the presence of an acute inflammatory condition. This is the first description of fecal loading as a radiological sign for acute appendicitis.

In conclusion, the results of the present work suggest that the presence of images of fecal loading in the cecum on plain abdominal radiographs may be a useful sign associated with acute appendicitis. This association should be emphasized, mainly considering that this sign is rare in the presence of other acute inflammatory abdominal

diseases and disappears when the inflamed appendix is removed.

REFERENCES

- 1 **Boleslawski E**, Panis Y, Benoist S, Denet C, Mariani P, Valleur P. Plain abdominal radiography as a routine procedure for acute abdominal pain of the right lower quadrant. *World J Surg* 1999; **23**: 262-264
- 2 **Birnbaum BA**, Wilson SR. Appendicitis at the millenium. *Radiology* 2000; **215**: 337-348
- 3 **Sivit CJ**. Imaging the child with right lower quadrant pain and suspected appendicitis. *Pediatr Radiol* 2004; **34**: 447-453
- 4 **Hayes R**. Abdominal pain. *Eur Radiol* 2004; **14**: L123-L137
- 5 **Rao PM**, Rhea JT, Rao JA, Conn AKT. Plain abdominal radiography in clinically suspected appendicitis. *Am J Emerg Med* 1999; **17**: 325-328
- 6 **Thorpe JA**. The plain abdominal radiograph in acute appendicitis. *Ann Roy Coll Surg Engl* 1979; **61**: 45-47
- 7 **Petroianu A**, Oliveira Neto JE. Prevalence of acute appendicitis in a mixed population. *Dig Surg* 1997; **14**: 195-197
- 8 **Shimkin PM**. Radiology of acute appendicitis. *Am J Roentgenol* 1978; **130**: 1001-1004
- 9 **Shorvon PJ**. Imaging of appendicitis. *Br J Radiol* 2002; **75**: 717-720
- 10 **Shelton T**, McKinlay R, Schwartz RW. Acute appendicitis. *Curr Surg* 2003; **60**: 502-505
- 11 **Petroianu A**, Oliveira Neto JE, Alberti LR. Incidência comparativa da apendicite aguda em população miscigenada, de acordo com a cor da pele. *Arq Gastroenterol* 2004; **41**: 24-26

Science Editor Guo SY Language Editor Elsevier HK

• BRIEF REPORTS •

Effect of autologous blood donation on the central venous pressure, blood loss and blood transfusion during living donor left hepatectomy

Bruno Jawan, Yu-Fan Cheng, Chia-Chi Tseng, Yaw-Sen Chen, Chih-Chi Wang, Tung-Liang Huang, Hock-Liew Eng, Po-Ping Liu, King-Wah Chiu, Shih-Hor Wang, Chih-Che Lin, Tsan-Shiun Lin, Yueh-Wei Liu, Chao-Long Chen

Bruno Jawan, Chia-Chi Tseng, Department of Anesthesiology, Chang Gung Memorial Hospital, Kaohsiung Medical Center, Taiwan, China

Yu-Fan Cheng, Yaw-Sen Chen, Chih-Chi Wang, Tung-Liang Huang, Hock-Liew Eng, Po-Ping Liu, King-Wah Chiu, Shih-Hor Wang, Chih-Che Lin, Yueh-Wei Liu, Tsan-Shiun Lin, Chao-Long Chen, Liver Transplantation Program, Chang Gung Memorial Hospital, Kaohsiung Medical Center, Taiwan, China

Correspondence to: Chao-Long Chen, MD, Superintendent, Chang Gung Memorial Hospital, Ta-pei Road 123, Niao Shung Hsiang, Kaohsiung, Taiwan, China. clchen@adm.cgmh.org.tw

Telephone: +886-7-7317123 Fax: +886-7-7320142

Received: 2004-11-18 Accepted: 2005-01-05

Key words: Patient; Living donor; Surgery; Hepatectomy; Blood; Autologous; Monitoring; Central venous pressure; Blood loss

Jawan B, Cheng YF, Tseng CC, Chen YS, Wang CC, Huang TL, Eng HL, Liu PP, Chiu KW, Wang SH, Lin CC, Lin TS, Liu YW, Chen CL. Effect of autologous blood donation on the central venous pressure, blood loss and blood transfusion during living donor left hepatectomy. *World J Gastroenterol* 2005; 11(27): 4233-4236

<http://www.wjgnet.com/1007-9327/11/4233.asp>

Abstract

AIM: Autologous blood donation (ABD) is mainly used to reduce the use of banked blood. In fact, ABD can be regarded as acute blood loss. Would ABD 2-3 d before operation affect the CVP level and subsequently result in less blood loss during liver resection was to be determined.

METHODS: Eighty-four patients undergoing living donor left hepatectomy were retrospectively divided as group I (GI) and group II (GII) according to have donated 250-300 mL blood 2-3 d before living donor hepatectomy or not. The changes of the intraoperative CVP, surgical blood loss, blood products used and the changes of perioperative hemoglobin (Hb) between groups were analyzed and compared by using Mann-Whitney *U* test.

RESULTS: The results show that the intraoperative CVP changes between GI ($n = 35$) and GII ($n = 49$) up to graft procurement were the same, subsequently the blood loss, but ABD resulted in significantly lower perioperative Hb levels in GI.

CONCLUSION: Since none of the patients required any blood products perioperatively, all the predonated bloods were discarded after the patients were discharged from the hospital. It indicates that ABD in current series had no any beneficial effects, in term of cost, lowering the CVP, blood loss and reduce the use of banked blood products, but resulted in significant lower Hb in perioperative period.

INTRODUCTION

Donor hepatectomy with maximal safety while preserving graft viability and adequacy, in terms of size and function for both recipient and donor, is of principal concern in living donor liver transplantation (LDLT). There are compelling reasons for avoiding surgical blood loss with subsequent blood transfusion^[1]. Allogenic blood transfusion cannot only transmit the infectious diseases, but also induce variety of immunologic responses, such as alloimmunization, transfusion-associated graft vs host diseases, and immunosuppression, which would result in malignant tumor recurrence and increased postoperative infection rate^[2]. Preoperative autologous blood donation (ABD) has been successfully applied in reducing the use of allogenic blood transfusion in liver resection^[3,4]. It is recommended that the last blood donation should not be collected later than 72 h before surgery, to allow for restoration of intravascular volume^[5]. Indeed, ABD can be regarded as acute blood loss. On the other side, low intraoperative central venous pressure (CVP) is associated with less surgical blood loss in hepatectomy surgery^[4,6,7]. Would preoperative ABD 2-3 d before living donor hepatectomy, without intravenous (IV) crystalloid replacement of the loss, affect the intraoperative CVP levels, subsequently reduce the blood loss and blood transfusion during living donor hepatectomy is to be determined. Aims of this retrospective study were to compare the intraoperative CVP levels, blood loss, and the requirement of blood transfusion in patients with and without preoperative ABD during living donor hepatectomy.

MATERIALS AND METHODS

Only consanguineous relatives up to the fifth degree and

lawfully wedded spouses are considered legal live donors in Taiwan. Donor volunteers underwent anthropometric measurements, thorough laboratory analysis, psychosocial evaluation, and detailed imaging studies including Doppler ultrasonography to check the quality of liver parenchyma and patency of blood vessels, and magnetic resonance, venography, arteriography, and cholangiography to check hepatic and portal venous anatomy and hepatic artery and biliary tree branching patterns as previously reported^[8]. Donors should be free of the active liver disease and the donor-recipient pair must be blood group identical or compatible.

After obtaining approval from the Ethics Committee of the Department of Health, Taiwan and written informed consent for surgery and anesthesia from the patients, the patients came into operation room without premedication and IV line. After establishment of the IV line, the anesthesia was induced with thiopental and fentanyl. Succinylcholine was used for facilitating the tracheal intubation. The anesthesia was maintained with isoflurane in oxygen-air mixture and atracurium was used as muscle relaxant. All patients were monitored with electrocardiography, arterial line for continuous blood pressure monitoring, CVP, pulse oximetry, end tidal CO₂, body temperature and urine output.

IV fluids restriction combined with the use of furosemide were applied to lower the intraoperative CVP levels. The deficit of the insensible fluids loss from no per os intake of the patients was not replaced before graft procurement; the intraoperative fluids were maintained to 2-4 mL/(kg · h) before the liver graft is dissected. If the CVP was higher than 10 cm H₂O, furosemide was given; second dose of furosemide was also given if the urine output was lower than 0.5 mL/(kg · h). After the liver graft was procured, IV fluid was increased to approximately 10 mL/(kg · h) until the end of the surgery to replace the cumulative deficits from the procedure. Concerning the surgical procedure and liver parenchymal transection with strict adherence to a meticulous surgical technique without vascular inflow, occlusion to either side of the liver has been previously published^[1].

The anesthesia records were retrospectively reviewed. Patients who had donated 250-300 mL blood 2-3 d before operation was grouped in group I (GI), while no blood donation in group II (GII). The grouping was not at random or blinded; ABD was performed without normovolemic replacement of the loss by IV infusion of the crystalloid in the first 37 cases. Since none of those patients required blood transfusion after successful LDLT, the protocol of ABD was stopped. Data such as anesthesia time, CVP levels (hourly), blood loss, blood transfusion, crystalloids, doses of furosemide and urine output were collected, compared and analyzed between groups by using Mann-Whitney *U* test. All the data were given in mean±SD. Statistical calculations were performed using the SPSS advanced statistics module (SPSS Inc., Chicago, IL, USA). *P* value <0.05 was regarded as significant.

RESULTS

From June 1994 to October 2002, 123 LDLT were performed. Only patients with healthy liver (Table 1) and

undergoing left hepatectomy were enrolled in this study. Right hepatectomy (2/37 in GI and 37/86 in GII) was excluded due to most of the patients of ABD received left hepatectomy. Thirty-five patients were included in ABD group (GI) and 49 in non-ABD group (GII). Table 1 shows the characteristics of the patients of GI and GII. The age, weight, liver functions, anesthesia time, blood loss, and mean dose of furosemide used was not significantly different. Likewise, the crystalloids infusion before and after graft procurement was not significantly different either, but the preoperative hemoglobin (Hb) as well as postoperative d 1-4 of GI was significantly lower in GI in comparison to GII. Figure 1 shows the changes of the CVP levels of both groups, the initial CVP of both groups were higher than 10 cm H₂O, it decreased gradually, under the influence of fluids restriction and diuresis effect of furosemide, and reached a level of 7.9±2.5, 7.7±2.2 and 7.8±1.7, 8.3±1.8 cm H₂O at 6th-7th h after anesthesia begin for GI and GII respectively. It was at that time that the parenchymal transection was performed. After procurement of the liver graft, the IV infusion rate was increased from 3.0±2.3 and 3.4±0.9 to 9.4±6.3 and 10±3.7 mL/(kg · h) for GI and GII respectively. The recovery of the CVP of GI was significantly slower after graft procurement in comparison to GII.

Table 1 Characteristics of patients of GI and GII

	GI (n = 35)	GII (n = 49)
Age (yr)	31.1±5.9	33.9±8.7
Weight (kg)	59.1±9.1	56±8.8
Gender (female/male)	24/11	31/18
SGOT (U/L)	17±6.5	46.3±4.7
SGPT (U/L)	15±11.2	20.9±4.4
ALP (U/L)	53.9±21	56.4±15.7
Total bilirubin (mg, %)	0.58±0.22	0.67±0.2
BUN (mg, %)	12.8±3.3	15.8±13.9
Creatinine (mg, %)	0.79±0.7	0.75±0.1
Anesthesia time (h)	10.4±1.5	10±1.1
Blood loss (mL)	63.8±56	67±63
Fluid 1 [mL/(kg · h)]	3.0±2.3	3.4±0.9
Fluid 2 [mL/(kg · h)]	9.4±6.3	10±3.7
Urine 1 [mL/(kg · h)]	1.6±0.7	1.6±0.7
Urine 2 [mL/(kg · h)]	2.0±1.8	1.7±1.3
Preoperative Hb (g/dL)	11.9±1.8 ^a	12.3±1.5
Postoperative d 1 Hb (g/dL)	11.4±1.83 ^a	12.4±1.6
Postoperative d 2 Hb (g/dL)	11.2±2.0 ^a	12.3±1.5
Postoperative d 3 Hb (g/dL)	10.5±1.6 ^a	11.7±1.4
Postoperative d 4 Hb (g/dL)	9.8±0.9 ^a	11.7±1.69
Furosemide (mg)	11.6±5.0	12.2±1.5

1: Before graft procurement, 2: after graft procurement. ^a*P*<0.05 vs others. SGOT: serum glutamic oxaloacetic transaminase; SGPT: serum glutamic pyruvic transaminase; ALP: alkaline phosphatase.

DISCUSSION

LDLT is a new form of therapy for pediatric and adult patients with end-stage liver diseases to overcome the problem of organ donor shortage. However, the major medical and ethical concern of this technique is the risk to the healthy donor. This concern is legitimate, since

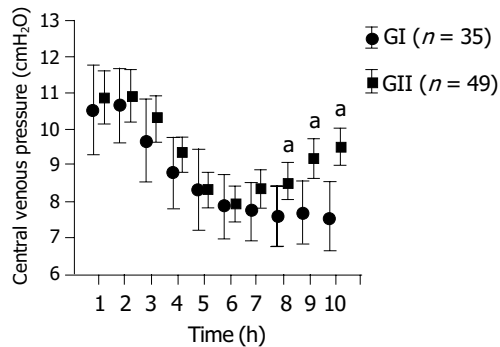


Figure 1 The CVP changes were not significantly different between GI and GII from the first measurement up to the graft procurement, but the recovery of the CVP of GI was slower in comparison to GII after increasing the infusion rate from T8 till the end of the operation ^a $P < 0.05$ vs GI.

hepatectomy is a major upper abdominal surgery with potential risk of massive blood loss and subsequent requirement for blood transfusion, which is correlated significantly with postoperative morbidity and mortality^[9]. It is known that low CVP resulted in significant less blood loss during liver resection. Therefore, maintaining a low CVP has been regarded as a simple and effective way to reduce blood loss during parenchymal transection^[3,4,6]. A low CVP is accompanied by low pressure in the hepatic veins and sinusoids, theoretically favoring less blood loss during parenchymal transection and allows easier control of inadvertent venous injury^[1]. Low CVP indicates less intravascular volume and ABD is in fact a kind of acute blood loss. If the volume loss is not replaced, theoretically would result in lowering of the intravascular volume, subsequently the CVP and blood loss of liver resection. Our results show that donation of 250-300 mL of blood 2-3 d before donor hepatectomy without IV fluids replacement seemed not to affect the changes of the CVP levels during the surgical procedure in comparison to the group without ABD (Figure 1). The mechanism is probably due to the fact that the volume loss of the donated blood has been fully compensated by the oral intake of the healthy donors within 2-3 d. Figure 1 shows that, under the same anesthesia, same regime in lowering the CVP by fluids restriction and forced diuresis with furosemide, the changes of the CVP, from the first measurement to graft procurement, were not significantly different between GI and GII. The CVP of both groups decreased gradually from 10.5 ± 3.6 and 10.8 ± 2.8 to 7.9 ± 2.5 , 7.7 ± 2.2 and 7.8 ± 1.7 , 8.3 ± 1.8 cm H₂O at the time of parenchymal transection (around T6-7) for GI and GII respectively. The recovery of the CVP level after procurement of the liver graft to the end of the operation was slower in GI after increasing the infusion rate aimed to replace the cumulative fluid deficit to expand intravascular volume and to preserve renal function. Table 1 shows that the blood loss was not significantly different between groups. Both had only minimal blood loss with a mean loss of 63.8 ± 56 and 67 ± 63 mL for GI and GII respectively.

Current results indicated that ABD itself did not have favorable effect in lowering the intraoperative CVP levels and likewise the blood loss in comparison to non-ABD

group. In contrary, it significantly lowered the preoperative Hb level as well as its levels at postoperative d 1-4 (Table 1). It indicated that GI patients would reach earlier low Hb and transfusion threshold. Heiss *et al.*, reported that the blood transfusion rate was indeed higher in the autologous blood group than in the homologous group in patients undergoing colorectal cancer surgery, mainly because these patients had lower preoperative Hb concentrations owing to the blood donation^[10].

Allogenic blood transfusion is often life saving and crucial in the treatment of major blood loss^[11]. Although the safety of the banked blood supply has been improved recently but it can still have adverse effects^[2,12]. The risks of autologous transfusion are less than those of allogenic RBC transfusions^[12,13], but it is still not risk free^[13-16]. Complications such as bacterial contamination, hemolysis due to administrative error, volume overload were reported^[14]. Furthermore, studies have unexpectedly shown similar postoperative infectious complications and immunosuppression in patients receiving autologous blood donated before surgery, as with those receiving homologous blood^[13,17]. Factors such as histamine, plasminogen activator, superoxide and eosinophil cation protein, released into the plasma during storage may be of major importance in enhancing overall immunosuppression^[18]. The best policy in avoiding blood transfusion is to improve the surgical and anesthetic technique to minimize blood loss. Anyway, ABD is still an acceptable alternative measurement to reduce the use of allogenic blood if the amount of expected surgical blood loss is large enough requiring blood transfusion^[3,4]. Since none of our patients required any blood products perioperatively, the predonated autologous bloods of GI were discarded after the patients being discharged from the hospital. In contrary to previous reports^[3,4], ABD in current series had no any beneficial effect, in terms of cost, lowering the CVP, blood loss and reducing the use of banked blood products, but resulted in significant lower Hb in perioperative period, subsequently increasing the chance of getting autologous blood transfusion from their anemia.

In conclusion. Autologous donation of 250-300 mL blood 2-3 d before liver hepatectomy in LDLT seemed not to affect the intraoperative CVP level and subsequently no favorable effect in reducing the blood loss during liver resection. In contrary, it resulted in significant lower Hb in perioperative period, subsequent increasing the chance of getting autologous blood transfusion from their anemia. ABD in living donor left hepatectomy is not recommended if minimal surgical bleeding can be maintained.

REFERENCES

- 1 **Chen CL**, Chen YS, de Villa VH, Wang CC, Lin CL, Goto S, Wang SH, Cheng YF, Huang TL, Jawan B, Cheung HK. Minimal blood loss living donor hepatectomy. *Transplantation* 2000; **69**: 2580-2586
- 2 **Klein HG**. Immunomodulatory aspects of transfusion: a once and future risk? *Anesthesiology* 1999; **91**: 861-865
- 3 **Chan AC**, Blumgart LH, Wuest DL, Melendez JA, Fong Y. Use of preoperative autologous blood donation in liver resections for colorectal metastases. *Am J Surg* 1998; **175**: 461-465
- 4 **Itamoto T**, Katayama K, Nakahara H, Tashiro H, Asahara T. Autologous blood storage before hepatectomy for hepato-

- cellular carcinoma with underlying liver disease. *Br J Surg* 2003; **90**: 23-28
- 5 **Vanderlinde ES**, Heal JM, Blumberg N. Autologous transfusion. *Bmj* 2002; **324**: 772-775
- 6 **Jones RM**, Moulton CE, Hardy KJ. Central venous pressure and its effect on blood loss during liver resection. *Br J Surg* 1998; **85**: 1058-1060
- 7 **Melendez JA**, Arslan V, Fischer ME, Wuest D, Jarnagin WR, Fong Y, Blumgart LH. Perioperative outcomes of major hepatic resections under low central venous pressure anesthesia: blood loss, blood transfusion, and the risk of postoperative renal dysfunction. *J Am Coll Surg* 1998; **187**: 620-625
- 8 **Chen YS**, Cheng YF, De Villa VH, Wang CC, Lin CC, Huang TL, Jawan B, Chen CL. Evaluation of living liver donors. *Transplantation* 2003; **75**: S16-19
- 9 **Gozzetti G**, Mazziotti A, Grazi GL, Jovine E, Gallucci A, Gruttadauria S, Frena A, Morganti M, Ercolani G, Masetti M. Liver resection without blood transfusion. *Br J Surg* 1995; **82**: 1105-1110
- 10 **Heiss MM**, Mempel W, Jauch KW, Delanoff C, Mayer G, Mempel M, Eissner HJ, Schildberg FW. Beneficial effect of autologous blood transfusion on infectious complications after colorectal cancer surgery. *Lancet* 1993; **342**: 1328-1333
- 11 **Greenburg AG**. Benefits and risks of blood transfusion in surgical patients. *World J Surg* 1996; **20**: 1189-1193
- 12 **Goodnough LT**, Brecher ME, Kanter MH, AuBuchon JP. Transfusion medicine. First of two parts-blood transfusion. *N Engl J Med* 1999; **340**: 438-447
- 13 **Goodnough LT**, Brecher ME, Kanter MH, AuBuchon JP. Transfusion medicine. Second of two parts-blood conservation. *N Engl J Med* 1999; **340**: 525-533
- 14 **Linden JV**, Kruskall MS. Autologous blood: always safer? *Transfusion* 1997; **37**: 455-456
- 15 **Domen RE**. Adverse reactions associated with autologous blood transfusion: evaluation and incidence at a large academic hospital. *Transfusion* 1998; **38**: 296-300
- 16 **Goldman M**, Remy-Prince S, Trepanier A, Decary F. Autologous donation error rates in Canada. *Transfusion* 1997; **37**: 523-527
- 17 **Nielsen HJ**. Influence on the immune system of homologous blood transfusion and autologous blood donation: impact on the routine clinical practice/differences in oncological and non-tumour surgery? *Anesthesiol Intensivmed Notfallmed Schmerzther* 2000; **35**: 642-645
- 18 **Nielsen HJ**. Detrimental effects of perioperative blood transfusion. *Br J Surg* 1995; **82**: 582-587

Science Editor Guo SY Language Editor Elsevier HK

• BRIEF REPORTS •

Colchicine sensitizes human hepatocellular carcinoma cells to damages caused by radiation

Chia-Yuan Liu, Hui-Fen Liao, Shou-Chuan Shih, Shee-Chan Lin, Wen-Hsiung Chang, Cheng-Hsin Chu, Tsang-En Wang, Yu-Jen Chen

Chia-Yuan Liu, Shou-Chuan Shih, Shee-Chan Lin, Wen-Hsiung Chang, Cheng-Hsin Chu, Tsang-En Wang, Division of Gastroenterology, Department of Internal Medicine, Mackay Memorial Hospital, Taipei, Taiwan, China
Chia-Yuan Liu, Hui-Fen Liao, Yu-Jen Chen, Department of Medical Research, Mackay Memorial Hospital, Taipei, Taiwan, China
Shou-Chuan Shih, Mackay Medicine, Nursing and Management College, Taipei, Taiwan, China
Hui-Fen Liao, Yu-Jen Chen, Graduate Institute of Sports Coaching Science, Chinese Culture University, Taipei, Taiwan, China
Yu-Jen Chen, Department of Radiation Oncology, Mackay Memorial Hospital, Taipei, Taiwan, China
Hui-Fen Liao, Department of Molecular Biology and Biochemistry, National Chiayi University, Chiayi, 300 Taiwan, China
Supported by the MMH grant from Mackay Memorial Hospital, No. 9252

Correspondence to: Dr. Yu-Jen Chen, Department of Radiation Oncology, Mackay Memorial Hospital, 92, Section 2, Chung San North Road, Taipei 104, Taiwan, China. chenmdphd@yahoo.com
Telephone: +886-2-28094661 Fax: +886-2-28096180

Received: 2004-11-24 Accepted: 2004-12-20

Abstract

AIM: We studied the effect of colchicine combined with radiation on the survival of human hepatocellular carcinoma (HCC) HA22T/VGH cells.

METHODS: Twenty-four hours after treatment with 0-8 ng/mL colchicine, HA22T/VGH cells were irradiated at various doses (0, 1, 2, 4, and 8 Gy). Colony assay was performed to assess the surviving cell fraction. Survival curves were fitted by using a linear-quadratic model to estimate the sensitizer enhancement ratio (SER). Flow cytometry was used for cell cycle analysis.

RESULTS: Colchicine at lower concentrations (1 and 2 ng/mL) had obvious synergy with radiation to inhibit HCC cell growth, whereas higher concentrations (4 and 8 ng/mL) had only additive effect to radiation. Pretreatment with 1 and 2 ng/mL colchicine for 24-h enhanced cell killing by radiation with SERs of 1.21 and 1.53, respectively. G₂/M arrest was only observed with higher colchicine doses (8 and 16 ng/mL) after 24-h treatment; this effect was neither seen with lower doses (1, 2, and 4 ng/mL) nor with any dose after only 1 h of treatment.

CONCLUSION: Our results suggest that colchicine has potential as an adjunct to radiotherapy for HCC treatment. Lower doses of colchicine possess radiosensitizing effects via some mechanism other than G₂/M arrest. Further study is necessary to elucidate the mechanism.

© 2005 The WJG Press and Elsevier Inc. All rights reserved.

Key words: Colchicine; Radiation sensitizer; Hepatocellular carcinoma

Liu CY, Liao HF, Shih SC, Lin SC, Chang WH, Chu CH, Wang TE, Chen YJ. Colchicine sensitizes human hepatocellular carcinoma cells to damages caused by radiation. *World J Gastroenterol* 2005; 11(27): 4237-4240

<http://www.wjgnet.com/1007-9327/11/4237.asp>

INTRODUCTION

Colchicine interferes with microtubule formation, thereby affecting mitosis and other microtubule-dependent functions^[1]. It has been used in clinical practice for a long time, including for the treatment of acute gout^[2], prophylaxis of recurrent gout^[3], Behcet's disease^[4], chronic hepatitis B^[5], and primary biliary cirrhosis^[6]. It is a relatively safe and an effective drug when used with appropriate dosage^[7].

Hepatocellular carcinoma (HCC) is a highly malignant tumor with poor prognosis and high mortality. It is a common malignancy in Asian countries. In China, the incidence has been increasing over the past two decades. The age-adjusted rate of death per 100 000/year was 20.37 in the 1990s. In the USA, the incidence of HCC has approximately doubled over the past three decades^[8]. Aggressive treatment with a variety of modalities, including surgery, transarterial chemoembolization, percutaneous ethanol injection, radiofrequency ablation, microwave coagulation therapy, and laser-induced thermotherapy have all been used in an attempt to control this disease. However, the overall 5-year survival is still around 5%. Few tumors are resectable because of advanced stage or the presence of associated liver disease^[9,10].

Radiation therapy (RT) has not played an important role in HCC treatment in the past because normal liver tissue has low tolerance to radiation. Radiation hepatitis usually develops with whole liver irradiation at or above 35 Gy, yet this dose level may not be sufficient to eradicate the tumor. However, small portions of the liver can be irradiated with 50-60 Gy without significant long-term morbidity. Recent advances in RT including three-dimensional conformal radiation therapy (3DRT) limits the exposure of normal liver tissue and allows delivery of higher RT doses (40-80 Gy)^[11]. 3DRT has improved treatment outcome and reduced normal liver damage in unresectable HCC^[12]. There is a dose-response relationship with 3-DRT for primary HCC, with only the

radiation dose being a significant factor for predicting treatment response^[13]. It is important to develop novel ways to improve the efficacy of RT, not only by physical technique but also by pharmacological agents. The development of radiosensitizers in order to reduce the required cytotoxic RT dose for HCC is especially important for this disease that arises in the midst of radiosensitive normal tissue.

Other studies have demonstrated that cells are most radiosensitive in the G₂/M phase, whereas the most resistant are in late S phase^[14]. Because colchicine arrests the cell cycle at the G₂/M phase, we designed this study to assess its effect in combination with radiation on HA22T/VGH, a poorly differentiated HCC cell line^[15,16].

MATERIALS AND METHODS

Preparation of colchicine

Colchicine (C₂₂H₂₅NO₆, molecular weight 399.4, purity 95%) was purchased from Sigma Co. (St. Louis, MO, USA). The powder was dissolved in distilled water to form an aqueous stock solution and diluted with PBS before use.

Cell culture

The human poorly differentiated HCC cell line HA22T/VGH^[15,16] was cultured in DMEM (GIBCO, Grand Island, NY, USA) supplemented with 10% heat-inactivated fetal calf serum (FCS, Hyclone, Logan, UT, USA), NaHCO₃ (10 mmol/L) and HEPES (20 mmol/L) at 37 °C in a humidified 50 mL/L CO₂ incubator. For routine subculturing, the cells were grown to near confluence, collected by 0.25% trypsin, counted using the trypan blue exclusion test, and adjusted to an initial density of approximately 10⁴ cells/mL.

Colchicine treatment and radiation delivery

In preliminary work, we determined the cytotoxic effect of different colchicine concentrations on HA22T/VGH HCC cells by using a 3-(4,5-dimethylthiazol-2-yl)-2,5-diphenyl-tetrazolium bromide (MTT) assay and found that concentrations up to 2 ng/mL were non-toxic. Based on these preliminary results, we used colchicine concentrations of 0-8 ng/mL to test for radiosensitization. HA22T/VGH HCC cells were treated with 0, 1, 2, 4, and 8 ng/mL colchicine for 24 h, and the colchicine was washed out before RT. RT with 6 MeV electron beam energy was delivered by a linear accelerator (Clinac® 1800, Varian Associates, Inc., CA, USA; dose rate 2.4 Gy/min) at various doses (0, 1, 2, 4, and 8 Gy) in a single fraction. Full electron equilibrium was ensured for each fraction by a parallel plate PR-60C ionization chamber (CAPINTEL, Inc., Ramsey, NJ, USA). One hundred and fifty viable tumor cells were plated onto 35-mm six-well culture dishes and were allowed to grow in DMEM medium containing 10% heat-inactivated FCS and the various concentrations of colchicine at 37 °C in a humidified 50 mL/L CO₂ incubator for 24 h. Then the cells were treated with various radiation doses. Following radiation, a colony assay was performed.

Colony assay

After 10-14 d, the culture dishes were stained with 3%

crystal violet and colonies (≥ 50 cells) were counted. The surviving fraction was calculated as mean colonies/cells inoculated. The mean plating efficiency for untreated HA22T/VGH HCC cells was 43%. Survival curves were fitted by using a linear-quadratic model^[17]. The sensitizer enhancement ratio (SER) was calculated as the radiation dose needed for radiation alone divided by the dose needed for colchicine plus radiation at a surviving fraction of 37% (D₀ in radiobiology).

Cell cycle analysis by flow cytometry

Cells were treated with various doses of colchicine (0, 1, 2, 4, 8, and 16 ng/mL) for 1 or 24 h, then harvested and fixed at 4 °C for 1 h with 70% ethanol. The cells were stained for 30 min with propidium iodide (PI) solution (PI, 0.5 mg/mL; RNase, 0.1 mg/mL; Sigma Co.) from a CycleTEST plus DNA reagent kit (Becton Dickinson, Lincoln Park, NJ, USA). Analysis of DNA content was performed using a FACScalibur flow cytometer (Becton Dickinson). The data from 10⁴ cells were collected and analyzed using ModFit software (Becton Dickinson).

Statistical analysis

Data were expressed as percentage and mean \pm SE.

We used Sigma Plot software (version 8.0, SPSS Inc., Chicago, IL, USA) to fit survival curves with a linear-quadratic model. One-way analysis of variance was used to compare the colony formation between different groups (SPSS, version 10.0, Chicago, IL, USA).

RESULTS

Cell survival and SER

The results of colony assays of various doses colchicine combined with radiation are shown in Table 1. There was an obvious synergistic effect of low-dose colchicine (1 and 2 ng/mL) plus radiation. When the dose was increased to 4 and 8 ng/mL, only mild additive effects were noted.

As the survival curves in Figure 1 demonstrate, low-dose colchicine sensitized HA22T/VGH HCC cells to radiation in a dose-dependent manner. The RT doses required for a surviving fraction of 37% (D₀ in radiobiology) after pretreatment with 0, 1, and 2 ng/mL colchicine were 9.45, 7.80, and 6.16 Gy respectively. The calculated SERs of colchicine were 1.21 for 1 ng/mL and 1.53 for 2 ng/mL.

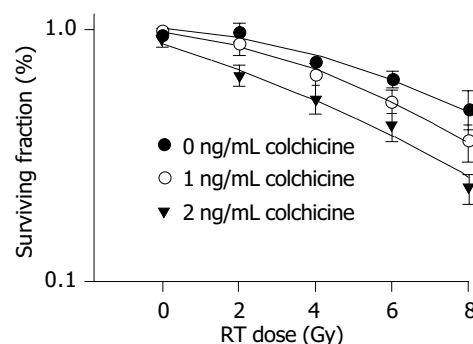


Figure 1 Radiation survival curves for human HA22T/VGH hepatocellular carcinoma cells. Cells were treated with vehicle (●), colchicine 1 ng/mL (○) and 2 ng/mL (▼) for 1 h before radiation.

Table 1 Colony assay of human HA22T/VGH hepatocellular carcinoma cells. Data are expressed as mean±SE

Colchicine (ng/mL)	0	1	2	4	8
RT 0 Gy	81.0±4.0	78.7±1.0	72.8±3.3	57.5±4.0	29.2±2.7
1	78.3±4.1	70.5±5.1	52.7±4.5	43.3±4.3	22.3±3.0
2	59.8±3.5	53.5±4.2	42.3±3.6	33.2±2.5	12.8±3.0
4	51.2±3.0	41.5±3.2	32.8±3.2	27.0±3.3	11.5±2.7
8	38.2±5.6	27.3±3.5	18.5±1.8	15.3±2.4	6.7±1.8

Cell cycle analysis after varying doses of colchicine

Although colchicine is reported to arrest mitosis, no HA22T/VGH HCC cells were clearly seen in the G₂/M phase 1-h treatment (data not shown). After 24 h of colchicine treatment, significant G₂/M arrest was induced by higher doses (8 and 16 ng/mL) but not by doses, which were less than 8 ng/mL (Table 2). The DNA histograms after 24 h of treatment with varying doses of colchicine are shown in Figure 2.

Table 2 Cell cycle analysis of human HA22T/VGH hepatocellular carcinoma cells. Cell were treated with various doses of colchicine for 24 h and analyzed by flow cytometry

Colchicine (ng/mL)	Cell cycle distribution (%)		
	G ₀ /G ₁	S	G ₂ +M
0	49.0±1.4	24.6±1.1	26.4±1.0
1	51.4±1.1	21.7±1.4	26.9±1.0
2	52.2±1.5	21.5±1.4	26.3±0.9
4	51.6±1.9	22.0±1.5	26.5±0.9
8	43.0±2.1 ^a	21.7±1.7	35.4±1.2 ^b
16	17.6±1.3 ^b	23.5±1.3	58.9±2.2 ^b

^aP<0.05, ^bP<0.01 vs colchicine treatment with 0 ng/mL.

DISCUSSION

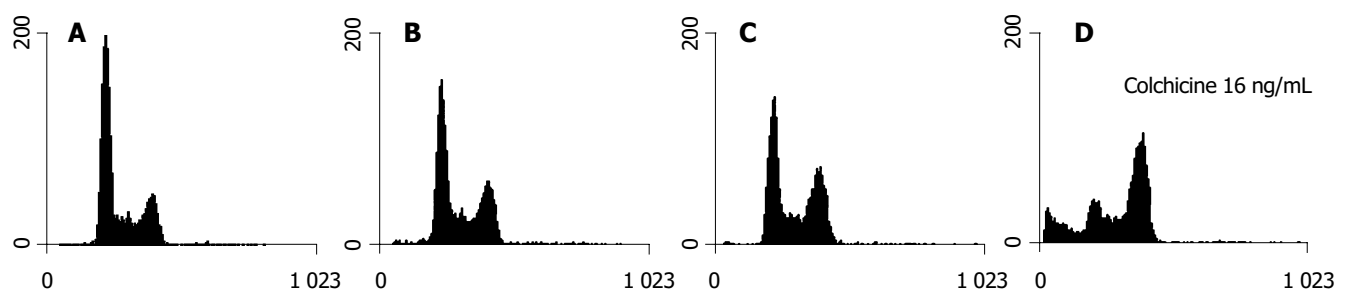
The present study demonstrates that pretreatment with colchicine is capable of reducing the survival of irradiated human HCC HA22T/VGH cells. The combined effect varies with the dose of colchicine. Pretreatment with colchicine at lower doses (1-2 ng/mL) 1 h prior to RT yielded a synergistic effect on radiation-induced cytotoxicity. Higher doses gave only a mild additive effect. However,

the G₂/M arrest phenomenon was not found with low doses or short-term (1 h) colchicine treatment. Evident G₂/M arrest was observed after treatment with higher doses (8 and 16 ng/mL) of colchicine for 24 h. Alteration of cell cycle distribution therefore may not play a major role in the radiosensitizing effect of colchicine in this combined therapy.

RT plays an important role in combined treatment for several malignant tumors^[18,19]. However, the risk of radiation-induced toxicity limits its use in liver tumors^[20]. While 3DRT is increasingly used for HCC, limiting the volume of irradiated normal liver and allowing adjustment of the radiation dose to improve the therapeutic index, it still has many limitations. Advanced liver cirrhosis or poor liver reserve is a common problem in patients with HCC^[21]. The risk of hepatic failure after cytotoxic doses of RT therefore remains as a great problem. Radiosensitizers may give patients with poor liver reserve a better chance of controlling their tumor. Pentoxifylline and ganglioside GD3 have been shown to act as radiosensitizers in the human HCC cell line HepG2. Pentoxifylline may do so by causing cell cycle arrest in the G₂/M phase. Ganglioside GD3 may have a dual action in producing radiosensitization by interacting with mitochondria and by inactivating NF-κB^[22,23].

The safety and therapeutic range of colchicine are well established. The doses of colchicine (0-8 ng/mL) we used before RT are much lower than those in previous reports for other *in vitro* disease models^[7]. Our results demonstrate that colchicine enhances the radiation effect *in vitro*, thus reducing the radiation dose needed to inhibit tumor growth. Most RT-related complications develop not early in the course of RT but rather after a high cumulative dose. Using colchicine at low doses yielded an SER of 1.21 at 1 ng/mL and 1.53 at 2 ng/mL. This means that if the original planned RT dose was 50 Gy, the same cytotoxic effect would be achieved by only 32.68 Gy after pretreatment with 2 ng/mL of colchicine. This reduced RT dose is close to 30 Gy, the threshold for whole liver irradiation, which may result in lethal liver damage with a 5% probability in 5 years (TD 5/5)^[20].

Our results suggest that lower doses of colchicine sensitize HA22T/VGH HCC cells to radiation. At lower doses (1 and 2 ng/mL), 24 h of treatment with colchicine did not change the G₂/M phase distribution significantly. At higher doses (8 and 16 ng/mL), the drug arrested that cell cycle at the G₂/M phase. There was an accompanying evident sub-G₁ peak noted on the DNA histogram (Figure 2). This implies that the synergistic effect of colchicine and RT may involve multiple mechanisms,

**Figure 2** DNA histograms in cell cycle analyses of HA22T/VGH cells by flow cytometry. A: Control; B: Colchicine 2 ng/mL; C: Colchicine 8 ng/mL;

D: Colchicine 16 ng/mL.

perhaps including cell cycle regulation, induction of apoptosis, and others.

In conclusion, colchicine at optimal doses sensitizes human HA22T/VGH HCC cells to radiation by a mechanism other than cell cycle arrest at the G₂/M phase.

ACKNOWLEDGMENTS

The authors wish to thank Dr. Mary Jeanne Buttrey for critical reading and correction of the manuscript.

REFERENCES

- 1 Ben-Chetrit E, Levy M. Colchicine: 1998 update. *Semin Arthritis Rheum* 1998; **28**: 48-59
- 2 Emmerson BT. The management of gout. *N Engl J Med* 1996; **334**: 445-451
- 3 Yu TF, Gutman AB. Efficacy of colchicine prophylaxis in gout. Prevention of recurrent gouty arthritis over a mean period of five years in 208 gouty subjects. *Ann Intern Med* 1961; **55**: 179-192
- 4 Masuda K, Nakajima A, Urayama A, Nakae K, Kogure M, Inaba G. Double-masked trial of cyclosporin versus colchicine and long-term open study of cyclosporin in Behcet's disease. *Lancet* 1989; **1**: 1093-1096
- 5 Floreani A, Lobello S, Brunetto M, Aneloni V, Chiaramonte M. Colchicine in chronic hepatitis B: a pilot study. *Aliment Pharmacol Ther* 1998; **12**: 653-656
- 6 Lee YM, Kaplan MM. Efficacy of colchicine in patients with primary biliary cirrhosis poorly responsive to ursodiol and methotrexate. *Am J Gastroenterol* 2003; **98**: 205-208
- 7 Wallace SL, Singer JZ. Review: systemic toxicity associated with the intravenous administration of colchicine-guidelines for use. *J Rheumatol* 1988; **15**: 495-499
- 8 El-Serag HB. Hepatocellular carcinoma: an epidemiologic view. *J Clin Gastroenterol* 2002; **35**(5 Suppl 2): S72-S78
- 9 Faivre J, Forman D, Esteve J, Obradovic M, Sant M. Survival of patients with primary liver cancer, pancreatic cancer and biliary tract cancer in Europe. *Eur J Cancer* 1998; **34**: 2184-2190
- 10 El-Serag HB, Mason AC, Key C. Trends in survival of patients with hepatocellular carcinoma between 1977 and 1996 in the United States. *Hepatology* 2001; **33**: 62-65
- 11 Nguyen MH, Keffe EB. Treatment of Hepatocellular cancer. In: Rustgi AK, Crawford JM. *Gastrointestinal Cancers*. London: Saunders 2003: 615
- 12 Cheng SH, Lin YM, Chuang VP, Yang PS, Cheng JC, Huang AT, Sung JL. A pilot study of three-dimensional conformal radiotherapy in unresectable hepatocellular carcinoma. *J Gastroenterol Hepatol* 1999; **14**: 1025-1033
- 13 Park HC, Seong J, Han KH, Chon CY, Moon YM, Suh CO. Dose-response relationship in local radiotherapy for hepatocellular carcinoma. *Int J Radiat Oncol Biol Phys* 2002; **54**: 150-155
- 14 Sinclair WK, Morton RA. X-ray sensitivity during the cell generation cycle of cultured Chinese hamster cells. *Radiat Res* 1966; **29**: 450-474
- 15 Lin YM, Hu CP, Chou CK, Lee TW, Wu KT, Chen TY, Peng FK, Lin TJ, Ko JL, Chang CM. A new human hepatoma cell line: establishment and characterization. *Zhonghua Minguo Weisheng Wuji Mianyixue Zazhi* 1982; **15**: 193-201
- 16 Chang C, Lin Y, Lee TW, Chou CK, Lee TS, Lin TJ, Peng FK, Chen TY, Hu CP. Induction of plasma protein secretion in a newly established human hepatoma cell line. *Mol Cell Biol* 1983; **3**: 1133-1137
- 17 Hall EJ. Cell survival curves. In: *Radiobiology for the radiologist*. 5th ed. Philadelphia: Lippincott Williams & Wilkins 2000: 32-37
- 18 Kuban DA, Dong L. High-dose intensity modulated radiation therapy for prostate cancer. *Curr Urol Rep* 2004; **5**: 197-202
- 19 Olmi P, Fallai C, Cerrotta AM, Lozza L, Badii D. Breast cancer in the elderly: the role of adjuvant radiation therapy. *Crit Rev Oncol Hematol* 2003; **48**: 165-178
- 20 Emami B, Lyman J, Brown A, Coia L, Goitein M, Munzenrider JE, Shank B, Solin LJ, Wesson M. Tolerance of normal tissue to therapeutic irradiation. *Int J Radiat Oncol Biol Phys* 1991; **21**: 109-122
- 21 Alsowmely AM, Hodgson HJ. Non-surgical treatment of hepatocellular carcinoma. *Aliment Pharmacol Ther* 2002; **16**: 1-15
- 22 Wu DH, Liu L, Chen LH. Radiosensitization by pentoxifylline in human hepatoma cell line HepG2 and its mechanism. *Diyi Junyi Daxue Xuebao* 2004; **24**: 382-385
- 23 Paris R, Morales A, Coll O, Sanchez-Reyes A, Garcia-Ruiz C, Fernandez-Checa JC. Ganglioside GD3 sensitizes human hepatoma cells to cancer therapy. *J Biol Chem* 2002; **277**: 49870-49876

Science Editor Guo SY Language Editor Elsevier HK

• BRIEF REPORTS •

Co-infection of SENV-D among chronic hepatitis C patients treated with combination therapy with high-dose interferon-alfa and ribavirin

Chia-Yen Dai, Wan-Long Chuang, Wen-Yu Chang, Shinn-Cherng Chen, Li-Po Lee, Ming-Yen Hsieh, Nei-Jen Hou, Zu-Yau Lin, Ming-Yuh Hsieh, Liang-Yen Wang, Ming-Lung Yu

Chia-Yen Dai, Wan-Long Chuang, Wen-Yu Chang, Shinn-Cherng Chen, Li-Po Lee, Ming-Yen Hsieh, Nei-Jen Hou, Zu-Yau Lin, Ming-Yuh Hsieh, Liang-Yen Wang, Ming-Lung Yu, Hepatobiliary Division, Department of Internal Medicine, Kaohsiung Medical University Hospital, Kaohsiung, Taiwan, China
Chia-Yen Dai, Nei-Jen Hou, Department of Internal Medicine, Kaohsiung Municipal Hsiao-Kang Hospital, Kaohsiung, Taiwan, China

Chia-Yen Dai, Department of Occupational Medicine, Kaohsiung Municipal Hsiao-Kang Hospital, Kaohsiung, Taiwan, China
Supported by the National Science Council Grant, No. NSC-91-2314-B037-344

Correspondence to: Ming-Lung Yu, MD, PhD, Hepatobiliary Division, Department of Internal Medicine, Kaohsiung Medical University Hospital, No. 100, Shih-Chuan 1st Road, Kaohsiung 807, Taiwan, China. d780178@kmu.edu.tw

Telephone: +886-7-3121101-7475 Fax: +886-7-3123955

Received: 2004-11-08 Accepted: 2004-12-20

Abstract

AIM: The clinical significance of co-infection of SENV-D among patients with chronic hepatitis C (CHC) and response of both viruses to combination therapy with high-dose interferon-alfa (IFN) plus ribavirin remain uncertain and are being investigated.

METHODS: Total 164 (97 males and 67 females, the mean age 48.1 ± 11.4 years, range: 20-73 years, 128 histologically proved) naive CHC patients were enrolled in this study. SENV-D DNA was tested by PCR method. Detection of serum HCV RNA was performed using a standardized automated qualitative RT-PCR assay (COBAS AMPLICOR HCV Test, version 2.0). HCV genotypes 1a, 1b, 2a, 2b, and 3a were determined by using genotype-specific primers. Pretreatment HCV RNA levels were determined by using the branched DNA assay (Quantiplex HCV RNA 3.0). There are 156 patients receiving combination therapy with IFN 6 MU plus ribavirin for 24 wk and the response to therapy is determined.

RESULTS: Sixty-one (37.2%) patients were positive for SENV-D DNA and had higher mean age than those who were negative (50.7 ± 10.6 years vs 46.6 ± 11.6 years, $P = 0.026$). The rate of sustained viral response (SVR) for HCV and SENV-D were 67.3% (105/156) and 56.3% (27/48), respectively. By univariate analysis, the higher rate of SVR was significantly related to HCV genotype non-1b ($P < 0.001$), younger ages ($P = 0.014$), lower

pretreatment levels of HCV RNA ($P = 0.019$) and higher histological activity index (HAI) score for intralobular regeneration and focal necrosis ($P = 0.037$). By multivariate analyses, HCV genotype non-1b, younger age and lower pretreatment HCV RNA levels were significantly associated with HCV SVR (odds ratio (OR)/95% confidence interval (CI): 12.098/0.02-0.19, 0.936/0.890-0.998, and 3.131/1.080-9.077, respectively). The SVR of SENV-D was higher among patients clearing SENV-D than those who had viremia at the end of therapy ($P = 0.04$).

CONCLUSION: Coexistent SENV-D infection, apparently associated with higher ages, is found in more than one-third Taiwanese CHC patients. Both HCV and SENV-D are highly susceptible to combination therapy with high-dose IFN and ribavirin and SENV-D co-infection does not affect the HCV response. HCV genotype, pretreatment HCV RNA levels and age are predictive factors for HCV SVR.

© 2005 The WJG Press and Elsevier Inc. All rights reserved.

Key words: Chronic hepatitis C; Combination therapy; Interferon; Ribavirin; SENV-D

Dai CY, Chuang WL, Chang WY, Chen SC, Lee LP, Hsieh MY, Hou NJ, Lin ZY, Hsieh MY, Wang LY, Yu ML. Co-infection of SENV-D among chronic hepatitis C patients treated with combination therapy with high-dose interferon-alfa and ribavirin. *World J Gastroenterol* 2005; 11(27): 4241-4245
<http://www.wjgnet.com/1007-9327/11/4241.asp>

INTRODUCTION

A new family of DNA viruses was recently isolated and designated as SEN virus (SENV)^[1,2]. SENV is a single-stranded circular DNA virus distantly related to the large TT virus family with eight different variants (A-H) shown by phylogenetic analysis^[3]. Two strains of SENV (SENV-D and SENV-H) are more prevalent among patients with transfusion-associated non-AE hepatitis than in healthy blood donors that suggested the significant associations between SENV-D/H and transfusion-associated hepatitis^[2,4]. Nevertheless, the clinical implication and etiological importance in association with liver diseases of SENV infection still remain undetermined.

HCV is the major etiologic agent of post-transfusion hepatitis and leads to chronic liver disease and primary

hepatocellular carcinoma^[5,6]. With the prevalence rate of chronic hepatitis C (CHC) ranging from 0.95% to 2.6% among the general population^[7,8], we had previously reported a positive rate of anti-HCV up to 57.9% in some communities in southern Taiwan^[9]. For CHC, the combination therapy with interferon-alfa (IFN) and ribavirin has been considered as first-line therapy. Previous reports have demonstrated the increased rate of sustained viral response (SVR) to 31-43% after combination therapy for 24 or 48 wk than 6-19% of IFN monotherapy^[10,11]. Lai *et al.*, reported a SVR rate of 43% after combination therapy with standard IFN dose in Taiwan^[12]. In our previous study, the rate of HCV SVR with a high-dose IFN monotherapy achieved 41.2% among Taiwanese CHC patients^[13] and the tailored-dose IFN monotherapy according to the virological characteristics of CHC patients yielded a better efficacy^[14]. The benefits of high-dose IFN may be gained in the combination therapy for CHC.

The clinical significance of SENV infection in combination with HCV infection remains controversial. For patients with CHC, Rigas *et al.*, reported that co-infection with SENV might adversely affect the outcome of treatment with combination therapy^[15]. Another study, however, did not support their findings^[16]. The aims of the present study are to survey the prevalence and clinical implications of SENV-D co-infection on biochemical, pathological, and virological profiles among CHC patients. The response of HCV and SENV-D to combination therapy with high-dose IFN and ribavirin are also investigated. Furthermore, we elucidate the predictive factors for HCV SVR and the influence of concurrent SENV-D infection on HCV response to combination therapy.

MATERIALS AND METHODS

Patients

Between May 1998 and May 2001, a total of 164 Taiwanese CHC patients in the clinics of hepatological division of the Kaohsiung Medical University Hospital, 97 men and 67 women, aged between 20 and 73 years (mean 48.1 ± 11.4 years) were enrolled in the study. All patients were diagnosed with chronic HCV infection based on continuous positivity for second-generation antibody to HCV (anti-HCV) in serum for more than 6 mo and positive for HCV RNA. Liver biopsies were carried out in 128 patients and the disease activity grade and fibrosis stage were quantitatively scored according to the histological activity index (HAI) scoring system^[17]. Patients who were positive for hepatitis B surface antigen (HBsAg) had human immunodeficiency virus type I infection, autoimmune liver disease, metabolic liver diseases including α -1 anti-trypsin deficiency hemochromatosis or Wilson's disease, alcoholic liver disease or intravenous drug abuse were excluded. All the serum samples, when collected from patients at the time of their evaluation, were stored at -70°C before testing. The study had been approved by the Ethics Committee of Kaohsiung Medical University Hospital and all patients had given their informed consent.

Methods

Laboratory tests Serum HBsAg was assayed using

commercially available kits (General Biological HBsAg radio-immunoassay; General Biological Cooperation, Taiwan) and second-generation HCV antibody (anti-HCV) was detected with commercially available ELISA kits (Abbott, North Chicago, IL, USA). Alanine aminotransferase (ALT, normal upper limit of serum ALT = 34 IU/L) was measured on a multichannel autoanalyzer.

Detection of SENV-D DNA and detection/quantification/genotyping of serum HCV RNA The presence of SENV-D DNA was determined by PCR as described previously^[18]. Detection of serum HCV RNA was performed using a standardized automated qualitative RT-PCR assay (COBAS AMPLICOR HCV Test, version 2.0; Roche, Branchburg, NJ, USA). The detection limit was 50 IU/mL. HCV genotypes 1a, 1b, 2a, 2b, and 3a were determined by amplification of the core region using genotype-specific primers described by Okamoto *et al.*^[19]. Pretreatment HCV RNA levels were determined by using the branched DNA assay (Quantiplex HCV RNA 3.0, Bayer, Emeryville, CA, USA), performed strictly in accordance with the manufacturer's instructions. The quantification limit was 615 IU of HCV RNA per milliliter.

Combination therapy with high-dose IFN and ribavirin Total 156 CHC-naïve patients (92 males, 64 females, mean age: 48.0 ± 11.5 years, 122 patients with liver biopsies) received combination therapy for 24 wk using IFN subcutaneously at a dosage of 6 MU thrice a week and ribavirin by mouth at a dosage of 1 000-1 200 mg daily. After the cessation of therapy, all of them received 24 wk of follow up for evaluation of the response. A SVR for HCV was defined as clearance of serum HCV RNA at the end of the therapy and 24 wk after the cessation of combination therapy. All other patients were defined as non-responders (NR). To evaluate the response of SENV-D, the presence of SENV-D DNA was determined at wk 24 and 48. An end-of-treatment viral response (ETVR) and a SVR for SENV-D were indicated by negative PCR results at wk 24 and 48, respectively.

Statistical analysis

Serum HCV RNA levels were expressed as the mean \pm SD after logarithmic transformation of original values. Frequency was compared between groups using the χ^2 test or Fisher's exact test, and group means were compared using the *t*-test. For all tests a *P* value lesser than 0.05 was considered to be significant. Stepwise logistic regression was used to analyze factors associated with response to combination therapy in CHC patients. Odds ratios (ORs) and their associated 95% confidence intervals (CIs) were used to quantify the magnitude of their associations.

RESULTS

Study population

The mean pretreatment ALT and HCV RNA levels of the 164 CHC patients was 136.9 ± 168.9 IU/L and 5.79 ± 0.67 log IU/mL, respectively. There were 140 (85.4%) patients with abnormal ALT levels. The HCV genotype distribution was as follows: 1b in 80 (48.8%) patients, 2a in 48 (29.3%) patients, 2b in 18 (11.0%) patients, mixed in 13 (7.9%)

patients and unclassified in 5 (3.0%) patients. Of 128 patients undergoing liver biopsies, the mean scores for peri-portal necrosis, intralobular necrosis, portal inflammation (grading) and fibrosis were 1.11 ± 1.34 , 0.52 ± 0.88 , 1.91 ± 1.24 , 3.51 ± 2.55 , and 1.25 ± 1.36 , respectively.

SENV-D viremia in chronic hepatitis C patients

Of 164 CHC patients, 61 patients were positive for SENV-D DNA showing a prevalence of 37.2%. The comparison of clinical characteristics between patients with and without SENV-D co-infection was shown in Table 1. The mean age was higher among patients with positive SENV-D DNA than those who were negative for SENV-D DNA (50.7 ± 10.6 years *vs* 46.6 ± 11.6 years, $P = 0.026$). No other clinical and virological factor was related to positive SENV-D DNA. Among 128 patients that underwent liver biopsies, all the mean scores were similar between SENV-D DNA-positive and -negative patients.

Table 1 Comparison of clinical characteristics between individuals with and without SENV-D viremia in 164 CHC patients

	SENV-D viremia		<i>P</i>
	Positive (<i>n</i> = 61)	Negative (<i>n</i> = 103)	
Sex (male) (%)	36 (59.0)	61 (59.2)	NS
Age (yr)	50.7 ± 10.6	46.6 ± 11.6	0.026
Serum ALT (IU/L)	144.0 ± 164.3	125.8 ± 164.2	NS
Normal (≤ 34 IU/L) (%)	8 (33.3)	16 (66.7)	NS
Abnormal (> 34 IU/L) (%)	53 (37.9)	87 (62.1)	
HCV RNA levels (log IU/mL)	5.72 ± 0.70	5.85 ± 0.63	NS
HCV genotype 1b (%)	26 (42.6)	54 (52.4)	NS
Histology (HAI scores)	46	82	
Peri-portal necrosis	1.11 ± 1.34	1.11 ± 1.35	NS
Intralobular necrosis	0.70 ± 1.00	0.41 ± 0.78	NS
Portal inflammation	1.80 ± 1.31	1.98 ± 1.21	NS
Total score (grading)	3.54 ± 2.65	3.49 ± 2.52	NS
Fibrosis	1.39 ± 1.50	1.16 ± 1.28	NS

Results are expressed as mean \pm SD. HAI: histological activity index, NS: no significance.

HCV virological response to combination therapy

Of all 156 naive CHC patients receiving combination therapy, the HCV genotype distribution was as follows: 1b in 76 (48.7%) patients, 2a in 47 (30.1%) patients, 2b in 16 (10.3%) patients, mixed in 12 (7.7%) patients, and unclassified in 5 (3.2%) patients. The mean pretreatment ALT and HCV RNA levels were 134.8 ± 166.8 IU/L and 5.79 ± 0.66 log IU/mL, respectively with 133 (85.3%) and

99 (63.5%) patients having abnormal ALT levels and high serum HCV levels ($\geq 200\,000$ IU/mL). Of 122 patients undergoing liver biopsies, the mean scores for peri-portal necrosis, intralobular necrosis, portal inflammation (grading), and fibrosis were 1.09 ± 1.31 , 0.52 ± 0.89 , 1.93 ± 1.22 , 3.52 ± 2.48 , and 1.23 ± 1.33 , respectively. After combination therapy with high dose IFN and ribavirin for 24 wk, 105 (67.3%) of 156 patients achieved SVR. The clinical and virological features between CHC patients with HCV SVR and those with NR are shown in Table 2. In comparison between these two groups by univariate analysis, the higher rate of SVR was significantly related to younger ages ($P = 0.014$), lower pretreatment levels of HCV RNA ($< 200\,000$ IU/mL, $P = 0.019$), HCV genotype non-1b ($P < 0.001$) and higher HAI score for intralobular regeneration and focal necrosis ($P = 0.037$). No significant association between other clinical and virological factors and HCV response of combination therapy was observed. Based on multivariate regression analyses, the significant factors associated with HCV SVR after combination therapy were HCV genotype non-1b, younger age and pretreatment HCV RNA levels less than $200\,000$ IU/mL with the OR and 95%CI of these factors summarized in Table 3.

Table 2 Comparison of clinical and virological features between sustained viral responders (SVR) and non-responders (NR) of CHC patients after combination therapy

	HCV response		<i>P</i>
	NR (<i>n</i> = 51)	SVR (<i>n</i> = 105)	
Sex (male) (%)	31 (60.8)	61 (58.1)	NS
Age (yr)	51.24 ± 11.3	46.4 ± 11.3	0.014
Serum ALT (IU/L)	122.2 ± 105.0	140.9 ± 189.9	NS
Normal (≤ 34 IU/L) (%)	4 (18.2)	18 (81.8)	NS
Abnormal (> 34 IU/L) (%)	47 (34.6)	87 (65.4)	
HCV RNA levels (log IU/mL)	5.90 ± 0.62	5.73 ± 0.68	NS
High level ($\geq 200\,000$ IU/mL) (%)	39 (39.4)	60 (60.6)	0.019
Low level ($< 200\,000$ IU/mL) (%)	12 (21.1)	45 (78.9)	
HCV genotype 1b (%)	44 (86.3)	32 (30.5)	< 0.0001
Positive SENV-D DNA (%)	16 (31.4)	41 (39.0)	NS
Histology (HAI scores)			
Patients no.	37	85	
Peri-portal necrosis	1.08 ± 1.30	1.091 ± 1.323	NS
Intralobular necrosis	0.278 ± 0.61	0.64 ± 0.97	0.037
Portal inflammation	2.03 ± 1.17	1.89 ± 1.25	NS
Total score (grading)	3.32 ± 2.22	3.60 ± 2.59	NS
Fibrosis	1.41 ± 1.38	1.157 ± 1.31	NS

Results are expressed as mean \pm SD. HAI: histological activity index, NS: no significance.

Table 3 Stepwise logistic regression analysis of factors significantly associated with HCV sustained virologic response (SVR) after combination therapy in 156 CHC patients

Dependent variable	Independent variable	Comparison	OR (95%CI) ¹	<i>P</i>
HCV SVR	HCV genotypes	1b = 0 Non-1b = 1	12.098 (0.02–0.19)	< 0.001
	Age	Per year increased	0.936 (0.890–0.998)	0.011
	HCV RNA level	High ($\geq 200\,000$ IU/mL) = 0	3.131 (1.080–9.077)	0.036
	Low ($< 200\,000$ IU/mL) = 1			

¹CI: Confidence interval.

Clearance of SENV-D DNA after combination therapy

SENV-D DNA was followed in 48 CHC patients (28 males, 20 females, mean age: 50.2 ± 10.5 years) concomitant with SENV-D viremia before combination therapy. Their mean ALT level was 154.6 ± 179.8 IU/L (range: 16-112 years) and 41 patients were abnormal. The HCV genotype distribution is as follows: 1b in 19 patients, 2a in 19 patients, 2b in 4 patients, mixed in 5 patients, and unclassified in 1 patient. The clinical characteristics and virological features between individuals with and without SENV-D DNA after combination therapy were analyzed and shown in Table 4. At the end of treatment, SENV-D DNA was negative in 37 patients (77.1%). Thirteen of thirty-seven patients (35.1%) had reappearance of serum SENV-D DNA when followed 24 wk after the cessation of therapy. Three of eleven patients (27.3%) with positive SENV-D DNA at the end of treatment were cleared of SENV-D DNA 24 wk after the cessation of therapy. The rate of SVR of SENV-D DNA after combination therapy was 56.3% (27/48). As shown in Table 4, the SVR of SENV-D was higher among patients with ETVR than those who were SENV-D viremia at the end of treatment (88.9% *vs* 61.9%, $P = 0.04$). No other clinical and virological factor was related to SVR for SENV-D.

Table 4 Comparison of clinical characteristics and virological features between 48 CHC patients with and without sustained clearance of SENV-D after combination therapy

	SENV-D response		<i>P</i>
	NR (<i>n</i> = 21)	SVR (<i>n</i> = 27)	
Sex (male) (%)	15 (71.4)	13 (48.2)	NS
Age (yr)	48.3 ± 10.6	51.7 ± 10.3	NS
Serum ALT (IU/L)	157.6 ± 122.9	152.4 ± 216.3	NS
High HCV RNA level ($\geq 200\ 000$ IU/mL) (%)	9 (42.9)	18 (66.7)	NS
HCV genotype 1b (%)	7 (33.3)	12 (44.4)	NS
SENV-D ETVR (%)	13 (61.9)	24 (88.9)	0.04
HCV SVR (%)	17 (81.0)	18 (66.7)	NS

Results are expressed as mean \pm SD. ETVR: end-of-treatment viral response, SVR: sustained viral responder, NR: non-responders, NS: no significance.

DISCUSSION

The geographic distribution of different SENV variants has been noted. In Japan, SENV-D is more prevalent than SENV-H^[20-23], but the predominant strain of SENV-H has been reported in the USA^[4]. Kao *et al.*, reported that the prevalence of SENV-H was 2-7 times higher than that of SENV-D in different northern Taiwanese individuals^[16,24]. The findings of the present study revealed that 37.1% of Taiwanese patients with CHC were co-infected with SENV-D which is higher by 28% than reports by Kao *et al.*^[16]. Our previous studies have shown that the prevalence of SENV-D was also higher than SENV-H not only among southern Taiwan blood donors (19.7% and 5.8%)^[18] but also among patients on maintenance hemodialysis (46.5% and 27.3%)^[25]. Furthermore, we found the prevalence of SENV-H was 19.2% among Taiwanese CHC patients (unpublished data) which is lower than that of SENV-D. It is interesting that a

marked difference of genotypic distribution of SENV between southern and northern Taiwan exists.

There was a higher mean age among CHC patients who were SENV-D viremic than non-viremic. We found similar results among blood donors too^[18]. However, we did not observe significant correlation between age and the prevalence of SENV-H among blood donors^[18] and CHC patients (unpublished data). The cause of discrepancy between trends of change in the prevalence of SENV-D and -H was not clear. Whether the possible assumptions such as the different exposure rate or routes of infection or different rates of spontaneous clearance between these two strains can clarify the issues needs further large-scale and longitudinal studies.

The clinical significance of SENV infection in combination with HCV infection remains unclear^[15,16]. Kao *et al.*, reported the relevance between HCV genotype 2a and SENV co-infection^[16]. The present study revealed that the pretreatment mean ALT levels and HCV RNA levels, and the histological scores between CHC patients with and without SENV-D co-infection were compatible and failed to show association between SENV-H and HCV genotype. Nevertheless, we have found a correlation between SENV-H co-infection and HCV genotype 1b among CHC patients (unpublished data). The discrepancy needs further studies. The biochemical and histological characteristics of CHC patients were not influenced by SENV-D co-infection that indicated the irrelevance between severity of liver disease and SENV-D co-infection.

As previous reports from researchers in Taiwan, the SVR rate of CHC patients was high (40-43%) after combination therapy with IFN 3 MU and ribavirin for 24 wk^[12,16]. In the present study, the HCV SVR rate was 67.3% after combination therapy with 6 MU IFN and ribavirin for 24 wk, which may further indicate the favorable results of combination therapy for Taiwanese CHC patients. The positive predictors of SVR to combination therapy with high-dose IFN were elucidated as HCV genotype non-1b, lower pretreatment HCV RNA levels and younger age. HCV genotype non-1b, having 12 times of SVR rate than genotype 1b in the present study, is the most important factor predicting SVR. Previous reports have demonstrated that HCV with SENV co-infection affected HCV response to combination therapy with IFN plus ribavirin adversely^[15] but the other report denied the relevance between HCV response and SENV co-infection^[16,22]. Our data here indicates that SENV-D co-infection does not affect the HCV response in the combination therapy with high dose IFN and ribavirin. In addition to co-infection with GB virus C/hepatitis G virus or TT virus that had no impact on the response to IFN monotherapy in CHC patients in our previous studies^[13,26,27], it seems unnecessary to determine whether CHC patients coinfect these viruses or not before they received combination therapy.

After combination therapy with 6 MU IFN and ribavirin for 24 wk among 48 CHC patients concomitant with SENV-D viremia, the rates of viral clearance at the end of follow-up achieved 56.3%. In an earlier study on the response of SENV-D among CHC patients, the sustained response rate of SENV-D has recently been reported by Umemura

et al., (73.3%) after high-dose IFN monotherapy^[22] and by Kao *et al.*, (87.5%) after combination therapy with 3 MU IFN and ribavirin for 24 wk^[16]. The lower SVR rate of SENV-D than SENV-H (78.3%, unpublished data) in our study from southern Taiwan was different from results from northern Taiwan that showed higher SENV-D SVR rate (87.5%) than SENV-H (26.8%)^[16]. The causes of different response to combination therapy, in addition to the different prevalence, of these two strains in southern and northern Taiwan need further research.

In conclusion, we find that more than one-third Taiwanese patients with CHC are coinfectd with SENV-D and coexistent SENV-D infection is apparently associated with higher ages but does not have an influence on the clinico-pathological characteristics of HCV infection. SENV-D is highly susceptible and does not affect the HCV response to combination therapy. After combination therapy with high dose IFN and ribavirin, two-thirds of Taiwanese CHC patients achieve SVR and HCV genotype non-1b, lower pretreatment HCV RNA levels and younger age are predictive factors for SVR.

REFERENCES

- Mushahwar IK. Recently discovered blood-borne viruses: are they hepatitis viruses or merely endosymbionts? *J Med Virol* 2000; **62**: 399-404
- Bowden S. New hepatitis viruses: contenders and pretenders. *J Gastroenterol Hepatol* 2001; **16**: 124-131
- Tanaka Y, Tanaka Y, Primi D, Wang RY, Umemura T, Yeo AE, Mizokami M, Alter HJ, Shih JW. Genomic and molecular evolutionary analysis of a newly identified infectious agent (SEN virus) and its relationship to the TT virus family. *J Infect Dis* 2001; **183**: 359-367
- Umemura T, Yeo AE, Sottini A, Moratto D, Tanaka Y, Wang RY, Shih JW, Donahue P, Primi D, Alter HJ. SEN virus infection and its relationship to transfusion-associated hepatitis. *Hepatology* 2001; **33**: 1303-1311
- Alter MJ, Margolis HS, Krawczynski K, Judson FN, Mares A, Alexander WJ, Hu PY, Miller JK, Gerber MA, Sampliner RE. The natural history of community-acquired hepatitis C in the United States. *New Engl J Med* 1992; **327**: 1899-1905
- Lauer GM, Walker BD. Hepatitis C virus infection. *N Engl J Med* 2001; **345**: 41-52
- Chuang WL, Chang WY, Lu SN, Lin ZY, Chen SC, Hsieh MY, Wang LY, You SL, Chen CJ. The role of hepatitis C virus in chronic hepatitis B virus infection. *Gastroenterol Jpn* 1993; **28** (Suppl 5): 23-27
- Chen DS, Chen DS, Wang JT, Chen PJ, Wang TH, Sung JL. Hepatitis C virus infection in Taiwan. *Gastroenterol Jpn* 1991; **26**(Suppl 3): 164-166
- Wang JH, Lu SN, Wu JC, Huang JF, Yu ML, Chen SC, Chuang WL. A hyperendemic community of hepatitis B virus and hepatitis C virus infection in Taiwan. *Trans R Soc Trop Med Hyg* 1999; **93**: 253-254
- McHutchison JG, Gordon SC, Schiff ER, Shiffman ML, Lee WM, Rustgi VK, Goodman ZD, Ling MH, Cort S, Albrecht JK. Interferon alfa-2b alone or in combination with ribavirin as initial treatment for chronic hepatitis C. *N Engl J Med* 1998; **339**: 1485-1492
- Poynard T, Marcellin P, Lee SS, Niederau C, Minuk GS, Ideo G, Bain V, Heathcote J, Zeuzem S, Trepo C, Albrecht J. Randomised trial of interferon alpha2b plus ribavirin for 48 wk or for 24 wk versus interferon alpha2b plus placebo for 48 wk for treatment of chronic infection with hepatitis C virus. *Lancet* 1998; **352**: 1426-1432
- Lai MY, Kao JH, Yang PM, Wang JT, Chen PJ, Chan KW, Chu JS, Chen DS. Long-term efficacy of ribavirin plus interferon alfa in the treatment of chronic hepatitis C. *Gastroenterology* 1996; **111**: 1307-1312
- Dai CY, Yu ML, Lin ZY, Chen SC, Hsieh MY, Lee LP, Hou NJ, Hsieh MY, Wang LY, Tsai JF, Chuang WL, Chang WY. Clinical significance of TT Virus (TTV) infection in chronic hepatitis C patients with high dose interferon-alpha therapy in Taiwan: re-evaluated by using new set of TTV primers. *Hepatol Res Hepatol Res* 2003; **27**: 95-100
- Yu ML, Dai CY, Chen SC, Lee LP, Huang JF, Lin ZY, Hsieh MY, Wang LY, Chuang WL, Chang WY. A prospective study on treatment of chronic hepatitis C with tailored and extended interferon-alpha regimens according to pretreatment virological factors. *Antiviral Res Antiviral Res* 2004; **63**: 25-32
- Rigas B, Hasan I, Rehman R, Donahue P, Wittkowski KM, Lebovics E. Effect on treatment outcome of coinfection with SEN viruses in patients with hepatitis C. *Lancet* 2001; **358**: 1961-1962
- Kao JH, Chen W, Chen PJ, Lai MY, Chen DS. SEN virus infection in patients with chronic hepatitis C: preferential coinfection with hepatitis C genotype 2a and no effect on response to therapy with interferon plus ribavirin. *J Infect Dis* 2003; **187**: 307-310
- Knodel RG, Ishak KG, Black WC, Chen TS, Craig R, Kaplowitz N, Kiernan TW, Wollman J. Formulation and application of a numerical scoring system for assessing histological activity in asymptomatic chronic active hepatitis. *Hepatology* 1981; **1**: 431-435
- Dai CY, Yu ML, Lin ZY, Chen SC, Hsieh MY, Wang LY, Tsai JF, Chuang WL, Chan WY. Prevalence and clinical significance of SEN virus infection among volunteer blood donors in southern Taiwan. *Dig Dis Sci* 2004; **49**: 1181-1185
- Okamoto H, Tokita H, Sakamoto M, Horikita M, Kojima M, Iizuka H, Mishiro S. Characterization of the genomic sequence of type V (or 3a) hepatitis C virus isolates and PCR primers for specific detection. *J Gen Virol* 1993; **74**(Pt 11): 2385-2390
- Kobayashi N, Tanaka E, Umemura T, Matsumoto A, Iijima T, Higuchi M, Hora K, Kiyosawa K. Clinical significance of SEN virus infection in patients on maintenance haemodialysis. *Nephrol Dial Transplant* 2003; **18**: 348-352
- Umemura T, Alter HJ, Tanaka E, Yeo AE, Shih JW, Oriei K, Matsumoto A, Yoshizawa K, Kiyosawa K. Association between SEN Virus Infection and Hepatitis C in Japan. *J Infect Dis* 2001; **184**: 1246-1251
- Umemura T, Alter HJ, Tanaka E, Oriei K, Yeo AE, Shih JW, Matsumoto A, Yoshizawa K, Kiyosawa K. SEN virus: response to interferon alfa and influence on the severity and treatment response of coexistent hepatitis C. *Hepatology* 2002; **35**: 953-959
- Shibata M, Wang RY, Yoshida M, Shih JW, Alter HJ, Mitamura K. The presence of a newly identified infectious agent (SEN virus) in patients with liver diseases and in blood donors in Japan. *J Infect Dis* 2001; **184**: 400-404
- Kao JH, Chen W, Chen PJ, Lai MY, Chen DS. Prevalence and Implication of a Newly Identified Infectious Agent (SEN Virus) in Taiwan. *J Infect Dis* 2002; **185**: 389-392
- Dai CY, Chuang WL, Chang WY, Chen SC, Sung MH, Hsieh MY, Lin ZY, Hsieh MY, Wang LY, Tsai JF, Yu ML. SEN virus infection among patients on maintenance hemodialysis in southern Taiwan. *J Infection* 2005: (in press)
- Yu ML, Chuang WL, Dai CY, Chen SC, Lin ZY, Hsieh MY, Tsai JF, Wang LY, Chang WY. GB virus C/hepatitis G virus infection in chronic hepatitis C patients with and without interferon-alpha therapy. *Antiviral Res* 2001; **52**: 241-249
- Dai CY, Yu ML, Chuang WL, Hou NJ, Hou C, Chen SC, Lin ZY, Hsieh MY, Wang LY, Chang WY. The response of hepatitis C virus and TT virus to high dose and long duration interferon-alpha therapy in naive chronic hepatitis C patients. *Antiviral Res* 2002; **53**: 9-18

• BRIEF REPORTS •

Composition of common bile duct stones in Chinese patients during and after endoscopic sphincterotomy

Wei-Lun Tsai, Kwok-Hung Lai, Chiun-Ku Lin, Hoi-Hung Chan, Ching-Chu Lo, Ping-I Hsu, Wen-Chi Chen, Jin-Shiung Cheng, Gin-Ho Lo

Wei-Lun Tsai, Kwok-Hung Lai, Chiun-Ku Lin, Hoi-Hung Chan, Ching-Chu Lo, Ping-I Hsu, Wen-Chi Chen, Jin-Shiung Cheng, Gin-Ho Lo, Division of Gastroenterology, Department of Internal Medicine, Kaohsiung Veterans General Hospital, School of Medicine, National Yang Ming University, Taiwan, China

Supported by the Grants From National Science Council, No. NSC 89-2314-B-075B-007, No. NSC 89-2315-13-075B-003, and No. NSC 90-2314-B-075B-001

Correspondence to: Kwok-Hung Lai, Division of Gastroenterology, Department of Internal Medicine, Kaohsiung Veterans General Hospital, 386 Ta-Chung 1st Road, Kaohsiung 813, Taiwan, China. khlai@isca.vghks.gov.tw

Telephone: +886-7-3468366 Fax: +886-7-3456888

Received: 2004-12-10 Accepted: 2005-01-05

CONCLUSION: Bilirubinate stone is the predominant composition of initial or recurrent CBD stone in Chinese patients. The composition of CBD stones may be different from initial stones after ES.

© 2005 The WJG Press and Elsevier Inc. All rights reserved.

Key words: Endoscopic sphincterotomy; Common bile duct stone; Bilirubinate stone; Cholesterol stone

Tsai WL, Lai KH, Lin CK, Chan HH, Lo CC, Hsu PI, Chen WC, Cheng JS, Lo GH. Composition of common bile duct stones in Chinese patients during and after endoscopic sphincterotomy. *World J Gastroenterol* 2005; 11(27): 4246-4249

<http://www.wjgnet.com/1007-9327/11/4246.asp>

Abstract

AIM: Endoscopic sphincterotomy (ES) is a well-established therapeutic modality for the removal of common bile duct (CBD) stones. After ES there are still around 10% of patients that experience recurrent CBD stones. The aim of this study is to investigate the composition of CBD stones before and after ES and its clinical significance in Chinese patients.

METHODS: From January 1996 to December 2003, 735 patients with CBD stones received ES at Kaohsiung Veterans General Hospital and stone specimens from 266 patients were sent for analysis. Seventy-five patients had recurrent CBD stones and stone specimens from 44 patients were sent for analysis. The composition of the stones was analyzed by infrared (IR) spectrometry and they were classified as cholesterol or bilirubinate stones according to the predominant composition. Clinical data were analyzed.

RESULTS: In the initial 266 stone samples, 217 (82%) were bilirubinate stones, 42 (16%) were cholesterol stones, 3 were calcium carbonate stones, 4 were mixed cholesterol and bilirubinate stones. Patients with bilirubinate stones were significantly older than patients with cholesterol stones (66 ± 13 years vs 56 ± 17 years, $P = 0.001$). In the 44 recurrent stone samples, 38 (86%) were bilirubinate stones, 3 (7%) were cholesterol stones, and 3 were mixed cholesterol and bilirubinate stones. In 27 patients, both initial and recurrent stone specimens can be obtained, 23 patients had bilirubinate stones initially and 2 became cholesterol stones in the recurrent attack. In the four patients with initial cholesterol stones, three patients had bilirubinate stones and one patient had a cholesterol stone in the recurrent attack.

INTRODUCTION

The prevalence of gallstone diseases varied from 10% to 30% in the normal population and increased with age^[1-3]. Most gallstones are asymptomatic, but symptomatic gallstones may occur due to either cystic duct obstruction or common bile duct (CBD) stone formation. Endoscopic sphincterotomy (ES) is a well-established therapeutic modality for the removal of CBD stones. In follow-up studies after ES, 3-21% of patients developed recurrent CBD stones^[4-6] and most of them can be treated successfully by endoscopy^[4,7].

The main composition of gallstones is cholesterol and bile pigments^[8]. The major composition of GB stones obtained from Western patients is cholesterol (consisting of more than 50% cholesterol)^[8]. However, in the Asian patients, most gallstones are pigmented stones^[9]. Pigmented stones can be classified as black stones, associated with hemolysis or brown stones, associated with infection or bile stasis^[10-13]. Stones in the CBD are often brown, pigmented stones^[14-16]. After ablation of sphincter, bactobilia may happen and the pathogenesis of CBD stone formation may be different from the patients with intact sphincters^[17,18]. There have been few studies reporting the composition of recurrent CBD stones in patients after ES.

The aim of this study is to determine the composition of initial and recurrent CBD stones by infrared (IR) spectrometry and investigate the relationship of clinical characteristics and the change of the composition of recurrent stones after ES.

MATERIALS AND METHODS

Since January 1996 to December 2003, total 735 patients

with CBD stones received successful ES with clearance of CBD stones in Kaohsiung Veterans General Hospital and 266 stone specimens were collected and sent for stone analysis. During clinical follow-up, 75 patients had recurrent stones and 44 stone specimens were collected for stone analysis. Clinical data such as age, sex, diameter of CBD, size, number and color of stones, presence of juxtaepapillary diverticulum (JPD), gallbladder (GB) status, and GB stones were recorded. GB stone was detected by sonogram or computed tomography of abdomen. Diameter of CBD and size and number of stones were measured during endoscopic retrograde cholangiopancreatography.

The stone sample was retrieved by Dormia basket (FG-22Q-1, Olympus) or snarenet (Roth snarenet, U.S.E.) from the bile duct. The stone specimen was pulverized into a homogenous powder, mixed with KBr and ground into fine particles. The mixed powder was pressed with a hydraulic pressure of 400 psi for 1 min to form a disc. Sample disc was analyzed with IR spectrometer. The stones were classified as cholesterol or bilirubinate stone according to the predominant composition. The characteristic band features and key band locations were in accordance with those reported in the literature^[9,19]. Bilirubinate stones had characteristic IR absorption bands at 970, 1 186, 1 250, 1 568, 1 627, and 1 650/cm with a key band at 1 250/cm; cholesterol stones had characteristic IR absorption bands at 728, 836, 952, 1 050, 1 375, 1 470, and 2 950/cm with key bands at 1 050 and 1 470/cm.

This protocol was approved by the Department of Medical Research and Education of Kaohsiung Veterans General Hospital. The values are expressed as mean±SD. Categorical variables were analyzed with χ^2 -test or Fisher's exact test and continuous variables were analyzed by Student's *t*-test. A *P* value <0.05 was regarded as significant.

RESULTS

Among the 735 patients with CBD stones and receiving successful ES, there were no significant differences in age, sex, presence of JPD, or cholecystectomy between the patients whose stones were collected for analysis or not (Table 1). In the group of patients with stone collection, their CBD diameter and stone size were larger.

Table 1 Patients' characteristics between stone collected and uncollected groups

	Collected (n = 266)	Uncollected (n = 469)	<i>P</i>
Age (yr)	64±14	65±14	0.454
Sex (M/F)	156/110	297/172	0.210
JPD ¹ (%)	105 (39) ²	158 (34)	0.116
Cholecystectomy (%)	65 (24) ²	108 (23)	0.665
CBD size (cm)	1.7±0.6	1.5±0.6	<0.001
CBD stone size (cm)	1.2±0.6	0.6±0.7	<0.001

¹JPD: Juxtaepapillary diverticulum; CBD: common bile duct. ²Number of cases; the number inside the parenthesis shows the percentage.

In the 266 stone samples, 217 (82%) were bilirubinate stones, 42 (16%) were cholesterol stones, 3 were calcium carbonate stones, 4 were mixed cholesterol and bilirubinate

stones. Patients with bilirubinate stones were significantly older than patients with cholesterol stones (66±13 years *vs* 56±17 years, *P* = 0.001). There were no significant differences in sex, CBD diameter, size or number of CBD stones, presence of JPD, GB status, or presence of gallstones between patients with bilirubinate or cholesterol stones (Table 2).

Table 2 Patients' characteristics and initial stone compositions

	Bilirubinate (n = 217)	Cholesterol (n = 42)	<i>P</i>
Age (yr)	66±13	56±17	0.001
Sex (M/F)	130/87	22/20	0.365
CBD diameter (cm)	1.7±0.5	1.6±0.6	0.119
Stone size (cm)	1.2±0.6	1.2±0.7	0.410
Stone number (S/M)	111/106	16/26	0.121
JPD			0.084
Present	93 (43) ¹	12 (29)	
Absent	124 (57) ¹	30 (71)	
GB status			0.323
Cholecystectomy	57 (26) ¹	8 (19)	
Intact GB	160 (74)	34 (81)	
With stone	111 (51)	20 (48)	

Seven patients were excluded (three were calcium carbonate stones, four were mixed cholesterol and bilirubinate stones). CBD: Common bile duct; S/M: single/multiple; JPD: juxtaepapillary diverticulum; GB: gallbladder. ¹Number of cases; the number inside the parenthesis shows the percentage.

A total 75 patients had recurrent CBD stones and received another endoscopic treatment. Stone specimens were collected from 44 patients for stone analysis. In the 44 recurrent stone samples, 38 (86%) were bilirubinate stones, 3 (7%) were cholesterol stones, and 3 were mixed cholesterol and bilirubinate stones. Among the three patients with recurrent cholesterol stones, two patients had intact GBs with stones and one had received a cholecystectomy 6 mo prior to recurrence. There were no significant differences in age, sex, CBD diameter, size or number of CBD stones, GB status, or presence of gallstones between patients with recurrent bilirubinate or cholesterol stones (Table 3).

Table 3 Patients' characteristics and compositions of recurrent CBD stones

	Bilirubinate (n = 38)	Cholesterol (n = 3)	<i>P</i>
Age (yr)	66±10	65±6	0.836
Sex (M/F)	21/17	3/0	0.254
CBD diameter (cm)	1.9±0.6	1.4±0.2	0.159
Stone number (S/M)	16/22	1/2	1.000
Stone size (cm)	1.4±0.8	0.8±0.4	0.096
JPD			0.543
Present	13 (34) ¹	2 (67)	
Absent	25 (66)	1 (33)	
GB status			1.000
Cholecystectomy	18 (47) ¹	1 (33)	
Intact GB	20 (53)	2 (67)	
With stone	15 (39)	2 (67)	

Three patients with mixed cholesterol and bilirubinate stones were excluded. CBD: Common bile duct; S/M: single/multiple; JPD: juxtaepapillary diverticulum; GB: gallbladder. ¹Number of cases; the number inside the parenthesis shows the percentage.

In 27 patients, both initial and recurrent stone specimens can be obtained and sent for analysis, 23 patients had bilirubinate stones at initial treatment, 21 of them still had bilirubinate stones and 2 patients had cholesterol stones after recurrence. Both the patients with recurrent cholesterol stones also had GB stones. Four patients had cholesterol stones in the initial attack, three of them had bilirubinate stones, one patient still had cholesterol stones with recurrence and this patient had received cholecystectomy 6 mo prior to recurrence (Table 4).

Table 4 Change of stone compositions between initial and recurrent stone

Recurrent	Initial	
	Bilirubinate (n = 23)	Cholesterol (n = 4)
Bilirubinate (n = 24)	21	3
Cholesterol (n = 3)	2	1

Among the initial 266 stone samples, colors of stones were recorded. In the 217 patients with bilirubinate stones, 55 were yellowish, 93 were blackish, 64 were brownish and 5 were greenish. In the 42 patients with cholesterol stones, 15 were yellowish, 12 were blackish, 15 were brownish. In patients with mixed bilirubinate and cholesterol stones, two were yellowish and two were blackish. In patients with calcium carbonate stones, two were yellowish and one was blackish (Table 5).

Table 5 Compositions and color of stones

	Bilirubinate stone (n = 217)	Cholesterol stone (n = 42)	Mixed bilirubinate and cholesterol stone (n = 4)	Calcium carbonate stone (n = 3)
Yellow	55	15	2	2
Black	93	12	2	1
Brown	64	15	0	0
Green	5	0	0	0

DISCUSSION

We found that 82% of our patients had bilirubinate stones in the first attack, so the mechanism of CBD stone formation is different from the Western countries, but it is similar to some Asian studies^[9,20,21]. After ablation of sphincter of Oddi by ES, bactobilia may happen from direct extension of duodenal organisms into the CBD and β -glucuronidase released by the bacteria can promote the formation of bilirubinate stones^[17,18,22-24]. This explains why bilirubinate stone is the predominant composition of recurrent CBD stones (86%) after ES. Unlike the cholesterol stones, bilirubinate stones are often soft and easily broken^[16], so complete clearance of bilirubinate stones even after ES may be inadequate; some radiologically undetectable small fragments of bilirubinate stones may be left in the CBD; in addition to impaired biliary emptying, it may lead to bilirubinate stone formation at a later time.

Among the initial 42 patients with cholesterol stones, 8

patients received cholecystectomy at least 3 mo (median: 60 mo, range: 3-120 mo) before ES and 14 patients had intact GB but no GB stones. Besides spontaneous pass-out of stones, *de novo* formation of cholesterol stones from CBD may also be possible in these patients^[14,16].

In previous reports, JPD may facilitate primary CBD stone, but not GB stones formation^[16,25]. In our study, patients with initial bilirubinate stones had higher incidence of JPD than patients with initial cholesterol stones (43% *vs* 29%), but the difference did not reach statistical significance ($P = 0.084$).

In the 23 patients with initial bilirubinate stones, 21 had bilirubinate stones at recurrence, 2 had cholesterol stones when recurrence and these 2 patients also had GB stones at the time of recurrence, so stone pass-out from the GB may possibly explain the cholesterol composition of their CBD stones. In the four patients with initial cholesterol stones, three patients had bilirubinate stones and one had cholesterol stones at recurrence. The patient, who had recurrent cholesterol stones, had received cholecystectomy 6 mo before. It is difficult to determine whether the cholesterol stone is formed in the bile duct or GB. Our results indicated that different mechanism of CBD stone formation might occur in the same patient after ablation of sphincter leading to the formation of a different composition of stones.

In this study, we found that patients with bilirubinate stones are older than patients with cholesterol stones. Similar data have been found in Western patients with cholesterol *vs* pigment GB stones^[26]. It is well known that the duodenum is usually sterile in young healthy patients, but immunological and motor function of the alimentary tract may deteriorate gradually with age^[27]. The bacterial colonization of the CBD is an age-dependent phenomenon^[23] and this may explain the higher incidence of bilirubinate stones in older patients.

Cholesterol stones were usually yellowish or brownish^[15,28], but 12 out of 42 (29%) cholesterol stones in our patients were black in color, whereas 93 out of 217 (43%) bilirubinate stones were black in color. The nature of CBD stones cannot be completely determined by gross appearance alone^[28,29] and the IR spectroscopy is an important tool to determine the exact composition of stones.

For most patients, endoscopic retrieval of stones for analysis is more difficult than surgical procedure. In our study, only 266 out of 735 patients had received the analysis of stones. It could be speculated that different stone composition may influence the collection of stone for analysis during extraction procedure. Cholesterol stones are often smoother and harder while bilirubinate stones, on the other hand, are softer and tend to be broken down into small fragments when retrieved by basket or even a snarenet. This infers that the real percentage of bilirubinate stones in our patients may be actually higher. However, our analysis does not show significant difference in age, sex, presence of JPD, or cholecystectomy between patients whose stones were collected for analysis or not. Even though the CBD diameter and stone size are larger in the patients with stone analysis, there is no difference in CBD size or stone size between bilirubinate or cholesterol stones. We believe that little selection bias has taken place in our patients, despite only about 36% of patients' stones were collected for analysis.

In conclusion, bilirubinate stones are the predominant composition of initial and recurrent CBD stone after ES in Chinese patients. Patients with bilirubinate stones are older than those with cholesterol stones. The composition of stones may change after ES.

ACKNOWLEDGMENTS

The authors thank Mr. E-Ming Wang, Miss. Min-Ching Wei, and Ming-Ti Fu for their assistance in follow-up visits and data management and Dr. Ying-Huei Lee for stone analysis.

REFERENCES

- 1 **Bates T**, Harrison M, Lawson C, Padley N. Longitudinal study of gall stone prevalence at necropsy. *Gut* 1992; **33**: 103-107
- 2 **Heaton KW**, Braddon FEM, Mountford RA, Hughes AO, Emmett PM. Symptomatic and silent gall stones in the community. *Gut* 1991; **32**: 316-320
- 3 **Su CH**, Lui WY, P'eng FK. Relative prevalence of gallstone diseases in Taiwan: A nationwide cooperative study. *Dig Dis Sci* 1992; **37**: 764-768
- 4 **Lai KH**, Peng NJ, Lo GH, Cheng JS, Huang RL, Lin CK, Huang JS, Chiang HT, Ger LP. Prediction of recurrent choledocholithiasis by quantitative chlescintigraphy in patients after endoscopic sphincterotomy. *Gut* 1997; **41**: 399-403
- 5 **Hawes RH**, Cotton PB, Vallon AG. Follow-up 6-11 years after duodenoscopic sphincterotomy for stones in patients with prior cholecystectomy. *Gastroenterology* 1990; **98**: 1008-1012
- 6 **Seifert E**. Long-term follow-up after endoscopic sphincterotomy (EST). *Endoscopy* 1988; **20**: 232-235
- 7 **Lai KH**, Lo GH, Lin CK, Hsu PI, Chan HH, Cheng JS, Wang EM. Do patients with recurrent choledocholithiasis after endoscopic sphincterotomy benefit from regular follow-up. *Gastrointest Endosc* 2002; **55**: 523-526
- 8 **Carey MC**. Pathogenesis of gallstones. *Am J Surg* 1993; **165**: 410-419
- 9 **Huang SM**, Su CH, Wu LH, Chang TJ, Wu CW, Lee CH, Lui WY. Polarising microscopy versus infrared absorption spectroscopy in gallstone analysis- a preliminary report. *Asian J Surg* 1989; **12**: 172-177
- 10 **Cahalane MJ**, Neubrand MW, Carey MC. Physical-chemical pathogenesis of pigment gallstones. *Semin Liver Dis* 1988; **8**: 317-328
- 11 **Crowther RS**, Soloway RD. Pigment gallstone pathogenesis: from man to molecules. *Semin Liver Dis* 1990; **10**: 171-180
- 12 **Trotman BW**. Pigments gallstone disease. *Gastroenterol Clin N Am* 1991; **20**: 111-126
- 13 **Leuschner U**, Guldutuna S, Hellstern A. Pathogenesis of pigment stones and medical treatment. *J Gastroenterol Hepatol* 1994; **9**: 87-98
- 14 **Malet PF**, Dabezies MA, Huang G, Long WB, Gadacz TR, Soloway RD. Quantitative infrared spectroscopy of common bile duct gallstones. *Gastroenterology* 1988; **94**: 1217-1221
- 15 **Bernhoft RA**, Pellegrini CA, Motson RW, Way LW. Composition and morphologic and clinical features of common duct stones. *Am J Surg* 1984; **148**: 77-85
- 16 **Sandstd O**, Osnes T, Skar V, Urdal P, Osnes M. Common bile duct stones are mainly brown and associated with duodenal diverticula. *Gut* 1994; **35**: 1464-1467
- 17 **Gregg JA**, Girolami PD, Carr-Locke DL. Effects of sphincteroplasty and endoscopic sphincterotomy on the bacteriologic characteristics of the common bile duct. *Am J Surg* 1985; **149**: 668-671
- 18 **Skar V**, Skar AG, Midtvedt T, Osnes M. Bacterial growth in the duodenum and in the bile of patients with gallstone disease treated with endoscopic papillotomy (EPT). *Endoscopy* 1986; **18**: 10-13
- 19 **Lee YH**, Chen MT, Huang JK, Chang LS. Analysis of urinary calculi by infrared spectroscopy. *Chin Med J* 1990; **45**: 157-165
- 20 **Tanaka M**, Takahata S, Konomi H, Matsunaga H, Yokohata K, Takeda T, Utsunomiya N, Ikeda S. Long-term consequence of endoscopic sphincterotomy for bile duct stones. *Gastrointest Endosc* 1998; **48**: 465-469
- 21 **Kim DI**, Kim MH, Lee SK, Seo DW, Chol WB, Lee SS, Park SJ, Joo YH, Yoo KS, Kim HJ. Risk factors for recurrence of primary bile duct stones after endoscopic biliary sphincterotomy. *Gastrointest Endosc* 2001; **54**: 42-48
- 22 **Cetta F**. Do surgical and endoscopic sphincterotomy prevent or facilitate recurrent common duct stone formation? *Arch Surg* 1993; **128**: 329-336
- 23 **Cetta F**. The possible role of sphincteroplasty and surgical sphincterotomy in the pathogenesis of recurrent common duct brown stones. *HPB Surg* 1991; **4**: 261-270
- 24 **Ho KJ**, Lin XZ, Yu SC, Chen JS, Wu CZ. Cholelithiasis in Taiwan: Gallstone characteristics, surgical incidence, bile lipid composition and role of B-glucuronidase. *Dig Dis Sci* 1995; **40**: 1963-1973
- 25 **Lotveit T**. The composition of biliary calculi in patients with juxtapapillary duodenal diverticula. *Scand J Gastroenterol* 1982; **17**: 653-656
- 26 **Trotman BW**, Ostrow JD, Soloway RD. Pigment vs cholesterol cholelithiasis: comparison of stone and bile composition. *Am J Dig Dis* 1974; **19**: 585-590
- 27 **Cetta F**. The route of infection in patients with bactibilia. *World J Surg* 1983; **7**: 562
- 28 **Wei TC**. Quantitative determination of chemical composition of gallstones by infrared absorption spectrophotometry. *J Formos Med Assoc* 1982; **81**: 145-157
- 29 **Chen YJ**, Liu MH, Chen PH, Lo HW, Wang CS, Yuan J, Wen KL. Composition analysis of gallstones by fourier transformed infrared spectroscopy. *Chin J Gastroenterol* 1992; **9**: 1-8

• BRIEF REPORTS •

Clinical evaluation of serum concentrations of intercellular adhesion molecule-1 in patients with colorectal cancer

Xu Kang, Fang Wang, Jin-Dong Xie, Jun Cao, Pei-Zhong Xian

Xu Kang, Jin-Dong Xie, Pei-Zhong Xian, Department of Gastro-intestinal Surgery, Affiliated Hospital, Guangdong Medical College, Zhanjiang 524001, Guangdong Province, China

Fang Wang, South China Sea Institute of Oceanology, Chinese Academy of Sciences, Guangzhou 510301, Guangdong Province, China

Jun Cao, Department of Pathology, Affiliated Hospital, Guangdong Medical College, Zhanjiang 524001, Guangdong Province, China

Supported by the Youth Science Foundation of Guangdong Medical College, No. 2002110

Co-first-author: Fang Wang

Correspondence to: Dr. Xu Kang, Department of Gastro-intestinal Surgery, Affiliated Hospital, Guangdong Medical College, Zhanjiang 524001, Guangdong Province, China. kangxuwf@163.com

Telephone: +86-759-2387416 Fax: +86-759-2231754

Received: 2004-12-25 Accepted: 2005-01-12

Abstract

AIM: To investigate the correlation between the serum soluble intercellular adhesion molecule-1 (sICAM-1) and the clinicopathologic features and to evaluate the possible prognostic significance of sICAM-1 concentration in colorectal cancer.

METHODS: A total of 56 patients (mean age 57.3 years) having transitional cell carcinoma of the colorectal and 25 control patients (mean age 42.6 years) were enrolled in the study. The serum samples of the patients were obtained on the day before surgery. Sera were obtained by centrifugation, and stored at -80 °C until assay. Serum concentrations of ICAM-1 were measured with enzyme-linked immunoassay. Differences between the two groups were analyzed by Student's *t*-test.

RESULTS: No significant increase of serum sICAM-1 could be demonstrated in the Dukes A₁ patients (352.63±61.82 µg/L) compared to the control group (345.72±49.81 µg/L, *P*>0.05), Dukes A₁ patients (352.63±61.82 µg/L) compared to Dukes A_{2,3} patients (491.17±86.36 µg/L, *P*<0.05). Furthermore, the patients with Dukes B had significantly higher serum concentrations of sICAM-1 than those of the control group (496.82±93.04 µg/L vs 345.72±49.81 µg/L, *P*<0.01). Compared with Dukes A_{2,3}, B colorectal cancer patients, patients with more advanced clinical stage (Dukes C and D) had higher levels of sICAM-1 (743.68±113.74 µg/L vs 491.17±86.36 µg/L and 496.82±93.04 µg/L, *P*<0.001). The difference was statistically significant in sICAM-1 levels between patients with positive lymph node status and those without lymph node involvement (756.25±125.57 µg/L vs 445.62±69.18 µg/L, *P*<0.001). Patients with poorly differentiated colorectal cancer had

a higher level of sICAM-1 than those with differentiated and highly differentiated cancer (736.49±121.97 µg/L vs 410.23±67.47 µg/L, *P*<0.001).

CONCLUSION: In this study, serum ICAM-1 levels were found to be related to tumor presence, clinical stages, and grade. Increased ICAM-1 in patients with colorectal cancer which should be considered when the diagnostic and/or prognostic usefulness of soluble ICAM-1 is to be evaluated. sICAM-1 should prove useful for monitoring malignant disease stage and for evaluating the effectiveness of various therapeutic approaches for colorectal carcinomas.

© 2005 The WJG Press and Elsevier Inc. All rights reserved.

Key words: sICAM-1; Colorectal cancer; Tumor metastasis; Clinicopathological factors

Kang X, Wang F, Xie JD, Cao J, Xian PZ. Clinical evaluation of serum concentrations of intercellular adhesion molecule-1 in patients with colorectal cancer. *World J Gastroenterol* 2005; 11(27): 4250-4253

<http://www.wjgnet.com/1007-9327/11/4250.asp>

INTRODUCTION

Colorectal cancer is the third most common malignant neoplasm worldwide^[1] and has a higher incidence rate in Guangdong, Shanghai, Jiangsu, and Zhejiang Province. Moreover, with the development of economy, diets are high in total fat, protein, calories, alcohol, and meat (both red and white) and low in calcium and folate, which incline to increased incidence of colorectal cancer. The prevalence of colorectal cancer increased gradually in recent years. Efforts to identify causes and to develop effective preventive measures have led scientists pay much attention to it.

Intercellular adhesion molecule-1 (ICAM-1) is a monomeric, transmembrane molecule of the immunoglobulin superfamily with a molecular weight of 95-110 ku. Two ligands, the lymphocyte function-associated antigen-1 and the membrane adhesion complex-1, mediate adhesion and transvascular migration^[2]. This protein mediates adhesion and transmigration of leukocytes through the endothelium. Surface expressed ICAM-1 is apparently shed from the cells and then circulates as soluble ICAM-1 (sICAM-1). Although the source of sICAM-1 has not been fully elucidated, it can be released by cancer cells and also by mononuclear blood, endothelial, and fibroblastic cells^[3]. It has been reported that

the upregulated expression of ICAM-1 on cell surfaces occurred in a variety of diseases, including autoimmune diseases, endocrine diseases, and some cancers^[4,5]. A soluble form of ICAM-1 (sICAM-1) lacking cytoplasmic tail and transmembrane region has also been found^[5]. sICAM-1 can compete with membranous ICAM-1 to bind LFA-1, so that it can block leukocyte LFA-1 and prevent effective recognition and lysis of target cells by effector leukocyte. This phenomenon represents an important mechanism for tumor escape from immune surveillance^[6,7]. Shedding of ICAM-1 by circulating tumor cells may allow their escape from surveillance by cytotoxic T cell and natural killer cells and thus promote metastasis^[8]. In our research, we have found that some anticancer gene and proto-oncogene have different expression in colorectal cancer^[9,10]. In this study, we investigate the clinical significance of serum adhesion molecule levels at the time of diagnosis in patients with colorectal carcinoma and to evaluate the usefulness of these assays in terms of prognosis and survival.

MATERIALS AND METHODS

Patients and specimens

Serum samples were taken from 56 patients (32 men, 24 women, average age 57.3 years) with colorectal cancer admitted to the Affiliated Hospital of Guangdong Medical College from 2001 to 2002. In all patients the diagnosis was proven by histology. Staging was performed according to the criteria of Dukes system (Table 1). The reference group consisted of 25 others with non-malignant diseases (9 women and 16 men, average age 42.6 years). Blood samples were obtained from patients before the initial treatment. All blood samples were processed immediately for centrifugation. All sera were stored at -80 °C until assayed and determined not taking clinical information into account.

Table 1 Colorectal cancer patients and disease characteristics

Stage	n	%
Dukes A ₁	3	5.36
Dukes A _{2,3}	6	10.71
Dukes B	21	37.50
Dukes C and D	26	46.43
Histologic differentiation		
Highly	22	39.29
Moderate	24	42.86
Poorly	10	17.85
Localization		
Right colon	17	30.36
Left colon	21	37.50
Rectum	18	32.14

Measurement of sICAM-1

The serum levels of soluble receptors were determined quantitatively by specific enzyme-linked immunosorbent assay (ELISA). The serum samples were diluted 10 times according to the manufacturer's instructions (R&D Systems), and as described previously^[11]. Soluble receptor concentrations were calculated from standard curves generated by standard dilutions of known concentrations. The mean intra-assay CV, determined by assaying the sICAM-1 concentration in three serum samples in replicates of 10, is reported to be

4.4%. The mean inter-assay CV, determined by assaying three serum samples in duplicate in 18 separate assays by four operators, has been determined to be 7.4%. The cut-off values were calculated as the mean±SD were 860 ng/mL for sICAM-1. The reported sensitivity of the ELISA is less than 0.35 ng/mL.

Statistical analysis

The Student's *t*-test was used for statistical significance of differences between groups. *P*<0.05 was considered to be significant.

RESULTS

We studied the correlation between the sICAM-1 levels and clinicopathological factors, Table 1 shows the relationships between the concentration of sICAM-1 antigen in the sera and various clinicopathologic features of the patients. No significant increase of serum sICAM-1 could be demonstrated in the Dukes A₁ patients (352.63±61.82 µg/L) compared to a control group (345.72±49.81 µg/L, *P*>0.05). There is a significant statistic difference when Dukes A₁ patients (352.63±61.82 µg/L) compared to Dukes A_{2,3} patients (491.17±86.36 µg/L, *P*<0.05). Furthermore, serum sICAM-1 levels were significantly higher in patients with Dukes B when compared to the control group (496.82±93.04 µg/L *vs* 345.72±49.81 µg/L, *P*<0.01). Among patient groups, while there was no significant difference between Dukes A_{2,3} and Dukes B, a significant difference was found between Dukes B and Dukes C and D. Compared with Dukes A_{2,3}, B colorectal cancer patients, the patients with more advanced clinical stage Dukes C and D, had higher levels of sICAM-1 (743.68±113.74 µg/L *vs* 491.17±86.36 µg/L and 496.82±93.04 µg/L, *P*<0.001). Difference was statistically significant in sICAM-1 levels between patients with positive lymph node status and those without lymph node involvement (756.25±125.57 µg/L *vs* 445.62±69.18 µg/L, *P*<0.001). Poor differentiation was observed to have a higher level of sICAM-1 than moderated and highly differentiated patients *P*<0.001. The positive rates of each group were calculated with mean±SD of normal control sICAM-1 as a limit. The results are shown in Table 2.

Table 2 Correlation between soluble ICAM-1 concentrations and clinicopathologic factors in colorectal cancer

Factors	n	ICAM-1 (mean±SD, µg/L)	χ ²	P
Clinical staging				
Dukes A ₁	3	352.63±61.82 ^a		
Dukes A _{2,3}	6	491.17±86.36	2.88	<0.05
Dukes B	21	496.82±93.04 ^d	0.18	>0.05
Dukes C and D	26	743.68±113.74	12.38	<0.001
Grade of differentiation				
Highly differentiated	22	410.23±67.47 ^b		
Differentiated	24	486.53±103.64 ^d	4.08	<0.01
Poorly differentiated	10	736.49±121.967	10.48	<0.001
Metastasis				
Liver	3	769.19±127.32		
Lymph node positive	23	756.25±125.57 ^d	0.32	>0.05
Lymph node negative	30	445.62±69.18	16.98	<0.001

^a*P*<0.05, Dukes A₁ *vs* Dukes A_{2,3}; ^b*P*<0.01, highly differentiated *vs* differentiated;

^d*P*<0.001, Dukes B *vs* Dukes C and D; Differentiated *vs* poorly differentiated; lymph node positive *vs* lymph node negative.

DISCUSSION

Soluble forms of cell adhesion molecules have been identified in the circulation and may be monitored as markers of inflammation and endothelial dysfunction^[4]. Neoplastic transformation and the evolution to metastatic disease are characterized by a dramatic aberration in cellular cohesive interactions. The adhesion molecules have also been shown to facilitate tumor cell motility, adhesion of tumor cells to endothelium, neovascularization at the metastatic sites, and host inflammatory response to cancer. Evaluation of sICAM-1 has shown important clinical implications in many types of cancer. In particular, the measurement of serum concentrations of ICAM-1 might provide important prognostic values independent of conventional pathologic factors in cancer patients^[12-14].

In the present study of colorectal cancer, revealed that serum sICAM-1 levels were elevated in patients with colorectal cancer. These parameters were elevated in both local and metastatic disease and significant correlations between the parameters and stage of disease were seen. The data of the present study are in agreement with those previously reported which described an increase in the sICAM-1 content of serum in colorectal carcinoma^[15,16]. We have also demonstrated that concentrations of sICAM-1 are increased in colorectal cancer, particularly in patients with distant metastasis. Our study also showed that sICAM-1 levels were correlated with both clinical staging and lymph node during liver metastasis involvement. Basoglu^[17] reported that the concentrations of sICAM-1 and TSA were significantly higher in patients with Dukes C and D, and they presume that sICAM-1 and TSA are the best of the tested markers. These markers should prove useful for monitoring malignant disease stage and for evaluating the effectiveness of various therapeutic approaches for colorectal carcinomas. In contrast to our study, it was demonstrated that the expression of sICAM-1 was inversely correlated with lymph node metastasis^[18].

With regard to prognosis, Liu reported in gastric cancer that serum sICAM-1 concentration may be a valuable parameter for predicting the prognosis and degree of the gastric cancer. Liu^[19] measured the circulating ICAM-1 in the sera of nasopharyngeal, oral, and laryngeal cancer cases and indicated that the circulating ICAM-1 was not elevated in the sera of oral and laryngeal cancer patients, but increased in nasopharyngeal cancer patients. They speculated that the discrepancy in the level of ICAM-1 among these three groups of patients with head and neck carcinoma might be attributed to either the different immunological reaction profiles or a cell-specific response. The cellular source and the mechanisms for releasing the soluble components of these endothelial adhesion molecules, although not well known, could involve either shedding or enzymatic cleavage from endothelial cells, leukocyte surfaces or tumor cells^[20]. Some mechanisms have been proposed concerning the elevation of sICAM-1 in serum, such as enzymatic cleavage of cell surface adhesion molecules or secretion of alternatively spliced forms lacking the transmembrane domain. Additionally, that sICAM-1 has been described on malignant epithelial tissue may be the source of at least some of the sICAM-1 present in sera of cancer patients^[21]. It is widely accepted

that histological stage is a powerful prognostic factor in colorectal cancer. In this study, it was revealed that ICAM-1 status has prognostic value coincide with histological stage. Therefore, these results suggested that it may be possible to add ICAM-1 status to conventional clinicopathological factors to predict recurrence.

In conclusion, our study demonstrates that ICAM-1 expression may be a useful indicator of prognosis in patients with colorectal cancer. Patients with lymph node, liver invasion, and advanced clinical stage of tumors had significantly higher serum concentrations of sICAM-1. Invasion status and clinical stage are significant prognostic indicators. Though serum level of sICAM-1 cannot be served as a specific parameter for colorectal cancer, it is no doubt that the measurement of the ICAM-1 level may provide a convenient means to obtain a general indication of colorectal cancer. Therefore, sICAM-1 may be a valuable predictor for colorectal cancer clinically.

REFERENCES

- 1 Shike M, Winawer SJ, Greenwald PH, Bloch A, Hill MJ, Swaroop SV. Primary prevention of colorectal cancer: the WHO collaborating centre for the prevention of colorectal cancer. *Bull World Health Organ* 1990; **68**: 377-385
- 2 Wollenberg B, Jan N, Sutier W, Hofmann K, Schmitt UM, Stieber P. Serum levels of intercellular adhesion molecule-1 squamous cell carcinoma of the head and neck. *Tumour Biol* 1997; **18**: 88-94
- 3 Nakata B, Hori T, Sunami T, Ogawa Y, Yashiro M, Maeda K, Sawada T, Kato Y, Ishikawa T, Hirakawa K. Clinical significance of serum soluble intercellular adhesion molecule 1 in gastric cancer. *Clin Cancer Res* 2000; **6**: 1175-1179
- 4 Springer TA. Adhesion receptors of the immune system. *Nature* 1990; **346**: 425-434
- 5 Rothlein R, Mainolfi EA, Czajkowski M, Marlin SD. A form of circulating ICAM-1 in human serum. *J Immunol* 1991; **147**: 3788-3793
- 6 Becker JC, Dummer R, Hartmann AA, Burg G, Schmidt RE. Shedding of ICAM-1 from human melanoma cell lines induced by IFN- γ and tumor necrosis factor- α : functional consequences on cell-mediated cytotoxicity. *J Immunol* 1991; **147**: 4398-4401
- 7 Becker JC, Christian T, Schmidt RE, Brocker EB. Soluble intercellular adhesion molecule-1 inhibits MHC-restricted specific T cell/tumor interaction. *J Immunol* 1993; **151**: 7224-7232
- 8 Banks RE, Gearing AJH, Hemingway IK, Norfolk DR, Perren TJ, Selby PJ. Circulating intercellular adhesion molecule-1 (ICAM-1), E-selectin and vascular cell adhesion molecule-1 (vcam-1) in human malignancies. *Br J Cancer* 1993; **68**: 122-124
- 9 Kang X, Xie PZ, Cao J. Relationship between expression p53 protein, c-erbB2, PCNA, and bcl-2 in colorectal cancer and clinical pathological features. *Hainan Med J* 2004; **15**: 14-16
- 10 Kang X, Xie PZ, Xu FP. Study of p16/MTS1 gene inactivation in Colorectal Carcinoma. *Chinese New Med* 2004; **5**: 1345-1346
- 11 Koundouros E, Odell E, Coward PY, Wilson RF, Palmer RM. Soluble adhesion molecules in serum of smokers and nonsmokers, with and without periodontitis. *J Periodontal Res* 1996; **31**: 596-599
- 12 Benekli M, Gullu IH, Tekuzman G, Savas MC, Hayran M, Hascelik G, Firat D. Circulating intercellular adhesion molecule-1 and E-selectin levels in gastric cancer. *Br J Cancer* 1998; **78**: 267-271
- 13 Dwivedi C, Dixit M, Hardy RE. Plasma lipid-bound sialic acid alterations in neoplastic diseases. *Experientia* 1990; **46**: 91-97
- 14 Tsujisaki M, Imai K, Hirata H, Hanzawa Y, Masuya J, Nakano T, Sugiyama T, Matsui M, Hinoda Y, Yachi A. Detection of

- circulating intercellular adhesion molecule-1 antigen in malignant diseases. *Clin Exp Immunol* 1991; **85**: 3-8
- 15 **Velikova G**, Banks RE, Gearing A, Hemingway I, Forbes MA, Preston SR, Hall NR, Jones M, Wyatt J, Miller K, Ward U, Al-Maskatti J, Singh SM, Finan PJ, Ambrose NS, Primrose JN, Selby PJ. Serum concentrations of soluble adhesion molecules in patients with colorectal cancer. *Br J Cancer* 1998; **77**: 1857-1863
- 16 **Reinhardt KM**, Steiner M, Zillig D, Nagel HR, Blann AD, Brinckmann W. Soluble intercellular adhesion molecule-1 in colorectal cancer and its relationship to acute phase proteins. *Neoplasma* 1996; **43**: 65-67
- 17 **Basoglu M**, Yildirgan MI, Taysi S, Yilmaz I, Kiziltunc A, Balik AA, Celebi F, Atamanalp SS. Levels of soluble intercellular adhesion molecule-1 and total sialic acid in serum of patients with colorectal cancer. *J Surg Oncol* 2003; **83**: 180-184
- 18 **Maeda K**, Kang SM, Sawada T, Nishiguchi Y, Yashiro M, Ogawa Y, Ohira M, Ishikawa T, Hirakawa YS, Chung K. Expression of intercellular adhesion molecule-1 and prognosis in colorectal cancer. *Oncol Rep* 2002; **9**: 511-516
- 19 **Liu CM**, Sheen TS, Ko JY, Shun CT. Circulating intercellular adhesion molecule-1 (ICAM-1), E-selectin and vascular cell adhesion molecule-1 (VCAM-1) in head and neck cancer. *Br J Cancer* 1999; **79**: 360-362
- 20 **Ferdeghini M**, Gadducci A, Prontera C, Annicchiarico C, Galletti O, Bianchi M, Facchini V, Genazzani AR. Preoperative serum intercellular adhesion molecule-1 (ICAM-1) and E-selectin (Endothelial cell leukocyte adhesion molecule, ELAM-1) in patients with epithelial ovarian cancer. *Anticancer Res* 1995; **15**: 2255-2260
- 21 **Ros-Bullon MR**, Sanchez-Pedreno P, Martinez-Liarte JH. Serum sialic acid in malignant melanoma patients: an ROC curve analysis. *Anticancer Res* 1999; **19**: 3619-3622

Science Editor Guo SY Language Editor Elsevier HK

• BRIEF REPORTS •

Immunization of mice with concentrated liquor from male zooid of *Antheraea pernyi*

Sheng Li, Bo Zhang, Wei-Dong Zhang, Ting-Hang Ma, Yong Huang, Long-Hai Yi, Jin-Ming Yu

Sheng Li, Bo Zhang, Ting-Hang Ma, Yong Huang, Long-Hai Yi, Jin-Ming Yu, Shandong Tumor Hospital, Jinan 250117, Shandong Province, China
Wei-Dong Zhang, Basic Medical Institute of Shandong Academy of Medical Sciences, Jinan 250062, Shandong Province, China
Supported by the National Natural Science Foundation of China, No. 30472260
Co-correspondence: Jin-Ming Yu
Correspondence to: Sheng Li, Shandong Tumor Hospital, Jinan 250117, Shandong Province, China. drlisheng@sohu.com
Fax: +86-531-8550649
Received: 2004-11-02 Accepted: 2004-12-21

Abstract

AIM: To study the effects of concentrated liquor from male zooid of *Antheraea pernyi* on immunological mice.

METHODS: For each experiment, 40 mice were randomly divided into normal saline group (control group) and three tested groups that were administered different dosages of concentrated liquor from male zooid of *A. pernyi* and food for 15 d. The typical FSR and HC_{50} value, monocyte-phagocytic exponent K and emendated monocyte-phagocytic exponent α were determined and calculated respectively.

RESULTS: After 24 and 48 h, the FSR values of the three tested groups improved significantly in comparison to the control group by variance analysis. The HC_{50} values showed a significant difference between the high dosage group and the control group, as well as between the high dosage group and other two tested groups. The monocyte-phagocytic exponent K and emendated exponent α showed rising tendencies, but no significant differences were found by variance analysis.

CONCLUSION: The concentrated liquor from male zooid of *A. pernyi* can significantly enhance cellular and humoral immune function in mice, but has no distinct influence on the monocyte-phagocytic system in mice.

© 2005 The WJG Press and Elsevier Inc. All rights reserved.

Key words: *Antheraea pernyi*; Male zooid; Concentrated liquor; Mice; Immune function

Li S, Zhang B, Zhang WD, Ma TH, Huang Y, Yi LH, Yu JM. Immunization of mice with concentrated liquor from male zooid of *Antheraea pernyi*. *World J Gastroenterol* 2005; 11 (27): 4254-4257
<http://www.wjgnet.com/1007-9327/11/4254.asp>

INTRODUCTION

The concentrated liquor from male zooid of *Antheraea pernyi* is a pure preparation of traditional Chinese medicine, which possesses many health-care functions. According to The Great Dictionary of Traditional Chinese Medicine, *A. pernyi* is the matured insect of silkworm. The major components of male zooid are proteins and more than 20 kinds of free amino acids, cytochrome $C^{[1]}$, with the actions of tonifying the liver and invigorating the kidney, strengthening Yang Qi and astringing essence^[2]. So male zooid is mainly employed to treat impotence, seminal emission, and stranguria with hematuria. This agent is made from unmated male zooid of *A. pernyi*. The effective components are extracted from its combined lixivium of edible level, then isolated, purified, and concentrated with advanced cryogenic techniques. The qualitative and quantitative analyses are tested by thin-layer chromatography. We undertook this animal experiment to study the effects of the concentrated liquor on cellular, humoral, and monocyte-phagocytic immune functions in mice.

MATERIALS AND METHODS

Experimental materials

Raw materials from male zooid of *A. pernyi* were provided by the Silkworm Research Institute of Shandong Agriculture Science Academy, purified and concentrated in our laboratory^[3].

The whole blood of Guinea pig was sampled and centrifuged. The concentrated RBCs of mice were added to 5 mL of extracted Guinea pig serum and stored at 4 °C for 30 min before use, then centrifuged at 1 500 r/min for 15 min. Preclusion of unspecific hemolysis caused by complement was eliminated by extraction of supernatant. The processed serum diluted in normal saline at 1:10 served as the experimental complement.

Effects of concentrated liquor from male zooid of *Antheraea pernyi* on cellular immune function of mice

Forty Kunming mice (6-8 wk) weighing 18-20 g were randomized into three tested groups (high-, medium-, and low-dosage group), and treated with 16.53, 2.62, and 0.564 mg/kg of concentrated liquor from male zooid of *A. pernyi* respectively. During the 15-d process of continuous oral filling, a dosage of 2% 0.2 mL (1×10^6 /mL) (V/V) SRBC was injected into the abdominal cavity of each mouse on the 10th d. Four days later, sizes of the left plantars of the immunized mice were measured with slide gaud, then another dosage of 20 μ L (1×10^6 /mL) 20 mol/L (V/V)

SRBC was injected subcutaneously at the measured site of each mouse. Twenty-four and forty-eight hours after injection, thickness of the left plantar of each treated mouse was measured respectively. Each site was measured thrice, and the average value was used to calculate the FSR. $\text{FSR} = \text{thickness of the left plantar before injection} - \text{thickness of the left plantar after injection (mm)}$.

Effects of concentrated liquor from male zooid of *Antheraea pernyi* on humoral immune function of mice

Kunming mice (6–8 wk) weighing 18–22 g were randomized into three testing groups and fed with concentrated liquor from male zooid of *A. pernyi* at the dosages of 16.53, 2.62, and 0.564 mg/kg, respectively. During the 15-d process of continuous oral filling, a dosage of 0.2 mL (1×10^6 /mL) 20 mol/L (V/V) SRBC was injected into the abdominal cavity of each mouse on the 10th d. Five days later, whole blood was sampled from each mouse by eye extraction, and then the serum was prepared. Hemolysis in serum was determined as follows: the prepared serum from each mouse was diluted at 1:50, 1 mL of the diluted serum was added into a 10-mL test tube, and then 0.5 and 1 mL complement of 10% SRBC was added into the tube. A control tube was added with normal saline instead of serum. After incubation at 37 °C for 30 min, the reaction was stopped in ice bath, centrifuged at 2 000 r/min for 10 min, the supernatant was extracted and 3 mL of Du's reagent was added. At the same time, 0.25 mL 10% SRBC was added into Du's reagent to a final volume of 4 mL and placed at room temperature. The optical densities of all preparations were tested by type-722 spectrophotometer in 1-cm color matching cups, the optical density of the control test tube was defined as zero value. The semi-hemolytic value (HC_{50}) was calculated as: $\text{HC}_{50} = \frac{\text{optical density value of each sample tube}}{\text{the optical density value of SRBC at semi-hemolysis} \times \text{dilution multiples}}$.

Effects of concentrated liquor from male zooid of *Antheraea pernyi* on monocyte-phagocytic function of mice

Kunming mice (6–8 wk) weighing 18–22 g were randomized into three tested groups and fed with concentrated liquor from male zooid of *A. pernyi* for 15 d at the same dosages as the above. After the last dosage was given, charcoal particle clearance test was performed. The detailed procedure was as follows: Each mouse was injected with diluted Chinese ink through its tail vein, 20 μL whole blood was sampled from the medial canthus of each mouse at the 2nd and 10th min respectively, distilled water was added to a final volume of 2 mL, and the A value at 600 nm was determined. Then, the mice were killed by dearticulation, the liver, and spleen were removed and weighed. The monocyte-phagocytic exponent K was calculated as $K = (\lg A_2 - \lg A_{10}) / (t_2 - t_1)$, and the emended monocyte-phagocytic exponent α as $\alpha = \text{body weight} / (\text{liver weight} + \text{spleen weight}) \times K^{1/3}$. The A_2 and A_{10} were the values at the 2nd and 10th min respectively, t_1 and t_2 represented the sampling time (both representing the ability of monocyte-phagocytic system to clear colloid charcoal particles in mice).

Statistical analysis

Variance analysis was performed with the statistical software

SPSS (version 10.0). The data were expressed as mean \pm SD, $P < 0.05$ was considered statistically significant.

RESULTS

Effects of concentrated liquor from male zooid of *Antheraea pernyi* on cellular immune function of mice

Twenty-four and forty-eight hours after immunization with SRBC, the FSR values of the three tested groups improved significantly compared to the control group by variance analysis (Table 1), indicating that the cellular immune function of mice could be improved obviously by concentrated liquor from male zooid of *A. pernyi*.

Table 1 Effects of concentrated liquor from male zooid of *A. pernyi* on cellular immune function of mice (mean \pm SD)

Group	Dosage (mg/kg)	Animal (n)	FSR (mm)	
			24 h	48 h
Control	dH ₂ O	10	0.66 \pm 0.25 ^b	0.20 \pm 0.16 ^d
Low-dosage	0.564	10	1.22 \pm 0.28	0.61 \pm 0.26
			<0.01	<0.01
Medium-dosage	2.62	10	1.24 \pm 0.23	0.61 \pm 0.19
			<0.01	<0.01
High-dosage	16.53	9	1.45 \pm 0.25	0.66 \pm 0.26
			<0.01	<0.01

^b $P < 0.01$, FSR (mm) of control group vs that of high-, medium- and low-dosage groups at 24 h respectively. ^d $P < 0.01$, FSR (mm) of control group vs that of high-, medium- and low-dosage groups at 48 h respectively.

Effects of concentrated liquor from male zooid of *Antheraea pernyi* on humoral immune function of mice

As shown in Table 2, the HC_{50} values representing the humoral immune function of mice showed a significant difference between the high dosage group and the control group by variance analysis ($F = 7.965$, $P < 0.01$). The same results were also observed between the high-dosage group and the other two tested groups ($P < 0.01$). The concentrated liquor from male zooid of *A. pernyi* had certain positive effect on the humoral immune function of mice.

Table 2 Effects of concentrated liquor from male zooid of *A. pernyi* on humoral immune function of mice (mean \pm SD)

Group	Dosage (mg/kg)	Animal (n)	HC_{50}
Control	dH ₂ O	7	42.2 \pm 18.2 ^b
Low-dosage	0.564	8	46.4 \pm 23.01 ^b
Medium-dosage	2.62	8	40.13 \pm 15.16 ^b
High-dosage	16.53	8	91.16 \pm 37.6
			<0.01 ^{b,d}

^b $P < 0.01$, high-dosage group vs control group. ^d $P < 0.01$, high-dosage group vs low- and medium-dosage groups respectively.

Effects of concentrated liquor from male zooid of *Antheraea pernyi* on monocyte-phagocytic function of mice

The monocyte-phagocytic exponent K and emended

Table 3 Effects of concentrated liquor from male zooid of *A. pernyi* on monocyte-phagocytic function of mice (mean±SD)

Group	Dosage (mg/kg)	Animal (n)	K	α
Control	dH ₂ O	10	0.0514±0.0122 ^a	6.249±0.772 ^c
Low-dosage	0.56	10	0.0527±0.0157 <i>P</i> >0.05	6.304±0.967 <i>P</i> >0.05
Medium-dosage	2.62	10	0.0517±0.0104 <i>P</i> >0.05	6.354±0.761 <i>P</i> >0.05
High-dosage	16.53	10	0.0570±0.0111 <i>P</i> >0.05	6.438±0.690 <i>P</i> >0.05

^a*P*>0.05, *K* value, high-, medium-, and low-dosage groups vs control group respectively. ^c*P*>0.05, α value, high-, medium-, and low-dosage groups vs control group respectively.

monocyte-phagocytic exponent α (both representing the ability of monocyte-phagocytic system to clear colloid charcoal particles in mice) are shown in Table 3. Both exponent *K* and emendated exponent α displayed a rising tendency, but no significant differences were observed among the groups by variance analysis (*P*>0.05).

DISCUSSION

The male zooid is an animal material medicine in China, whose functions are well documented in Compendium of Materia Medica as follows^[4]: invigorating essential Qi, strengthening vagina, untiring of sexual intercourse, and arresting essence. In Ri Hua Zi Ben Cao (Ri Hua Zi Materia Medica), it is documented to have the following actions: strengthening sexual function, checking spermatorrhea and stranguria with hematuria, warming kidney, extinguishing sore and scar, indications: wound from metal instrument injury, acute catarrhal and allergic conjunctivitis, and frostbite, heat-induced sore. Thus, male zooid can tonify the liver and invigorate the kidney, consolidate essence and strengthen Yang, check bleeding and promote muscle growth. The male zooid of *A. pernyi* contains many active substances, such as brain hormone, pro-thymosin, hormone of *A. pernyi*, diuretics, which can adjust metabolism and restore immune functions^[5-10].

Hu *et al.*^[11], using the fruit fly (*Drosophila melanogaster*) as a longevity model, examined the effect of hu-bao (HB) and seng-bao (SB), two marketed health products made from a mixture of natural ingredients, and found that the effect of HB and SB are specific for the male fly. The life-span of the male significantly increased when HB or SB was added to the culture medium. When the male silkworm moth ingredient was removed from HB or SB, the life-span prolongation effect of HB and SB drastically diminished, suggesting that the male silkworm moth is a key ingredient in combination with other components for specific prolongation of the life-span of male flies. The immune system in the Chinese oak silk moth, *A. pernyi*, originated from a single ancestral gene with that of the Cecropia moth whose antibacterial activity has been tested against nine different bacterial species^[12]. Zhang *et al.*^[13], reported that the cecropins from Chinese oak silkworm *A. pernyi* possess effective anti-tumor activity with no cytotoxicity against normal eukaryotic cells, and impede the neoplastic process in murine large intestines.

T cells play a role in immune response, killing tumor cells and suppressing tumor growth. Due to the actions of

estrogen, paracrine of tumor, negative nitrogen balance, the immune functions of patients can be suppressed and lead to immune escape, proliferation, and metastasis of tumor cells^[14]. Th1 and Th2 are two subgroups of CD4+Th cells. Most tumor tissues can secrete functional cytokine of Th2, causing the shift from Th1 to Th2 and immune suppression. Thus, promoting shift from Th2 to Th1 may be a method of tumor immunotherapy. The androgen-like action of male zooid can antagonize the immuno-suppression of high-level E2, promote high-expression of IL-18, induce production of IFN- γ , IL-2, IL-12, IL-18, and GM-CSF by monocytes, enhance cytotoxicity of NK and Th1 cells, accelerate proliferation of T cells and induce differentiation of Th1 cells^[15]. Amino acids in male zooid can adjust negative nitrogen balance and restore immune functions. Peptides in male zooid can also improve immune functions, enhance T cell activity by killing tumor cells^[16].

In general, the concentrated liquor from male zooid of *A. pernyi* can enhance non-specific immunity and CTL-mediated specific immunity, and has therapeutic functions in tumor therapy and adjuvant therapy.

Our study showed that the concentrated liquor from male zooid of *A. pernyi* could suppress tumor growth and improve immune function in mice. For immune modulation, it was observed in animal experiments that it could enhance cellular immunity significantly in all the three tested groups. In the high dosage group, the humoral immunity also obviously improved. A rising tendency was shown without significant difference.

In conclusion, the concentrated liquor from male zooid of *A. pernyi* is a potential anti-tumor agent by strengthening anti-pathogenic Qi. Further researches should be performed on its immuno-modulating effects on pancreatic and liver cancer.

REFERENCES

- 1 Piao HS, Ju Y, Zheng YH, Li YJ, Zheng CJ, Shen GH. Extraction separation and identification of amino acid components in the semen of male silk moths. *Yanbian Daxue Yixue Xuebao* 1997; **20**: 147-148
- 2 Li QY, Hu PL. The study of antheraea pernyi and boxbyxmori. *Shanghai Zhongyiyao Zazhi* 1996; **11**: 45-47
- 3 Xu SY, Bian RL, Chen X. Experimental methodology of pharmacology. Beijing: the People's Health Press 1991: 1233-1238
- 4 Ming D, Li SZ. Compendium of materia medica. 4TH edition. Beijing: the People's Health Press 1981: 2247-2255
- 5 Tang JH. The effect of antheraea pernyi. *Huaxia Yixue* 1999; **12**: 341

- 6 **Liu TY**, Li DJ. Chinese medicine: *Antheraea Pernyi*. *Beijing Zhongyiyao Daxue Xuebao* 1994; **17**: 22-23
- 7 **Mao G**, Cui DJ, Xu QM. The effect of *Antheraea Pernyi*. *Liaoning Zhongyi Zazhi* 1994; **21**: 231-232
- 8 **Liu XM**, Zhou LS. The anti-fatigue function of the capsule Wei Li Kang. *Guangdong Yiyao* 2003; **24**: 248-249
- 9 **Mo ZQ**, Zhou SY, Sang T, Wen SK. The pharmacological investigation and application of *Antheraea Pernyi*. *Zhongyiyao* 1995; **18**: 101-103
- 10 **Cao Cai**, Wei HY. Pharmacological study of *Antheraea Pernyi*. *Zhongguo Zhongyi Zazhi* 1991; **16**: 368-370
- 11 **Hu K**, Wang Q, Hu PQ. The male silkworm moth (*Antheraea pernyi*) is a key ingredient in hu-bao and sheng-bao for specific prolongation of the life-span of the male fruit fly (*Drosophila melanogaster*). *Am J Chin Med* 2002; **30**: 263-270
- 12 **Qu Z**, Steiner H, Engstrom A, Bennich H, Boman HG. Insect immunity: isolation and structure of cecropins B and D from pupae of the Chinese oak silk moth, *Antheraea pernyi*. *Eur J Biochem* 1982; **127**: 219-224
- 13 **Zhang WM**, Lai ZS, He MR, Xu G, Huang W, Zhou DY. Effects of the antibacterial peptide cecropins from Chinese oak silkworm, *Antheraea pernyi* on 1, 2-dimethylhydrazine-induced colon carcinogenesis in rats. *Diyi Junyi Daxue Xuebao* 2003; **23**: 1066-1068
- 14 **Vermeiren J**, Ceuppens JL, Van Ghelue M, Witters P, Bullens D, Mages HW, Kroczeck RA, Van Gool SW. Human T cell activation by costimulatory signal-deficient allogeneic cells induces inducible costimulator-expressing anergic T cells with regulatory cell activity. *J Immunol* 2004; **172**: 5371-5378
- 15 **Makar KW**, Wilson CB. DNA methylation is a nonredundant repressor of the Th2 effector program. *J Immunol* 2004; **173**: 4402-4406
- 16 **Xie ZW**. The effects of Chinese traditional medicine on the Th1/Th2 balance. *Guowai Yixue* 2002; **24**: 335-337

Science Editor Wang XL and Guo SY Language Editor Elsevier HK

• BRIEF REPORTS •

Surgical treatment of giant esophageal leiomyoma

Bang-Chang Cheng, Sheng Chang, Zhi-Fu Mao, Mao-Jin Li, Jie Huang, Zhi-Wei Wang, Tu-Sheng Wang

Bang-Chang Cheng, Sheng Chang, Zhi-Fu Mao, Jie Huang, Zhi-Wei Wang, Tu-Sheng Wang, Department of Thoracic Cardiovascular Surgery, Renmin Hospital of Wuhan University, Wuhan 430060, Hubei Province, China
Mao-Jin Li, Department of Radiology, Renmin Hospital of Wuhan University, Wuhan 430060, Hubei Province, China
Supported by the Science and Technology Foundation of Hubei Province, No. 992P1203
Co-first-author: Sheng Chang
Correspondence to: Professor Bang-Chang Cheng, Department of Thoracic Cardiovascular Surgery, Renmin Hospital of Wuhan University, Wuhan 430060, Hubei Province, China. dr_cheng@126.com
Telephone: +86-27-88041919-2240
Received: 2004-12-25 Accepted: 2005-01-12

Abstract

AIM: To summarize the operative experiences for giant leiomyoma of esophagus.

METHODS: Eight cases of giant esophageal leiomyoma (GEL) whose tumors were bigger than 10 cm were treated surgically in our department from June 1980 to March 2004. All of these cases received barium swallow roentgenography and esophagoscopy. Leiomyoma located in upper thirds of the esophagus in one case, middle thirds of the esophagus in five cases, lower thirds of the esophagus in two cases. Resection of tumors was performed successfully in all of these cases. Operative methods included transthoracic extramucosal enucleation and buttressing the muscular defect with pedicled great omental flap (one case), esophagectomy and esophago-gastrostomy above the arch of aorta (three cases), total esophagectomy and esophageal replacement with colon (four cases). Histological examination confirmed that all of these cases were leiomyoma.

RESULTS: All of the eight patients recovered approvingly with no mortality and resumed normal diet after operation. Vomiting during meals occurred in one patient with esophagogastronomy, and remained 1 mo. Reflux esophagitis occurred in one patient with esophago-gastrostomy and was alleviated with medication. Thoracic colon syndrome (TCS) occurred in one patient with colon replacement at 15 mo postoperatively. No recurrence occurred in follow-up from 6 mo to 8 years.

CONCLUSION: Surgical treatment for GEL is both safe and effective. The choices of operative methods mainly depend on the location and range of lesions. We prefer to treat GEL via esophagectomy combined with esophago-gastrostomy or esophagus replacement with colon. The long-time quality of life is better in the latter.

© 2005 The WJG Press and Elsevier Inc. All rights reserved.

Key words: Giant esophageal leiomyoma; Esophagus; Greater omentum; Esophageal replacement with colon

Cheng BC, Chang S, Mao ZF, Li MJ, Huang J, Wang ZW, Wang TS. Surgical treatment of giant esophageal leiomyoma. *World J Gastroenterol* 2005; 11(27): 4258-4260
<http://www.wjgnet.com/1007-9327/11/4258.asp>

INTRODUCTION

Leiomyoma is the most common benign tumor found in the esophagus but it is, however, a rare neoplasm. It is found mainly in the lower and middle thirds of the esophagus and, in most cases are single lesions^[1]. Leiomyoma can occur at any age but 90% of cases occur in patients between the ages of 20 and 69 years, with peak incidence in the third to fifth decades^[2]. The male-to-female ratio is approximately 2:1. About half the patients with leiomyoma are asymptomatic and malignant change is rare. Transthoracic extramucosal enucleation is a safe and effective procedure for about 96% of esophageal leiomyoma^[3]. However, few of esophageal leiomyoma becomes giant-sized gradually (diameter of tumor larger than 10 cm) and show the symptoms caused by compression of tumor, obstruction of esophagus or dysfunction of cardia. The surgical treatment strategy of such GEL is not the same of common esophageal leiomyoma, especially when mucosa is damaged by leiomyoma or lesions have potential sarcomatous change. This report summarized the operative experience of GEL in our department.

MATERIALS AND METHODS

Materials

Between June 1980 and March 2004, there were 8 cases of GEL whose tumors were larger than 10 cm that underwent surgical treatment in our department. These patients comprised five males and three females, whose age ranged from 25 to 58 years (mean age, 42.5 years). Duration of symptoms was from 5 to 12 years. All of the eight patients had dysphagia and complained of retrosternal pain and backache in five cases, superior belly distention in five cases, weight loss in four cases, heartburn in three cases, cough in two cases, took normal diet in two cases, semi-liquid diet in four cases, liquid diet in two cases. All of the eight patients received barium swallow roentgenography and esophagoscopy. CT scan was performed in five cases, MRI in three cases, endoscopic ultrasonography (EUS) in one case. Leiomyoma located in upper thirds of the esophagus

in one case, middle thirds of the esophagus in five cases, lower thirds of the esophagus in two cases. The shapes of tumors were multinode-like in four cases, spiral-like in three cases, horseshoe-like in one case.

Methods

All patients received operation under general anesthesia. One patient underwent extramucosal enucleation of tumor and buttressing of the muscular defect with pedicled greater omental flap. In this case, the tumor located in lower thirds of the esophagus (Figure 1). Left posterolateral thoracotomy was performed through the sixth intercostal space. After removing the tumor, the muscular defect was found too large to allow a tension-free suture. Through a radial incision near esophageal hiatus, we made the great omentum into a pedicle flap (26 cm×9 cm) and pulled it up into thoracic cavity to cover the muscular defect. Three patients accepted esophagectomy and esophagogastrostomy above the arch of aorta through left posterolateral thoracotomy. Nasogastric tube and plasmatic canal were placed to aid in drainage and nutrition. Another four patients underwent total esophagectomy and esophageal replacement with colon. In these cases, patients were laid in supine position at the beginning. Esophageal interposition was performed with left colon (isoperistaltic, retrosternal) through left cervical abdominal incision. Then the patient's position was changed to full left lateral decubitus. Tumor and total esophagus were resected through right posterolateral thoracotomy. A feeding jejunostomy was used in these four patients, and enteral feeding was begun after 24 h with 5% dextrose in water and continued with an elemental diet after 48 h. The minimum size of tumor was 10 cm×10 cm×6 cm, the maximum was 20 cm×15 cm×15 cm. Histological examination confirmed that all of these were leiomyoma.

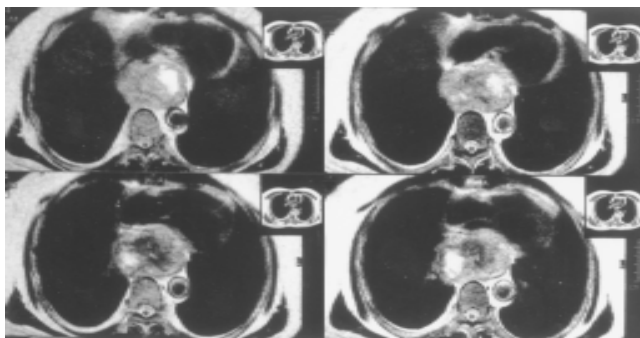


Figure 1 A 42-year-old male with giant esophageal leiomyoma. MRI image shows the tumor located in lower thirds of the esophagus. The size of tumor is 10 cm×10 cm×6 cm.

RESULTS

All of the eight patients recovered approvingly with no mortality and resumed normal diet after operation. Postoperative complications included leakage of cervical esophageal stoma (one case), pulmonary atelectasis (one case), thoracic infection (one case), chylothorax (one case). They all healed with conservative interventions and drainage. Patients were followed up from 6 mo to 8 years. Vomiting

after meals occurred in one patient with esophagogastrostomy, and remained for 1 mo. Vomiting after meals was not seen in patients with colonic interposition. Reflux esophagitis occurred in one patient with esophagogastrostomy and was alleviated with medication. Thoracic colon syndrome (TCS) occurred in one patient with colon replacement at 15 mo postoperatively, and recovered with re-operation. No recurrence occurred.

DISCUSSION

Leiomyoma is the most common benign tumor found in the esophagus but is nonetheless rare. Of all esophageal tumors, benign tumors account for fewer than 10%, of which 4% are leiomyomas^[4]. These tumors are usually found in middle age and are almost twice as common in men. They are located mainly in the lower and middle thirds of the esophagus. Leiomyoma may undergo cystic degeneration, calcification occurs infrequently and malignant change is rare^[5]. Leiomyoma is a slow growing tumor and the size of the lesion may not change for many years. Approximately one-half of all tumors are smaller than 5 cm, but 5% may be larger than 10 cm. Giant leiomyoma involving the entire esophagus and weighing up to 5 kg have been reported^[6]. Giant leiomyoma of esophagus should be removed when diagnosed, but its operative method is not the same of common leiomyoma.

Since most leiomyomas are intramural, eccentric, and well encapsulated, they can be easily shelled out (enucleated) without resorting to esophageal resection. One concern after enucleation of a large leiomyoma is that the myotomy may result functionally in achalasia. It is generally accepted that tumors up to 8 cm can be safely enucleated without significant postoperative dysphagia as long as the mucosa is intact and the myotomy is reapproximated^[3,7]. Larger lesions can be removed via enucleation but often result in the muscular defects too large to allow a tension-free suture, requiring a tissue flap to prevent mucosal bulging. We resected a 10 cm×10 cm×6 cm esophageal leiomyoma successfully with extramucosal enucleation and buttressing the muscular defect with pedicled greater omental flap. No postoperative dysphagia occurred during follow-up.

The greater omentum (GO) square is large and allows the covering of various tissue defects. The pedicled GO flap has the advantages of its own blood supply and anti-inflammatory effect^[14]. Using the GO to fill or buttress tissular defect is not novel in thoracic surgery^[14]. Angiography shows many types of vascular supply for the GO. Therefore, the GO flap exsection technique is very important. The flap transposition through the diaphragm is not difficult. The opening should not be very wide for good great omentum tissue adhesion and too narrow to prevent compression of the vessels.

Majority of GEL may require esophageal resection. The choices of this method depend on several factors: (1) The esophageal leiomyoma is too large to allow a resection without damaging the mucosa; (2) Adhesion between leiomyoma and the esophageal mucosa is tight and extensive; (3) Unrepairable mucosal defect caused by resection of tumor; (4) Large leiomyomas locate in the distal esophagus and extend downward across the cardia; (5) Leiomyosarcoma

is suspected. Resection for GEL is typically performed with esophagectomy and gastric pull-up through left posterolateral thoracotomy. In our experience, blood supply of the GEL was abundant, especially at the region posterior to the arch of aorta and upper part of the diaphragm. Careful dissection and hemostasia was necessary. Be cautious not to damage thoracic duct. For this purpose, transfixing the trunk of thoracic duct above the diaphragm between descending aorta and azygos vein was helpful. Gastric pull-up has some postoperative morbidity including reflux esophagitis, stricture formation, dumping, diarrhea, reduced meal capacity, and weight loss^[8]. Many of these complications are thought to be caused by division of the vagal nerves and the subsequent loss of parasympathetic innervation to the foregut^[9].

The rationale for use of the colon is that there will be fewer complications related to acid reflux than when the stomach is used for esophageal replacement. If the GEL is located in the upper thirds of the esophagus and the mucosa is damaged by GEL, esophageal replacement with colon (ERC) might be the best choice in this situation. Our techniques of ERC are different to others. The retrosternal colon replacement is performed through left cervical abdominal approaches in supine position at first, and then resects tumor and total esophagus through right posterolateral thoracotomy in full left lateral decubitus. We prefer this approach to synchronous abdominothoracic incision, for the former has allowed better exposure.

Several factors are important to decrease the mortality and postoperative complications of ERC: (1) Choosing suitable colonic segment and ensuring an adequate arterial supply. Before cutting the mesocolon, we usually clamp the communicating branches for 3~5 min in order to ensure that blood supply is enough; (2) Adopting isoperistaltic interposition. Studies show that isoperistaltic interposition is superior to antiperistaltic interposition and the long-time quality of life is better in the former^[10,13]; (3) Single-layer esophagocolonic anastomosis. Our studies show that single-layer anastomosis can reduce the morbidity of fistula and stricture^[11]; (4) Choosing colonic pull-up approach properly. The upward approach of colonic segment is decided by the condition of individual patient and the experience of the surgeon; (5) Avoiding redundancy of the colonic segment. Colon redundancy can be due to technical error at the time of operation (i.e., leaving redundancy in the interposition graft), intrathoracic herniation of colon, or differential colon growth. Proper attention to the length of the colon segment is important to prevent intrathoracic redundancy^[16]. Yildirim *et al.*^[17], suggest that the colon is one of the best substitutes for the esophagus, and there is no need to perform a routine pyloroplasty or antireflux procedure as an adjunct to the primary surgery. Our patients

healed satisfactorily and the long-time quality of life was good during follow-up and it was coincident with the literature^[12,13,15].

REFERENCES

- 1 **Hatch GF 3rd**, Wertheimer-Hatch L, Hatch KF, Davis GB, Blanchard DK, Foster RS Jr, Skandalakis JE. Tumors of the esophagus. *World J Surg* 2000; **24**: 401-411
- 2 **Lawrence SL**, Sunil S, Clayton JB, Blair M, Michael LK, Larry RK, John CK. Current management of esophageal leiomyoma. *J Am Coll Surg* 2004; **198**: 136-146
- 3 **Bonavina L**, Segalin A, Rosati R, Pavanello M, Peracchia A. Surgical therapy of esophageal leiomyoma. *J Am Coll Surg* 1995; **181**: 257-262
- 4 **Jesic R**, Randjelovic T, Gerzic Z, Zdravkovic DJ, Krstic M, Milinic N, Pavlovic A, Svejic T, Bulajic M. Leiomyoma of the esophagus. Case report. *Srp Arh Celok Lek* 1997; **125**: 113-115
- 5 **Nagashima R**, Takeda H, Motoyama T, Tsukamoto O, Takahashi T. Coexistence of superficial esophageal carcinoma and leiomyoma: case report of an endoscopic resection. *Endoscopy* 1997; **29**: 683-684
- 6 **Aurea P**, Grazia M, Petrella F, Bazzocchi R. Giant leiomyoma of the esophagus. *Euro J Cardiothorac Surg* 2002; **22**: 1008-1010
- 7 **Roviaro GC**, Maciocco M, Varoli F, Rebuffat C, Vergani C, Scarduelli A. Videothoracoscopic treatment of oesophageal leiomyoma. *Thorax* 1998; **53**: 190-192
- 8 **Watson TJ**, Peters JH, DeMeester TR. Esophageal replacement for end-stage benign esophageal disease. *Surg Clin North Am* 1997; **77**: 1099-1113
- 9 **Banki F**, Mason RJ, DeMeester SR, Hagen JA, Balaji NS, Crookes PF, Bremner CG, Peters JH, DeMeester TR. Vagal-sparing esophagectomy: a more physiologic alternative. *Ann Surg* 2002; **236**: 324-335
- 10 **Cheng BC**, Lu SQ, Gao SZ, Tu ZF, Lin DM, Wang TS. Colon replacement for esophagus: clinical experience from 240 cases. *Chin Med J* 1994; **107**: 216-218
- 11 **Gao SZ**, Wang TS, Yao Z, Cheng BC, Tu ZF, Ling DM, Peng SY. Experimental study and clinical application of a single-row suturing esophagogastrostomy. *J Surg Oncol* 1990; **43**: 167-171
- 12 **Cheng BC**, Gao SZ, Tu ZF, Lu DT, Zhou SG, Cai XT, Huang ZR, Wang CX. The clinical study on the route of colon segment for replacement of the esophagus. *Chin J Thorac Cardiovasc Surg* 2000; **16**: 283-285
- 13 **Cheng BC**, Shao K. Evaluation of the quality of life after esophageal replacement with colon. *Chin J Clin Rehabilitation* 2002; **6**: 2676-2677
- 14 **Levashev YN**, Akopov AL, Mosin IV. The possibilities of greater omentum usage in thoracic surgery. *Eur J Cardiothorac Surg* 1999; **15**: 465-468
- 15 **Thomas P**, Fuentes P, Giudicelli R, Reboud E. Colon interposition for esophageal replacement: current indications and long-term function. *Ann Thorac Surg* 1997; **64**: 757-764
- 16 **Domreis JS**, Jobe BA, Aye RW, Deveney KE, Sheppard BC, Deveney CW. Management of long-term failure after colon interposition for benign disease. *Am J Surg* 2002; **183**: 544-546
- 17 **Yildirim S**, Koksall H, Celayir F, Erdem L, Oner M, Baykan A. Colonic Interposition vs Gastric Pull-Up After Total Esophagectomy. *J Gastrointest Surg* 2004; **8**: 675-678

• BRIEF REPORTS •

Mutations outside the YMDD motif in the P protein can also cause DHBV resistant to Lamivudine

Jin-Yang He, Yu-Tong Zhu, Rui-Yi Yang, Li-Ling Feng, Xing-Bo Guo, Feng-Xue Zhang, Hong-Shan Chen

Jin-Yang He, Yu-Tong Zhu, Rui-Yi Yang, Li-Ling Feng, Xing-Bo Guo, Feng-Xue Zhang, Tropical Medicine Institute of Guangzhou University of Traditional Chinese Medicine, Guangzhou 510405, Guangdong Province, China
Hong-Shan Chen, Institute of Medical Biotechnology of CAMS and PUMC, Beijing 100050, China
Correspondence to: Jin-Yang He, MD, Tropical Medicine Institute of Guangzhou University of Traditional Chinese Medicine, Guangzhou 510405, Guangdong Province, China. sunny12345678_89@yahoo.com.cn
Telephone: +86-20-31774402
Received: 2004-12-22 Accepted: 2005-01-12

Abstract

AIM: To observe the Lamivudine resistance character of a DHBV strain *in vitro* and *in vivo*, and to analyze if the Lamivudine resistance character is caused by gene mutation or by abnormality of the Lamivudine metabolism.

METHODS: Congenitally DHBV-negative Guangdong brown ducks and duck embryo liver cells were respectively taken as animal and cell model. The Lamivudine-susceptible DHBV and Lamivudine-resistant DHBV (LRDHBV) were infected and Lamivudine was administrated according to the divided groups. The changes of DHBV quantity in the animal and cell model were tested. Three Lamivudine-resistant and two Lamivudine-susceptible DHBV complete genomes were successfully amplified, sequenced and then submitted to GenBank. All the DHBV complete sequences in the GenBank at present were taken to align with the three LRDHBV to analyze the mutational points related to the Lamivudine-resistant mutation.

RESULTS: Both the animal and cell model showed that the large and the small dosage Lamivudine have no significant inhibitory effect on the LRDHBV. Five sequences of DHBV complete genomes were successfully cloned. The GenBank accession numbers of the three sequences of LRDHBV are AY521226, AY521227, and AY433937. The two strains of Lamivudine-susceptible DHBV are AY392760 and AY536371. The correlated mutational points are KorR86Q and AorE591T in the P protein.

CONCLUSION: The Lamivudine resistance character of this DHBV strain is caused by genome mutation; the related mutational points are KorR86Q and AorE591T and have no relations with the YMDD motif mutation.

He JY, Zhu YT, Yang RY, Feng LL, Guo XB, Zhang FX, Chen HS. Mutations outside the YMDD motif in the P protein can also cause DHBV resistant to Lamivudine. *World J Gastroenterol* 2005; 11(27): 4261-4267
<http://www.wjgnet.com/1007-9327/11/4261.asp>

INTRODUCTION

More than 400 million people worldwide are chronically infected by HBV^[1]. HBV infections, the 10th leading cause of death worldwide, result in 500 000 to 1.2 million deaths per year caused by chronic hepatitis, cirrhosis, and hepatocellular carcinoma^[2]. Lamivudine had been considered to be a great progress in the area of anti-virus drug. It can make the blood HBV DNA of more than 90% of patients changed to negative when administrated for 1 year by 100 mg/d^[3,4]. But it can also lead to YMDD mutant and cause Lamivudine resistance. YMDD mutations developed in 12.1%, 49.7% and 70.5% of the patients respectively at year 1, 2, and 3^[5]. So the searching of Lamivudine-resistant problem is very important. It is believed consistently that the cause of Lamivudine resistance is HBV gene mutation. The main mutant motif is the YMDD in the P protein of HBV^[6-8]. But there are no animal and cell models of Lamivudine-resistant HBV which can be conveniently used, which cause very little progress that has been the problem of Lamivudine-resistant HBV.

After the finding of the DHBV by Summers *et al.*^[9,10], the process of replication and genome sequence of DHBV had been discovered rapidly. These facilitated the understanding of the related aspects of HBV. Because of the similarity of the DHBV and HBV in the replicating manner and pathogenesis, the duck hepatitis B model had been used as animal model of anti-HBV drug screening and HBV pathogenesis searching. When we persistently used the congenitally infected duck as animal model to screen anti-HBV drug, one congenitally infected duck had been found to have the character of Lamivudine resistance. We named it Lamivudine-resistant duck (LRD). The LRD-infected virus was named as Lamivudine-resistant DHBV (LRDHBV). We proved the character of Lamivudine resistance of LRDHBV in embryo duck liver cell model and postnatally infected duck model. Then the complete genome of LRDHBV and Lamivudine-susceptible DHBV were cloned and sequenced. The LRDHBV-related mutant points were analyzed.

MATERIALS AND METHODS

Animals

One-day-old Guangdong brown ducks were obtained from

a duck factory on the Shi-Jing town of Guangzhou city. Congenitally DHBV-negative ducks were chosen by dot blot assay to be experimental animals. The ducks were fed a standard duck diet and water according to the guidelines approved by the China Association of Laboratory Animal Care.

Primary hepatocytes

Guangdong brown duck eggs were purchased from a commercial supplier. The eggs were incubated for 20 d in the environment of 37.6 °C and 50-60% humidity. The eggs were opened and were proved to be congenitally DHBV negative using PCR method. The duck embryo liver was plucked out and digested with 0.2% collagenase (type II, Gibco) in 3 mL of serum-free William E medium (Sigma) supplemented with 2 mol/L L-glutamine, 15 mol/L HEPES (N-2-hydroxyethylpiperazine-N'-2-ethane-sulfonic acid [pH 7.2]), 100 U of penicillin per mL, 100 µg of streptomycin, 10⁻⁵ mol/L hydrocortisone, 1 µg of insulin per mL, and 1.5% dimethyl sulfoxide (all from Sigma, Germany) for 30 min at 37 °C. After washing twice with 5 mL of medium, the cells from one liver were suspended in 20-24 mL of medium, seeded onto 10-12 tissue culture dishes (60-mm diameter; 2 mL per dish, the density is 5×10⁵ cells per well), and cultivated at 37 °C and 50 mL/L CO₂. The medium was first changed 30 min after seeding, and further medium changes were done daily. Cellular toxicity was tested daily by light microscope examination and MTT assay of Mosmann^[11] as described by Alley *et al.*^[12].

Serum and DHBV infection

Lamivudine-susceptible DHBV serum was from congenitally infected ducks that had been proved to be DHBV positive by dot blot method. LRDHBV serum was from LRD at the time point of 10-d Lamivudine administration. In the animal model, 0.2 mL of Lamivudine-susceptible DHBV or LRDHBV was injected to the shank vein of every duck that were 2 d old. The primary hepatocytes were infected between 24 and 48 h after seeding by adding 50 µL Lamivudine-susceptible DHBV or LRDHBV per dish directly to the medium. After 3-h incubation at 37 °C, the inoculum was removed, and 2 mL of fresh medium was added.

Groups and dot blot assay

Twelve ducks infected with Lamivudine-susceptible DHBV and 18 ducks infected with LRDHBV were chosen and randomly divided into five groups. Group A were infected with Lamivudine-susceptible DHBV; group B were infected with LRDHBV; group C were infected with LRDHBV and fed with large dosage Lamivudine (100 mg/kg, b.i.d.); group D were infected with LRDHBV and fed with small dosage Lamivudine (20 mg/kg, b.i.d.); group E were infected with Lamivudine-susceptible DHBV and fed with small dosage Lamivudine (20 mg/kg, b.i.d.). The serum samples were collected at time points of 1 d before drug administration (D0), 5th d of drug administration (D5), 10th d of drug administration (D10) and 3rd d post stopping of drug administration (P3). The primary hepatocytes were also divided into five groups similar to the animal experiment. The hepatocytes were also

treated with two concentrations of Lamivudine (100 and 1 000 µmol/L) starting from 3 d after virus inoculation. The hepatocytes were collected and DNA was extracted at the time points of 3, 6, 9, and 12 d after virus inoculation respectively. Forty microliters of serum or twenty-five microliters of hepatocytes DHBVDNA extraction dissolution was spotted, and DHBVDNA was detected with a full-length DHBV genomic DNA probe labeled with [α -³²P] dCTP as described previously^[13]. A quantity analysis was carried out using enzyme photometer. The limit of detection of serum viral DNA by this assay is 100 pg/mL.

Amplification of the DHBV complete genome

Three samples of LRDHBV DNA were extracted from the serum of LRD which was the same as the LRDHBV serum used to infect the congenitally DHBV-negative ducks and duck embryo liver cells. Two samples of Lamivudine-susceptible DHBVDNA were extracted from serum of two ducks that were susceptible to Lamivudine. One pair of primers was used to test if there was DHBVDNA in the extraction solutions. The primer sequences^[14] are: P1 -5'-GCG CTT TCC AAG ATA CTG GAG CCC AA-3' (sense) and P2-5'-CTG GAT GGG CCG TCA GCA GGA TTA TA-3' (anti-sense). The PCR condition is: 94 °C 30 s, 55 °C 30 s, 72 °C 1 min, 30 cycles. One pair of primers was designed to amplify the complete genome of DHBV. The primer sequences are Q1-5'-ACC CCT CTC TCG AAA GCA ATA-3' (sense) and Q2-5'-GTG TAT GTA AGA GCC GTC CAA TC-3' (anti-sense). The LAPCR condition is: 94 °C 30 s; 52 °C 1 min; 72 °C 3.5 min, after 30 cycles, another 72 °C 5 min was supplemented. One percent agarose gel was used to analyze the LAPCR product.

Cloning and sequencing of DHBV complete genome

The 3.0-kb PCR product was inserted into the pMD18-T vector using the TAKARA Ligation kit. JM109 competent cells were made with the method of CaCl₂ which was found by Mandel *et al.*^[15,16]. Three LRDHBV DNA recombinants and two Lamivudine-susceptible DHBV DNA recombinants were transformed into the JM109 competent cells. The five kinds of *E. coli* containing the five kinds of recombinants were conserved and sent to TAKARA to do bidirectional sequencing. The sequencing results were analyzed with related software.

Statistical analysis

Results were expressed as mean±SD. Statistical comparisons between the groups were done using Nemenyi method. *P* values less than 0.05 were considered statistically significant.

RESULTS

Lamivudine could not inhibit LRDHBV in duck animal model

We first examined if the LRDHBV could be inhibited in body of the other duck. We injected the LRDHBV-positive serum to the congenitally DHBV-negative ducks. These ducks were infected with LRDHBV and treated with Lamivudine. Lamivudine were used in large and small dosage groups. The feeding was maintained for 10 d. Serum samples were collected at four time points from 1 d before administration to 3rd d post stopping of administration. The DHBV in the

serum samples were quantified by dot blot assay. After 10 d of Lamivudine administration, the quantity of Lamivudine-susceptive DHBV in the duck blood markedly got down. But 3 d after stopping of administration, the quantity of susceptible DHBV rose up to former level. No significant effect was observed when the large and small dosage of Lamivudine was fed to the LRDHBV-infected ducks (Table 1 and Figure 1). So it can be concluded that the LRDHBV can also show the character of Lamivudine resistance in the ducks postnatally infected with the LRDHBV.

Table 1 and Figure 1 showed that no significant effect was observed when the large and small dosage of Lamivudine was fed to the LRDHBV-infected ducks. While the 10-d Lamivudine administration could make the Lamivudine-susceptive DHBV markedly get down in the duck model.

The dynamic change of the DHBV quantity in the blood before and after lamivudine administration

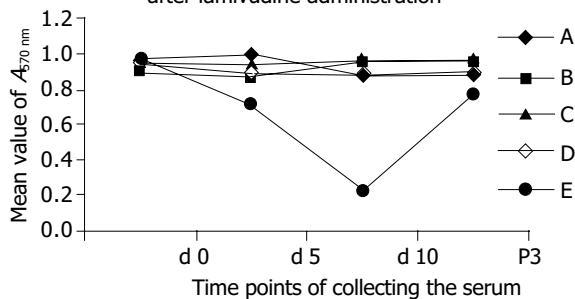


Figure 1 A: Lamivudine-susceptive DHBV control group; B: LRDHBV control group; C: LRDHBV-infected group administrated by large dose Lamivudine group; D: LRDHBV-infected group administrated by small dose Lamivudine group; E: Lamivudine-susceptive DHBV-infected group administrated by small dose Lamivudine group.

Lamivudine could not inhibit LRDHBV in the duck embryo liver cells

We inoculated the LRDHBV to the primary duck embryo liver cells and administrated Lamivudine according to the divided groups to observe if the LRDHBV have the Lamivudine-resistant character in the liver cells. Lamivudine administration was started from 3rd d post DHBV inoculation and maintained for 9 d. The liver cells were collected at four time points from 3 to 12 d post DHBV inoculation. The total DHBV in the cells was extracted immediately after cell collection. The DHBV quantity was tested by dot blot assay. The results showed that the Lamivudine-susceptive DHBV got down markedly at the time points of 6th, 9th, and 12th d post DHBV inoculation, while both the small and large dosage Lamivudine have no significant effect on the LRDHBV in the duck embryo liver cells (Figure 3). So

the LRDHBV showed Lamivudine-resistant character in the duck embryo liver cells too. We also tested the cytotoxicity of Lamivudine to the embryo liver cells. However, no significant cytotoxicity was detected in liver cells cultured with different concentrations of Lamivudine for 9 d by daily microscope examination (Figure 2) and by MTT method.

Lamivudine-susceptive DHBV was inhibited markedly at the time points of 6th, 9th, and 12th d post DHBV inoculation, while both the small and large dosage Lamivudine have no significant effect on the LRDHBV in the duck embryo liver cells.

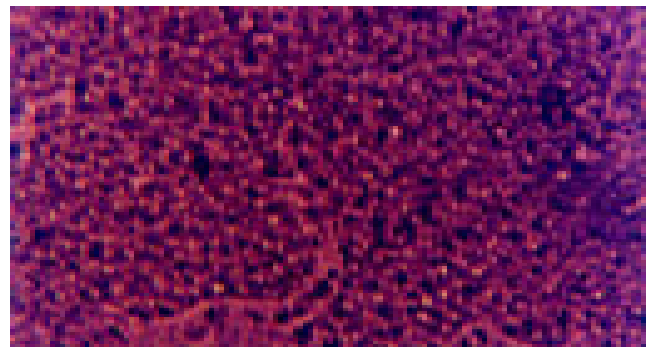


Figure 2 Duck embryo liver cells (5 d after DHBV inoculation, optic microscope ×40). They have no significant effect of Duck embryo liver cells infected with DHBV or LRDHBV.

Effects of lamivudine to the lamivudine susceptible and resistant DHBV in duck embryo liver cell culture

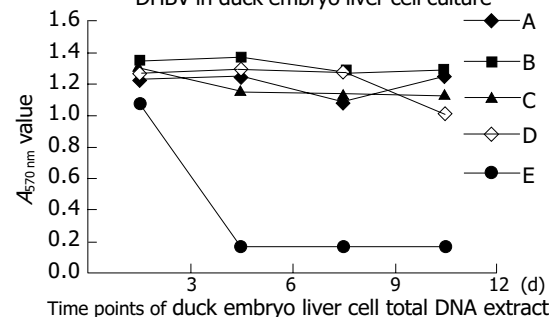


Figure 3 A: Lamivudine-susceptive DHBV control; B: LRDHBV control; C: LRDHBV-infected cells administrated by large dosage Lamivudine; D: LRDHBV-infected cells administrated by small dosage Lamivudine; E: Lamivudine-susceptive DHBV-infected cells administrated by small dosage Lamivudine.

DHBV complete genomes were successfully amplified and cloned

We designed two pairs of primer to amplify the DHBV complete genome. One was designed according to the method

Table 1 DHBV quantity in the duck blood of various groups expressed by $A_{570\text{ nm}}$ value (mean±SD)

Groups	D0	D5	D10	P3
Lamivudine-susceptive DHBV control	0.96±0.31	1.00±0.06	0.87±0.05	0.87±0.02
LRDHBV control	0.91±0.03	0.86±0.01	0.95±0.01	0.95±0.04
LRDHBV-infected group administrated by large dose Lamivudine	0.96±0.03	0.94±0.02	0.97±0.05	0.97±0.03
LRDHBV-infected group administrated by small dose Lamivudine	0.96±0.02	0.88±0.02	0.87±0.01	0.90±0.05
Lamivudine-susceptive DHBV-infected group administrated by small dose Lamivudine	0.96±0.05	0.73±0.05 ^b	0.22±0.03 ^b	0.69±0.02 ^b

^bP<0.01 group A vs group E.

of Gunther to amplify the HBV complete genome^[17]. It covered the DR1 of DHBV genome. Another pair of primer covered the DR2 of DHBV genome and LAPCR was used to amplify. We found that the primer covering the DR1 could not amplify the DHBV genome after optimizing the LAPCR condition. However, when we used the primer covering the DR2, the complete genome of DHBV was easily amplified (Figure 4). So we amplified three strains of LRDHBV and two strains of Lamivudine-susceptible DHBV complete genome. Then we inserted these DHBV complete genomes into the pMD18-T vector and transformed them to the JM 109 competent cells (Figure 4). Then the *E. coli* that included the five DHBV complete genomes were sent to the TAKARA to sequencing. The five complete sequences of DHBV complete genomes were submitted to the GenBank. Three strains of LRDHBV are AY521226, AY521227, and AY433937. Two strains of Lamivudine-susceptible DHBV are AY392760 and AY536371.

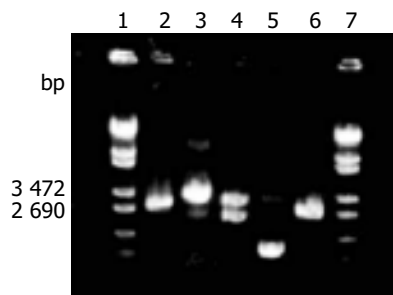


Figure 4 Electrophoresis graph of the amplification of DHBV complete genome and enzyme cutting of the recombinant. Lanes 1 and 7: λ -EcoT14I digest marker; lane 2: the LAPCR product of DHBV complete genome; lane 3: the cloning product of DHBV complete genome; lane 4: *EcoRI* enzyme cutting product of DHBV complete genome recombinants; lane 5: loop product of pMD18-T vector; lane 6: *EcoRI* enzyme cutting product of loop product of pMD18-T vector.

Analyze the related mutant points in the LRDHBV genome

Firstly, we compared the complete nucleotide sequences of the AY521226, AY521227, and AY433937, and the identity is the same 98%. The identity of the AY392760 and the AY536371 is also 98%. But comparing the nucleotide sequences of the LRDHBV (AY521226, AY521227, and AY433937) with the Lamivudine-susceptible DHBV (AY392760 and AY536371), the identity in the nucleotide level is the same 92%. So it seems that there are marked differences between LRDHBV and the Lamivudine-susceptible DHBV in nucleotide level. As the HBV or DHBV P protein is the target of Lamivudine, we turned to the P protein sequences of these DHBV. We initially aligned the P protein sequences of AY521226, AY521227, AY433937 with AY392760, AY536371. There were too many mutant points to analyze which points were related to the Lamivudine-resistant character. As the identities of AY392760 and AY433937 is only 88%, alignment should be done in a wider range. We downloaded all the DHBV protein sequences and aligned with the three Lamivudine-resistant sequences AY521226, AY521227, and AY433937. We found that there were two mutational points in the P protein. The two mutational points are KorR86Q and AorE591T (Figures 5A and B). We have not found any

significant mutational points in S or C protein sequences. The KorR86Q is located in the TP (terminal protein) domain, and the AorE591T is located in the RT (reverse transcriptase) domain. So we guessed that these two mutational points were related to the character of Lamivudine resistance.

DISCUSSION

We referred to Gunther's method^[17] when we designed the primers of amplifying the DHBV complete genome. This method noted that only the primers cover the DR1 sequence of HBV, the HBV genome can be wholly amplified. We first used one pair of primers that cover the DR1 of DHBV to amplify DHBV complete genome. Though all kinds of methods of optimizing the PCR condition were tested, the DHBV complete genome could not be amplified. So we guessed that the DR2 of DHBV sequence is also an important obstacle of amplifying the DHBV complete genome. In our experience, it is very hard to get the target products when the primers are located at both sides of the DR2. Additionally, the DR2 is located at the terminal of DHBV-positive strand. There is nick part followed by DR2 in the positive strand of DHBV. So we designed one pair of primers to cover the DR2 to amplify the whole DHBV genome. To our surprise, the complete genomes of DHBV were easily amplified. This phenomenon may be because the genome structure of DHBV is different to the HBV.

If Lamivudine-resistant character of LRDHBV was caused by unusual metabolism of Lamivudine in the duck body and did not correlate with virus genome mutation, it should not have the Lamivudine-resistant character in duck embryo liver cells and other ducks infected with the LRDHBV. Our results showed that the LRDHBV resistant to the Lamivudine appeared both in duck embryo liver cells and in duck body. So we concluded that the Lamivudine-resistant character is caused by DHBV mutation.

To our present knowledge, most of the Lamivudine-resistant phenomena of HBV are related to the YMDD motif mutation^[6-8,18]. Similar to HBV, mutagenesis *in vitro* in the YMDD motif of DHBV can also cause Lamivudine resistance^[19]. So we speculate that the mutational points were also located in the YMDD motif of LRDHBV. But the sequencing results denied this speculation.

After we obtained the five DHBV complete sequences, we found that there are no YMDD motif mutations in the P protein sequences of the three LRDHBV sequences. Then we aligned the P protein sequences of three LRDHBV with the two Lamivudine-susceptible DHBV P protein sequences. There were too many different points to analyze the mutational points related to the character of Lamivudine resistance. So we planned to align these three LRDHBV P protein sequences with more DHBV P protein sequences. There should be a prerequisite that the DHBV P protein sequences aligned with the three LRDHBV P protein sequences come from the DHBV which are susceptible to Lamivudine. Because it was never reported that there was a naturally occurred LRDHBV and we found only one strain of DHBV that have the Lamivudine-resistant character in so many years of laboratory work, we believed that the LRDHBV that occurred naturally is very few. So we

A	AF493986	61	VRAPLSHVRAATIDLRLGNKLP	B	538	ELGIRINFDKTTPSPVNEIRFLGYQID
	AY294656		RHHLGKLSGLYQMGCTFNPEWKVPDISDTHFNLD			ENFMKIEESRWKELRTVIKKIKVGEWYDWKCIQ
			VRAPLSHVRAATIDLRLGNKLP			ELGIRINFDKTTPSPVNEIRFLGYQID
	AF047045		RHHLGKLSGLYQMGCTFNPEWKVPDISDTHFNLD			ENFMKIEESRWKELRTVIKKIKVGEWYDWKCIQ
			VRAPLSHVRAATIDLRLGNKLP			ELGIRINFDKTTPSPVNEIRFLGYQID
	AF505512		RHHLGKLSGLYQMGCTFNPEWKVPDISDTHFNLD			ENFMKIEESRWKELRTVIKKIKVGEWYDWKCIQ
			VRAPLSHVRAATIDLRLGNKLP			ELGIRINFDKTTPSPVNEIRFLGYQID
	AY294029		RHHLGKLSGLYQMGCTFNPEWKVPDISDTHFDLD			ENFMKIEESRWKELRTVIKKIKVGEWYDWKCIQ
			VRAPLSHVRAATIDLRLGNKLP			ELGIRINFDKTTPSPVNEIRFLGYQID
	K01834		RHHLGKLSGLYQMGCTFNPEWKVPDISDTHFNLD			ENFMKIEESRWKELRTVIKKIKVGEWYDWKCIQ
			VRAPLSHVRAATIDLRLGNKLP			ELGIRINFDKTTPSPVNEIRFLGYQID
	AY250901		RHHLGKLSGLYQMGCTFNPEWKVPDISDTHFNLD			ENFMKIEESRWKELRTVIKKIKVGEWYDWKCIQ
			VRAPLSHVRAATIDLRLGNKLP			ELGIRINFDKTTPSPVNEIRFLGYQID
	AY250902		RHHLGKLSGLYQMGCTFNPEWKVPDISDTHFNLD			ENFMKIEESRWKELRTVIKKIKVGEWYDWKCIQ
			VRAPLSHVRAATIDLRLGNKLP			ELGIRINFDKTTPSPVNEIRFLGYQID
	AY250903		RHHLGKLSGLYQMGCTFNPEWKVPDISDTHFNLD			ENFMKIEESRWKELRTVIKKIKVGEWYDWKCIQ
			VRAPLSHVRAATIDLRLGNKLP			ELGIRINFDKTTPSPVNEIRFLGYQID
	AY250904		RHHLGKLSGLYQMGCTFNPEWKVPDISDTHFNLD			ENFMKIEESRWKELRTVIKKIKVGEWYDWKCIQ
			VRAPLSHVRAATIDLRLGNKLP			ELGIRINFDKTTPSPVNEIRFLGYQID
	AY294028		RHHLGKLSGLYQMGCTFNPEWKVPDISDTHFNLD			ENFMKIEESRWKELRTVIKKIKVGEWYDWKCIQ
			VRAPLSHVRAATIDLRLGNKLP			ELGIRINFDKTTPSPVNEIRFLGYQID
	M60677		RHHLGKLSGLYQMGCTFNPEWKVPDISDTHFNLD			ENFMKIEESRWKELRTVIKKIKVGEWYDWKCIQ
			VRAPLSHVRAATIDLRLGNKLP			ELGIRINFDKTTPSPVNEIRFLGYQID
	X74623		RHHLGKLSGLYQMGCTFNPEWKVPDISDTHFNLD			ENFMKIEESRWKELRTVIKKIKVGEWYDWKCIQ
			VRAPLYHVRAATIDLRLGNKLP			ELGIRINFDKTTPSPVNEIRFLGYQID
	X12798		RHHLGKLSGLYQMGCTFNPEWKVPDISDTHFNLD			ENFMKIEESRWKELRTVIKKIKVGEWYDWKCIQ
			VRAPLSHVRAATIDLRLGNKLP			ELGIRINFDKTTPSPVNEIRFLGYQID
	X58567		RHHLGKLSGLYQMGCTFNPEWKVPDISDTHFDLE			ENFMKIEESRWKELRTVIKKIKVGEWYDWKCIQ
			VRAPLSHVRAATIDLRLGNKLP			ELGIRINFDKTTPSPVTEIRFLGYQID
	AY494850		RHHLGKLSGLYQMGCTFNPEWKVPDISDTHFKSE		539	EQFMKIEESRWKELRTVIKKIKIGEWYDWKCIQ
			VRAPLSHVRAATIDLRLGNKLP			ELGVRINFDKTTPSPVNEIRFLGYQID
	AY494851		RHHLGKLSGLYQMGCTFNPEWKVPDISDTHFKSE		539	QKYLKIEDDRWKELRTVIKKIKVGEWYDWKCIQ
			VRAPLSHVRAATIDLRLGNKLP			ELGVRINFDKTTPSPVNEIRFLGYQID
	AY521226		RHHLGKLSGLYQMGCTFNPEWKVPDISDTHFKSE			QRYMKIEESRWKELRTVIKKIKIGEWYDWKCIQ
			VRAPLSHVRAATIDLRLGNRLPA		540	ELGIRINFDKTTPSPVTDIRFLGNQID
	AY521227		QHHLGKLSGLYQMGCSFNPEWKVPDISDTHFDLQ			EKYMKIEESRWKELRTVIKKIKVG 7WYDWKCIQ
			VRAPLSHVRAATIDLRLGNRLPA			ELGIRINFDKTTPSPVNDIRFLGYQID
	AY433937		QHMGKLSGLYQMGCSFNPEWKVPDISDTHFDLQ			EKYMKIEESRWKELRTVIKKIKVG 7WYDWKCIQ
			VRAPLSHVRAATIDLRLGNRLPA			ELGIRINFDKTTPSPVTDIRFLGYQID
	NC_001344		QHMGKLSGLYQMGCSFNPEWKVPDISDTHFDLQ			EKYMKIEESRWKELRTVIKKIKVG 7WYDWKCIQ
			VRAPLSHVRAATIDLRLGNKLP			ELGIRINFDKTTPSPVNDIRFLGYQID
	X60213		KHHLGKLSGLYQMGCTFNPEWKVPDISDTHFDLQ			QKFMKIEESRWIELRTVIKKIKIGAWYDWKCIQ
			VRAPLSHVRAATIDLRLGNKLP			ELGIRINFDKTTPSPVNDIRFLGYQID
	M32990		KHHLGKLSGLYQMGCTFNPEWKVPDISDTHFDLQ			QKFMKIEESRWIELRTVIKKIKIGAWYDWKCIQ
			VRAPLSHVRAATIDLRLGNKLP			ELGIRINFDKTTPSPVNDIRFLGYQID
	M32991		KHHLGKLSGLYQMGCTFNPEWKVPDISDTHFDLQ			QKFMKIEESRWKELRTVIKKIKIGAWYDWKCIQ
			VRAPLSHVRAATIDLRLGNKLP			ELGIRINFDKTTPSPVNDIRFLGYQID
	AJ006350		KHHLGKLSGLYQMGCSFNPEWKVPDISDTHFDLQ			QKFMRIEESRWKELRTVIKKIKIGAWYDWKCIQ
			VRAPLSHVRAATIDLRLGNKLP			ELGVRINFDKTTPSPVNDIRFLGYQID
	AF404406		KHHLGKLSGLYQMGCTFNPEWKVPDISDTHFDLQ			QKFMKIEESRWKELRTVIKKIKIGAWYDWKCIQ
			VRAPLSHVRAATIDLRLGNKLP		539	ELGIRINFDKTTPSPVTEIRFLGYQID
	M21953		KHHLGKLSGLYQMGCTFNPEWKVPDISDTHFDLQ			QKFMKIEESRWKELRTVIKKIKIGAWYDWKCIQ
			VRAPLSHVRAATIDLRLGNKLP		539	ELGIRINFDKTTPSPVTEIRFLGYQID
	AY392760		KHHLGKLSGLYQMGCTFNPEWKVPDISDTHFDLQ			QKFMKIEEDRWKELRTVIKKIKVGEWYDWKCIQ
			VRAPLSHVRAATVDLRLGNRLPA		540	ELGIRINFDKTTPSPVNEIRFLGYQID
	AY536371		RHHLGKLSGLYQMGCTFNPEWKVPDISDTHFDMQ			QKYMKIEESRWSELRTVIKKIKVGEWYDWKCIQ
			VRAPLSHVRAATVDLRLGNRLPA		540	ELGIRINFDKTTPSPVNEIRFLGYQID
			RHHLGKLSGLYQMGCTFNPEWKVPDISDTHFDMQ			QKYTKIEESRWSELRTVIKKIKIGEWYDWKCIQ
	X58568		VRAPLSHVRAATEDLRLGNKLP		539	ELGIRINFDKTTPSPVNEIRFLGYQID
			RHHLGKLSGLYQMGCTFNPDWKVPDISDTHFDMQ			HRFMKIEESRWKELRTVIKKIKIGEWYDWKCIQ
	X58569		VRAPLSRVRAATEDLRLGNRLPA		539	ELGIRINFDKTTPSPVNEIRFLGYQID
			RHHLGKLSGLYQMGCTFNPEWKVPDISDTHFDMQ			QRFMKIEESRWKELRTVIKKIKIGEWYDWKCIQ

Figure 5 A: KorR86Q mutant point in the P protein of the LRDHBV;

mutant point in the P protein of the LRDHBV.

presumed that the DHBV sequences in the GenBank up to now come from DHBV that are susceptible to Lamivudine. So we downloaded all the DHBV sequences in the GenBank and aligned the P protein sequences of these DHBV. The results showed that there were two mutational points that occurred in the P protein sequences of LRDHBV. It is KorR86Q in the TP domain and AorE591T in the RT domain. The TP domain of DHBV P protein mainly acts as a primer to originate the synthesis of DHBV-negative strand^[20]. But it is the tyrosine residue in 96aa of TP domain that primed the reverse transcription of negative strand^[21,22]. AorE591T is located in the lower reaches of YMDD motif. So the roles of KorR86Q and AorE591T in the Lamivudine-resistant phenomenon need deeper research.

For both hepadnaviruses and HIV, the mechanism of action of Lamivudine requires phosphorylation to 3TC-5'-triphosphate (3TC-TP), which in turn specifically inhibits the viral polymerase^[23-26]. The specificity is conferred by the much lower affinity of 3TC-TP for the cellular α - and β -polymerase^[25,27]. The mechanism of inhibition of hepadnavirus involves inhibition of the viral polymerase^[26,28,29]. Acting as a chain terminator for the DNA polymerase activities, the Lamivudine inhibit the reverse transcriptase in a manner that resemble competitive inhibition with respect to dCTP^[30]. The side groups of isoleucine and valine of the YMDD mutants sterically prevent Lamivudine from appropriately configuring into the nucleotide binding site of the reverse transcriptase^[31]. This can cause Lamivudine resistance. Can the KorR86Q and AorE591T mutants also prevent Lamivudine from appropriately configuring into the nucleotides binding site of the reverse transcriptase? It needs more research.

A 4-year clinical research showed that YMDD mutants only could explain the 75% of Lamivudine resistances. Polymerase gene mutations were observed in 82.5% of virological breakthroughs but also in 75% of the non-responders^[32]. So the mutations outside the YMDD motif in the P protein can independently cause DHBV resistant to Lamivudine is not very strange.

REFERENCES

- Lin KW, Kirchner JT. Hepatitis B. *Am Fam Physician* 2004; **69**: 75-82
- Lavanchy D. Hepatitis B virus epidemiology, disease burden, treatment, and current and emerging prevention and control measures. *J Viral Hepat* 2004; **11**: 97-107
- Nevens F, Main J, Honkoop P, Tyrrell DL, Barber J, Sullivan MT, Fevery J, De Man RA, Thomas HC. Lamivudine therapy for chronic hepatitis B: α six month randomized dose-ranging study. *Gastroenterology* 1997; **113**: 1258-1263
- Yao G, Wang B, Cui Z. Long-term effect of Lamivudine treatment in chronic hepatitis B virus infection. *Chin J Hepatol* 1999; **7**: 80-83
- Yao GB, Wang BE, Cui ZY, Yao JL, Zeng MD. The long-term efficacy of Lamivudine in chronic hepatitis B: interim analysis of 3-year's clinical course. *Chin J Intern Med* 2003; **42**: 382-387
- Allen MI, Deslauriers M, Andrews CW, Tipples GA, Walters KA, Tyrrell DL, Brown N, Condreay LD. Identification and characterization of mutations in hepatitis B virus resistant to Lamivudine. Lamivudine Clinical Investigation Group. *Hepatology* 1998; **27**: 1670-1677
- Honkoop P, Niesters HG, de Man RA, Osterhaus AD, Schalm SW. Lamivudine resistance in immunocompetent chronic hepatitis B. Incidence and patterns. *J Hepatol* 1997; **26**: 1393-1395
- Fu L, Cheng YC. Role of additional mutations outside the YMDD motif of hepatitis B virus polymerase in L-SddC(3TC) resistance. *Biochem Pharmacol* 1998; **55**: 1567-1572
- Summers J, Mason WS. Replication of the genome of a hepatitis B-like virus by reverse transcription of an RNA intermediate. *Cell* 1982; **20**: 403-415
- Mason WS, Seal G, Summers J. Virus of Pekin ducks with structural and biological relatedness to human hepatitis B virus. *J Virol* 1980; **36**: 829-836
- Mosmann T. Rapid colorimetric assay for cellular growth and survival: application to proliferation and cytotoxicity assays. *J Immunol Methods* 1983; **65**: 55-63
- Alley MC, Scudireo DA, Monks A, Hursey ML, Czerwinski MJ, Fine DL, Abbott BJ, Mayo JG, Shoemaker RH, Boyd MR. Feasibility of drug screening with panels of human tumor cell lines using a microculture tetrazolium assay. *Cancer Res* 1988; **48**: 589-601
- Lambert V, Fernholz D, Sprengel R, Fourel I, Deleage G, Wildner G, Peyret C, Trepo C, Cova L, Will H. Virus-neutralizing monoclonal antibody to a conserved epitope on the duck hepatitis B virus pre-S protein. *J Virol* 1990; **64**: 1290-1297
- Kock J, Schlicht HJ. Analysis of the earliest steps of hepadnaviral replication: genome repair after infectious entry into hepatocytes does not depend on viral polymerase activity. *J Virol* 1993; **67**: 4876-4874
- Mandel M, Higa A. Calcium-dependent bacteriophage DNA infection. *J Mol Biol* 1970; **53**: 154
- Cohen SN, Chang AC, Hsu L. Nonchromosomal antibiotic resistance in bacteria: Genetic transformation of *Escherichia coli* by R-factor DNA. *Proc Natl Acad Sci USA* 1972; **69**: 2110
- Gunther S, Li BC, Miska S, Kruger DH, Meisel H, Will H. A novel method for efficient amplification of whole hepatitis B virus genomes permits rapid functional analysis and reveals deletion mutants in immunosuppressed patients. *J Virol* 1995; **69**: 5437-5444
- Niesters HG, Honkoop P, Haagsma EB, de Man RA, Schalm SW, Osterhaus AD. Identification of more than one mutation in the hepatitis B virus polymerase gene arising during prolonged Lamivudine treatment. *J Infect Dis* 1998; **177**: 1382-1385
- Seigneres B, Aguesse-Germon S, Pichoud C, Vuillermoz I, Jarnard C, Trepo C, Zoulim F. Duck hepatitis B virus polymerase gene mutants associated with resistance to Lamivudine have a decreased replication capacity *in vitro* and *in vivo*. *J Hepatol* 2001; **34**: 114-122
- Wang GH, Seeger C. The reverse transcriptase of hepatitis B virus acts as a protein primer for viral DNA synthesis. *Cell* 1992; **71**: 663-670
- Weber M, Bronsema V, Bartors H, Bosserhoff A, Bartenschlager R, Schaller H. Hepadnavirus P protein utilizes a tyrosine residue in the Tpdomain to primer reverse transcription. *J Virol* 1994; **68**: 2994-2999
- Zoulim F, Seeger C. Reverse transcription in hepatitis B viruses is primed by a tyrosine residue of the polymerase. *J Virol* 1994; **68**: 6-13
- Cammack N, Rouse P, Marr CL, Reid PJ, Boehme RE, Coates JA, Penn CR, Cameron JM. Cellular metabolism of (-)-enantiomeric 2'-deoxy-3'-thiacytidine. *Biochem Pharmacol* 1992; **43**: 2509-2604
- Chang CN, Skalski V, Zhou JH, Cheng YC. Biochemical pharmacology of (+)- and (-)-2'-deoxy-3'-thiacytidine as anti-hepatitis B virus agents. *J Biol Chem* 1992; **267**: 22414-22420
- Hao ZD, Cooney DA, Hartman NR, Perno CF, Fridland A, DeVico AL, Sarngadharan MG, Broder S, Johns DG. Factors determining the activity of 2'-deoxy-3'-dideoxynucleosides in suppressing human immunodeficiency virus *in vitro*. *Mol Pharmacol* 1988; **34**: 431-435
- Coates JA, Cammack N, Jenkinson HJ, Mutton IM, Pearson BA, Storer R, Cameron JM, Penn CR. The separated enanti-

- omers of 2'-deoxy-3'-thiacytidine(BCH189)both inhibit human immunodeficiency virus replication *in vitro*. *Antimicrob Agents Chemother* 1992; **36**: 202-205
- 27 **Hart GJ**, Orr DC, Penn CR, Figueiredo HT, Gray NM, Boehme RE, Cameron JM. Effects of (-) 2',3'-dideoxy-3'-thiacytidine (3TC) 5'-triphosphate on human immunodeficiency virus reverse transcriptase and mammalian DNA polymerase alpha, beta and gamma. *Antimicrob Agents Chemother* 1992; **36**: 1688-1694
- 28 **Chang CN**, Doong SL, Zhou JH, Beach JW, Jeong LS, Chu CK, Tsai CH, Cheng YC, Liotta D, Schinazi R. Deoxycytidine deaminase-resistant stereoisomer is the active form of (\pm)-2', 3'-dideoxy-3'-thiacytidine in the inhibition of hepatitis B virus replication. *J Biol Chem* 1992; **267**: 13938-13942
- 29 **Coates JA**, Cammack N, Jenkinson HJ, Jowett AJ, Jowett MI, Pearson BA, Penn CR, Rouse PL, Viner KC, Cameron JM. (-)-2'-dideoxy-3'-thiacytidine is a potent ,highly selective inhibitor of human immunodeficiency virus type 1 and type 2 replication *in vitro*. *Antimicrob Agents Chemother* 1992; **36**: 733-739
- 30 **Severini A**, Liu XY, Wilson JS, Tyrrell DL. Mechanism of inhibition of duck hepatitis B virus polymerase by (-)- α -L-2', 3'-dideoxy-3'-thiacytidine. *Antimicrob Agents Chemother* 1995; **39**: 1430-1435
- 31 **Doo E**, Liang TJ. Molecular anatomy and pathophysiologic implications of drug resistance in hepatitis B virus infection. *Gastroenterology* 2001; **120**: 1000-1008
- 32 **Gaia S**, Marzano A, Smedile A, Barbon V, Abate ML, Olivero A, Lagget M, Paganin S, Fadda M, Niro G, Rizzetto M. Four years of treatment with Lamivudine: clinical and virological evaluations in HBe antigen-negative chronic hepatitis B. *Aliment Pharmacol Ther* 2004; **20**: 281-287

Science Editor Guo SY Language Editor Elsevier HK

• BRIEF REPORTS •

Genetic polymorphisms of *N*-acetyltransferase 2 and colorectal cancer risk

Lu-Jun He, Yue-Ming Yu, Fang Qiao, Jing-Shan Liu, Xiao-Feng Sun, Ling-Ling Jiang

Lu-Jun He, Ling-Ling Jiang, Department of Biochemistry, Hebei Medical University, Shijiazhuang 050017, Hebei Province, China
Fang Qiao, Jing-Shan Liu, Laboratory of HLA, Hebei Province Blood Center, Shijiazhuang 050071, Hebei Province, China
Yue-Ming Yu, Department of Surgery, No. 4 Hospital of Hebei Medical University, Shijiazhuang 050011, Hebei Province, China
Xiao-Feng Sun, Department of Oncology, Institute of Biomedicine and Surgery, University of Linköping, S-581 85 Linköping, Sweden
Correspondence to: Dr. Ling-Ling Jiang, Department of Biochemistry, Hebei Medical University, Shijiazhuang 050017, Hebei Province, China. guiyang1959@yahoo.com
Telephone: +86-311-6265639 Fax: +86-311-7061014
Received: 2004-10-19 Accepted: 2004-11-26

Abstract

AIM: To identify the distribution of *N*-acetyltransferase 2 (NAT2) polymorphism in Hebei Han Chinese and the effects of the polymorphism on the development of colorectal cancer.

METHODS: We performed a hospital-based case-control study of 237 healthy individuals and 83 colorectal cancer patients of Hebei Han Chinese. DNA was extracted from peripheral blood and cancer tissues. The genotypes of the polymorphisms were assessed by PCR-restriction fragment length polymorphism (RFLP).

RESULTS: There were four NAT2 alleles of WT, M1, M2, and M3 both in the healthy subjects and in the patients, and 10 genotypes of WT/WT, WT/M1, WT/M2, WT/M3, M1/M1, M1/M2, M1/M3, M2/M2, M2/M3, M3/M3. M2 allele was present in 15.61% of healthy subjects and 29.52% of patients ($\chi^2 = 15.31$, $P < 0.0001$), and M3 allele was present in 30.59% of healthy subjects and 16.87% of patients ($\chi^2 = 25.33$, $P < 0.0001$). There were more WT/M2 ($\chi^2 = 34.42$, $P < 0.0001$, odd ratio = 4.99, 95%CI = 2.27-9.38) and less WT/M3 ($\chi^2 = 3.80$, $P = 0.03$) in the patients than in the healthy subjects. In 70.3% of the patients, there was a difference in NAT2 genotype between their tumors and blood cells. Patients had more WT/M2 ($\chi^2 = 5.11$, $P = 0.02$) and less M2/M3 ($\chi^2 = 4.27$, $P = 0.039$) in their blood cells than in the tumors. Furthermore, 53.8% (7/13) of M2/M3 in tumors were from WT/M2 of blood cells.

CONCLUSION: There is a possible relationship between the NAT2 polymorphisms and colorectal cancer in Hebei Han Chinese. The genotype WT/M2 may be a risk factor for colorectal cancer.

Key words: NAT2 gene; Colorectal cancer; RFLP

He LJ, Yu YM, Qiao F, Liu JS, Sun XF, Jiang LL. Genetic polymorphisms of *N*-acetyltransferase 2 and colorectal cancer risk. *World J Gastroenterol* 2005; 11(27): 4268-4271
<http://www.wjgnet.com/1007-9327/11/4268.asp>

INTRODUCTION

Colorectal cancer is one of the common tumors in Hebei Province of China. *N*-acetyltransferase 2 (NAT2) is polymorphic and catalyzes both *N*-acetylation (usually deactivation) and *O*-acetylation (usually activation) of a variety of heterocyclic amine drugs and carcinogens^[1]. Heterocyclic amines which are found mainly in well-cooked meat, require metabolic activation to function as mutagens and animal carcinogens. Enzymes such as cytochrome P4501A2 (CYP1A2) and NAT2 perform this task. Genetic studies in humans have shown that individuals may be classified as rapid or slow acetylators according to the rates at which drugs are acetylated by NAT2^[2]. NAT2 polymorphism is a representative genetic trait of individual's susceptibility to several cancers^[3]. Epidemiological studies suggest that the NAT2 acetylation polymorphisms modify the risk of developing carcinoma of urinary bladder, colorectal and breast cancer, head and neck cancer, pulmonary and prostatic cancer. Associations between slow NAT2 acetylator genotypes and urinary bladder cancer as well as between rapid NAT2 acetylator genotypes and colorectal cancer are the most consistently reported^[3]. However, whether there is a true association between colorectal cancer and NAT2 polymorphism is controversial. Human epidemiological studies suggest that rapid acetylator phenotypes may be associated with higher incidences of colorectal cancer in American populations^[4]. Researchers in UK^[5] found that no significant differences in NAT2 allelic frequencies (WT, M1, M2, M3 alleles) or genotypes are observed between colorectal cancer patients and the healthy population. Ethnic differences exist in NAT2 genotype frequencies that may be a factor in cancer incidence, emphasizing the need to investigate the distribution frequency of NAT2 genotypes and the association of their polymorphism with colorectal cancer in Hebei Han Chinese population.

We identified the distribution of NAT2 polymorphisms in Chinese healthy individuals and colorectal cancer patients from Hebei Province. We also performed a case-control study to investigate whether the NAT2 genetic polymorphism was a risk factor for colorectal cancer in these Chinese population.

MATERIALS AND METHODS

Subjects

We conducted a case-control study of colorectal cancer patients between April 2001 and April 2003. Both patients and controls were Hebei Han Chinese. Eighty-three patients (46 males, 37 females) with histopathologically confirmed diagnosis of colorectal cancer, were recruited from the Department of Surgery at Hebei No. 4 Hospital. Their mean age was 47.5 years (ranging 25-77 years). The control group consisted of 237 (124 males, 113 females) healthy individuals selected from the blood donors in Hebei Province Blood Center. Their average age was 42.6 years (ranging 20-80 years).

DNA extraction

The peripheral blood was treated with EDTA. Tumor samples were obtained from colorectal cancer patients and immediately frozen in liquid nitrogen and stored at -80 °C until used. Genomic DNA was isolated from peripheral leukocytes by PEL-FREEZE reagent protocol or from the tumor samples by the standard procedure of proteinase K/RNase digestion and phenol/chloroform extraction.

Typing NAT2 polymorphism

PCR-RFLP was performed to investigate the NAT2 allele. PCR was performed in 40 µL reaction mixture containing 50-200 ng DNA, 20 mmol/L of each primer, 1.25 mmol/L of dNTPs, 25 mmol/L of MgCl₂, 1 PCR buffer, 5U of thermostable Taq DNA polymerase using a programmable thermocycler. The primer sequences were 5'-GGA ACA AAT TGG ACT TGG-3' and 5'-TCT AGC ATG AAT CAC TCT GC-3'. PCR conditions were 5 min at 95 °C; 35 cycles of 1 min at 95 °C, 1 min at 57 °C and 1.5 min at 72 °C; followed by a final extension for 5 min at 72 °C. After amplification, the 1 093 bp PCR-products were digested with *Kpn*I (M1 allele), *Bam*HI (M3 allele), *Msp*I/*A*luI (M4 allele) for 16-18 h at 37 °C and *Taq*I (M2 allele) for 16-18 h at 65 °C separately in a 25 µL final volume. Digested fragments were then separated by electrophoresis on 20 g/L agarose gel (M1, M3) or 40 g/L agarose gel (M2, M4) and visualized by ethidium bromide staining. All the experiments included positive and negative controls for each studied polymorphism.

Statistical analysis

Statistical analysis was performed with SAS 6.0 for Windows. Hardy-Weinberg equilibrium test was carried out using statistical software for linkage analysis. χ^2 and Fisher's exact test were used for comparisons of frequencies. Associations were expressed as odd ratios (OR) with 95% confidence interval (95%CI). $P < 0.05$ was considered statistically significant.

RESULTS

Polymorphism of NAT2 gene in Hebei Han Chinese

The results of genotype analysis are shown in Figure 1. In 237 healthy and 83 colorectal cancer patients of Hebei Han Chinese, there were four kinds of NAT2 alleles including wild-type gene WT allele and polymorphisms of M1, M2, and M3 alleles (Table 1). No M4 polymorphism was found. Ten genotypes including WT/WT, WT/M1, WT/M2, WT/M3, M1/M1, M1/M2, M1/M3, M2/M2, M2/M3, M3/M3 and their frequencies in both groups are shown in Table 2. M3 (59.67%) was the major polymorphism in healthy group. The distribution of NAT2 genotypes in healthy group was consistent with Hardy-Weinberg equilibrium ($\chi^2 = 7.2533$, $g = 8$, $P > 0.5$). In healthy group, 71.3% and 28.7% were classified as rapid-acetylators genotypes (WT/WT, WT/M_x, $x = 1, 2, 3$) and slow-acetylators genotypes (M_x/M_x), respectively. The frequency of WT/M3 (29.1%) in the rapid-acetylators genotypes was the highest.

The frequency of allele M2 (29.5%) was the highest in the 83 patients, 18 (21.7%) were slow-acetylators genotypes (M_x/M_x), and 65 (78.3%) were rapid-acetylators genotypes (WT/WT, WT/M_x), 35 (53.8%) of them being WT/M2 (Table 2).

Association of NAT2 polymorphism with susceptibility to colorectal cancer in Hebei Han Chinese

M3 allele was present in 30.59% (154/474) of the healthy subjects and in 16.87% (28/166) of the patients ($\chi^2 = 25.33$, $P < 0.0001$). The M2 allele frequency was significantly different between healthy (15.61%) and patient groups (29.52%) ($\chi^2 = 15.31$, $P < 0.0001$). There was no difference in rapid-acetylators or slow-acetylators frequency between healthy and patient groups. However, there was a significant

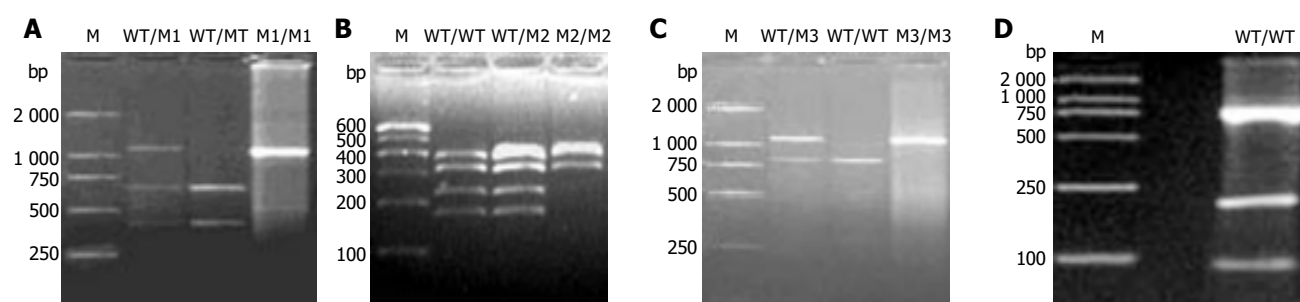


Figure 1 NAT2 genotype analysis by PCR-RFLP. M: DNA Marker (100, 250, 500, 750, 1 000, 2 000 bp); **A**: digest with *Kpn*I (M1 allele) shows wildtype genotype (lane 2: 660 and 433 bp, WT/WT), variant genotype (lane 3: 1 093 bp, M1/M1) and heterozygote genotype (lane 1: 1 093, 660 and 433 bp, WT/M1); **B**: digest with *Taq*I (M2 allele) shows wildtype genotype (lane 1: 380, 317, 226 and 170 bp, WT/WT), variant genotype (lane 3: 396, 380 and

317 bp, M2/M2) and heterozygote genotype (lane 2: 396, 380, 317, 226 and 170 bp, WT/M2); **C**: digest with *Bam*HI (M3 allele) shows wildtype genotype (lane 2: 811 and 282 bp, WT/WT), variant genotype (lane 3: 1 093 bp, M3/M3) and heterozygote genotype (lane 1: 1 093, 811 and 282 bp, WT/M3); **D**: digest with *Msp*I/*A*luI (M4 allele) shows wildtype genotype (lane 1: 759, 189, 91 and 53 bp, WT/WT).

Table 1

Alleles	Healthy controls		Patients	
	Number	Frequency	Number	Frequency
WT	231	0.4874	80	0.4819
M1	24	0.0506	9	0.0542
M2	74	0.1561 ^{1b}	49	0.2952
M3	145	0.3059 ^{2d}	28	0.1687
M4	0	0	0	0
SUM	474	1.0000	166	1.0000

¹ $\chi^2=15.31$, ^b $P<0.0001$ and ² $\chi^2=25.33$, ^d $P<0.0001$ vs patients.

Table 2

	Rapid-acetylase genotype					Slow-acetylase genotype						
	WT/WT	WT/M1	WT/M2	WT/M3	Sum	M1/M1	M1/M2	M1/M3	M2/M2	M2/M3	M3/M3	Sum
Controls <i>n</i>	62	9	29	69	169	1	4	9	5	31	18	68
%	26.2	3.8	12.2	29.1	71.3	0.4	1.7	3.8	2.1	13.1	7.6	28.7
Patients <i>n</i>	15	1	35	14	65	1	2	4	3	6	2	18
%	18.1	1.2	42.2	16.9	78.3	1.2	2.4	4.8	3.6	7.2	2.4	21.7
χ^2	2.20	0.64	34.42	3.80	1.54	0.00	0.00	0.007	0.12	2.06	2.01	1.54
<i>P</i>	0.14	0.42	<0.0001	0.03	0.22	1.00	1.00	0.94	0.73	0.15	0.16	0.22

difference between WT/M2 ($\chi^2=34.42$, $P<0.0001$) and WT/M3 ($\chi^2=3.80$, $P<0.05$) compared to the healthy controls. The risk associated with combinations of NAT2 genotypes is shown in Table 3. The genotype WT/M2 might be a risk factor for colorectal cancer (OR = 4.99, 95%CI = 2.27-9.38).

Comparable analysis of WT/M2 and M2/M3 genotypes in blood cells and cancer tissues of colorectal cancer patients

In 70.4% of patients, there was a difference in NAT2 genotype between tumor tissues and blood cells. The frequency of NAT2 genotypes, especially WT/M2 and M2/M3, was significantly different between tumor tissues and blood cells ($\chi^2=5.11$, $P<0.05$; $\chi^2=4.27$, $P<0.05$, Table 4). The frequency of genotype M2/M3 was 9.3% in

peripheral blood cells and 24.1% in cancer tissue. Furthermore, 53.8% (7/13) of the tumors had M2/M3 while the corresponding blood cells had WT/M2.

DISCUSSION

Human NAT2 is a genetic polymorphism. Different genotypes (WT/WT, WT/Mx, Mx/Mx, x = 1, 2, 3, 4) are composed of different NAT2 alleles (wild type allele WT, mutation allele Mx). According to the intensity of acetyl action, a different genotype shows a different phenotype (rapid-acetylase genotype and slow-acetylase genotype). Genotypes composed of any two mutation alleles (Mx/Mx) show slow-acetylase genotypes, while those consisted of WT/WT or WT/Mx show rapid-acetylase genotypes. Bell

Table 3

Genotypes	Control		Patients		OR (95%CI)
	<i>n</i>	%	<i>n</i>	%	
WT/WT	62	26.2	15	18.1	1.00
WT/M2	29	12.2	35	42.2	4.99 (2.27-9.38)
WT/M1	9	3.8	1	1.2	0.46 (0.05-3.92)
WT/M3	69	29.1	14	16.9	0.84 (0.38-1.88)
WT/WT and WT/Mx	169	71.3	65	78.3	1.59 (0.85-2.99)
Mx/Mx	68	28.7	18	21.7	1.09 (0.51-2.35)

x = 1, 2, 3, 4, OR: odds ratio; CI: confidence interval.

Table 4

	WT/M2		M2/M3		Others	
	<i>n</i>	%	<i>n</i>	%	<i>n</i>	%
Blood cells	23	42.6	5	9.3	26	48.2
Cancer tissues	12	22.2 ¹	13	24.1 ²	29	53.7

¹ $\chi^2=5.11$, $P=0.020$ and ² $\chi^2=4.27$, $P=0.039$ vs blood cells.

et al.^[6], reported that there are significant differences in the frequency of WT, M1, and M4 alleles between Caucasian and African-Americans, while the frequency of M2 and M3 alleles is similar. The M4 allele is not detectable in Caucasian-Americans, while 18% African-Americans carry at least one M4 allele. The frequencies of NAT2 WT, M1, M2, M3, and M4 alleles in Singapore Chinese are 0.51, 0.07, 0.32, 0.10, and 0.00, respectively^[7]. The proportions of rapid and slow acetylators do also vary remarkably between ethnic groups as well as between populations of different geographical origins^[8]. For example, the percentage of slow acetylators is 5% in Canadian Eskimos, over 80% in Egyptians and 90% in Moroccans^[9,10]. Singapore Chinese have 72% of rapid-acetylator genotypes. In our study, four NAT2 alleles (WT, M1, M2, M3) and ten NAT2 genotypes (WT/WT, WT/M1, WT/M2, WT/M3, M1/M1, M1/M2, M1/M3, M2/M2, M2/M3, M3/M3) were found in Hebei Han Chinese. M4 was not present in Hebei Han Chinese, while 29.1% of healthy controls carried at least one M3 allele. Hebei Han Chinese had 71.3% of rapid-acetylator genotypes. The frequencies of the NAT2 M4 allele and rapid-acetylator genotypes are similar in both Hebei Han Chinese and Singapore Chinese, but there are significant differences in the frequencies of WT, M1, M2, and M3 between the two populations.

NAT2 is an important enzyme for the detoxification and/or bioactivation of several carcinogenic arylamines, its activity directly affects metabolic response of carcinogen *in vivo* and intensity of toxic reaction^[11]. It was reported that the polymorphism of NAT2 gene is associated with the occurrence of colorectal cancer^[12]. Genetic epidemiological studies suggest that rapid acetylator phenotype may be associated with the higher incidence of colorectal cancer in the UK populations^[12]. Lee *et al.*^[7], also showed that the rapid acetylator genotype is associated with cancer occurring in Singapore Chinese. However, our results suggest that rapid-acetylator genotype or slow-acetylator genotype does not appear to be associated with colorectal cancer development, but there is an association between the WT/M2 genotype and colorectal cancer. The M2 allele was more frequent in the patients than in the healthy subjects ($\chi^2 = 15.31$, $P < 0.0001$). Odds ratio (OR) for genotype WT/M2 was 4.99 (95%CI = 2.27-9.38). The data suggest that genotype WT/M2 may be a risk factor for colorectal cancer in Hebei Han Chinese.

Schnakenberg *et al.*^[13], detected the loss of heterozygosity in slow and rapid acetylator genotypes in bladder cancer patients. They observed allelic loss at the NAT2 locus in 11 of 60 tumor samples (18.3%), but not in controls. The

present study also demonstrated changes of NAT2 genotypes in 70.4% of the tumor specimens. The rising M2/M3 in tumors seems to be transformed from genotype WT/M2 of blood cells, and also suggests that WT/M2 may be a risk factor for colorectal cancer. Our findings may contribute to the early diagnosis of colorectal cancer.

REFERENCES

- 1 Pande JN, Pande A, Singh SP. Acetylator status, drug metabolism and disease. *Natl Med J India* 2003; **16**: 24-26
- 2 Hein DW. Molecular genetics and function of NAT1 and NAT2: role in aromatic amine metabolism and carcinogenesis. *Mutant Res* 2002; **30**: 65-77
- 3 Hein DW, Doll MA, Fretland AJ, Leff MA, Webb SJ, Xiao GH, Devanaboyina US, Nangju NA, Feng Y. Molecular genetics and epidemiology of the NAT1 and NAT2 acetylation polymorphisms. *Cancer Epidemiol Biomarkers Prev* 2000; **9**: 29-42
- 4 Rodriguez JW, Kirilin WG, Ferguson RJ, Doll MA, Gray K, Rustan TD, Lee ME, Kemp K, Urso P, Hein DW. Human acetylator genotype: relationship to colorectal cancer incidence and arylamine N-acetyltransferase expression in colon cytosol. *Arch Toxicol* 1993; **67**: 445-452
- 5 Sachse C, Smith G, Wilkie MJ, Barrett JH, Waxman R, Sullivan F, Forman D, Bishop DT, Wolf CR. A pharmacogenetic study to investigate the role of dietary carcinogens in the etiology of colorectal cancer. *Carcinogenesis* 2002; **23**: 1839-1849
- 6 Bell DA, Taylor JA, Butler MA, Stephens EA, Wiest J, Brubaker LH, Kadlubar FF, Lucier GW. Genotype/phenotype discordance for human arylamine N-acetyltransferase (NAT2) reveals a new slow-acetylator allele common in African-Americans. *Carcinogenesis* 1993; **14**: 1689-1692
- 7 Lee EJ, Zhao B, Seow-Choen F. Relationship between polymorphism of N-acetyltransferase gene and susceptibility to colorectal carcinoma in a Chinese population. *Pharmacogenetics* 1998; **8**: 513-517
- 8 Fretland AJ, Leff MA, Doll MA, Hein DW. Functional characterization of human N-acetyltransferase 2 (NAT2) single nucleotide polymorphisms. *Pharmacogenetics* 2001; **11**: 207-215
- 9 Weber WW, Hein DW. N-acetylation pharmacogenetics. *Pharmacol Rev* 1985; **37**: 25-79
- 10 Evans DA. N-acetyltransferase. *Pharmacol Ther* 1989; **42**: 157-234
- 11 Zhao B, Seow A, Lee EJ, Lee HP. Correlation between acetylation phenotype and genotype in Chinese women. *Eur J Clin Pharmacol* 2000; **56**: 689-692
- 12 Barrett JH, Smith G, Waxman R, Gooderham N, Lightfoot T, Garner RC, Augustsson K, Wolf CR, Bishop DT, Forman D. Colorectal Cancer Study Group. Investigation of interaction between N-acetyltransferase 2 and heterocyclic amines as potential risk factors for colorectal cancer. *Carcinogenesis* 2003; **24**: 275-282
- 13 Schnakenberg E, Ehlers C, Feyerabend W, Werdin R, Hubotter R, Dreikorn K, Schloot W. Genotyping of the polymorphic N-acetyltransferase (NAT2) and loss of heterozygosity in bladder cancer patients. *Clin Genet* 1998; **53**: 396-402

• BRIEF REPORTS •

Expression of albumin, IGF-1, IGFBP-3 in tumor tissues and adjacent non-tumor tissues of hepatocellular carcinoma patients with cirrhosis

Shi-Min Luo, Wei-Min Tan, Wei-Xiong Deng, Si-Min Zhuang, Jian-Wei Luo

Shi-Min Luo, Wei-Min Tan, Wei-Xiong Deng, Si-Min Zhuang, Jian-Wei Luo, Department of Cadre Surgery, The First Municipal People's Hospital of Guangzhou, Guangzhou 510180, Guangdong Province, China

Correspondence to: Wei-Min Tan, Department of Cadre Surgery, The First Municipal People's Hospital of Guangzhou, 1 Panfu Lu, Guangzhou 510180, Guangdong Province, China. lsmin@gzsums.edu.cn
Telephone: +86-20-81048285 Fax: +86-20-81048285

Received: 2004-11-12 Accepted: 2005-01-05

Abstract

AIM: To explore the expression of albumin (ALB), insulin-like growth factor (IGF)-1, and insulin-like growth factor binding protein (IGFBP)-3 in tumor tissues and adjacent non-tumor tissues of hepatocellular carcinoma (HCC) patients with cirrhosis.

METHODS: Twenty-four HCC patients with cirrhosis who underwent hepatectomy were studied. ALB mRNA, IGF-1 mRNA, and IGFBP-3 mRNA in liver tissues (including tumor tissues and adjacent non-tumor tissues) were detected by reverse transcriptase-polymerase chain reaction (RT-PCR). Liver Ki67 immunohistochemistry staining was studied. At the same time, 12 patients with cholelithiasis or liver angioma who underwent operation were segregated as normal control.

RESULTS: In HCC patients with cirrhosis, hepatic ALB mRNA, IGF-1 mRNA, and IGFBP-3 mRNA of tumor tissues or adjacent non-tumor tissues were lower than the normal liver tissues, while in tumor tissues, hepatic ALB mRNA and IGFBP-3 mRNA were lower, hepatic IGF-1 mRNA was higher than in adjacent non-tumor tissues. Liver Ki67 labeling index (Ki67 LI) in tumor tissues or adjacent non-tumor tissues were higher than that in the normal liver tissues, while in tumor tissues it was higher than that in adjacent non-tumor tissues.

CONCLUSION: Imbalance of IGF-1 and IGFBP-3 may play a role in hepatocarcinogenesis and tumor development of liver cirrhosis patients.

© 2005 The WJG Press and Elsevier Inc. All rights reserved.

Key words: Hepatocellular carcinoma; Insulin growth factor-1; Insulin-like growth factor binding protein-3

Luo SM, Tan WM, Deng WX, Zhuang SM, Luo JW. Expression

of albumin, IGF-1, IGFBP-3 in tumor tissues and adjacent non-tumor tissues of hepatocellular carcinoma patients with cirrhosis. *World J Gastroenterol* 2005; 11(27): 4272-4276
<http://www.wjgnet.com/1007-9327/11/4272.asp>

INTRODUCTION

Extensive research on insulin-like growth factors (IGFs) during the last decade has greatly advanced our understanding of these peptides that are not only the endocrine mediators of growth hormone (GH)-induced metabolic and anabolic actions but also polypeptides that act in a paracrine and autocrine manner to regulate cell growth, differentiation, apoptosis, and transformation^[1]. In biological fluids, IGFs are complexed with specific binding proteins (IGFBPs)^[2-4]. The functions of IGFBPs are to modulate the biologic activity of IGFs. Imbalance of these diverse processes may preferentially favor uncontrolled cell proliferation leading to malignant transformation. Recent evidence from epidemiologic studies has confirmed an association between serum levels of IGFs and several malignancies at the population level and has resulted in a resurgence of scientific interest in this field.

IGF-1 and IGF-2 are single chain polypeptides, which have 62% homology with proinsulin. Serum concentrations of IGF-2 are higher than IGF-1 (400-600 ng/mL *vs* 100-200 ng/mL) in humans of all ages, are relatively stable after puberty and are not regulated by GH. IGF-2 has proliferative and antiapoptotic actions similar to IGF-1 since its effects are exerted by the IGF-1R^[5]. However, IGF-2 plays a fundamental role in embryonic and fetal growth, whereas its role in the postnatal period is less important as it is substituted by IGF-1.

The liver is the central organ of the endocrine GH/IGF-1 axis. GH is secreted by the somatotrophic cells of the anterior pituitary, transported in the circulation by the high affinity growth hormone binding protein and acts through the hepatic GH receptor to regulate the production of the potent mitogenic growth factor IGF-1. The availability of IGF-1 to its tissue receptors is further regulated by the high affinity IGFBPs (IGFBP-1 to -6) of which the liver is also a significant source, with IGFBP-3 being most abundant^[6]. Epidemiologic studies have found high circulating IGF-1 and low IGFBP-3 levels to be associated with an increased risk of developing breast, endometrial, lung, colorectal, and prostate cancer. IGFBP-3 was reported to be a growth suppressor in variable pathways^[7,8].

Hepatocellular carcinoma (HCC) is the fifth most common cancer worldwide, with estimated 467 000 new cases per year^[9]. HCC is one of the most common malignant tumors in the world. Since the 1990s HCC has become the second killer in various cancers in China. Most HCC cases arise in HBV and liver cirrhosis. In carcinogenesis induced by viral infection, the frequency of gene mutation is considered to increase as the mitotic activity of cells gets greater. Under conditions that increase the proliferative activity of hepatocytes such as chronic hepatitis and liver cirrhosis, the probability of mutation increases, resulting in increased occurrence of HCC.

Albumin (ALB) is the major protein produced in the liver, and its primary functions include transportation of a variety of substances in the blood and maintenance of osmotic pressure. In normal adults, ALB constitutes more than 65% of the total plasma protein content. The plasma concentration of ALB reflects its synthesis, degradation, and distribution. Thus, the expression of hepatic ALB mRNA was more useful in reflecting the degree of liver injury or liver functional reserve than serum ALB.

In this study, we used the reverse transcriptase-polymerase chain reaction (RT-PCR) technique to detect ALB mRNA, IGF-1 mRNA, IGFBP-3 mRNA in tumor tissues and adjacent non-tumor tissues of HCC patients with cirrhosis. At the same time, we have immunochemically detected Ki67 antigen which appears in all phases of the cell cycle of proliferating cells but is negative in G₀^[10] on paraffinized section by microwave antigen retrieval method and compared the proliferative activity between adjacent non-tumor tissue as well as tumor tissues. We explored the roles of IGF-1 and IGFBP-3 in hepatocarcinogenesis and tumor development of liver cirrhosis patients.

MATERIALS AND METHODS

Patients and tissue samples

Of the patients at our department who underwent curative resection for HCC with liver cirrhosis between September 2002 and June 2003. Curative resection was defined as complete resection of all macroscopically detectable tumor with histological tumor clearance (the entire tumor mass was included in the surgical specimen without exposure of tumor cells on the cut edge). At the time of study entry, the inclusion criteria had no evidence of endocrine disease. Twenty-four HCC patients with liver cirrhosis who underwent hepatectomy were studied. At the same time, 12 patients with cholelithiasis or liver angioma who underwent operation were segregated as normal control and these patients had no liver cirrhosis and endocrine disease.

Liver samples (including HCCs and adjacent non-tumor tissues) were excised at the operation, immediately freeze clamped with liquid nitrogen, and stored at -70 °C for analysis of ALB mRNA, IGF-1 mRNA, and IGFBP-3 mRNA. For histological examination, some liver samples were fixed in 10% neutral-buffered formalin, embedded in paraffin.

Reverse transcriptase polymerase chain reaction (RT-PCR)

RT-PCR was performed to measure the expression levels

of ALB mRNA, IGF-1 mRNA, and IGFBP-3 mRNA in liver tissues. The primers used were deduced from the cDNA sequence. The sequences of the primers for ALB sense and antisense were 5'-CCCAAGTGTCAACTCCAAC-3' (sense) and 5'-GCAGGTCTCCTTATCGTCAG-3' (antisense), a 456 bp long fragment was amplified. The sequences of the primers for IGF-1 sense and antisense were 5'-AGCAGTCTTCCAACCCAATTA-3' (sense) and 5'-CACGGACAGAGCGAGCTG-3' (antisense), a 355 bp long fragment was amplified. The sequences of the primers for IGFBP-3 sense and antisense were 5'-ATATGGTCCCTGCCGTAGA-3' (sense) and 5'-AAATCGAGGCTGTAGCCAG-3' (antisense), a 345 bp long fragment was amplified. The sequences of the primers for β -actin sense and antisense were 5'-ACTCTTCCAGCCTTCCTTCCT-3' (sense) and 5'-TCACCTTCACCGTTCAGTTT-3' (antisense), a 513 bp long fragment was amplified.

Total RNA was extracted from frozen liver specimens by the guanidinium isothiocyanate method. The RNA was quantified and checked for purity by spectrophotometry at 260 and 280 nm. Aliquots of total RNA were reverse transcribed using *SperSriptII* Reverse Transcriptase (Invitrogen Corp.) and subsequently amplified by PCR using the Taq DNA polymerase (Promega Corp.).

The PCR was carried out in 25 μ L of reaction mixture containing 0.5 μ L cDNA template, 2.5 μ L 10 \times PCR-Buffer, 1.5 μ L 25 mmol/L MgCl₂, 0.5 μ L 10 mmol/L dNTPs, 0.5 μ L 10 μ mol/L ALB or IGF-1 or IGFBP-3 primers, 0.15 μ L 10 μ mol/L β -actin primers, 0.5 μ L 5 IU/ μ L Taq DNA polymerase. The mixture was heated for 5 min at 94 °C for initial DNA denaturation, followed by 30 cycles of denaturation (at 94 °C for 45 s), annealing (ALB at 50 °C for 45 s, IGF-1 at 48 °C for 45 s, IGFBP-3 at 55 °C for 45 s), polymerization (at 72 °C for 1 min) and then a final extension of 10 min at 72 °C. PCR reactions were stored frozen until analysis by agarose gel electrophoresis.

PCR reactions were electrophoresed on 1.5% agarose gel, stained with ethidium bromide and quantitated using the interactive build analysis system. The band intensity of the ALB or IGF-1 or IGFBP-3 was compared with the band intensity of the β -actin, and the amount of ALB mRNA, IGF-1 mRNA, and IGFBP-3 mRNA was estimated.

Immunohistochemistry

Two-step immunohistochemical staining technique was used. Main reagent included rabbit polyclonal antibody Ki67 Ab-4 (Neomarkers Corp.) and PV-6000 PicTureTM Kits. Briefly, sections were deparaffinized, rehydrated, and then immersed in 0.1 mol/L citric acid buffer (pH 6.0) and boiled for 5-10 min in a microwave oven. The slides were then rinsed gently with PBS at pH 7.2-7.4, and treated with 0.3% hydrogen peroxide in absolute methanol for 1 h at room temperature to remove endogenous peroxidase. The sections were then incubated with the primary antibody Ki67 Ab-4 (1:200 dilution) for 30 min at 37 °C. After rinsing thrice with PBS, each for 2 min, the sections were incubated with PV-6000 for 30 min at 37 °C. They were then rinsed thrice with PBS for 2 min, and visualized with DAB. Finally, the sections were then counterstained with hematoxylin.

On each slide, Ki67-positive nuclei were evaluated by

means of light microscopy at 400 magnification. A minimum of 1 000 cells, evaluated through a minimum of 200 cells per field in five different fields. The Ki67 labeling index (Ki67 LI) is the number (%) of positive cells.

Statistical analysis

Data are expressed as mean \pm SE. The statistical software SPSS 10.0 was used. Statistical significance was set at $P<0.05$.

RESULTS

In HCC patients with cirrhosis, hepatic ALB mRNA, IGF-1 mRNA, IGFBP-3 mRNA of tumor tissues or adjacent non-tumor tissues were lower than the normal liver tissues, while in tumor tissues, hepatic ALB mRNA and IGFBP-3 mRNA were lower, hepatic IGF-1 mRNA was higher than in adjacent non-tumor tissues. Liver Ki67 LI in tumor tissues was higher than that in adjacent non-tumor tissues, while in adjacent non-tumor tissues it was higher than that in the normal liver tissues (Table 1).

Table 1 Comparison of hepatic ALB mRNA, IGF-1 mRNA, IGFBP-3 mRNA and liver Ki67 LI

	<i>n</i>	ALB mRNA	IGF-1 mRNA	IGFBP-3 mRNA	Liver Ki67 LI (%)
Normal liver tissues	12	0.69 \pm 0.05	0.95 \pm 0.02	2.02 \pm 0.04	0 \pm 0
Tumor tissues	24	0.38 \pm 0.01 ^a	0.76 \pm 0.03 ^a	0.45 \pm 0.13 ^a	17.3 \pm 5.9 ^a
Adjacent non-tumor tissues	24	0.50 \pm 0.05 ^{a,c}	0.43 \pm 0.06 ^{a,c}	0.72 \pm 0.17 ^{a,c}	0.2 \pm 0.1 ^{a,c}

^a $P<0.05$, tumor tissues or adjacent non-tumor tissues vs normal liver tissues;

^c $P<0.05$, adjacent non-tumor tissues vs tumor tissues.

DISCUSSION

The liver is probably the major source of circulating IGF-1 with GH confirmed as the dominant regulator of IGF-1 gene expression and serum levels in human disease^[11-13]. IGF-1 is an important anabolic polypeptide with various effects. IGF-1 synthesis is disturbed in liver cirrhosis and reflects the severity of the clinical stage. It represents a good marker of hepatic function. The etiology of cirrhosis does not seem to influence its levels^[14]. Serum IGFBP-3 proves to be a better marker for the hepatic synthetic capacity than serum ALB or cholinesterase^[15]. Serum IGF-1, IGF-2, and IGFBP-3 may provide a new dimension in the assessment of liver dysfunction. Combined detection of serum IGF-1, IGF-2, and IGFBP-3 with Child-Pugh score is more effective in predicting prognosis than Child-Pugh score alone.

Giovannucci presented a model integrating nutrition, insulin and IGF-1 physiology ("bioactive" IGF-1), and carcinogenesis based on the following: (1) insulin and the IGF-1 axis function in an integrated fashion to promote cell growth and survival; (2) chronic exposure to these growth properties enhances carcinogenesis; and (3) factors that influence bioactive IGF-1 will affect cancer risk. The model presented here summarizes the data that chronic exposure to high levels of insulin and IGF-1 may mediate many of the risk factors for some cancers that are high in

Western populations. This hypothesis may help explain some of the epidemiologic patterns observed for these cancers, both from a cross-national perspective and within populations^[16]. In HCC, HBV stimulates IGF-1R expression^[17] and enhances IGF-2 gene expression^[18]. Hepatitis C virus has also been related to increased IGF-2 transcription in HCC^[19]. HCC is associated with a higher IGF-1:IGFBP-3 ratio than that found in patients with liver cirrhosis and a similar degree of liver failure^[20].

IGF-1 and IGFBP-3 play a crucial role in the regulation of growth, cellular proliferation and transformation, and apoptosis. The local tissue expression of IGF-1 and IGFBP-3 has been associated with tumor grade, pathologic stage, and disease progression for patients with various malignancies. Epidemiologic studies have found high circulating IGF-1 and low IGFBP-3 levels to be associated with an increased risk of developing breast, endometrial, lung, colorectal, and prostate cancer. IGFBP-3 was reported to be a growth suppressor in variable pathways^[7,8]. In the IGF receptor dependent pathway, IGFBP-3 binds to IGF-1 and 2 and suppresses its growth signal. In the IGF receptor independent pathways, the IGFBP-3 mediates wide varieties of growth suppression signal.

This study showed hepatic IGF-1 mRNA, IGFBP-3 mRNA of tumor tissues or adjacent non-tumor tissues were lower than the normal liver tissues, while in tumor tissues, hepatic IGFBP-3 mRNA was lower but hepatic IGF-1 mRNA was higher than in adjacent non-tumor tissues. Thus, imbalance of IGF-1 and IGFBP-3 are thought to be important in hepatocarcinogenesis and tumor development of liver cirrhosis patients. IGFBP-3 mRNA which decreased in local tissues may take part in important roles in carcinogenesis. As the IGFBP-3 is produced mainly in the liver, IGFBP-3 may play an important role in the carcinogenesis of HCC. IGFBP-3 functions as a general mediator of growth inhibitory and apoptosis-inducing pathways.

IGFBP-3 is the most abundant IGFBP in human serum and has been shown to be a growth inhibitory, apoptosis-inducing molecule, capable of acting via IGF-dependent and IGF-independent mechanisms. Over the last decade, several clinical studies have proposed that individuals with IGFBP-3 levels in the upper normal range may have a decreased risk for certain common cancers. This includes evidence of a protective effect against breast, prostate, colorectal, and lung cancer. In addition, a series of *in vitro* studies and animal experiments point towards an important role for IGFBP-3 in the regulation of cell growth and apoptosis. Epidemiologic and experimental evidence suggesting a role for IGFBP-3 as an anti-cancer molecule^[21]. At the intracellular level this may either involve modulation of the bcl-2/bax ratio^[22] or the p53 protein^[23]. Kuemmerle *et al.*, reported that endogenous IGFBP-3 directly inhibits proliferation of human intestinal smooth muscle cells by activation of TGF-betaRI and Smad 2, an effect which is independent of its effect on IGF-1 stimulated growth^[24]. Interestingly, IGFBP-3 has been localized in the nucleus, implying a more direct transcriptional regulatory role, but it remains largely unknown how extracellular IGFBP-3 enters the cell^[25].

The liver has the unique capacity to regulate its growth

and mass both in humans and in animals. This property is particularly remarkable because hepatocytes are cells which in their normal state rarely divide. However, their proliferative capacity and the ability of the liver to adapt to variable metabolic demands are not lost. To assess the proliferating cells, we have immunochemically detected Ki-67 nuclear antigen. Characterization of the Ki-67 antibody revealed an interesting staining pattern. The antibody was reactive with a nuclear structure present exclusively in proliferating cells. A detailed cell cycle analysis revealed that the antigen was present in the nuclei of cells in the G₁, S, and G₂ phases of the cell division cycle as well as in mitosis. Quiescent or resting cells in the G₀ phase did not express the Ki-67 antigen. Because the Ki-67 antigen was present in all proliferating cells (normal and tumor cells), it soon became evident that the presence of this structure is an excellent operational marker to determine the growth fraction of a given cell population. For this reason, antibodies against the Ki-67 protein were increasingly used as diagnostic tools in cell proliferation.

ALB is a ubiquitous protein that is synthesized only by hepatocytes. ALB is a polypeptide chain of 580 amino acids that is produced by hepatocytes^[26]. The number of ALB molecules produced by a single hepatocyte has been estimated to be ~40 000^[27]. The expression of ALB gene is reduced in various liver diseases and the degree of reduction in the hepatic ALB mRNA level is generally correlated with the severity of the disease^[28]. This study showed that liver Ki67 LI in tumor tissues was higher than that in adjacent non-tumor tissues, which was higher than that in normal liver tissues, but hepatic ALB mRNA in tumor tissues was lower than that in adjacent non-tumor tissues, which was higher than that in normal liver tissues. It represented that proliferating hepatocytes or tumor tissues had less function.

The IGF system performs a fundamental role in the regulation of cellular proliferation, differentiation, and apoptosis. Disruptions in the balance of IGF system components leading to excessive proliferation and survival signals have been implicated in the development of different tumor types. This study represented the imbalance of IGF-1 and IGFBP-3 which are thought to be important in hepatocarcinogenesis and tumor development of liver cirrhosis patients. Epidemiologic evidence indicates that increased levels of IGF-I, reduced levels of IGFBP-3 or an increased ratio of IGF-1 to IGFBP-3 in the circulation are associated with an increased risk for the development of several common cancers, including those of the breast, prostate, lung, and colon. The results of preclinical studies indicate that a diversity of interventions which antagonize IGF-1R signaling or augment IGFBP-3 function inhibit tumor cell growth in models of human cancers. A more comprehensive understanding of the interplay between cellular targets of the IGF system and antineoplastic agents will facilitate the development of novel strategies for the prevention and treatment of cancer^[29]. Thus, the GH/IGF-I axis may be a target for cancer prevention and treatment.

REFERENCES

- Holly JM, Wass JA. Insulin-like growth factors: autocrine, paracrine or endocrine? New perspectives of the somatome-
- din hypothesis in the light of recent developments. *J Endocrinol* 1989; **122**: 611-618
- Zapf J, Waldvogel M, Froesch ER. Binding of nonsuppressible insulinlike activity to human serum. Evidence for a carrier protein. *Arch Biochem Biophys* 1975; **168**: 638-645
- Martin JL, Baxter RC. Insulin-like growth factor-binding protein from human plasma. Purification and characterization. *J Biol Chem* 1986; **261**: 8754-8760
- D'Ercole AJ, Stiles AD, Underwood LE. Tissue concentrations of somatomedin C: further evidence for multiple sites of synthesis and paracrine or autocrine mechanisms of action. *Proc Natl Acad Sci USA* 1984; **81**: 935-939
- O'Dell SD, Day IN. Insulin-like growth factor II (IGF-II). *Int J Biochem Cell Biol* 1998; **30**: 767-771
- Rajaram S, Baylink DJ, Mohan S. Insulin-like growth factor-binding proteins in serum and other biological fluids: regulation and functions. *Endocr Rev* 1997; **18**: 801-831
- De Mellow JS, Baxter RC. Growth hormone-dependent insulin-like growth factor (IGF) binding protein both inhibits and potentiates IGF-I-stimulated DNA synthesis in human skin fibroblasts. *Biochem Biophys Res Commun* 1988; **156**: 199-204
- Valentinis B, Bhalra A, DeAngelis T, Baserga R, Cohen P. The human insulin-like growth factor (IGF) binding protein-3 inhibits the growth of fibroblasts with a targeted disruption of the IGF-I receptor gene. *Mol Endocrinol* 1995; **9**: 361-367
- Murray CJ, Lopez AD. Mortality by cause for eight regions of the world: Global Burden of Disease Study. *Lancet* 1997; **349**: 1269-1276
- Gerdes J, Schwab U, Lemke H, Stein H. Production of a mouse monoclonal antibody reactive with a human nuclear antigen associated with cell proliferation. *Int J Cancer* 1983; **31**: 13-20
- Mathews LS, Norstedt G, Palmiter RD. Regulation of insulin-like growth factor I gene expression by growth hormone. *Proc Natl Acad Sci USA* 1986; **83**: 9343-9347
- Kratzsch J, Blum WF, Schenker E, Keller E, Jahreis G, Hausteil B, Ventz M, Rotzsch W. Measurement of insulin-like growth factor I (IGF-I) in normal adults, patients with liver cirrhosis and acromegaly: experience with a new competitive enzyme immunoassay. *Exp Clin Endocrinol* 1993; **101**: 144-149
- Schoenle EJ, Zapf J, Prader A, Torresani T, Werder EA, Zachmann M. Replacement of growth hormone (GH) in normally growing GH-deficient patients operated for craniopharyngioma. *J Clin Endocrinol Metab* 1995; **80**: 374-378
- Vyzantiadis T, Theodoridou S, Gioulema O, Harsoulis P, Evgenidis N, Vyzantiadis A. Serum concentrations of insulin-like growth factor-I (IGF-I) in patients with liver cirrhosis. *Hepatology* 2003; **50**: 814-816
- Sidlova K, Pechova M, AKotaska K, Prusa R. Insulin-like growth factor binding protein-3 in patients with liver cirrhosis. *Physiol Res* 2002; **51**: 587-590
- Giovannucci E. Nutrition, insulin, insulin-like growth factors and cancer. *Horm Metab Res* 2003; **35**: 694-704
- Kim SO, Park JG, Lee YI. Increased expression of the insulin-like growth factor I (IGF-I) receptor gene in hepatocellular carcinoma cell lines: implications of IGF-I receptor gene activation by hepatitis B virus X gene product. *Cancer Res* 1996; **56**: 3831-3836
- Kang-Park S, Lee JH, Shin JH, Lee YI. Activation of the IGF-II gene by HBV-X protein requires PKC and p44/p42 map kinase signalings. *Biochem Biophys Res Commun* 2001; **283**: 303-307
- Tanaka S, Takenaka K, Matsumata T, Mori R, Sugimachi K. Hepatitis C virus replication is associated with expression of transforming growth factor-alpha and insulin-like growth factor-II in cirrhotic livers. *Dig Dis Sci* 1996; **41**: 208-215
- Mattera D, Capuano G, Colao A, Pivonello R, Manguso F, Puzziello A, D'Agostino L. Increased IGF-I: IGFBP-3 ratio in patients with hepatocellular carcinoma. *Clin Endocrinol* 2003; **59**: 699-706
- Ali O, Cohen P, Lee KW. Epidemiology and biology of insulin-like growth factor binding protein-3 (IGFBP-3) as an anti-

- cancer molecule. *Horm Metab Res* 2003; **35**: 726-733
- 22 **Butt AJ**, Firth SM, King MA, Baxter RC. Insulin-like growth factor-binding protein-3 modulates expression of Bax and Bcl-2 and potentiates p53-independent radiation-induced apoptosis in human breast cancer cells. *J Biol Chem* 2000; **275**: 39174-39181
- 23 **Williams AC**, Collard TJ, Perks CM, Newcomb P, Moorghen M, Holly JM, Paraskeva C. Increased p53-dependent apoptosis by the insulin-like growth factor binding protein IGFBP-3 in human colonic adenoma-derived cells. *Cancer Res* 2000; **60**: 22-27
- 24 **Kuemmerle JF**, Murthy KS, Bowers JG. IGFBP-3 activates TGF-beta receptors and directly inhibits growth in human intestinal smooth muscle cells. *Am J Physiol Gastrointest Liver Physiol* 2004; **287**: G795-802
- 25 **Moschos SJ**, Mantzoros CS. The role of the IGF system in cancer: from basic to clinical studies and clinical applications. *Oncology* 2002; **63**: 317-332
- 26 **Yamaguchi K**, Nalesnik MA, Carr BI. *In situ* hybridization of albumin mRNA in normal liver and liver tumors: identification of hepatocellular origin. *Virchows Arch B Cell Pathol Incl Mol Pathol* 1993; **64**: 361-365
- 27 **Sell S**, Thomas K, Michalson M, Salatrepat J, Bonner J. Control of albumin and alpha-fetoprotein expression in rat liver and in some transplantable hepatocellular carcinomas. *Biochim Biophys Acta* 1979; **564**: 173-178
- 28 **Ozaki I**, Motomura M, Setoguchi Y, Fujio N, Yamamoto K, Kariya T, Sakai T. Albumin mRNA expression in human liver diseases and its correlation to serum albumin concentration. *Gastroenterol Jpn* 1991; **26**: 472-476
- 29 **Jerome L**, Shiry L, Leyland-Jones B. Deregulation of the IGF axis in cancer: epidemiological evidence and potential therapeutic interventions. *Endocr Relat Cancer* 2003; **10**: 561-578

Science Editor Guo SY Language Editor Elsevier HK

• BRIEF REPORTS •

Nuclear factor-kappaB activation on the reactive oxygen species in acute necrotizing pancreatitis rats

Jin Long, Na Song, Xi-Ping Liu, Ke-Jian Guo, Ren-Xuan Guo

Jin Long, Na Song, Xi-Ping Liu, Ke-Jian Guo, Ren-Xuan Guo, Department of Surgery, The First Affiliated Hospital, China Medical University, Shenyang 110001, Liaoning Province, China
Correspondence to: Jin Long, MD, Department of Surgery, The First Affiliated Hospital, China Medical University, Shenyang 110001, Liaoning Province, China. ljcmu@sina.com
Telephone: +86-24-23256666-6237 Fax: +86-24-22717355
Received: 2004-12-30 Accepted: 2005-01-12

Abstract

AIM: To investigate the potential role of nuclear factor kappa-B (NF- κ B) activation on the reactive oxygen species in rat acute necrotizing pancreatitis (ANP) and to assess the effect of pyrrolidine dithiocarbamate (PDTC, an inhibitor of NF- κ B).

METHODS: Rat ANP model was established by retrograde injection of 5% sodium taurocholate into biliopancreatic duct. Rats were randomly assigned to three groups (10 rats each): Control group, ANP group and PDTC group. At the 6th h of the model, the changes of the serum amylase, nitric oxide (NO), malondialdehyde (MDA), superoxide dismutase (SOD) and pancreatic morphological damage were observed. The expressions of inducible nitric oxide (iNOS) were observed by SP immunohistochemistry. And the expressions of NF- κ B p65 subunit mRNA were observed by hybridization *in situ*.

RESULTS: Serum amylase and NO level decreased significantly in ANP group as compared with PDTC administrated group [(7 170.40 \pm 1 308.63) U/L vs (4 074.10 \pm 1 719.78) U/L, P <0.05], [(76.95 \pm 9.04) μ mol/L vs (65.18 \pm 9.02) μ mol/L, P <0.05] respectively. MDA in both ANP and PDTC group rose significantly over that in control group [(9.88 \pm 1.52) nmol/L, (8.60 \pm 1.41) nmol/L, vs (6.04 \pm 1.78) nmol/L, P <0.05], while there was no significant difference between them. SOD levels in both ANP and PDTC group underwent a significant decrease as compared with that in control [(3 214.59 \pm 297.74) NU/mL, (3 260.62 \pm 229.44) NU/mL, vs (3 977.80 \pm 309.09) NU/mL, P <0.05], but there was no significant difference between them. Though they were still higher than those in Control group, pancreas destruction was slighter in PDTC group, iNOS expression and NF- κ B p65 subunit mRNA expression were lower in PDTC group as compared with ANP group.

CONCLUSION: We conclude that correlation among NF- κ B activation, serum amylase, reactive oxygen species level and tissue damage suggests a key role of NF- κ B in the pathogenesis of ANP. Inhibition of NF- κ B activation

may reverse the pancreatic damage of rat ANP and the production of reactive oxygen species.

© 2005 The WJG Press and Elsevier Inc. All rights reserved.

Key words: Pancreatitis; Acute necrotizing; Nuclear factor-kappaB; Reactive oxygen species

Long J, Song N, Liu XP, Guo KJ, Guo RX. Nuclear factor-kappaB activation on the reactive oxygen species in acute necrotizing pancreatitis rats. *World J Gastroenterol* 2005; 11(27): 4277-4280

<http://www.wjgnet.com/1007-9327/11/4277.asp>

INTRODUCTION

Acute pancreatitis is clinically classified into mild and severe forms. Mild or edematous acute pancreatitis is a self-limiting disease with a low complication and mortality rate. However, ANP has an unacceptably high morbidity and mortality rate. Multiple therapeutic modalities have been suggested for acute pancreatitis, but none has been unambiguously proven to be effective yet. The major problem is that the pathophysiology of the disease is not fully understood^[1,2].

Oxygen free radicals are molecules produced continuously in cells by several mechanisms. The generation of oxygen free radicals is physiologic. In most circumstances, oxygen free radicals are neutralized immediately by enzymatic scavengers. But when formation of oxygen free radicals overwhelms radical neutralization in cells, oxidative stress occurs. As they are very reactive, they react well with all biological substances such as proteins, polysaccharides, and nucleic acids, resulting in tissue injury. It has been suggested that oxygen free radicals are responsible for a wide variety of diseases or conditions, for they play an important role in the pathogenesis of pancreatitis in some experimental models, and they are involved in the initiation of pancreatitis. Also, it was reported that oxygen free radicals acted as important mediators of tissue damage in experimental acute pancreatitis^[3,4].

Nuclear factor kappa-B (NF- κ B) is a sequence-specific transcription factor known to be involved in inflammatory and immune responses. It plays an important role in physiologic and pathologic conditions as an inducible nuclear factor. NF- κ B is able to mediate a variety of inflammatory mediators involved in acute pancreatitis, including cytokines and adhesion molecules, as well as specific inducible isoform of nitric oxide synthase enzymes. Recent experimental studies appeared to have shed some light on the intracellular signaling

pathway in the inflammatory cascade in acute pancreatitis^[5-7]. Hence, the role of NF- κ B in acute pancreatitis has attracted more and more attention.

Therefore, this study was conducted to evaluate the role of NF- κ B in experimental model of rat ANP and to analyze the role of NF- κ B activation on nitric oxide (NO) and other reactive oxygen species in the pathogenesis of ANP.

MATERIALS AND METHODS

Experimental groups and models

We randomized 30 male Wistar rats (weighing 250-300 g) to three groups, Control group, ANP group, and PDTC group. After having fasted for 24 h before the experiment, and allowed only drinking water freely, all rats were intraperitoneally infused with 2.5% pentobarbital sodium. When the abdominal cavity was opened through the median incision, the common bile duct and the pancreatic duct were found. After intubation from the end of pancreatic duct, the pancreatic duct was shut both at the duodenal ampulla and near the hepatic hilum transiently to prevent regurgitation of the infusion into the liver or duodenum. The ANP and PDTC group were induced by slow and even infusion of 5% sodium taurocholate (Sigma, St. Louis, MO, USA) into the pancreatic duct. The Control group received infusion of saline of the same amount instead of sodium taurocholate. In addition to sodium taurocholate, PDTC group received intravenous infusion of PDTC (Sigma, St. Louis, MO, USA) 10 mg/kg, while Control and ANP group received the same amount of saline instead.

Tested parameters

At the 6th h of the model, blood was collected from the abdominal aorta of rats, and the pancreas was removed according to the following measurement: (1) Serum amylase detected by HITACHI 7170 automatic biochemical analyzer; (2) Ratio of NO₂⁻ to NO₃⁻ determined by copper-zinc-cadmium reductive chromatometry, which reflects NO level; (3) Malondialdehyde (MDA) detected by TBA chromatometry; (4) Superoxide dismutase (SOD) detected by hydroxylamine chromatometry; (5) Morphological damage to pancreas observed microscopically after fixation in 10% neutral formaldehyde solution and HE stain, morphological alterations were graded using a scale of the degree of inflammation, necrosis and edema; (6) Expressions of iNOS in pancreatic tissue detected by iNOS immunohistochemical kits (Beijing Zhongshan Biotechnology Co., Ltd. Beijing, China) iNOS antibody was diluted 50 fold, tested with SP method, and cells stained with brown-yellow granules were considered to be positive; (7) Expressions of NF- κ B p65 subunit mRNA in pancreatic tissue: After fixation in 4%

citromint and 1% DEPC, expression of NF- κ B p65 subunit mRNA *in situ* kits (Wuhan Boster Bioengineering Co., Ltd. Wuhan, Hubei, China) Plasma and nucleus of pancreatic acinar stained with brown-yellow granules were considered to be positive. All immunohistochemistry or *in situ* images were analyzed and processed using MetaMorph v4.6 software (Universal Imaging Corp.). The intensity of expression was represented by average gray value, and the difference of average gray value reflected the difference of expression. Two pathologists assessed all of histopathologic sections in 20 fields/organ, and they were not aware as to which groups the sections belonged.

Statistical analysis

SASS 6.12 statistical analytic software was applied to process the data collected, and $P < 0.05$ was considered statistically significant.

RESULTS

Change of serum amylase, NO, MDA, and SOD (Table 1)

After the above treatment, serum amylase in ANP group rose rapidly. Although it was significantly higher than that in control group ($P < 0.05$), serum amylase of PDTC group was still significantly lower than that in ANP group ($P < 0.05$). NO levels in both ANP and PDTC group increased. The former, however, was significantly higher than the latter ($P < 0.05$). MDA in both ANP and PDTC group rose significantly over that in control group ($P < 0.05$), while there was no significant difference between the two results themselves. SOD levels in both ANP and PDTC group underwent a significant decrease as compared with that in control group ($P < 0.05$), but there was no significant difference between either of them.

Morphological change of the pancreatic tissue (Figure 1)

The only gross change in the abdominal cavity in control group was the mildly edematous pancreas. No structural damage was found microscopically in the pancreatic tissue, except for some local interstitial edema. In ANP group, bloody ascites, necrotic foci in pancreas, and fat necrosis in mesentery and omentum were found grossly. Interstitial lobular inflammatory infiltrations were observed in pancreas microscopically, as well as diffusive bleeding and piecemeal necrosis. In PDTC group, ascites and fat necrosis diminished notably compared with those in ANP group. Microscopically, slight bleeding, mild acinar degeneration and mild structure damage to lobules were observed together with declining inflammatory infiltration. The damage of ANP group is obviously grave than PDTC group [Histopathologic score: (5.76 ± 1.12) *vs* (4.00 ± 1.50) , $P < 0.05$].

Table 1 Changes of serum amylase, NO, MDA, SOD

Group	Amylase (U/L)	NO (umol/L)	MDA (nmol/L)	SOD (NU/mL)
Control	990.20 \pm 189.32	56.97 \pm 13.31	6.04 \pm 1.78	3977.80 \pm 309.09
ANP	7170.40 \pm 1308.63 ^c	76.95 \pm 9.04 ^c	9.88 \pm 1.52 ^c	3214.59 \pm 297.74 ^c
PDTC	4074.10 \pm 1719.78 ^{a,c}	65.18 \pm 9.02 ^a	8.60 \pm 1.41 ^c	3260.62 \pm 229.44 ^c

^a $P < 0.05$ vs ANP group; ^c $P < 0.05$ vs control group.

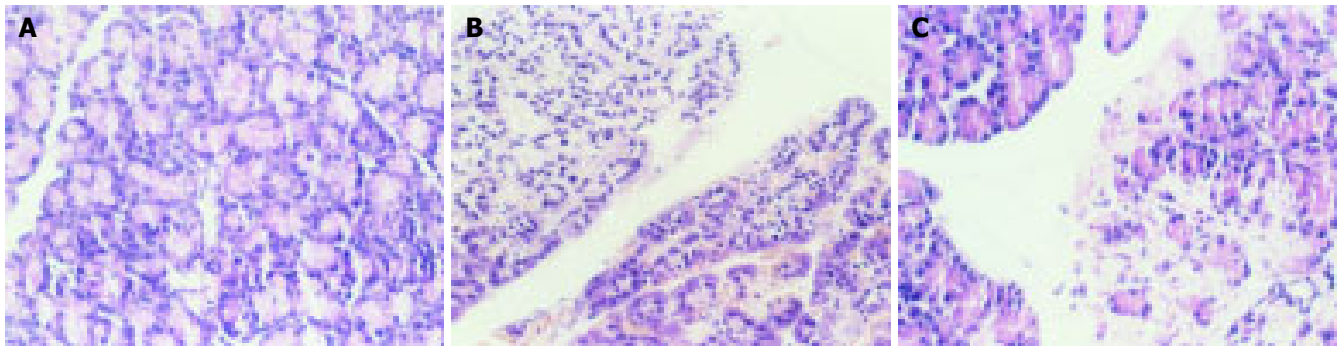


Figure 1 Morphological change of the pancreatic tissue (original magnification, $\times 400$). A: Control group; B: ANP group; C: PDTC group.

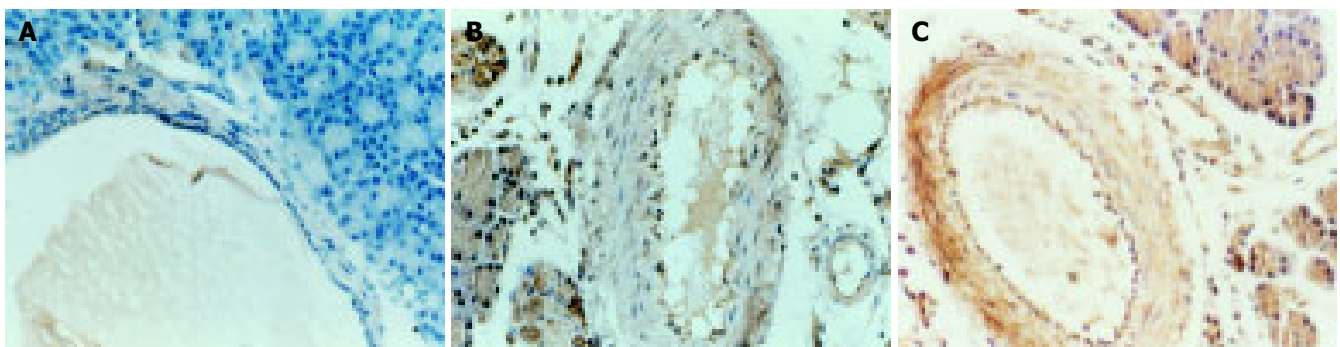


Figure 2 Expression of NOS in pancreatic tissue (DAB, original magnification, $\times 400$). A: Control group; B: ANP group; C: PDTC group.

Expressions of iNOS in pancreatic tissue (Figure 2)

Expression of iNOS was negative in control group while positive in both ANP and PDTC group, mainly found in endotheliums and smooth muscle cells. The iNOS expression is significantly lower with PDTC group than ANP group [Average gray value: (80.43 ± 10.48) *vs* (64.26 ± 9.18) , $P < 0.05$].

Expressions of NF- κ B p65 subunit mRNA in pancreatic tissue (Figure 3)

In control group, expression of NF- κ B was negative in all acinar nuclei, and positive only in some plasma. In ANP group, however, the expression was positive in both nucleus and plasma of pancreatic acinar. And the expression in nucleus and plasma decreased significantly in PDTC group [Average gray value: (104.25 ± 19.08) *vs* (67.28 ± 8.95) , $P < 0.05$].

DISCUSSION

One of the most severe complications of ANP is multiple system organ failure (MSOF) in early stage. The early systemic complication is the major cause of death in ANP, which leads to a mortality rate of 20%. Although it has been indicated that trypsin activation, auto-digestion of pancreas, cytokines, endotoxin, reactive oxygen species, and arachidnate^[8-11] play an important role in the progression of MSOF in ANP, the mechanisms of the development of this disease remain obscure.

Like what happens in other inflammatory diseases, reactive oxygen species are generated in the early stage of

ANP, and they play quite a vital role in the onset and development of ANP^[11]. During ANP, activated neutrophils are attached to endothelial cells, infiltrate into tissues, and produce large amount of reactive oxygen species and a kind of cytokines, which may cause severe damage to the pancreatic tissue. NO, in addition to potent function of vasodilation, can also inhibit the adherence, infiltration, and activation of white blood cells, and affect the production of reactive oxygen species^[11,12]. NO is generated by two classes of nitric oxide synthase (NOS): One that is constitutive, Ca^{2+} -dependent and physiologically activated (cNOS) and the other is inducible (iNOS). cNOS produces temperate amount of NO relieving ANP, whereas iNOS produces excess NO exacerbating the damage of ANP to the body^[12].

Excessive production of NO causes vasodilatation and hypotension leading to organ hypoperfusion, edema, and organ dysfunction. Moreover, the reaction of NO with superoxide causes the formation of peroxynitrite, which is a powerful oxidant and cytotoxic agent and may play an important role in the cellular damage associated with the overproduction of NO. The spontaneous reaction of peroxynitrite with proteins makes the nitration of tyrosine residues to form nitrotyrosine, which is a specific nitration product of peroxynitrite and a marker for peroxynitrite-induced oxidative tissue damage. In this study, we found the concentration of SOD as an antioxidant decreased and that of MDA as the lipid peroxide increased, indicating the role of NO on the free radical reaction and oxidation response could intensify ANP.

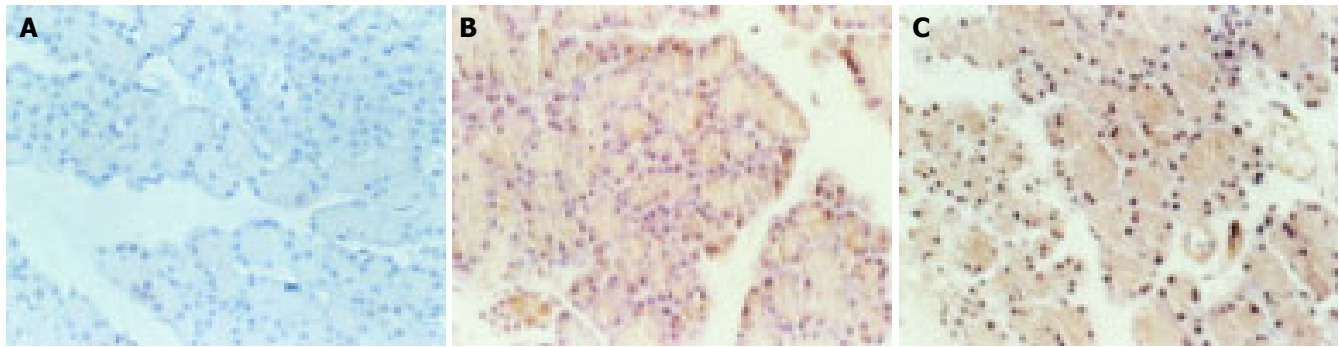


Figure 3 Expression of NF- κ B p65 mRNA in pancreatic tissue (DAB, original

magnification, $\times 400$). **A:** Control group; **B:** ANP group; **C:** PDTC group.

NF- κ B is a kind of pleiotropic regulative protein of transcription. Its activation takes part in the pathogenesis of ANP. Inhibition of the action can ameliorate the rat ANP^[13,14]. NF- κ B is also capable of regulating the expression of multiple inflammatory genes, such as tumor necrosis factor α (TNF- α), interleukin-6,8 (IL-6,8), and iNOS^[15]. Over-expressions of these discussed genes, however, can cause damage to the pancreatic and extra-pancreatic tissues in ANP. NF- κ B activation does relate to the reactive oxygen species in ANP.

Our study provides evidence that the injection of sodium taurocholate can cause ANP, with manifestation of the rise of serum amylase and NO, MDA level, damage to pancreas, inflammatory infiltration, and the decrease of SOD. Hybridization *in situ* and immunohistochemical results suggest that NF- κ B is activated immediately at the onset of ANP, accompanied by high expression of iNOS. And there is otherwise no expression of NF- κ B and iNOS under physiological conditions. The lower expression of NF- κ B p65 subunit mRNA in PDTC group indicates that the administration of PDTC may inhibit the NF- κ B activation. PDTC also leads to lower increase in serum amylase and slighter histological damage to pancreas. All these results are consistent with previous studies, substantiating that NF- κ B activation is involved in the pathogenesis of ANP, and inhibition of the activation may reverse rat ANP^[13,14]. Compared with those in ANP group, the NO and MDA level decreases, SOD level increases, and iNOS expression decreases. It is the increase of iNOS expression that aggravates ANP. Expression of iNOS is regulated by NF- κ B activation and inhibition of the activation may reduce iNOS expression, thus relieve ANP. Correlation among NF- κ B activation, NO, MDA, SOD level, tissue damage, and iNOS expression suggests a key role of NF- κ B activation in the pathogenesis of ANP model. By inhibiting iNOS expression, NF- κ B activation sets back over-production of reactive oxygen species like NO, therefore it reverses the damage of ANP to rats.

We may finally draw the conclusion from the above study that NF- κ B activation in rat ANP may reduce over-production of reactive oxygen species, thus ameliorate the

severity of ANP, all of which is achieved by inhibiting iNOS expression. The drug that can inhibit the activation of NF- κ B may become a way of the therapy of ANP.

REFERENCES

- 1 **Yousaf M**, McCallion K, Diamond T. Management of severe acute pancreatitis. *Br J Surg* 2003; **90**: 407-420
- 2 **Banks PA**. Practice guidelines in acute pancreatitis. *Am J Gastroenterol* 1997; **92**: 377-386
- 3 **Schoenberg MH**, Birk D, Beger HG. Oxidative stress in acute and chronic pancreatitis. *Am J Clin Nutr* 1995; **62** (6 Suppl): 1306S-1314S
- 4 **Sweiry JH**, Mann GE. Role of oxidative stress in the pathogenesis of acute pancreatitis. *Scand J Gastroenterol Suppl* 1996; **219**: 10-15
- 5 **Jaffray C**, Yang J, Carter G, Mendez C, Norman J. Pancreatic elastase activates pulmonary nuclear factor kappa B and inhibitory kappa B, mimicking pancreatitis-associated adult respiratory distress syndrome. *Surgery* 2000; **128**: 225-231
- 6 **Frossard JL**, Pastor CM, Hadengue A. Effect of hyperthermia on NF-kappaB binding activity in cerulein-induced acute pancreatitis. *Am J Physiol Gastrointest Liver Physiol* 2001; **280**: G1157-1162
- 7 **Algul H**, Tando Y, Schneider G, Weidenbach H, Adler G, Schmid RM. Acute Experimental Pancreatitis and NF-kappaB/Rel Activation. *Pancreatology* 2002; **2**: 503-509
- 8 **Karne S**, Gorelick FS. Etiopathogenesis of acute pancreatitis. *Surg Clin North Am* 1999; **79**: 699-710
- 9 **Denham W**, Norman J. The potential role of therapeutic cytokine manipulation in acute pancreatitis. *Surg Clin North Am* 1999; **79**: 767-781
- 10 **Norman J**. The role of cytokines in the pathogenesis of acute pancreatitis. *Am J Surg* 1998; **175**: 76-83
- 11 **Schulz HU**, Niederau C, Klonowski-Stumpe H, Halangk W, Luthen R, Lippert H. Oxidative stress in acute pancreatitis. *Hepatogastroenterology* 1999; **46**: 2736-2750
- 12 **Jaworek J**, Jachimczak B, Tomaszewska R, Konturek PC, Pawlik WW, Sendur R, Hahn EG, Stachura J, Konturek SJ. Protective action of lipopolysaccharides in rat caerulein-induced pancreatitis: role of nitric oxide. *Digestion* 2000; **62**: 1-13
- 13 **Gukovsky I**, Gukovskaya AS, Blinman TA, Zaninovic V, Pandolfi SJ. Early NF-kappaB activation is associated with hormone-induced pancreatitis. *Am J Physiol* 1998; **275** (6 Pt 1): G1402-1414
- 14 **Dunn JA**, Li C, Ha T, Kao RL, Browder W. Therapeutic modification of nuclear factor kappa B binding activity and tumor necrosis factor-alpha gene expression during acute biliary pancreatitis. *Am Surg* 1997; **63**: 1036-1043
- 15 **Abraham E**. NF-kappaB activation. *Crit Care Med* 2000; **28**: N100-104

• CASE REPORT •

Metastatic liver cancer: A rare case

Bong-Wan Kim, Hee-Jung Wang, In-Ho Jeong, Sang-Ick Ahn, Myoung-Wook Kim

Bong-Wan Kim, Hee-Jung Wang, In-Ho Jeong, Sang-Ick Ahn, Myoung-Wook Kim, Department of Surgery, Ajou University School of Medicine, Suwon, South Korea

Correspondence to: Hee-Jung Wang, MD, PhD, Department of Surgery, Ajou University School of Medicine, San-5 Youngtong ku, Wonchon dong, Suwon 442-749, South Korea. wanghj@ajou.ac.kr
Telephone: +82-31-219-5011 Fax: +82-31-219-5755

Received: 2004-11-29 Accepted: 2005-01-05

Abstract

Hemangiopericytoma is a rare tumor especially when it rises in the peritoneal cavity. We present a case of a 60-year-old woman with an isolated recurrent hemangiopericytoma of the liver. The patient presented with a palpable right upper quadrant abdominal mass, which occurred 7 years after undergoing resection of a malignant hemangiopericytoma arising from the greater omentum. She had not followed up 6 mo after surgery. Various imaging studies showed a single large, well-capsulated liver tumor with central necrosis, accompanied by hypervascularity typical of a vascular tumor. Preoperative laboratory HBsAg and anti-HCV workup were both negative. Under the impression of recurrent malignant hemangiopericytoma, right trisegmentectomy was performed to completely resect the tumor. Pathological examination confirmed the diagnosis of recurrent hemangiopericytoma. Even though the incidence of the hemangiopericytoma is relatively low, malignant hemangiopericytoma has a tendency to recur frequently after a long-term disease-free interval. Also, the recurrent hemangiopericytoma is not easily detected early during follow-up until it becomes symptomatic because there are no specific tumor markers, and because of the diversity with regard to site of recurrence. The authors suggest that Positron Emission Tomogram (PET) may be a useful tool for the detection of recurrent hemangiopericytoma. We describe herein some characteristics and behaviors of malignant hemangiopericytoma, particularly after surgical resection.

© 2005 The WJG Press and Elsevier Inc. All rights reserved.

Key words: Hemangiopericytoma; Greater omentum; Hepatic metastasis; Follow-up; Positron emission tomography

Kim BW, Wang HJ, Jeong IH, Ahn SI, Kim MW. Metastatic liver cancer: A rare case. *World J Gastroenterol* 2005; 11 (27): 4281-4284

<http://www.wjgnet.com/1007-9327/11/4281.asp>

INTRODUCTION

Hemangiopericytoma was first described in 1942 by Stout

and Murray, and approximately 1 000 cases have been reported to date in the literature. Hemangiopericytomas arise from the pericyte of Zimmermann, and although it may occur in any part of the human body, the frequency of occurrence has been reported to be the lower extremities, pelvic cavity, retro-peritoneum, thoracic cavity, and upper extremities, in descending order. Most tumors have been reported to occur in the deep portions of the body, and those arising within the peritoneum are rare^[1]. Generally, although hemangiopericytomas arising in the peritoneal cavity show better prognosis compared to adenocarcinomas that occur in the gastrointestinal tract, surgery seems to be the only effective mode of therapy.

Histologically benign hemangiopericytomas are known to be curable by complete surgical resection, while the malignant type, albeit characterized by slow growth, has been known to recur frequently after curative surgical resection. Another reported characteristic of hemangiopericytomas is the development of non-islet-cell-tumor hypoglycemia in the latter phase of the natural course^[1], and this has been related to the production of the insulin-like growth factor II by the tumor^[2,3]. Malignant hemangiopericytomas are characterized by an indolent rate of growth, but recurrence has been demonstrated in more than half of the cases which had been followed up. In addition, the diversity of the sites of recurrence via hematological and lymphatic routes and lack of specific tumor markers has contributed to the difficulty in detecting recurrent disease. The lungs have been shown to be the most common distal site of recurrence, while other sites include the brain, scalp, chest wall, liver, subcutaneous lymph node, gastrointestinal tract, and ovaries^[4,5].

The authors report a surgically treated case of hemangiopericytoma of the greater omentum, and which recurred as a metachronous solitary liver metastasis 7 years after complete resection. We also suggest the employment of the positron emission tomography (PET) method as a useful tool in the post-operative follow-up of patients with a history of hemangiopericytomas, as there is no other definite established mode of follow-up.

CASE REPORT

A gravida 6, para 5, at present 60-years old, female patient had presented with a palpable lower abdominal mass referred initially from a private gynecologic clinic in March 1997, under the impression of a myoma of the uterus. Her past gynecologic history showed that she had entered menopause at 49 years of age. Physical examination showed a mobile, solid mass in the lower abdomen. Transvaginal ultrasonography demonstrated that the mass did not originate from the uterus. A magnetic resonance imaging was performed to determine if the mass was of ovarian origin, and which

showed that an 8 cm sized, solitary mass of unknown origin was present in the pelvic cavity. There was no evidence of lymph node enlargement. The tumor markers β -HCG, CA19-9, CA-125, CEA were all within the normal range. The patient subsequently underwent exploratory laparotomy under the impression of a possible ovarian malignancy, upon which a 10 cm \times 8 cm \times 7 cm mass originating from the greater omentum was observed. There was no gross evidence of other pathology such as surrounding adhesions or lymph node pathology, and the patient consequently underwent tumor excision including a portion of the omentum. Pathologic examination revealed necrosis in the central portion of the tumor, atypical hyperplasia of spindle-shaped tumor cells, and five mitoses per 10 HPF, suggestive of a malignant hemangiopericytoma. The patient was discharged 7 d after surgery and no further adjuvant anti-cancer therapy was administered. She had not followed up 6 mo after surgery.

The patient was asymptomatic until October 2004, when she began to complain of a palpable right upper quadrant mass, and she visited our department for evaluation. Initial abdominal computerized tomography (CT) demonstrated a large mass in the right hepatic lobe. To ascertain whether this lesion was a possible hepatocellular carcinoma, a common cause of liver tumors in Korea, viral marker studies were conducted, and which showed HBsAg (-), anti-HBs (+), anti-HBc (+), and anti-HCV (-). Also, the tumor markers

AFP, CEA, CA19-9, and CA125 were all within normal limits. Plain chest X-ray was also normal.

Abdominal CT scan showed that the tumor was of a hypervascular nature, with active contrasting from the periphery of the tumor in the arterial phase, and remaining contrast in the delayed phase suggesting a tumor of vascular origin. The hepatic artery angiogram confirmed that the tumor was hypervascular, with vessels from major arteries providing branches surrounding and entering into the deep portions of the tumor (Figure 1). These findings were highly suggestive of a recurrent malignant hemangiopericytoma. To determine the presence of any distant metastatic lesion, a head and neck CT (normal) was performed, while the 18 F-FDG PET scan showed a standardized uptake value (SUV) of 4.8 in the right hepatic lobe indicative of 18 F-FDG uptake. There were no other suspicious sites other than the liver (Figure 2). The patient therefore underwent laparotomy and right trisegmentectomy of the liver under the impression of recurrent malignant hemangiopericytoma. Gross findings showed a 15 cm, large solitary sarcomatous lesion with central necrosis. Microscopic examination of the tumor confirmed the presence of malignant hemangiopericytoma identical to that of the lesion of 1997, with free resection margins (Figures 3 and 4). The patient was discharged on the 20th postoperative day without complications.

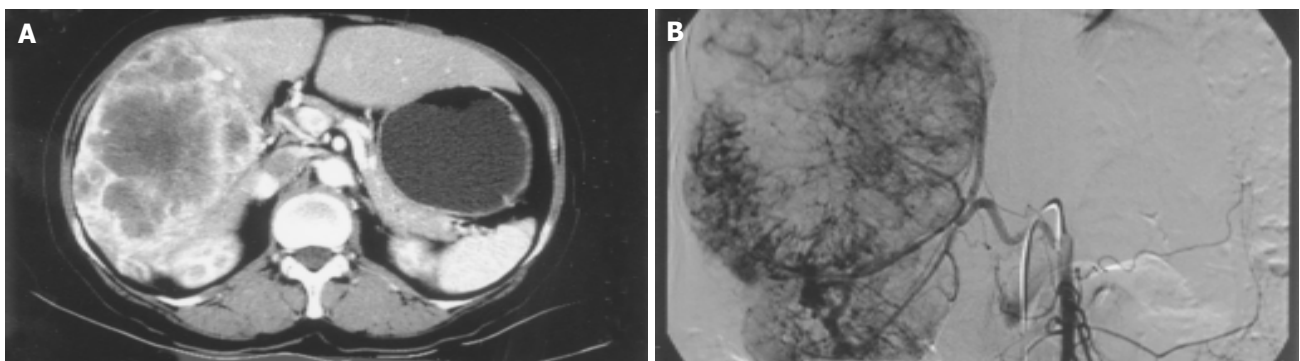


Figure 1 A: Liver CT scan showed a huge tumor in the right lobe of the liver with enhancement from the periphery in the arterial phase; B: The hepatic arteriogram

demonstrated numerous feeding vessels surrounding and entering into the tumor. The patient had variation of the right hepatic artery from the superior mesenteric artery.

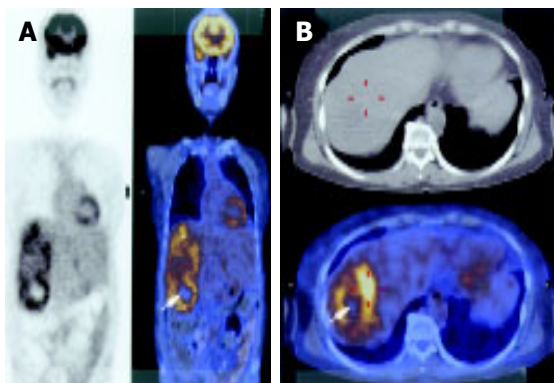


Figure 2 A: 18 F-FDG PET showed high uptake at the tumor without any distant lesions. The silent area in the center of the tumor suggests central necrosis (arrow); B: The highest uptake area measured 4.8 SUV (red line mark).



Figure 3 Resected specimen showed a huge single tumor with sarcomatous consistency. The margin was irregular because of the constrictive envelopment of feeding vessels. The central necrosis is indicated (arrow).

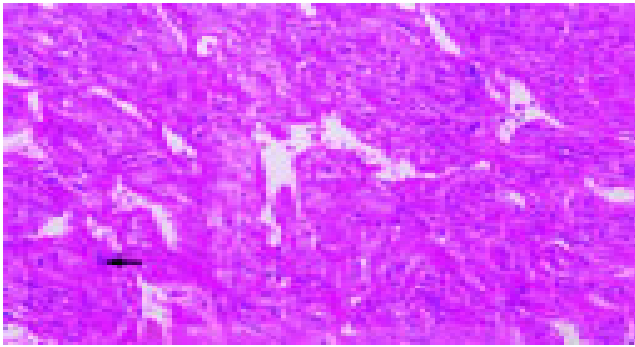


Figure 4 Microscopic examination demonstrated numerous atypical vessels (stag-horn appearance) in the high population of spindle-shaped tumor cells. A mitotic figure is seen (arrow), H&E, $\times 200$.

DISCUSSION

Hemangiopericytomas primarily occurring in the abdominal cavity are very rare, and only 12 cases in the world-wide literature have reported those occurring in the greater omentum. It is thought that surgical removal of the tumor is the most effective mode of therapy for hemangiopericytomas, but as yet there is no established range of surgical resection for malignant types that occur in the abdomen. As demonstrated in our case, in light of the fact that secondary surgery confirmed recurrent metastatic liver tumor 7 years after initial simple excision, and that there was no local recurrence in the omentum and the peritoneal cavity, we do not feel that complete anatomical removal of the total greater omentum would lead to superior prognosis compared to simple excision only. This finding is similar to previously reported cases of greater omental hemangiopericytomas^[6].

Grossly, malignant hemangiopericytomas have been reported usually as a solitary lesion, but in some series, several hundred, multiple nodules have also been observed^[7]. In most cases, the tumor is observed as smoothly encapsulated, while the areas where the vessels enter into the tumor surface are characterized as irregular due to local tumor retraction. As hemangiopericytomas are hypervascular tumors, angiography demonstrates a feature of numerous feeding vessels surrounding and entering into the tumor, sometimes being observed as multiple cork-screw type feeding vessels. These findings, however, are not common findings, and are not highly regarded as a distinctive diagnostic feature^[8,9]. Moreover, it is difficult to ascertain both a diagnosis of hemangiopericytoma and malignant characteristic with these radiological and gross findings alone.

Microscopic observation of H&E staining demonstrates numerous neovascularized vessels within a highly concentrated area of tumor cells, and which also frequently show a stag-horn feature. The tumor cells are mostly spindle-shaped, but may be spherical or other shapes, the nuclear to cytoplasm ratio is increased, while the cytoplasm is pale staining. Differential diagnosis includes glomus tumor, fibrous histiocytoma, synovial sarcoma, and mesenchymal sarcoma, and advances in immunohistochemical techniques usually allows differentiation from a malignant hemangiopericytoma. It has been reported in the previous literature that malignant

hemangiopericytomas comprise about half of all cases, and that after local excision and long-term follow-up, approximately 60% of patients experience local or distant recurrence^[4]. The disease-free interval has been reported to vary markedly between 2 mo and 26 years^[10]. Specific features that qualify a hemangiopericytoma as a malignant lesion are more than four mitoses per 10 HPF, pleomorphic cells with abnormal chromatin pattern, and accompanied by either central tumor necrosis or intra-tumoral hemorrhage.

Observations of previous data regarding hemangiopericytomas arising in the greater omentum have shown that the presence of more than four mitoses per 10 HPF is closely related to recurrence of disease. Also, the number of increased mitoses has also been suggested to be related with increased tumor size, and that tumors of more than 20 cm in diameter imply poor prognosis^[6].

Other modes of therapy for malignant hemangiopericytoma may consist of anticancer chemotherapy and radiotherapy for residual or metastatic tumors^[11,12], and these are usually the preferred mode of adjuvant therapy after surgery because of limited efficacy.

From the clinical perspective, compared to other common malignant tumors of the gastrointestinal tract, malignant hemangiopericytomas have a comparatively longer disease-free interval after surgical resection and an indolent natural history^[13]. However, it should be mentioned that in many cases of recurrent disease after a long disease-free interval, it is common that either the qualified gastrointestinal surgeon concludes that the disease has been completely cured after a certain length of follow-up, or that the patient refuses further follow-up. This is also reflected in our case, whereby the patient presented with a recurrent large intra-abdominal mass, or with related cancer symptoms such as hypoglycemia.

Another difficulty involving postoperative management of hemangiopericytoma is that since there is no established follow-up protocol after surgery, the length of follow-up and the diagnostic methods employed varies from surgeon to surgeon. Moreover, the absence of specific tumor markers makes it all the more difficult to detect recurrent disease. The authors of this study suggest that the PET scan is a valid, non-invasive diagnostic procedure in the ascertainment of recurrent malignant hemangiopericytoma. This may be particularly true in patients where if the preoperative PET demonstrates a hemangiopericytoma, the presence of a recurrent tumor of a similar character will be detected by PET in the follow-up. However, it should be noted that there may be differences in the degree of uptake between histologically identical hemangiopericytomas. In our case ^{18}F -FDG uptake was increased within the tumor, but other series have shown that ^{11}C -methionine and ^{15}O - H_2O uptake was increased rather than ^{18}F -FDG^[14]. That report is different from ours, so we think further evaluations about useful radio-isotope of PET for malignant hemangiopericytoma are needed. Another study suggested the correlation between the high uptake of ^{18}F -FDG in hemangiopericytomas and poor prognosis^[15]. Consequently, it is the opinion of the authors that such variable uptakes by malignant hemangiopericytoma as seen in PET scans contribute more to the detection of recurrent disease after surgical removal, rather than to the

establishment of preoperative differential diagnosis. Also, the PET scans the whole body, and therefore allows detection of recurrent hemangiopericytoma, which has a wide pattern of recurrence.

In conclusion, although the pattern of recurrent malignant hemangiopericytoma is diverse, surgical intervention after early detection may allow another long disease-free period. For this to be accomplished, long-term follow-up is imperative, and we suggest that yearly PET scans are useful in attaining this goal.

REFERENCES

- 1 **Enzinger FM**, Smith BH. Hemangiopericytoma. An analysis of 106 cases. *Hum Pathol* 1976; **7**: 61-82
- 2 **Sohda T**, Yun K. Insulin-like growth factor II expression in primary meningeal hemangiopericytoma and its metastasis to the liver accompanied by hypoglycemia. *Hum Pathol* 1996; **27**: 858-861
- 3 **Grunenberger F**, Bachellier P, Chenard MP, Massard G, Caraman PL, Perrin E, Zapf J, Jaeck D, Schlienger JL. Hepatic and pulmonary metastases from a meningeal hemangiopericytoma and severe hypoglycemia due to abnormal secretion of insulin-like growth factor: a case report. *Cancer* 1999; **85**: 2245-2248
- 4 **McMaster MJ**, Soule EH, Ivins JC. Hemangiopericytoma. A clinicopathologic study and long-term follow up of 60 patients. *Cancer* 1975; **36**: 2232-2244
- 5 **Begum M**, Katabuchi H, Tashiro H, Suenaga Y, Okamura H. A case of metastatic malignant hemangiopericytoma of the ovary: recurrence after a period of 17 years from intracranial tumor. *Int J Gynecol Cancer* 2002; **12**: 510-514
- 6 **Kaneko K**, Shirai Y, Wakai T, Hasegawa G, Kaneko I, Hatakeyama K. Hemangiopericytoma arising in the greater omentum: report of a case. *Surg Today* 2003; **33**: 722-724
- 7 **Matsuda S**, Usui M, Sakurai H, Suzuki H, Ogura Y, Shiraishi T. Insulin-like growth factor II-producing intra-abdominal hemangiopericytoma associated with hypoglycemia. *J Gastroenterol* 2001; **36**: 851-855
- 8 **Marc JA**, Takei Y, Schechter MM, Hoffman JC. Intracranial hemangiopericytomas. Angiography, pathology and differential diagnosis. *Am J Roentgenol Radium Ther Nucl Med* 1975; **125**: 823-832
- 9 **Guthrie BL**, Ebersold MJ, Scheithauer BW, Shaw EG. Meningeal hemangiopericytoma: histopathological features, treatment, and long-term follow-up of 44 cases. *Neurosurgery* 1989; **25**: 514-522
- 10 **Schirger A**, Uihlein A, Parker HL, Kernohan JW. Hemangiopericytoma recurring after 26 years; report of a case. *Mayo Clin Proc* 1958; **33**: 347-352
- 11 **Wong PP**, Yagoda A. Chemotherapy of malignant hemangiopericytoma. *Cancer* 1978; **41**: 1256-1260
- 12 **Staples JJ**, Robinson RA, Wen BC, Hussey DH. Hemangiopericytoma-the role of radiotherapy. *Int J Radiat Oncol Biol Phys* 1990; **19**: 445-451
- 13 **Spitz FR**, Bouvet M, Pisters PW, Pollock RE, Feig BW. Hemangiopericytoma: a 20-year single-institution experience. *Ann Surg Oncol* 1998; **5**: 350-355
- 14 **Kracht LW**, Bauer A, Herholz K, Terstegge K, Friese M, Schroder R, Heiss WD. Positron emission tomography in a case of intracranial hemangiopericytoma. *J Comput Assist Tomogr* 1999; **23**: 365-368
- 15 **Reisser C**, Haberkorn U, Strauss LG. Diagnosis of energy metabolism in ENT tumors-a PET study. *Hno* 1992; **40**: 225-231

Science Editor Guo SY Language Editor Elsevier HK

• CASE REPORT •

Successful endoscopic hemostasis for gastric arterial bleeding due to invasion of malignant lymphoma

Kenichi Nomura, Shinya Yamada, Daisuke Shimizu, Takashi Okuda, Yuri Kamitsuji, Naohisa Yoshida, Yosuke Matsumoto, Naoki Wakabayashi, Kazuya Mikami, Shigeo Horiike, Takeshi Okanoue, Masafumi Taniwaki

Kenichi Nomura, Shinya Yamada, Daisuke Shimizu, Yuri Kamitsuji, Yosuke Matsumoto, Shigeo Horiike, Masafumi Taniwaki, Molecular Hematology and Oncology, Kyoto Prefectural University of Medicine Graduate School of Medical Science, Kyoto, Japan
Yuri Kamitsuji, Inflammation and Immunology, Kyoto Prefectural University of Medicine Graduate School of Medical Science, Kyoto, Japan

Takashi Okuda, Naohisa Yoshida, Naoki Wakabayashi, Takeshi Okanoue, Molecular Gastroenterology and Hepatology, Kyoto Prefectural University of Medicine Graduate School of Medical Science, Kyoto, Japan

Kazuya Mikami, Department of Urology, Kyoto Prefectural University of Medicine Graduate School of Medical Science, Kyoto, Japan

Daisuke Shimizu, Masafumi Taniwaki, Clinical Molecular Genetics and Laboratory Medicine, Kyoto Prefectural University of Medicine Graduate School of Medical Science, Kyoto, Japan

Correspondence to: Kenichi Nomura, MD, PhD, Molecular Hematology and Oncology, Kyoto Prefectural University of Medicine Graduate School of Medical Science, Kawaramachi-Hirokoji, Kamigyo-ku, Kyoto, 602-0841, Japan. nomuken@sun.kpu-m.ac.jp
Telephone: +81-75-251-5521 Fax: +81-75-251-0710

Received: 2004-09-23 Accepted: 2004-10-13

Abstract

A 75-year-old male with malignant lymphoma (ML) accompanied with gastric lesion was treated with combination chemotherapy. The patient produced tarry stool on the 4th d, and emergency gastroscopy showed arterial bleeding from the lesion. Hemostasis was achieved by injecting pure ethanol and using hemostatic clips. There is only one previous report on endoscopic hemostasis being effective for bleeding due to lymphoma. Since gastric bleeding causes significant mortality, endoscopic hemostasis should be considered as first-line treatment for ML patients who were treated with chemotherapy.

© 2005 The WJG Press and Elsevier Inc. All rights reserved.

Key words: Malignant lymphoma; Endoscopic hemostasis; Pure ethanol injection; Hemostatic clips

Nomura K, Yamada S, Shimizu D, Okuda T, Kamitsuji Y, Yoshida N, Matsumoto Y, Wakabayashi N, Mikami K, Horiike S, Okanoue T, Taniwaki M. Successful endoscopic hemostasis for gastric arterial bleeding due to invasion of malignant lymphoma. *World J Gastroenterol* 2005; 11(27): 4285-4286
<http://www.wjgnet.com/1007-9327/11/4285.asp>

INTRODUCTION

Patients with stage I-II primary gastric lymphoma are

commonly treated with chemotherapy alone or in combination with radiation therapy to avoid long-term sequelae after gastric resection^[1,2]. Although gastrointestinal bleeding during chemotherapy has been observed in only 3% of cases^[2], it is a definite cause of mortality. However, only emergency gastrectomy may be able to rescue patients with neutropenia and thrombocytopenia after chemotherapy^[3].

Endoscopic hemostasis has been established as a first-line treatment for acute bleeding in all patients with peptic ulcer. Among various methods employed, injection with pure ethanol or the use of hemostatic clips is one of the most effective treatments for achieving definitive hemostasis^[4-8]. However, there has been only one report describing a case of successful endoscopic hemostasis for bleeding from lymphoma in the stomach. However, this case underwent hemostatic treatment before chemotherapy^[9].

Our report concerns an elderly patient with gastric bleeding due to invasion of lymphoma after standard chemotherapy. Although this patient was considered inoperable before chemotherapy, we managed to achieve hemostasis by injecting pure ethanol and using hemostatic clips.

CASE REPORT

A 75-year-old man was admitted to our hospital in January 2004 because of lumbar pain. Computed tomography detected a huge mass at the kidney and swelling of the paraaortic lymph nodes. He was diagnosed as having renal cell carcinoma with lymph node invasion and underwent surgical treatment in March. However, the swelling of the lymph nodes was histologically diagnosed as diffuse large B-cell lymphoma (DLBCL), and because ⁶⁷Ga-citrate scintigraphy showed uptake at the stomach, we performed upper gastrointestinal endoscopy. An ulcerative lesion was detected in the upper body (Figure 1), which, although suspected of being invasion of lymphoma, a biopsy sample showed to be a benign ulcer. Because there were no other signs of lymphoma, the patient was treated with interferon therapy for renal cell carcinoma as adjuvant therapy. Omeprazole and cimetidine were administered for the gastric lesion. After 2 mo, multiple superficial lymph node swelling was observed. Biopsy of the cervical lymph node indicated recurrence of DLBCL, but because our patient was considered inoperable, we started CHOP therapy (cyclophosphamide, adriamycin, vincristine, and prednisolone) on 6th July. However, the patient produced massive tarry stool on d 4, resulting in a drop in the hemoglobin level to 44 g/L. Emergency endoscopy was performed that detected arterial bleeding from the ulcerative lesion in the upper body (Figure 2).

The condition had not changed since the previous examination in spite of the treatment with antipeptic agents. Ethanol injections (0.1 mL at a time) into the surrounding tissue close to the bleeding vessels, at a few injecting sites 2 mm from the bleeding vessels, suppressed the pulsatile bleeding, and definitive hemostasis was achieved with the concomitant use of hemostatic clips. During the following 2 weeks, the ulcerative lesions became smaller and no further bleeding was detected (Figure 3).

The second biopsy samples were histologically compatible with lymphoma.



Figure 1 Giant ulcer at cardia of stomach.



Figure 2 Emergency gastroscopy showed pulsatile arterial bleeding.



Figure 3 No bleeding was observed in the ulcer injected with ethanol.

DISCUSSION

This report concerns a patient with arterial bleeding from the stomach due to lymphoma invasion. We had considered surgical resection of the stomach before chemotherapy to avoid bleeding, but we performed chemotherapy as first treatment instead, because surgery was considered to carry serious risks. The reasons for these were that (1) the patient had previously undergone laparotomy for renal cell carcinoma and adhesion of viscera was suspected to be severe, (2) paraaortic lymph nodes were swollen making it difficult to create anastomoses for a gastroduodenostomy, and (3) lymphoma was expected to progress rapidly during recovery from the operation.

Because the mechanism of hemostasis is thought to consist of solidification caused by vascular shrinking resulting from the direct action of ethanol and degeneration of the vascular endothelial cells, there is good reason for attempting endoscopic hemostasis for bleeding due to lymphoma. We successfully achieved hemostasis with ethanol injection and clips, although the fundus of the ulcer remained fragile due to necrosis of the lymphoma after chemotherapy. Because lymphoma is curable with chemotherapy alone, endoscopic hemostasis should be considered as a first-line treatment for bleeding due to lymphoma.

ACKNOWLEDGMENT

The authors are grateful to Ms. Yuko Kanbayashi for her pharmacological advice.

REFERENCES

- 1 Maor MH, Velasquez WS, Fuller LM, Silvermintz KB. Stomach conservation in stages IE and IIE gastric non-Hodgkin's lymphoma. *J Clin Oncol* 1990; **8**: 266-271
- 2 Ferreri AJ, Cordio S, Ponzoni M, Villa E. Non-surgical treatment with primary chemotherapy, with or without radiation therapy, of stage I-II high-grade gastric lymphoma. *Leuk Lymphoma* 1999; **33**: 531-541
- 3 Sakakura C, Hagiwara A, Nakanishi M, Yasuoka R, Shirasu M, Togawa T, Taniwaki M, Yamagishi H. Bowel perforation during chemotherapy for non-hodgkin's lymphoma. *Hepatogastroenterology* 1999; **46**: 3175-3177
- 4 Exon DJ, Sydney Chung SC. Endoscopic therapy for upper gastrointestinal bleeding. *Best Pract Res Clin Gastroenterol* 2004; **18**: 77-98
- 5 Asaki S. Tissue solidification in coping with digestive tract bleeding: hemostatic effect of local injection of 99.5% ethanol. *Tohoku J Exp Med* 1981; **134**: 223-227
- 6 Hepworth CC, Swain CP. Mechanical endoscopic methods of haemostasis for bleeding peptic ulcers: a review. *Baillieres Best Pract Res Clin Gastroenterol* 2000; **14**: 467-476
- 7 Raju GS, Gajula L. Endoclips for GI endoscopy. *Gastrointest Endosc* 2004; **59**: 267-279
- 8 Shimoda R, Iwakiri R, Sakata H, Ogata S, Kikkawa A, Ootani H, Oda K, Ootani A, Tsunada S, Fujimoto K. Evaluation of endoscopic hemostasis with metallic hemoclips for bleeding gastric ulcer: comparison with endoscopic injection of absolute ethanol in a prospective, randomized study. *Am J Gastroenterol* 2003; **98**: 2198-2202
- 9 Nishimura H, Saito M, Shibata K, Ueno K, Maeura Y, Murata A. A case of malignant lymphoma accompanied with arterial bleeding from the gastric lesion. *Jpn J Med* 1989; **28**: 604-607

• CASE REPORT •

Imaging features of ciliated hepatic foregut cyst

Song-Hua Fang, Dan-Jun Dong, Shi-Zheng Zhang

Song-Hua Fang, Dan-Jun Dong, Shi-Zheng Zhang, Department of Radiology, Sir Run Run Shaw Hospital, Zhejiang University, Hangzhou 310016, Zhejiang Province, China

Correspondence to: Song-Hua Fang, Department of Radiology, Sir Run Run Shaw Hospital, Zhejiang University, Hangzhou 310016, Zhejiang Province, China. fangsonghua@163.com
Telephone: +86-571-86090073-4609

Received: 2004-10-09 Accepted: 2004-11-26

Abstract

Ciliated hepatic foregut cyst (CHFC) is a very rare cystic lesion of the liver that is histologically similar to bronchogenic cyst. We report one case of CHFC that was hard to distinguish from solid-cystic neoplasm in imaging features. Magnetic resonance imaging was helpful in differentiating these cysts from other lesions.

© 2005 The WJG Press and Elsevier Inc. All rights reserved.

Key words: Ciliated foregut cyst; Liver; Magnetic resonance imaging; X-ray computed tomography

Fang SH, Dong DJ, Zhang SZ. Imaging features of ciliated hepatic foregut cyst. *World J Gastroenterol* 2005; 11(27): 4287-4289

<http://www.wjgnet.com/1007-9327/11/4287.asp>

INTRODUCTION

Ciliated hepatic foregut cyst (CHFC) is a very rare, benign and solitary cyst^[1,2]. It is most often unilocular^[2]. To our knowledge, 5 cases of CHFC were reported in the 19th century, 53 cases in the 20th century and 5 cases in the 21st and its medical imaging findings are seldom reported^[1,3]. It is difficult to differentiate the CHFC from malignant tumor^[1,4,5]. Herein, we present the radiologic features from one CHFC that was not similar to other nonparasitic cysts, but rather mimicked cystic-solid mass of the liver on the images obtained.

CASE REPORT

A 30-year-old man presented with a 5-mo history of left upper abdominal discomfort and mild fatigue. Physical examination and laboratory studies had no positive findings including hepatitis.

A plain radiograph of the abdomen was normal. Sonographic examination revealed a well-delineated hypoechoic mass, 3 cm×4 cm in size, in the liver. It was located in the medial segment of the left lobe (segment IV),

just adjacent to the surface of the liver. Unenhanced computed tomographic (CT) scan was obtained, and the lesion appeared slightly hypoattenuating relative to surrounding liver parenchyma (Figure 1A). The attenuation value of the lesion was 47 HU. At contrast material-enhanced CT, this lesion was not enhanced and appeared slightly hypoattenuating with well-defined margin (Figure 1B). On delayed CT scan, it had still no enhancement. Magnetic resonance (MR) imaging at 1.5 T was performed for more detailed examination. The lesion appeared isointense relative to surrounding liver parenchyma on T1-weighted imaging (Figure 1C) and markedly homogeneously hyperintense on T2-weighted imaging (Figure 1D). It was also not enhanced after Gd-DTPA administration (Figure 1E).

The lesion was resected surgically because the possibility of hypovascular neoplasm could not be excluded completely according to the imaging. The resected specimen revealed an unilocular cystic lesion containing a mucinous fluid.

On pathologic examination, the cyst had a fibrous wall lined by ciliated pseudostratified columnar epithelial cells, which was consistent with a CHFC (Figure 1F).

DISCUSSION

The histogenesis of CHFC is still unclear, but most authors consider that it arises from the embryonic foregut in the liver^[1,2,5]. CHFC is usually a benign, solitary cyst consisting of a ciliated pseudostratified columnar epithelium, a subepithelial connective tissue layer, a smooth muscle layer and an outer fibrous capsule^[2,6]. It is often smaller than 3 cm in diameter and found most commonly in the medial segment of the left hepatic lobe, just beneath the hepatic surface^[5,7]. CHFC is not actually a neoplasm and usually found incidentally on radiologic imaging during surgical exploration or autopsy. It is mostly asymptomatic and surgical resection should be avoided^[5]. However, on the other hand, it was reported recently that one case causes portal vein compression and the other shows malignant transformation through squamous metaplasia (it is not surprising to find squamous mucosa because tracheobronchial tree derives from the embryologic foregut), which warns to examine CHFC cautiously^[8,9], and suggests that a large-sized symptomatic CHFC should be excised, especially when radiologic studies yield equivocal results^[10].

Generally CHFC is a well-delineated anechoic or slightly hypoechoic small mass on ultrasonography. Because CHFC can contain various elements ranging from clear serous material to milky white to brown mucoid material, and these have variable viscosities, and the different CT attenuation numbers can be shown^[5]. The lesion can be hypoattenuating as our case or isoattenuating relative to surrounding liver parenchyma at unenhanced CT. Even it has very high

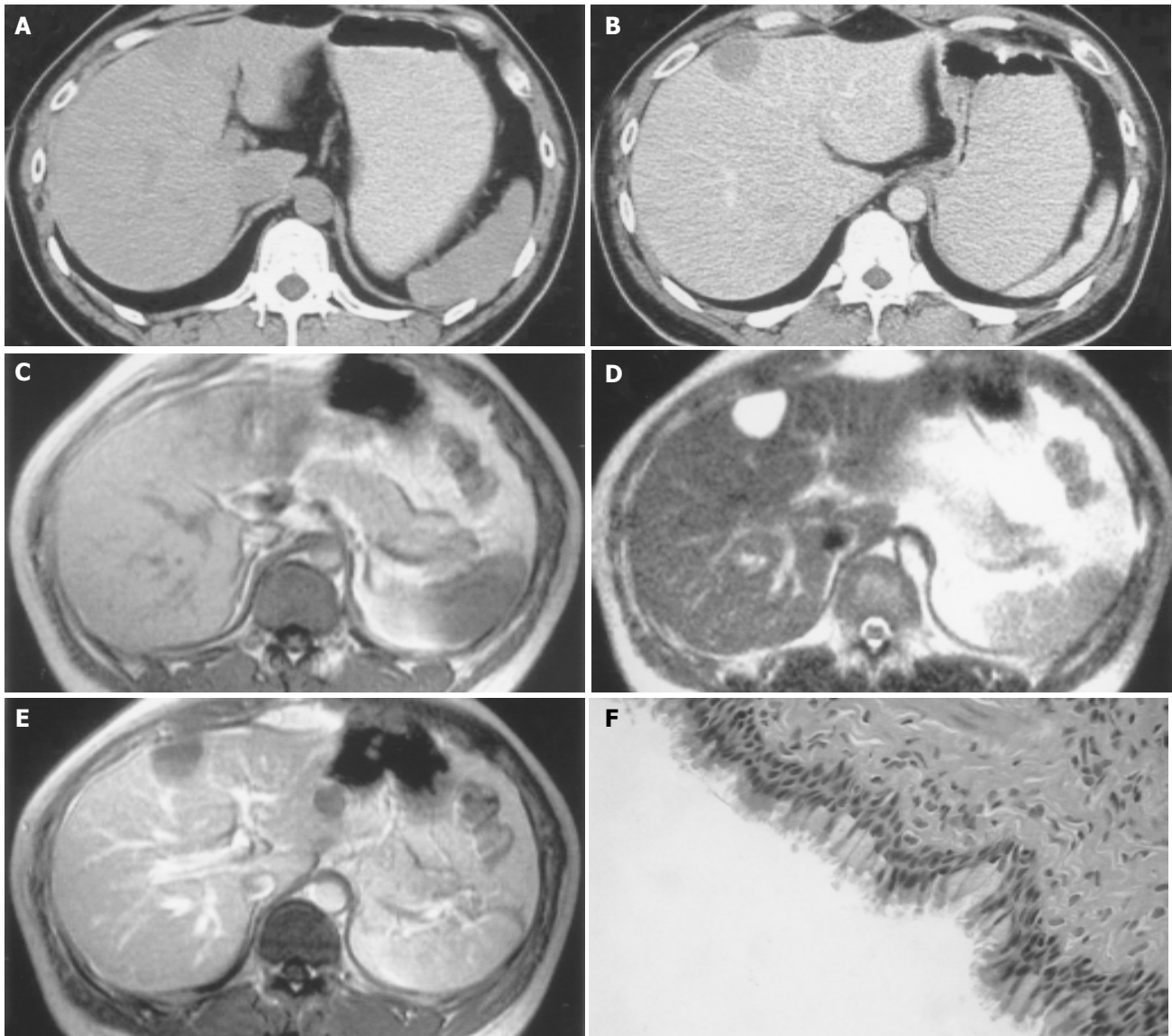


Figure 1 CHFC in a 30-year-old man. **A:** Unenhanced CT scan shows a slightly hypoattenuating (47 HU) mass in the medial segment beneath the hepatic surface; **B:** On enhanced CT scan, a well-defined hypoattenuating mass is revealed with no enhancement; **C:** On axial T1-weighted imaging, the lesion appears isointense relative to surrounding liver parenchyma; **D:** Axial

T2-weighted imaging shows markedly homogeneously hyperintense mass in the left liver; **E:** Enhanced T1-weighted imaging delineates slightly hypointense mass just beneath the hepatic surface; **F:** Photomicrograph reveals a cyst lined by ciliated pseudostratified columnar epithelial cells (HE $\times 400$).

attenuation numbers because the lesion contains calcium^[5]. All the CHFCs have no enhancement after injection of contrast materials, which is one of the characteristics of CHFC and has significance in the differential diagnosis. On MR imaging, all lesions are hyperintense on T2-weighted sequences. However, on T1-weighted images, they may be hypointense, isointense, or hyperintense according to the various elements the lesions contain, including clear serous material or milky white or brown mucous with abundant protein and lipid sometimes^[5,11,12].

When a CHFC appears hypoechoic at US and the attenuation at CT ranges from that of soft tissue to very high attenuation, it is hard to differentiate the CHFC from a solid lesion. However, MR imaging is found to be useful in differential diagnosis, especially on T2-weighted imaging. When a CHFC is demonstrated as anechoic lesion at US,

cystadenoma may be included in the differential diagnosis because the lesion may be malignant. Differential points are that cystadenomas are usually multilocular and sometimes reveal mural nodules, and these features are well revealed on radiologic imaging^[5].

CHFC occurs more frequently in men and is found most commonly in the medial segment of the left hepatic lobe just beneath the hepatic surface, unlike most other solitary cysts that show a female predominance and greater occurrence in the right hepatic lobe^[7]. Therefore, this location is also one of the characteristics of CHFC and probably an important diagnostic consideration. Meanwhile, MRI is helpful to differentiate CHFC from other solitary cysts that usually show markedly homogeneously hypointense on T1-weighted imaging.

In conclusion, when a well-demarcated subcapsular

lesion of the left hepatic lobe with the varied internal appearance as we described above is demonstrated, CHFC should be considered.

REFERENCES

- 1 **Horii T**, Ohta M, Mori T, Sakai M, Hori N, Yamaguchi K, Fujino H, Oishi T, Inada Y, Nakamura K, Okanoue T, Kashima K. Ciliated hepatic foregut cyst. A report of one case and a review of the literature. *Hepatol Res* 2003; **26**: 243-248
- 2 **Bogner B**, Hegedus G. Ciliated hepatic foregut cyst. *Pathol Oncol Res* 2002; **8**: 278-279
- 3 **Hirata M**, Ishida H, Konno K, Nishiura S. Ciliated hepatic foregut cyst: case report with an emphasis on US findings. *Abdom Imaging* 2001; **26**: 594-596
- 4 **Wu ML**, Abecassis MM, Rao MS. Ciliated hepatic foregut cyst mimicking neoplasm. *Am J Gastroenterol* 1998; **93**: 2212-2214
- 5 **Kadoya M**, Matsui O, Nakanuma Y, Yoshikawa J, Arai K, Takashima T, Amano M, Kimura M. Ciliated hepatic foregut cyst: radiologic features. *Radiology* 1990; **175**: 475-477
- 6 **Rosai J**. Liver. In: Rosai J, ed. *Ackerman's surgical pathology*. 8th ed. St Louis: *Mosby* 1996: 898-899
- 7 **Vick DJ**, Goodman ZD, Deavers MT, Cain J, Ishak KG. Ciliated hepatic foregut cyst: a study of six cases and review of the literature. *Am J Surg Pathol* 1999; **23**: 671-677
- 8 **Harty MP**, Hebra A, Ruchelli ED, Schnauffer L. Ciliated hepatic foregut cyst causing portal hypertension in an adolescent. *Am J Roentgenol* 1998; **170**: 688-690
- 9 **Furlanetto A**, Dei Tos AP. Squamous cell carcinoma arising in a ciliated hepatic foregut cyst. *Virchows Arch* 2002; **441**: 296-298
- 10 **de Lajarte-Thirouard AS**, Rioux-Leclercq N, Boudjema K, Gandon Y, Ramee MP, Turlin B. Squamous cell carcinoma arising in a hepatic foregut cyst. *Pathol Res Pract* 2002; **198**: 697-700
- 11 **Murakami T**, Imai A, Nakamura H, Tsuda K, Kanai T, Wakasa K. Ciliated foregut cyst in cirrhotic liver. *J Gastroenterol* 1996; **31**: 446-449
- 12 **Shoenut JP**, Semelka RC, Levi C, Greenberg H. Ciliated hepatic foregut cysts: US, CT, and contrast-enhanced MR imaging. *Abdom Imaging* 1994; **19**: 150-152

Science Editor Wang XL and Guo SY Language Editor Elsevier HK

• ACKNOWLEDGMENTS •

Acknowledgments to Reviewers of *World Journal of Gastroenterology*

Many reviewers have contributed their expertise and time to the peer review, a critical process to ensure the quality of *World Journal of Gastroenterology*. The editors and authors of the articles submitted to the journal are grateful to the following reviewers for evaluating the articles (including those were published and those were rejected in this issue) during the last editing period of time.

Yasuji Arase, M.D.

Department of Gastroenterology, Toranomon Hospital, 2-2-2 Toranomon minato-ku, Tokyo 105-8470, Japan

Takeshi Azuma, Associate Professor

Second Department of Internal Medicine, University of Fukui, Faculty of Medical Sciences, Matsuoka-cho, YoshIDA-gun, Fukui 910-1193, Japan

Xian-Ming Chen, M.D.

Mayo Medical School, Clinic and Foundation, 200 First Street, SW, Rochester, MN 55905, United States

Jaime Guardia, Professor

Internal Medicine and Liver Unit, Hospital Universitari 'Vall d'Hebron'. Universitat Autònoma de Barcelona, Hospital Universitari Vall d'Hebron, Pg Vall d'Hebron, 119, Barcelona 08035, Spain

Hajime Isomoto,

Basic Research Center for Digestive Diseases, Division of Gastroenterology and Hepatology, Mayo Clinic, 200 First Street, Rochester 55905, United States

Seigo Kitano, Professor

Department of Surgery I, Oita University Faculty of Medicine, 1-1 Idaigaoka Hasama-machi, Oita 879-5593, Japan

Zahariy Krastev, Professor

Department of Gastroenterology, Universiti Hospital "St. Ivan Rilski", #15, blvd "Acad. Ivan Geshov", Sofia 1431, Bulgaria

Ai-Ping Lu, Professor

China Academy of Traditional Chinese Medicine, Dongzhimen Nei, 18 Beixincang, Beijing 100700, China

Reza Malekzadeh, Professor

Director, Digestive Disease Research Center, Tehran University of Medical Sciences, Shariati Hospital, Kargar Shomali Avenue, 19119 Tehran, Iran

Timothy H Moran, Professor

Department of Psychiatry, Johns Hopkins University School of Medicine, Ross 618, 720 Rutland Ave, Baltimore, Maryland

21205, United States

Yoshiharu Motoo, Associate Professor

Cancer Research Institute, Kanazawa University, 13-1 Takaramachi, Kanazawa 920-0934, Japan

Hiroshi Nakagawa, Assistant Professor

Gastroenterology Division, University of Pennsylvania, 415 Curie Blvd. 638B CRB, Philadelphia 19104, United States

Pankaj Jay Pasricha, M.D.

Department of Internal Medicine, The University of Texas Medical Branch, 301 University Boulevard, Rt. 0764, Galveston, TX 77555-0764, United States

Michiie Sakamoto, Professor

Department of Pathology, Keio University School of Medicine, 35 Shinanomachi, Shinjuku-ku, Tokyo 160-8582, Japan

Qin Su, Professor

Department of Pathology, Cancer Hospital and Cancer Institute, Chinese Academy of Medical Sciences and Peking Medical College, PO Box 2258, Beijing 100021, China

Kiichi Tamada, M.D.

Department of Gastroenterology, Jichi Medical School, 3311-1 Yakushiji, Minamikawachi, Kawachigun, Tochigi 329-0498, Japan

Hans Ludger Tillmann, Professor

Medizinische Klinik und Poliklinik II, University Leipzig, Philipp Rosenthal Str. 27, Leipzig 04103, Germany

Karel van Erpecum, M.D.

Department of Gastroenterology and Hepatology, University Hospital Utrecht, Utrecht 3508GA, The Netherlands

Yuan Wang, Professor

Institute of Biochemistry and Cell Biology, Shanghai Institutes for Biological Sciences, Chinese Academy of Sciences, Shanghai 200031, China

Hiroyuki Watanabe, Assistant Professor

Department of Internal Medicine, Cancer Research Institute, Kanazawa University, 13-1 Takaramachi, Kanazawa University, Kanazawa 920-8641, Japan

Harry H-X Xia, M.D.

Department of Medicine, The University of Hong Kong, Pokfulam Road, Hong Kong, China

Hiroshi Yoshida, M.D.

First Department of Surgery, Nippon Medical School, 1-1-5 Sendagi, Bunkyo-ku, Tokyo 113-8603, Japan